STATE OF MAINE

LAND USE PLANNING COMMISSION

IN RE: PICKETT MOUNTAIN MINE REZONING APPLICATION	)	
	)	PRE-FILED DIRECT TESTIMONY
Applicant: Wolfden Mt. Chase LLC	)	OF ANN MAEST
Location: T6R6 WELS	)	
Commission Application Number: ZP 779A	)	

I. INTRODUCTION

This pre-filed direct testimony of Dr. Ann Maest of Buka Environmental is submitted on behalf of Intervenors Penobscot Nation, Houlton Band of Maliseet Indians, Natural Resources Council of Maine, and Conservation Law Foundation, in opposition to the rezoning application ("Application") filed with the Land Use Planning Commission ("LUPC") by Wolfden Mt. Chase LLC, a wholly owned subsidiary of Wolfden Resources LLC (collectively "Wolfden").

My testimony focuses on the geochemical characteristics of the Pickett Mountain deposit, its acid mine drainage (AMD) and contaminant leaching potential, the reliability of water quality predictions, the proposed water treatment and water balance estimate, and the fate and transport of mine contaminants from mine sources to nearby water resources. Due to shortcomings in its Application on these and other topics, Wolfden has failed to demonstrate that the project will avoid significant adverse environmental impacts and that its technical approaches to minimize or mitigate these impacts are reasonably feasible.

II. QUALIFICATIONS

Ann S. Maest is Vice President of Buka Environmental in Telluride, Colorado, and has over 35 years of research and professional experience. She is an aqueous geochemist with expertise in the environmental effects of hard rock mining; the fate and transport of natural and

anthropogenic contaminants in groundwater, surface water, and sediment; mineralogy and mine waste characterization; sampling and analysis of water, sediment, soil, and wastes; geochemical modeling; and responsible mining initiatives. Dr. Maest worked as a research geochemist with the U.S. Geological Survey, where she conducted research on metal-organic interactions, metal and metalloid speciation, and redox geochemistry in surface water and groundwater. She was also a Senior Scientist at the Environmental Defense Fund where she designed approaches to minimize the release of toxics from mining and manufacturing facilities. The results of her research have been published in peer-reviewed journals including *Applied Geochemistry*, *Minerals*, and *Chemical Geology*. Dr. Maest has served on several National Academy of Sciences committees and a board related to earth resource and mining and minerals research issues and was an invited speaker on technical challenges and solutions for the mining sector at the United Nations. She is a member of the American Chemical Society, the International Mine Water Association, and the Society for Mining, Metallurgy & Exploration (SME). Ann holds an undergraduate degree in geology from Boston University and a PhD in geochemistry and water resources from Princeton University.

III. GEOCHEMICAL CHARACTERISTICS OF THE PICKETT MOUNTAIN DEPOSIT

The Pickett Mountain deposit is a volcanogenic massive sulfide (VMS) deposit that initially formed on the seafloor and is similar to modern-day "black smokers" that form chimneys and other sulfide deposits in the deep submarine environment (A-Z Mining Professionals, 2019, pp. 30–31; Plumlee et al., 1999, pp. 381–82). Of the three types of VMS deposits, Pickett Mountain is a member of the Kuroko-type VMS deposit (McCormick, 2021, p. 3). Kuroko-type VMS deposits occur in intermediate to felsic volcanic rocks that have higher acid drainage potential than the other types of VMS deposits (Cyprus-type and Besshi-type) that

occur in basaltic and sedimentary rocks, respectively (Plumlee et al., 1999, pp. 381-82). The Preliminary Economic Assessment by A-Z Mining Professionals Limited notes that the deposit is hosted primarily by intermediate to felsic volcanic units (Stantec Consulting Services Inc., 2023 ("Application") at 544 (all page references to the Application are to the pdf pagination, not to internal document pagination)).

The Pickett Mountain deposit contains high percentages of pyrite (iron sulfide), which is typical of VMS deposits. As noted in Section IV, pyrite is the primary source of AMD. The minerals of primary economic interest are chalcopyrite (copper iron sulfide), galena (lead sulfide), and sphalerite (zinc iron sulfide). Pyrite is intimately associated with the minerals of economic interest in the deposit, which contains 45 – 60% pyrite, 4% chalcopyrite, 3% galena, and 15% sphalerite (Application at 544). The sulfides of economic interest are overlain and in sharp contact with massive pyrite (A-Z Mining Professionals, 2019, p. 25). The association of large amounts of pyrite with the material that would likely be removed as ore indicates that pyrite will remain on the walls of the underground mine and will also be an important part of waste rock, ore, and tailings.

Minor amounts of other sulfides, including tetrahedrite, tennantite,[1] and arsenopyrite,[2] occur in the deposit (Application at 544) and can also form AMD (Plumlee, 1999, p. 3-4, Tables 3.2 and 3.3). In addition to iron, copper, zinc, arsenic, and antimony, the next most abundant metals in tetrahedrite-tennantite are mercury and lead; cadmium, cobalt, manganese, and selenium concentrations are also elevated in these two sulfide minerals (George et al., 2017).

It is unclear whether the minor sulfides would be mostly associated with the ore that is planned to be removed from the site or remain on the site with the waste rock and as part of the

[1] Tetrahedrite and tennantite are copper-iron-zinc arsenic and antimony sulfides, respectively.
[2] Arsenic iron sulfide

walls of the underground mine. Even though the deposit is relatively compact, as defined by the limited exploration conducted to date, ore cannot be surgically removed from the deposit, and it is certain that the major and minor sulfides would also be present in mined materials and surfaces remaining on the site. The mineralogy and geochemistry of the deposit tell us that once mined, the major and minor sulfides will be sources of many toxic constituents – including copper, lead, zinc, arsenic, antimony, mercury, cadmium, cobalt, manganese, and selenium. These toxic elements will leach from the mined materials on- and off-site and potentially affect downgradient water resources.

The deposit, as currently defined, is the smallest of the known VMS deposits in the Maine/New Brunswick/Newfoundland area. As shown in Figure 1, the Pickett Mountain deposit is currently estimated to contain only 2.05 million metric tonnes (Mt) of indicated ore (also see A-Z Mining Professionals, 2019, Table 1.1, p. 2). As noted in the Preliminary Economic Assessment, “The potential quantity and grade of the target is conceptual in nature. There has been insufficient exploration of this target to define a Mineral Resource and it is uncertain if further local exploration will result in this target being delineated as a Mineral Resource.” (Application at 622). The lack of a proven reserve, the small deposit size, and the high likelihood that acid drainage will form and require long-term treatment and management make development of the project economically risky.

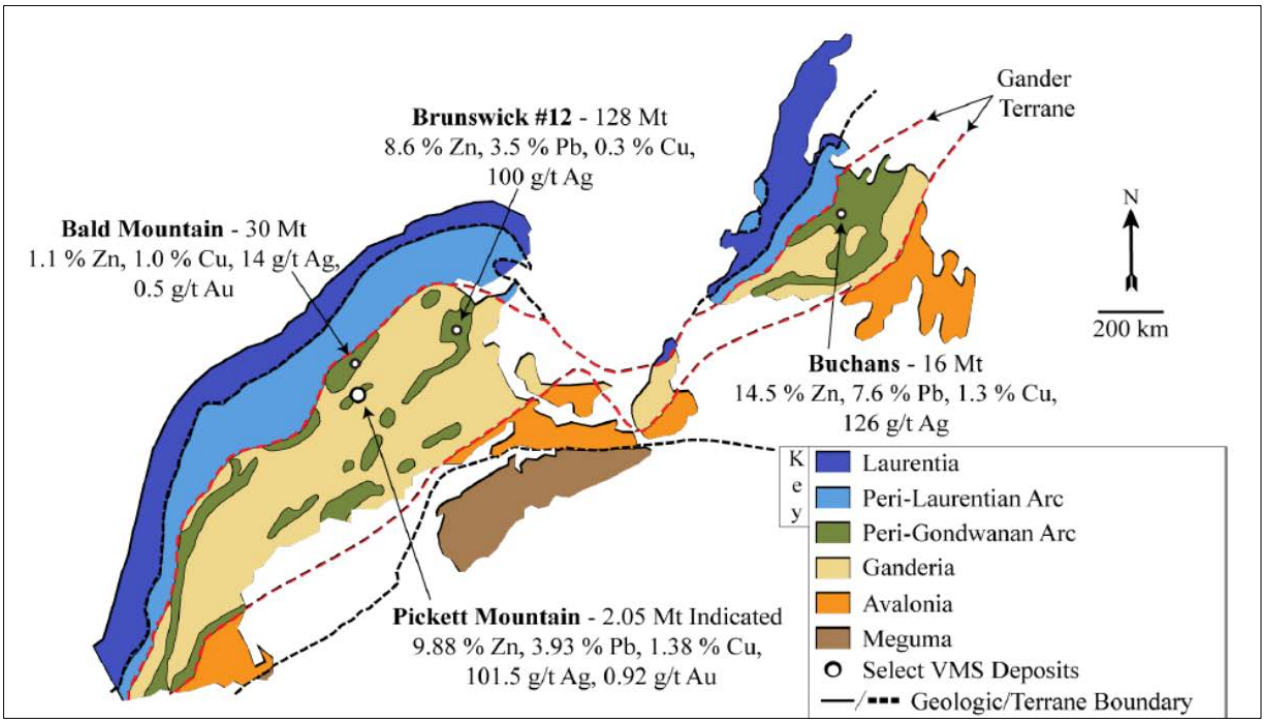

Figure 1. Map showing volcanogenic massive sulfide (VMS) deposits and mines in geologic terranes from Maine, including the Pickett Mountain deposit, through New Brunswick and Newfoundland, Canada. Deposit names, sizes, and ore grades are shown.
Source: McCormick, 2021, Figure 2.1, p. 12.

Zinc is the only metal identified as a critical mineral in the Pickett Mountain deposit. Zinc was added to the U.S. critical mineral list in 2022 (U.S. Department of the Interior, 2022) and was not on the previous list in 2018 (the list is updated every three years). However, according to the U.S. Geological Survey's Mineral Commodity Summaries (U.S. Geological Survey, 2023, p. 201), zinc mine production in the U.S. increased by 9% in 2022 compared to 2021. Several other zinc exploration and mine expansion projects were in development in the U.S. in 2022, and zinc production at the Red Dog zinc-lead mine in Alaska (largest zinc mine in the U.S. and second largest in the world) increased in 2022. In addition, the Empire State zinc mine in New York gained approval to add open pit mining to its active underground mine. In terms of domestic production, the small predicted production from Pickett Mountain would not meaningfully change the overall U.S. mine production and would not change the amount of U.S.

refined zinc because the concentrate from Pickett Mountain is planned to be refined in Canada. In addition, the United States is already the world's fifth largest exporter of zinc.[3]

IV. ACID MINE DRAINAGE POTENTIAL FROM THE PICKETT MOUNTAIN DEPOSIT AND WATER QUALITY FROM SIMILAR DEPOSITS

Based on the limited information on mineralogy, deposit type, lithology, and alteration, the Pickett Mountain deposit is nearly certain to generate acid mine drainage. Because of the catalysis of the reaction by microbes, which are ubiquitous in groundwater and surface water (Nordstrom and Alpers, 1999), the reaction is very difficult to stop once it has begun. The reaction will take place at the mine site, in wastes and ore temporarily stored on the site, in the underground workings, and at the tailings disposal site and can adversely affect downgradient water quality at both locations.

A. Acid mine drainage potential for the Pickett Mountain Deposit

Pyrite is the primary cause of AMD, which is often considered the most environmentally damaging and enduring water quality problem associated with metal mining (see, e.g., USDA, 1993, p. 3; INAP, 2023). The effects of AMD on aquatic life are substantial, and it is considered the largest environmental liability facing the Canadian mining industry (Jennings et al., 2008, p. 4; Tremblay, 2001). Developing mines in sulfide deposits can require perpetual management and treatment, and careful consideration and experience must be applied to AMD prediction, monitoring, management, and prevention (Australian Government, 2016, p. 3). For example, mines that operated during the Bronze Age in Spain (5000 years ago) and in Bolivia nearly 500 years ago are still producing acid drainage (Davis et al., 2000; Strosnider et al., 2007). The

[3] World Bank, 2021. https://wits.worldbank.org/trade/comtrade/en/country/ALL/year/2021/tradeflow/Exports/partner/WLD/product/260800

mining district discussed in Davis et al. (2000), the Iberian Pyrite Belt in Spain, which is still producing acid drainage after nearly 5000 years, is, like Pickett Mountain, a VMS deposit.

1. Forgotten or ignored sources of AMD

As noted in Section III, the Pickett Mountain deposit has high percentages of pyrite and other metal sulfides that will produce acid mine drainage when extracted and handled at the site. Acid-base accounting tests are normally applied to all mined materials – including ore, waste rock, the walls of the underground workings or pits, tailings, and overburden – to estimate the potential for the materials to produce acid during and after mining. Importantly, Wolfden fails to mention all potential sources of AMD, stating that "Within the Project Area, the potential sources of acid rock drainage are limited to mineralize rock from underground being temporarily stored on the surface." (Application at 289). This statement ignores leaching of the walls of the underground workings as a source of acid drainage. Mining the deposit will require dewatering of the area that will become the underground mine (to allow mining to proceed). Lowering the groundwater table will bring much more oxygen into the mined-out area, thus creating the ideal environment to produce acid mine drainage from the sulfides that will inevitably be exposed on the walls of the underground workings. As noted by Price (2009, p. 4-2) and many other practitioners, samples of the walls of the underground mine should be a part of geochemical testing.

Wolfden additionally states that their approach for handling the mineralized rock temporarily stored on the surface (lined rock pads, leachate collection, treatment, discharge) will "remove potentially acid generating material and thereby remove the risk related to acid rock drainage." (Application at 289) It is important to realize that even with trucking the ore offsite for concentrating and storing removed mineralized rock on the surface in a protective manner, releases of mine-related contaminants can and do occur, as described in Section V for the Eagle

Mine in Michigan and Sections VI and VIII for the Buckhorn Mine in Washington State. None of the mitigation measures proposed by Wolfden Resources address the AMD risk from leaching of the walls of the underground mine.

2. Inadequate number of samples

Wolfden has provided results for only seven geochemistry samples in the Application in Attachment 10-B, Research Productivity Council (RPC) Report (Application at 399). In an August 2023 letter to LUPC (Wolfden, 2023, p. 7), Wolfden states that a more comprehensive metal leaching and acid rock drainage (MLARD) testing program will be completed on fresh cores, once collected, but at this point, only seven samples have been analyzed. These minimal results cannot be used to demonstrate that the project will avoid significant adverse effects.

Geochemical testing is the only way the potential environmental effects of a proposed mining project can be predicted (because the project does not yet exist), and the results are typically used to design protective management approaches to prevent and minimize the effects of mining on natural resources, especially on water quality. Geochemical test samples during the early phases of mining are derived from exploration drill cores and bench-scale metallurgical testing used to produce tailings. For the Pickett Mountain mineral resource estimate in 2019, 940 of the total 2,550 samples from the 148 drill holes[4] were used, and a block model of the deposit was created (A-Z Mining Professionals, 2019, p. 3). Clearly, there is no shortage of material available for geochemical testing, yet results for only seven samples are available. According to Price (2009, p. 8-5–8-6), when discussing sampling of mined materials for geochemistry, "…the most cost-effective way to characterize geologic materials, waste materials and walls will be an

[4] Note that Wolfden added only 38 new drill holes, from 2017-2018; the remainder were historic drill holes (A-Z Mining Professionals, 2019, p.1)

iterative phased process of sampling and analysis similar to that used to determine other geologic characteristics such as ore reserves."

Acid-base accounting and other geochemical testing should begin during the exploration phase (Price, 2009, pp. 3-12, 4-10 - 4-13). Geochemical characterization usually peaks during the development phase; testing during this phase includes laboratory testing of waste and ore materials (static and kinetic) (INAP, 2009, Chapter 4, Table 4-2). The Pickett Mountain Project appears to be in advanced exploration or in the early stages of mine development. Although strict numbers of recommended sample numbers do not exist and are dependent on the deposit's characteristics, the variety in geologic units and alteration chemistry indicate that many more than seven samples should have been analyzed for acid drainage and contaminant leaching potential using static and kinetic testing methods.

3. Lack of information on sample locations and representativeness

To help understand the potential acid drainage and contaminant leaching of a deposit, geochemical samples should be representative of the deposit's variability in geologic and geochemical characteristics (including mineralogy and metal identity and content). The geochemical sampling efforts presented in the Application are not. Wolfden does not even identify the location of the seven samples, except that four are collected more than 100 ft from the deposit and three are closer to the deposit (Application at 289). In the response to agency questions (Wolfden, August, 2023, p. 7), Wolfden adds that five samples were collected from cores in the footwall and two from the hanging wall, but no information on lithology (rock types) or mineralogy is provided.

A 2019 document called a "NI 43-101," prepared by A-Z Mining Professionals (p. 1) for submission by Wolfden to a Canadian regulatory body, identifies many relevant geologic units and rock types, and these should be tested. The NI 43-101 notes, on p. 1, "The mineral zone at

Pickett Mountain is a stratabound volcanogenic massive sulphide deposit that has been traced by drilling approximately 900 metres along strike and 750 metres down dip. It consists of 4 primary lenses (W1, W2, E1, and E2) and several minor lenses."[5] In addition to the four massive sulfide lenses, the same document describes at least four rock types: mudstone & siltstone, massive mafic rock, mixed breccia unit, massive sulfide, felsic fragmental rock, as shown in Figure 2. The massive sulfide lenses are more directly in contact with felsic fragmental rock and mixed breccia unit (see Figure 2), but portions of the massive mafic rock and potentially the mudstone and siltstone units could also be disturbed during mining. Figure 2 shows that many drill core samples have been collected in each unit, yet only seven samples have been tested. The identity of the seven samples, even in terms of general geologic unit and ultimate mined material have not been presented. We must therefore assume that the geochemical sampling results in the Application are not representative of the variability of geological and geochemical characteristics of the deposit. It is clear that none of the samples are representative of the massive sulfide lenses or any rocks in contact with the lenses. If they were, the %S (sulfur) values would be much higher. As noted in Section III, the deposit contains 45 – 60% pyrite, 4% chalcopyrite, 3% galena, and 15% sphalerite (Application at 544). For example, a sample with 45% pyrite would be 54%S, yet the highest %S value in the seven samples is only 2.7%. Wolfden does add in its responses to agency questions (Wolfden, August, 2023, p. 7) that additional samples will be collected in ore, waste rock, and low-grade ore, including typical rock types to be encountered during underground development and production – but no information is yet available.

[5] A *lens* is a lenticular geological body that tapers out markedly in all directions; its thickness is slight compared to its length.

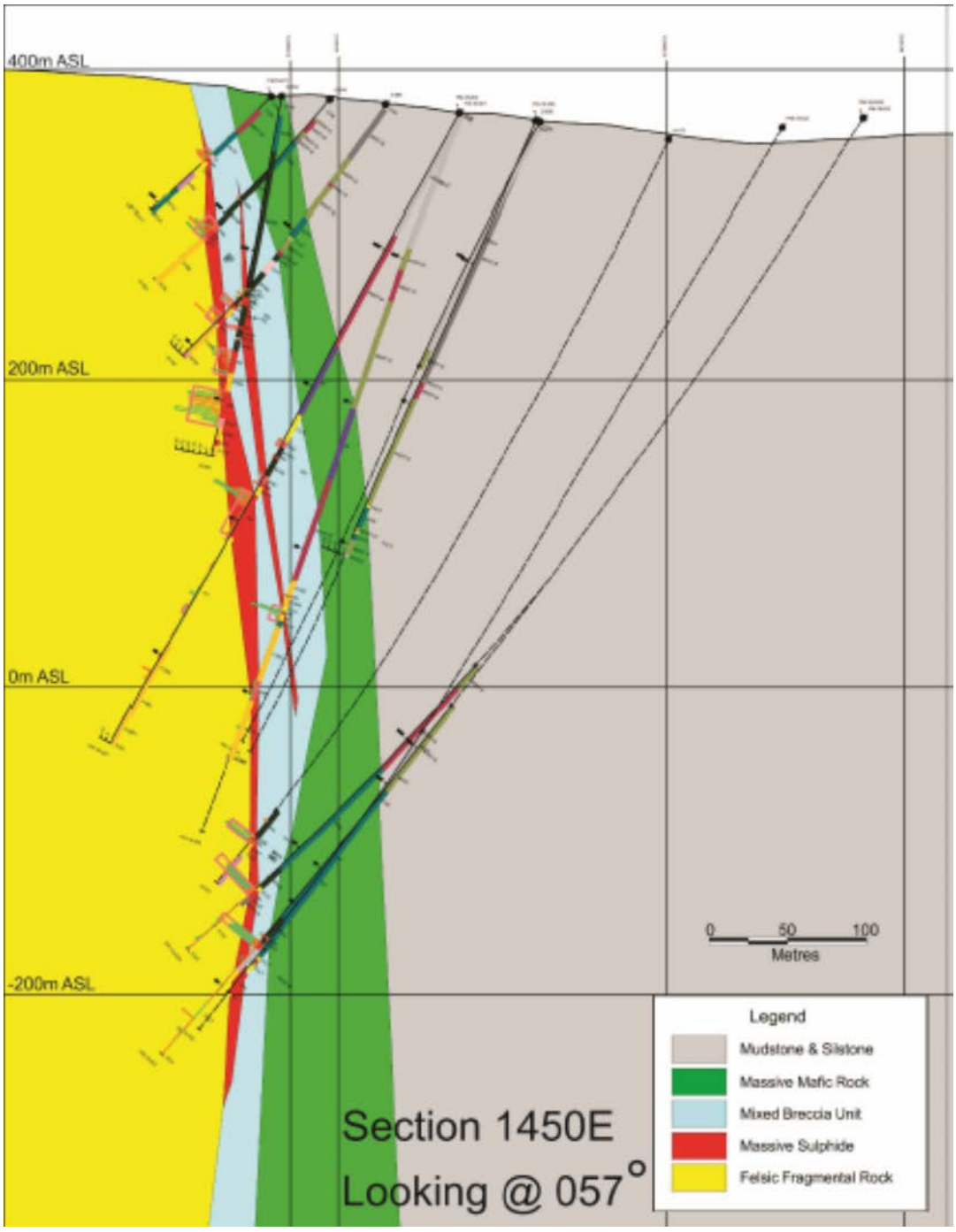

Figure 2. Cross-section of the Pickett Mountain deposit showing drill cores and sampling locations.
Source: A-Z Mining Professionals, 2019, Figure 7.5, p. 22.

4. Interpretation of limited geochemical testing results

In this section I provide an interpretation of the limited geochemical testing results presented in the RPC report (Attachment 10-B of the Application).

Acid-base accounting

The acid-base accounting (ABA) results for the seven samples are provided in Table 2 of the RPC report (Application at 402).[6]

Wolfden's consultants did use the most recommended method for ABA testing (Modified Sobek). According to the RPC report, three samples are potentially acid generating, and the remaining four are "not net acid producers." These conclusions are not supported by the data. All seven samples exhibit characteristics that should trigger additional testing, especially for mineralogy and long-term testing, to understand the samples' acid generating potential, according to Maest et al. (2005, p. 28) and Plante et al. (2012). Either none of this testing has been conducted on the Pickett Mountain deposit samples, or the results have not been made publicly available. In either case, because of the lack of additional testing, Wolfden cannot make reliable statements about the acid-generating potential of any of the samples presented in the Application. Wolfden's contractor, RPC, seems to understand that they are not equipped to interpret the ABA results. The report states, "It is recommended that a specialized consultant be contacted for the full MEND Report 1.20.1 analysis and interpretation prior to follow up with the regulatory agent." (Application at 402) Even though the lack of follow-up sampling is troubling, what is more concerning is the low number of samples and the fact that we have no idea where these samples were collected, including their depth or geologic unit.

Total metals analysis

Whole rock and total metals analysis results for the seven samples are presented in Tables 3 and 4 of the RPC report (Application at 403 and 404). The methods used to prepare the samples are not described. At least five different methods of sample digestion can be used, and

[6] Note that the calculated NP/AP ratio for sample ABA-007 in Table 2 is incorrect. It should be 82 rather than 131 (the sample is less net neutralizing than shown).

the method used will affect the results (Price, 2009, Chapter 10.0). The samples were analyzed by ICP (I assume this is inductively coupled plasma atomic emission spectroscopy, ICP-AES), which is generally an acceptable method. The detection limits noted in Table 3 are generally acceptable, with the exception of selenium and silver. Ideally, these detection limits should be 0.01 mg/kg, which would require using ICP-MS, because average concentrations in unmineralized rock types are quite low (Yaroshevsky, 2006, pp. 50–51). The geochemical characteristics of the samples are not described, and it is not known if the samples are from mineralized or unmineralized locations.

The RPC report does not interpret these results in terms of the potential for metal leaching. My review shows that there is a potential for metal leaching from these samples. In my review, I compared the results to the appropriate values in Yaroshevsky (2006, pp. 50-51), which presents average metal concentrations in different rock types on a global basis, including overall average crustal abundance (average metal content of all rocks on Earth). The comparison shows that total concentrations of antimony, arsenic, cadmium, cobalt, mercury, lead, thallium, and zinc were at least twice as high as average values for the types of rocks present at the Pickett Mountain site. These elements are known to be toxic to human health (antimony, arsenic, cadmium, mercury, lead, thallium) and aquatic life (cadmium, mercury, lead, zinc) at relatively low concentrations.

Lead values were up to 63 times higher, cadmium values were up to 47 times higher, and zinc values were up to 30 times higher than average crustal abundances for these metals. The high values were not limited to the three samples identified as potentially acid generating (PAG; ABA-003, -004, -006), although the highest values were often in these samples. Sample ABA-001 had the highest concentrations of mercury and thallium. The results suggest that leaching of

these samples, even under neutral pH conditions, may produce elevated concentrations of certain metals and metalloids, and more testing – including long-term (kinetic) leach testing – is needed.

B. Water quality from similar deposits

Because Wolfden has not described the provenance of the samples in the RPC report and because no leach testing has been conducted (short-term or long-term/kinetic), or is publicly available for the Pickett Mountain deposit, it is helpful to examine water quality associated with similar VMS deposits to begin to understand the leachate chemistry that could be generated from mining of the Pickett Mountain deposit.

As noted in Section III, the Pickett Mountain deposit is a Kuroko-type VMS deposit. One of the most well-known Kuroko-type VMS deposits is the Iron Mountain Mine in California. This mine has produced negative pH values (as low as -3.5) due to the extremely high acidity and leachate with very high concentrations of arsenic, zinc, copper and other elements. The Iron Mountain Mine is similar to the Pickett Mountain deposit in terms of its mode of formation, but it is a very large and old mine, has high temperatures in the mine stopes due to the heat generated by exothermic pyrite oxidation, and has experienced evaporative concentration (Plumlee et al., 1999, p.382).

The Holden Mine in Washington State is a Kuroko-type VMS deposit in a wetter climate with greater groundwater recharge into the mine workings. The water quality data in the Plumlee et al. (1999, pp. 409, 415, 421, 427) appendix for the Holden Mine are from tailings leachate, adit water, and mine dump water (waste rock). The pH values ranged from 2.9 to 4.6, and copper concentrations ranged from 0.003 to greater than 40 mg/L. The values for the protection of aquatic life for copper in Maine Department of Environmental Protection Chapter 584 are hardness dependent (hardness can protect against toxicity), but the default value to protect aquatic life from acute toxicity is 3.07 micrograms per liter, more than 1000 times lower than the

higher values from the Holden Mine (See Code Me. R. § 06-096 Ch. 584, App. A, Table 1). Sulfate and cadmium concentrations for the Holden Mine were also high and are shown in Figure 3 plotted against pH. Sulfate is an indication of acid mine drainage, and cadmium is toxic to humans at low concentrations and to aquatic life at even lower concentrations. Federal drinking water standards for sulfate and cadmium are shown for comparison purposes to indicate how much the mine waters would need to be diluted or treated to attain concentrations that are acceptable for human consumption. Wolfden's water releases would have to meet even lower background values.

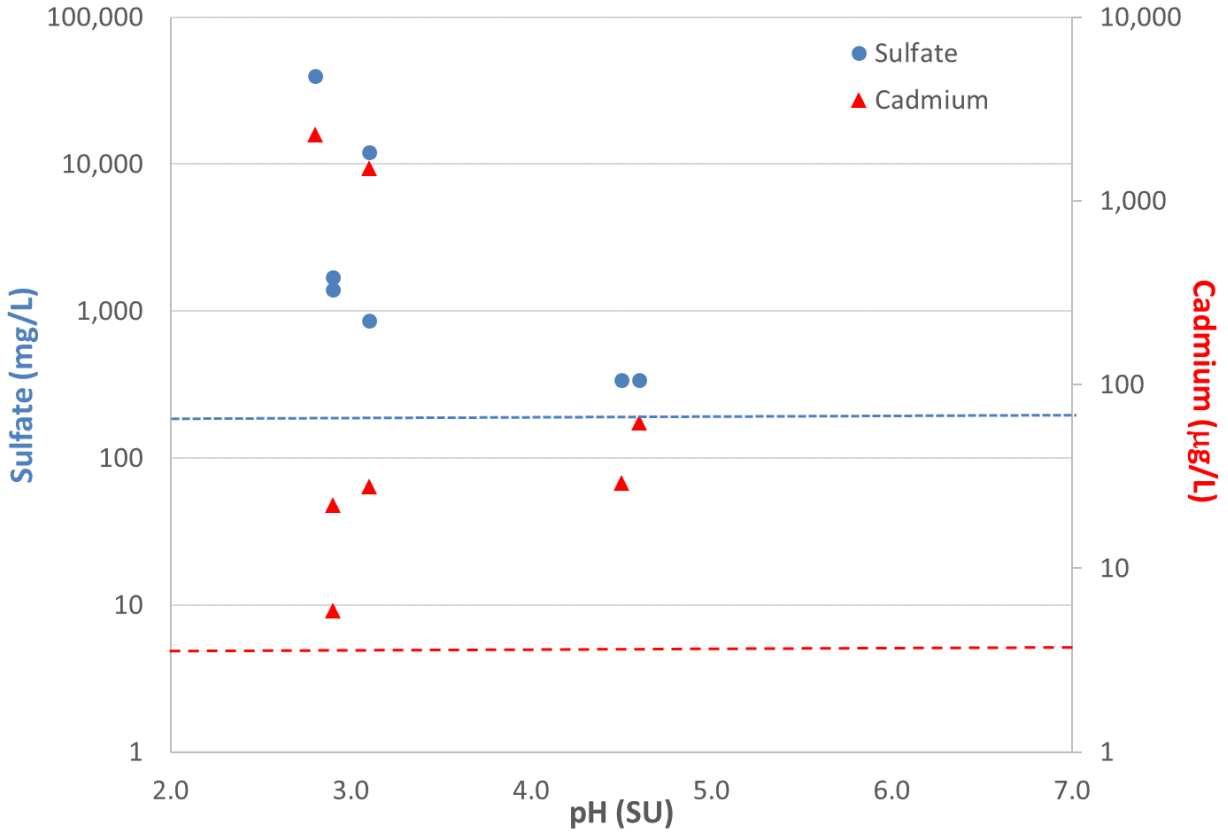

Figure 3. Sulfate and cadmium concentrations versus pH for mine water from the Holden Mine, Washington State. Note the logarithmic axes, used to be able to see the lower concentrations and the U.S. federal drinking water standard lines for sulfate (blue) and cadmium (red). The line shown for sulfate is a secondary maximum contaminant level.
Data source: Plumlee et al., 1999, Appendix, pp. 409, 415, 421, 427.

V. PREDICTIONS VS REALITY

A. Predictions for large-scale U.S. mines

In a 2006 study, James Kuipers and I evaluated the environmental performance at large U.S. hardrock mines for 183 major mines (Kuipers and Maest, 2006). The study included review of 104 Environmental Impact Statements (EISs) and collection of water quality data and associated information from state agencies to compare predicted and actual water quality at 25 case study mines.[7] The results showed that overall, 76% of the mines had mine-related exceedences of water quality standards in groundwater and surface water (i.e. contaminant levels were worse than water quality standards). Of these mines with exceedences, nearly half underestimated or ignored the potential for contaminant leaching potential in EISs (Kuipers and Maest, 2006, p. ES-10). The study also found that mines with certain inherent characteristics (proximity to surface water and groundwater; moderate to high acid drainage and contaminant leaching potential) were even more likely to exceed water quality standards. For example, for case study mines with close proximity to groundwater and moderate to high acid drainage/contaminant leaching potential, 93% had exceedences of water quality standards in groundwater, and 86% of those mines predicted there would be no exceedences (Kuipers and Maest, 2006, p. ES-12. Notably, the Pickett Mountain site would be in close proximity to groundwater and surface water, and the deposit has high acid drainage and contaminant leaching potential.

The study further found that one of the primary causes of exceedences was failure of planned and implemented mitigation measures:[8] this failure mode occurred at 64% of the sites.

[7] The case study mines were based on ability to access water quality data, variability in geographic location, commodity type, extraction and processing methods; variability in EIS elements related to water quality (climate, proximity to water, acid drainage and contaminant leaching potential); and best professional judgment.
[8] Mitigation measures include facility liners, leachate collection systems, run-on/run-off controls, land application of mine water, mine water capture and treatment.

In fact, the water quality predictions without considering mitigation measures (predictions with and without mitigation measures are required for EISs) were closer to actual water quality monitoring results. Although the study is 17 years old, it remains the most comprehensive study conducted on this issue. The implications of the findings are that (1) mines with close proximity to water with moderate to high acid drainage/contaminant leaching potential, like the proposed Pickett Mountain mine, need special attention from regulators, (2) geochemical and hydrologic characterization testing (upon which predictions are based) need improvement, and (3) a better understanding is needed of why mitigation measures so often fail.

These conclusions are very relevant to LUPC's evaluation of Wolfden's application. First, the Pickett Mountain mine would be the type of mine that the study showed is highly likely to exceed water quality standards and fail to meet its water quality predictions. Second, Wolfden has failed to provide adequate geologic and hydrologic testing to support its environmental claims. And third, as discussed in Section VI below, Wolfden has not demonstrated that its primary mitigation measure—water treatment—will be able to ensure that the mine's discharges will meet Maine's requirements.

B. Predictions and groundwater quality for the Eagle Mine, Michigan

A comparison of predicted and actual water quality at an active mine, the Eagle Mine in the Upper Peninsula of Michigan, owned and operated by Lundin Mining, provides a more recent example. The Eagle Mine is similar to the Picket Mountain deposit due to its high sulfide content, high concentration of base metals, it is an underground mine that ships all ore offsite to a mill (Humboldt Mill, ~38 miles away by road), and has close proximity to water and moderate to high acid drainage and contaminant leaching potential. Unlike Wolfden Resources, Lundin Mining is a well-established base metal mining company with operations and projects in South America, Europe, and the United States, primarily producing copper, zinc, gold, and nickel.

Water quality for the inflow to the underground mine and waste rock leachate was predicted before mining began (Foth & Van Dyke, 2005). The mine significantly underpredicted sulfate concentrations in the mine inflow and the waste rock leachate. Sulfate is an indication of the development of acid drainage, and values have continued to increase over time. In addition to higher than predicted concentrations for certain constituents in mine sources, concentrations in some groundwater sampling locations have also increased, including arsenic, nitrate, sulfate, mercury, and chloride.

The results for large-scale U.S. mines and the Eagle Mine demonstrate that mine water quality predictions are highly uncertain, and that a modern mine owned and operated by an experienced mining company can have water quality challenges on the mine site – even when all ore is being removed from the site for offsite processing.

VI. WATER TREATMENT AND MINE WATER CAPTURE

The primary mitigation measure proposed by Wolfden Resources at this point is treatment of mine influenced water using ultrafiltration and reverse osmosis (UF/RO). Although these methods are expensive and require experienced on-site personnel to operate and maintain the treatment systems, they are generally reliable and effective methods for treatment of mine influenced water, including for the treatment of acid mine drainage. However, the information presented in the Water Treatment Scoping Study in the Application (at 444), which is included as Attachment 10-D of the Application, does not instill confidence in the success of site-specific treatment of mine water generated from the Pickett Mountain deposit.

Mine water treatment appears to be the only mitigation measure proposed to avoid adverse environmental effects at the proposed site. Additional methods to effectively capture mine influenced water will also be needed but have not been planned.

A. Shortcomings of the MWS Water Treatment Scoping Study

1. Use of Halfmile Mine water quality

The water treatment scoping study attempts to illustrate through modeling that Wolfden will be able to use UF/RO to enable all water discharges from the Pickett Mountain mine to meet natural background water quality. Because actual water resulting from operation of the Pickett Mountain mine does not exist, the study uses water quality data from the Halfmile Mine in New Brunswick, Canada, as a surrogate. The use of Halfmile Mine water quality as a surrogate for expected Pickett Mountain mine water quality is not substantiated.

The only information provided in the Application is that it is a "relevant operating mine" (Application at 444), and that its "water quality data is similar to other mine only operations and provides an appropriate comparison to water quality data expected from Pickett Mountain." (Application at 452). No references or citations are provided. The Halfmile Mine was an underground polymetallic mine in northern New Brunswick, Canada. Unlike the Pickett Mountain deposit, the Halfmile deposit is considered a basaltic and sediment-hosted massive sulfide deposit, which, as noted in Section III and Plumlee et al. (1999, p. 383) has a lower acid generation potential than the Pickett Mountain deposit, which is generally hosted in intermediate to felsic volcanic rocks.

In addition to providing no information about the characteristics of the Halfmile Mine, the input water quality used for the Halfmile Mine is missing important key parameters, including total alkalinity, total dissolved solids, mercury, chloride, fluoride, nitrate, ammonia, and sulfate (Application at 453, Table 1). Because all major anions have no data, the validity of the model is in question; without having all major cations and anions (sodium, calcium, magnesium, alkalinity, sulfate, chloride at a minimum), a charge balance – one method used to ensure the overall water quality results are reasonable – cannot be conducted on the influent

water quality data from the Halfmile Mine. Because samples were collected from the Halfmile Mine during construction and operation (Application at 451), concentrations of nitrate and ammonia are important as a measure of the effects of blasting in the underground mine, yet these analyte concentrations are not included. Five metals are “Not Detectable” in Table 1, and no numeric detection limit is provided. Because the typical rejection (removal) rates for ammonium (NH_4^+) are lower than some of the other projected rates (80-90%; Application at 451; Figure 6), and concentrations would likely be high in water in the underground mine, it is important to include this analyte in the model. In addition, no rejection rate is given for ammonia (NH_3, uncharged ion) in Figure 6 of the water treatment scoping study. At higher pH values (>9.3), concentrations of the uncharged ammonia are higher than the cationic ammonium, and the uncharged form, ammonia, is what causes toxicity to aquatic life (U.S. EPA, 2013, pp. 6-8). Because of the proposed addition of cemented rock fill to the underground mine for the Pickett Mountain Project, mine influent water could have higher pH values, so it is very important to understand the ability of the proposed treatment system to effectively remove both nitrate and ammonia.

Another example of the failure to substantiate the use of Halfmile Mine water quality as a surrogate is that, while the highest value of Halfmile Mine samples was used as the influent water quality for the water treatment modeling, the number of Halfmile Mine samples evaluated and the time period over which the samples were collected are not mentioned. Not enough information is provided to determine if Halfmile Mine is a reasonably comparable mine or to know if the influent water quality used in the Water Treatment Scoping Study is representative of the kinds of mine-influenced inputs (both volume and quality) to the treatment plant at the proposed Pickett Mountain Project.

2. Water treatment modeling

My understanding from the water treatment scoping study is that the Halfmile Mine water itself was not put through an UF/RO treatment system, but instead the effluent water quality that hypothetically would result from treating water with contaminant levels presented for the Halfmile Mine was predicted using models. Of the 192 possible analyte results produced from the four models used (Application at 456, Table 2), at least 85% of the results are either not reported or are reported as 0 or 0.000. Of the few results reported as non-zero values, many are created by the program itself (basis not explained) because the influent water quality had "Not Reported" values. One of the few results reported by all four models is pH, with results of 5.76, 4.600, 5.230, and 8.140. Because each pH unit is 10 times different in hydrogen ion concentration (activity), these reported model results vary by three and half orders of magnitude in hydrogen ion concentration and show the high variability in model outputs.

One of the stated benefits of one of the models, hyd-RO-Dose, is "modeling of water chemistry parameters to five decimal places making it especially effective for ultra-pure water" (Application at 455). This benefit is meaningless if the majority of the results are zero and key input values are missing.

As noted in the previous section on the input values used from the Halfmile Mine, many of the major cation and anion values are missing or "Not Reported." The Texas Water Development Board (2014, p.6) report cited in the Application attachment (Application at 454) states, "The mineral data required by the computer models constitute the major cations and anions found in natural waters. The validity of the analytical data entered into the software model and the subsequent mineral scaling (solubility) calculations used to determine the maximum recovery that can be achieved, both depend on the accuracy of these inputs." Models for the

effectiveness of RO treatment could be more reliable, depending on several factors, but the lack of information about the influent water quality, renders the modeling effort essentially useless.

3. Source of the target water quality values is not defined

In its Application, Wolfden is making a comparison between the predicted effluent from the proposed UF/RO mine water treatment plant and local water quality to determine if the discharge could meet background values, as required by Maine law. The target values for water treatment in the Water Treatment Scoping Study are from "groundwater sampling efforts in September 2021" (Application at 452). Table 1 in Attachment 10-D (Application at 453) lists average and maximum constituent values from the 10 samples collected in 2021, and the full analytical results are stated to be in Appendix 1 of the Water Treatment Scoping Study (Application at 452). However, Appendix 1 does not contain water quality data for the 10 samples – only a fuzzy map showing the locations of 10 water sampling points, with no labelling of the water bodies they were collected from. Using the location map in A-Z Mining Professionals (2019, Figure 4.2, p. 10), Figure 6 shows that three samples were collected from Pleasant Lake, one from the stream flowing into Pleasant Lake, one in Mud Lake, one in a stream south of Mud Lake, two in Pickett Mountain Pond, one in a stream flowing into Pickett Mountain Pond, and one in a stream on the east side of Pickett Mountain Pond.

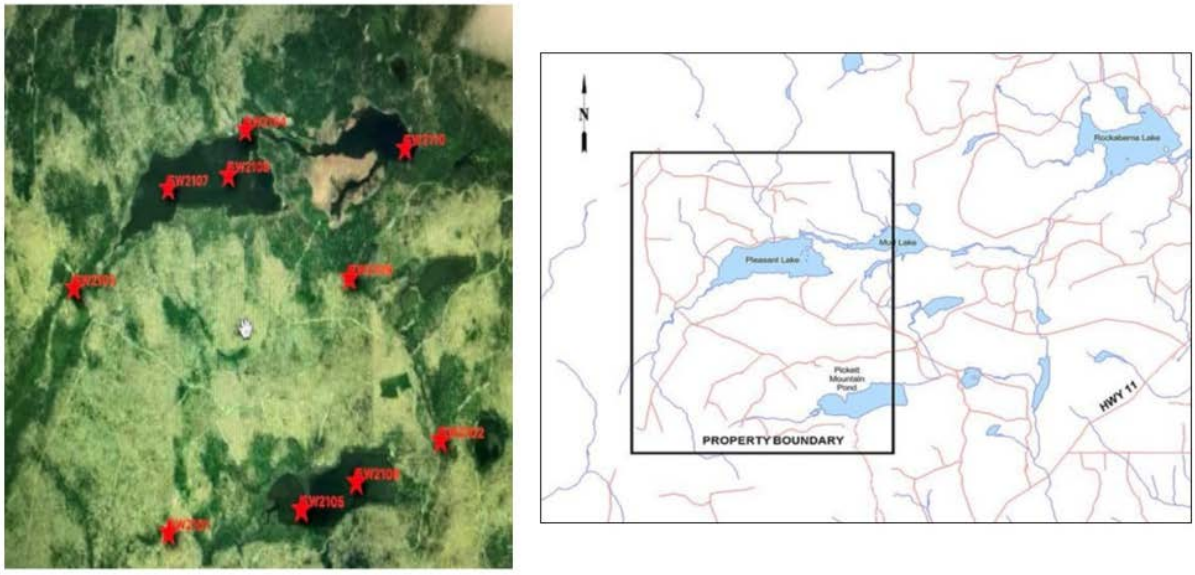

Figure 6. Locations from "groundwater study" conducted by Wolfden, Sept. 2021 (left) and location map showing ponds in and near the property boundary (right).
Sources: Left: Application at 469 (Attachment 10-D, Appendix 1); Right: A-Z Mining Professionals, 2019, Fig. 4.2, p. 10.

The samples used in the Water Treatment Scoping Study as target water quality appear to be from surface water, not groundwater – yet the proposed plan is to discharge treated water to groundwater using a combination of spray irrigation and snowmaking. Assuming that the average and maximum values in Table 1 in Attachment 10-D (Application at 453) are from the 10 samples shown on the map and that the results in the tables are accurate, the results show that surface waters in nearby streams and lakes/ponds have very low solute concentrations with low buffering capacity, neutral pH, and high dissolved organic carbon content. Groundwater should have somewhat higher concentrations of inorganic ions (e.g., calcium, sulfate) because of its longer residence time in soils or aquifers. As noted in the memorandum from the Department of Environmental Protection (2023, p. 6-7), the surface water streams on the project site are classified as Class A waterbodies, and any direct discharges are permitted only if (in addition to other requirements) the discharge effluent will be equal to or better than the existing water quality of the receiving waters. Similarly, the memorandum states that discharge to a wetland

must also meet the Class A criteria, and "given that streams are expression of ground water, the characteristics of the Class A surface water bodies must not be adversely impacted by changes in the characteristics of the ground water as a result of the disposal of treated wastewater via spray irrigation or snowmaking."

Because of the lack of information on local water quality, including groundwater quality, the Water Treatment Scoping Study does not demonstrate whether treated effluent could meet background water quality. And due to the lack of key parameters in the input water quality and a better demonstration that Halfmile Mine water quality is an appropriate surrogate, more work is needed to demonstrate that UF/RO treatment will be technically feasible for treatment of mine water from the Pickett Mountain mine and tailings facility.

Because of the noted shortcomings in the Water Treatment Scoping Study, it would be important for Wolfden Resources to provide examples of comparable mines that use UF/RO treatment and can meet the strict treat-to-background requirements of the State of Maine, but no similar mines have been put forth.

B. Other challenges with UF/RO treatment and mine water capture

1. Management and composition of water treatment plant brine

One of the challenges with UF/RO treatment of high-solute waters, like those expected if the Pickett Mountain deposit is developed, is the production and management of brine from the MWTP. Two UF/RO systems are proposed for the Pickett Mountain Project: one at the mine site and one at the tailings disposal site (Application at 723). According to the U.S. Environmental Protection Agency (U.S. EPA, 2014, p. 43), brine is typically 20-30% of the influent water volume. While the amount of effluent from the mine water treatment plant at the mine site is estimated to be 3,072 gallons/day (Application at 464), the amount of permeate (treated water) versus brine is not provided, and no information is included about the composition of the brine.

In addition, Wolfden proposes to use the brine to make cemented rock fill for backfilling the underground mine, but no information is provided on how the brine's composition might affect the backfill chemistry and leaching. The cemented rock fill placed in the underground mine will remain in the underground in perpetuity, and in some locations the backfill will be close to the ground surface (see Figure 2). The lack of information about the brine composition and volume adds to the uncertainty about the proposed water treatment plan.

Results from long-term leach tests conducted on cemented rockfill used to backfill the Buckhorn Mine show that over time, the neutralization potential decreased markedly, and the leached arsenic concentrations increased, as shown in Figure 7. The effects of using brine in the backfill for the Pickett Mountain mine need to be evaluated to determine if contaminant leaching could adversely affect downgradient groundwater and surface water quality over time.

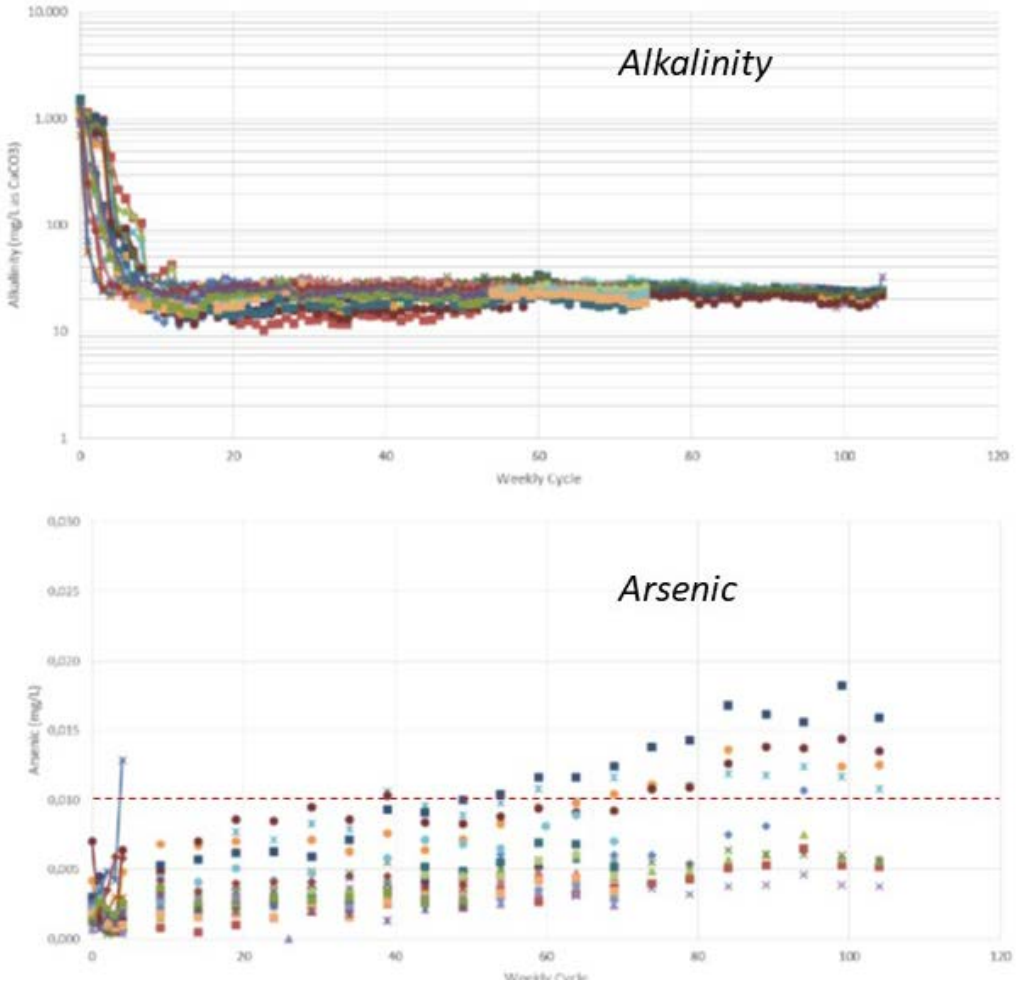

Figure 7. Results from long-term leach tests on cemented rockfill at the Buckhorn Mine, Washington. The alkalinity, a measure of the neutralization potential of the leachate, decreased by nearly two orders of magnitude and the arsenic concentrations rose over the approximately 100-week long testing period. A dashed line at 0.010 mg/L arsenic, the site permit limit, is shown for comparison.
Source: Golder Associates, 2016. 4th Quarter DRMP Report, Figures 2 and 4, pdf 20 and 22.

2. Potential for mine influenced water to evade treatment

Whenever a compliance monitoring location downstream or downgradient of a mining operation shows increasing concentrations of mine-related constituents, it is an indication that not all mine influenced water is being effectively captured by the water management system. If the Pickett Mountain Project aims to avoid adverse impacts to water quality, it must effectively capture all mine-related pollution from its temporary storage facilities for ore and development

rock, contact water ponds, the batch plant, stormwater management features, and the underground mine on the site and from its tailings storage facility, which is planned to be located off-site in an undisclosed location. Captured water can be treated and returned to the environment in a cleaner condition, but uncaptured mine influenced water will contaminate downgradient water resources and lead to undue adverse impacts to water resources.

Land Use Planning Commission (LUPC) guidelines for a zone change application specific to metallic mineral mining require "A description of general measures that may be undertaken to assure that mining in the specified location will not have undue adverse impacts on existing uses and resources and measures that a permittee may take to avoid, minimize or mitigate any adverse impacts of existing uses and features (Chapter 12)." (Application at 286).

Exhibit 10.0 of the Application, Surrounding Uses and Anticipated Impacts, notes in multiple places that surrounding water will not be adversely impacted from mine development:

- "The Project's water treatment approach is designed to capture, treat, and return mine water and contact water while maintaining existing hydrology and water quality to the Project area's wetlands, streams, and surrounding natural environment." (Application at 291)
- "Untreated or contaminated water will not be allowed to return to the natural environment." (Application at 293)
- "…the Project does not anticipate any adverse impacts to the quantity or quality of water received by local aquifers." (Application at 294)
- "Given the capture, collection, and treatment of impacted water to background level quality, the Project will not adversely impact surrounding water resources." (Application at 297)

These statements appear to be primarily based on the treatment of mine water using UF/RO, which is generally a good approach but does not consider mine influenced water that will escape capture, often referred to as “bypass flows.” Bypass flows or seepage can occur from mine water facilities on the surface that could leak or overflow and from mine influenced groundwater that bypasses dewatering wells, among other sources.

A study conducted by Earthworks (Gestring, 2019, p. 1) found that 93% of operating copper mines in the United States failed to capture and control mine wastewater and resulted in adverse water quality impacts. Many of these impacts were from nonpoint source seepage that was not captured from tailings, waste rock, and other mine facilities that were designed to control seepage. Other sources included releases from leaks and spills of process water, tailings spills, runoff, and infiltration through tailings and waste stockpiles and releases associated with extreme storm events. Groundwater contamination sources from the Continental Pit in Montana, included the underground workings, the walls of the open pits, and mine water in the underground workings.

The Buckhorn Mine in Washington State has failed to maintain its groundwater capture zone created by deep dewatering wells. Groundwater compliance monitoring locations outside the designated capture zone have recorded violations of chloride, nitrate, sulfate, and certain metals and arsenic during and after mine operations. The mine closed in 2017, and NPDES permit violations are continuing (Washington State, Office of the Attorney General, 2022). Like the proposed Pickett Mountain Project, the Buckhorn Mine hauled all its ore offsite for concentrating and tailings disposal and backfilled cemented and uncemented waste rock in the underground mine after storing it temporarily on the surface.

VII. WATER BALANCE

Water balance estimates require the use of water balance models, which are highly uncertain – especially in advance of mine development – and should be updated regularly as part of adaptive management.

A. Lack of foundation for 30-gpm dewatering estimate

Errors in water balance estimates affect estimates of the amount of water that will require capture and treatment. An estimated hydrologic budget is presented in the Application at 292 in Table 10-1. The budget includes an estimate for dewatering of the underground mine and surrounding groundwater at only 30 gallons per minute (gpm). The basis for this estimate is not provided in the Application. Safeeq et al. (2021) demonstrate the lack of reliability of water balance estimates, especially in small headwater catchments, in part due to lack of consideration of deep groundwater flow in water balance models. Small catchments are defined by Safeeq et al. (2021) as 0.5-5km^2, or 124-1,236 acres. The combined watersheds in the project area are larger, approximately 10,485 acres, but the project area where water will be collected, treated, and returned to the watershed is 28.4 acres (Application at 290).

The water balance discussion in the Application at 290 does not use any site-specific information or measurements. For example, it estimates that approximately 42% of precipitation is lost to evapotranspiration and surface runoff, but the reference provided (footnote 6) is simply from the Northeast Regional Climate Center for average monthly potential evapotranspiration (PET) for a grass-covered surface, not a site-specific study, and it says nothing about infiltration (or runoff for that matter), which must be determined for the specific site, taking geology, topography, soils, and hydraulic conductivity at different depths into account.

In addition to dewatering estimates, the water balance should include estimates of bypass flows from mine influenced water holding ponds, and mine influenced groundwater that is not

captured by dewatering wells. The stormwater analysis completed by Wood (Attachment 10-C of the Application) includes contact water from ore, low grade ore, and waste rock stored on lined pads that will require treatment (Application at 293). However, the analysis assumes no leakage from these facilities and does not consider mine influenced groundwater that will not be captured by the planned dewatering wells.

B. Failure to consider climate change

In response to LUPC questions regarding the volume of spray irrigation and its potential impact on wetland and stream hydrology, consultants to Wolfden (April, 2023, p. 6), SME, assessed the variation in naturally occurring precipitation using historical precipitation data for Caribou, Maine, from 1939 to 2018. This evaluation does not consider climate change, which could cause increasing or decreasing precipitation, extreme precipitation events, and different seasonal precipitation patterns. Any calculations of water balance must consider climate change and should use the most recent data and interpretation from the Intergovernmental Panel on Climate Change (IPCC, 2023).

VIII. FATE AND TRANSPORT OF CONTAMINANTS

A. Overview

The study of the fate and transport of contaminants in the environment is often conceptualized as: Sources ➔ Pathways ➔ Receptors. Sources and pathways are specific to the mining operation and surrounding environment, and receptors are site-specific and are natural resources such as streams, wetlands, lakes, and other receiving water bodies.

For the Pickett Mountain Project, the potential contaminant **sources** at the mine site include temporary storage facilities for ore and development rock, contact water ponds, blasting, chemical storage areas (e.g., for blasting agents, chemicals for the mine water treatment plant, cement), the batch plant, stormwater management features, inadequately treated effluent,

construction fill used to create the mine facilities (depending on the material used), and the underground mine. Sources at the tailings disposal facility include the mill, the filtered (referred to as “dry stack” in the Application, at 523) tailings storage facility, chemical storage areas (e.g., chemicals used for the flotation operation), ore storage facilities, and concentrator storage and loading platforms.

Potential contaminant **pathways** include leaching of ore and development rock; leakage through and runoff from ore and development rock stockpiles; leaching of sulfide and other minerals on the walls of the underground workings and along fractures produced from blasting; chemical spills; movement of mine influenced water along faults, through fractured bedrock, and through soils and other surficial geologic materials to downgradient groundwater and surface water; bypass flows of mine influenced groundwater not captured by dewatering wells; and spills of contact stormwater from the batch plant to soils and groundwater. Pathways at the tailings disposal facility include infiltration through the tailings storage facility to downgradient groundwater and surface water; chemical spills (chemicals used for flotation and the treatment plant); windblown dust from the tailings facility; leakage and spills from ore and concentrator storage areas and loading platforms. The haul road between the mine site and the tailings facility is also a potential contaminant pathway related to dust from the road and possible spills from the ore trucks.

Potential **receptors** include shallow and deeper groundwater below and downgradient of mine sources; surface water, including the streams, lakes, and ponds sampled during the 2021 sampling event. Specific receptors at the tailings disposal area cannot be identified at this time because the location has not been identified.

B. Contaminant pathways at the proposed mine site

The presence of faults in the project area is not mentioned at all in the Application, but a 1989 study of the Pickett Mountain deposit (then called the Mount Chase massive sulfide

prospect), Scully (1989, pp. 77-78) discusses several steeply dipping faults and fault gouge areas adjacent to the Pickett Mountain deposit that could transport contaminants from the underground mine to downgradient groundwater and surface water. The Scully study mentions one major fault that strikes through the deposit area, has been intercepted several times in drill holes, and appears to be an important regional structural feature (Scully, 1989, p. 77-78). This is the kind of structural feature that could transport water from the underground mine to downgradient groundwater and surface water. Water moves more rapidly along these preferential pathways, which have been proposed as contaminant pathways at many mines, including the Buckhorn Mine in Washington State. According to a complaint against the Buckhorn Mine (Washington State Office of the Attorney General, 2021, p. 8): "Discharges to groundwater travel anywhere from a few hundred to a few thousand feet to ultimately discharge to surface waters at or near the Buckhorn Mine site via hydraulic connectivity." This hydraulic connectivity refers to movement through faults and fractures.

The fate and transport of contaminants, or even the movement of groundwater, is barely discussed in the Application. A tacit acknowledgment of groundwater-surface water interactions is found in the Application at 295: "the Project's water treatment approach will return clean, treated water back to the environment using WRAs.[9] The siting and release of water from these WRAs is designed to maintain current hydrology to wetlands, streams, PVPs,[10] and vernal pools." In the same way that infiltrated treated water will move through groundwater to surface waters, any mine influenced water at the mine site that escapes capture will move through groundwater to downgradient groundwater and surface water, thus increasing the risk of adverse water quality effects.

[9] WRAs = water recharge areas
[10] PVPs = potential vernal pools

C. Risk of receptor impacts at the proposed mine site

Pickett Mountain Pond and the stream feeding it appear to be downgradient of the deposit (see McCormick, 2021, Figure 2.5, p. 19). Other high-quality fisheries and water resources (e.g., Pleasant Lake, Mud Lake, Grass Pond, and the streams leading to and from them, which include the headwaters of the West Branch Mattawamkeag River) are also nearby and could be adversely affected via groundwater contamination from the proposed project.

Based on the limited water quality results presented in Table 1 in the Water Treatment Scoping Study (Application at 453), streams, lakes, and ponds in the project area are poorly buffered: that is, they have very low total alkalinity (average of 6.92 and maximum of 9.2 mg/L as $CaCO_3$). The low buffering capacity of surface waters means that if acid mine drainage escapes capture, the receiving water will not be able to counteract the increase in acidity, and the pH of the streams will drop rapidly. In addition, hardness values are very low in local surface waters. Hardness, which is a measure of the calcium and magnesium content of the water, protects aquatic life against the toxic effects of metals. Aquatic biota are more susceptible to metals, even at very low concentrations, in streams with low hardness. The available data show that hardness values average 9.8 and have a maximum of 12.7 mg/L as $CaCO_3$.[11] The formulae for calculating hardness-based aquatic life criteria are for hardness values in the range of 25 to 400 mg/L as $CaCO_3$; special testing is recommended for waters with hardness values less than 20-25 mg/L as $CaCO_3$ (U.S. EPA, 2002, pp. 7-9). The very low hardness in these surface water bodies strongly suggests that site-specific toxicity tests should be conducted to better understand the effects of increasing metal concentrations (e.g., zinc, lead, copper and possibly cadmium) on

[11] Hardness (as $CaCO_3$) = 2.49728 x (Ca mg/L) + 4.117918 x (Mg mg/L), using values in Table 1 (Application at 453)

aquatic life. The relatively high dissolved organic carbon (Application at 453) will counteract this effect to some extent, but site-specific aquatic toxicity studies are needed.

Potential expansion of the Pickett Mountain Project, based on geophysical and soil surveys, would bring the operation and potential adverse water quality effects even closer to Pickett Mountain Pond, Mud Lake, Pleasant Lake, and Grass Pond (Figure 8, and compare with Figure 6, right). Locations in Figure 8 circled in red and labelled A, B, C, D are potential future targets for new or additional drilling (Application at 565). Once a mining project begins, it is very common for them to expand over time as additional drilling takes place.

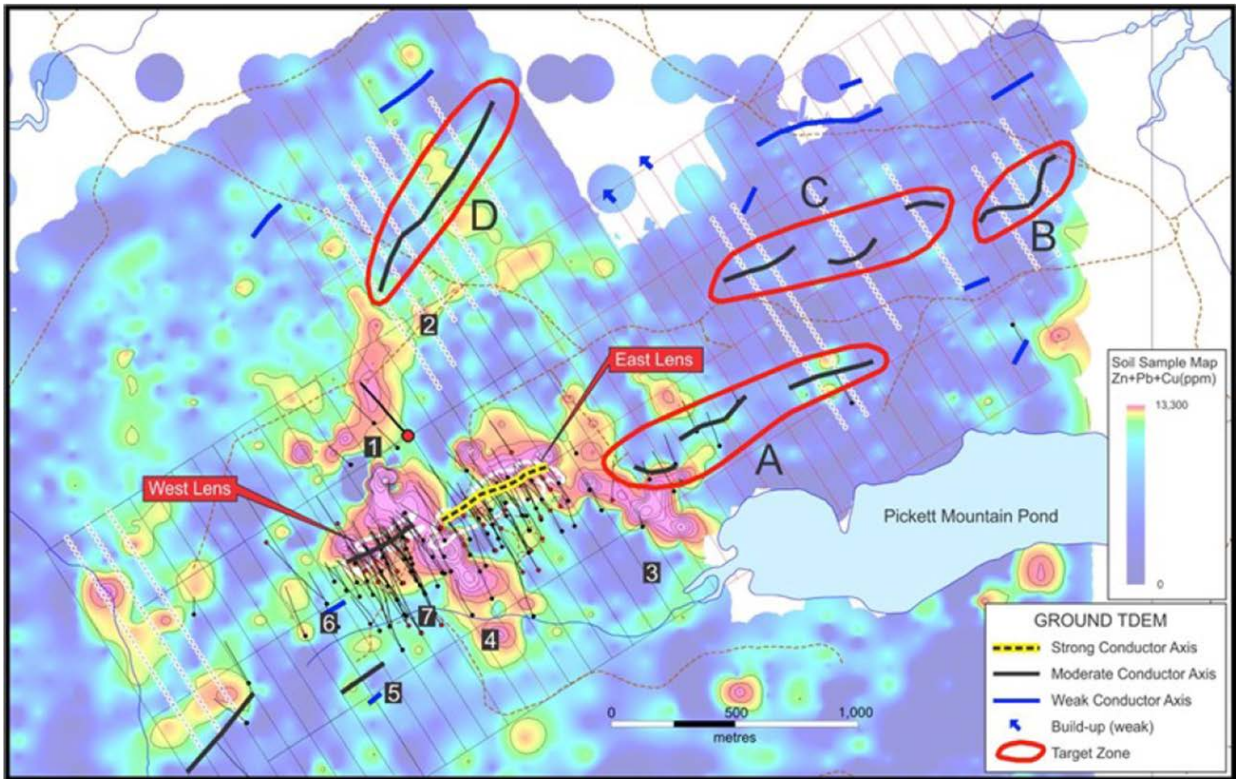

Figure 8. Future target zones (A, B, C, D) and Zn-Pb-Cu soil map. Higher composite Zn-Pb-Cu concentrations in soil overlay the identified East and West lenses and additional areas to the southeast toward Pickett Mountain Pond and to the north toward Mud Lake and Pleasant Lake. *Source: Application at 565, Figure 9.13.*

Wolfden plans to treat mine water using UF/RO, but it has not presented a plan for capture of bypass flows from onsite and offsite mine facilities to minimize the adverse

environmental effects of blasting agents (nitrate and ammonia) and the leaching of metals, metalloids (especially arsenic), and sulfate from the walls of the underground mine that could reach downgradient groundwater and surface water at the mine site. Wolfden has also not presented a plan to minimize the adverse effects of releases from the tailings facility at the undisclosed offsite location. Without these important mitigation measures, Wolfden has failed to demonstrate that it will avoid significant adverse effects on natural resources.

IX. SUMMARY POINTS:

- The Pickett Mountain deposit is a volcanogenic massive sulfide deposit with inherently high acid generation and contaminant leaching potential. The deposit area is also close to groundwater and surface water resources. These inherent characteristics increase the likelihood of adverse environmental impacts.
- More work is needed to understand the specific leaching characteristics of the ore, waste rock, tailings, and walls of the underground mine. Only seven samples have been tested for acid generation and contaminant leaching potential, even though 2,550 samples have been analyzed and used for ore delineation. The results of additional testing are needed for designing effective treatment methods.
- Wolfden is proposing to use ultrafiltration and reverse osmosis as the treatment method for removing contaminants from mine influenced water at the mine site and at the tailings facility location. Although this approach can in theory produce high-quality effluent, Wolfden provides no example of a comparable mine that accomplishes the levels required at this site. In addition, the water treatment study has so many shortcomings that it does not reasonably demonstrate the ability to meet the strict discharge requirements of the State of Maine.

- Estimating water balance in advance of mine development is notoriously difficult and requires updating throughout the entire mining process. The water balance presented in the Application does not lay a foundation using any site-specific data for the 30-gpm estimate for dewatering of the underground mine. This figure seems low, and improved estimates are needed because the amount directly affects how much water will require treatment at the mine site. The water balance also does not include “bypass” flows from mine influenced water that escapes capture from the underground mine and the temporary ore and development rock storage pads. Importantly, the mine water balance also does not take climate change into account.
- The Application fails to consider the walls of the underground mine and blasting as sources of mine contaminants or preferential contaminant pathways such as faults at the Pickett Mountain site. The proposed mine and potential future ore targets are in close proximity to high-quality fisheries and water resources (Pleasant Lake, Mud Lake, Grass Pond, and the streams leading to and from them), which, based on limited available water quality data, have very low ability to resist the effects of acid mine drainage. Effective measures to capture mine influenced water as close to sources as possible and to minimize the use of blasting agents have not been provided. Without these additional measures, Wolfden has failed to demonstrate that it will avoid significant adverse effects on natural resources.

X. REFERENCES

A-Z Mining Professionals, 2020. Preliminary Economic Assessment for Pickett Mountain Project, Penobscot County, Maine, USA. Prepared for Wolfden Resources Corporation. Attachment 14-A of Land Use Planning Commission Application for Zone Change, Pickett Mountain Metallic Mine, T6 R6 WELS, Penobscot County.

A-Z Mining Professionals, 2019. National Instrument 43-101 Technical Report, Pickett Mountain Project Resource Estimation Report. Penobscot County, Maine, USA. Prepared for: Wolfden Resources Corporation. 131 pp. https://www.wolfdenresources.com/wp-content/uploads/2019/02/Pickett-Mountain-Resource-Estimate-Wolfden-NI43-101.pdf

Australian Government, 2016. Preventing acid and Metalliferous Drainage. Leading Practice Sustainable Development Program for the Mining Industry. September. 221 pp. https://www.industry.gov.au/sites/default/files/2019-04/lpsdp-preventing-acid-and-metalliferous-drainage-handbook-english.pdf

Davis et al., 2000. Rio Tinto estuary (Spain): 5000 years of pollution. *Environmental Geology* 39, (10) 1107-1116.

Department of Environmental Protection, 2023. Memorandum: Department comments on Wolfden Mt. Chase, LLC's petition to rezone portion of Township 6, Range 6 Penobscot County, Maine for development of an underground metallic mineral deposit, January 18, 2023, July 5. To Tim Carr, Senior Planner, Land Use Planning Commission. From: Michael Clark, Mining Coordinator, Bureau of Land Resources.

Foth & Van Dyke, 2005. Eagle Mine Groundwater Discharge Permit Application, Appendix G. WWTP Influent and Effluent Calculations.

George L.L., Cook N.J., Ciobanu C.L., 2017. Minor and Trace Elements in Natural Tetrahedrite-Tennantite: Effects on Element Partitioning among Base Metal Sulphides. *Minerals* 7(2), 17. https://doi.org/10.3390/min7020017

Gestring, B., 2019. U.S. operating copper mines: Failure to capture & treat wastewater. 9pp. for Earthworks. https://www.congress.gov/116/meeting/house/110436/documents/HHRG-116-II06-20200205-SD036.pdf

Golder Associates, 2016. Buckhorn Mine Development Rock Management Program, 4th Quarter, Water Year 2016. July 1st to September 30th, 2016. Progress Report. October 11. 24 pp.

INAP (International Network for Acid Prevention), 2023. https://www.inap.com.au/

INAP, 2009. GARD Guide. Chapter 4. http://www.gardguide.com/index.php?title=Chapter_4

IPCC, 2023. Sixth Assessment Report. Released on 20 March. https://www.ipcc.ch/assessment-report/ar6/

Jennings, S.R., Neuman, D.R., Blicker, P.S., 2008. Acid Mine Drainage and Effects on Fish Health and Ecology: A Review. Reclamation Research Group Publication, Bozeman, MT. Prepared for U.S. Fish and Wildlife Service, Anchorage Fish and Wildlife Field Office, Anchorage, Alaska. 29 pgs. https://easternbrooktrout.org/science-data/science-publications/acid-mine-drainage-and-effects-on-fish-health-and-ecology-a-review/view

Kuipers, J.R. and A.S. Maest (primary), K.A. MacHardy, and G. Lawson (contributing). 2006. Comparison of Predicted and Actual Water Quality at Hardrock Mines: The Reliability of Predictions in Environmental Impact Statements. Prepared for Earthworks, Washington, DC.

Available: https://earthworks.org/wp-content/uploads/2021/09/ComparisonsReportFinal.pdf. Peer-reviewed by US EPA as part of their Bristol Bay Watershed Assessment, 2012.

Maest, A.S. and J.R. Kuipers (primary), C.L. Travers, and D.A. Atkins (contributing). 2005. Predicting Water Quality at Hardrock Mines: Methods and Models, Uncertainties, and State-of-the-Art. Earthworks, Washington, DC. Available: https://earthworks.org/publications/predicting_water_quality_at_hardrock_mines/.

Maine Administrative Code. 06 096 DEPARTMENT OF ENVIRONMENTAL PROTECTION, Chapter 200: METALLIC MINERAL EXPLORATION, ADVANCED EXPLORATION AND MINING.

McCormick, M.J., 2021. Geology and Lithogeochemistry of the Pickett Mountain Volcanogenic Massive Sulfide Deposit, Northern Maine. Electronic Theses and Dissertations. 3413. Available: https://digitalcommons.library.umaine.edu/etd/3413. Accessed 9/9/2023.

Nordstrom, D.K. and Alpers, C.N., 1999. Geochemistry of acid mine waters. *Reviews in Economic Geology*. 6A. Chapter 6, 133-160. https://www.resolutionmineeis.us/sites/default/files/references/nordstorm-alpers-1999.pdf

Plante, B., Bussiere, B., Benzaazoua, M., 2012. Static tests response on 5 Canadian hard rock mine tailings with low net acid-generating potentials. Journal of Geochemical Exploration 114 (2012) 57–69. http://dx.doi.org/10.1016/j.gexplo.2011.12.003

Plumlee, G., Smith, K., Montour, M.R., Ficklin, W.H., Mosier, E.L., 1999. Geologic controls on the composition of natural waters and mine waters draining diverse mineral-deposit types. *Reviews in Economic Geology*. 6B. 373-432. https://doi.org/10.5382/Rev.06.19

Plumlee, G., 1999. The environmental geology of mineral deposits. *Reviews in Economic Geology*. 6A. 71-116. https://www.researchgate.net/publication/264046895_The_environmental_geology_of_mineral_deposits

Price, W.A., 2009. Prediction Manual for Drainage Chemistry from Sulphidic Geologic Materials. MEND Report 1.20.1. 579pp. https://mend-nedem.org/wp-content/uploads/1.20.1_PredictionManual.pdf

Safeeq, M., Bart, R.R., Pelak, N.F., Singh, C.K., Dralle, D.N., Hartsouth, P., Wagenbrenner, J.W., 2021. How realistic are water-balance closure assumptions? A demonstration from the southern sierra critical zone observatory and kings river experimental watersheds. Hydrological Processes. 35e14100. https://doi.org/10.1002/hyp.14199

Scully, M., 1989. Geology and Petrochemistry of the Mount Chase Massive Sulfide Prospect, Penobscot County, Maine: M.Sc. thesis, University of Missouri-Rolla, 117 p. https://scholarsmine.mst.edu/cgi/viewcontent.cgi?article=1732&context=masters_theses

Stantec Consulting Services Inc., 2023. Land Use Planning Commission Application for Zone Change. Pickett Mountain Metallic Mine, T6 R6 WELS, Penobscot County, January 18. Prepared for Wolfden Mount Chase, LLC. 1198pp. (“Application”)

State of Maine, Department of Inland Fisheries & Wildlife, 2023. Letter to Tim Carr, LUPC, June 27. RE: Wolfden Mt. Chase LLC, Rezoning Request ZP 779A, Pickett Mountain Metallic Mineral Mine, T6R6 WELS. In: ZP779A Agency Review Memoranda.

Strosnider, W., Nairn, R., Llanos, F.S., 2007. A legacy of nearly 500 years of mining in Potosí, Bolivia: Acid mine drainage source identification and characterization. Journal American Society of Mining and Reclamation. 788-803. 10.21000/JASMR07010788. Available: https://www.asrs.us/Publications/Conference-Proceedings/2007/0788-Strosnider.pdf

Texas Water Development Board, 2014. Part II. Performance Evaluation of Reverse Osmosis Membrane Computer Models. Final Report. By E. Mancha, D. DeMichele, W. Shane Walker, T.F. Seacord, J. Sutherland, A. Cano. 89pp. https://www.twdb.texas.gov/publications/reports/contracted_reports/doc/1148321310_Part%20II_Performance%20Evaluation.pdf

Tremblay, G.A., 2001. The Canadian Mine Environment Neutral Drainage (MEND) initiative. VI SHMMT I XVIII ENTMME- 2001 -Rio de Janeiro/Brazil, 8pp. https://www.artigos.entmme.org/download/2001/special_session/1099%20-%20Gilles%20A.%20Tremblay%20-%20THE%20CANADIAN%20MINE%20ENVIRONMENT%20NEUTRAL%20DRAINAGE%20(MEND)%20INITIATIVE.pdf

U.S. Department of Agriculture, Forest Service, 1993. Acid Mine Drainage from Impact of Hardrock Mining on the National Forests: A Management Challenge. https://archive.org/details/CAT31108485

U.S. Department of the Interior, 2022. 2022 Final List of Critical Minerals. Federal Register, Vol. 87, No. 37, February 24. 10381-10382. https://www.federalregister.gov/documents/2022/02/24/2022-04027/2022-final-list-of-critical-minerals

U.S. Environmental Protection Agency (U.S. EPA), 2014. Reference Guide to Treatment Technologies for Mining-Influenced Water, Office of Superfund Remediation and Technology Innovation. March. EPA 542-R-14-001. https://www.epa.gov/sites/default/files/2015-08/documents/reference_guide_to_treatment_technologies_for_miw.pdf

U.S. EPA, 2013. Aquatic life ambient water quality criteria for ammonia – Freshwater. 2013. EPA-822-R-13-001. 255pp. https://www.epa.gov/sites/default/files/2015-08/documents/aquatic-life-ambient-water-quality-criteria-for-ammonia-freshwater-2013.pdf

U.S. EPA, 2002. National Recommended Water Quality Criteria: 2002. Office of Water, Office of Science and Technology, EPA-822-R-02-047. 36pp. https://www.epa.gov/sites/default/files/2018-12/documents/national-recommended-hh-criteria-2002.pdf

U.S. Geological Survey, 2023. Mineral Commodity Summaries 2023. 214pp. https://doi.org/10.3133/mcs2023

Washington State, Office of the Attorney General, 2022. Court rules gold mining company violated the law more than 3,000 times in Okanogan County.

https://www.atg.wa.gov/news/news-releases/court-rules-gold-mining-company-violated-law-more-3000-times-okanogan-county

Washington State, Office of the Attorney General, 2021. Case 2:20-cv-00147-RMP ECF No. 58 filed 03/04/21. 99pp.

Wolfden, 2023. Response to LUPC Comments of February 24, 2023. April 13. 78pp.

Wolfden, 2023. Pickett Mountain Mine Rezone Petition, ZP779A. August 11. 35pp.

Yaroshevsky, A.A., 2006. Abundances of chemical elements in the Earth's crust. *Geochemistry International*, Vol. 44, No. 1, pp. 48–55. https://www.researchgate.net/publication/226858508_Abundances_of_chemical_elements_in_the_Earth's_crust

VERIFICATION

I, Ann Maest Cooney, being first duly sworn, affirm that the above testimony is true and accurate to the best of my knowledge.

Date: 22 September 2023 Signed: Ann Maest Cooney

Personally appeared the above-named Ann Maest Cooney and made oath that the foregoing testimony was true and correct to the best of their knowledge and belief.

Dated: September 22, 2023

Notary Public

AUDREY MORTON
Notary Public
State of Colorado
Notary ID # 20074028244
My Commission Expires 08-13-2027

INDEX OF ATTACHMENTS FOR ANN MAEST PRE-FILED TESTIMONY

Jennings, S.R., Neuman, D.R. and Blicker, P.S., 2008. Acid Mine Drainage and Effects on Fish Health and Ecology: A Review. https://easternbrooktrout.org/science-data/science-publications/acid-mine-drainage-and-effects-on-fish-health-and-ecology-a-review/view.....Attachment 12

Kuipers, J.R. and A.S. Maest (primary), K.A. MacHardy, and G. Lawson (contributing). 2006. Comparison of Predicted and Actual Water Quality at Hardrock Mines: The Reliability of Predictions in Environmental Impact Statements. https://earthworks.org/wp-content/uploads/2021/09/ComparisonsReportFinal.pdf. (excerpted) .....Attachment 13

Maest, A.S. and J.R. Kuipers (primary), C.L. Travers, and D.A. Atkins (contributing). 2005. Predicting Water Quality at Hardrock Mines: Methods and Models, Uncertainties, and State-of-the-Art. Earthworks, Washington, DC. https://earthworks.org/publications/predicting_water_quality_at_hardrock_mines/. (excerpted) .....Attachment 14

McCormick, Michael J., "Geology and Lithogeochemistry of the Pickett Mountain Volcanogenic Massive Sulfide Deposit, Northern Maine" (2021). Electronic Theses and Dissertations. 3413. https://digitalcommons.library.umaine.edu/etd/3413. (excerpted) .....Attachment 15

Nordstrom, D.K. and Alpers, C.N., 1999. Geochemistry of acid mine waters. *Reviews in Economic Geology*. 6A. Chapter 6, 133-160. https://www.resolutionmineeis.us/sites/default/files/references/nordstorm-alpers-1999.pdf. .....Attachment 16

Plante, B., Bussiere, B. Benzaazoua.2012. Static tests response on 5 Canadian hard rock mine tailings with low net acid-generating potentials. Journal of Geochemical Exploration 114 (2012) 57–69. http://dx.doi.org/10.1016/j.gexplo.2011.12.003 .....Attachment 17

Plumlee, G., Smith, K., Montour, M.R., Ficklin, W.H., Mosier, E.L. 1999. Geologic controls on the composition of natural waters and mine waters draining diverse mineral-deposit types. *Reviews in Economic Geology*. 6B. 373-432. https://doi.org/10.5382/Rev.06.19. (excerpted) .....Attachment 18

Plumlee, G. 1999. The environmental geology of mineral deposits. *Reviews in Economic Geology*. 6A. 71-116. https://www.researchgate.net/publication/264046895_The_environmental_geology_of_mineral_deposits. (excerpted).....Attachment 19

Price, W.A. 2009. Prediction Manual for Drainage Chemistry from Sulphidic Geologic Materials. MEND Report 1.20.1. 579pp. https://mend-nedem.org/wp-content/uploads/1.20.1_PredictionManual.pdf. (excerpted).....Attachment 20

Safeeq, M., Bart, R.R., Pelak, N.F., Singh, C.K., Dralle, D.N., Hartsouth, P., Wagenbrenner, J.W., 2021. How realistic are water-balance closure assumptions? A demonstration from the southern sierra critical zone observatory and kings river experimental watersheds. https://doi.org/10.1002/hyp.14199. .....Attachment 21

Scully, M., 1989. Geology and Petrochemistry of the Mount Chase Massive Sulfide Prospect, Penobscot County, Maine: M.Sc. thesis, University of Missouri-Rolla. https://scholarsmine.mst.edu/cgi/viewcontent.cgi?article=1732&context=masters_theses. (excerpted).....Attachment 22

Stantec Consulting Services Inc., 2023. Land Use Planning Commission Application for Zone Change. Pickett Mountain Metallic Mine, T6 R6 WELS, Penobscot County, January 18. ("Application") (excerpted).....Attachment 23

State of Maine, Department of Inland Fisheries & Wildlife, 2023. Letter to Tim Carr, LUPC, June 27. RE: Wolfden Mt. Chase LLC, Rezoning Request ZP 779A, Pickett Mountain Metallic Mineral Mine, T6R6 WELS. In: ZP779A Agency Review Memoranda .....Attachment 24

Strosnider, W. Nairn, R., Llanos, F.S., 2007. A legacy of nearly 500 years of mining in Potosí, Bolivia: Acid mine drainage source identification and characterization. Journal American Society of Mining and Reclamation. https://www.asrs.us/Publications/Conference-Proceedings/2007/0788-Strosnider.pdf.....Attachment 25

Texas Water Development Board, 2014. Part II. Performance Evaluation of Reverse Osmosis Membrane Computer Models. Final Report. By E. Mancha, D. DeMichele, W. Shane Walker, T.F. Seacord, J. Sutherland, A. Cano. https://www.twdb.texas.gov/publications/reports/contracted_reports/doc/1148321310_Part%20II_Performance%20Evaluation.pdf. (excerpted) .....Attachment 26

Tremblay, G.A., 2001. The Canadian Mine Environment Neutral Drainage (MEND) initiative. https://www.artigos.entmme.org/download/2001/special_session/1099%20-%20Gilles%20A.%20Tremblay%20-%20THE%20CANADIAN%20MINE%20ENVIRONMENT%20NEUTRAL%20DRAINAGE%20(MEND)%20INITIATIVE.pdf.....Attachment 27

U.S. Department of Agriculture, Forest Service, 1993. Acid Mine Drainage from Impact of Hardrock Mining on the National Forests: A Management Challenge. https://archive.org/details/CAT31108485.....Attachment 28

U.S. Environmental Protection Agency (U.S. EPA), 2014. Reference Guide to Treatment Technologies for Mining-Influenced Water, Office of Superfund Remediation and Technology Innovation. https://www.epa.gov/sites/default/files/2015-08/documents/reference_guide_to_treatment_technologies_for_miw.pdf. (excerpted) ..... Attachment 29

U.S. EPA, 2013. Aquatic life ambient water quality criteria for ammonia – Freshwater. 2013. https://www.epa.gov/sites/default/files/2015-08/documents/aquatic-life-ambient-water-quality-criteria-for-ammonia-freshwater-2013.pdf. (excerpted) ..... Attachment 30

U.S. EPA, 2002. National Recommended Water Quality Criteria: 2002. Office of Water, Office of Science and Technology, EPA-822-R-02-047. 36pp. https://www.epa.gov/sites/default/files/2018-12/documents/national-recommended-hh-criteria-2002.pdf (excerpted) ..... Attachment 31

U.S. Geological Survey, 2023. Mineral Commodity Summaries 2023. https://doi.org/10.3133/mcs2023. (excerpted) ..... Attachment 32

Washington State, Office of the Attorney General, 2022. Court rules gold mining company violated the law more than 3,000 times in Okanogan County. https://www.atg.wa.gov/news/news-releases/court-rules-gold-mining-company-violated-law-more-3000-times-okanogan-county ..... Attachment 33

Washington State, Office of the Attorney General, 2021. Case 2:20-cv-00147-RMP ECF No. 58 filed 03/04/21. (excerpted). ..... Attachment 34

Wolfden, 2023. April: Response to LUPC Comments of February 24, 2023. (excerpted) ..... Attachment 35

Wolfden, 2023. August: Pickett Mountain Mine Rezone Petition, ZP779A (Response to Comments). (excerpted) ..... Attachment 36

World Bank, 2021. Zinc ores and concentrates exports by country |2021 (worldbank.org) ..... Attachment 37

Yaroshevsky, A.A., 2006. Abundances of chemical elements in the Earth's crust. *Geochemistry International*, Vol. 44, No. 1, pp. 48–55. https://www.researchgate.net/publication/226858508_Abundances_of_chemical_elements_in_the_Earth's_crust ..... Attachment 38

ATTACHMENT 1

National Instrument 43-101 Technical Report

Pickett Mountain Project
Resource Estimation Report

Penobscot County, Maine, USA

Located at:
68.468°W Longitude
46.134°N Latitude

Prepared For:
Wolfden Resources Corporation

Prepared By:
Finley Bakker, P. Geo.
Jerry Grant, P. Geo.
Brian LeBlanc, P. Eng.

Effective Date:
January 7, 2019

1.0 SUMMARY

The Pickett Mountain Property is located in northeastern Maine, USA, in the southeast quarter of Township 6, Range 6, Penobscot County. It is about 153 km north of Bangor and approximately 53 kilometres (km) from the Canadian border. The Property consists of 2,781 hectares of private land that was acquired for US$8.5 million in 2017 by Wolfden Mt. Chase LLC (a wholly-owned subsidiary of Wolfden Resources Corporation) and included all of the mineral, timber, oil, and surface rights, exclusive of the surface area of any lakes ("ponds").

The project is located within the Ganderia zone of the northern Appalachian orogenic belt, formed during the Paleozoic orogen. The area is underlain by Late Neoproterozoic to Early Ordovician rocks that have undergone multiple stages of deformation, metamorphism, and plutonism and record the development and destruction of a continental margin. The Property covers a portion of the southeast limb of the southwest-plunging Weeksboro-Lunksoos Lake Anticlinorium that is cored by Early Cambrian shale and siltstone with interbedded quartzite that are unconformably overlain by a sequence of quartz-feldspar crystal tuff, rhyolite, volcanic breccia, and lapilli tuff, a massive sulphide horizon that varies from 0 to about 15 metres thick dominated by sphalerite-galena-chalcopyrite-pyrite mineralisation, hanging wall tuffs, mafic flows, and shale.

The mineral zone at Pickett Mountain is a stratabound volcanogenic massive sulphide deposit that has been traced by drilling approximately 900 metres along strike and 750 metres down dip. It consists of 4 primary lenses (W1, W2, E1, and E2) and several minor lenses. This style of deposit is a major source of Cu, Zn, and to a lesser extent Pb, Ag, Au, Cd, Se, Sn, Bi, and minor amounts of other metals. This style of mineralisation typically has a high value due to its multi-element character and concentrated value per tonne mined.

Between 1978 and 1989, the Property was explored by Getty Mineral Company (Getty) and then by Chevron Resources Company (Chevron). Over this period, 111 holes totalling 34,058 metres were drilled. An historical resource estimate was prepared by Getty and estimated the deposit to contain approximately 3.15 million tons with an average grade of 9.66% Zn, 4.30% Pb, 1.24% Cu, 2.96 opt Ag, and 0.029 opt Au. In 1989, Chevron completed another historical resource estimate using an updated geological interpretation and more rigorous controls. This estimate was 2.5 million tons averaging 11.42% Zn, 4.94% Pb, 1.62% Cu, and 3.3 opt Ag. Wolfden is not treating these historical estimates as current Mineral Resources and the historical estimates are not NI 43-101 compliant.

Since acquiring the Property in December 2017, Wolfden has completed an exploration program consisting of an airborne geophysical survey (VTEM™), ground Time-Domain (TDEM) electromagnetic surveys, bore-hole TDEM electromagnetic surveys, ground induced polarization surveys (IP), and geological mapping as well as diamond drilling.

To date, 111 historical drill holes and 38 drill holes completed by Wolfden in 2017-2018, have tested the Pickett Mountain deposit and other regional exploration targets. Total footage for these combined drilling campaigns is 49,655 metres.

A current National Instrument 43-101 compliant Mineral Resource estimate (January 7, 2019) calculated on the Pickett Mountain deposit is based on a 9.0% Zn equivalent cut-off and is tabulated below (Table 1.1).

TABLE 1.1
MINERAL RESOURCE STATEMENT – JANUARY 7, 2019

Category	Tonnes	% Zn	% Pb	% Cu	g/t Ag	g/t Au	Density	% ZnEq
Indicated	2,050,000	9.88	3.93	1.38	101.58	0.92	3.99	19.32
Inferred	2,030,000	10.98	4.35	1.20	111.45	0.92	4.00	20.61

A number of potential cut-off grades for Zinc Equivalent were calculated for each resource category as represented in the sensitivity tables below (Table 1.2 and Table 1.3). The tonnage and grade are robust over the intervals chosen. A 9% Zinc Equivalent cut-off was considered to be conservative until further technical studies have been completed.

TABLE 1.2
SENSITIVITY TO CUT-OFF GRADES – INDICATED MINERAL RESOURCE – JANUARY 7, 2019

% ZnEq Cut-off Grade	Tonnes	% Zn	% Pb	% Cu	g/t Ag	g/t Au	Density	% ZnEq
3% ZnEq	3,970,000	6.03	2.38	1.02	65.39	0.68	4.02	12.39
5% ZnEq	2,820,000	7.89	3.12	1.21	83.61	0.81	4.00	15.79
7% ZnEq	2,320,000	9.11	3.62	1.32	95.04	0.88	3.98	17.99
9% ZnEq	2,050,000	9.88	3.93	1.38	101.58	0.92	3.99	19.32
11% ZnEq	1,770,000	10.77	4.29	1.41	109.32	0.96	4.00	20.79

TABLE 1.3
SENSITIVITY TO CUT-OFF GRADES – INFERRED MINERAL RESOURCE – JANUARY 7, 2019

% ZnEq Cut-off Grade	Tonnes	% Zn	% Pb	% Cu	g/t Ag	g/t Au	Density	% ZnEq
3% ZnEq	4,020,000	6.59	2.58	0.94	69.91	0.68	4.03	13.03
5% ZnEq	2,980,000	8.35	3.29	1.06	87.12	0.79	4.01	16.14
7% ZnEq	2,450,000	9.67	3.83	1.15	99.99	0.86	4.00	18.43
9% ZnEq	2,030,000	10.98	4.35	1.20	111.45	0.92	4.00	20.61
11% ZnEq	1,740,000	12.06	4.77	1.24	121.42	0.97	4.00	22.39

1.1 MINERAL RESOURCE ESTIMATE PARAMETERS AND ASSUMPTIONS

- Mineral Resources are not Mineral Reserves and do not have demonstrated economic viability. There is no certainty that all or any part of the Mineral Resources will be converted into Mineral Reserves.
- Resources are presented as undiluted and in-situ for an underground mining scenario and are considered having reasonable prospects for economic extraction.

- The metal prices used to determine Zinc Equivalent (ZnEq) grades were US$1.20/pound for Zn, US$1.00/pound for Pb, US$2.50/pound for Cu, US$16.00/troy ounce for Ag, and US$1200/troy ounce for Au. The base case utilised a calculated cut-off grade of 9.00% ZnEq.
- Indicated Resources were estimated using a maximum distance of 25 metres from a drill hole and meeting a single hole minimum.
- Inferred Resources were estimated utilising a no hole minimum and using a minimum of 25 metres and maximum of 200 metres from a drill hole.
- The MRE encompasses 3 mineralised massive sulphide lenses.
- A total of 148 drill holes comprise the database including 2,550 samples; of these 940 samples were utilised in the estimate.
- Grade capping was not utilised as it was noted that the general uniformity of grade was fairly consistent with no significant outliers in the assay results.
- The specific gravities used in the MRE were based on a total of 253 physically measured specific gravities within the mineralised lenses.
- Wolfden is not aware of any legal, political, environmental, or other risks that could materially affect the potential development of the Mineral Resources.

The compliant Mineral Resource estimate represents a signficiant increase from the previous historical, unqualified resources prepared by Getty Minerals and Chevron Resources in the 1980s.

Continued expansion and infill drilling will have significant potential to expand and upgrade the Mineral Resource. Additionally, several high-quality exploration targets situated near the deposit as well as elsewhere on the Property and volcanic belt, offer excellent potential for the discovery of additional massive sulphide lenses.

Based on the positive results of the 2018 diamond drill program, the resulting updated resource estimate, new geological theories, and geophysical targets identified by the airborne and ground surveys, additional work is warranted and recommended as follows:

- To upgrade the Inferred Mineral Resource, a limited infill drill program with a 25 metres by 25 metres pattern is required to confirm if the current 50 metre by 50 metre drill pattern is sufficient.
- Complete down-hole EM surveying of several completed drill holes in order to test for the potential to expand mineralisation outside of the current modeled lenses. Drill test the higher priority down-hole plate conductors.
- Drill untested areas immediately adjacent to the modeled Inferred Resource domains in order to test for potential expansion, continuity, and grades of the mineralised lens.
- Drill untested, higher priority regional geophysical anomalies after further ground trothing and verification.
- Collection of a representative metallurgical sample from drill core rejects for further testing and more advanced studies. As part of the metallurgical testing, investigate various pre-concentration techniques that could be assessed in future studies.
- Following completion of the metallurgical test work, commission an engineering study to undertake a basic mine design and a Preliminary Economic Assessment of the resource. The geometry of the resource appears amenable to bulk mining techniques. These should be investigated to determine the most cost effective mining methods and processing techniques.

4.2 LAND TENURE

Wolfden acquired, through its indirect wholly-owned subsidiary Wolfden Mt. Chase LLC, all of the mineral, timber, oil, and surface rights, exclusive of the surface area of great ponds (lakes that include the waters of Pickett Mountain Pond, Pleasant Lake and Mud Lake) covering approximately 2,781 hectares (Figure 4.2). More specifically, the Property consists of the southeast quarter of Township 6, Range 6, in Penobscot County, Maine. The only known encumbrances are two small surface rights parcels on the north shore of Pleasant Lake and a small surface rights lease on the south side of Pleasant Lake for recreation purposes.

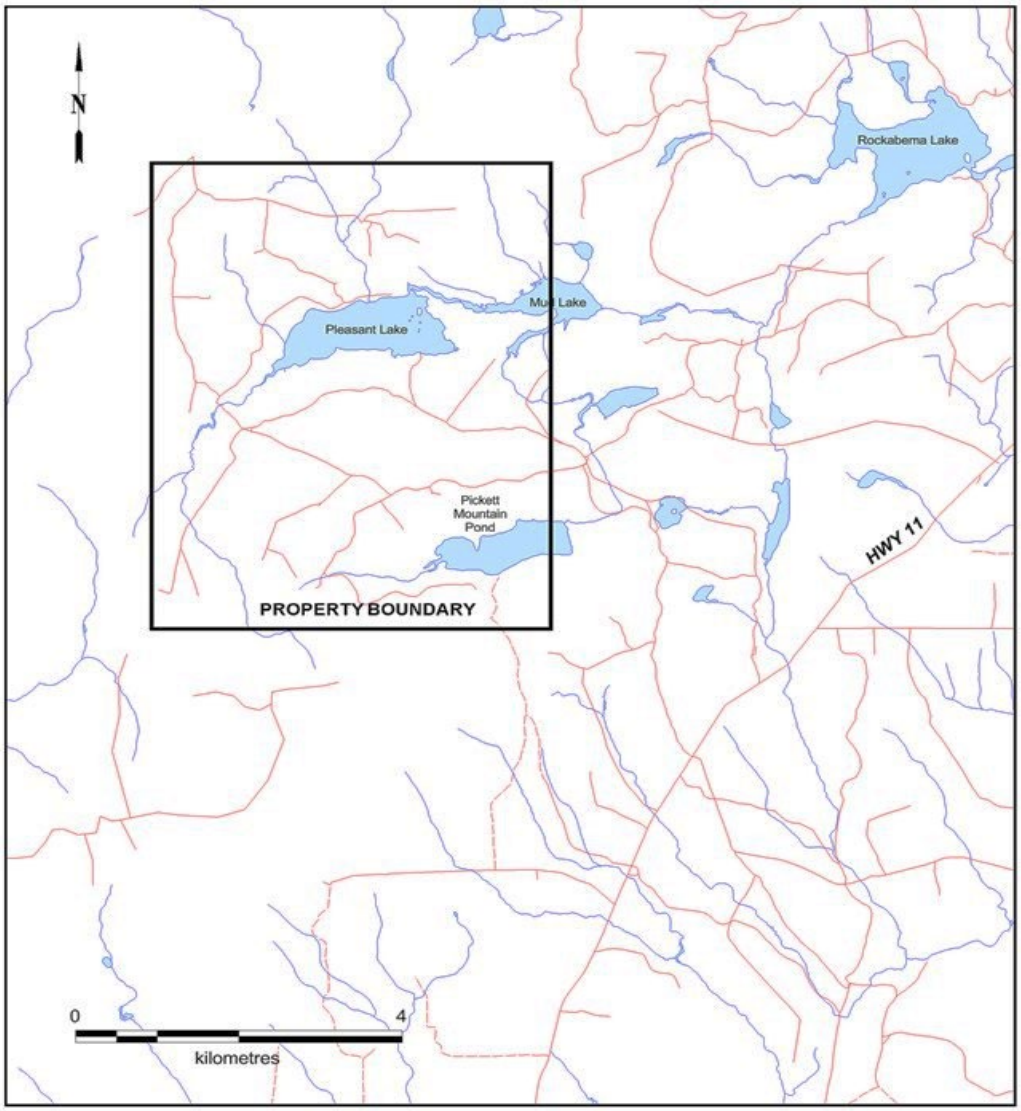

Figure 4.2 Pickett Mountain Property map

Wolfden advises that it does not require any permits to complete the contemplated exploration work on the Property. The authors are not aware of any other significant factors and risks that may affect access, title, or the right or ability to perform work on the Property as currently contemplated. There are no known environmental liabilities to which the Property is subject to.

4.3 PURCHASE AGREEMENT

On November 15, 2017, Wolfden Mt. Chase LLC acquired a 100% interest in the Pickett Mountain Project for a cash purchase price of US$8.5 million (the “Acquisition”) from a third party vendor. To fund the acquisition, the Company granted a 1.35% gross sales royalty on the Pickett Mountain Project to a subsidiary of Altius Minerals Corporation for cash consideration of US$6 million and completed a non-brokered private placement of 20,200,000 subscriptions at a price of C$0.25 per subscription receipt for gross proceeds of C$5,050,000.

7.0 GEOLOGICAL SETTING AND MINERALISATION

7.1 REGIONAL GEOLOGY

The Pickett Mountain project is located in the northern Appalachian orogenic belt. The Appalachians are a Paleozoic orogen that formed along the northern margin of Gondwana in the Neoproterozoic and early Paleozoic. It has been subdivided into 5 domains based on stratigraphic and structural contrasts: Humber, Notre Dame, Ganderia, Avalonia, and Meguma, as shown in Figure 7.1 (Hibbard, et al., 2007; Fyffe, et al., 2009). The Pickett Mountain project is located within the Ganderia zone.

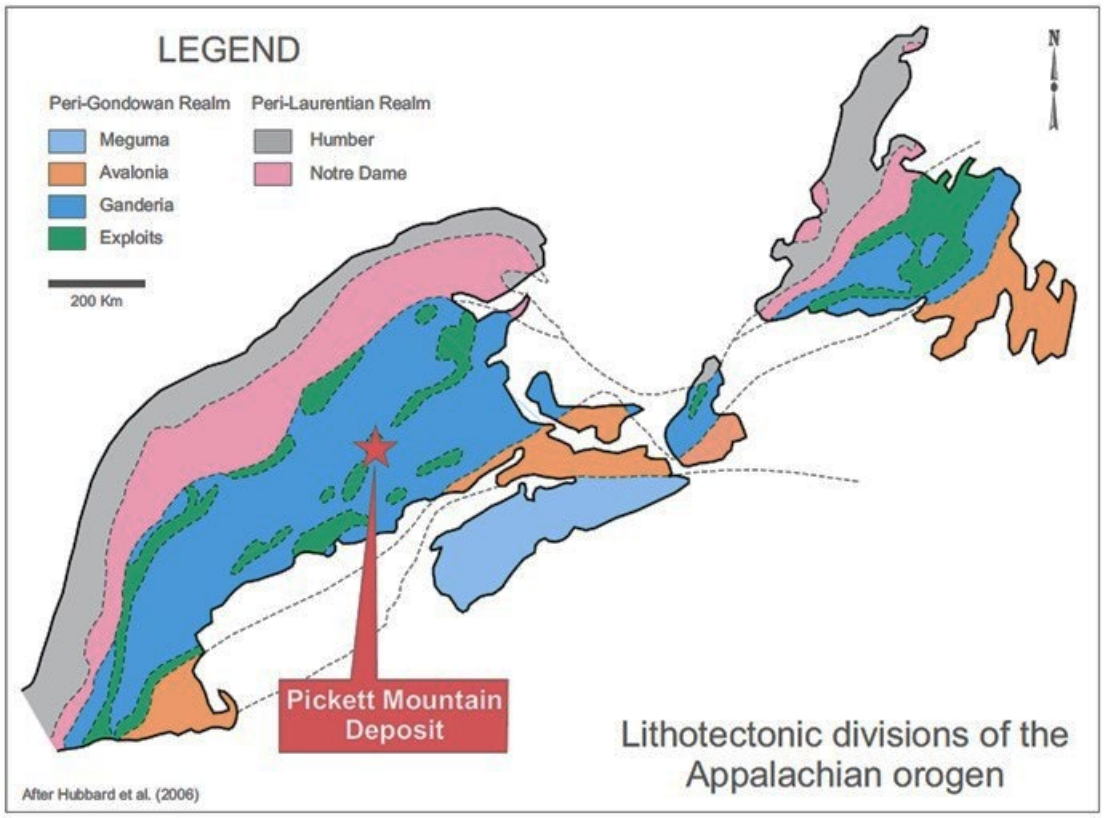

Figure 7.1 Lithotectonic divisions of the northern Appalachian orogen (Source: Adapted from Hibbard, et al., 2006)

The Ganderia Zone consists of Late Neoproterozoic to Early Ordovician rocks that are predominantly continent-derived, quartz-rich sediments and with Neoproterozoic volcanic and plutonic rocks (Fyffe, et al., 2009). These have undergone multiple stages of deformation, metamorphism, and plutonism and record the development and destruction of a continental margin (Williams, 1978).

The Property covers a portion of the southeast limb of the southwest plunging Weeksboro-Lunksoos Lake Anticlinorium that is cored by the Grand Pitch Formation, made up of complexly folded shale and siltstone with interbedded quartzite and greywacke and believed to be of Early Cambrian age (Figure 7.2). The stratigraphic sequence within the Anticlinorium and above the unconformity is illustrated in Figure 7.3.

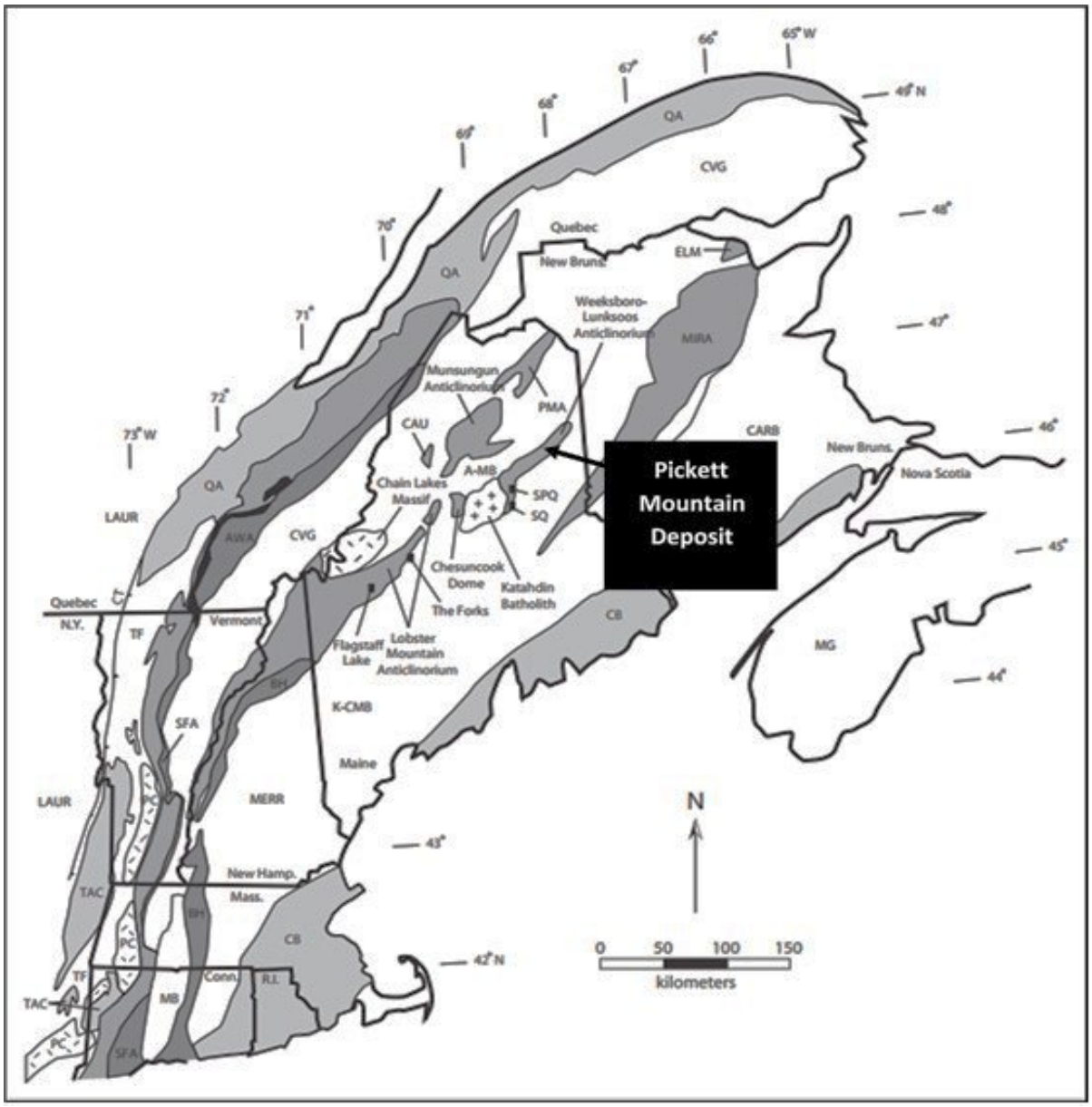

Figure 7.2 Generalised geology of the northern Appalachians

(Source: Schoonmaker, et al., 2017)

Pre-Devonian units are shaded. LAUR = autochthonous Laurentian margin, QA = Quebec Allochthons, TAG = Taconic Allochthons, TF = transported Laurentian margin and basin deposits, PC = Precambrian massifs, SFA-AWA = Shelburne Falls arc, Ascot-Weedon arc, and related oceanic rocks, including ophiolitic fragments (black), MB = Mesozoic basin, CVG = Connecticut Valley Gaspe Synclinorium, BH = Bronson Hill Arc, MERR = Merrimack Synclinorium, CAU = Caucomgomoc inlier, A-MB = Aroostook-Matapedia belt, SPQ = Shin Pond quadrangle, SQ = Stacyville quadrangle, PMA = Pennington Mtn. Anticlinorium, MIRA = Miramichi Highlands, K-CMB = Kearsarge–Central Maine belt, ELM = Elmtree-Belledune inlier, CARB = Carboniferous cover rocks, CB = Coastal belt, MEG = Meguma terrane

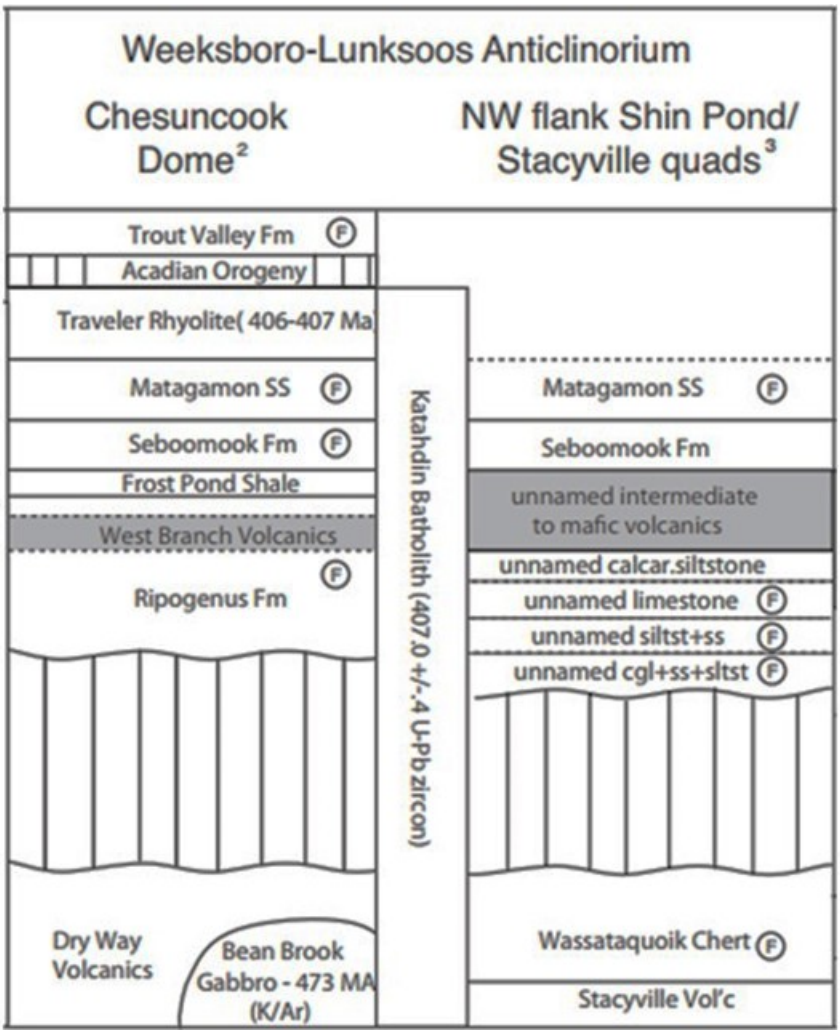

Figure 7.3 Stratigraphic section for the Weeksboro-Lunksoos Lake Anticlinorium, north-central Maine, showing Ordovician through Devonian rocks
All units shown lie unconformably above the Cambrian Grand Pitch Formation
(Source: Adapted from Schoonmaker, et al., 2011)

7.2 LOCAL GEOLOGY

The local stratigraphy documented in this section is thought to be equivalent to the lower-most Ordovician-age volcanic rocks (Dry Way Volcanics and Stacyville Volcanics) illustrated on Figure 7.3. The geology of the Pickett Mountain deposit locale, as mapped in 2018, is illustrated in Figure 7.4 and a cross section of the deposit and associated lithotypes are depicted on Figure 7.5.

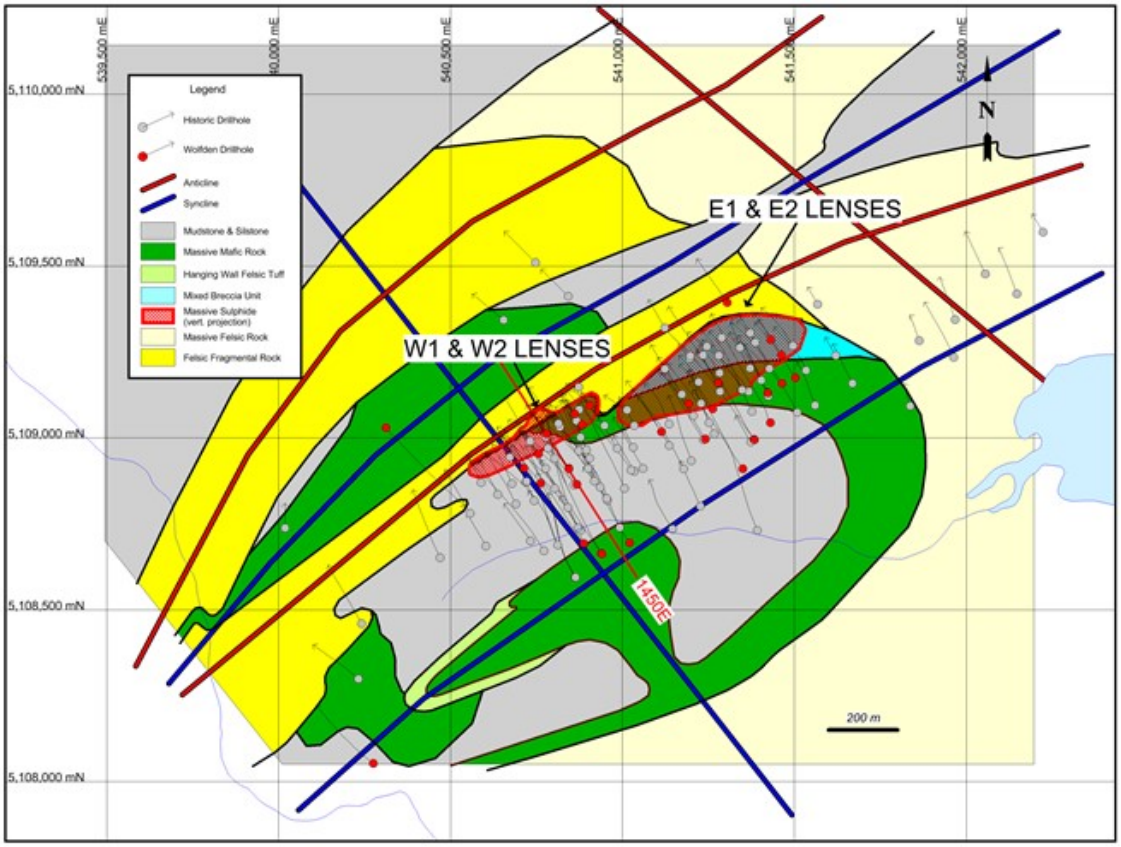

Figure 7.4 Geology plan map of the Pickett Mountain deposit

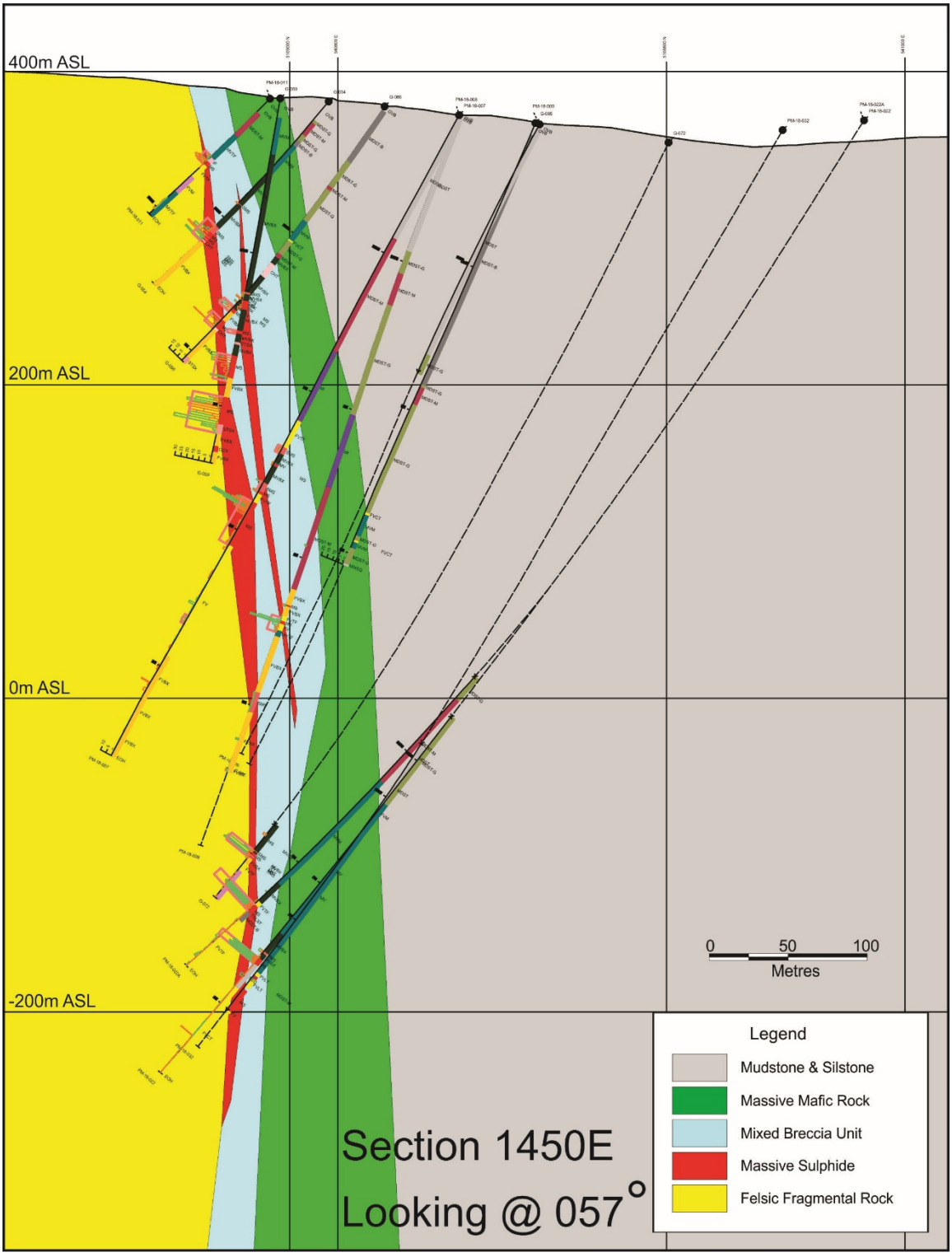

Figure 7.5 Cross Section of the Pickett Mountain deposit

In 2018, geological mapping was completed in the deposit area as well as in the northwest portion of the Property. Outcrop exposure is quite poor; mapping was augmented with the logged drill-hole geology in

the deposit area. Three main rock units were observed in the outcrop: footwall felsic volcanic rock, hanging wall mudstone-siltstone, and hanging wall massive mafic rock.

In the deposit area, the contact between the footwall and hanging wall rocks is occupied by an assemblage of mafic and felsic flows and breccia, mudstone, and massive sulphide. Generally, contacts and bedding strike northeast and dip steeply to the southeast. Repetitions of the contact between the footwall and hanging wall rocks suggest folding. The W1 and W2 Lenses are planar and steeply dipping. The E1 Lens is similarly oriented at its west edge, but the strike rotates clockwise and the dip shallows eastward, as it becomes affected by an interpreted synclinal fold nose with an axis that plunges towards the southwest.

7.2.1 STRATIGRAPHY

7.2.1.1 Footwall Felsic Rocks

The lowermost rock units are felsic volcanic fragmental rocks and a unit of massive, quartz-feldspar porphyritic rock described herein as QFP.

The fragmental rock is commonly felsic volcanic breccia, consisting of rounded, oblate fragments in a matrix of similar composition and texture, but a slightly different colour. Quartz and more commonly, feldspar phenocrysts, are generally round and less than 1 mm. Sections of the breccia contain abundant blocky patches of dark, fine-grained felsic rock with scattered 0.5 mm plagioclase phenocrysts thought to be fiamme, although wall rock rip-ups have also been reported. The fragmental rock also includes sections of tuff and lapilli tuff, which are compositionally similar to the volcanic breccia. Thin aplite dykes are reported in the drill logs. The foliation is usually penetrative and the aspect ratio of the fragments is 2:1:1. Sericitisation is always present and commonly minor, but increases to strong in the deposit area.

The QFP is massive and hard, with abundant 1-2 mm rounded quartz and feldspar phenocrysts in a fine-grained, hard, felsic matric. The quartz eyes tend to clump together in 0.5-1.0 cm masses somewhat resembling raspberries. The foliation appears as anastomosing 0.5 cm-spaced cleavage, and alteration is not observed.

7.2.1.2 Massive Sulphide

The massive sulphide is fine-grained and weakly to moderately banded, with the banding defined by centimetre to decimetre scale variations in the content of pyrite, sphalerite, galena, chalcopyrite, and gangue minerals. Other minerals present in varying amounts include calcite, chlorite, tetrahedrite, arsenopyrite, and magnetite.

The massive sulphide attains a maximum horizontal width of up to 25 metres (E1 Lens).

7.2.1.3 Breccia Unit

In the deposit area, a disrupted assemblage of rock types separates the deposit contact and a stratigraphically overlying massive mafic flow. The unit is 150 metres wide horizontally in the footwall to the East Zone, but thins to the west, pinching out near the West Zone.

The unit is not exposed on the surface; the drill logs suggest the unit is dominantly mafic breccia, with fist-sized mafic bombs in hyaloclastite. Other rocks include massive felsic and pyroclastic flows (which have Zr/Ti ratios distinctly lower than those of the footwall felsic rock), black and maroon mudstone (similar to those in the mudstone-siltstone unit), maroon chert, and semi-massive and massive sulphide.

A tentative interpretation of this unit is a flow breccia at the front of, and then overridden by the overlying mafic flow.

7.2.1.4 Massive Mafic Flow

This thick unit was initially mapped as anorthosite, as it consists almost entirely of fine-grained, equant plagioclase with <5% clinopyroxene. The rock is featureless and massive and has been named massive mafic flow because of the associated breccias.

7.2.1.5 Mudstone and Siltstone

Mudstone, with lesser siltstone, is the uppermost unit observed. The mudstone is dark green to black or, in a 200 metre thick horizon, alternating medium green and maroon. The siltstone is light beige and occurs in 5 cm to 30 cm beds. Bedding is otherwise faint to absent.

7.2.2 METAMORPHISM

Chlorite is the only possible prograde metamorphic mineral observed suggesting at most, lower greenschist grade metamorphism.

7.2.3 STRUCTURE

Similar felsic volcanic rocks and mudstone-siltstone are repeated across several contacts throughout the mapped area. Regional USGS mapping of nearby stratigraphic units indicate contacts repeated by closely spaced anticlines and synclines, or folding, in nearby stratigraphic units rather than a history of alternating volcanism and sedimentation. The deposit horizon is rotated into an interpreted syncline east of the East Zone, also arguing for fold repetitions of the contact.

Foliations in the rocks are axial planar to the interpreted folds near contacts but tend to be more northerly away from contacts. It is suggested that these foliations record a later flattening that produced cross-folding in the deposit area.

7.3 MINERALISATION

The mineral zone at Pickett Mountain is a volcanogenic massive sulphide deposit that strikes at approximately 057°. It has been traced by drilling approximately 900 metres along strike and to 750 vertical metres below surface. It consists of 4 primary lenses and several minor lenses that likely

reflect the original formation of the mineralisation. It is stratabound and is hosted primarily by an intermediate to felsic lapilli tuff to volcanic breccia unit (Scully, 1988).

Primary minerals of economic interest are chalcopyrite, galena, and sphalerite intercalated with variable amounts of pyrite. Accessory minerals include tetrahedrite and minor arsenopyrite. There are four primary lenses of massive sulphide that have been discovered to date (W1, W2, E1, and E2). These vary from 0.5 metres to about 25 metres in horizontal width and with the highest base metal grades situated at or near the base of the massive sulphide lenses. The high-grade Cu-Pb-Zn sulphides are typically finely laminated and are overlain and in sharp contact with massive pyrite (Scully, 1988).

The high-grade sulphides typically include 45% to 60% pyrite, 15% sphalerite, 3% galena, and 4% chalcopyrite. There are also minor amounts of tetrahedrite, tennantite, arsenopyrite, magnetite, and barite. Laminations are typically 2 mm to 5 cm in thickness and are compositionally defined (Scully, 1988).

The W1 Lens is the most prominent massive sulphide lens discovered to date having been traced by drilling over a 300 metre strike length and to a vertical depth of 750 metres. Notably, it also is the highest grade of all lenses based on current and historic drilling. The W2 Lens is situated in the hanging wall, or slightly to the south of the W1 Lens. It also has been traced over a 300 metre strike length and to a vertical depth of approximately 600 vertical metres.

The E1 and E2 Lenses are situated at the same stratigraphic level; the E2 Lens is located close to the surface while the E1 Lens sits at greater depth. Collectively, they have been traced over a strike-length of close to 550 metres and to a maximum vertical depth of about 400 metres below the surface.

Longitudinal sections for all 4 massive sulphide lenses are depicted in Figure 7.6 and Figure 7.7.

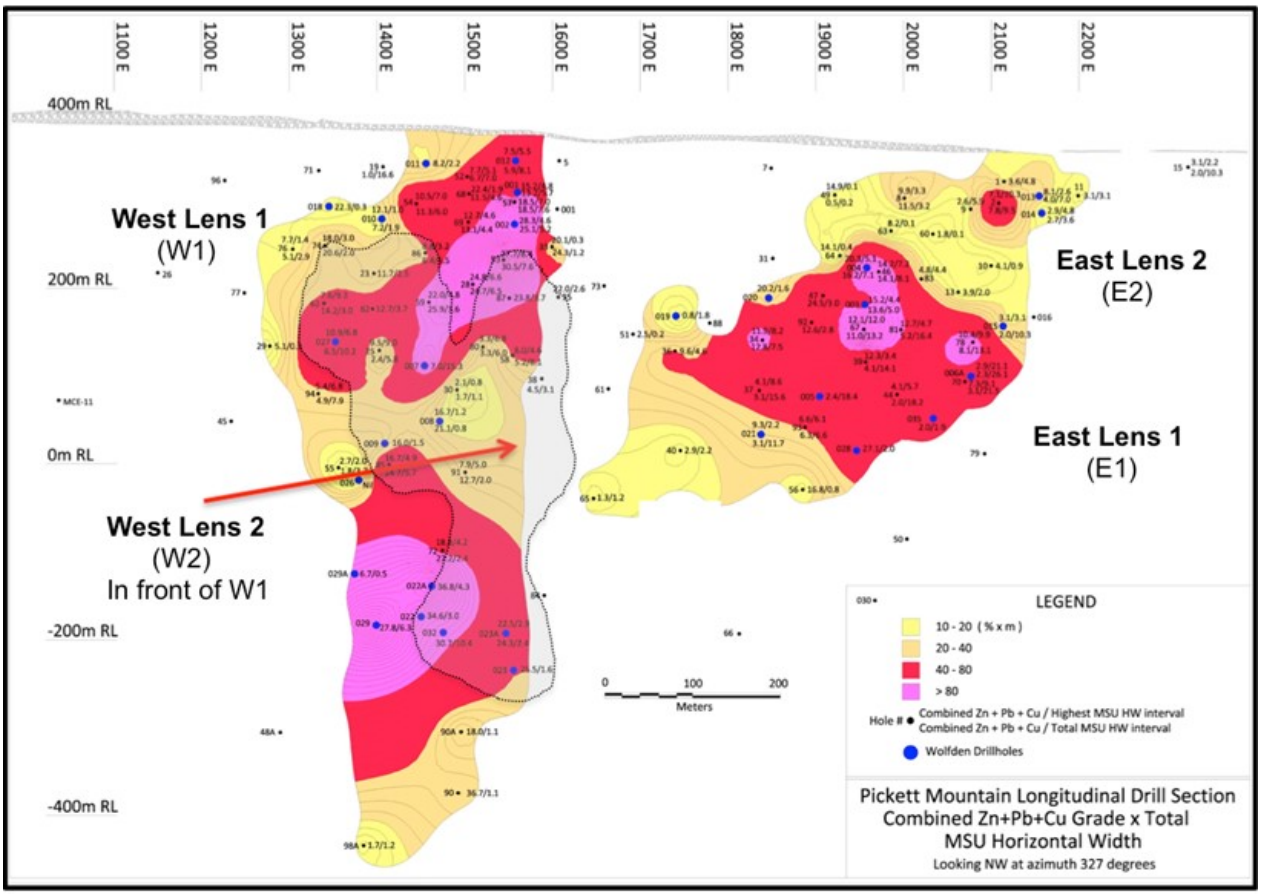

Figure 7.6 Longitudinal section of the W1, E1, and E2 massive sulphide lenses

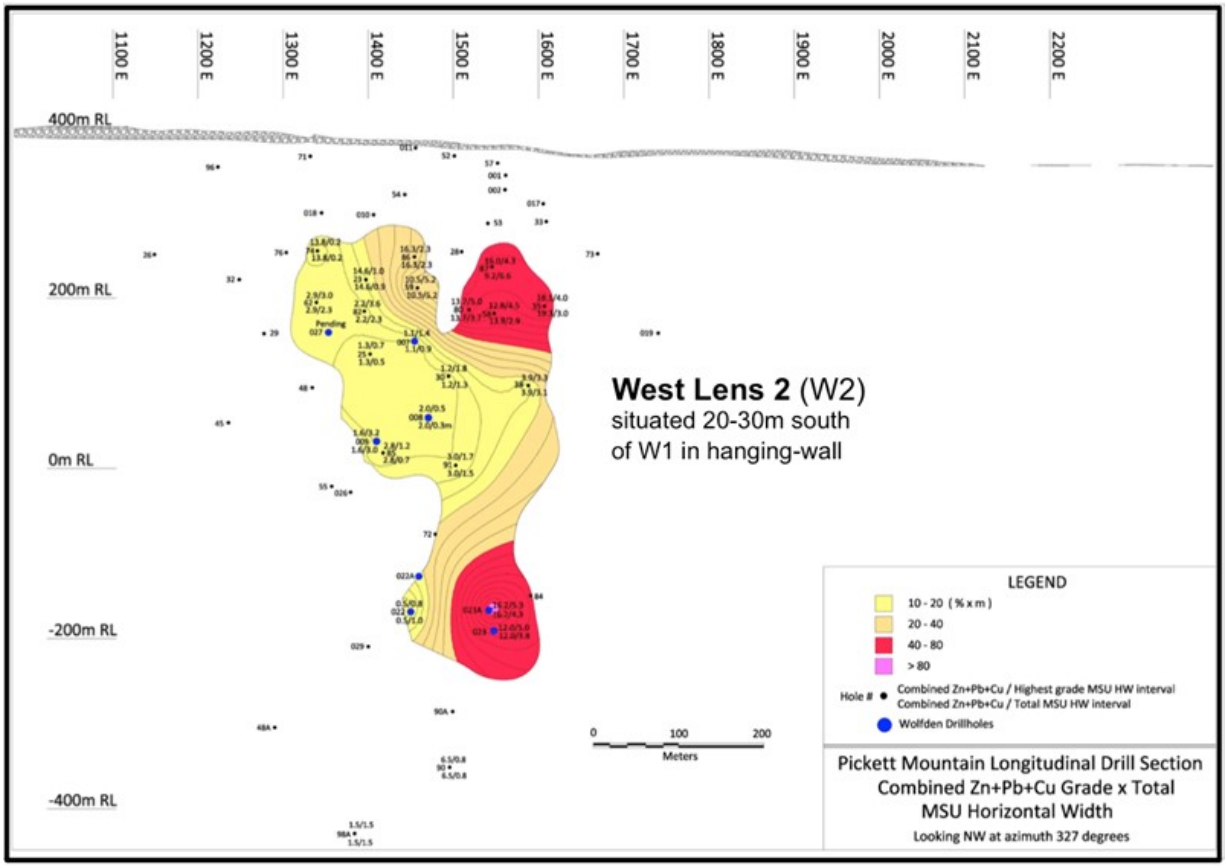

Figure 7.7 Longitudinal section of the W2 massive sulphide lens

Table 7.1 tabulates the most significant intersections obtained from the 4 massive sulphide lenses based on historic drilling (Getty and Chevron) and by recent drilling completed by Wolfden.

TABLE 7.1
SIGNIFICANT DRILL INTERCEPTS FROM HISTORIC DRILLING AND WOLFDEN DRILLING
(PM SERIES OF HOLES)

Pickett Mountain Massive Sulphide Zone Comprehensive Drill Results - Historical and Recent

Section	Zone	Hole #	From (m)	To (m)	Length (m)	Long HW (m)	Zn (%)	Pb (%)	Cu (%)	Ag (%)	Au (%)	Cu + Pb + Zn (%)	(Cu + Pb + Zn) * HW (%m)
1250E	MS-W1	29	279.04	279.65	0.45	0.28	3.50	1.30	0.26	8.57	0.34	5.06	1.40
1300E	MS-W1	76	162.89	168.30	5.41	2.89	1.67	0.57	2.88	38.24	0.36	5.12	14.79
1350E	MS-W1	55	457.60	462.77	5.18	3.71	0.99	0.33	0.56	8.96	0.18	1.88	6.99
1350E	MS-W1	62	212.59	219.91	7.31	3.00	8.59	4.55	1.09	76.88	0.87	14.23	42.69
1350E	MS-W1	74	158.20	161.54	3.34	1.98	13.53	5.11	1.95	167.80	0.98	20.58	40.75
1350E	MS-W1	94	316.43	332.25	15.82	7.89	2.71	1.08	1.09	44.55	0.73	4.89	38.61
1350E	MS-W1	PM-18-018	110.10	110.60	0.49	0.29	11.70	8.31	2.25	100.00	0.46	22.26	6.48
1350E	MS-W1	PM-18-027	254.99	279.40	13.20	10.21	6.47	2.72	1.41	96.92	0.56	10.60	108.28
1350E	MS-W1	PM-18-029A	612.46	613.42	0.95	0.70						Pending	Pending
1400E	MS-W1	23	197.92	201.32	3.40	2.45	6.32	3.22	2.12	65.37	0.71	11.66	28.61
1400E	MS-W1	25	314.55	321.47	6.92	5.78	1.35	0.33	0.72	10.74	0.24	2.39	13.83
1400E	MS-W1	82	254.20	259.10	4.90	3.66	7.22	2.85	2.64	115.21	0.95	12.71	46.53
1400E	MS-W1	85	398.50	411.21	12.71	5.70	8.81	4.04	1.88	92.74	1.02	14.72	83.88
1400E	MS-W1	98A	925.92	927.32	1.40	1.16	1.58	0.01	0.10	1.30	0.10	1.69	1.96
1400E	MS-W1	PM-18-010	123.60	126.89	3.30	1.91	5.02	1.63	0.50	40.10	0.30	7.15	13.68
1400E	MS-W1	PM-18-026	492.49	497.20	4.71	3.21						Nil	Nil
1400E	MS-W1	PM-18-029	657.60	668.15	10.55	6.34	19.32	7.24	1.24	206.36	1.28	27.80	176.37
1450E	MS-W1	54	112.93	121.30	8.37	6.01	7.76	2.27	1.23	44.25	0.71	11.26	67.65
1450E	MS-W1	59	194.28	211.99	17.70	3.60	14.98	7.80	3.14	150.75	1.19	25.92	93.30
1450E	MS-W1	72	526.77	530.69	3.92	2.44	18.10	8.54	0.56	210.05	1.13	27.20	66.30
1450E	MS-W1	86	172.20	180.20	8.00	5.53	3.04	1.11	2.23	35.78	0.59	6.38	35.30
1450E	MS-W1	PM-18-007	279.70	311.19	31.49	15.32	4.41	1.65	0.97	60.54	0.61	7.03	107.69
1450E	MS-W1	PM-18-008	342.29	344.70	2.41	0.79	16.78	3.98	0.37	68.38	0.53	21.13	16.78
1450E	MS-W1	PM-18-009	380.90	384.40	3.50	1.50	10.58	4.14	1.26	85.15	0.59	15.97	23.96
1450E	MS-W1	PM-18-011	56.59	59.59	3.00	2.15	4.22	1.42	2.60	34.26	0.54	8.24	17.75
1450E	MS-W1	PM-18-022	662.20	666.91	4.71	3.01	23.83	9.88	0.88	262.59	1.52	34.58	104.25
1450E	MS-W1	PM-18-022A	639.40	645.30	5.90	4.25	23.95	11.84	0.95	324.08	1.35	36.73	156.13
1500E	MS-W1	28	200.75	210.82	10.06	6.53	15.91	7.41	1.42	181.06	1.83	24.74	161.57
1500E	MS-W1	30	342.35	344.00	1.62	1.13	0.90	0.40	0.36	22.00	0.27	1.67	1.89
1500E	MS-W1	52	54.03	68.00	13.79	6.96	4.03	1.71	0.92	33.75	0.50	6.66	46.39
1500E	MS-W1	68	64.77	85.64	20.87	4.55	7.80	2.59	1.13	44.75	0.52	11.51	52.44
1500E	MS-W1	69	91.28	121.60	30.32	4.37	8.40	3.55	1.16	107.32	0.95	13.11	57.34
1500E	MS-W1	80	283.46	293.06	9.61	6.04	1.61	1.09	0.58	14.74	0.44	3.27	19.76
1500E	MS-W1	90	812.43	814.34	1.91	1.10	25.21	10.66	0.87	140.53	0.85	36.75	40.27
1500E	MS-W1	91	432.51	435.12	2.62	1.95	8.26	3.00	1.45	70.65	1.45	12.72	24.81
1500E	MS-W1	90A	761.76	763.13	1.37	1.05	12.50	4.75	0.77	93.24	0.79	18.02	18.96
1500E	MS-W1	PM-18-023	722.00	724.40	2.40	1.60	20.39	3.75	1.39	107.14	1.05	25.53	40.82
1500E	MS-W1	PM-18-023A	686.90	690.19	3.29	2.42	15.83	7.78	0.70	167.87	0.93	24.30	58.78
1550E	MS-W1	53	157.89	171.79	13.90	7.58	18.61	10.25	1.63	229.89	1.62	30.49	230.94
1550E	MS-W1	57	81.40	95.98	14.58	7.64	11.06	5.91	1.54	145.75	0.92	18.51	141.36
1550E	MS-W1	58	278.07	292.61	14.54	8.15	2.97	1.30	0.94	78.25	0.45	5.21	42.48
1550E	MS-W1	87	214.97	220.70	5.73	3.71	15.53	6.02	2.25	191.42	0.88	23.80	88.19
1550E	MS-W1	PM-17-001	84.25	92.20	7.95	5.69	7.88	3.83	1.51	104.01	0.85	13.23	75.25
1550E	MS-W1	PM-17-002	109.80	119.69	9.90	5.19	16.31	7.09	1.73	185.61	1.42	25.13	130.40
1550E	MS-W1	PM-18-012	37.30	48.70	11.40	8.14	3.63	1.43	0.83	34.84	0.30	5.89	47.94
1600E	MS-W1	33	156.88	158.44	0.76	1.25	13.60	9.78	0.90	186.76	1.01	24.28	30.25
1650E	MS-E1	65	413.30	416.59	3.29	1.16	0.77	0.26	0.32	4.86	0.53	1.35	1.57
1750E	MS-E1	36	275.97	282.30	6.33	4.52	6.11	2.46	1.07	63.61	0.72	9.64	43.60
1750E	MS-E1	40	385.66	388.90	3.20	2.22	1.54	0.59	0.77	0.00	0.55	2.90	6.43
1750E	MS-E1	PM-18-019	235.90	238.80	2.90	1.83	0.40	0.08	0.28	3.88	0.05	0.76	1.39
1850E	MS-E1	34	245.04	259.10	14.06	7.53	8.68	3.28	0.82	78.59	0.99	12.78	96.23
1850E	MS-E1	37	320.03	341.99	21.96	15.62	1.64	0.69	0.72	51.18	0.73	3.05	47.71
1850E	MS-E1	PM-18-020	194.60	197.80	3.20	1.65	13.15	5.34	1.70	124.66	1.14	20.20	33.24
1850E	MS-E1	PM-18-021	350.00	371.00	21.00	11.68	1.99	0.69	0.34	15.02	0.30	3.02	35.25
1900E	MS-E1	47	181.19	187.60	6.40	3.02	17.09	6.42	1.02	128.91	1.40	24.53	74.20
1900E	MS-E1	49	67.21	67.57	0.30	0.22	0.21	0.17	0.12	0.17	0.14	0.50	0.11
1900E	MS-E1	56	396.85	398.80	1.95	0.81	12.00	4.08	0.67	96.38	1.30	16.76	13.53
1900E	MS-E1	64	118.06	130.82	12.77	0.35	8.24	3.71	1.36	83.84	0.78	13.32	4.72
1900E	MS-E1	92	225.31	229.50	4.19	2.82	8.41	3.29	0.87	76.64	0.81	12.57	35.48
1900E	MS-E1	93	330.04	343.70	13.66	6.62	3.94	1.46	0.85	72.97	1.12	6.25	41.38
1900E	MS-E1	PM-18-005	278.11	323.91	45.80	18.39	1.30	0.51	0.59	24.04	0.43	2.41	44.28
1950E	MS-E1	39	236.52	268.70	32.15	14.09	2.31	0.90	0.85	22.46	0.44	4.06	57.26
1950E	MS-E1	46	161.85	171.91	9.30	8.08	9.58	3.66	0.79	86.27	0.72	14.04	113.34
1950E	MS-E1	67	172.66	254.12	68.28	13.20	6.78	3.04	1.20	50.22	0.65	11.02	145.65
1950E	MS-E1	PM-18-003	192.89	202.60	9.71	4.99	9.27	3.39	0.99	58.78	0.73	13.64	68.10
1950E	MS-E1	PM-18-004	170.61	180.89	10.29	7.12	10.96	4.06	1.23	117.31	0.96	16.25	115.76
1950E	MS-E1	PM-18-028	390.89	394.30	3.41	2.04	19.14	7.37	0.60	151.04	1.16	27.12	55.22

TABLE 7.1
SIGNIFICANT DRILL INTERCEPTS FROM HISTORIC DRILLING AND WOLFDEN DRILLING
(PM SERIES OF HOLES)
(CONTINUED)

Section	Zone	Hole #	From (m)	To (m)	Length (m)	Long HW (m)	Zn (%)	Pb (%)	Cu (%)	Ag (%)	Au (%)	Cu + Pb + Zn (%)	(Cu + Pb + Zn) * HW (%m)
2000E	MS-E1	8	88.09	91.74	2.74	3.25	7.27	2.62	1.63	60.61	1.47	11.53	37.46
2000E	MS-E1	44	292.46	318.21	25.69	18.19	0.94	0.52	0.53	8.50	0.41	1.99	36.24
2000E	MS-E1	63	95.71	95.90	0.20	0.04	5.30	2.40	0.54	30.17	0.45	8.24	0.35
2000E	MS-E1	81	230.12	255.60	25.01	16.44	3.16	1.22	0.78	32.11	0.59	5.16	84.81
2000E	MS-E1	83	204.37	209.85	5.48	4.41	3.14	1.24	0.43	29.45	0.33	4.81	21.23
2050E	MS-E2	9	78.03	85.95	7.62	5.88	2.08	0.28	0.30	20.16	0.75	2.66	15.63
2050E	MS-E2	13	183.79	186.69	2.74	2.14	2.62	0.54	0.72	57.90	0.57	3.88	8.30
2050E	MS-E1	60	94.49	96.31	1.82	0.13	0.79	0.28	0.75	5.14	0.17	1.82	0.24
2050E	MS-E2	70	263.05	304.80	35.35	21.53	1.76	0.58	0.69	20.40	0.49	3.03	65.22
2050E	MS-E2	78	229.51	252.56	23.05	13.10	5.01	2.00	1.10	48.88	0.62	8.12	106.32
2050E	MS-E2	PM-18-006A	255.70	308.10	52.40	26.09	1.33	0.48	0.50	18.63	0.30	2.31	60.28
2100E	MS-E2	1	40.84	47.55	6.58	4.90	2.08	0.73	0.72	29.36	0.20	3.54	17.36
2100E	MS-E2	2	64.16	76.96	12.65	9.50	5.02	1.87	0.91	49.63	0.63	7.80	74.08
2100E	MS-E2	10	168.86	170.08	1.07	1.02	2.49	0.67	0.93	48.48	0.20	4.09	4.18
2150E	MS-E2	PM-18-013	59.10	68.50	9.40	7.01	2.38	0.83	0.75	32.17	0.41	3.96	27.78
2150E	MS-E2	PM-18-014	86.70	91.70	5.00	3.61	1.70	0.55	0.47	24.66	0.28	2.72	9.84
2100E	MS-E2	PM-18-015	229.00	245.50	16.50	10.33	1.10	0.42	0.52	18.58	0.27	2.04	21.08
2200E	MS-E2	11	53.04	57.45	4.41	3.06	2.15	0.56	0.42	30.43	0.41	3.13	9.58
1350E	MS-W2	62	199.33	205.13	5.80	2.37	1.47	0.50	0.94	20.53	0.72	2.91	6.90
1350E	MS-W2	74	151.27	151.64	0.01	0.22	9.30	3.65	0.84	82.96	0.62	13.79	3.03
1350E	MS-W2	PM-18-027	242.80	246.00	3.20	1.32						Pending	Pending
1400E	MS-W2	23	192.02	193.32	1.30	0.92	8.08	5.01	1.58	101.95	0.87	14.66	13.51
1400E	MS-W2	25	308.46	309.07	0.61	0.50	0.60	0.23	0.50	14.23	0.33	1.33	0.67
1400E	MS-W2	82	242.83	245.97	3.15	2.32	0.94	0.32	0.91	26.52	0.46	2.17	5.03
1400E	MS-W2	85	382.21	383.87	1.34	0.72	1.75	0.85	0.23	7.54	0.24	2.83	2.03
1400E	MS-W2	PM-18-009	369.60	376.40	6.79	2.92	0.78	0.25	0.53	16.53	0.23	1.56	4.56
1450E	MS-W2	59	167.19	181.66	14.47	2.88	6.16	2.75	1.58	88.43	0.62	10.49	30.17
1450E	MS-W2	86	162.00	164.59	2.59	1.76	11.18	3.86	1.28	85.01	1.03	16.31	28.63
1450E	MS-W2	PM-18-007	251.60	253.39	1.80	0.85	0.63	0.15	0.34	9.03	0.14	1.12	0.96
1450E	MS-W2	PM-18-008	331.88	332.88	0.98	0.33	0.96	0.36	0.73	17.60	0.17	2.05	0.67
1450E	MS-W2	PM-18-022	656.80	658.30	1.50	0.96	0.00	0.00	0.54	28.92	0.58	0.54	0.52
1500E	MS-W2	30	309.67	311.63	1.95	1.31	0.39	0.08	0.74	0.00	0.17	1.22	1.60
1500E	MS-W2	80	217.63	223.87	6.24	3.73	8.15	3.90	1.64	110.32	1.00	13.68	51.01
1500E	MS-W2	91	413.00	415.10	2.10	1.51	1.00	0.37	1.65	9.25	0.38	3.02	4.56
1550E	MS-W2	58	212.63	218.45	5.82	2.93	8.08	3.31	2.40	123.54	1.12	13.79	40.43
1550E	MS-W2	87	151.27	163.37	12.10	6.63	5.54	2.35	1.28	56.94	0.56	9.17	60.81
1550E	MS-W2	PM-18-023	661.14	667.06	5.92	3.79	7.48	3.21	1.31	62.66	0.73	12.00	45.44
1550E	MS-W2	PM-18-023A	646.60	652.60	6.00	4.33	10.19	4.69	1.28	52.93	0.49	16.17	70.01
1600E	MS-W2	35	210.65	215.10	4.39	3.03	12.82	5.65	0.86	87.84	0.83	19.34	58.61
1600E	MS-W2	38	327.57	331.55	3.98	3.09	2.26	0.88	0.73	32.37	0.45	3.87	11.98

Notes: The historical drill results included in this table were generated between 1979 to 1989 by Getty Mining Company and Chevron Resources. The historic drill core samples were cut in half using a diamond saw or core splitter and sent to Skyline Laboratories in Tucson, Arizona for analyses. Copper, lead, and zinc were analyzed utilising atomic absorption spectrometry (AA) while gold and silver were analysed utilising the fire-assay technique. High-grade copper, lead, and zinc assays obtained by AA were checked routinely utilising wet chemistry techniques. Wolfden is not aware of the quality assurance and quality control programs undertaken with these results, if any. The historical data, which does include most of the drill core in storage, does not include the original assay certificates. The historical results were compiled by Wolfden utilising original drill logs, drill sections, working files and reports, and databases prepared by the former owners of the Property at that time and subsequently acquired by Wolfden. Wolfden has not independently verified the historic results. Holes drilled by Wolfden begin with PM-17 and PM-18.

ATTACHMENT 2

Australian Government

PREVENTING ACID AND METALLIFEROUS DRAINAGE

Leading Practice Sustainable Development Program for the Mining Industry

September 2016

INDUSTRY.GOV.AU | DFAT.GOV.AU

AMD may be very acidic (low pH) and contain elevated concentrations of metals, metalloids and major ions and low concentrations of dissolved oxygen. Hence, it can present a major risk to aquatic life, riparian vegetation and human uses of the water resource for many kilometres downstream from where it enters a waterway. In many parts of the world, local communities depend on waterways for their livelihood. Clean water is essential for drinking, crop irrigation and stock watering, and is vital to sustain aquatic ecosystems, including aquatic life used for food.

Mining activities in the past have sometimes damaged ecosystems and had very heavy impacts on communities. Today, such poor practice should not occur if mining is to be accepted by society as part of an economically sustainable development framework. Successful management of AMD is vital to ensure that mining activities meet increasingly stringent environmental regulations and community expectations, and that the industry's social licence to operate is maintained.

Once a mining operation has ceased, poor-quality water from the production of AMD may continue to damage the environment, human health and livelihoods for decades or even centuries. A mine site in the Iberian Pyrite Belt in Spain, for example, has been generating AMD for more than 2,000 years.

The crucial step in leading practice management of AMD is to assess the risk as early as possible. 'Risk' includes environmental, human health, commercial, reputation, legal and regulatory risks. The progressive evaluation of AMD risk, begun during exploration and continuing through the feasibility evaluation stage, provides the data necessary to quantify potential impacts and management costs before significant disturbance of sulfidic material. When projects proceed at sites where AMD is a potential risk, efforts should focus on prevention or minimisation, rather than on control or treatment.

At decommissioned and older operating mine sites where the characterisation of mined materials for AMD potential and/or management of resultant drainage has been inadequate, high remediation and treatment costs can continue to reduce the profitability of the operating companies. The term 'treatment in perpetuity' has entered modern mining vocabulary as a result of intractable AMD issues that prevent the relinquishment of mining leases, despite the cessation of mining operations. Such situations are inconsistent with sustainable mining practice and must be avoided at new mines by the application of appropriate materials characterisation and AMD minimisation strategies.

Leading practice management of AMD continues to evolve, and that evolution has been captured in the content of successive editions of this series of handbooks and elsewhere (Jones & Taylor 2008; Jones 2011; Miller 2014). This handbook outlines current leading practice approaches for predicting and minimising the occurrence of AMD from a risk management perspective and contains case studies highlighting the application of leading practice strategies for the management of sulfidic wastes that are currently being, or have been, implemented by the industry. In particular, a number of the case studies document strategies that were implemented during the operating life of a mine, and for which longer term monitoring data is now available to demonstrate good performance over at least a decade. There are also updates of previous case studies that indicate the benefits of the early implementation of leading practice concepts. This contrasts with the previous two editions of this handbook, which by necessity used case studies of management strategies that had just been implemented and for which there had been insufficient time to fully assess their performance.

Specialist expertise may be needed to help plan and implement many of the strategies described in this handbook. It is particularly important that expert advice be sought during the characterisation and prediction process (Section 4), in assessing the risk posed by AMD (Section 5), and before the selection and implementation of long-term minimisation and control strategies (Section 6).

ATTACHMENT 3

9-2000

Rio Tinto Estuary (Spain): 5000 Years of Pollution

Richard A. Davis
University of South Florida, rdavis@usf.edu

A. T. Welty
University of South Florida

J. Borrego
University de Huelva

J. A. Morales
University de Huelva

J. G. Pendon
University de Huelva

See next page for additional authors

Rio Tinto estuary (Spain): 5000 years of pollution

R.A. Davis Jr. · A.T. Welty · J. Borrego · J.A. Morales · J.G. Pendon · J.G. Ryan

Abstract Mining of massive sulfide deposits in southwestern Spain extending back to the Copper and Bronze Ages has resulted in the pollution of the Rio Tinto fluvial-estuarine complex, the site of Columbus' departure for the New World in 1492. Additional sources of potential pollution include the large industrial complex at Huelva near the lower portion of the estuary. Extensive analysis of surface sediment samples and cores has established that there are no geographic trends in the distribution of the pollutants, which include Cu, Fe, Pb, Zn, Ti, Ba, Cr, V and Co. These data have, however, demonstrated that tidal flux within the estuary carries phosphorus and perhaps other elements from the industrial complex at Huelva to the tidal limit of the system, several kilometers upstream from the discharge site. Radiometric analysis of short cores shows that sedimentation rates over at least the past couple of centuries have been about 0.3 cm/year. These data and that from a single deep core demonstrate that the estuary was polluted from mining activity long before the large-scale operations began in the late nineteenth century.

Key words Sediment pollution · Massive sulfides · Phosphate · Open-pit mining · Estuary

Received: 3 May 1999 · Accepted: 18 October 1999

R.A. Davis Jr. (✉) · A.T. Welty · J.G. Ryan
Department of Geology, University of South Florida,
4202 E. Fowler Ave, SCA 203, Tampa, FL 33620, USA
e-mail: rdavis@chuma.cas.usf.edu
Tel.: +813-914-2159
Fax: +813-914-2654

J. Borrego · J.A. Morales · J.G. Pendon
Departmento de Geologia, University de Huelva,
21819 Huelva, Spain

Present address: A.T. Welty, Department of Geology,
Northern Arizona University, Flagstaff, AZ 86011, USA

Introduction

The Rio Tinto system in the province of Huelva, southwestern Spain, has great historical significance as well as environmental interest. It is one of the most polluted fluvial-estuarine systems in the world and most likely has been so for thousands of years. It is in the headwaters of this river that mining supporting the Copper Age and Bronze Age took place. The estuary, at the town of Palos de la Frontera, was the origin of Columbus' expedition in 1492 and for subsequent trips. Most recently, the city of Huelva has become the site of one of the most polluted industrial areas of the world. It is possible, however, that the pollution of the system began thousands of years ago with the original mining of the massive sulfide deposits near the headwaters of the Rio Tinto.

This investigation was conducted in order to answer the following questions:

1. What is the level and distribution of metals and other important pollutants in the sediments of the system?
2. What is the influence, if any, of tidal transport of the pollutants being discharged in and near the industrial complex at Huelva?
3. What is the chronology associated with the pollutants and to what extent, if any, have they been incorporated into the sediments that have accumulated in the estuary?

Study area

The massive sulfide deposit called the Iberian Pyrite Belt is one of the largest and most famous of such deposits in the world. It extends in essentially an east to west orientation across about 250 km of southwestern Spain and southern Portugal (Fig. 1) with an average width of 30–40 km. The thickness of the complex ranges up to hundreds of meters. The rich ore body is limited to a length of 5 km and is 750 m wide and 40 m thick. These sulfides were formed in the early Carboniferous, about 300–350 Ma, over a sequence of Devonian shales and quartz arenites and are overlain by Lower Carboniferous turbidites (Moreno 1993). The mineralization was produced by tremendous hydrothermal activity on the sea floor during a period of intense volcanic activity. The

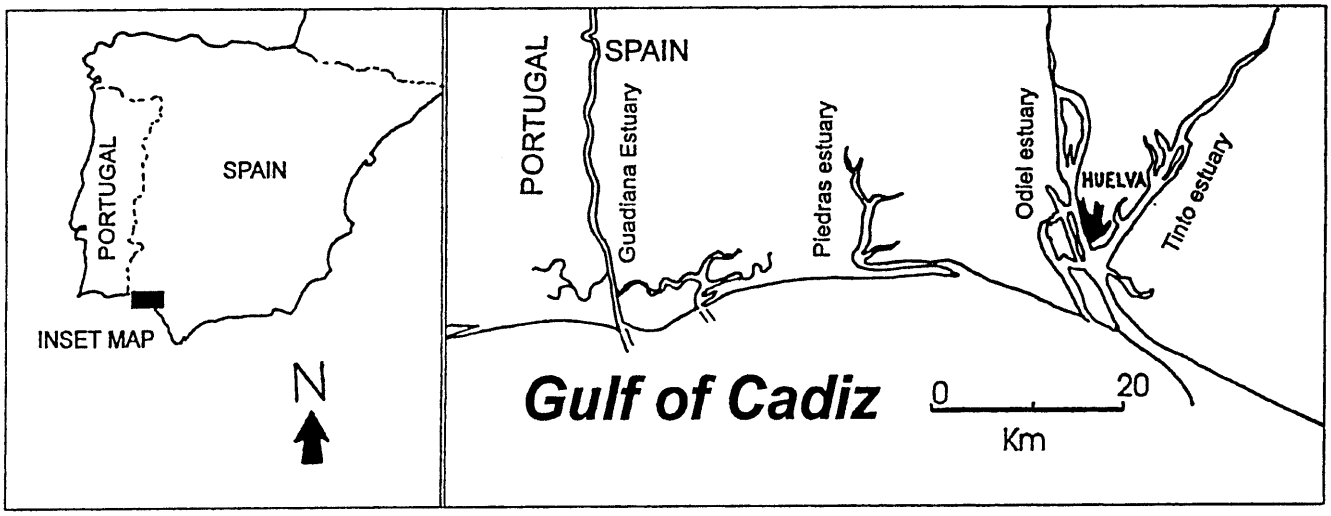

Fig. 1
Map showing the location of the Rio Tinto system in south-western Spain

massive deposit is very rich in Fe, Cu, Zn, As, Pb, Ag and Au. Deformation of this complex took place during the Hercenian Orogeny (Strauss and others 1977).

Historical perspective

Mining of these massive sulfide deposits has been going on for about 5000 years, beginning with the Iberians and Tartessans who developed the first mine about 3000 b.c. near the present community of Nerva (Fig. 2). This underground, small-scale operation was followed by that of the Phoenicians (2800–2600 b.p.) and the Romans (2000–1800 b.p.). The area is the site of the beginnings of the Copper Age and the Bronze Age (Coles and Harding 1979), and the Romans made some of their first coins from materials mined here, especially the silver and gold. Subsequent cultures, including the Visigoths (1600–1300 b.p.) and Moors (1300–500 b.p.P), essentially abandoned the mining operations. Then in the nineteenth century the mining was taken over by the United Kingdom, and large-scale, open-pit operations prevailed until the deposits had been essentially depleted about a century later. Peak production for the large volume products such as pyrite was between 1875 and 1930 (Ferrero 1988). The copper production was stopped in 1986 and silver and gold production ended in 1996. A much smaller-scale copper production was initiated again in 1994 but proved uneconomic and was halted in 1998.
The amount of material excavated from these ancient operations has been estimated from the volume of waste produced. The Tartessans removed about 3 million tons using small galleries and shallow depths with typically only one or two people working the mine. The Romans expanded the operations with larger galleries and greater depths. They dug below the water table and used clever water-wheel systems to pump the galleries dry. These operations accounted for about 24.5 million metric tons of material (Flores 1979). The expansion of the mining to open-pit methods led to the total production of about 1600 million metric tons of material.
The other and recent aspect of the potential pollution of this fluvial-estuarine system is the industrialization of the Huelva area beginning in 1967. Within only a few years, operations began of (1) a huge phosphate beneficiation plant which processes raw ore from nearby Morocco and other locations, (2) a plant for processing Australian heavy minerals such as magnetite and ilmenite ("black sand") and (3) a large paper mill located at San Juan del Puerto (Fig. 2). Each of these industries is contributing huge volumes of pollutants to the local estuaries. The phosphate plant has produced millions of tons of phospho-gypsum which is piled along the west margin of the Rio Tinto estuary (Fig. 2). Tailings of the pyrite plant are similarly located and the paper plant discharges a large volume of contaminated wastewater.

Rio Tinto system

The Rio Tinto drainage system includes an area of 1670 km^2 and the river/estuary extends for 95 km to the mouth near Huelva. The headwaters of the river are in the area of intense mining from which the river descends from elevations near 400 m down to about 40 m at the town of Niebla (Fig. 2) below which meandering begins with a modest flood plain. The annual discharge of the Rio Tinto, as gauged at Niebla, has ranged from almost nothing to about 350 Hm^3 over the period of record (Fig. 3a). There is great variation in discharge during the hydrological year with most taking place during the winter whereas during the summer it is almost nothing (Fig. 3b). Floods have played a major role in the Rio Tin-

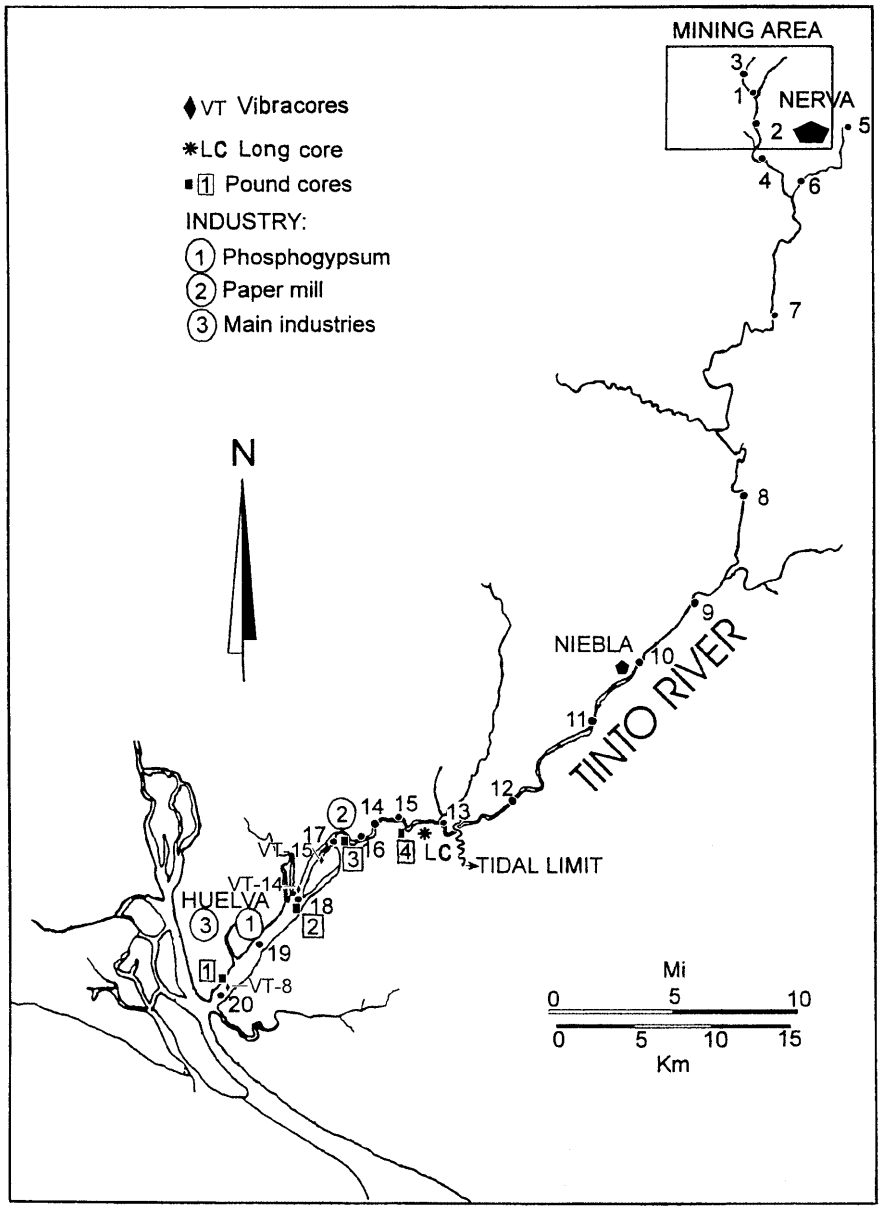

Fig. 2
Map of the Rio Tinto system showing the locations of mining and polluting industries, surface sediment samples, short pound cores and the long core

to with the most recent taking place in 1995 (Schell and others 1996).

Tidal influence begins a few kilometers upstream from the community of San Juan del Puerto (Fig. 2). The estuarine portion of this system consists of extensive intertidal and supratidal flats with marsh fringes typically just above neap high tide. Mean tidal range is 2.2 m at the mouth of the estuary with some decrease upstream (Fig. 4). Water quality of this estuary is extremely poor with low tide pH values typically at 2.0–2.5. Flood tides bring in Atlantic water and raise the pH to near neutral levels in the lower portion of the estuary. There is no macrobenthic community and only during flood tides are there nekton or plankton in the estuary. The only organisms in the river portion of the system are microalgae, bacteria and fungi (Moreira and others 1997).

The estuarine portion of the Rio Tinto system is characterized by braided channel systems of gravel, sand and mud with terrigenous gravel being limited to the uppermost portion. Tidal channels are typically floored by bedforms in sand with mud concentrated on the channel margins and in the lower intertidal zones. Shell material is conspicuously absent from the surface sediments of the estuary.

Previous work

The scientific literature on the Rio Tinto is quite sparse until about 1990. During the 1990s, there was an explosion of research effort invested into this region, much of

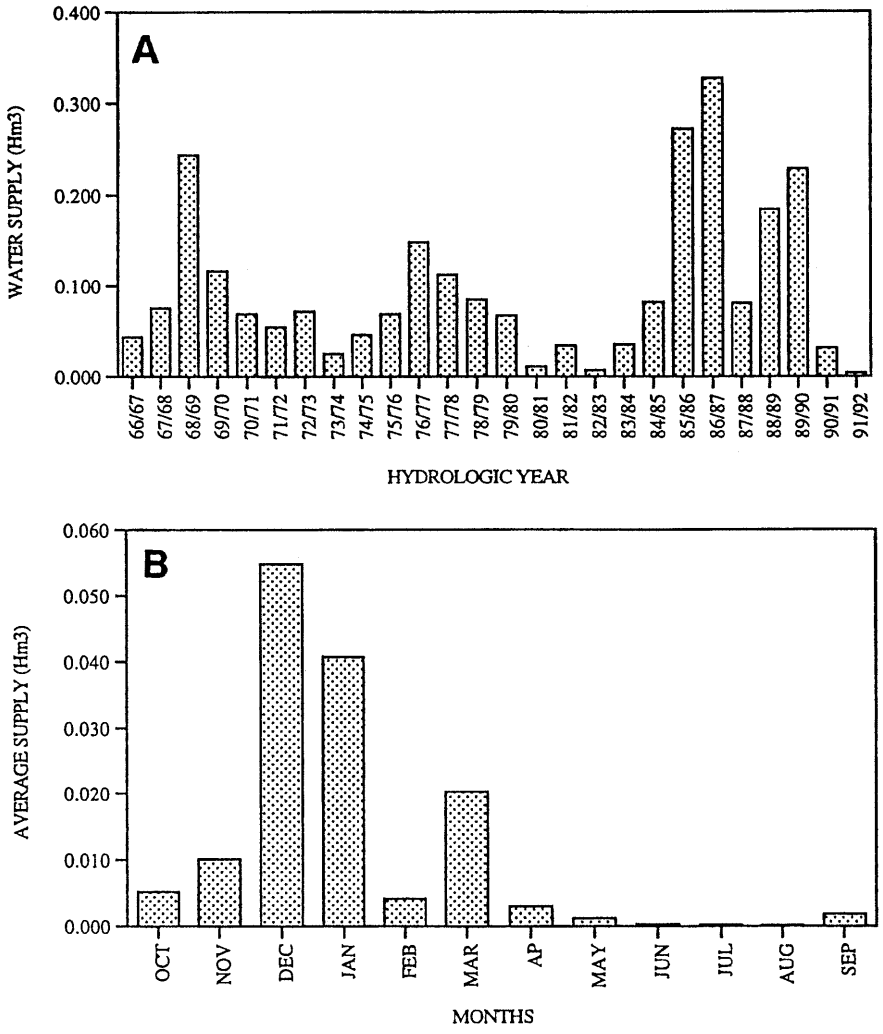

Fig. 3
Hydrologic data for **a** long-term discharge and **b** annual discharge patterns over the period of 1966–1992 for the Rio Tinto taken at the town of Niebla (see Fig. 2 for location)

it aimed at the pollution of the Rio Tinto and the adjacent Odiel River. Efforts have included analyses of both the water and the sediments of the estuary but none have been very comprehensive.

Although there had been considerable effort directed toward the ore body itself (e.g. Strauss and others 1977, 1981; Klau and Large 1980) and to the history of the mining in the region (e.g. Flores 1979; Harvey 1981; Morral 1990) there had been no significant attempt to assess the influence of the mining activities on the river and estuary of the Rio Tinto system until recently.

A group led by R. Amils from the University of Automona Madrid has been investigating the microbial community of the estuary with surprising results (e.g. Lopez-Arcilla and others 1994; Moreira and others 1997). They have found an abundant and diverse assemblage of bacteria, algae and fungi inhabiting these very acidic waters.

Water chemistry of the Rio Tinto has been well documented and the database is growing rapidly. The local environmental authorities have been collecting water samples on a weekly basis from a single station in the middle of the estuary near the phospho-gypsum stacks (Fig. 2) since 1977. They measure pH, dissolved oxygen and salinity, but their sampling is weekly, regardless of the tidal situation, thus giving a great range in these parameters depending on tidal stage.

Most of the data on water samples are from the river and estuary and few from the mining region. Published data of the analyses and the locations of the samples within the estuary are not shown in detail (Leblanc and others 1995; van Geen and others 1997). Both investigations conclude that the estuary system is discharging high concentrations of metal pollutants into the Gulf of Cadiz and beyond. High levels of radioactivity have also been documented in estuarine waters as a consequence of the beneficiation process being carried out at the phosphate plant where effluent is discharged into both the Odiel and Rio Tinto systems (Martinez-Aguirre and Garcia-Leon 1991). Borrego and others (1999) have analyzed samples from seven locations near the industrial complexes along the Odiel, the Rio Tinto and the combined estuaries (Huelva estuary) for numerous parameters and have found very elevated concentrations from industrial and domestic waste. Visual indications of the high levels of pollution

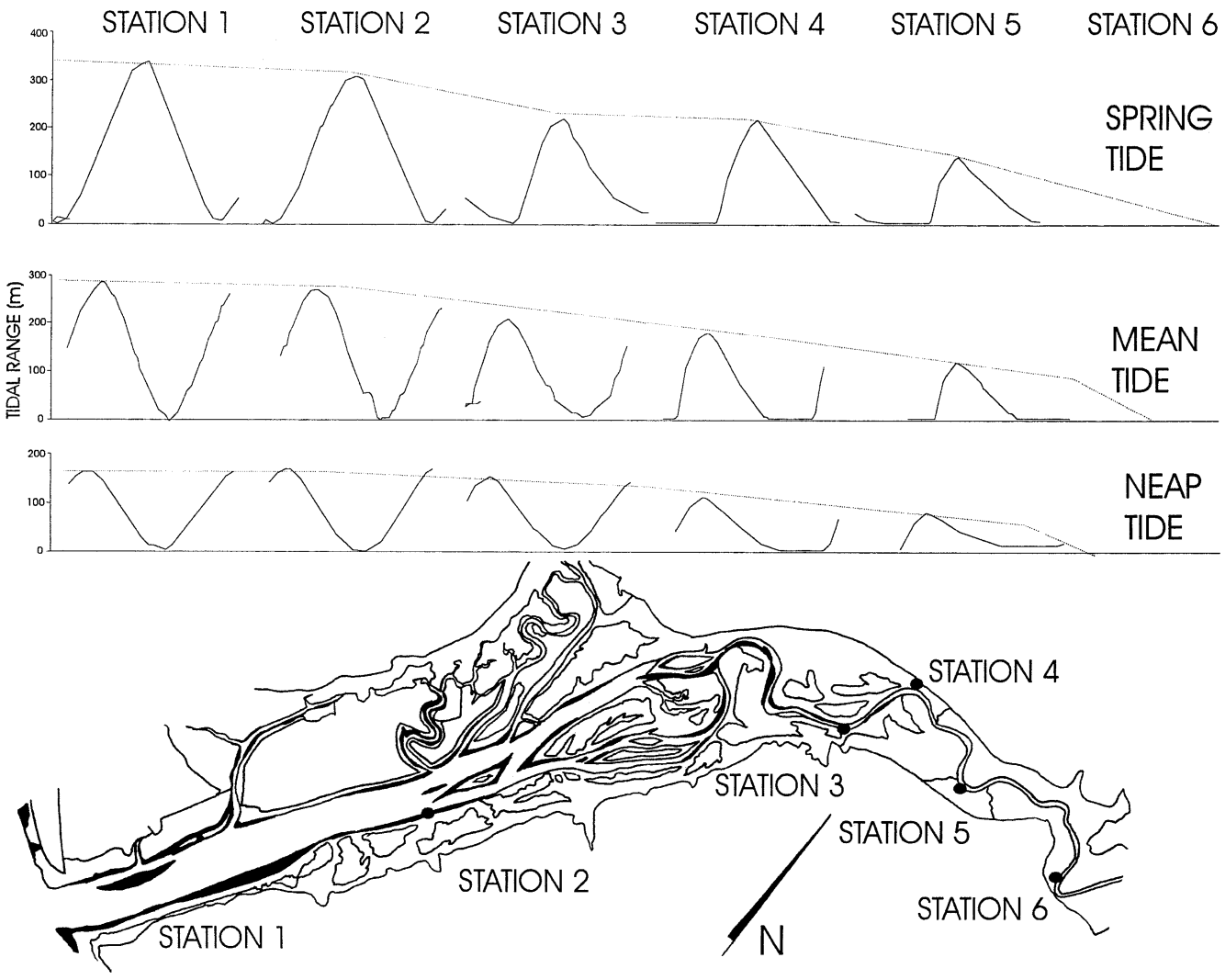

Fig. 4
Tidal curves showing the change in range up the estuary for spring, mean and neap conditions

are the red color of the water in the river and the presence of large amounts of sulfur in modern fluvial sediments (Fig. 5).

Sediment samples have been analyzed from several locations throughout both the Odiel and Rio Tinto systems. Probably the most geographically comprehensive study to date has considered both of these fluvial-estuarine complexes (Lissen 1991). The data set extends from the headwaters of both drainage systems to the open sea. More recently, Nelson and Lamothe (1993) looked at the anomalous heavy metal concentrations along both systems as well, but had a limited number of samples (11 samples from 6 locations). Another recent investigation of heavy metals was undertaken for 12 sites from the mine area to the mouth of the estuary (Schell and others 1996). These studies all concluded that there were quite elevated concentrations of many heavy metals (e.g. Pb, Cu, Ca, Mn, As, Zn, Fe, Ag) in the estuaries as a consequence of the mining activities. They did not address the contributions of the phosphate plant at Huelva nor the influence, if any, of tidal flux in distributing these pollutants.

All authors agree that the mining began about 5000 years ago but few have tried to unravel the chronology of the significant pollution in the fluvial-estuarine system. Two publications have considered the time framework of this pollution using limited data and reaching conflicting results. Detailed examination and analysis of a 50-m core taken from the marsh adjacent to the Odiel estuary at Huelva City go a long way toward interpreting the history of mining pollution (Ruiz and others 1998). Twenty samples were taken from the core and analyzed for 11 oxides and 16 elements, many of which might have had their origins in the mining operations or in the nearby industrial complex. The beginning of significant contributions of heavy metals from the mining activity is about 5 m below the top of the core. A 14-C date of $5390 + 155$ years b.p. was obtained at 10 m down the core. The authors interpret the first occurrence of the concentrations of pollutants to represent the beginnings of mining about 4800 years ago, although there is no radiomet-

Fig. 5
Photographs showing pollution in the Rio Tinto; **a** the red color from which the river gets its name shown here above the influence of tides and **b** abundant sulfur that has accumulated in the fine sediments near the landward limit of tidal influence

ric data to corroborate this interpretation. Recent pollution is assigned to the 0.3–0.4-m layer at the top of the natural portion of the core and therefore is assigned a date of about 1967, although no Pb or Cs series dating was done on the core.

A more distant pair of short cores was collected from the continental shelf in the Gulf of Cadiz off the mouth of the estuary at water depths of 56 and 69 m (van Geen and others 1997). The analyses for metal pollutants and Pb-210 series dating showed that the earliest level with detectable Zn contamination accumulated between 1840 and 1890, the period when large-scale mining operations began. This is in marked contrast to the data of Ruiz and others (1998) which show considerable contamination beginning at about the time of the start of mining practices thousands of years ago.

Database

Surface sediment samples for geochemical analysis were taken from throughout the fluvial-estuarine system (Fig. 2). Effort was made to include sites within the mining area, from an apparently pristine stream near the headwaters of the Rio Tinto and from throughout the fluvial-dominated portion of the system. Samples were also taken of the country rock in the mining area. Some limitations were posed by access, especially in the area of high relief just below the mining areas. The estuarine portion of the system where current industry is located was sampled so as to include material from both sides of the estuary (Fig. 2).

Short pound cores were taken from the channel margins of the estuary and near its upper limits. Geochemical analyses and radiometric dating were done for three vibracores taken from various locations in the estuary (Fig. 2).

Initial geochemical analyses included the sand fraction of the samples but it was apparent that there were very low concentrations of pollutants in this portion of the sediment, a conclusion also reached by Nelson and Lamothe (1993). The mud fraction (<63 μm) of the surface samples and of two of the pound cores was analyzed for nine oxides and eight trace elements by using an ARL DC plasma-emission spectrometer at the University of South Florida. The samples were dissolved in a 4:1 mixture of HF:$HClO_4$, evaporated to dryness and brought to final dilutions in 1 M HNO_3. Solutions were diluted by a factor of 20 for analysis of major elements. Calibration curves were constucted using the US Geological Survey standards G-2, QLO, MAG-1 and SCO-1 which were prepared and analyzed with the samples. Precision for all major elements is within 1–2% except for phosphorus which is within 10%. Trace element precision is variable but is at least within 25%.

In addition to the geochemical analysis, Pb-210 series dating was conducted on the four pound cores in order to determine the recent chronology of pollution associated with the industrialization of Huelva in 1967 and the huge expansion of mining in the late nineteenth century. These analyses were conducted at Florida State University, Department of Oceanography by W. Burnett and associates.

Geochemical analysis of the vibracore samples included Cu, Zn, As and this was done at the University of Huelva by los Servicios Centrales using an ICP mass spectrometer.

Distribution of pollutant species in surface sediments

The obvious first step in trying to determine the source of pollutant species in the Rio Tinto system is to consider the distribution of the various elements downstream from the mining activities. A total of 43 sediment samples from 18 different distances from the mine area formed the database for determining if any downstream trends in concentration are present. There is no question

from these data that there are very elevated levels of most of the elements contained in the sulfide ore bodies throughout the Rio Tinto system. Some are orders of magnitude above normal background levels (Schell and others 1996). Important pollutants included in the analyses are Fe, Ti, Ba, Ni, Co, Cr, V, Zn and Cu. Other species concentrations that were determined, such as Al, Mg, Ca, K and Na, are either not important constituents of the ore body, or are not major pollutants, or they could come from sources such as the turbidites associated with the massive sulfide deposits.

As was stated by others (Nelson and Lamothe 1993; Schell and others 1996), there seems to be no downstream pattern to the concentrations (Table 1). Plots show way too much scatter to be significant (Fig. 6).

Influence of the phosphate industry

Phosphorus is not present in elevated levels in the upper reaches of the Rio Tinto but it is in the estuary (Table 1). The huge beneficiation plant in the Huelva industrial complex produces both large volumes of phospho-gyp-

Table 1
Chemical analyses of surface sediment samples. Rio Tinto fluvial/estuarine system. Geochemical data from the 43 surface sediment samples analyzed. Note that they are arranged with the top of the table representing the mining site and the bottom being the mouth of the estuary. Elevated P_2O_5 values begin near the limit of tidal influence

Distance (km)	Sample	Site description	Al_2O_3 (wt%)	Fe_2O_3 (wt%)	MgO (wt%)	CaO (wt%)	MnO (wt%)	K_2O (wt%)	Na_2O (wt%)	TiO_2 (wt%)	P_2O_5 (wt%)	Sr (ppm)	Ba (ppm)	Ni (ppm)	Co (ppm)	Cr (ppm)	V (ppm)	Zn (ppm)	Cu (ppm)
11	3	Spoil pile outwash	5.25	3.86	0.2	0.11	0.006	1.76	0.14	0.62	0.08	76	12660	15	6	8	43	3200	325
3.6	5	Rio Jarama	15.46	1.83	1.9	1.27	0.385	2.66	O.91	0.64	0.13	73	682	34	15	16	111	2500	114
5.2	2	Fluvial	9.49	15.42	1.32	0.32	0.073	1.78	0.49	0.47	0.41	81	5908	48	21	19	107	14200	877
10	4	Open-pit mine	7.47	21.55	2.02	0.37	0.091	1.51	0.32	0.29	0.26	49	1768	63	37	53	109	23200	1090
12	6	Rio Jarama	25.44	2.29	2.27	2.02	0.258	2.5	3.4	1.4	0.15	143	572	49	24	0	158	14000	971
22.2	7 A	Fluvial	14.13	3.55	1.24	1.73	0.061	2.06	1.81	1.31	0.16	153	1380	33	18	27	155	2750	255
22.2	7B	Fluvial	4.94	8.1	0.6	0.26	0.026	0.98	0.34	0.35	0.11	42	444	25	13	61	54	10600	480
42.2	8 A	Fluvial	11.47	10.92	1.02	1.16	0.115	2.51	0.8	0.78	0.21	164	1993	49	24	0	158	14000	971
42.2	8B	Fluvial	6.27	7.64	0.4	0.17	0.022	1.44	0.35	0.27	0.14	38	589	24	9	27	93	8000	4 28
50.4	9 A	Fluvial	9.83	11.59	0.81	0.49	0.066	1.89	0.69	0.44		65	793	32	5	47	74	720	952
50.4	9B	Fluvial	7.03	11.72	0.71	0.35	0.035	1.39	0.46	0.33		49	570	36	6	62	82	10600	1040
50.4	9 C	Fluvial	11.63	13.87	0.72	0.27	0.039	2.05	1.09	0.57	0.29	211	1207	43	18	99	185	8260	241
50.4	9D	Fluvial	8.69	11.77	0.97	0.34	0.08	1.42	0.48	0.32		47	662	37	7	49	86	17800	1080
58.8	10 A	Fluvial	12.21	11.18	1.03	0.65	0.048	2.73	0.79	0.8	0.26	105	2210	36	17	0	165	13100	812
58.8	10B	Fluvial	7.36	18.6	0.49	0.15	0.023	1.56	0.46	0.35		50	748	33	5	46	99	6140	227
61.6	11 A	Fluvial	8.6	9.87	0.92	0.88	0.042	1.52	0.61	0.46	0.15	61	381	30	4	37	53	797	1150
61.6	11B	Fluvial	3.42	13.22	0.46	0.2	0.023	0.55	0.25	0.17		27	220	20	7	25	41	7830	476
61.6	11 C	Fluvial	11.75	9.48	0.89	0.47	0.036	2.51	0.9	0.64		102	1162	44	5	82	114	10000	552
68	12 A	Above tidal limit	10.38	10.77	1.07	1.02	0.046	2.07	0.83	0.65	0.18	83	345	16	2	27	33	233	341
68	12B	Above tidal limit	9.71	10.71	1.23	0.59	0.05	2.26	0.82	0.55		97	702	34	5	51	81	18200	604
71.4	13 A	Within tidal limit	7.87	14.65	0.81	0.84	0.043	1.75	0.61	0.49	0.27	78	333	17	2	27	42	400	317
71.4	13B	Within tidal limit	19.54	4.93	0.72	0.11	0.021	2.86	0.49	0.72	0.74	110	530	36	10	24	141	3250	181
75	15 A	Estuary	14.73	9.36	0.94	0.3	0.03	2.8	0.85	0.47	0.96	169	400	29	3	99	113	259	598
75	15B	Estuary	12.45	9.74	1.09	0.46	0.037	2.77	0.99	0.29	0.61	207	416	35	4	80	108	574	522
75	15C-1	Estuary	15.17	6.25	1.43	0.9	0.053	3.05	1.72	0.76		113	783	34	5	69	84	731	1160
75	15C-2	Estuary	14.74	9.5	1.31	0.34	0.038	3.53	1.74	0.52	0.2	134	758	41	5	84	125	602	775
76	14 A	Estuary	8.31	8.88	1.07	0.87	0.024	3.13	4.71	0.68	0.39	169	1246	32	6	50	73	4470	475
76	14B	Estuary	14.57	9.13	0.97	0.27	0.022	2.03	0.83	0.58	2.42	83	444	31	4	108	109	7410	293
76	14 C	Estuary	17.58	3.37	1.62	0.32	0.028	3.32	0.98	0.89	0.2	77	384	36	4	94	117	493	569
76	14D	Estuary	15.16	8.33	0.7	0.16	0.016	1.98	0.62	0.58	2.95	104	674	270	6	55	57	653	1100
78.2	16 A	Estuary	16.69	6.5	1.1	0.33	0.03	2.14	1.4	0.59	3.28	149	609	41	6	97	131	293	738
78.2	16B	Estuary	8.59	10.4	1.87	0.38	0.056	1.31	0.59	0.17	2.46	144	469	25	4	41	101	774	1020
78.2	16C-1	Estuary	13.9	5.7	1.47	0.69	0.05	2.28	3.03	0.64	0.15	109	354	34	5	89	87	369	275
78.2	16C-2	Estuary	16.97	3.6	2.86	2.21	0.121	2.93	1.73	0.64	0.15	112	379	45	7	102	97	213	213
81	17 A	Estuary	5.43	6.44	2.81	1.46	0.024	2.34	13.82	0.21	1.08	515	216	40	4	204	124	1110	990
81	17B	Estuary	7.59	10.62	2.9	0.38	0.072	0.68	3.39	0.16	1.26	192	652	34	7	46	136	2490	3000
81	17C-1	Estuary	17.69	4.73	2.09	0.34	0.046	2.95	2.44	0.61	0.2	86	388	39	4	92	100	725	2150
81	17C-2	Estuary	10.33	9.7	1.43	0.36	0.023	1.74	5.12	0.43	2.34	228	675	28	3	67	167	276	509
84.8	18 A	Gysum stacks	15.35	5.28	1.54	0.45	0.035	2.46	2.25	0.66	1.37	96	508	45	5	89	128	5030	1340
84.8	18B-1	Gysum stacks	8.03	8.16	2.63	0.78	0.047	1.66	9.01	0.22	1.56	397	479	34	7	51	108	1360	2930
84.8	18B-2	Gysum stacks	12.87	9.81	1.37	0.38	0.036	2	1.08	0.38	2.4	101	384	39	3	71	90	300	496
84.8	18D-1	Gysum stacks	15.11	3.36	2.56	9.7	0.036	2.25	3.15	0.51	0.27	140	302	56	15	113	74	278	140
92.4	20-A	Iron foundry	1.67	41.64	0.49	0.82	0.101	0.16	0.71	0.04	0.96	171	751	60	16	36	325	14700	3420

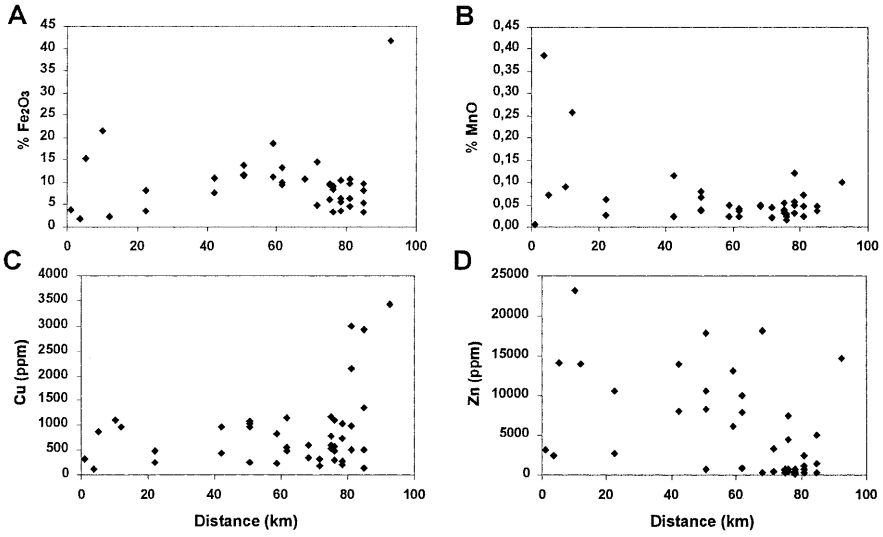

Fig. 6
Plots of the distribution downstream of selected pollutants showing the absence of any geographic trend. The highly elevated values for Fe_2O_3 and Cu near the mouth of the estuary reflect the proximity of the industrial complex where ore was processed

sum waste adjacent to the estuary and discharges fluids into it. The geographic distribution of the elevated phosphate concentrations (Table 1) extends to almost the tidal limit of the estuary at sample site 13B (Fig. 2). This indicates that the phosphate industry is polluting the Rio Tinto throughout the entire estuarine portion.
It should also be noted that the analyses of the long core in the Odiel estuary adjacent to the Huelva industrial complex did not show any high levels of phosphate indicating that Rio Tinto waters do not travel into the Odiel estuary.

Rates of sediment accumulation

The four pound cores were collected in order to determine if a chronology could be developed for two important events in the Rio Tinto environments: (1) the expansion of mining to large-scale, open-pit procedures in the late nineteenth century and (2) the development of the major industrial complex at Huelva City beginning in 1967. Cores nearly 1 m long were taken and dated by Pb-210 methods with the expectation that their length would include at least a century of sediment accumulation. Each core was photographed, cut, described and sampled for analysis. Both geochemical analysis and dating were conducted for each of the samples taken.
Although there are individual spurious values, overall the results of the Pb-210 analyses are quite consistent for three of the cores (1–3) which show nearly the same rate of sediment accumulation; about 0.3 cm/year (Fig. 7). The fourth core, which was taken near the limit of tidal influence in the system, did not provide any stratigraphic trends based on the Pb-210 analysis (Fig. 7). This suggests that the sediment in the core accumulated as the result of a major discharge event that reworked sediment at least several decimeters in thickness. Although the most recent important flood events prior to the sampling

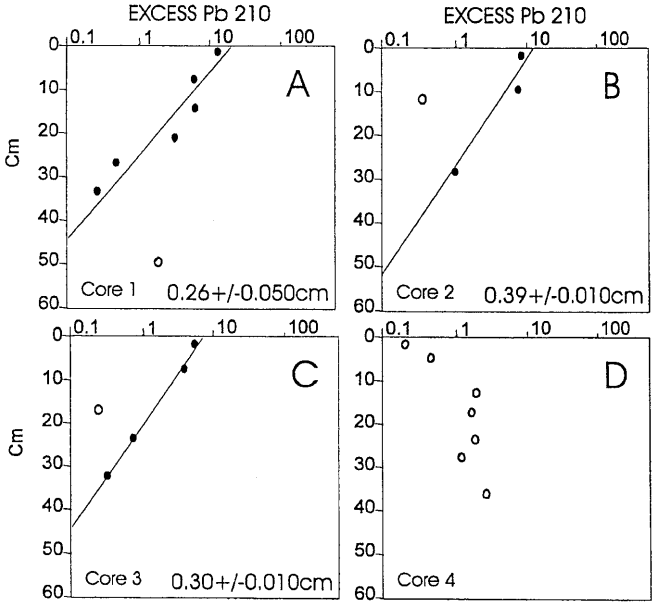

Fig. 7
Plots of Pb-210 analyses for four short-pound cores taken from along the tidal portion of the estuary. See Fig. 2 for locations of the cores. Note that there is no stratigraphic trend for core no. 4 and thus, no sedimentation rate was obtained for it

were in 1988 and 1989, it is likely that little sediment accumulated since that time because of (1) the location near the limit of tidal influence and (2) the absence of sediment discharge in this part of the system except during major flood events.
Using the rates of sediment accumulation determined for each of the cores, it is clear that the cores do represent more than 100 years of the accumulation of sediment in the Rio Tinto system. The lowermost sample analyzed in each of the two cores accumulated in 1830 (2) and 1810 (3), well before the large-scale mining operations began

in the headwaters area. These data compare with the dates of large-scale copper production in the early 1880s (Harvey 1981) and the first occurrence of excess zinc (1840–1890) in shelf cores as determined by van Geen and others (1997).

Of significance is the fact that the geochemical analyses of the push-core samples show that extremely elevated levels of the various pollutants produced by mining activity accumulated before the large-scale mining began in the late nineteenth century (Table 2). These data show that the Rio Tinto was polluted as the result of mining activities in its headwater areas that predate the large-scale, open-pit mining of the United Kingdom operators. Further testimony to this conclusion is provided by geochemical analysis of sediment samples from the vibracores (Fig. 8). Samples from throughout the cores show elevated concentrations of Cu and Zn. Specifically core VT-8, near the mouth of the Rio Tinto, had high concentrations of Cu and Zn to depths of 1.6 m and then a very high level of Cu (970 ppm) near the base of the core (2.4 m) with a 14-C date of 2020 years b.p. Core VT-14 taken from several kilometers upstream showed similar results. High concentrations of Cu and Zn are in the upper 0.5 m, then there is a decrease ending with a large concentration of Cu (978 ppm) at 3.2 m, near the base of the core. A 14-C date from this horizon yielded an age of 840 years b.p. The other core to be dated (15) is from the vicinity of core VT-14 and showed high levels of both Cu and Zn, with the latter remaining about the same throughout the core whereas Cu increased to 2466 ppm near the base (Fig. 8). That horizon was dated at 3640 years b.p. This apparent reverse trend is real. The surface of the location from which this core was taken is an area of erosion indicating that the upper part of the heavily polluted sequence was removed. The radiometric date (3640 YBP) shows that pollution was present in pre-Roman times.

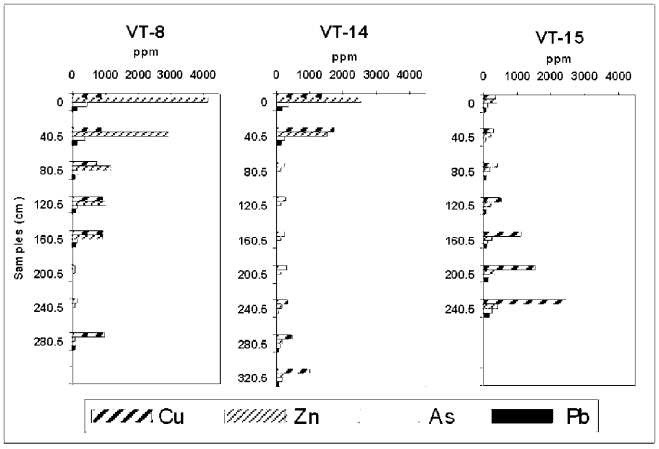

Fig. 8
Stratigraphic geochemical data from three vibracores taken from various locations in the Rio Tinto estuary. (see Fig. 2 for locations)

An important aspect of these stratigraphic data is the fact that abundant shells, including articulated *Cerastoderma* and thick oyster accumulations, are present throughout the range of the high concentrations of Cu and Zn. This means that these organisms must have been able to exist and reproduce under such benthic conditions. Data from other studies indicate that the waters of the current estuary are highly contaminated with Cu and Zn, as well as other metals. It should be expected that if sediment was highly contaminated in the past, the water was also. This raises a significant question: are these taxa typically toler-

Table 2
Elemental analyses from selected vibracores. Geochemical data obtained from analysis of the three vibracores cores shown in Fig. 7. Elevated levels of pollutants appear much before the large-scale mining operations

Sample	1	3	5	7	9	11	13	15	17
VT-8 (A)									
Depth (cm)	0	39.5	80.5	120.5	160.5	200.5	240.5	280.5	
Cu (ppm)	863.2	875	729.5	893.6	948.7	73.1	118.2	970	
Zn (ppm)	4122.9	2913.3	1175.3	1004.9	904.5	68.6	65.7	68.6	
As (ppm)	441	366.9	171.2	136	131.7	22.4	22.4	97.1	
Pb (ppm)	122.9	143.1	77.1	87.8	101.5	24.7	25.9	79.7	
VT-14 (B)									
Depth (cm)	0	39.5	80.5	120.5	160.5	200.5	240.5	280.5	320.5
Cu (ppm)	1349.4	1709.9	243.5	259.4	222.8	289.2	340.9	463.3	978.4
Zn (ppm)	2537.8	1508.2	147.9	138.4	119	136.3	150.4	168.4	208
As (ppm)	375.6	218.1	37.6	46.6	37	42.5	57.4	84	158.6
Pb (ppm)	170.2	125.8	47.2	43.9	39.4	47.2	49	54.1	71.6
VT-15 (C)									
Depth (cm)	0	39.5	80.5	120.5	160.5	200.5	240.5		
Cu (ppm)	355	286.7	419.3	513.3	1115.5	1546.9	2465.9		
Zn (ppm)	383	216.3	200.2	213.8	262.9	337.3	425		
As (ppm)	128	65.3	90.4	113.3	141.4	148.7	262.2		
Sample (ppm)	73.1	48	59.3	68.9	104.6	117.8	168.6		

ant of such high concentrations or were these populations genetically adapted to these toxic conditions? These core data demonstrate that pollution extended back well before the large-scale mining; at least to before the Roman activities and probably to the beginning of the original small, shaft mines.

Conclusions

Analysis and interpretation of a system-wide suite of surface sediment samples, four pound cores and three vibracores from the Rio Tinto fluvial-estuarine system permits the following important conclusions:

1. The data collected from the mines themselves to the mouth of the estuary corroborate that of other investigators in that there are highly elevated concentrations of numerous pollutant oxides and trace elements in surface sediments.
2. Likewise, our data do not show any downstream trends, high concentrations occur throughout the system.
3. Effluent produced by the phosphate beneficiation system in the Huelva industrial complex is being transported upstream to the tidal limit of the estuary as evidenced by elevated phosphorus concentrations.
4. Benthic fauna, especially oysters and clams, were able to exist and reproduce under very polluted estuarine conditions
5. Most importantly, it has been determined that the Rio Tinto system was polluted by mining activities well before the large-scale, open-pit practices of the late nineteenth century.

Acknowledgements This project has benefited from the field assistance of numerous students from the University of Huelva including Mercedes Lopez, Immaculata Jimenez, Josep Pascual and Elena Urbina. Funding was provided by grant CICYT PB93–1205 from the Andalusian Government and by the University of South Florida overhead rebate system. Chemical analyses of the vibracores were provided by the E.C. ELOISE program and the TOROS project (E.C. contract number ENV4-CT96–0217) by Dr. Marc Leblanc.
Davis conceived and organized the project and provided funding from USF. The funding in Spain was organized by Pendon. Both of them, along with Borrego and Morales, conducted the fieldwork and some of the laboratory analysis. Most of the geochemical analyses were conducted by Welty under the supervision of Ryan.

References

Borrego J, Ceron JC, Morales JA (1999) Impacts of human activities on the Tinto and Odiel estuary waters (Huelva, south-west Spain). Environ Geol (in press)
Coles JM, Harding AF (1979) The Bronze Age in Europe. St Martin Press, London
Ferrero MD (1988) Los conflictos de Febrero de 1888 en Riotinto: distintas versiones de los hechos. HuelvaHist 2:603–623
Flores M (1979) Las minas de Riotinto hasta su venta a los ingleses. PhD ThesisUniversity of Sevilla
Geen A van, Adkins JF, Boyle EA, Nelson CH, Palanques A (1997) A 120-year record of widespread contamination from mining of the Iberian pyrite belt. Geology 25:291–291
Harvey CE (1981) The Rio Tinto Company: an economic history of a leading international mining concern, 1873–1954. A Hodge, Penzance, UK
Klau W, Large DE (1980) Submarine exhalative Cu-Pb-Zn deposits, a discussion of their classification and metallogenesis. Geol Jahrb 40:13–58
Leblanc M, Benothman D, Elbaz-Poulichet F, Luck JM, Cravajal D, Gonzalez AJ, Grande JA, Ruiz de Almodovar G, Saiz R (1995) Rio Tinto (Spain), an acidic river from the oldest and the most important mining area of Western Europe: preliminary data on metal fluxes. In: Pasava J, Kribek B, Zak K (eds) Mineral deposits: from their origin to their environmental impacts. Balkema, Rotterdam, pp 669–670
Lissen JM (1991) Contaminacion por metales en los sedimentos de los Rios Tinto y Odiel. PhDThesis, University of Sevilla
Lopez-Arcilla AI, Marin U, Amils R (1994) Bioleaching and interrelated acidophilic microorganisms from Rio Tinto (Spain). Geomicrobiol J 11:223–233
Moreira D, Lopez-Archilla AI, Amils R, Martin I (1997) Characterization of two new thermoacidophilic microalgae: genome organization and comparison with *Galdieria sulphuraria*. FEMS Microbiol Lett 122:109–114
Moreno C (1993) Postvolcanic Paleozoic of the Iberian pyrite belt: an example of Basin morphologic control on sediment distribution in a turbidite basin. J Sed Pet 63:1118–1128
Morral FM (1990) A mini-history of Rio Tinto. Can Mining Metall Bull 83:150–154
Nelson CH, Lamothe PH (1993) Heavy metal anomalies in the Tinto and Odiel river and estuary system, Spain. Estuaries 16:496–511
Ruiz F, Gonzalez-Regalado ML, Borrego J, Morales JA, Pendon JG, Munoz JM (1998) Stratigraphic sequence, elemental concentrations and heavy metal pollution in Holocene sediments from the Tint-Odiel Estuary, south-western Spain. Environ Geol 34:270–278
Schell C, Macklin MG, Hudson-Edwards KA (1996) Flood dispersal and alluvial storage of heavy metals in an acid ephemeral river: Rio Tinto, SW Spain. Proceedings of the 4th International Symposium on the Geochemistry of the Earth's Surface. Ilkley, UK, pp 475–479
Strauss GK, Madel J, Alonso FF (1977) Exploration practice for strata-bound volcanogenic sulfide deposits in the Spanish-Portuguese pyrite belt, In: Klemm DD, Scheinder H-J (eds) Time and strata-bound ore deposits. Springer, Berlin Heidelberg New York, pp 55–93
Strauss GK, Roger G, Lecolle M, Lopera E (1981) Geochemical and geologic study of the volcano-sedimentary sulfide orebody of La Zarza, Huelva Province, Spain. Econ Geol 76:1975–2000

ATTACHMENT 4

STATE OF MAINE
DEPARTMENT OF ENVIRONMENTAL PROTECTION

JANET T. MILLS
GOVERNER

MELANIE LOYZIM
COMMISSIONER

MEMORANDUM

To: Tim Carr, Senior Planner, Land Use Planning Commission

From: Michael Clark, Mining Coordinator, Bureau of Land Resources

Date: July 5, 2023

Re: Department comments on Wolfden Mt. Chase, LLC's petition to rezone portion of Township 6, Range 6 Penobscot County, Maine for development of an underground metallic mineral deposit, January 18, 2023

The Department of Environmental Protection (Department or DEP) has reviewed the above noted zoning petition (the Petition), submitted to the Land Use Planning Commission (Commission or LUPC) by Wolfden Mt. Chase, LLC (Wolfden or Applicant). The Petition provides information in support of Wolfden's request to rezone approximately 374 acres that are currently within the General Management subdistrict, to allow construction, mining, closure, and reclamation activities over an estimated 10-15 years. The project is named Pickett Mountain and is located north of Patten, in Penobscot County near the border with Aroostook County. The Department's comments on the Petition follow.

In preparing these comments, the Department has attempted to (a) provide observations based on its experience and expertise that may assist the LUPC in its review, (b) identify any obvious issues with the proposed project that, if not addressed, would automatically preclude the Department from permitting the project under the Maine Metallic Mineral Mining Act (Mining Act), and (c) note additional information the Department would require before it could accept an application for the proposed project as complete for processing. This Petition review is similar to a Department memorandum dated January 28, 2021, which provided comments on a previously submitted, and subsequently withdrawn, petition revised June 30, 2020. The current Petition presents a notable difference from the prior petition in that no beneficiation structures, processes or activity is proposed for the mine site; the current Petition is for the underground mine and associated aboveground infrastructure only. The Petition makes several acknowledgements that much more detail and information would be provided in any permit application to the Department. Considering that context, the Department is providing proportionately fewer comments with respect to (c) above.

When considering the Department's comments, it is important to understand that the Department conducted a high-level review of the Petition. This is far more limited than the type of review the Department conducts when reviewing permit applications. Recognizing this, there may be important environmental considerations associated with the project, including considerations that could be identified from a closer review of the Petition, that are not reflected in the comments below.

As noted appropriately throughout the Petition, it is also important to recognize that far more information would be required as part of any permit application filed pursuant to the Mining Act and the Department's accompanying rules, 06-096 CMR ch. 200, *Metallic Mineral Exploration, Advanced Exploration and Mining* (Chapter 200). This is inherent in the difference between a zoning petition and a metallic mineral mining permit application. The Department recognizes, however, that the Commission may require some similar information and that there is overlap between the information needed by the Commission to review a zoning petition and by the Department to review a permit application. Therefore, the Department includes references to Chapter 200 and notes some of the information that a permit applicant would be required to provide pursuant to this rule. This may help the Commission when evaluating its own information needs and assessing whether similar information, or a subset of similar information, is necessary as part of the rezoning process or more appropriately deferred to any subsequent permitting process.

Finally, should an application for a mining permit ever be filed with the Department by Wolfden or any other person, the Department would review that application under the governing statute and rules based on the information in that application and the accompanying record materials. Nothing in these comments is intended to prejudge any future application, should one be filed.

A. Clarity and Consistency

The Petition is voluminous and contains several sub-documents with Attachments. The Department suggests efforts be made to improve accessibility for readers, including the public, such as creating tabs to separate exhibits and using a whole-document page numbering system.

The Preliminary Economic Assessment (PEA) contains references to aspects of the prior petition, and while the Introduction in the Petition itself states that the current Petition is for the mine only, it still contains references to a Tailings Management Facility (TMF) and subsurface wastewater disposal options that are not part of the updated proposal. Suggestions include an edited PEA, or a preface to the PEA that identifies which aspects are no longer relevant or are revised for the current proposal.

There is a potential inconsistency pertaining to the applicant's intentions for providing potable water. According to Section 2.5.2, the Applicant apparently does not intend to operate a public water well at this site during the construction phase but will be providing drinking water from an offsite source, although this section of the application refers to "potable water via a drilled well and storage tank…within the footprint of the office complex." However, Section 16.14.2 of the PEA states that a "drilled well will be used to meet all of the potable water demand at the mine." If the Applicant does not intend to operate a public water system at this site, at a minimum, all taps served by on-site water sources would need to be clearly labelled as non-potable water or otherwise marked so that they are not used for drinking water. The applicant should review this proposal with the Drinking Water Program of the Maine Department of Health and Human Services to determine whether this or additional procedures are required for this well to not be considered a public water supply. Also note that, according to Section 17.4 of the PEA, the facility will require 325m^3/day (approximately 86,000 gallons/day) of makeup water, the source

for which is not identified. Again, it is possible that these noted inconsistencies are rooted in parts of the PEA which may or may not be applicable to the current proposal.

A similar potential relic is described in Section 16.14.2 of the PEA, which states that the facility will include a "mine laydown yard…constructed near the portal." This is not clearly labeled on the preliminary site plans received for review. Is this intended to be a portion of the main infrastructure pad (PEA Section 13.3, Figure 18-2)?

The PEA indicates that exploration for exploitable resources is ongoing. If this is still the case, Wolfden should consider the availability of space or need for expansion of at least some proposed development areas if additional areas of the deposit are identified.

Figure 2-7 provides details for wastewater disposal, including an infiltration gallery without identifying that it is for a septic system design for the aboveground infrastructure sanitary wastewater disposal, as noted in the text of Exhibit 24, 'Sewage Water/Wastewater Disposal'. This led more than one DEP staff member to question if a subsurface mine and process water treatment option is also proposed.

B. Chapter 200 Prohibitions

The General Prohibitions section of Chapter 200 states, in relevant part, that:

> The Department may not approve a mining permit in an unorganized or deorganized area of the State unless the Maine Land Use Planning Commission certifies to the Department that:
>
> (1) The proposed mine is an allowed use within the subdistrict or subdistricts in which the project is located; and
> (2) The proposed mine meets any land use standard established by the Maine Land Use Planning Commission applicable to the project that is not considered in the Department's review.

If the LUPC grants rezoning approval and subsequently affirms the above criteria, Wolfden has indicated that it will file an application for a mining permit, subject to the provisions and requirements of Chapter 200. The Department has not identified any proposal within the Petition that is prohibited under Subchapter 1 (1)(B). The listed prohibitions include:

(1) Heap, Percolation or in-situ leaching;
(2) Mining for Thorium or Uranium ore;
(3) Block caving;
(4) Open-pit mining; and
(5) Wet mine waste units and tailings impoundments.

The Department also did not identify any aspects of the currently proposed mine location that would not meet the siting criteria of being greater than ¼-mile from the jurisdictional limits of specific geographical, ecological, or recreational features such as National and state parks, state

or national historical sites, and wildlife refuges or management areas. The complete list of these areas is found in Chapter 200, Subchapter 5 (B)(4). Similarly, the Department has not identified that the proposed mine site is located wholly or partially in, on or under any state land listed in 12 M.R.S §549-B(7)(C-1), as would be prohibited by Chapter 200, Subchapter 5 (B)(5).

C. Ore processing and Waste Rock management

The Petition does not propose Beneficiation or other ore processing on-site, nor does it propose a specific off-site location for such. Any application to the Department for a mining permit under Chapter 200 must include a Mining Operation Plan to include processing of the metallic mineral ore and disposal of associated reactive mine waste. Processing and waste disposal may be proposed for an off-site location(s). If the off-site location(s) is within the state of Maine, the application must provide sufficient evidence that the processing and disposal activities will meet the Chapter 200 standards. Regardless of location, the plan must also include a Transportation Plan, including transport of lean ore, ore concentrate, or metallic product, as well as proposals to prevent leaks, fugitive dust, and contingency in the event of a transportation accident.

Attachment 10-B of the Petition presents limited mine waste characterization (Final Report: Static Acid Rock Drainage (ARD) Testing, April 16, 2021). While the testing did use material from the site, no information is presented showing the location of the samples and the extent to which they are representative of the likely waste rock, lean ore, and other rock materials requiring disposal on the site. An application for a mining permit would require more detailed ARD testing and characterization as part of a Mining Operation Plan.

Chapter 200 Subchapter 1 (1)(B) prohibition 5 states that a mining operation may place into a mine shaft waste rock that is neutralized or otherwise treated to prevent contamination of groundwater or surface water. Wolfden is proposing to backfill waste rock into the mine, with or without cement, as indicated in Section 2.5.3.1.2, 'Production Activities'. However, in the following section, 'Backfilling and Source of Backfill Material', there is not a specific discussion of the criteria that would be used to make a determination regarding whether cement will be necessary for neutralization of some waste rock; only whether the cement is needed for additional structural stability (Note: this section is also identified as Section 2.5.3.1.2 and is likely a typo that should be 2.5.3.1.3) Additional detailed discussion would be needed in any application under Chapter 200 in order to ensure that reactive mine waste would be properly characterized, neutralized and appropriately managed.

This section also indicates that an offsite borrow source will be used. Note that the letter in Attachment 2-C describing this material indicates that the estimate "is contingent on the ability of Sargent to successfully permit and utilize the quarry", suggesting that the proposed site is not a currently licensed quarry. If permitting under 38 M.R.S. Article 8-A is required for this quarry, the applicant and fill contractor should schedule this permitting so that the source would be available for use in a timely manner. For certain quarrying activities, a monitoring program with at least one year of background data may be required for excavation below certain depths, in addition to review and approval of other information.

D. Solid Waste

As presented, the Petition generally addresses solid waste disposal requirements and there are options near the mine site for management of the identified waste. "Organics Storage" is identified on the site plans, but without a specific description. If this is for temporary storage of ground land-clearing debris until being transported off site for the indicated use as erosion control material, that should be clarified.

E. Air Emissions / Licensing

The air quality within the area of the requested rezoning is currently designated as attainment/unclassifiable for all national ambient air quality standards (NAAQS), meaning the existing levels of air contaminants for which NAAQS have been established are below the levels which would trigger air quality concerns.

Exhibit 9.4.1, 'Air and Climate Resources,' addresses air quality almost exclusively with respect to dust control, including from rock crushing operations. Crushers and other heavy equipment may require air emissions licenses, and there may be other aspects of the mining operation that could generate air contaminants. Regulated air pollutants expected to be emitted from such equipment and activities include particulate matter (PM), particulate matter less than 10 microns (PM_{10}), particulate matter less than 2.5 microns ($PM_{2.5}$), sulfur dioxide (SO_2), nitrogen oxides (NO_x), carbon monoxide (CO), volatile organic compounds (VOC), and lead (Pb), as well as hazardous air pollutants (HAP).

Chapter 200, Subchapter 5 (20)(L) Air Quality Standards, requires that mining operations not discharge air contaminants into the ambient air in such a manner as to violate the Maine ambient air quality standards or emissions standards established pursuant to 38 M.R.S §§ 585, 585-B or 585-K. The Petition's exhibit section states, as Policy 1: "Require compliance with all state and federal air quality standards. Require compliance with more stringent standards where necessary to preserve the air quality or unique values of identified sensitive areas, or to improve the air quality of identified nonattainment areas."

Based on the limited information provided by Wolfden to the LUPC, the Department expects that the proposed facility would emit regulated air pollutants at levels requiring Wolfden to apply for and obtain an air emissions license in accordance with *Major and Minor Air Emission License Regulations*, 06-096 C.M.R. ch. 115 (Chapter 115). Chapter 115 provides for different application and licensing procedures depending on whether the proposed facility would be a minor source or a major source of emissions. The Chapter 115 licensing process would require Wolfden to provide additional information to the Department that would allow the Department to determine applicable requirements to control air pollution pursuant to state and federal laws and regulations, including control technology, emission standards and limitations, ambient air quality standard compliance demonstration, monitoring, equipment and operational restrictions, and recordkeeping and reporting.

F. Water Treatment (permitting)

Water resources within the area of the requested rezoning are currently classified as described in 38 M.R.S. § 464, Classification of Maine waters and 38 M.R.S. § 470, Classification of ground water. Standards associated with each of these waterbodies can be found in 38 M.R.S. § 465, Standards for classification of fresh surface waters; 38 M.R.S. § 465-A, Standards for classification of lakes and ponds; and 38 M.R.S. § 465-C, Standards of classification of ground water.

The surface water streams on the project site are classified as Class A waterbodies pursuant to 38 M.R.S. § 464. Maine law 38 M.R.S. § 465 for Class A waterbodies states in relevant part;

C. Except as provided in this paragraph, direct discharges to these waters licensed after January 1, 1986 are permitted only if, in addition to satisfying all the requirements of this article, the discharged effluent will be equal to or better than the existing water quality of the receiving waters. Prior to issuing a discharge license, the department shall require the applicant to objectively demonstrate to the department's satisfaction that the discharge is necessary and that there are no other reasonable alternatives available. Discharges into waters of this classification licensed prior to January 1, 1986 are allowed to continue only until practical alternatives exist.

(1) This paragraph does not apply to a discharge of storm water that is in compliance with state and local requirements.

D. Storm water discharges to Class A waters must be in compliance with state and local requirements.

E. Material may not be deposited on the banks of Class A waters in any manner that makes transfer of pollutants into the waters likely.

In addition to Maine statutes, Maine Department of Environmental Protection rule 06-098 C.M.R 586 establishes criteria for discharges to Class A waterbodies as follows;

1. Scope. Under 38 MRSA section 464 discharges to class A waters must be equal to or better than the receiving water in order to ensure that habitat, aquatic life, and bacteria are as naturally occurs. The following sections define effluent criteria necessary to ensure these requirements are met.

2. Criterion for pH. The pH of the discharged effluent shall not be greater than or less than a 0.2 pH unit difference from that of the seasonal median value of the receiving water upstream of the discharge.

3. Criterion for plant nutrients. Nutrients in the discharged effluent shall not exceed the seasonal median concentration of nutrients in the receiving water, or a value demonstrated by the applicant to be better than the seasonal median and which does not cause the aquatic life to be other than as naturally occurs.

The effluent shall not significantly alter the particle size distribution of the downstream floral community or otherwise alter the natural character of the downstream biotic community.

4. Criterion for temperature. The temperature of the discharged effluent shall not vary by more than 0.5°F from the temperature of the receiving water at the time of discharge.

5. Criterion for dissolved oxygen. In addition to the requirements of 38 MRSA section 465(2)(B) the dissolved oxygen content of the discharged effluent shall not be less than that of the receiving water at the time of discharge.

6. Criteria for other water quality parameters. Except as provided above, the concentration in the discharged effluent of biochemical oxygen demand and all constituents listed in Quality Criteria for Water 1986 (EPA 440/5-86-001) shall not exceed the seasonal median concentration as measured in the receiving water upstream of the discharge or prior to a discharge where a suitable upstream site is not available.

7. Establishment of seasonal values. For the purpose of establishing seasonal values in the receiving water pursuant to Sections 2, 3, and 6 of this rule, an applicant will provide data based on seasons and sample frequencies approved by the Department on a case-by-case basis.

The applicant has indicated the shallow ground water and surrounding wetlands will be recharged by way of treated wastewater being disposed of on-site via spray irrigation and snowmaking activities covering 15-29 acres. The Department has taken a long-standing position that wetlands that are hydraulically connected to a surface waterbody take on the same classification as the surface waterbody. For this project, any discharge to a wetland must meet the Class A criteria cited above. Given that streams are expression of ground water, the characteristics of the Class A surface waterbodies must not be adversely impacted by changes in the characteristics of the ground water as a result of the disposal of treated wastewater via spray irrigation or snowmaking. And lastly, as previously stated in the Department of Environmental Protection's January 28, 2021, memorandum to the Land Use Planning Commission, effluent discharged to wetlands or groundwater that reaches surface waters must be characterized as natural and may not alter the flow or the habitat of the surface waters. See 38 M.R.S. §§ 465(1 & 2), 465-A.

The Department notes that depending on final design, the proposed facility may be subject to the requirements of the Department's Multi-Sector General Permit (MSGP) for Stormwater Discharge Associated with Industrial Activity and the requirements of the Environmental Protection Agency's Ore Mining and Dressing Effluent Guidelines and Standards (40 CFR Part 440).

G. Water Treatment (proposal and site considerations)

Detailed soils mapping of application areas at a Class A level will be necessary to define application rates for any spray application or snowmaking area. Note that the soils analysis reports oxyaquic soils in many areas of the site (Soil Suitability Evaluation page 3-8, for example) proposed for wastewater application; the higher water table in these soils, often not

associated with redoximorphic features in many cases, will need to be determined and used to define areas that can meet the necessary minimum depth to the seasonal high water table for spray application. In particular, high seasonal water tables during periods of extended snowmelt can lead to saturation of large areas of soil, with potential impacts on soil and vegetation characteristics, slope stability, and downgradient potential for seepage erosion. The Petition presents information regarding mine water treatment using the water chemistry obtained from a mine in generally similar deposits in New Brunswick (Water Treatment Scoping Study, Attachment 10-D). However, no information is presented demonstrating chemical similarity between this water and potential mine water at this site. It is expected that these waters would be generally similar, and the proposed treatment methods are known to be effective in general in systems designed, operated, and maintained correctly, but final approval by the Department will require analysis of waters from the site and generated from leaching tests and other means more accurately simulating conditions that could obtain at the site of the proposed development. It is also not explicitly stated whether the treatment goals (Water Treatment Scoping Study, Table 1) reflect ambient water quality, aquatic life criteria, or other factors relevant to specific conditions at the proposed mine site. Final approval of a wastewater treatment system will require more explicit evaluation of possible water inflow to the mine than is presented in this application (see for example Preliminary Economic Assessment Section 16.6.5, which does not include or reference a source for the values used), possible revision of the pre-and post-development runoff values and description of the volume available for contingency storage due to mechanical failures or other issues in the treatment system (Note that contingency sizing of the plant, rather than of water storage requirements, is discussed on p. 21 ff. of the Water Treatment Scoping Study).

H. Surface Water and Aquatic Life Protection

Chapter 200, Subchapter 3, Permits, Section 9(C) requires submission of a Baseline Site Characterization Report, which, among other things, must include documentation of aquatic and terrestrial flora and fauna species presence, distribution, and abundance, including the existence of endangered and threatened species and significant wildlife habitats. It must also contain a water balance of the affected area including, but not limited to, consideration of precipitation, evapotranspiration, infiltration, runoff, surface and groundwater flow, hydraulic gradients, velocity, flowpaths, elevations, and groundwater/surface water interactions. The report must contain an ambient water quality monitoring plan and monitoring results that provide baseline water quality information for any surface or groundwater that potentially may be impacted as a result of the mining activity. The baseline water quality monitoring shall include at least two (2) years of data collected over 24 or more consecutive months unless pre-existing data are approved for use by the Department. For this proposed project, potential impacts of concern to aquatic resources include erosion/sedimentation, nutrient enrichment, contamination of surface and groundwater from roads (e.g., road salt, petroleum, etc.,), stormwater and mine water, and impacts to vegetative communities caused by spray irrigation (water level changes, conversion of community type, introduction of invasive species, erosion/gullying).

The following comments are specific to Attachment 6A, Wetland and Watercourse Delineation and Potential Vernal Pool Survey Report, July 28, 2022:

Section 4.1. State and Federal Regulations: Under the Water Classification Program, all waters of the State are assigned a statutory water quality class by the Maine Legislature with associated management goals (designated uses) and water quality criteria, including criteria for aquatic habitat and aquatic life (biological criteria). Riverine waters and associated freshwater wetlands are assigned to Class AA, A, B, or C. There is a single classification for lakes and ponds (Class GPA).

Streams and freshwater wetlands in the vicinity of the project area are assigned statutory Class A (see §465-2 under Standards for classification of fresh surface waters: http://www.mainelegislature.org/legis/statutes/38/title38sec465-A.html). In addition, Chapter 579 Classification Attainment Evaluation Using Biological Criteria for Rivers and Streams (https://www.maine.gov/dep/water/rules/index.html) includes assessment methods based on aquatic macroinvertebrate communities to determine if rivers and streams attain numeric biological criteria for their assigned statutory class. Standards for classification of lakes and ponds are found in §465-A: http://www.mainelegislature.org/legis/statutes/38/title38sec465-A.html.

Section 6.1.1. Water Features: It is not clear from this section which waterbodies are in the project area as well as which are within a 3-mile radius. More details would be needed to fully evaluate potential impacts to aquatic resources.

Figure 1. Delineated Wetlands and Streams Map does not show connectivity with waterbodies outside the project area. This is pertinent information that is needed to evaluate potential adverse impacts to downstream waters. A comprehensive map depicting aquatic resources within the project area and 3-mile radius (required under LUPC guidance), including streams, lakes, and ponds (labeled with waterbody names if available), and wetlands (labeled with NWI classification) should be provided in any application for a mining permit.

Section 6.1.3 Wetlands: The Department was unable to locate a summary of acreages for various mapped wetland types. Is this information available?

The following comments are specific to Exhibit 10.0. Surrounding Uses and Anticipated Impacts:

Section 10.5.4. Wetlands/Streams/Waterbodies: Although lakes and ponds in the project area and 3-mile radius are listed, no details are provided regarding streams in the project area or within a 3-mile radius.

Section 10.5.2. Hydrology and Water Quality: It would be helpful to see discussion of the potential for unanticipated groundwater flow direction and depth and factors that may increase risks of contamination to aquatic resources.

Section 10.5.2.1. Water Treatment and Management Approach: Stormwater and mine water are proposed to be collected and stored in a lined 3.25-acre pond, then fed to an on-site wastewater treatment facility and tested before discharging via spray irrigation and snowmaking. Discharges would be upgradient of wetlands and streams so that existing hydrology is maintained, and at

least 75 feet from the edge of the waterbody. An estimated 15-29 acres of land would be needed for recharge of treated water. Given the large extent of the area to be used for wastewater storage and discharge of treated water, are there contingency plans for accidental release of untreated or partially treated water due to unanticipated circumstances such as system failure or extreme weather events?

I. Stormwater Management

Chapter 200, Subchapter 5 (20)(C)(2) requires that stormwater management practices meet the standards of 06-096 C.M.R. ch. 500. While significantly more information would be needed for a complete review, the Department generally finds that the concept plan and preliminary calculations presented in the Petition can be reviewed under Chapter 500 and could meet the applicable standards.

J. Fuel Storage and Spill Prevention

The Petition identifies several above-ground and below-ground fuel and oil storage locations, including diesel storage, a fuel station, a maintenance facility, emergency power, an electrical substation, various transformer pads, and possibly facilities associated with the proposed solar array (see Section 2.3). A complete Spill Prevention Control and Countermeasures program, together with all elements of Groundwater Protection Plan (see Site Location Application Section 15(B)), would be required as part of the application for the mine; this would require significantly more detail than indicated in Section 18.9 of the Preliminary Economic Assessment.

K. Soils

The applicant has presented a Class D-level soils map for the facility, with field verification and additional analysis of site suitability prepared by a Maine Certified Soil Scientist. This information is consistent with the surficial geology and observations at the site, but additional information would be required for the Department to process any mining permit application. Although the Site Location of Development Law (M.R.S. 38 §§481-489-E) does not apply to the proposed development, developments such as that proposed for this site would be expected to meet comparable criteria for soils mapping levels and other relevant aspect of the development as those described in Section 11(B) of the Site Location of Development application, including Class A soil mapping in areas proposed for wastewater disposal. Where more detailed soils mapping exists or is performed for the application, the more detailed mapping should be used in preference to the Class D mapping for the purposes of evaluating predevelopment runoff conditions and other relevant information for the application; this could require substantial revision of, for example, Figure 10-1 and any predevelopment runoff calculations based on that figure and/or level of soils mapping, depending on the areas used for wastewater management or other purposes that would require more detailed soils mapping.

L. Closure / Reclamation

Section 2.5.4 of the Petition states that reclamation activities will be based on a reclamation plan that will be submitted as part of an application to the Department under Chapter 200.

Reclamation plans are required as part of the Mining Operation Plan and Reclamation standards are found in Chapter 200, Subchapter 5 (23).

Section 18.22.7 of the Preliminary Economic Assessment describes possible breaching of collection ponds as part of reclamation, as does Section 2.5.4 of the Petition itself. The permitting process under Chapter 200 could, however, identify stormwater management features that must be retained and maintained on the site as part of the long-term post-development hydrology management of the site, and it is premature to consider regrading of all such features at this time.

ATTACHMENT 5

RESPONDENT
EXHIBIT NO. 151

Appendix G

WWTP Influent and Effluent Calculations

Appendix G-1

Calculations

Foth & Van Dyke

Client: Kennecott Minerals Company Scope ID.: 04W018
Project: Eagle Project
Prepared by: JJF1 Date: 12/06/05
Checked by: HJA Date: 12/08/05

Wastewater Treatment Plant Water Quality Estimates

	04EA-054A[1] (µg/L)	04EA-054B[1] (µg/L)	04EA-054D[1] (µg/L)	04EA-054E[1] (µg/L)	18-34 m 05EA-107[2] (µg/L)	97-114 m 05EA-107[2] (µg/L)	Upper Bedrock Leakage Composite[3] (µg/L)	86 purges 249 - 302 m 04EA-084[2] (µg/L)	Lower Bedrock Leakage[4] (µg/L)	Total Leakage Composite[5] (µg/L)	Incremental Change[6] (µg/L)	Composite Mine Drainage[7] (µg/L)	TDRSA Contact Runoff[8] (µg/L)	WWTP Influent Wastewater[9] (µg/L)	Lime Clarifier Effluent[10] (µg/L)	RO Effluent[11] (µg/L)	Evaporator Distillate[12] ug/L	Effluent ug/L	Part 22 Std (µg/L)	Effluent % of Part 22 (%)
Aluminum	100	100	100	100	50	50	**83**	50	**50**	**68**	88	156	1.0	140	140	2	0.07	1.85	150	1%
Antimony	5	5	5	5	5	5	**5.0**	5	**5**	**5.0**	16	21	0.4	19	19	1.00	0.12	0.97	3	33%
Arsenic	2	2	2	2	2	2	**2.0**	19	**19**	**10**	17.0	27	83	33	33	1.70	0.21	1.66	25	7%
Barium	27	60	20	20	20	20	**28**	20	**20**	**24**	4.0	28	30	28	28	1.40	0.19	1.37	1,000	0%
Beryllium	1.0	1.0	1.0	1.0	1.0	1.0	**1.0**	1.0	**1.0**	**1.0**		1.0		1.0	1	0.05	0.01	0.05	2	3%
Boron	1,340	1,370	2,720	3,910	940	4,100	**2,397**	5,900	**5,900**	**3,973**	70	4,043	580	3,671	3,671	178	23.97	173.60	250	**71%**
Cadmium	0.5	0.5	0.5	0.5	0.5	0.5	**0.5**	5.0	**5.0**	**2.5**	10.0	13	0.2	11	11	0.60	0.07	0.58	2.5	24%
Calcium	8,900	34,000	25,000	19,000	5,900.0	3,100.0	**15,983**	76,000	**76,000**	**42,991**	4,000	46,991	199,000	63,345	***14,000***	26	9.68	25.53	n.a.	
Chloride	18,000	26,000	64,000	42,000	1,200	97,000	**41,367**	2,000,000.0	**2,000,000**	**922,752**	1,580	924,332	10,000	825,963	825,963	45,239	5,360.61	44,099.62	250,000	18%
Chromium	5	5	5	5	5	5	**5.0**	5	**5.0**	**5.0**	4.5	10	0.45	8.5	9	0.50	0.06	0.49	50	1%
Cobalt	10	10	10	10	10	10	**10.0**	10	**10.0**	**10**	720	730	0.80	652	***500***	9	4.41	9.26	20	**47%**
Copper	5	5	5	5	5	5	**5.0**	5	**5.0**	**5.0**	150	155	60	145	145	7.40	0.94	7.22	500	1%
Fluoride	170	190	140	120	530	850	**333**	1,000	**1,000**	**633**	98	731	500	706	706	42	4.56	40.93	1,000	4%
Iron	22	20	130	61	88	79	**67**	1,800	**1,800**	**847**	6,400	7,247	2.0	6,467	***1,000***	3	0.07	3.21	300	1%
Lead	1.0	1.0	1.0	1.0	1.0	1.0	**1.0**	1.0	**1.0**	**1.0**	9.0	10	0.40	9.0	9	0.50	0.06	0.49	2	25%
Lithium	10	14	23	14	13	16	**15**	130	**130**	**67**	26	93	19	85	85	4.30	0.55	4.19	85	5%
Magnesium	3,600	2,500	4,100	3,800	2,400	980	**2,897**	61,000	**61,000**	**29,043**	5,000	34,043	18,000	32,317	***8,000***	17	5.53	16.67	200,000	0%
Manganese	20	20	20	20	22	20	**20**	68	**68**	**42**	950	992		992	***500***	***2.50***	0.07	2.43	50	5%
Mercury	0.000653	0.000428	0.000651	0.00495	0.00081	0.00351	**0.00183**	0.00021	**0.00021**	**0.00110**	0.04000	0.04110	0.04000	0.0410	0.0410	0.00210	0.00027	0.00205	***1.0***	**0%**
Molybdenum	10	10	11	10	10	10	**10**	10	**10**	**10**	13	23	1.5	21	21	1.10	0.13	1.07	18.5	6%
Nickel	25	29	25	25	25	25	**26**	25	**25**	**25**	36,400	36,425	8,330	33,403	***2,000***	5.00	0.07	4.86	50	10%
Nitrogen, Ammonia					76	93	**85**	260	**260**	**163**	10,000	10,163		10,163	10,163	2,367	1,000.00	2,327.94	***5,000***	47%
Nitrogen, Nitrate					50	50	**50**	50	**50**	**50**		50		50	50	31	0.13	30.12	***5,000***	1%
Phosphorus, total					10	33	**22**	15	**15**	**18**		18		18.5	18	0.80	0.12	0.78	1,000	0%
Potassium	2,000	8,100	7,100	4,300	2,900	1,700	**4,350**	9,200	**9,200**	**6,533**	1,000	7,533	29,000	9,842	9,842	1,241	59.03	1,207.23	n.a.	
Selenium	1.0	1.0	1.1	1.0	1.0	1.0	**1.0**	17.0	**17**	**8.2**	20.0	28	4.0	26	26	1.30	0.17	1.27	25	5%
Silver	0.2	0.2	0.2	0.2	0.2	0.2	**0.2**	0.5	**0.5**	**0.3**	4.5	4.8	0.05	4.3	4.3	0.20	0.03	0.20	17	1%
Sodium	24,000	27,000	41,000	40,000	21,000	80,000	**38,833**	970,000	**970,000**	**457,858**	1,000	458,858	19,000	411,536	411,536	30,804	3,380.57	30,020.47	120,000	26%
Strontium					170	91	**131**	4,800	**4,800**	**2,232**	20	2,252	200	2,031	2,031	97	13.27	94.61	2,300	4%
Sulfate	5,600	6,300	28,000	12,000	5,000	5,000	**10,317**	5,000	**5,000**	**7,924**	110,000	117,924	575,000	167,099	167,099	1,700	1,135.15	1,683.86	250,000	1%
Thallium							~		~	-	8.0	8.0	0.05	7.1	7	0.40	0.05	0.39	1	40%
Vanadium							~		~	-	7.0	7.0	0.75	6.3	6	0.30	0.04	0.29	2	14%
Zinc	10	10	11	12	10	12	**11**	19	**19**	**15**	150	165	1,900	351	351	18.00	0.07	17.49	1,200	2%

Flows:

Percentage of leakage from upper bedrock:	55%
Percentage of leakage from lower bedrock (brackish):	45%
Mine Drainage Flow (gpm)	180
TDRSA Flow (gpm)	21.7

Notes:

[1] Data from holes 04EA-054A, -054B, -054D, and -054E from Table 6.2 Golder Associates, Eagle Project Bedrock Hydrogeologic Investigation, 2005.

[2] Data from holes 05EA-107 and 04EA-084 from Appendix F-1.

[3] The upper bedrock leakage composite is the average of holes 04EA-054A, 04EA-054B, 04EA-054D, 04EA-054E, 05EA-107 (60 ft - 115 ft) and 05EA-107 (320 ft - 375 ft).

[4] The lower bedrock leakage is from hole 04EA-084, 817-991 ft.

[5] The total leakage composite is estimated as 55% from the upper bedrock leakage and 45% from the lower bedrock leakage.

[6] The incremental change is the incremental water quality for underground mine during operations due to rock wall leachings. Data from Table 2, Geochimica Technical Memorandum titled Water Quality in Underground Mine During Operational Conditions. , November 7, 2005. (Appendix F-2) The incremental change for nitrogen (ammonia) is the estimated increase in ammonia due to blasting residuals.

[7] The composite mine drainage is the sum of the total leakage composite and the incremental change.

[8] The TDRSA contact runoff is the water quality for the development Rock stockpile with limestone addition. Data from Table 3, Geochimica Technical Memorandum titled Water Quality from the Development Rock Storage Pad During Operations, November 7, 2005. (Appendix F-2)

[9] The WWTP influent wastewater is the water quality of the of the combined 180 gpm mine drainage water and the 21.7 gpm TDRSA runoff water.

[10] Estimated concentration following metals precipitation process. Treatment reductions are estimated for cobalt, nickel and manganese. Additional treatment will occur for other metals including calcium and magnesium. The lime treatment reduction for these other metals were conservatively not estimated.

[11] Estimated concentration of the combined second stage RO permeate and the concentrate reduction process RO permeate.

[12] Estimated concentration in the evaporator distillate based on 10 ppm estimated total dissolved solids carryover in the evaporator. The 10 ppm is proportioned using the mass flow for each parameter feeding the evaporator.

ATTACHMENT 6

minerals

MDPI

Article

Minor and Trace Elements in Natural Tetrahedrite-Tennantite: Effects on Element Partitioning among Base Metal Sulphides

Luke L. George [1,*], Nigel J. Cook [2] and Cristiana L. Ciobanu [2]

[1] School of Physical Sciences, The University of Adelaide, Adelaide, SA 5005, Australia
[2] School of Chemical Engineering, The University of Adelaide, Adelaide, SA 5005, Australia; nigel.cook@adelaide.edu.au (N.J.C.); cristiana.ciobanu@adelaide.edu.au (C.L.C.)
* Correspondence: luke.george@adelaide.edu.au; Tel.: +61-4-3510-1187

Academic Editor: Antonio Simonetti
Received: 21 December 2016; Accepted: 23 January 2017; Published: 29 January 2017

Abstract: Minerals of the tetrahedrite isotypic series are widespread components of base metal ores, where they co-exist with common base metal sulphides (BMS) such as sphalerite, galena, and chalcopyrite. We used electron probe microanalysis and laser-ablation inductively-coupled plasma mass spectrometry to obtain quantitative multi-trace element data on tetrahedrite-tennantite in a suite of 37 samples from different deposits with the objective of understanding which trace elements can be incorporated, at what levels of concentration, and how the presence of tetrahedrite-tennantite influences patterns of trace element partitioning in base metal ores. Apart from Fe and Zn, Hg and Pb are the two most abundant divalent cations present in the analysed tetrahedrite-tennantite (up to 10.6 wt % Hg and 4 wt % Pb). Cadmium, Co and Mn are also often present at concentrations exceeding 1000 ppm. Apart from one particularly Te-rich tetrahedrite, most contained very little Te (around 1 ppm), irrespective of prevailing assemblage. Bismuth is a common minor component of tetrahedrite-tennantite (commonly > 1000 ppm). Tetrahedrite-tennantite typically hosts between 0.1 and 1000 ppm Se, while Sn concentrations are typically between 0.01 and 100 ppm. Concentrations of Ni, Ga, Mo, In, Au, and Tl are rarely, if ever, greater than 10 ppm in tetrahedrite-tennantite and measured W concentrations are consistently <1 ppm. Taking into account the trace element concentrations in co-crystallizing BMS, the results presented allow the partitioning trends between co-crystallized sphalerite, galena, chalcopyrite, and tetrahedrite-tennantite to be defined. In co-crystallizing BMS assemblages, tetrahedrite-tennantite will always be the primary host of Ag, Fe, Cu, Zn, As, and Sb, and will be the secondary host of Cd, Hg, and Bi. In contrast, tetrahedrite-tennantite is a poor host for the critical metals Ga, In, and Sn, all of which prefer to partition to co-crystallizing BMS. This study shows that tetrahedrite-tennantite is a significant carrier of a range of trace elements at concentrations measurable using contemporary instrumentation. This should be recognized when establishing protocols for trace element analysis of tetrahedrite-tennantite, and when assessing the main hosts of trace elements in any given assemblage, e.g., for geometallurgical purposes.

Keywords: tetrahedrite-tennantite; trace elements; laser-ablation inductively-coupled plasma mass spectrometry; element partitioning

1. Introduction

The tetrahedrite isotypic series [1–4] can be expressed by the general formula $A_6(B,C)_6X_4Y_{12}Z$, where A = Cu or Ag in triangular coordination, B = Cu or Ag in tetrahedral coordination, C = Fe or Zn, or more rarely Pb, Hg, Cd or Mn also in tetrahedral coordination, X = Sb, As, or more rarely Bi or Te in

trigonal pyramidal coordination, *Y* = S or Se in tetrahedral coordination, and *Z* is S or Se in a special octahedral coordination [4], i.e., $(Cu,Ag)_6(Cu,Ag,Fe,Zn,Pb, etc.)_6(Sb,As,Bi,Te)_4(S,Se)_{13}$. Any excess of Cu above 10 atoms per formula unit (*apfu*) ("Cu-excess tetrahedrite-tennantite"; e.g., [5,6]) is taken to indicate the presence of Cu^{2+} [7]. Divalent metals are limited to 2 *apfu* in the tetrahedrite-tennantite structure [4].

The tetrahedrite isotypic series currently comprises eight named minerals: tetrahedrite ($Cu_6[Cu_4(Fe,Zn)_2]Sb_4S_{13}$), tennantite ($Cu_6[Cu_4(Fe,Zn)_2]As_4S_{13}$), freibergite ($Ag_6[Cu_4Fe_2]Sb_4S_{13-x}$), hakite ($Cu_6[Cu_4Hg_2]Sb_4Se_{13}$), giraudite ($Cu_6[Cu_4(Fe,Zn)_2]As_4Se_{13}$), goldfieldite ($Cu_{10}Te_4S_{13}$), argentotennantite ($Ag_6[Cu_4(Fe,Zn)_2]As_4S_{13}$), and argentotetrahedrite ($Ag_{10}(Fe,Zn)_2Sb_4S_{13}$; Table 1). The series is notable among sulphides for extensive fields of solid solution and broad ranges of metals that can be incorporated within the structure (e.g., [8–10]). This diversity is borne out by the range of minor and trace elements measured in natural specimens. Perhaps most noteworthy, the tetrahedrite isotypic series is an important concentrator of silver, and may also be the main host for antimony and arsenic in many ore deposits. Research interest in tetrahedrite-tennantite has also been generated by the observation of compositional variations across an orefield that may be tied to ore-forming processes (e.g., [11–14]), and which offer insights into ore genesis as well as potential as exploration vectors in, for example, porphyry-epithermal environments.

Table 1. Named minerals in the tetrahedrite isotypic series.

Mineral	Ideal Formula	References
Tetrahedrite	$Cu_6[Cu_4(Fe,Zn)_2]Sb_4S_{13}$	[1,3,15,16]
Tennantite	$Cu_6[Cu_4(Fe,Zn)_2]As_4S_{13}$	[2,7]
Freibergite	$Ag_6[Cu_4Fe_2]Sb_4S_{13-x}$	[15,17]
Hakite	$Cu_6[Cu_4Hg_2]Sb_4Se_{13}$	[18]
Giraudite	$Cu_6[Cu_4(Fe,Zn)_2]As_4Se_{13}$	[19]
Goldfieldite	$Cu_{10}Te_4S_{13}$	[20–22]
Argentotennantite	$Ag_6[Cu_4(Fe,Zn)_2]As_4S_{13}$	[23]
Argentotetrahedrite *	$Ag_{10}(Fe,Zn)_2Sb_4S_{13}$	[24]

* Argentotetrahedrite differs from freibergite in that Ag is contained within both the A and B sites as opposed to the A site only. This endmember has only been described on the basis of electron probe microanalysis (EPMA) data. A proper definition through the IMA Commission on New Minerals, Nomenclature and Classification (CNMNC) based on X-ray powder or reflectance data is required.

The tetrahedrite isotypic series is also, undeniably, one of the most thoroughly studied among the sulphides, notably in a series of articles [10,25–29] that have explored, through experiment, how minor elements are incorporated into the tetrahedrite-tennantite (fahlore) structure.

The present contribution seeks to build on these extensive foundations, using electron probe microanalysis (EPMA) and laser-ablation inductively-coupled plasma mass spectrometry (LA-ICP-MS) on a suite of 37 samples from different locations, to address two interdependent goals. Firstly, we seek to understand the range of minor and trace elements which can be incorporated into natural tetrahedrite-tennantite, including those seldom reported in the literature for either natural or synthetic specimens. Secondly, we investigate how the preferred trace element partitioning trends among the common base metal sulphides (BMS) sphalerite, galena, and chalcopyrite outlined in George et al. (2016) [30], are modified if tetrahedrite-tennantite is present in a mineral assemblage and co-crystallizes with BMS.

2. Background

2.1. Crystal Structure

Members of the tetrahedrite isotypic series are classified as sulfosalts; a group of sulphides containing As^{3+}, Sb^{3+}, Bi^{3+} or Te^{4+}, where one or more of these metalloid cations is associated with one or more metallic cations [4]. The metalloids are not bonded to the metals; both exclusively bond to

the anion S^{2-} (or more rarely Se^{2-} or Te^{2-}). They are thus distinct from sulphide minerals such as arsenopyrite (FeAsS), löllingite ($FeAs_2$), gudmundite (FeSbS) or enargite/luzonite (Cu_3AsS_4) where trivalent metalloids bond directly to Fe or Cu.

Moëlo et al. (2008) [4] classify the tetrahedrite isotypic series as sulfosalts with an excess of small (univalent) cations (Ag,Cu) relative to (As,Sb,Bi), and further sub-group them as Cu(Ag)-rich sulfosalts. The tetrahedrite isotypic series is the most complex isostructural series among sulfosalts due to the extensive iso- and heterovalent substitutions that are possible.

In Cu pure tetrahedrite (i.e., $Cu_{12}Sb_4S_{13}$), the structure is most simply understood as linked polyhedra of metal atoms about sulphur atoms [1]. The S^{2-} anion is bonded to six Cu^{2+} cations in octahedral coordination, while each S^{-} anion is coordinated tetrahedrally to two Cu^{+} cations, one Cu^{2+} cation and one Sb^{3+} cation. The angles between bonds in the tetrahedron are significantly distorted from the ideal 109.28°. Each tetrahedron shares a corner with the octahedron, while the remaining three corners of each tetrahedron share corners with two adjacent tetrahedrons (Figure 1). Antimony cations are positioned at the tetrahedron corners closest to the octahedron. The crystal structure of tennantite is analogous to that of tetrahedrite (with As substituted for Sb), although the degree of tetrahedron distortion is generally less in tennantite [2].

Additional investigations on how the tetrahedrite-tennantite structure is changed through incorporation of major elements such as Ag, Fe, Zn or Hg have been carried out (e.g., [31–34]), as has research into the possible oxidation and coordination states of such elements (e.g., [35–37]).

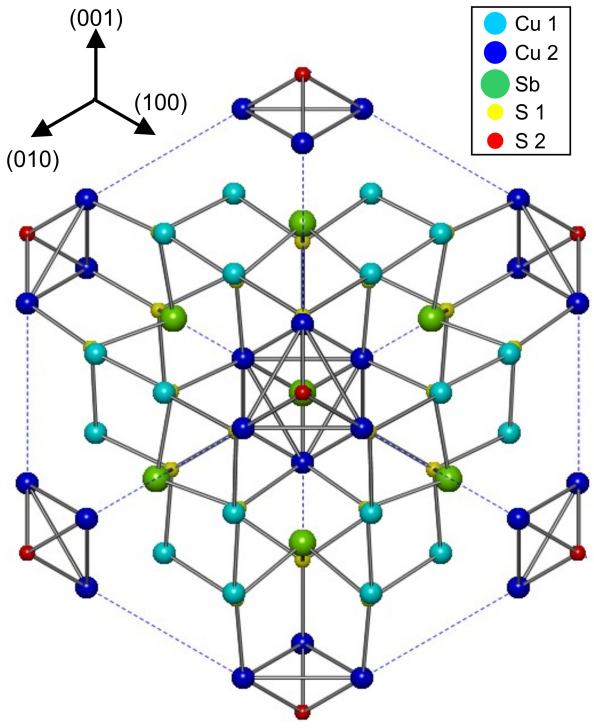

Figure 1. Crystal structure of tetrahedrite drawn from .cif file in American Mineralogist Crystal Structure Database after data in [31].

2.2. Documented Substitutions

Major metal/metalloid components of the tetrahedrite-tennantite series are copper, iron, zinc, antimony, and arsenic. Silver readily enters the tetrahedrite-tennantite structure, with argentotetrahedrite and argentotennantite the Ag end-member analogues of tetrahedrite and tennantite, respectively.

Bismuthian tetrahedrite or tennantite (the latter referred to as "*annivite*") are known from a number of localities (e.g., [38–42]), with Bi substituting into the (Sb,As) site. Staude et al. (2010) [13] document

granite-hosted tetrahedrite-tennantite containing up to 22.17 wt % (1.83 *apfu*) Bi from the Schwarzwald ore district, SW Germany. Gołębiowska et al. (2012) [43] report tetrahedrite containing up to 15.86 wt % (1.36 *apfu*) Bi and tennantite containing up to 18.41 wt % (1.51 *apfu*) Bi from Rędziny, Lower Silesia, Poland. At Rędziny, Bi-poor tennantite is generally interpreted as crystallizing at lower temperatures, with the most Bi-rich varieties crystallizing between 230 and 300 °C. Bismuth incorporation in tetrahedrite-tennantite has been studied experimentally [29], with concentrations of up to 1 *apfu* attained irrespective of the Sb/As ratio, consistent with observations in natural specimens [43].

Plumbian tetrahedrite-tennantite is also commonly reported in the literature (e.g., [44–47]). Vavelidis and Melfos (1997) [48] document 1.55 wt % Pb in tennantite, and up to 12.31 wt % Pb in tetrahedrite from the Maronia area of Thrace, Greece, and advocate that Pb^{2+} is incorporated in the (Fe,Zn) site. As much as 4.64 and 5.5 wt % Pb was measured in tennantite from Sark, Channel Islands, by Bishop et al. (1977) [49] and Ixer and Stanley (1983) [50], respectively.

Mercury is frequently reported in tetrahedrite-tennantite, where it substitutes for (Fe,Zn). Mercurian giraudite and hakite containing as much as 15.32 wt % and 14.98 wt %, respectively, are documented by Förster et al. (2002) [51] from the Niederschlema-Alberoda uranium deposit, Erzgebirge, Germany. Compositions almost span the entire solid solution range between the two minerals. They infer complete miscibility between mercurian giraudite and hakite in nature, analogous to tetrahedrite and tennantite. Jurković et al. (2011a) [52] report mercurian tetrahedrite from the Duboki Vagan barite deposit, south of Kreševo, Bosnia, containing up to 3.795 wt % Hg.

Both Mn [47,53] and Cd [54] are occasionally reported as minor elements in tetrahedrite-tennantite, substituting for (Fe,Zn). Pattrick (1978; 1985) [55,56], Huiwen and Chunpei (1988) [57] and Voudouris et al. (2011) [58] each report tetrahedrite-tennantite with Cd concentrations reaching up to ~12 wt %, representing approximately 2 *apfu* Cd. Dobbe (1992) [59] reports an unusual manganoan-cadmian tetrahedrite from Tunaberg, Bergslagen, Sweden, containing up to 2.4 wt % Mn and 5 wt % Cd.

Tellurian tetrahedrite has been widely described (e.g., [6,22] and references therein). A complete solid solution exists between tetrahedrite and the telluride-bearing end-member goldfieldite [60]. Tellurium occupies the (Sb,As) site and is incorporated through the coupled substitution $(Cu,Fe,Zn)^{2+} + (As,Sb)^{3+} = Cu^{+} + Te^{4+}$ [20,61,62]. Shimizu and Stanley (1991) [63] report tetrahedrite from the Iriki mine, Japan, with compositions varying from Te-free tetrahedrite to goldfieldite containing up to 18.5 wt % Te. Similarly, Knittel (1989) [62] measure up to 17.68 wt % Te in arsenian goldfieldite from the Marian gold mine, northern Luzon, Philippines.

Hakite and giraudite are the Se-dominant analogues of tetrahedrite and tennantite, respectively. Förster et al. (2002) [51] measure up to 39.98 wt % Se (10.86 *apfu*) and 37.55 wt % Se (11.1 *apfu*) in mercurian giraudite and hakite, respectively, from the Niederschlema-Alberoda uranium deposit, Erzgebirge, Germany. Selenium-bearing goldfieldite is reported by Pohl et al. (1996) [64] suggesting extensive solid solution among the less-common members of the tetahedrite group.

Indium-bearing tetrahedrite-tennantite is occasionally recorded (e.g., [65–68]). Gaspar (2002) [69] document up to 2.7 and 0.2 wt %. In tennantite and tetrahedrite, respectively, from Neves-Corvo, Portugal.

Tin, Co and Ni have been measured in tetrahedrite-tennantite up to a few thousand ppm. Gaspar (2002) [69] report tetrahedrite and tennantite from Neves-Corvo, Portugal, carrying up to 4784 and 1300 ppm Sn, respectively. Tetrahedrite from the same deposit contains up to 4300 ppm Co. Serranti et al. (2002) [66] also measure 4784 ppm Sn in tetrahedrite from the Corvo orebody, Portugal, as well as up to 1369 ppm Ni in tennantite. Up to 3800 ppm Co was measured in tetrahedrite-tennantite in a fluorite vein from Oberwolfach, Clara, SW Germany, and up to 6900 ppm Ni was measured from nearby Urberg, Gottesehre [13].

Gold is occasionally present in tetrahedrite-tennantite, usually only at a few ppm at most. Knittel (1989) [62], however, measured up to 0.02 wt % Au in tellurian tennantite from the Marian gold mine, northern Luzon, Philippines, while Jurković et al. (2011b) [70] record up to 39 ppm Au in mercurian tetrahedrite from the Duboki Vagan deposit, Bosnia. Wohlgemuth-Ueberwasser et al. (2015) [71] also measured up to 19.4 ppm Au in tetrahedrite-tennantite from black smokers in the Manus Basin,

Papua New Guinea, and infer that tetrahedrite-tennantite may control Au distributions in a sulphide assemblage. Unique tetrahedrite from Saski Rad, Bosnia, has also been documented containing 92 ppm Tl, 20 ppm W, 7.3 ppm Mo, and 0.5 ppm Ga, elements that are rarely if ever reported as a trace component in tetrahedrite-tennantite [70].

3. Approach and Methodology

The published data above show that alongside the essential constituents Cu, Fe, Zn, Sb, As, and S, the tetrahedrite isotypic series may incorporate up to wt % levels of Ag, Mn, Cd, Bi, Pb, In, Hg, Se, and Te, thousands of ppm Ni, Co, and Sn, at least ppm-level concentrations of Au, Tl, W, and Mo, and possibly also Ga. We have sought to analyse the concentrations of these 23 elements in a suite of 37 samples (Table 2). Sample material mostly derives from collections of the South Australian Museum and the Tate Museum (The University of Adelaide; as indicated in Table 2), while some material originates from the author's personal collections. Although some samples comprise solely tetrahedrite-tennantite (i.e., without other sulphides present), most were selected because they consist of tetrahedrite-tennantite co-existing with other base metal sulphides. Textural evidence suggests that these assemblages co-crystallized at equilibrium (~120° triple-junctions between sulphides; see Figure 2). The trace element partitioning rules for BMS outlined in George et al. (2016) [30] were employed as an additional check for assessing BMS co-crystallization. Thus through trace element analysis of the sulphides in each co-crystallized assemblage, the preferred partitioning of trace elements can be determined for a BMS assemblage comprising tetrahedrite-tennantite.

Quantitative analysis on tetrahedrite-tennantite was carried out using a Cameca SX-Five EPMA (Cameca, Gennevilliers, France), which utilizes five wavelength dispersive spectrometers (WDS). The elements analysed were S, Pb, Cd, As, Se, Fe, Cu, Mn, Ag, Sn In, Hg, Zn, Ni, Co, Sb, Te, Bi, Tl, and Ga. Beam operating conditions were maintained at 20 kV and 20 A with a beam size of 5 μm. Further details on EPMA methodology, including standards, count times and typical minimum limits of detection, are given as Electronic Appendix A. EPMA element maps were generated using the same instrument. An operating voltage of 20 kV and 224 nA were applied for EPMA mapping of selected grains, with a step size of 4 μm.

LA-ICP-MS instrumentation and analytical procedures followed those given in George et al. (2016) [30] and George et al. (in press) [72]. A Resonetics M-50-LR 193 nm Excimer laser (Resonetics, Nashua, NH, USA) and an Agilent 7700cx Quadrupole ICP mass spectrometer (Agilent, Santa Clara, CA, USA) were used for the LA-ICP-MS analysis of tetrahedrite-tennantite (Adelaide Microscopy, The University of Adelaide). An atmosphere of ultra-high purity (UHP) He (0.7 L/min) was created inside the ablation cell, and Ar (0.93 L/min) was mixed with the ablated material upon exiting the cell. The mixture then passed through a pulse-homogenizing device (squid) before being directed to the torch. Regular calibration of the ICP-MS was performed so that the sensitivity on the isotopes of interest was maximized, and formation of unwanted molecular oxide species was kept at a minimum.

Laser beam energy was kept at 100 mJ with a 26 μm spot size, while the repetition rate was maintained at 10 Hz. Each analysis was a total of 60 s, consisting of a 30 s background measurement and 30 s of sample ablation. A delay of 40 s was allowed between each analysis for cell washout and gas stabilization. The following isotopes were analysed: ^{34}S, ^{55}Mn, ^{57}Fe, ^{59}Co, ^{60}Ni, ^{65}Cu, ^{66}Zn, ^{69}Ga, ^{75}As, ^{82}Se, ^{95}Mo, ^{107}Ag, ^{111}Cd, ^{115}In, ^{118}Sn, ^{121}Sb, ^{125}Te, ^{182}W, ^{197}Au, ^{202}Hg, ^{205}Tl, ^{206}Pb, ^{207}Pb, ^{208}Pb, and ^{209}Bi. The dwell time for each element was 0.01 s, while In, Au, and Tl were set to 0.05 s. Unless tetrahedrite-tennantite was fine-grained and sparse within any given sample, we aimed to make 10 spot analyses on each sample. Electronic Appendix B shows the range of minimum detection limits and mean errors for the trace elements analysed. Electronic Appendix C shows the full tetrahedrite-tennantite LA-ICP-MS dataset, as well as the data for co-existing sphalerite, galena and chalcopyrite also analysed in each sample according to methodology outlined in George et al., (2016) [30].

Table 2. Summary of samples used in this study.

Sample	Tetrahedrite-Tennantite Composition	Assemblage	Locality	Ore Type
G16396 *	$(Cu_9,Ag_{1.2},Zn_{0.9},Fe_{0.9},Pb_{0.1})$ $(Sb_{3.8},As_{0.1})$ S_{13}	*Tet*, *Sp*, *Gn*, *Cp*	Broken Hill, NSW, Australia	SEDEX (recrystallized)
G11579 *	$(Cu_{9.6},Ag_{0.3},Zn_1,Fe_{0.9})$ $(Sb_{3.7},As_{0.2})$ $S_{13.2}$	*Tet*, *Sp*, *Cp*, *Gn*	Kalgoorlie, WA, Australia	Orogenic Au
G13289b *	$(Cu_{10.1},Zn_{1.7},Fe_{0.3})$ $(Sb_{3.2},As_{0.8})$ $S_{12.9}$	*Tet*, *Gn*, *Cp*, *Sp*	S. Wheal Exmouth, Devon, England	Low temperature replacement
G6940 *	$(Cu_{9.5},Ag_{0.5},Fe_{1.2},Zn_{0.8})$ $(Sb_{3.8},As_{0.2})$ S_{13}	*Tet*, *Cp*, *Sp*, *Gn*	Great Boulder Mine, WA, Australia	Orogenic Au
G13289a *	$(Cu_{10.1},Zn_{1.7},Fe_{0.3})$ $(Sb_{3.2},As_{0.7})$ S_{13}	*Tet*, *Cp*, *Sp*, *Gn*	S. Wheal Exmouth, Devon, England	Low temperature replacement
V446	$(Cu_{8.2},Ag_{1.9},Fe_{1.7},Zn_{0.4})$ $Sb_{3.9}$ S_{13}	*Sp*, *Gn*, *Cp*, *Tet*	Bleikvassli, Norway	SEDEX (recrystallized)
V538	$(Cu_{7.8},Ag_{2.2},Fe_{1.7},Zn_{0.4})$ $Sb_{3.9}$ $S_{13.1}$	*Sp*, *Gn*, *Cp*, *Tet*	Bleikvassli, Norway	SEDEX (recrystallized)
Hj13	$(Cu_{9.2},Ag_{0.6},Fe_{1.6},Zn_{0.4})$ $Sb_{3.9}$ $S_{13.2}$	*Gn*, *Cp*, *Sp*, *Tet*	Herja, Romania	Epithermal
G6951 *	$(Cu_{9.4},Ag_{0.5},Zn_{1.8},Cd_{0.1})$ $(Sb_{3.5},As_{0.4})$ $S_{13.2}$	*Tet*, *Sp*, *Gn*, *(Cp)*	Yerranderie, NSW, Australia	Epithermal
Bv97-52	$(Cu_9,Ag_{0.6},Fe_{1.6},Zn_{0.7},Pb_{0.2})$ $(As_{2.8},Sb_{1.5})$ $S_{13.2}$	*Ten*, *Sp*, *Gn*	Bleikvassli, Norway	SEDEX (recrystallized)
G10847 *	$(Cu_{10},Ag_{0.1},Zn_{1.7},Fe_{0.3})$ $(Sb_{2.1},As_{1.8})$ S_{13}	*Tet*, *Sp*, *Gn*	Mt. Camel, Heathcote, Vic., Australia	Greenstone hosted
EV8 **	$(Ag_{5.6},Cu_{4.6},Fe_{1.9},Zn_{0.3})$ $Sb_{3.9}$ $S_{12.6}$	*Gn*, *Sp*, *Tet*	Evelyn Mine, NT, Australia	VMS
Hj14	$(Cu_{6.8},Ag3.2,Fe_{1.8},Zn_{0.3})$ $Sb_{3.8}$ $S_{13.2}$	*Gn*, *Sp*, *Tet*	Herja, Romania	Epithermal
G6948 *	$(Cu_{9.6},Ag_{0.5},Fe_{1.4},Zn_{0.6})$ $(Sb_{3.9},As_{0.1})$ S_{13}	*Tet*, *Sp*, *Cp*, *(Gn)*	Medcritting, Tas., Australia	Unknown
G14549b *	$(Cu_{8.7},Ag1.8,Fe_{1.1},Zn_{0.7})$ $(Sb_{3.8},As_{2.8})$ $S_{12.8}$	*Tet*, *Sp*, *Cp*	Consols Mine, Broken Hill, NSW, Australia	SEDEX (recrystallized)
Mo17A	$(Cu_{7.2},Ag_{2.5},Fe_{1.6},Zn_{0.4},Pb_{0.4})$ $(Sb_{3.7},As_{0.1})$ $S_{13.1}$	*Cp*, *Gn*, *Tet*	Mofjell, Norway	SEDEX (recrystallized)
ORV1	$(Cu_{10.1},Ag_{0.1},Zn_{1.3},Fe_{0.4})$ $(Sb_{3.1},As_{0.8})$ $S_{13.2}$	*Cp*, *Gn*, *Tet*	Oravita, Romania	Skarn
G14549a *	$(Cu_{8.7},Ag_{2.4},Fe_{1.1},$ $Zn_{0.7})$ $Sb_{3.7}$ $S_{12.3}$	*Tet*, *Gn*, *(Sp)*	Consols Mine, Broken Hill, NSW, Australia	SEDEX (recrystallized)
G873 *	$(Cu_{9.5},$ $Ag_{0.7},$ $Zn_{1.2},$ $Fe_{0.7})$ $(Sb_3,As_{0.9})$ $S_{12.9}$	*Tet*, *Gn*	Yerranderrie, NSW, Australia	Epithermal
G16152 *	$(Cu_{10},Ag_{0.1},Zn_{1.1},Fe_{0.8},Co_{0.1})$ $(Sb_{2.2},As_{1.8})$ S_{13}	*Tet*, *Cp*, *(Gn)*	Siegen, Westphalia, Germany	SEDEX?
G871 *	$(Cu_{10.1},Hg_{0.9},Fe_{0.5},Zn_{0.5})$ $(Sb_{3.2},As_{0.7})$ $S_{13.1}$	*Tet*, *Cp*	Pulganbar, Grafton, NSW, Australia	Vein hosted
G874 *	$(Cu_{10.3},Zn_1,Hg_{0.5},Fe_{0.4})$ $(Sb_{3.3},As_{0.6})$ $S_{12.8}$	*Tet*, *Cp*	Pulganbar, Grafton, NSW, Australia	Vein hosted
G879 *	$(Cu_{9.6},Ag_{0.4},Fe_{1.6},Zn_{0.4})$ $(Sb_{3.8},As_{0.1})$ $S_{13.2}$	*Tet*, *Cp*	Ring Valley, Tas., Australia	Fissure fillings
G882 *	$(Cu_{10.3},Fe_1,Zn_{0.3},Hg_{0.2})$ $(Sb_{2.5},As_{1.4})$ $S_{13.1}$	*Tet*, *Cp*	Pulganbar, Grafton, NSW, Australia	Vein hosted
G6946 *	$(Cu_{10},Ag_{0.1},Zn_{1.3},Fe_{0.6})$ $(Sb_{3.7},As_{0.2})$ $S_{13.1}$	*Tet*, *Cp*	Siegen, Westphalia, Germany	SEDEX?
G6949 *	$(Cu_{9.7},Ag_{0.2},Fe_{1.7},Zn_{0.3})$ $(Sb_{3.9},As_{0.1})$ $S_{13.1}$	*Tet*, *Cp*	Webb's Ag Mine, Emmaville, NSW, Australia	Veins and dissemination
G11701 *	$(Cu_{5.2},Ag_{5.1},Fe_{1.6},Zn_{0.4})$ Sb_4 $S_{12.6}$	*Tet*, *Cp*	Broken Hill, NSW, Australia	SEDEX (recrystallized)
G14246 *	$(Cu_{9.8},Ag_{0.2},Fe_{1.5},Zn_{0.5})$ $(Sb_{3.8},As_{0.1})$ $S_{13.1}$	*Tet*, *Cp*	Curtin Davis Mine, Dundas, Tas., Australia	Intrusion related?
G14867 *	$(Cu_{10.5},Fe_{1.4},Zn_{0.2})$ $(As_{3.1},Sb_{0.8})$ S_{13}	*Ten*, *Cp*	Oraparinna, SA, Australia	Diapir related
Mo16	$(Cu_{7.3},Ag_{2.6},Fe_{1.8},Zn_{0.2})$ $(Sb_{3.8},As_{0.8})$ $S_{13.2}$	*Cp*, *Tet*, *(Gn)*	Mofjell, Norway	SEDEX (recrystallized)
G29851 *	$(Cu_{10.2},Fe_{1.1},$ $Zn_{0.5},Hg_{0.2})$ $(As_{3.6},Sb_{0.3})$ S_{13}	*Cp*, *Ten*	Gortdrum Mine, Ireland	Carbonate hosted
ORV4	$(Cu_{10.1},Zn_{1.4},Fe_{0.4})$ $(Sb_{2.7},As_{1.2})$ $S_{13.2}$	*Cp*, *Tet*	Oravita, Romania	Skarn
G12640 *	$(Cu_{10.2},Zn_{1.1},Fe_{0.9})$ $(As_{2.5},Sb_{1.4})$ $S_{12.9}$	*Ten*	Tinga, NSW, Australia	Unknown
G13301 *	$(Cu_{10.2},Fe_{1.2},Zn_{0.4})$ $(Sb_{3.3},As_{0.6})$ $S_{13.3}$	*Tet*	Allihies Mine, Castletown, Cork, Ireland	Unknown
G15977 *	$(Cu_{10.1},Zn_{1.2},Fe_{0.7})$ $(Sb_{3.2},As_{0.7})$ S_{13}	*Tet*	Mooloowatana HS, SA, Australia	Unknown
G16835 *	$(Cu_{10.1},Ag_{0.1},Zn_1,Fe_{0.7},$ $Hg_{0.1})$ $(As_2,Sb_{1.9})$ $S_{13.1}$	*Ten*	Grosskogel Mine, Austria	MVT?
VFI031 **	$(Cu_{8.4},Ag_{1.7},Zn_{1.9})$ $(Sb_{2.4},As_{1.4})$ $S_{13.1}$	*Tet*	Emperor Gold Mine, Fiji	Epithermal

Tet = tetrahedrite, *Ten* = tennantite, *Sp* = sphalerite, *Gn* = galena, *Cp* = chalcopyrite. Minerals in brackets are very minor phases. Tetrahedrite-tennantite composition determined by electron probe microanalysis. * Sample derives from the South Australian Museum. ** Sample derives from the Tate Museum. Other samples derive from the author's personal collection.

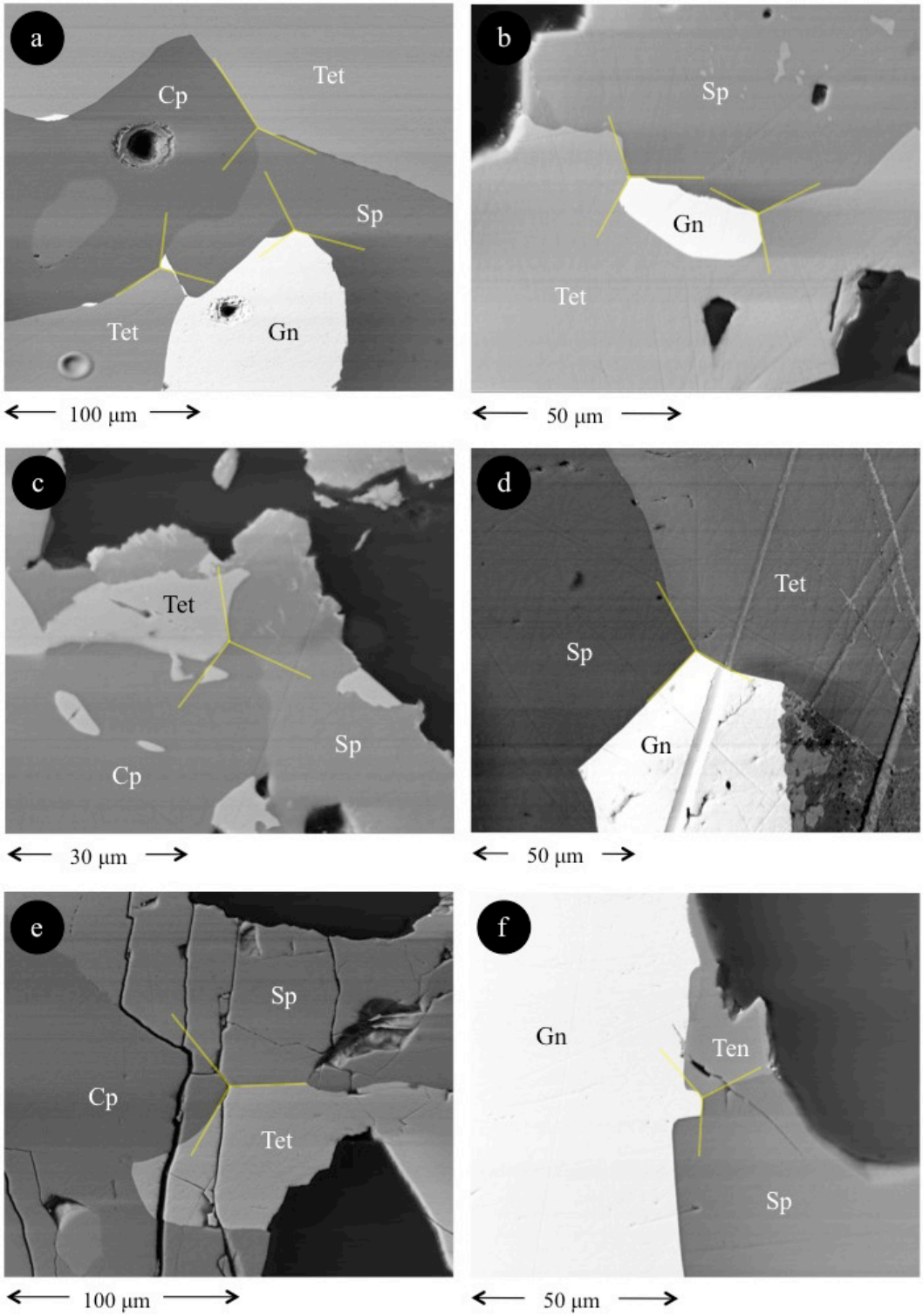

Figure 2. Representative back-scattered electron images illustrating textural evidence for tetrahedrite-tennantite and base metal sulphide (BMS) co-crystallization. (**a**) ~120° triple-junction grain boundaries as evidence for co-crystallization of tetrahedrite (Tet), sphalerite (Sp), galena (Gn) and chalcopyrite (Cp) in G11579 (Kalgoorlie, WA, Australia). Additional ~120° triple-junction grain boundaries between tetrahedrite, tennantite (Ten), sphalerite, galena, and chalcopyrite are illustrated from samples G6948 (Medcritting, Australia); (**b**,**c**) G10847 (Mt. Camel, Heathcote, Australia); (**d**) G6940 (Great Boulder Mine, WA, Australia); (**e**) and Bv97-52 (Bleikvassli, Norway); (**f**) Note grain boundaries curving towards the triple junction in order to approximate 120°.

The external standard used was MASS-1 (previously PS-1; [73]), utilizing the latest certificate of analysis [74]. Up to 10 unknown analyses were bracketed by multiple analyses of this reference material. Thus instrument drift was monitored, and a linear correction was applied to the unknown analyses. All data reduction was carried out using GLITTER [75]. Internal standardization was conducted using Cu concentration values obtained by EPMA on each individual sample. While certain interferences may have affected the reliability of some elements analysed by LA-ICP-MS (e.g., sulphur interference on ^{66}Zn; [76], or ^{59}Co^{16}O interference on ^{75}As; [77]), corrections were not applied as reliable measurements on these typically major elements were made by EPMA.

4. Results

As discussed in Cook et al. (2016) [78] and George et al. (in press) [72], mineral microanalysts are continually faced with the challenge of determining whether measurable concentrations of an element in any given mineral are present in solid solution, within microscale mineral inclusions hosted within the analysed mineral, or a mixture of both. Every effort has been made in the present study to report data that reflects elements in solid solution within the tetrahedrite-tennantite structure. This was done by examining all samples in back-scatter electron mode with a scanning electron microscope (SEM) prior to microanalysis so that only clean areas free of any noticeable inclusions were analysed. In addition, all downhole spectra from the LA-ICP-MS datasets were additionally checked for any peaks that suggest the presence of micro-inclusions beneath the sample surface (e.g., [72,79]). If present, such analyses were discarded. It is evident that some elements, notably Pb, are more commonly present as micro-inclusions in tetrahedrite-tennantite than others, perhaps due to the common presence of co-existing galena.

Table 3 summarizes the concentrations of 16 elements in tetrahedrite-tennantite as determined by EPMA. Nickel, Ga, In, and Tl were also measured, but analyses were consistently below the minimum limits of detection (average values of 0.022, 0.041, 0.031, and 0.126 wt %, respectively). Figure 3 shows the major element variation in the tetrahedrite-tennantite sample suite. Specimens spanning the entire tetrahedrite-tennantite solid solution range are represented (Figure 3a), as are samples ranging in composition from essentially Fe to Zn pure end-members (Figure 3b). Most tetrahedrite-tennantites here contain more Cu than Ag; only in sample EV8 (Evelyn Mine, NT, Australia) could freibergite be classified (Figure 3c; Table 3).

Concentrations of 20 trace and minor elements measured in tetrahedrite-tennantite by LA-ICP-MS are summarized in Table 4. Individual spot analyses are plotted as cumulative plots (Figures 4 and 5) that are sorted by the co-crystallized BMS assemblage. This allows a visualization of element concentrations and variation in different assemblages. In one sample (G871; Pulganbar, Grafton, NSW, Australia), clear oscillatory zoning was observed and mapped by EPMA (Figures 6 and 7). The zoning shows the inverse correlation between the trivalent cations Sb and As, such that Sb enriched zones are As depleted, and vice versa. Zones of high Cu, Fe, and Zn correlate with As enriched, Sb depleted zones, while high Hg zones correlate to Sb-enriched, As depleted zones. While such strong zoning appeared to be uncommon in the sample suite, other analysed tetrahedrite-tennantites may be considered as zoned to some degree based on variation of concentration values between spots. In general, grain-scale compositional zoning is common in tetrahedrite-tennantite, although this is more commonly observed as patchy heterogeneity (e.g., [80]). Micron-scale oscillatory zoning of the kind illustrated here is, however, well known from epithermal systems (e.g., [81]).

Table 3. Summary of element concentrations in tetrahedrite-tennantite determined by electron probe microanalysis (EPMA) (data in wt %).

Sample/Assemblage		S	Mn	Fe	Co	Cu	Zn	As	Se	Ag	Cd	Sn	Sb	Te	Hg	Pb	Bi	TOTAL
G16396 *	Mean (10)	24.4	0.016	3.07	-	33.3	3.59	0.237	0.021	7.25	0.051	-	27.3	-	0.069	0.994	-	100.1
Tet, Sp, Gn, Cp	*apfu*	*13.0*	*0.005*	*0.942*	-	*8.97*	*0.942*	*0.054*	*0.005*	*1.16*	*0.008*	-	*3.84*	-	*0.006*	*0.083*	-	*29.0*
G11579	Mean (10)	25.9	-	3.08	-	37.3	4.19	0.903	0.018	2.27	-	-	27.7	-	0.079	0.076	0.110	101.6
Tet, Sp, Cp, Gn	*apfu*	*13.2*	-	*0.902*	-	*9.59*	*1.05*	*0.197*	*0.004*	*0.344*	-	-	*3.72*	-	*0.006*	*0.006*	*0.009*	*29.0*
G13289b *	Mean (10)	25.5	-	1.06	-	39.5	6.71	3.47	-	0.243	-	-	23.6	-	0.076	0.066	-	100.1
Tet, Gn, Cp, Sp	*apfu*	*12.9*	-	*0.310*	-	*10.1*	*1.67*	*0.755*	-	*0.037*	-	-	*3.16*	-	*0.006*	*0.005*	-	*29.0*
G6940	Mean (10)	25.1	0.018	3.93	0.019	36.3	3.14	0.679	0.021	3.33	-	-	27.4	-	0.084	0.068	0.092	100.0
Tet, Cp, Sp, Gn	*apfu*	*13.0*	*0.005*	*1.18*	*0.005*	*9.55*	*0.801*	*0.151*	*0.004*	*0.516*	-	-	*3.76*	-	*0.007*	*0.005*	*0.007*	*29.0*
G13289a *	Mean (10)	25.7	-	0.976	-	39.4	6.77	3.20	0.031	0.212	-	-	24.1	-	0.073	0.079	-	100.4
Tet, Cp, Sp, Gn	*apfu*	*13.0*	-	*0.284*	-	*10.1*	*1.68*	*0.693*	*0.006*	*0.032*	-	-	*3.21*	-	*0.006*	*0.006*	-	*29.0*
V446	Mean (7)	24.1	0.031	5.36	0.022	30.0	1.69	-	-	11.6	-	-	27.5	0.032	0.098	0.108	-	100.5
Sp, Gn, Cp, Tet	*apfu*	*13.0*	*0.010*	*1.65*	*0.006*	*8.16*	*0.446*	-	-	*1.86*	-	-	*3.90*	*0.004*	*0.008*	*0.009*	-	*29.0*
V538	Mean (10)	24.2	0.020	5.42	0.023	28.7	1.33	-	0.033	13.5	-	0.029	27.3	-	0.100	0.086	-	100.6
Sp, Gn, Cp, Tet	*apfu*	*13.1*	*0.006*	*1.68*	*0.007*	*7.82*	*0.352*	-	*0.007*	*2.16*	-	*0.004*	*3.88*	-	*0.009*	*0.007*	-	*29.0*
Hj13	Mean (10)	25.4	0.021	5.39	0.025	35.2	1.76	-	0.025	3.88	-	0.053	28.7	-	0.118	0.088	-	100.5
Gn, Cp, Sp, Tet	*apfu*	*13.2*	*0.006*	*1.61*	*0.007*	*9.22*	*0.449*	-	*0.005*	*0.600*	-	*0.007*	*3.92*	-	*0.010*	*0.007*	-	*29.0*
G6951 *	Mean (10)	25.6	-	0.043	0.018	36.4	7.30	1.86	0.019	3.45	0.674	-	26.0	-	0.082	0.078	-	101.4
Tet, Sp, Gn, (Cp)	*apfu*	*13.2*	-	*0.013*	*0.005*	*9.44*	*1.84*	*0.408*	*0.004*	*0.526*	*0.099*	-	*3.51*	-	*0.007*	*0.006*	-	*29.0*
Bv97-52	Mean (10)	27.0	0.060	5.63	0.023	36.9	2.63	13.9	0.028	3.45	0.041	0.035	11.3	-	0.078	2.10	-	100.2
Ten, Sp, Gn	*apfu*	*13.2*	*0.017*	*1.58*	*0.006*	*9.01*	*0.650*	*2.80*	*0.006*	*0.568*	*0.005*	*0.004*	*1.53*	-	*0.006*	*0.199*	-	*29.0*
G10847	Mean (10)	26.8	-	1.00	-	40.7	6.98	8.43	-	0.745	-	-	16.6	-	0.230	0.076	-	101.6
Tet, Sp, Gn	*apfu*	*13.0*	-	*0.281*	-	*10.0*	*1.67*	*1.76*	-	*0.108*	-	-	*2.13*	-	*0.018*	*0.006*	-	*29.0*
EV8	Mean (10)	21.3	-	5.62	-	15.5	1.02	-	0.029	32.1	-	0.264	25.3	-	0.095	0.409	0.066	101.4
Gn, Sp, Tet	*apfu*	*12.6*	-	*1.91*	-	*4.63*	*0.294*	-	*0.007*	*5.64*	-	*0.042*	*3.94*	-	*0.009*	*0.038*	*0.006*	*29.0*
Hj14	Mean (6)	24.0	0.018	5.56	0.022	24.4	0.937	-	0.018	19.3	-	-	26.5	-	0.082	0.102	-	100.9
Gn, Sp, Tet	*apfu*	*13.2*	*0.006*	*1.76*	*0.007*	*6.77*	*0.253*	-	*0.004*	*3.15*	-	-	*3.85*	-	*0.007*	*0.009*	-	*29.0*
G6948	Mean (10)	24.9	0.047	4.60	-	36.3	2.33	0.234	0.027	3.39	-	-	28.1	-	0.086	0.071	0.091	100.0
Tet, Sp, Cp, (Gn)	*apfu*	*13.0*	*0.014*	*1.38*	-	*9.55*	*0.597*	*0.052*	*0.006*	*0.526*	-	-	*3.86*	-	*0.007*	*0.006*	*0.007*	*29.0*
G14549b	Mean (10)	24.0	-	3.73	-	32.5	2.66	0.134	0.017	11.1	0.147	-	27.3	-	0.094	0.255	0.129	101.7
Tet, Sp, Cp	*apfu*	*12.8*	-	*1.14*	-	*8.72*	*0.696*	*0.031*	*0.004*	*1.84*	*0.022*	-	*3.82*	-	*0.008*	*0.023*	*0.011*	*29.0*
Mo17A	Mean (7)	23.7	-	5.08	-	25.8	1.34	0.278	0.048	15.4	0.054	-	25.5	-	0.074	4.01	-	100.6
Cp, Gn, Tet	*apfu*	*13.1*	-	*1.62*	-	*7.21*	*0.363*	*0.065*	*0.012*	*2.54*	*0.009*	-	*3.73*	-	*0.007*	*0.390*	-	*29.0*
ORV1	Mean (10)	26.2	-	1.47	-	39.8	5.47	3.65	0.018	0.531	-	-	23.5	-	0.088	0.087	0.065	100.8
Cp, Gn, Tet	*apfu*	*13.2*	-	*0.427*	-	*10.1*	*1.34*	*0.783*	*0.004*	*0.079*	-	-	*3.11*	-	*0.007*	*0.007*	*0.005*	*29.0*
G14549a	Mean (10)	22.4	-	3.55	-	31.7	2.58	0.195	0.023	13.5	0.047	-	25.8	-	0.083	0.254	0.181	100.2
Tet, Gn, (Sp)	*apfu*	*12.3*	-	*1.12*	-	*8.74*	*0.694*	*0.045*	*0.005*	*2.36*	*0.008*	-	*3.73*	-	*0.007*	*0.021*	*0.016*	*29.0*
G873	Mean (10)	24.8	-	2.48	-	36.3	4.76	3.96	-	4.59	0.034	-	22.2	-	0.077	0.113	-	99.3
Tet, Gn	*apfu*	*12.9*	-	*0.740*	-	*9.52*	*1.21*	*0.881*	-	*0.710*	*0.005*	-	*3.04*	-	*0.006*	*0.009*	-	*29.0*
G16152	Mean (10)	26.6	-	2.82	0.362	40.7	4.38	8.48	-	0.449	-	-	16.8	-	0.185	0.066	-	100.9

Table 3. *Cont.*

Sample/Assemblage		S	Mn	Fe	Co	Cu	Zn	As	Se	Ag	Cd	Sn	Sb	Te	Hg	Pb	Bi	TOTAL
Tet, Cp, (Gn)	*apfu*	*13.0*	-	*0.792*	*0.096*	*10.0*	*1.05*	*1.77*	-	*0.065*	-	-	*2.17*	-	*0.014*	*0.005*	-	*29.0*
G871	Mean (10)	24.2	-	1.50	0.068	37.1	1.70	3.17	-	0.051	-	-	22.6	-	10.6	0.076	-	101.1
Tet, Cp	*apfu*	*13.1*	-	*0.464*	*0.020*	*10.1*	*0.449*	*0.726*	-	*0.008*	-	-	*3.23*	-	*0.922*	*0.006*	-	*29.0*
G874	Mean (10)	24.1	-	1.32	0.079	38.3	3.81	2.72	-	0.050	-	-	23.7	-	5.79	0.056	-	99.8
Tet, Cp	*apfu*	*12.8*	-	*0.404*	*0.023*	*10.3*	*1.00*	*0.621*	-	*0.008*	-	-	*3.33*	-	*0.494*	*0.005*	-	*29.0*
G879	Mean (10)	25.6	-	5.43	-	37.0	1.48	0.291	0.025	2.59	-	-	28.5	-	0.077	0.064	0.073	101.0
Tet, Cp	*apfu*	*13.2*	-	*1.60*	-	*9.58*	*0.371*	*0.064*	*0.005*	*0.395*	-	-	*3.85*	-	*0.006*	*0.005*	*0.006*	*29.0*
G882	Mean (10)	26.4	-	3.54	0.087	41.2	1.34	6.78	-	-	-	-	19.0	-	3.10	0.070	-	101.6
Tet, Cp	*apfu*	*13.1*	-	*1.01*	*0.024*	*10.3*	*0.327*	*1.44*	-	-	-	-	*2.50*	-	*0.247*	*0.005*	-	*29.0*
G6946	Mean (10)	25.7	-	2.05	-	39.0	5.14	1.04	0.023	0.600	-	-	27.5	-	0.158	0.059	-	101.3
Tet, Cp	*apfu*	*13.1*	-	*0.600*	-	*10.0*	*1.28*	*0.226*	*0.005*	*0.091*	-	-	*3.69*	-	*0.013*	*0.005*	-	*29.0*
G6949	Mean (10)	25.8	0.015	5.72	-	37.9	1.30	0.331	0.020	1.23	-	-	28.9	-	0.081	0.057	0.136	101.4
Tet, Cp	*apfu*	*13.1*	*0.004*	*1.67*	-	*9.75*	*0.326*	*0.072*	*0.004*	*0.186*	-	-	*3.87*	-	*0.007*	*0.005*	*0.011*	*29.0*
G11701	Mean (10)	21.5	-	4.72	0.026	17.6	1.48	-	0.025	29.2	-	-	26.1	-	0.081	0.055	-	100.6
Tet, Cp	*apfu*	*12.6*	-	*1.59*	*0.008*	*5.21*	*0.425*	-	*0.006*	*5.10*	-	-	*4.03*	-	*0.008*	*0.005*	-	*29.0*
G14246	Mean (10)	25.6	-	5.10	-	37.6	1.86	0.298	0.029	1.41	-	-	28.3	-	0.082	0.073	0.173	100.6
Tet, Cp	*apfu*	*13.1*	-	*1.50*	-	*9.76*	*0.470*	*0.065*	*0.006*	*0.215*	-	-	*3.83*	-	*0.007*	*0.006*	*0.014*	*29.0*
G14867	Mean (10)	28.0	-	5.06	0.023	44.7	0.765	15.5	0.020	0.049	-	-	6.40	-	0.392	0.073	0.135	101.0
Ten, Cp	*apfu*	*13.0*	-	*1.35*	*0.006*	*10.5*	*0.175*	*3.10*	*0.004*	*0.007*	-	-	*0.786*	-	*0.029*	*0.005*	*0.010*	*29.0*
Mo16	Mean (7)	24.3	-	5.62	0.024	26.5	0.933	3.60	0.024	15.9	0.054	-	26.7	-	0.089	0.088	-	100.6
Cp, Tet, (Gn)	*apfu*	*13.2*	-	*1.76*	*0.007*	*7.25*	*0.247*	*0.802*	*0.005*	*2.58*	*0.008*	-	*3.83*	-	*0.008*	*0.007*	-	*29.0*
G29851	Mean (10)	27.9	-	4.10	0.021	43.2	2.01	18.0	-	0.093	-	0.026	2.72	-	3.28	0.084	0.087	101.4
Cp, Ten	*apfu*	*13.0*	-	*1.10*	*0.005*	*10.2*	*0.461*	*3.60*	-	*0.013*	-	*0.003*	*0.337*	-	*0.246*	*0.006*	*0.006*	*29.0*
ORV4	Mean (10)	26.6	-	1.48	-	40.3	5.89	5.68	-	0.156	0.048	-	20.6	-	0.070	0.070	-	100.9
Cp, Tet	*apfu*	*13.2*	-	*0.419*	-	*10.1*	*1.43*	*1.20*	-	*0.023*	*0.007*	-	*2.70*	-	*0.006*	*0.005*	-	*29.0*
G12640	Mean (10)	27.1	0.017	3.46	-	42.3	4.53	12.1	-	0.212	-	-	11.2	-	0.122	0.072	-	101.1
Ten	*apfu*	*12.9*	*0.005*	*0.947*	-	*10.2*	*1.06*	*2.46*	-	*0.030*	-	-	*1.41*	-	*0.009*	*0.005*	-	*29.0*
G13301	Mean (10)	26.7	-	4.24	0.070	40.8	1.59	3.01	0.020	-	0.069	-	25.0	-	0.149	0.074	-	101.7
Tet	*apfu*	*13.3*	-	*1.21*	*0.019*	*10.2*	*0.387*	*0.639*	*0.004*	-	*0.010*	-	*3.27*	-	*0.012*	*0.006*	-	*29.0*
G15977	Mean (10)	26.0	-	2.53	-	39.8	5.07	3.45	-	0.102	0.243	-	24.2	-	0.117	0.083	-	101.3
Tet	*apfu*	*13.0*	-	*0.726*	-	*10.1*	*1.24*	*0.739*	-	*0.015*	*0.035*	-	*3.19*	-	*0.009*	*0.006*	-	*29.0*
G16835	Mean (10)	27.1	-	2.68	0.027	41.5	4.00	9.61	-	0.398	-	-	14.9	-	0.904	0.093	0.093	101.1
Ten	*apfu*	*13.1*	-	*0.746*	*0.007*	*10.1*	*0.952*	*1.99*	-	*0.057*	-	-	*1.90*	-	*0.070*	*0.007*	*0.007*	*29.0*
VFI031	Mean (5)	25.5	0.107	0.039	-	32.2	7.47	6.52	0.036	10.8	-	-	17.9	0.159	0.469	0.083	-	101.2
Tet	*apfu*	*13.1*	*0.032*	*0.011*	-	*8.37*	*1.89*	*1.43*	*0.008*	*1.65*	-	-	*2.43*	*0.020*	*0.039*	*0.007*	-	*29.0*

Tet = tetrahedrite, *Ten* = tennantite, *Sp* = sphalerite, *Gn* = galena, *Cp* = chalcopyrite, *apfu* = atoms per formula unit. Minerals in brackets are very minor phases. (X) = number of individual spot analyses in that sample. * Evidence suggests sulphides in sample did not co-crystallize (based on textures and partitioning trends among base metal sulphides). Dash = insufficient data to perform calculation (all analyses <mdl). Other <mdl values were ignored, thus data can be considered maximum concentrations. Totals are calculated by averaging the total for each spot in each sample. Hence each row will not add to the total.

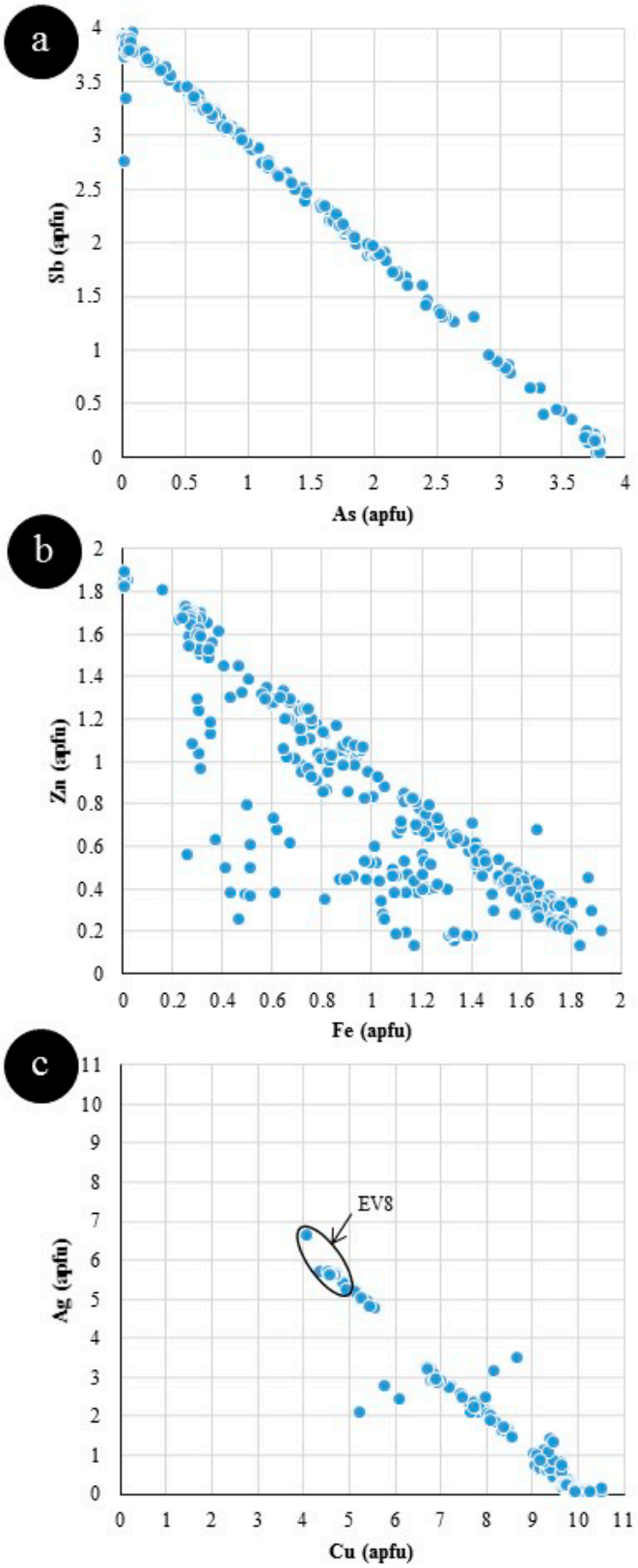

Figure 3. Scatter-plots showing the variation in major elements in the tetrahedrite-tennantite sample suite. (**a**) Sb vs. As; (**b**) Zn vs. Fe; and (**c**) Ag vs. Cu. Atoms per formula unit is calculated by normalizing mol % values to 29.

Table 4. Summary of trace element concentrations in tetrahedrite-tennantite determined by laser-ablation inductively-coupled plasma mass spectrometry (LA-ICP-MS) (data in ppm).

Sample/Assemblage		Mn	Fe	Co	Ni	Zn	Ga	As	Se	Mo	Ag	Cd	In	Sn	Te	W	Au	Hg	Tl	Pb	Bi
G16396 *	Mean (10)	1.4	ME	2.7	0.54	ME	0.09	4620	-	0.12	ME	4968	0.57	28	1.4	0.04	0.74	93	0.09	61	445
Tet, Sp, Gn, Cp	*St. Dev.*	*1.0*	*ME*	*1.1*	*0.78*	*ME*	*0.12*	*943*	*-*	*0.15*	*ME*	*751*	*0.16*	*39*	*1.1*	*0.06*	*0.53*	*20*	*0.16*	*40*	*768*
G11579	Mean (10)	32	ME	22	0.87	ME	0.06	28,446	53	0.09	ME	2692	7.0	0.54	50	-	0.03	93	0.05	3.1	3007
Tet, Sp, Cp, Gn	*St. Dev.*	*2.1*	*ME*	*4.5*	*1.0*	*ME*	*0.03*	*6725*	*23*	*0.08*	*ME*	*324*	*1.1*	*0.37*	*25*	*-*	*0.02*	*31*	*0.05*	*2.2*	*595*
G13289b *	Mean (10)	0.77	ME	44	0.14	ME	0.03	ME	11	0.03	2038	2187	0.25	0.80	0.07	0.01	0.02	9.3	0.15	270	8.2
Tet, Gn, Cp, Sp	*St. Dev.*	*0.54*	*ME*	*7.8*	*0.08*	*ME*	*0.02*	*ME*	*8.6*	*0.04*	*538*	*274*	*0.34*	*0.49*	*0.16*	*0.01*	*0.04*	*3.2*	*0.22*	*257*	*8.5*
G6940	Mean (10)	43	ME	0.55	0.33	ME	0.05	12,626	73	0.06	ME	1860	3.4	1.1	38	0.02	0.02	86	0.02	1.8	1539
Tet, Cp, Sp, Gn	*St. Dev.*	*7.9*	*ME*	*0.14*	*0.19*	*ME*	*0.04*	*5590*	*20*	*0.05*	*ME*	*231*	*0.92*	*0.71*	*21*	*0.03*	*0.02*	*28*	*0.02*	*0.68*	*142*
G13289a *	Mean (10)	0.83	10,116	38	0.25	ME	0.03	ME	21	0.04	1866	2052	0.17	0.47	0.09	0.01	0.01	13	0.05	108	11
Tet, Cp, Sp, Gn	*St. Dev.*	*0.65*	*1653*	*11*	*0.19*	*ME*	*0.03*	*ME*	*29*	*0.05*	*615*	*262*	*0.40*	*0.35*	*0.18*	*0.01*	*0.00*	*2.9*	*0.05*	*130*	*16*
V446	Mean (4)	204	ME	0.06	0.13	ME	0.19	38	12	0.02	ME	170	1.2	16	0.06	-	0.01	10	0.16	1.9	111
Sp, Gn, Cp, Tet	*St. Dev.*	*12*	*ME*	*0.05*	*0.25*	*ME*	*0.05*	*11*	*6.1*	*0.03*	*ME*	*24*	*0.21*	*1.7*	*0.09*	*-*	*0.02*	*1.5*	*0.21*	*-*	*22*
V538	Mean (3)	122	ME	0.02	0.00	ME	0.11	92	6.0	0.00	ME	158	0.64	22	0.13	-	0.00	10	0.21	21	45
Sp, Gn, Cp, Tet	*St. Dev.*	*6.9*	*ME*	*0.03*	*0.01*	*ME*	*0.10*	*44*	*2.6*	*0.00*	*ME*	*12*	*0.08*	*0.42*	*0.17*	*-*	*0.01*	*1.3*	*0.31*	*23*	*4.2*
Hj13	Mean (9)	109	ME	0.24	-	ME	0.03	117	8.9	0.08	ME	110	0.21	0.15	0.42	0.00	0.11	0.33	0.48	3.0	3.1
Gn, Cp, Sp, Tet	*St. Dev.*	*19*	*ME*	*0.38*	*-*	*ME*	*0.02*	*24*	*4.7*	*0.07*	*ME*	*18*	*0.08*	*0.23*	*0.73*	*0.01*	*0.13*	*0.10*	*0.24*	*1.4*	*1.0*
G6951 *	Mean (10)	1.5	369	27	-	ME	0.04	ME	-	0.06	ME	29,893	0.10	0.31	0.29	-	0.06	29	0.20	85	0.03
Tet, Sp, Gn, (Cp)	*St. Dev.*	*0.75*	*138*	*6.0*	*-*	*ME*	*0.02*	*ME*	*-*	*0.07*	*ME*	*7569*	*0.02*	*0.18*	*0.35*	*-*	*0.04*	*14*	*0.12*	*36*	*0.04*
Bv97-52	Mean (8)	389	ME	0.01	0.15	ME	0.32	ME	3.8	0.05	ME	682	1.9	46	-	-	0.00	46	0.00	ME	9.1
Ten, Sp, Gn	*St. Dev.*	*332*	*ME*	*0.01*	*0.37*	*ME*	*0.51*	*ME*	*1.9*	*0.05*	*ME*	*351*	*1.6*	*128*	*-*	*-*	*0.00*	*18*	*0.00*	*ME*	*5.9*
G10847	Mean (10)	18	ME	0.03	0.35	ME	0.34	ME	11	0.07	5164	1325	0.09	0.92	0.40	-	0.06	2668	0.11	13	1.3
Tet, Sp, Gn	*St. Dev.*	*4.7*	*ME*	*0.02*	*0.24*	*ME*	*0.13*	*ME*	*7.2*	*0.06*	*4579*	*169*	*0.02*	*0.78*	*0.41*	*-*	*0.09*	*493*	*0.22*	*9.3*	*0.22*
EV8	Mean (10)	7.6	ME	0.20	0.31	ME	0.21	121	19	-	ME	870	2.6	404	0.82	0.02	0.08	19	3.7	46,078	1174
Gn, Sp, Tet	*St. Dev.*	*3.0*	*ME*	*0.07*	*0.41*	*ME*	*0.11*	*142*	*16*	*-*	*ME*	*418*	*2.5*	*185*	*0.82*	*0.05*	*0.13*	*8.5*	*2.1*	*29,774*	*456*
Hj14	Mean (6)	80	ME	0.01	0.02	10,882	0.01	310	2.7	0.08	ME	161	0.05	18	0.09	-	11	0.26	0.24	39	0.03
Gn, Sp, Tet	*St. Dev.*	*22*	*ME*	*0.03*	*0.04*	*587*	*0.01*	*135*	*2.6*	*0.12*	*ME*	*22*	*0.05*	*16*	*0.15*	*-*	*5.2*	*0.09*	*0.58*	*10*	*0.06*
G6948	Mean (10)	517	ME	0.11	0.36	ME	0.06	8222	135	0.06	ME	1033	1.4	65	0.54	-	0.02	2.4	0.02	4.6	1933
Tet, Sp, Cp, (Gn)	*St. Dev.*	*71*	*ME*	*0.10*	*0.21*	*ME*	*0.06*	*5983*	*68*	*0.06*	*ME*	*89*	*0.17*	*28*	*0.47*	*-*	*0.01*	*2.6*	*0.01*	*3.9*	*621*
G14549b	Mean (10)	2.3	ME	1.2	0.56	ME	0.12	1921	11	0.10	ME	4731	0.33	19	0.14	-	0.39	47	0.83	871	475
Tet, Sp, Cp	*St. Dev.*	*1.2*	*ME*	*1.0*	*0.61*	*ME*	*0.09*	*805*	*9.0*	*0.13*	*ME*	*1272*	*0.24*	*19*	*0.18*	*-*	*0.22*	*23*	*0.58*	*775*	*386*
Mo17A	Mean (6)	0.50	ME	0.16	0.03	ME	0.01	20,439	5.8	0.03	ME	1751	0.02	0.06	0.83	-	0.06	1.9	0.12	ME	3.2
Cp, Gn, Tet	*St. Dev.*	*0.12*	*ME*	*0.20*	*0.07*	*ME*	*0.01*	*29,371*	*2.1*	*0.04*	*ME*	*373*	*0.01*	*0.06*	*0.71*	*-*	*0.10*	*1.1*	*0.15*	*ME*	*0.82*
ORV1	Mean (10)	0.18	ME	23	2.9	ME	0.04	ME	21	0.12	4023	979	0.40	0.11	0.34	-	0.01	36	0.00	4.0	12
Cp, Gn, Tet	*St. Dev.*	*0.13*	*ME*	*12*	*2.3*	*ME*	*0.05*	*ME*	*16*	*0.14*	*880*	*393*	*0.26*	*0.12*	*0.46*	*-*	*0.02*	*13*	*0.01*	*3.1*	*16*
G14549a	Mean (10)	1.4	ME	0.74	0.84	ME	0.13	3988	13	0.03	ME	3104	0.82	42	0.07	0.01	0.20	25	0.30	849	2794
Tet, Gn, (Sp)	*St. Dev.*	*0.61*	*ME*	*0.36*	*1.2*	*ME*	*0.07*	*1181*	*8.7*	*0.03*	*ME*	*929*	*1.5*	*41*	*0.10*	*0.01*	*0.13*	*11*	*0.16*	*106*	*1842*
G873	Mean (10)	1.6	ME	1.4	0.35	ME	0.09	ME	13	0.33	ME	4310	10	0.70	0.19	0.03	0.08	62	0.08	23	0.11
Tet, Gn	*St. Dev.*	*1.1*	*ME*	*2.0*	*0.25*	*ME*	*0.05*	*ME*	*11*	*0.89*	*ME*	*1422*	*1.9*	*0.37*	*0.20*	*0.03*	*0.07*	*25*	*0.09*	*5.7*	*0.10*
G16152	Mean (10)	0.47	ME	2512	12	ME	0.05	ME	13	1.9	4452	683	3.0	28	-	0.01	0.02	3456	0.02	16	29
Tet, Cp, (Gn)	*St. Dev.*	*0.32*	*ME*	*880*	*7.4*	*ME*	*0.03*	*ME*	*12*	*2.2*	*634*	*70*	*1.4*	*51*	*-*	*0.02*	*0.02*	*921*	*0.02*	*20*	*30*

Table 4. *Cont.*

Sample/Assemblage		Mn	Fe	Co	Ni	Zn	Ga	As	Se	Mo	Ag	Cd	In	Sn	Te	W	Au	Hg	Tl	Pb	Bi
G871	Mean (10)	0.46	ME	382	0.52	ME	0.04	ME	17	0.12	372	139	0.09	0.35	0.20	0.02	0.02	ME	0.02	1.8	0.25
Tet, Cp	*St. Dev.*	*0.45*	*ME*	*220*	*0.42*	*ME*	*0.03*	*ME*	*9.5*	*0.17*	*48*	*71*	*0.13*	*0.32*	*0.29*	*0.03*	*0.02*	*ME*	*0.01*	*1.4*	*0.21*
G874	Mean (10)	0.46	ME	557	0.20	ME	0.03	ME	14	0.11	206	263	1.8	0.47	0.17	0.02	0.01	ME	0.01	5.9	0.47
Tet, Cp	*St. Dev.*	*0.41*	*ME*	*397*	*0.12*	*ME*	*0.02*	*ME*	*15*	*0.07*	*40*	*157*	*1.2*	*0.35*	*0.16*	*0.02*	*0.01*	*ME*	*0.01*	*3.5*	*0.54*
G879	Mean (10)	7.1	ME	3.6	1.9	ME	0.14	8555	-	-	ME	380	15	1.4	0.29	0.04	0.09	20	0.11	18	1229
Tet, Cp	*St. Dev.*	*3.7*	*ME*	*2.6*	*2.9*	*ME*	*0.16*	*9952*	*-*	*-*	*ME*	*57*	*4.5*	*1.5*	*0.35*	*0.04*	*0.12*	*10*	*0.12*	*28*	*549*
G882	Mean (10)	0.70	ME	613	0.56	ME	0.13	ME	56	0.36	303	328	2.3	0.68	0.69	0.04	0.05	ME	0.03	37	4.8
Tet, Cp	*St. Dev.*	*0.62*	*ME*	*475*	*0.30*	*ME*	*0.10*	*ME*	*69*	*0.36*	*90*	*283*	*2.2*	*0.56*	*0.79*	*0.04*	*0.04*	*ME*	*0.04*	*40*	*3.3*
G6946	Mean (10)	1.4	ME	53	28	ME	0.14	ME	63	0.08	6202	1268	1.4	2.3	0.35	0.01	0.03	1917	0.01	7.3	98
Tet, Cp	*St. Dev.*	*1.2*	*ME*	*40*	*9.1*	*ME*	*0.09*	*ME*	*28*	*0.05*	*420*	*163*	*0.61*	*2.2*	*0.36*	*0.02*	*0.02*	*710*	*0.01*	*8.2*	*147*
G6949	Mean (10)	11	ME	0.32	2.6	ME	0.09	8922	16	0.09	ME	283	15	3.0	0.12	-	0.10	13	0.65	19	2821
Tet, Cp	*St. Dev.*	*7.9*	*ME*	*0.31*	*2.8*	*ME*	*0.07*	*2833*	*11*	*0.12*	*ME*	*47*	*5.9*	*2.5*	*0.13*	*-*	*0.08*	*4.5*	*0.39*	*15*	*1101*
G11701	Mean (10)	1.1	ME	78	0.55	ME	0.05	134	13	0.07	ME	1124	0.14	5.1	0.12	0.02	0.04	192	0.02	6.1	23
Tet, Cp	*St. Dev.*	*0.64*	*ME*	*21*	*0.56*	*ME*	*0.05*	*36*	*14*	*0.07*	*ME*	*902*	*0.05*	*7.5*	*0.22*	*0.02*	*0.06*	*91*	*0.04*	*3.0*	*23*
G14246	Mean (10)	18	ME	3.0	0.23	ME	0.06	5264	-	0.06	ME	365	7.3	1.5	0.22	0.01	0.02	58	0.08	3.2	2269
Tet, Cp	*St. Dev.*	*13*	*ME*	*1.4*	*0.13*	*ME*	*0.05*	*3493*	*-*	*0.06*	*ME*	*63*	*4.5*	*1.0*	*0.26*	*0.01*	*0.01*	*29*	*0.08*	*3.2*	*1035*
G14867	Mean (10)	0.36	ME	146	0.54	16,696	0.07	ME	376	0.15	70	183	3.0	0.68	0.34	-	0.02	5310	0.14	3.0	3768
Ten, Cp	*St. Dev.*	*0.15*	*ME*	*3.6*	*0.49*	*903*	*0.05*	*ME*	*293*	*0.12*	*20*	*19*	*0.35*	*0.44*	*0.53*	*-*	*0.01*	*3594*	*0.18*	*0.91*	*1038*
Mo16	Mean (3)	15	ME	7.0	1.7	8795	0.06	ME	11	0.01	ME	1213	0.03	0.10	2.0	-	0.02	31	0.03	2.2	2.7
Cp, Tet, (Gn)	*St. Dev.*	*6.6*	*ME*	*12*	*2.9*	*6021*	*0.09*	*ME*	*3.4*	*0.02*	*ME*	*599*	*0.01*	*0.04*	*1.2*	*-*	*0.02*	*10*	*0.06*	*1.0*	*1.0*
G29851	Mean (10)	0.88	ME	78	1.1	ME	0.10	ME	33	1.0	909	535	0.31	0.91	1.7	0.07	0.11	ME	0.12	108	1361
Cp, Ten	*St. Dev.*	*0.79*	*ME*	*28*	*0.75*	*ME*	*0.10*	*ME*	*22*	*1.0*	*382*	*97*	*0.12*	*0.77*	*1.3*	*0.07*	*0.22*	*ME*	*0.21*	*89*	*1471*
ORV4	Mean (10)	29	ME	3.3	1.9	ME	0.02	ME	12	0.19	1409	1269	4.5	0.07	3.0	-	-	37	0.01	2.9	140
Cp, Tet	*St. Dev.*	*29*	*ME*	*2.7*	*1.6*	*ME*	*0.04*	*ME*	*4.5*	*0.31*	*274*	*395*	*2.3*	*0.06*	*4.9*	*-*	*-*	*21*	*0.02*	*2.1*	*136*
G12640	Mean (10)	79	ME	3.1	0.62	ME	0.08	ME	107	0.15	1301	658	0.34	2.6	7.1	0.03	0.03	1654	0.14	7.3	54
Ten	*St. Dev.*	*13*	*ME*	*0.49*	*0.47*	*ME*	*0.06*	*ME*	*22*	*0.18*	*185*	*39*	*0.05*	*1.2*	*2.7*	*0.03*	*0.03*	*329*	*0.22*	*2.3*	*12*
G13301	Mean (10)	1.0	ME	633	31	ME	0.27	ME	127	-	158	7005	2.7	0.66	3.4	0.03	0.02	1747	0.02	11	100
Tet	*St. Dev.*	*2.2*	*ME*	*18*	*26*	*ME*	*0.20*	*ME*	*43*	*-*	*27*	*991*	*0.79*	*0.60*	*2.7*	*0.03*	*0.02*	*322*	*0.02*	*6.1*	*49*
G15977	Mean (10)	9.2	ME	19	0.28	ME	0.11	ME	32	0.06	630	1488	0.04	0.77	1.0	-	0.18	321	0.01	3.9	10.9
Tet	*St. Dev.*	*2.0*	*ME*	*2.7*	*0.16*	*ME*	*0.11*	*ME*	*15*	*0.08*	*181*	*114*	*0.03*	*0.42*	*0.73*	*-*	*0.05*	*129*	*0.02*	*2.4*	*1.0*
G16835	Mean (10)	2.0	ME	85	0.88	ME	0.11	ME	12	0.14	3942	331	1.1	0.70	1.1	0.05	0.18	14,761	0.06	61	2385
Ten	*St. Dev.*	*2.8*	*ME*	*8.4*	*0.76*	*ME*	*0.10*	*ME*	*11*	*0.13*	*314*	*45*	*0.19*	*0.65*	*1.3*	*0.12*	*0.13*	*2281*	*0.08*	*24*	*770*
VFI031	Mean (10)	1019	153	-	0.16	ME	1.2	ME	624	0.17	ME	1095	6.9	6.1	3648	0.01	2.2	8965	0.22	67	1.7
Tet	*St. Dev.*	*236*	*57*	*-*	*0.10*	*ME*	*0.42*	*ME*	*213*	*0.34*	*ME*	*129*	*2.1*	*11*	*3185*	*0.01*	*1.1*	*3439*	*0.13*	*76*	*0.11*

Tet = tetrahedrite, *Ten* = tennantite, *Sp* = sphalerite, *Gn* = galena, *Cp* = chalcopyrite, *St. Dev.* = standard deviation. Minerals in brackets are very minor phases. (X) = number of individual spot analyses in that sample. Dash = insufficient data to perform calculation (all analyses <mdl). Other <mdl values were treated as mdl/2. ME = major/minor element (concentration from EPMA > 1 wt %). * Evidence suggests sulphides in sample did not co-crystallize (based on textures and partitioning trends among base metal sulphides).

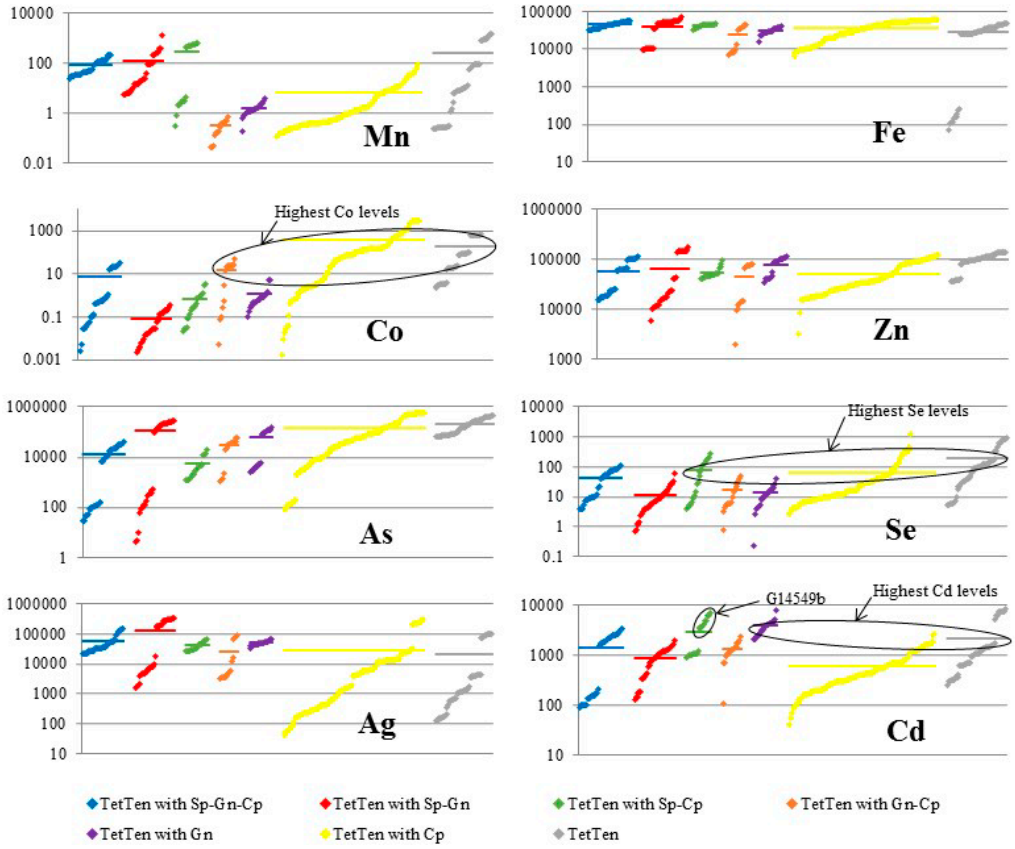

Figure 4. Cumulative plots showing individual spot concentrations of Mn, Fe, Co, Zn, As, Se, Ag and Cd in tetrahedrite-tennantite from different assemblages. Tetrahedrite-tennantite concentration data for each assemblage is sorted in ascending order and plotted in succession along the *X* axis. *Y* axis = concentration (parts per million). The average composition for each assemblage is given as a horizontal coloured line. TetTen = tetrahedrite-tennantite, Sp = sphalerite, Gn = galena, Cp = chalcopyrite.

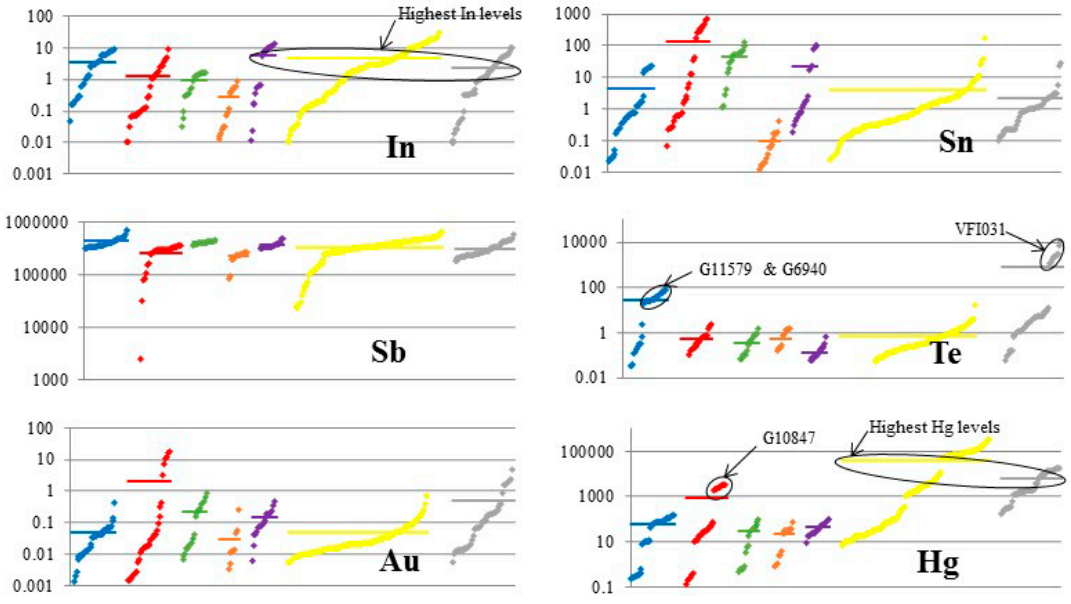

Figure 5. *Cont.*

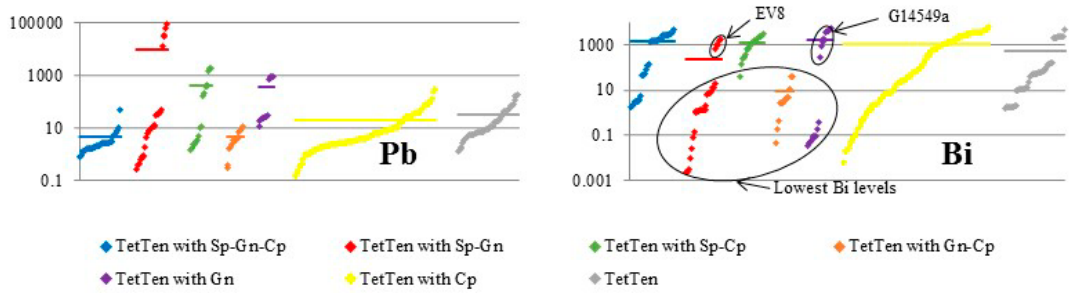

Figure 5. Cumulative plots showing individual spot concentrations of In, Sn, Sb, Te, Au, Hg, Pb, and Bi in tetrahedrite-tennantite from different assemblages. Tetrahedrite-tennantite concentration data for each assemblage is sorted in ascending order and plotted in succession along the *X* axis. *Y* axis = concentration (parts per million). The average composition for each assemblage is given as a horizontal coloured line.

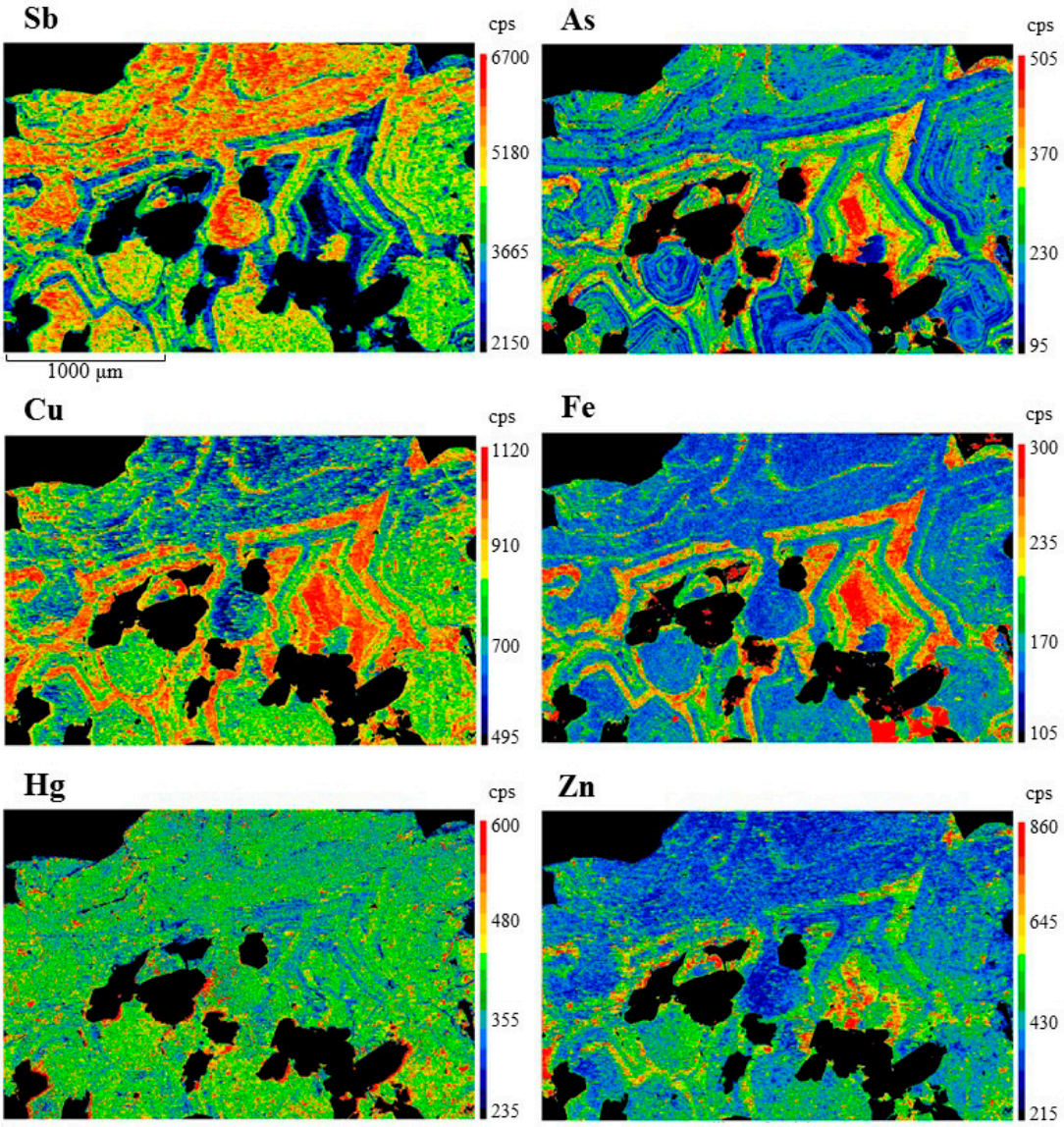

Figure 6. Electron probe microanalysis element maps showing chemical zoning of Sb, As, Cu, Fe, Hg, and Zn in tetrahedrite from sample G871 (Pulganbar, Grafton, NSW, Australia). Scales are in counts per second (cps).

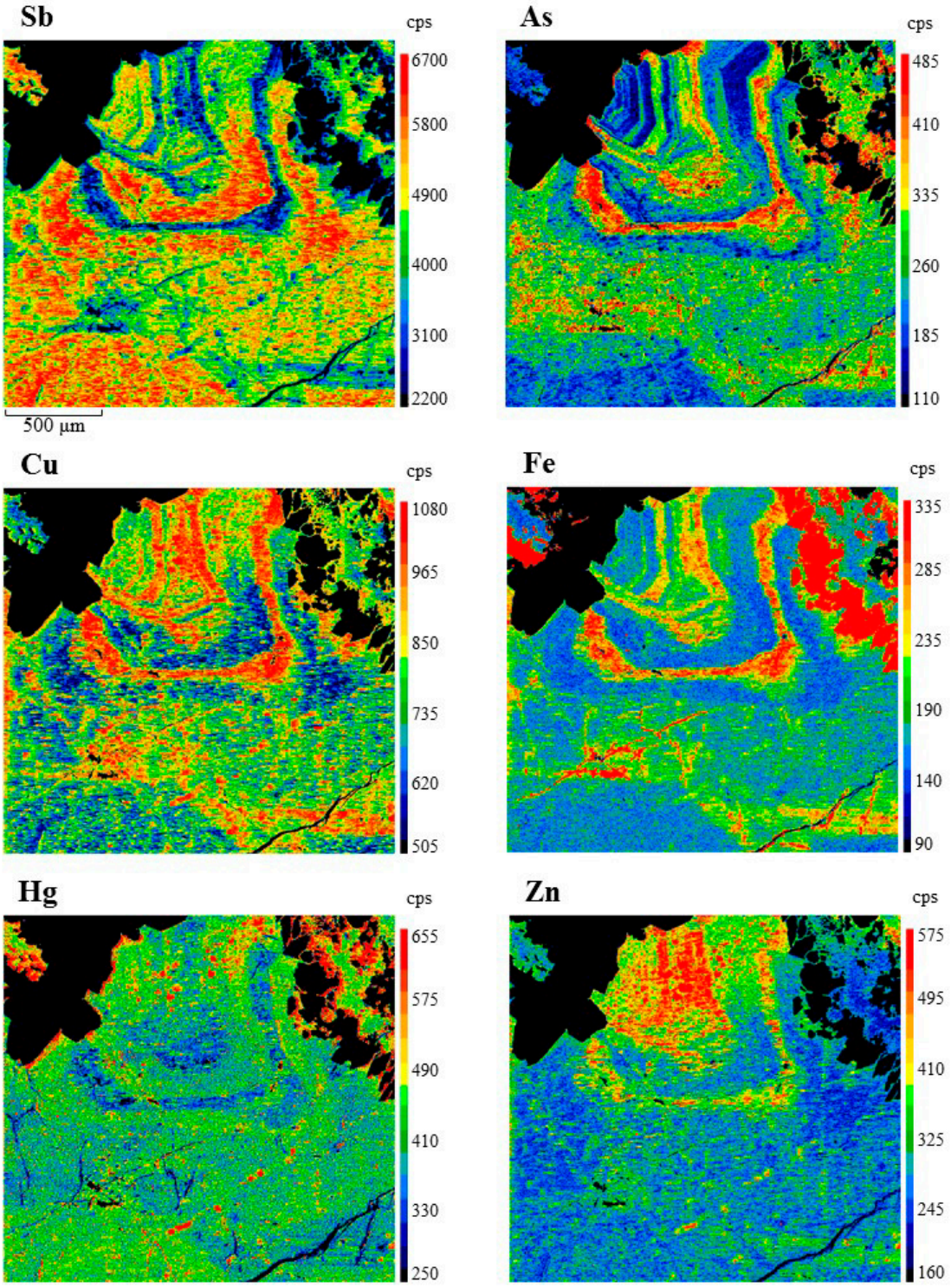

Figure 7. Electron probe microanalysis element maps showing chemical zoning of Sb, As, Cu, Fe, Hg, and Zn in tetrahedrite from sample G871 (Pulganbar, Grafton, NSW, Australia). Scales are in counts per second (cps).

Apart from Fe and Zn, Hg and Pb are the two most common divalent cations determined as present in tetrahedrite-tennantite. 10.6 wt % Hg and 4 wt % Pb are the highest measured levels of the two elements in tetrahedrite-tennantite, measured in samples G871 (Pulganbar, Grafton, NSW, Australia) and Mo17A (Mofjell, Norway), respectively. Tetrahedrite-tennantite (TetTen) crystallizing

in isolation, or with chalcopyrite (Cp; i.e., TetTen-Cp assemblages), hosts the most Hg (see Hg plot in Figure 5). While those tetrahedrite-tennantites crystallizing with sphalerite (Sp) and galena (Gn; TetTen-Sp-Gn assemblages) also host high levels of Hg, this trend is swayed by one population of Hg-rich tetrahedrites from sample G10847 (Mt. Camel, Heathcote, Australia; see Hg plot in Figure 5). The tetrahedrite in this sample co-crystallized with the most Hg-rich sphalerite of any sample here, implying a particularly Hg-rich crystallization environment. Thus, excluding this one sample, the highest Hg concentrations are present in tetrahedrite-tennantite, crystallizing without sphalerite or galena, which is in close agreement with Hg partitioning trends outlined in George et al. (2016) [30], where sphalerite is the preferred Hg host in BMS assemblages.

Cadmium, cobalt, and manganese are the other common divalent cations in tetrahedrite-tennantite. All may be present at concentrations greater than 1000 ppm. Whereas the EPMA data shows 0.674 wt % Cd in sample G6951 (Yerranderie, NSW, Australia), the LA-ICP-MS data shows almost 30,000 ppm in the same sample, hinting at heterogeneity from area to area of the sample. The highest Co and Mn in tetrahedrite-tennantite here is 0.362 wt % and 0.107 wt %, in samples G16152 (Siegen, Westphalia, Germany) and VF1031 (Emperor Gold Mine, Fiji), respectively. The LA-ICP-MS data for these samples is in close agreement. Cadmium concentrations are highest in tetrahedrite-tennantite that has not crystallized with sphalerite or chalcopyrite (see Cd plot in Figure 4). This is anticipated since Cd displays a strong preference for the sphalerite structure in BMS systems [30]. The only exception is the tetrahedrite from sample G14549b (Consols Mine, Broken Hill, NSW, Australia), which co-crystalized with sphalerite hosting up to 10,000 ppm Cd (see Cd plot in Figure 4). The exceptionally Cd-rich environment this assemblage formed in explains the high Cd concentrations in tetrahedrite, even though sphalerite co-crystallized. In a similar way, Co concentrations are also highest in those tetrahedrite-tennantites that have not crystallized with sphalerite (see Co plot in Figure 4), in line with findings reported by George et al. (2016) [30].

Tetrahedrite in sample VFI031 (Emperor Gold Mine, Fiji) contains as much as 3648 ppm Te, the highest concentration measured in this study. Apart from this sample, and two samples from the Kalgoorlie ore district, Western Australia (G11579 and G6940 with tetrahedrites containing 50 and 38 ppm Te, respectively), the mean Te concentrations in all tetrahedrite-tennantites from all assemblages are remarkably constant around the 1 ppm level (see Te plot in Figure 5).

Bismuth concentrations exceed 1000 ppm in tetrahedrite-tennantites from all assemblages except those co-crystallizing with galena and chalcopyrite, where concentrations only exceed 10 ppm in two spots. Bismuth concentrations in tetrahedrite-tennantite from TetTen-Sp-Gn and TetTen-Gn assemblages are also very low if samples EV8 (Evelyn Mine, NT, Australia) and G14549a (Consols Mine, Broken Hill, NSW, Australia) are excluded, both of which contain galena with up to 10,000 ppm Bi (see Bi plot in Figure 5). The Bi-rich galena co-crystallizing with high Bi tetrahedrite points at particularly Bi-rich crystallization environments for these samples. Such samples are anomalous for the otherwise Bi-depleted tetrahedrite-tennantites in TetTen-Sp-Gn and TetTen-Gn assemblages (see Bi plot in Figure 5). As shown in George et al. (2016) [30], the presence of galena can be considered the cause of this Bi depletion in tetrahedrite-tennantite since it is the preferred host of Bi in BMS assemblages.

Tetrahedrite-tennantite typically hosts between 0.1 and 1000 ppm Se. The most Se-rich tetrahedrite is recorded in sample VFI031 (Emperor Gold Mine, Fiji; 624 ppm). In general, the highest levels of Se in tetrahedrite-tennantite are reached when galena does not co-crystallize; i.e., from TetTen, TetTen-Sp-Cp, and TetTen-Cp assemblages (see Se plot in Figure 4). This is to be expected since galena is always the preferred host of Se in BMS assemblages [30].

Tin concentrations in tetrahedrite-tennantite are usually an order of magnitude lower than those of Se (typically between 0.01 and 100 ppm); they are the highest in EV8 (Evelyn Mine, NT, Australia; 404 ppm). Interestingly, the EPMA data records up to 0.264 wt % Sn in the tetrahedrite from EV8, though this may be due to inclusions of a Sn-rich phase (possibly stannite), since some were recognized on LA-ICP-MS downhole spectra from this sample.

The concentrations of Ni, In, Au, Tl, Mo and Ga are rarely, if ever, greater than 10 ppm in tetrahedrite-tennantite. The highest mean concentrations for these elements in tetrahedrite-tennantite are 31 ppm Ni (G13301; Allihies Mine, Castletown, Cork, Ireland), 15 ppm In (G879; Ring Valley, Tas., Australia, and G6949; Webb's Ag Mine, Emmaville, NSW, Australia), 11 ppm Au (Hj14; Herja, Romania), 3.7 ppm Tl (EV8; Evelyn Mine, NT, Australia), 1.9 ppm Mo (G16152; Siegen, Westphalia, Germany) and 1.2 ppm Ga (VFI031; Emperor Gold Mine, Fiji). Measured W concentrations never exceeded 1 ppm. The highest In concentrations are recorded in tetrahedrite-tennantites that crystallize without any sphalerite observed nearby (excluding 4-component assemblages); i.e., in TetTen-Gn, TetTen-Cp and TetTen assemblages (see In plot in Figure 5). This is concordant with George et al. (2016) [30] where sphalerite was shown to be the typical preferred host of In.

5. Discussion

5.1. Element Partitioning Between Tetrahedrite-Tennantite, Sphalerite, Galena, and Chalcopyrite

Figure 8 is a series of tri-plots that show where various elements are hosted in co-crystallized three-component assemblages in which one component is tetrahedrite-tennantite. Each individual point is a sample average, and where it plots shows how much of a given element is contained within the sulphides of that assemblage as a fraction of the overall amount of that element in the assemblage (using molar percentages for comparisons between sulphides). For example, in TetTen-Sp-Gn assemblages, sphalerite always concentrates more than 60% of the Mn budget, no more than 40% is ever contained in tetrahedrite-tennantite, and co-crystallizing galena essentially contains none of the available Mn. In the TetTen-Sp-Cp assemblage, sphalerite again always concentrates >50% of the Mn budget. We can thus say that whenever sphalerite is present, it is always the primary Mn host.

Apart from cases where chalcopyrite (or other Fe-sulphides such as pyrite and pyrrhotite) co-crystallizes, Fe is always hosted in either tetrahedrite-tennantite or sphalerite. In most cases tetrahedrite-tennantite is the primary host, but in four TetTen-Sp-Gn assemblages, sphalerite hosts > 50% of the Fe budget. Cobalt does not have a strong affiliation with any of the four sulphides, although it is never primarily hosted in chalcopyrite. In the absence of sphalerite, Zn always partitions to tetrahedrite-tennantite. Gallium seems to be most affiliated with sphalerite, although in TetTen-Sp-Cp assemblages, chalcopyrite hosts the larger share of Ga in four samples. Two of these samples (V446 and V538) come from the Bleikvassli deposit, Norway, a sedimentary-exhalative deposit which is interpreted to have recrystallized at conditions of granulite facies [82,83]. The other two (G6940 and G11579) come from Kalgoorlie, Western Australia, where Boulter et al. (1987) [84] describe recrystallization of pyrite during deformation associated with regional metamorphism. Thus, those assemblages in which chalcopyrite hosts more Ga than sphalerite, both come from environments where sulphides have recrystallized under regional metamorphism. Such conditions result in chalcopyrite becoming the primary Ga host, distinct from lower temperature/pressure environments where sphalerite is the preferred host [30,72].

Selenium is always concentrated in galena whenever that mineral is present, and tetrahedrite-tennantite seems to be the secondary host in most cases. Tetrahedrite-tennantite typically hosts > 90% of the Ag budget whenever it co-crystallizes with any combination of BMS. In all but one sample, Cd is principally hosted in sphalerite when present. In the single exception (sample G10847; Mt. Camel, Heathcote, Australia), tetrahedrite-tennantite is the preferred host. The same is true in assemblages in which sphalerite is absent.

As is the case in the three-component Sp-Gn-Cp assemblage, Sn does not have a strong affiliation with any sulphide [30]. It is concentrated in different phases in different samples. In most cases, however, Sn seems to prefer the BMS over tetrahedrite-tennantite. Tellurium has a strong affiliation with galena, while Hg appears to be preferentially incorporated into either sphalerite or tetrahedrite-tennantite in different samples. Galena will concentrate Bi whenever it is present, and in its absence tetrahedrite-tennantite always becomes the primary host.

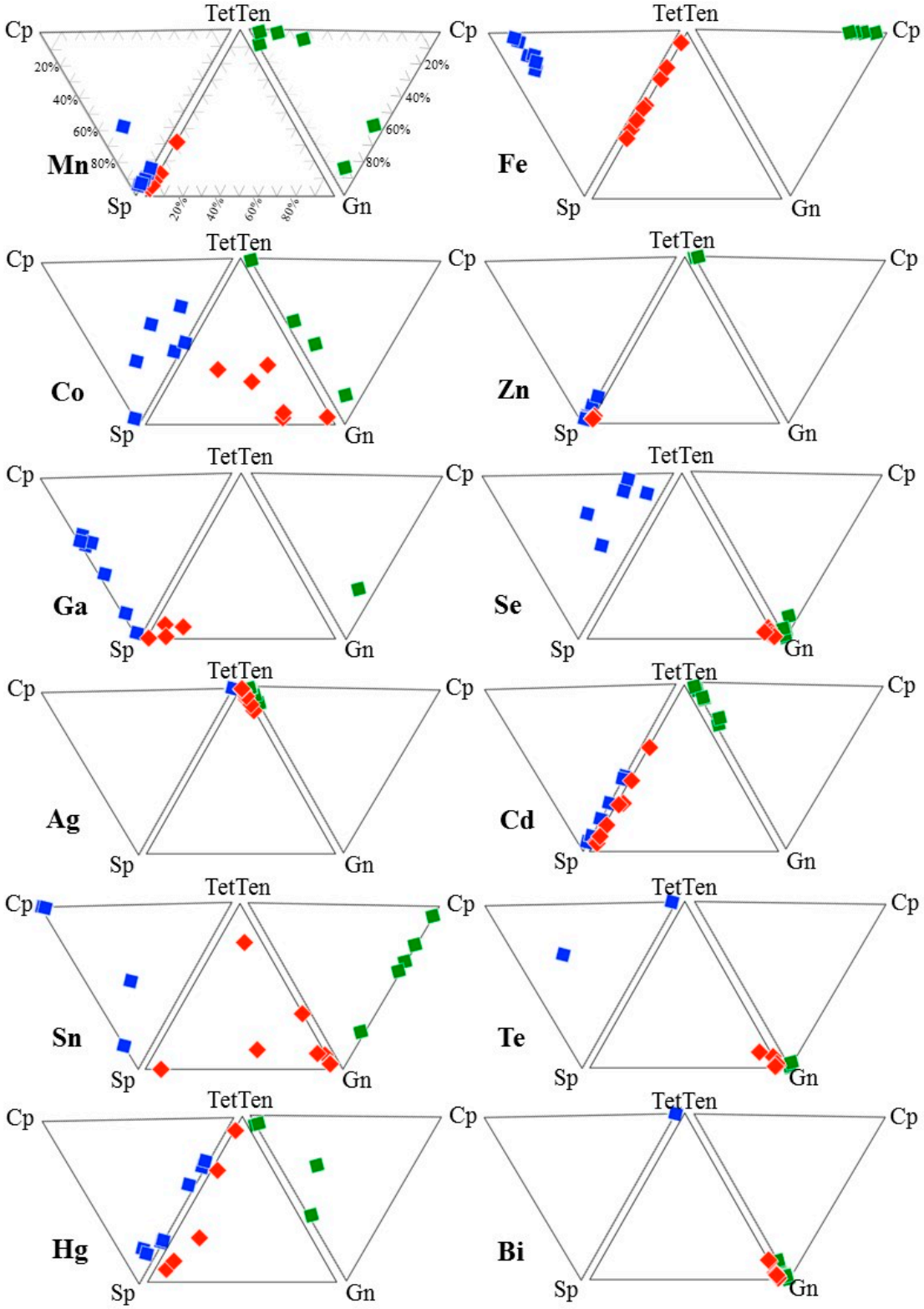

Figure 8. Series of tri-plots that show where the Mn, Fe, Co, Zn, Ga, Se, Ag, Cd, Sn, Te, Hg, and Bi budget is hosted in co-crystallized three-component assemblages comprising tetrahedrite-tennantite. Each individual point is a sample, and where it plots shows how much of a given element is contained within the sulphides of that assemblage as a fraction of the overall amount of that element in the assemblage (using molar percentages for comparisons between sulphides). TetTen = tetrahedrite-tennantite, Sp = sphalerite, Gn = galena, Cp = chalcopyrite.

5.2. Controls on Fe and Hg Partitioning

Both tetrahedrite-tennantite and sphalerite may be the primary host phase for Fe and Hg in different samples (excluding, of course, samples containing Fe-sulphides). Which mineral will host a greater molar percentage of Fe or Hg in a given system seems to depend on the amount of that element available in the system. In systems with lesser Fe, tetahedrite-tennantite is the primary Fe host, indicating that Fe prefers to partition into tetrahedrite-tennantite relative to sphalerite (Figure 9a). Sphalerite is the primary host of Fe only in those systems where Fe concentrations in tetrahedrite-tennantite approach 2 *apfu*, i.e., the maximum concentration of Fe allowed in the tetrahedrite-tennantite structure ([4]; Figure 9b). Thus, in assemblages free of Fe-sulphides, if there is more Fe than can be incorporated by tetrahedrite-tennantite, then the excess will partition to sphalerite such that sphalerite may host more Fe than tetrahedrite-tennantite.

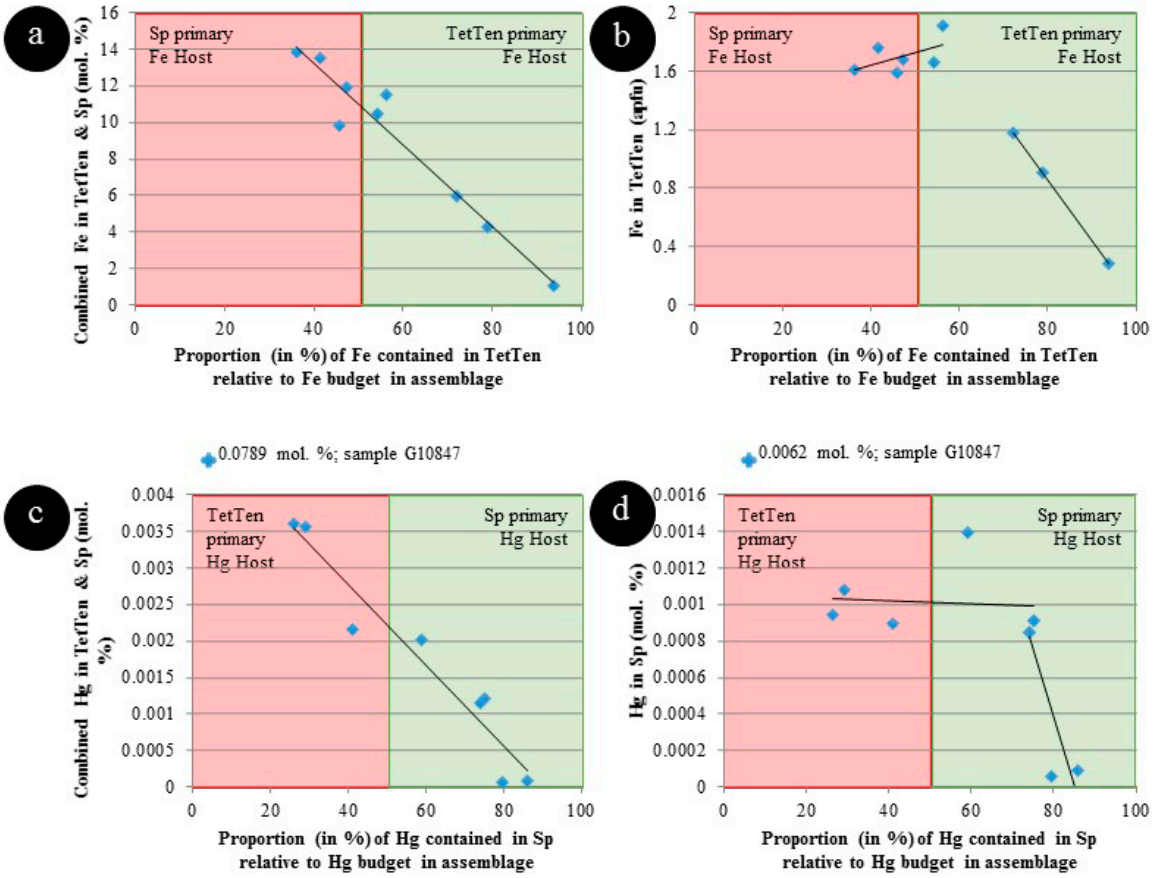

Figure 9. Scatter-plots that show the primary host of Fe and Hg depends on the concentration of Fe and Hg in tetrahedrite-tennantite and sphalerite. (**a**) Fe in tetrahedrite-tennantite and sphalerite vs. Fe in tetrahedrite-tennantite as a % of the assemblage Fe budget. (**b**) Fe in tetrahedrite-tennantite vs. Fe in tetrahedrite-tennantite as a % of the assemblage Fe budget. (**c**) Hg in tetrahedrite-tennantite and sphalerite vs. Hg in sphalerite as a % of the assemblage Hg budget. (**d**) Hg in sphalerite vs. Hg in sphalerite as a % of the assemblage Hg budget. TetTen = tetrahedrite-tennantite, Sp = sphalerite.

Similar patterns are observed for Hg. In systems with lesser Hg, sphalerite is the primary Hg host, indicating that Hg preferentially partitions into sphalerite (Figure 9c). Tetrahedrite-tennantite is the primary host of Hg only in those systems where Hg concentrations in sphalerite are ~0.001 mol% (Figure 9d). The present dataset may thus indicate that this is an approximate upper limit to Hg concentrations in sphalerite, at least when co-crystallizing with tetrahedrite-tennantite. Only in one sample is the concentration of Hg in sphalerite significantly higher than this; sample G10847

(Mt. Camel, Heathcote, VIC, Australia) which concentrates 0.0062 mol% Hg in sphalerite (equivalent to ~250 ppm Hg), and where co-crystallizing tetrahedrite hosts more than 0.07 mol% Hg (>2500 ppm Hg equivalent). This is the most Hg in any tetrahedrite-tennantite co-crystallizing with sphalerite analysed here. This particularly Hg-rich system seems to allow for exceptional Hg concentrations in sphalerite. In any case, if a given system contains more Hg than can be incorporated by sphalerite, then the excess will partition to tetrahedrite such that tetrahedrite may host more Hg than sphalerite.

6. Implications and Conclusions

This study shows that tetrahedrite-tennantite is a significant carrier of a range of trace elements at concentrations measurable using contemporary instrumentation. This should be recognized when establishing protocols for trace element analysis of tetrahedrite-tennantite, and when assessing the primary hosts for trace elements of interest in any given assemblage, e.g., for geometallurgical purposes. Most noteworthy, tetrahedrite-tennantite will always be the primary host of Ag in co-crystallizing BMS assemblages. Iron, Cu, Zn, As, Cd, Sb, Hg, and Bi are the additional elements that are controlled to some degree by the presence of tetrahedrite-tennantite. In contrast, tetrahedrite-tennantite does not appear, from the data here, to be a very good host for the critical metals Ga, In, and Sn, all of which prefer to partition to co-crystallizing BMS.

As an extension of arguments put forward by George et al. (2016) [30], the partitioning trends outlined here may be used as a tool to assess co-crystallization of a given TetTen ± Sp ± Gn ± Cp assemblage. If the hosts of various trace elements in such an assemblage do not match the preferred hosts outlined in Table 5, then it strongly suggests that assemblage did not co-crystallize. On the other hand, if the primary hosts do match those given here, that is typically suggestive of a co-crystallized assemblage.

Table 5. Preferred hosts of various trace elements in a co-crystallizing TetTen-Sp-Gn-Cp assemblage.

Trace Element	**Mn**	**Fe**	**Cu**	**Zn**
Preferred Host	Sp [1]	TetTen >Sp [3]	TetTen >Sp [3]	TetTen [1]
Trace Element	**Ga**	**As**	**Se**	**Ag**
Preferred Host	Sp [2]	TetTen >Gn [1]	Gn [1]	TetTen >Gn [1]
Trace Element	**Cd**	**In**	**Sn**	**Sb**
Preferred Host	Sp >TetTen [3]	Sp > Cp [2]	? *	TetTen >Gn [1]
Trace Element	**Te**	**Hg**	**Tl**	**Bi**
Preferred Host	Gn [1]	Sp >TetTen [3]	Gn [1]	Gn >TetTen [1]

Abbreviations: TetTen = tetrahedrite-tennantite, Sp = sphalerite, Gn = galena, Cp = chalcopyrite. [1] Trend observed in all examined samples. [2] Recrystallization increases element concentration in Cp and may make Cp primary host. [3] Trend generally, yet not always, true. * Recrystallization increases Sn concentration in Cp such that Cp is usually primary host in recrystallized samples. Below recrystallization conditions, no trend is observed.

Supplementary Materials: The following are available online at www.mdpi.com/2075-163X/7/2/17/s1.

Acknowledgments: We are deeply grateful to Ben Grguric and Ben McHenry for providing relevant sample material from the South Australian Museum. Similarly, Anthony Milnes is thanked for providing access to Tate Museum collections. We are also appreciative of microanalysis support from Ben Wade and Aoife McFadden.

Author Contributions: Nigel J. Cook conceived the research within the framework of Luke L. George's Ph.D. project. Luke L. George acquired the samples, performed all analytical work reported here, and interpreted the data. Luke L. George, and Nigel J. Cook wrote the paper with contributions from Cristiana L. Ciobanu.

Conflicts of Interest: The authors declare no conflict of interest.

References

1. Wuensch, B.J. The crystal structure of tetrahedrite, $Cu_{12}Sb_4S_{13}$. *Zeitschrift Krist. Cryst. Mater.* **1964**, *119*, 437–453. [CrossRef]
2. Wuensch, B.J.; Tackeuchi, Y.; Nowacki, W. Refinement of the crystal structure of binnite, $Cu_{12}As_4S_{13}$. *Zeitschrift Krist. Cryst. Mater.* **1966**, *123*, 1–20. [CrossRef]

3. Makovicky, E.; Skinner, B. Studies of the sulfosalts of copper. VII. Crystal structures of the exsolution products $Cu_{12.3}Sb_4S_{13}$ and $Cu_{13.8}Sb_4S_{13}$ of unsubstituted synthetic tetrahedrite. *Can. Mineral.* **1979**, *17*, 619–634.
4. Moëlo, Y.; Makovicky, E.; Mozgova, N.N.; Jambor, J.L.; Cook, N.J.; Pring, A.; Paar, W.; Nickel, E.H.; Graeser, G.; Karup-Møller, S.; et al. Sulfosalt systematics: A review. Report of the sulfosalt sub-committee of the IMA commission on ore mineralogy. *Eur. J. Mineral.* **2008**, *20*, 7–46. [CrossRef]
5. Repstock, A.; Voudouris, P.; Kolitsch, U. New occurrences of watanabeite, colusite, "arsenosulvanite" and "Cu-excess" tetrahedrite-tennantite at the Pefka high-sulfidation epithermal deposit, northeastern Greece. *Neues Jahrb. Miner. Abh. J. Miner. Geochem.* **2015**, *192*, 135–149. [CrossRef]
6. Repstock, A.; Voudouris, P.; Zeug, M.; Melfos, V.; Zhai, M.; Li, H.; Kartal, T.; Matuszczak, J. Chemical composition and varieties of fahlore-group minerals from Oligocene mineralization in the Rhodope area, Southern Bulgaria and Northern Greece. *Mineral. Petrol.* **2016**, *110*, 103–123. [CrossRef]
7. Makovicky, E.; Karanović, L.; Poleti, D.; Balić-Žunić, T.; Paar, W.H. Crystal structure of copper-rich unsubstituted tennantite, $Cu_{12.5}As_4S_{13}$. *Can. Mineral.* **2005**, *43*, 679–688. [CrossRef]
8. Sack, R.O.; Loucks, R.R. Thermodynamic properties of tetrahedrite-tennantites: Constraints on the interdependence of the Ag ↔ Cu, Fe ↔ Zn, Cu ↔ Fe, and As ↔ Sb exchange reactions. *Am. Mineral.* **1985**, *70*, 1270–1289.
9. Johnson, N.E.; Craig, J.R.; Rimstidt, J.D. Compositional trends in tetrahedrite. *Can. Mineral.* **1986**, *24*, 385–397.
10. Makovicky, E.; Karup-Möller, S. Exploratory studies on substitution of minor elements in synthetic tetrahedrite. Part I. Substitution by Fe, Zn, Co, Ni, Mn, Cr, V and Pb. Unit-cell parameter changes on substitution and the structural role of "Cu^{2+}". *Neues Jahrb. Miner. Abh.* **1994**, *167*, 89–123.
11. Hackbarth, C.J.; Petersen, U. A fractional crystallization model for the deposition of argentian tetrahedrite. *Econ. Geol.* **1984**, *79*, 448–460. [CrossRef]
12. Kovalenker, V.A.; Bortnikov, N.S. Chemical composition and mineral associations of sulphosalts in the precious metal deposits from different geological environment. *Geol. Carpathica* **1985**, *36*, 283–291.
13. Staude, S.; Mordhorst, T.; Neumann, R.; Prebeck, W.; Markl, G. Compositional variation of the tennantite-tetrahedrite solid-solution series in the Schwarzwald ore district (SW Germany): The role of mineralization processes and fluid source. *Mineral. Mag.* **2010**, *74*, 309–339. [CrossRef]
14. Apopei, A.I.; Damian, G.; Buzgar, N.; Buzatu, A. Mineralogy and geochemistry of Pb-Sb/As-sulfosalts from Coranda-Hondol ore deposit (Romania)—Conditions of telluride deposition. *Ore Geol. Rev.* **2016**, *72*, 857–873. [CrossRef]
15. Peterson, R.C.; Miller, I. Crystal structure and cation distribution in freibergite and tetrahedrite. *Mineral. Mag.* **1986**, *50*, 717–721. [CrossRef]
16. Pfitzner, A.; Evain, M.; Petricek, V. $Cu_{12}Sb_4S_{13}$: A temperature-dependent structure investigation. *Acta Cryst.* **1997**, *B53*, 337–345. [CrossRef]
17. Rozhdestvenskaya, I.V.; Zayakina, N.V.; Samusikov, V.P. Crystal structure features of minerals from the tetrahedrite-freibergite series. *Mineral. Zhurnal* **1993**, *15*, 9–17. (In Russian)
18. Johan, Z.; Kvaček, M. La hakite, un nouveau minéral du groupe de la tétraédrite. *Bull. Soc. Fr. Minéral.* **1971**, *94*, 45–48. (In French)
19. Johan, Z.; Picot, P.; Ruhlmann, F. Evolution paragénétique de la minéralisation uranifère de Chaméane (Puy-de-Dôme) France: Chaméanite, geffroyite et giraudite, trois séléniures nouveaux de Cu, Fe, Ag, and As. *Tscher. Miner. Petrog. Mitt.* **1982**, *29*, 151–167. (In French) [CrossRef]
20. Kalbskopf, R. Synthese und Kristallstruktur von $Cu_{12-x}Te_4S_{13}$, dem Tellur-Endglied der Fahlerze. *Tscher. Miner. Petrog. Mitt.* **1974**, *21*, 1–10. (In German) [CrossRef]
21. Dmitrieva, M.T.; Bojik, G.B. The crystallochemical mechanism of formation of vacancies in goldfieldite structure. *Zeitschrift Krist.* **1988**, *185*, 601.
22. Trudu, A.G.; Knittel, U. Crystallography, mineral chemistry and chemical nomenclature of goldfeldite, the tellurian member of the tetrahedrite solid-solution series. *Can. Mineral.* **1998**, *36*, 1115–1137.
23. Spiridonov, E.M.; Sokolova, N.F.; Gapeyev, A.K.; Dashevskaya, D.M.; Yevstigneyeva, T.L.; Chvileva, T.N.; Demidov, V.G.; Balashov, Y.P.; Shul'ga, V.I. The new mineral argentotennantite. *Dokl. Akad. Nauk SSSR* **1986**, *290*, 206–210. (In Russian)
24. Zhdanov, Y.Y.; Amuzinskii, V.A.; Andrianov, N.G. Discovery of a natural Ag-rich fahlore with the highest parameter of the unit cell. *Dokl. Akad. Nauk SSSR* **1992**, *326*, 337–340. (In Russian)

25. Karup-Møller, S. Exploratory studies on element substitutions in synthetic tetrahedrite. Part V. Mercurian tetrahedrite. *Neues Jahrb. Miner. Abh.* **2003**, *179*, 73–83. [CrossRef]
26. Karup-Møller, S.; Makovicky, E. Exploratory studies of element substitutions in synthetic tetrahedrite. Part II. Selenium and tellurium as anions in Zn-Fe tetrahedrites. *Neues Jahrb. Miner. Abh.* **1999**, *9*, 385–399.
27. Karup-Møller, S.; Makovicky, E. Exploratory studies of the solubility of minor elements in tetrahedrite: VI. Zinc and the combined zinc-mercury and iron-mercury substitutions. *Neues Jahrb. Miner. Mon.* **2004**, *11*, 508–524. [CrossRef]
28. Hansen, M.K.; Makovicky, E.; Karup-Møller, S. Exploratory studies on substitutions in tennantite-tetrahedrite solid solution. Part IV. Substitution of germanium and tin. *Neues Jahrb. Miner. Abh. J. Miner. Geochem.* **2003**, *179*, 43–71. [CrossRef]
29. Klünder, M.H.; Karup-Møller, S.; Makovicky, E. Exploratory studies on substitutions in the tetrahedrite-tennantite solid solution series Part III. The solubility of bismuth in tetrahedrite-tennantite containing iron and zinc. *Neues Jahrb. Miner. Mon.* **2003**, *2003*, 153–175. [CrossRef]
30. George, L.L.; Cook, N.J.; Ciobanu, C.L. Partitioning of trace elements in co-crystallized sphalerite–galena–chalcopyrite hydrothermal ores. *Ore Geol. Rev.* **2016**, *77*, 97–116. [CrossRef]
31. Foit, F.F., Jr.; Hughes, M.J. Structural variations in mercurian tetrahedrite. *Am. Mineral.* **2004**, *89*, 159–163. [CrossRef]
32. Johnson, M.L.; Burnham, C.W. Crystal structure refinement of an arsenic-bearing argentian tetrahedrite. *Am. Mineral.* **1985**, *70*, 165–170.
33. Johnson, N.E.; Craig, J.R.; Rimstidt, J.D. Crystal chemistry of tetrahedrite. *Am. Mineral.* **1988**, *73*, 389–397.
34. Pattrick, R.A.D.; Hall, A.J. Silver substitution into synthetic zinc, cadmium and iron tetrahedrites. *Mineral. Mag.* **1983**, *47*, 441–451. [CrossRef]
35. Charnock, J.M.; Garner, C.D.; Pattrick, R.A.D.; Vaughan, D.J. Co-ordination sites of metals in tetrahedrite minerals determined by EXAFS. *J. Solid State Chem.* **1989**, *82*, 279–289. [CrossRef]
36. Charnock, J.M.; Garner, C.D.; Pattrick, R.A.D.; Vaughan, D.J. EXAFS and Mössbauer spectroscopic study of Fe-bearing tetrahedrites. *Mineral. Mag.* **1989**, *53*, 193–199. [CrossRef]
37. Pattrick, R.A.D.; van der Lann, G.; Vaughan, D.J.; Henderson, C.M.B. Oxidation state and electronic configuration determination of copper in tetrahedrite group minerals by L-edge X-ray absorption spectroscopy. *Phys. Chem. Miner.* **1993**, *20*, 395–401. [CrossRef]
38. Oen, I.S.; Kieft, C. Bismuth-rich tennantite and tetrahedrite in the Mangualde pegmatite, Viseu district, Portugal. *Neues Jahrb. Miner. Mon.* **1976**, *2*, 94–96.
39. Bortnikov, N.S.; Kudryavtsev, A.S.; Troneva, N.V. Bi-rich tetrahedrite from the Tary-Ekan deposit (East Karamazar, central Asia). *Mineral. Zhurnal* **1979**, *198*, 61–64. (In Russian)
40. Kieft, K.; Eriksson, G. Regional zoning and metamorphic evolution of the Vindfall Pb-Zn ore, east central Sweden. *GFF* **1984**, *106*, 305–317. [CrossRef]
41. Spiridonov, E.M.; Chvileva, T.N.; Borodaev, Y.S.; Vinogradova, R.A.; Kononov, O.V. The influence of bismuth on optical properties of gray copper. *Dokl. Akad. Nauk SSSR* **1986**, *290*, 1475–1478. (In Russian)
42. Breskovska, V.V.; Tarkian, M. Compositional variation in Bi-bearing fahlores. *Neues Jahrb. Miner. Mon.* **1994**, *5*, 230–240.
43. Gołębiowska, B.; Pieczka, A.; Parafiniuk, J. Substitution of Bi for Sb and As in minerals of the tetrahedrite series from Rędziny, Lower Silesia, southwestern Poland. *Can. Mineral.* **2012**, *50*, 267–279. [CrossRef]
44. Nash, J.T. Geochemical studies in the Park City District; II, Sulfide mineralogy and minor-element chemistry, Mayflower Mine. *Econ. Geol.* **1975**, *70*, 1038–1049. [CrossRef]
45. Basu, K.; Bortnykov, N.; Mookherjee, A.; Mozgova, N.; Tsepin, A.I. Rare minerals from Rajpura-Dariba, Rajasthan, India III: Plumbian tetrahedrite. *Neues Jahrb. Miner. Abh.* **1981**, *141*, 280–289.
46. Mozgova, N.N.; Tsepin, A.I. *Fahlore (Features of Chemical Composition and Properties)*; Nauka: Moscow, Russia, 1983; p. 279. (In Russian)
47. Moh, G.H. Sulfosalts: Observations and mineral descriptions, experiments and applications. *Neues Jahrb. Miner. Abh.* **1984**, *150*, 25–64.
48. Vavelidis, M.; Melfos, V. Two plumbian tetrahedrite-tennantite occurrences from Maronia area (Thrace) and Milos island (Aegean sea), Greece. *Eur. J. Mineral.* **1997**, *9*, 653–658.
49. Bishop, A.C.; Criddle, A.J.; Clark, A.M. Plumbian tennantite from Sark, Channel Islands. *Mineral. Mag.* **1977**, *41*, 59–63. [CrossRef]

50. Ixer, R.A.; Stanley, C.J. Silver mineralization at Sark's Hope mine, Sark, Channel Islands. *Mineral. Mag.* **1983**, *47*, 539–545. [CrossRef]
51. Förster, H.J.; Rhede, D.; Tischendorf, G. Continuous solid-solution between mercurian giraudite and hakite. *Can. Mineral.* **2002**, *40*, 1161–1170. [CrossRef]
52. Jurković, I.B.; Garašić, V.; Jurković, I.M. Geochemical characteristics of mercurian tetrahedrite, barite and fluorite from the Duboki Vagan, Glumac and Dubrave-Dugi Dol barite deposits, south of Kreševo, Mid-Bosnian Schist Mts. *Geol. Croat.* **2011**, *64*, 49–59. [CrossRef]
53. Basu, K.; Bortnykov, N.; Mookherjee, A.; Mozgova, N.; Sivtsov, A.V.; Tsepin, A.I.; Vrublevskaja, Z.V. Rare minerals from Rajpura-Dariba, Rajasthan, India V: The first recorded occurrence of a manganoan fahlore. *Neues Jahrb. Miner. Abh.* **1984**, *149*, 105–112.
54. Voropayev, A.V.; Spiridonov, E.M.; Shchibrik, V.I. Cd-Tetrahedrite, first find in the USSR. *Dokl. Acad. Sci. USSR* **1988**, *300*, 1446–1468.
55. Pattrick, R.A. Microprobe analyses of cadmium-rich tetrahedrites from Tyndrum, Perthshire, Scotland. *Mineral. Mag.* **1978**, *42*, 286–288. [CrossRef]
56. Pattrick, R.A. Pb-Zn and minor U mineralization at Tyndrum, Scotland. *Mineral. Mag.* **1985**, *49*, 671–681. [CrossRef]
57. Huiwen, J.D.F.Z.Z.; Chunpei, Z. The first Discovery of Cd-Freibergite in China. *Acta Mineral. Sin.* **1988**, *2*, 005.
58. Voudouris, P.C.; Spry, P.G.; Sakellaris, G.A.; Mavrogonatos, C. A cervelleite-like mineral and other Ag-Cu-Te-S minerals [Ag_2CuTeS and $(Ag, Cu)_2TeS$] in gold-bearing veins in metamorphic rocks of the Cycladic Blueschist Unit, Kallianou, Evia Island, Greece. *Mineral. Petrol.* **2011**, *101*, 169–183. [CrossRef]
59. Dobbe, R.T. Manganoan-cadmian tetrahedrite from the Tunaberg Cu-Co deposit, Bergslagen, central Sweden. *Mineral. Mag.* **1992**, *56*, 113–115. [CrossRef]
60. Kovalenker, V.A.; Rusinov, V.L. Goldfieldite: Chemical composition, parageneses and conditions of formation. *Mineral. Zhurnal* **1986**, *8*, 57–70. (In Russian)
61. Kase, K. Tellurian tennantite from the Besshitype deposits in the Sambagawa metamorphic belt, Japan. *Can. Mineral.* **1986**, *24*, 399–404.
62. Knittel, U. Composition and association of arsenian goldfieldite from the Marian gold deposit, Northern Luzon, Philippines. *Mineral. Petrol.* **1989**, *40*, 145–154. [CrossRef]
63. Shimizu, M.; Stanley, C.J. Coupled Substitutions in Goldfieldite-Tetrahedrite Minerals from the Iriki Mine, Japan. *Mineral. Mag.* **1991**, *55*, 515–551. [CrossRef]
64. Pohl, D.; Liessmann, W.; Okrugin, V.M. Rietveld analysis of selenium-bearing goldfieldites. *Neues Jahrb. Miner. Mon.* **1996**, *1996*, 1–8.
65. Pinto, A.; Ferreira, A.; Bowles, J.F.W.; Gaspar, O.C. Mineralogical and textural characterization of the Neves-Corvo ores. Metallogenetic implications. In *Geology and VMS Deposits of the Lberian Pyrite Belt*; Ser. 27; Baniga, F.J.A.S., Carvalho, D., Eds.; SEG Neves Corvo Field Conference: Lisbon, Portugal, 1997; p. 90.
66. Serranti, S.; Ferrini, V.; Masi, U.; Cabri, L.J. Trace-element distribution in cassiterite and sulfides from rubané and massive ores of the Corvo deposit, Portugal. *Can. Mineral.* **2002**, *40*, 815–835. [CrossRef]
67. Figueiredo, M.O.; Silva, T.P.; de Oliveira, D.P.S.; Rosa, D.R.N. Searching for In-carrier minerals in polymetallic sulphide deposits: Digging deeper into the crystal chemistry of indium chalcogenides. In *Digging Deeper, Proceedings of the 9th Biennial SGA Meeting, Ferrara, Italy, 29–31 August 2007*; Andrew, C.J., Ed.; Irish Association Economic Geologists: Dublin, Ireland, 2007; pp. 1355–1358.
68. McClenaghan, S.H.; Lentz, D.R.; Martin, J.; Diegor, W.G. Gold in the Brunswick No. 12 volcanogenic massive sulfide deposit, Bathurst Mining Camp, Canada: Evidence from bulk ore analysis and laser ablation ICP-MS data on sulfide phases. *Miner. Depos.* **2009**, *44*, 523–557. [CrossRef]
69. Gaspar, O.C. Mineralogy and sulfide mineral chemistry of the Neves-Corvo ores, Portugal: Insight into their genesis. *Can. Mineral.* **2002**, *40*, 611–636. [CrossRef]
70. Jurković, I.B.; Garašić, V.; Jurković, I.M. Cobalt, nickel, wolfram, cadmium, selenium, silver and gold-bearing mercurian tetrahedrite from the Saski Rad barite-siderite deposit in the Mid-Bosnian Schist Mts. *Geol. Croat.* **2011**, *64*, 223–237.
71. Wohlgemuth-Ueberwasser, C.C.; Viljoen, F.; Petersen, S.; Vorster, C. Distribution and solubility limits of trace elements in hydrothermal black smoker sulfides: An in-situ LA-ICP-MS study. *Geochim. Cosmochim. Acta* **2015**, *159*, 16–41. [CrossRef]

72. George, L.L.; Cook, N.J.; Crowe, B.B.P.; Ciobanu, C.L. Trace elements in hydrothermal chalcopyrite. *Mineral. Mag.* **2017**, in press.
73. Wilson, S.; Ridley, W.; Koenig, A. Development of sulphide calibration standards for the laser ablation inductively-coupled plasma mass spectrometry technique. *J. Anal. At. Spectrom.* **2002**, *17*, 406–409. [CrossRef]
74. United States Geological Survey. Microanalytical Reference Materials and Accessories. Available online: http://crustal.usgs.gov/geochemical_reference_standards/microanalytical_RM.html (accessed on 6 October 2016).
75. Van Achterbergh, E.; Ryan, C.; Jackson, S.; Griffin, W. Data reduction software for LA-ICP-MS: Laser-Ablation-ICPMS in the earth sciences—Principles and applications. *Mineral. Ass. Can.* **2001**, *29*, 239–243.
76. Danyushevsky, L.; Robinson, P.; Gilbert, S.; Norman, M.; Large, R.; McGoldrick, P.; Shelley, M. Routine quantitative multi-element analysis of sulphide minerals by laser ablation ICP-MS: Standard development and consideration of matrix effects. *Geochem. Explor. Environ. Anal.* **2011**, *11*, 51–60. [CrossRef]
77. Patten, C.; Barnes, S.J.; Mathez, E.A.; Jenner, F.E. Partition coefficients of chalcophile elements between sulfide and silicate melts and the early crystallization history of sulfide liquid: LA-ICP-MS analysis of MORB sulfide droplets. *Chem. Geol.* **2013**, *358*, 170–188. [CrossRef]
78. Cook, N.; Ciobanu, C.L.; George, L.; Zhu, Z.Y.; Wade, B.; Ehrig, K. Trace element analysis of minerals in magmatic-hydrothermal ores by laser ablation inductively-coupled plasma mass spectrometry: Approaches and opportunities. *Minerals* **2016**, *6*, 111. [CrossRef]
79. George, L.; Cook, N.J.; Cristiana, L.; Wade, B.P. Trace and minor elements in galena: A reconnaissance LA-ICP-MS study. *Am. Mineral.* **2015**, *100*, 548–569. [CrossRef]
80. Plotinskaya, O.Y.; Grabezhev, A.I.; Seltmann, R. Fahlores compositional zoning in a porphyry-epithermal system: Biksizak occurrence, South Urals, Russia as an example. *Geol. Ore Depos.* **2015**, *57*, 42–63. [CrossRef]
81. Buzatu, A.; Damian, G.; Dill, H.G.; Buzgar, N.; Apopei, A.I. Mineralogy and geochemistry of sulfosalts from Baia Sprie ore deposit (Romania)—New bismuth minerals occurrence. *Ore Geol. Rev.* **2015**, *65*, 132–147. [CrossRef]
82. Vokes, F.M. Geological studies on the Caledonian pyritic zinc-lead orebody at Bleikvassli, Norland, Norway. *Nor. Geol. Unders.* **1963**, *222*, 1–126.
83. Vokes, F.M. On the possible modes of origin of the Caledonian sulfide ore deposit at Bleikvassli, Nordland, Norway. *Econ. Geol.* **1966**, *61*, 1130–1139. [CrossRef]
84. Boulter, C.A.; Fotios, M.G.; Phillips, G.N. The Golden Mile, Kalgoorlie; a giant gold deposit localized in ductile shear zones by structurally induced infiltration of an auriferous metamorphic fluid. *Econ. Geol.* **1987**, *82*, 1661–1678. [CrossRef]

ATTACHMENT 7

U.S. OPERATING COPPER MINES:

FAILURE TO CAPTURE & TREAT WASTEWATER

BY BONNIE GESTRING, MAY 2019

In 2012, Earthworks released a report documenting the failure to capture and treat mine wastewater at U.S. operating copper mines accounting for 89% of U.S. copper production.[1] The report found that 92% failed to capture and control mine wastewater, resulting in significant water quality impacts. This is an update to that effort. We reviewed government and industry documents for fifteen operating open-pit copper mines, representing 99% of U.S. copper production in 2015 – the most recent data on copper production available from the U.S. Geological Survey (see Table 1). **Our research found similar results: 14 out of 15 (93%) failed to capture and control wastewater, resulting in significant water quality impacts (see Table 2).** These unauthorized wastewater releases occurred from a number of different sources including uncontrolled seepage from tailings impoundments, waste rock piles, open pits, or other mine facilities, or failure of water treatment facilities, pipeline failures or other accidental releases.

TABLE 1:
Copper production from top 15 (as of 2015) U.S. open-pit copper mines (most recent data available from USGS).[2]

MINE	PRODUCTION (metric tons)
Morenci	481,000
Chino	142,000
Safford	91,600
Bagdad	95,300
Bingham Canyon	92,000
Sierrita	85,700
Ray	75,100
Pinto Valley	60,400
Mission Complex	68,300
Robinson	56,800
Tyrone	38,100
Continental pit	31,000
Phoenix	21,100
Miami	19,500
Silver Bell	19,300
Total (99% of U.S. production)	**1,377,000**
U.S. Total Copper Production	**1,380,000**

TABLE 2:
Wastewater capture and treatment failures at top 15 (as of 2015) producing U.S. open-pit copper mines.

MINE	DOCUMENTATION OF WASTEWATER CAPTURE AND TREATMENT FAILURE
Morenci	In 2012, the US Department of Justice and Department of Interior jointly announced that Freeport McMoRan agreed to pay $6.8 million to settle federal and state natural resource damages related to the Morenci Mine.[3] According to the complaint, the hazardous substance release, which included sulfuric acid and metals, injured, destroyed or led to the loss of "surface waters, terrestrial habitat and wildlife, and migratory birds."[4] The 2012 consent decree concluded that "mine tailings exposed to air and precipitation released hazardous substances on the surface of the tailings or that can percolate through the tailings to groundwater."[5] The consent decree found that "releases of hazardous substances at or from the Morenci Mine site have occurred and allege that such releases have caused injuries to natural resources at and in the vicinity of the site including surface water, sediments, soils, terrestrial habitats and terrestrial receptors." The investigation in support of the consent decree found that the main ore minerals are sulfide minerals, which have resulted in the development of acid mine drainage. According to the report, "Surface water has been, and most likely continues to be, exposed to hazardous substances released from the Morenci Mine through a variety of pathways."[6] It also found that "Concentrations of total and dissolved zinc have exceeded 1,000 ug/l in the Gila River and concentration of dissolved copper have exceeded 100 ug/l in the San Francisco River."[7] Contaminated groundwater is also released to surface water via seeps and springs. In 2011, the State of Arizona reached a settlement of $150,000 with the Morenci Mine for the release of acidic solution directly into Lower Chase Creek from a stormwater pipe.[8] The material travelled more than two miles, in violation of the mine's discharge permit. The discharge occurred due to an operator error, in which the process solution pipeline was connected to the stormwater pipeline. Pollutants in the discharge exceeded surface water quality standards for copper, zinc and pH in Lower Chase Creek.
Chino	In 2019, the Chino Mine released 2 million gallons of tailings slurry due to a failed coupling on the pipeline that carries tailings from the concentrator to the tailings pond.[9] The tailings flowed into a diversion of Whitewater Creek upstream from James Canyon Reservoir, and the report found that it was "likely that an unknown volume of the aqueous portion of the tailings slurry, some of the tailings solids entered the reservoir."[10] The reservoir is being pumped down to determine what volume of tailings solids entered the reservoir. In 2011, the U.S. Department of Justice and State of New Mexico issued a consent decree for damages to natural resources from hazardous substances from the Chino Mine.[11] The settlement followed an investigation of natural resource injuries related to the release of hazardous substances into the environment from acid mine drainage and process solution, among other sources. It found that, "surface water and associated sediments are exposed to hazardous substances released from the Chino Mine through a variety of pathways, including leaks and spills of process water, tailings spills; runoff, and infiltration or percolation from tailings and waste stockpiles."[12] Groundwater contamination from tailings pond #7, which became active in 1988, has occurred to the east, west and south of impoundment. It also found that hazardous substances have been released into groundwater at the Chino mine from multiple source areas.[13] Concentrations of hazardous substances in groundwater in exceedance of water quality standards confirm release to groundwater throughout the Chino Mine. Groundwater flow modeling for the North Mine area indicates that contaminated groundwater in four of these areas is not captured by dewatering in

MINE	DOCUMENTATION OF WASTEWATER CAPTURE AND TREATMENT FAILURE
Chino (cont'd)	the main pit. In the South Mine area, groundwater has exceeded standards for manganese and cadmium at Middle Whitewater Creek, Hurley and Lake One, and has exceeded standards for copper at Lake One. A 2012 assessment of groundwater impacts concluded that contaminated seepage from the mine will require water treatment in perpetuity.[14] In 2009, the State of New Mexico reached a settlement of $279,000 with the Chino Mine after the release of one million gallons of process solution that overflowed a containment sump and travelled more than 2 ½ miles down a surface water tributary near the mine in 2007.[15]A 2003 ecological risk assessment reported elevated concentrations of the hazardous substances copper and zinc in surface water from five different drainages at the Chino Mine, including Hanover/Whitewater Creek, Bayard Canyon, Bolton Draw, the unnamed drainage between Bolton Draw and Lampbright Draw and Lambright Draw.[16] The areal extent of injured alluvial and regional groundwater at the Chino Mine is 13,935 acres.
Safford	No documentation of unauthorized seepage or releases of unauthorized wastewater.
Bagdad	There have been numerous spills, including a broken pipeline in 2009 causing a release of 2.3 million gallons of sulfuric acid into the surrounding soils,[17] and a 1999 report of 12,000 gallons of process water with residual chlorine spilled into Bridle Creek.[18] According to a 2006 study, a tailings impoundment at the Bagdad Mine failed in 1991 and discharged to Copper Creek. Elevated concentrations of mercury, phenols, ammonia, copper and acidity occurred in Boulder and Copper creeks, resulting in a fish kill.[19] Water quality monitoring from 1998-2002 in Boulder Creek found water quality exceedances for arsenic, lead, mercury, and selenium. In Burro Creek, there were water quality exceedances for copper and mercury. In Butte Creek, there were water quality exceedances for mercury and selenium. In 1996, the EPA and the state of Arizona announced that Cyprus Bagdad Copper Corp., a subsidiary of Cyprus Mineral Corp., paid penalties totaling $760,000 for discharging contaminated water from the Bagdad Copper Mine.[20] The discharges involved various facilities including tailings ponds, leach dumps, and a sewage treatment plant.[21] According to an EPA report, seepage of pregnant leach solution from the Copper Creek Leaching System was discovered in a receiving pool in Boulder Creek in 1991.[22] Studies indicated that instead of being contained by the Copper Creek Flood Basin, the heavily contaminated solution seeped under the dam. The concentration of total copper in samples collected in the pool in Boulder Creek were as high as 76.4 mg/l. On March 29, 1993, U.S. EPA issued a Finding of Violation and Order against Cyprus.[23]
Bingham Canyon	Wastewater from the mine has escaped the site's collection system, contaminating groundwater with acid, metals and sulfates. The groundwater plume extends towards the Jordan River and covers and extensive area – contaminating the drinking water aquifer used by Salt Lake City residents.[24] Water treatment will be required in perpetuity.[25] In February 2008, the United States Fish and Wildlife Service took legal action against Kennecott for the release of hazardous substances from the mine's facilities, including selenium, copper, arsenic, lead, zinc and cadmium.[26] Groundwater contaminated by mine operations has been released from the mine site through artesian springs into areas that serve as fish and wildlife habitats. According to the federal biologists, the release of these hazardous pollutants has harmed natural resources, including migratory birds and their support ecosystems, which includes wetlands, marshes, freshwater wildlife habitats, playas and riparian areas and freshwater ponds.[27] The 2002 Record of Decision for the Kennecott North Zone Site, which includes the Magma tailings impoundment, describes leaching of contaminants through the berm and into

MINE	DOCUMENTATION OF WASTEWATER CAPTURE AND TREATMENT FAILURE
Bingham Canyon (cont'd)	groundwater and surface water, with adverse effects on biota.[28] The 2002 ROD also indicates that there were several incidences when poor-quality water was discharged from the south tailings pond into the Great Salt Lake in violation of state's water quality permit (UPDES). The 2002 ROD also documents discharges from the newer North tailings dam in violation of the discharge permit (UPDES permit).
Sierrita	Seepage from the 3,600-acre tailings pond at the Sierrita mine has sent a plume of contaminated groundwater toward the city of Green Valley, Arizona, causing drinking water wells to record high levels of sulfates.[29] The collection system failed to completely capture the contaminated mine seepage. Public water supply wells owned and operated by the Community Water Company and serving the community of Green Valley have been affected by the sulfate contamination. In 2006, the company signed a mitigation order on consent with the State of Arizona to address sulfate in drinking water. According to an ADEQ fact sheet, sulfate levels in monitoring wells have been about 1,000 – 2,000 mg/l.[30] High sulfate levels are known to cause diarrhea and harm the digestive system. From 1992-1994, the Sierrita Mine discharge contaminated process water and stormwater run-off to Demetrie Wash and its tributaries from various overflows, seepages and pipeline leaks and breaks.[31] In January 1993, a leak in a pipeline transporting process water discharged approximately 200,000 gallons of a mixture of process water and stormwater run-off to an unnamed tributary of Demetrie Wash.[32] Also in July 1993, a report of a discharge of approximately 2,700,000 gallons into the same wash as a result of another pipeline break.[33] Approximately 450,000 gallons were released to the wash in October 1993 by a broken pipeline. Each release involved contaminated water derived from a mixture of tailings reclaim water and groundwater pumped from an interceptor well.[34]
Ray	In 2012, seepage from the tailings impoundment was released into two catch basins and into a tributary of the Gila River.[35] At the time of the report, seepage into the tributary was estimated at 75 gpm.[36] The incident occurred as a result of operator error during the initiation of a new upstream construction method at its Elder Gulch Tailings Impoundment in 2011.[37] A delay in the completion of the tailings distribution line resulted in the uneven distribution of the tailings, which in turn caused the ponded water to migrate, and eventually be released from the impoundment into drainages. The seep was discovered on January 30, 2012, and seep flow from the embankment was observed to have stopped on February 7, 2012. All four surface water samples exceeded the limits for selenium. In 2011, a report of 6,000 to 8,000 tons of copper ore tailings released from one of the tailings ponds due to a breach in the dike. The company failed to operate and maintain all listed permitted facilities in its Aquifer Protection Permit No. P-100507 to prevent the unauthorized discharge of copper ore tailings.[38] In April 2009, the Department of the Interior and the State of Arizona, acting as natural resource trustees (Trustees) received a monetary settlement and three parcels of land from ASARCO, L.L.C. through the Natural Resource Damage Assessment and Restoration (NRDAR) program to account for injuries to trust resources incurred through multiple releases of hazardous substances by ASARCO L.L.C. into Mineral Creek and the Gila River in Pinal County, Arizona.[39] In 2007, a leak from a coupling in a tailings pipeline spilled tailings onto the banks and into the Gila River.[40] A $20,000 civil penalty was paid. According to the report, the pipeline had been in use since the construction of "d" tailings impoundment (about 1985), was in good condition, and was visually inspected on a frequent basis.

MINE	DOCUMENTATION OF WASTEWATER CAPTURE AND TREATMENT FAILURE
Ray Mine (cont'd)	According to a 2012 ecological risk assessment by the State of Arizona, "The site of injury stretches from the Ray Mine and the Hayden Facility, to the Gila River from the Ashurst- Hayden Diversion Dam, upstream past the confluence of the San Pedro and Gila Rivers, and for a distance of 5 miles up each of those rivers beyond the confluence and to Mineral Creek from its confluence with the Gila River upstream to a point one mile above the Big Box Canyon Dam."[41] The most substantial injuries occurred in the reach of Mineral Creek that extends from the tunnel outlet to the Gila River. The report finds that, "Dissolved copper concentrations in the surface water of this reach have been recorded up to 130 times surface water quality standards that will sustain aquatic life, and sediment copper concentrations have been recorded to exceed up to 22 times the level beyond which injury is inflicted on sediment-dwelling organisms (MacDonald et al. 2000)."[42] These concentrations of copper caused a complete loss of aquatic life in this reach. Overall, the report found that, "ecosystem services lost in the 117 acres that include Mineral Creek and its associated riparian habitat were estimated to be 100% from 1981- 2005, and up to 50% from 2005 to the present (Lipton 2009). Hazardous releases also affected the aquatic and riparian portions of the Gila River near the Ray Mine/Hayden Smelter Complex, including approximately 2,930 acres upstream of Mineral Creek to the confluence with the San Pedro River, and approximately 1,620 acres downstream of Mineral Creek to the Ashurst-Hayden Dam. The most substantial loss of ecosystem services in these areas occurred during the three years following the release of 300,000 tons of tailings in 1993, when ecosystem service losses were estimated at 10-25% (Lipton 2009)."[43]
Pinto Valley	In 2010, a report of a storm event that caused 5,362 tons of tailings to spill onto soil and Pinto Creek, including 214 pounds of arsenic and 11 pounds of lead.[44] According to the report, 500 cubic yards were released into water. Pinto Creek is a tributary to Roosevelt Lake. In 2007, a release of impounded storm and seepage water occurred due to a flange separation in a tailings line. The unexpected release washed out a section of the secondary containment, which allowed it to escape. An estimated 45,000 gallons of stormwater and tailings seepage reported to an unnamed tributary of Pinto Creek.[45] In 2007, the facility noticed that the action leakage rate for the Gold Gulch pond had been exceeded, documenting a leak in the pond. In February 2008 a wind and storm event ripped the top portion of the liner, requiring major repair, which was completed in February – March 2008.[46] The ALR exceedances continued on an intermittent basis throughout the remainder of 2008 and 2009. The leak rate was 26 gallons/minute on the day of the inspection. Since 1989, extreme storm events caused releases of copper bearing sediments and liquids to Pinto Creek from Pinto Valley operations. These releases resulted from partial tailings dam failures, pipeline breaks, seepage flows, conveyance blockages, and storm water overflows. Recent significant release events occurred in August 1989, July 1990, January 1991, August to September 1991, January to February 1993, and October 1997. In each of these events, materials were released in quantities sufficient to impact Pinto Creek or its tributaries."[47] Based on EPA's review of discharge monitoring reports between January 1990 and September 1991, Magma (now Pinto Valley) reportedly discharged effluent to Pinto Creek or its tributaries in excess of allowable effluent limitations on numerous occasions, and/or did not collect and analyze samples, in violation of permit conditions.[48] According to the report, during the first episode, approximately 3,000 gallons of effluent containing total suspended solids and copper of unknown concentrations was discharged from the ditch. A similar discharge of 24,000 gallons occurred on September 5, 1991. An estimated 39,000 gallons of effluent in exceedance of Arizona Surface Water Quality Standards and Aquifer Water Quality Standards for copper, zinc, and lead were discharged from the ditch on September 23, 1991.[49]

MINE	DOCUMENTATION OF WASTEWATER CAPTURE AND TREATMENT FAILURE
Pinto Valley (cont'd)	In 1997, a partial tailings failure deposited an estimated 276,000 cubic yards of tailings in Pinto Creek.[50] It buried 8.1 acres of creek bed and surrounding upland with material as deep as 42 feet.[51]
Mission Complex	In 2011, a report of a backup of a tailings line resulting in a release of tailings to a dry wash.[52] A news report stated that the release involved 811 cubic yards of tailings, containing 145 pounds of lead sulfide.[53] It travelled underneath the Interstate and onto private property. According to an EPA fact sheet released in 2008, the Mission Mine received a notice of violation in 2002 involving the discharge of primarily copper laden stormwater runoff and process water discharge to ephemeral tributaries of the Santa Cruz river near Tucson in violation of the facilities Multi Sector General Permit Case # 09-2002-0064. Discharges from mine (outfall 001A) contain significant levels of copper and lead, and TSS, which have been out of compliance since October, 2003.[54] Outfalls from the Mission complex discharge to ephemeral streams that are tributaries to the Santa Cruz River. Three large tailings ponds and several mine dumps are located on land leased from the Indian landowners approximately 1 mile south of the Arroyos project area. According to a report by the Bureau of Reclamation, leachate from these tailings has contributed to elevated levels of sulfate, TDS, and hardness in the aquifer below and adjacent to the ponds.[55]
Robinson	In 2015, the Robinson Mine in Nevada experienced seepage from its Tailings Storage Facility – resulting in groundwater degradation from sulfate at levels above the 500 mg/l requirement and resulting in the issuance of a Finding Of Alleged Violation and Order in April 2015.[56] In late May 2016, a 0.8 gpm flow of tailings solution was observed emanating from a small area of bedrock in a road-cut exposure immediately downslope of the downstream face of the Eastern Embankment Extension.[57] During the 2010 Permit renewal, the Liberty Pit lake exhibited poor water quality in the form of elevated metal concentrations and low pH (2-3 SU), which is out of compliance with requirements. To come into compliance the company was required to dewater the pit lake. NDEP also documents acid rock drainage seeps and puddles associated with the late-1990s to current Liberty Waste Rock Dump (WRD).[58] The mine experienced eight reported spills during 1996.[59] Most of these spills involved tailings solution and reclaim water releases due to equipment failures. The five spills resulting in releases of copper flotation tailings had spill volumes ranging from 1,500 gallons to 66,000 gallons. Four of these spills resulted in contamination of relatively small areas of soil. The largest spill resulted in contamination of a downstream drainage bed for 2.3 miles with an average flow path width of 3 ft. Two spills resulted in a combined release of 76,000 gallons of reclaim water.
Tyrone	In 2011, the U.S. Department of Justice and State of New Mexico issued a consent decree for damages to natural resources from hazardous substances from the Tyrone Mine.[60] The settlement followed an investigation of natural resource injuries related to the release of hazardous substances into the environment from acid mine drainage and process solution, among other sources. According to the investigation, "groundwater in both the regional aquifer and the perched groundwater aquifers at the site have been exposed to hazardous substances through a variety of pathways."[61] The assessment at the Tyrone Mine identified 14 different mine area sources that have affected water quality, including seepage from tailings impoundments, leach stockpiles and waste rock stockpiles. The areal extent of the contaminated groundwater plume at the Tyrone Mine is 6,280 acres. Groundwater seepage will require water treatment in perpetuity. A 2012 groundwater assessment concluded that contaminated seepage from the mine will require water treatment in perpetuity.[62] According to a 2013 report by the U.S. Fish and Wildlife Service and the State of New Mexico, "Riparian habitat resources have been exposed to hazardous substances through numerous

MINE	DOCUMENTATION OF WASTEWATER CAPTURE AND TREATMENT FAILURE
Tyrone (cont'd)	pathways at the Sites, including process water leaks and spills; tailings spills; dryfall from smelter emissions; windblown materials; runoff, infiltration, or percolation from tailings and waste stockpiles; and transport through erosional processes. Whitewater Creek and Mangas Creek are two important waterways at the Chino and Tyrone mines, respectively, where the riparian and associated streambed habitats have been exposed to hazardous substances from multiple sources. Those sources include direct inputs of contaminated water from the mines, tailings pond breaches during high-volume storm events, and deposition or spills of tailings directly into the streambed areas.[63] There have been multiple spills of tailings, releasing hazardous substances. The largest event occurred at the No. 3 tailings dam in 1980, releasing 2.6 million cubic yards of tailings into the Mangas Valley.[64] Tailings flowed 8 kilometers downstream and inundated farmland. The failure occurred as the result of a dam wall breach. In 2001, 5 tons of tailings spilled into the Mangas Wash from the stormwater containment dike at the tailings dam.[65]
Continental Pit	According to the Butte groundwater injury assessment report for the State of Montana's Natural Resource Damage Program, the walls of the Berkeley and Continental Pits were a source of groundwater contamination in the Butte Mine Flooding Operable Unit of the Superfund Site along with leaking solutions from the Yankee Doodle Tailings Pond.[66] Groundwater contamination is extensive, requiring the City of Butte to pipe its drinking water in from other watersheds. At current operations, mine tailings from the Continental Pit mine are placed in the Yankee Doodle tailings impoundment, which also contains the mine waste from previous mining at the Berkeley Pit. The tailings impoundment is unlined, and seepage from the impoundment travels through faults and fractures into the Berkeley Pit. When mining ceases, seepage from the tailings impoundment will continue to contribute contaminated water to the Berkeley pit. A consent decree requires contaminated water from the Berkeley Pit to be collected and treated in perpetuity.[67]
Phoenix	In 2002, groundwater from the gold tailings facility contain elevated concentrations of chloride, sodium, and sulfate, which is the result of a solute plume originating from the Gold Tailings facility – a copper and gold tailings storage facility.[68] In 2005, seepage of low pH and poor-quality solution emanating from a portion of the southern toe of the North Fortitude Waste Rock Facility was identified in June and formally inspected in August. Flow emanates from two locations along a 300-foot width of the toe and ultimately migrates to a natural drainage and eventually into the pit. In 2006, seepage of a small quantity of low pH and poor-quality water was discovered at the toe of the Box Canyon Waste Rock Facility following an intense precipitation event. Flow was estimated at 2 gallons per minute.
Miami	The Miami Mine, currently owned by Freeport McMoran, was formerly the Inspiration Mine owned and operated by the Inspiration Consolidated Copper Co. In 1986, the U.S. EPA issued a finding of violation and order under the Clean Water Act to the Inspiration Consolidated Copper Co. for discharges of acidic process solutions from Webster Lake (a large process solution impoundment) to Miami Wash and for acidic, metal contaminated groundwater surfacing near the confluence of Miami Wash and Pinal Creek.[69] Acidic water from this lake and other mining related sources generated a 15-kilometer-long plume of acidic groundwater in the alluvial aquifer.[70] In 1989, the Pinal Creek Site, which includes the Miami Mine, was placed on the WQARF Priority list.[71] The WQARF program is the state equivalent of the Federal "superfund" program. The Pinal Creek site was listed under the Arizona Water Quality Assurance Revolving Fund program for contamination in the shallow alluvial aquifers within the Pinal Creek drainage. According to the State of Arizona, "Releases of contaminants have occurred from all of the major mining sites from a variety of different sources, including, but not limited to, process solution

MINE	DOCUMENTATION OF WASTEWATER CAPTURE AND TREATMENT FAILURE
	impoundments, tailings piles, leach dumps, various spills, and as storm water runoff from waste and tailings piles."[72]
Silver Bell	In 2013, Asarco agreed to pay $110,000 to settle a spill in 2010 resulting from a rupture in a welded pipeline seam that allowed 70,000 gallons of process solution to escape from the Silver Bell Mine. The solution travelled more than a mile. Pollutants in the discharge exceed water quality standards for fluoride, arsenic, beryllium, cadmium, chromium, nickel and selenium.[73] In 2009, Silver Bell was fined $170,000 for three spills totaling 340,000 gallons of wastewater containing sulfuric acid and heavy metals into dry washes.[74] The pollutants seeped into soil, which endangered the groundwater in the aquifer below the mine and exceeded water quality standards. Two of the spills are described as such: Between Nov. 6 and Dec. 11, 2006, 150,000 gallons of leach solution containing sulfuric acid and metals escaped from a leaking impoundment. And between Nov. 11 and Dec. 13, 2006 another 100,000 gallons of stormwater containing sulfuric acid and heavy metals escaped from a storage pit. The EPA reports that a site inspection by the Arizona Department of Environmental Quality (ADEQ) in 1993 found water flowing in three unnamed washes below Silver Bell Mine. Samples taken from the two streams flowing under the waste rock dump showed violations of standards for total selenium, with one stream also violating standards for dissolved copper.[75] According to a 2000 report on native fish populations by Pima County, "The loss of native fish along Cocio Wash is a good example of the potentially damaging effects that mining can have on aquatic ecosystems. Summer floods in July and August 1981 swept gray clay sediments from a Silverbell Mine tailings pond into the wash. BLM biologist Bill Kepner later reported, "Our studies indicate that the Cocio Wash topminnow population is now extinct in that habitat due to recurrent mine spills and inundations by mine tailings... (Fonseca, 2000)."[76]

[1] Earthworks,U.S. Copper Porphyry Mines Report: The Track Record of Water Quality Impacts Resulting From Pipeline Spills, Tailings Failures and Water Collection and Treatment Failures. July 2012 (Revised 11/2012) Available at: https://earthworks.org/publications/us_copper_porphyry_mines/
[2] US Geological Survey, 2015 Minerals Yearbook, Copper (advance release), October 2017.
[3] US Department of Justice, Press Release: "Freeport-McMoran Corp and Freeport-McMoran Morenci Inc. will pay $6.8 million in Damages for Injuries to Natural Resources from the Morenci Copper Mine in Arizona. April 24, 2012. http://www.justice.gov/opa/pr/2012/April/12-enrd-527.html
[4] Id.
[5] United States and State of Arizona v. Freeport McMoran Corporation and Freeport McMoran Morenci Inc, Consent Decree, Case 4:12lcvl00307lHCE, April 2012.
[6] Id.
[7] Id.
[8] Arizona Department of Environmental Quality, Press Release: Freeport McMoran Morenci Inc. Agrees to $150,000 Settlement to Resolve Water Quality Violations from 2008 Spill, July 14, 2011.
[9] New Mexico Environmental Department, Corrective Action Response, DP-213, January 5, 2019 Unauthorized Discharge of Tailings Slurry from Tailing Spare Train Pipeline.
[10] Id.
[11] United States and State of New Mexico v. Freeport McMoran Corporations, et. al, Consent Decree, Case 1:11-cv-01140. December 2011.
[12] Stratus Consulting Inc., "Preassessment screen for the Chino, Tyrone and Cobre Mines Prepared for the US Fish and Wildlife Services, June 18, 2003. p. 3-3.
[13] Id. p. 2-16.
[14] Id. p. 2-18.
[15] New Mexico Environment Department, Press Release: Environment Department Reaches $276,000 Settlement with Freeport McMoran Chino Mines Co. Regarding Acid Spill that Contaminated Groundwater in Silver City," April 17, 2009.
[16] Stratus Consulting Inc., "Preassessment screen for the Chino, Tyrone and Cobre Mines Prepared for the US Fish and Wildlife Services, June 18, 2003.
[17] National Response Center, Incident No. 922634. And, https://cronkitenews.azpbs.org/2018/05/03/agencies-respond-to-scores-of-spills-and-accidents-in-arizona-every-year/
[18] National Response Center, Incident No. 476104
[19] Kuipers, J.R., Maest, A.S., MacHardy, K.A., and Lawson, G. 2006. Comparison of Predicted and Actual Water Quality at Hardrock Mines: The reliability of predictions in Environmental Impact Statements.
[20] US EPA, press release, "Cyprus Bagdad to pay $760,000 to settle water pollution charges," 9/16/1996.

[21] Id.
[22] US EPA, Damage Cases and Environmental Releases from Mine and Mineral Processing sites, 1997.
[23] Id.
[24] Interstate Technology and Regulatory Council Mining Waste Team, Bingham Canyon Wastewater Treatment Plant, Kennecott South Zone, August 2010,
International Conference on Acid Rock Drainage, March 26–30, St. Louis, MO. Available at: https://www.itrcweb.org/miningwaste-guidance/cs48_kennecott_south.pdf
[25] Borden, R.K, Peacey, V. and Vinton, B. 2006. "Groundwater response to the end of forty years of copper heap leach operations, Bingham Canyon, Utah. 2006. " Proceedings, 7th International Conference on Acid Rock Drainage, March 26–30, St. Louis, MO. Available at: http://www.imwa.info/docs/imwa_2006/0214-Borden-AU.pdf
[26] United States v. Kennecott Utah Copper Corporation. Complaint Case: 2:08cv00122. February 14, 2008.
[27] United States v. Kennecott Utah Copper Corporation. Complaint Case: 2:08cv00122. February 14, 2008.
www.fws.gov/.../r_r_Kennecott_Utah_Copper_ComplaintFinal.pdf
[28] US EPA, Kennecott North ROD, September 2002.
[29] Arizona Department of Environmental Quality, Phelps Dodge Sierrita Aquifer Protection Permit, Fact Sheet, Publication No. FS-05-17. Available at:
https://legacy.azdeq.gov/environ/water/download/phelps.pdf
[30] Id.
[31] US EPA, Damage Cases and Environmental Releases from Mines and Mineral Processing Sites, 1997.
[32] Id.
[33] Id.
[34] Id.
[35] Personal Communication, Peter Jagow, Compliance inspector, Arizona DEQ, July 10, 2012, based on February 2012 inspection.
[36] Arizona Department of Environmental Quality, Notice of Violation, Case ID #130170, May 9, 2012.
[37] Arizona Department of Environmental Quality, Inspection Report, May 6, 2011.
[38] Arizona Department of Environmental Quality, Inspection Report, May 6, 2011.
[39] State of Arizona and US Department of Interior, "Draft Restoration Plan and Environmental Assessment for the Hazardous Substances Releases from the Hayden Smelter and Ray Mine Facilities," February 2012.
[40] Arizona Department of Environmental Quality, Notice of Violation, Case ID 79745, July 12, 2007.
[41] Id.
[42] Id.
[43] Id.
[44] National Response Center Incident No. 929841.
[45] BHP Billiton, Follow Up Report, Environmental Release, National Response Center, Letter to EPA, October 31, 2007.
[46] US EPA, Region 9, Total Maximum Daily Load for Copper into Pinto Creek, Arizona, April 2001. p. 11.
[47] Ibid. p. 14.
[48] US EPA, Damage Cases and Environmental Releases from Mine and Mineral Processing sites, 1997. p. 32.
[49] Ibid.
[50] US EPA, Region 9 Total Maximum Daily Load for Copper into Pinto Creek, Arizona, April 2001. P. 14
[51] US Fish and Wildlife Service, Environmental Contaminants Program website, Pinto Creek Restoration, News and Activities, Arizona. Posted on December 22, 1999.
[52] National Response Center, Incident No. 986438.
[53] Arizona Daily Star, "Tailings spill blamed on Asarco valve issue" August 5, 2011. Available at:
https://tucson.com/business/local/tailings-spill-blamed-on-asarco-valve-issue/article_fea75159-fcb9-5b7f-a9d2-7f6422e9b8db.html
[54] US EPA, ASARCO Mission Complex Fact Sheet: EPA PERMIT NO. AZ0024635, September 22, 2008.
[55] US Department of Interior, Bureau of Reclamation, San Xavier District Arroyos Recharge Project, Final Environmental Assessment, May 2009. p. 16.
[56] Nevada Department of Environmental Protection, NDEP Fact Sheet, Robinson Mine, Permit No. NEV0092105.
https://ndep.nv.gov/uploads/documents/NEV0092105_fsFY18.pdf
[57] Id.
[58] Id. p. 88
[59] US EPA, Damage Cases and Environmental Releases from Mines and Mineral Processing Sites, 1997, p. 170. The Robinson Mine was formerly owned by BHP Copper, Magma Nevada Mining Company.
[60] United States and State of New Mexico v. Freeport McMoran Corporations, et. al, Consent Decree, Case 1:11-cv-01140. December 2011.
[61] Stratus Consulting, Preassessment Screen for the Chino, Tyrone, and Morenci Mine Sites, Grant County, New Mexico, and Morenci, Arizona, Prepared for US Fish and Wildlife Service, June 18, 2003.
[62] New Mexico Office of Natural Resources Trustee, "Final Groundwater Restoration Plan for the Chino, Cobre and Tyrone Mine Facilities, January 4, 2012. Table 2.1. p. 2-14.
[63] U.S. Fish and Wildlife Service and State of New Mexico, Wildlife and and Wildlife Habitat Restoration Plan and Environmental Assessment for the Chino, Cobre and Tyrone Mine Facilities, October 2013: https://onrt.env.nm.gov/wp-content/uploads/FMIWildlifeRPEAOctober2013.pdf
[64] Stratus Consulting, Preassessment Screen for the Chino, Tyrone, and Morenci Mine Sites, Grant County, New Mexico, and Morenci, Arizona, Prepared for US Fish and Wildlife Service, June 18, 2003. Table 2.3. p. 2-11.
[65] Stratus Consulting, Preassessment Screen for the Chino, Tyrone, and Morenci Mine Sites, Grant County, New Mexico, and Morenci, Arizona, Prepared for US Fish and Wildlife Service, June 18, 2003.
[66] Maest, Ann S. and John Metesch, Butte Groundwater Injury Assessment Report, Clark Fork River Basin NPL Sites, Prepared for the State of Montana Natural Resources Damage Program, April 1993. p. 2-1.
[67] https://www.itrcweb.org/miningwaste-guidance/References/2079-ZickPA.pdf
[68] US Department of Interior, Bureau of Land Management, Greater Phoenix Project, Draft Environmental Impact Statement, Volume 1, September 2017, p. 3-22.
[69] Arizona Department of Environmental Quality, Website: Pinal Creek Site Overview. http://static.azdeq.gov/wqarf/pnlck_rr.pdf
[70] USGS, Hydrogeology and Geochemistry of Aquifer and Stream Contaminated Related to Acidic Water in Pinal Creek Basin Near Globe Arizona, 1996.
[71] Arizona Department of Environmental Quality, Website: Pinal Creek Site Overview. http://static.azdeq.gov/wqarf/pnlck_rr.pdf
[72] http://static.azdeq.gov/wqarf/pnlck_rr.pdf
[73] Arizona Daily Star, "Asarco Unit to pay $110,000 to settle mine spill charges," January 9, 2013
https://tucson.com/business/local/asarco-unit-to-pay-k-to-settle-mine-spill-charges/article_0dc1c34e-6a53-11e2-a438-0019bb2963f4.html
[74] ADEQ, Press Release: Silver Bell Mining to Pay $170,000 in civil penalties for water quality violations in Pima County. April 7, 2009

[75] US EPA, Damage Cases and Environmental Releases from Mines and Mineral Processing Sites, 1997. p. 23.
[76] Pima County, Arizona Board of Supervisors, Historical Occurrence of Native Fish in Pima County, December 2000. p. 19

ATTACHMENT 8

KINROSS Kettle River – Buckhorn

Crown Resources Corporation
A Kinross company
363 Fish Hatchery Road
Republic, WA, USA 99166

phone: (509) 775-3157
fax: (509) 775-3447

CERTIFIED MAIL: Uploaded to Ecology's WebDMR portal

October 14, 2016

Mr. Sanjay Barik
Water Quality Program
Department of Ecology
Central Regional Office
1250 W. Alder Street
Union Gap, WA 98903

Re: **Development Rock Management Quarterly Report – 4th, Quarter, Water Year 2016**

Dear Mr. Barik,

Attached please find the Development Rock Management quarterly report for 4th quarter, Water Year 2016 for the Buckhorn Mine.

The Department of Ecology (Ecology) issued the original NPDES Permit for the Buckhorn Mountain Mine on September 27, 2007. Ecology renewed that Permit on February 27, 2014 (Renewed Permit). Crown filed an appeal of the Renewed Permit with the Pollution Control Hearings Board (PCHB) on February 28, 2014. On July 30, 2015, the PCHB issued its decision on the appeal. Crown has appealed the PCHB's decision to Superior Court and believes the Renewed Permit will be deemed invalid by the Court.

Nonetheless, Crown wishes to continue working with Ecology on resolving the disputed permit issues, and has voluntarily modified its sampling and monitoring procedures to be consistent with the terms of the Renewed Permit while the appeal is pending. Accordingly, the attached DRMP quarterly report follows the new requirements set forth in the Renewed Permit. By submitting the DRMP quarterly report, Crown does not waive any of its rights or appeal issues, and reserves the right to submit revised DRMP quarterly report based on the rulings of the PCHB, Court or as Crown otherwise deems appropriate.

Please contact me at 509-775-8575 if you have any questions or require additional information.

Sincerely,

Jacquelyn J. Nutt

Jacquelyn J. Nutt
Environmental Superintendent

cc: File
John Bromley

BUCKHORN MINE

DEVELOPMENT ROCK MANAGEMENT PROGRAM

4th Quarter, Water Year 2016

July 1st to September 30th, 2016

Progress Report

Prepared By:

Kinross Gold Corporation

Kettle River – Buckhorn Operations

October 11, 2016

TABLE OF CONTENTS

1. INTRODUCTION

This report summarizes the underground mining progress that took place at the Buckhorn Mine between July 1 and September 30 of 2016 (4th Quarter, Water Year 2016) and presents the associated analytical results obtained from drift and composite samples, as required by the Development Rock Management Plan (DRMP) (Golder November 2006) and the First Addendum of the DRMP (Washington Department of Ecology and Department of Natural Resources, 2011).

Consistent with established reporting Water Year conventions, each quarter refers to the following months of the calendar year:

- Quarter 1 – October 1 through December 31
- Quarter 2 – January 1 through March 31
- Quarter 3 – April 1 through June 30
- Quarter 4 – July 1 through September 30

During WY2016 Q4, active mining occurred in the Upper, Main, and Gold Bowl Portals. Mining progress consisted of 6,457 linear feet (145,687 tons), of which 597 feet (8,927 tons) were development rock.

Drawing 1, *Locations of Mine Developments – Fourth Quarter WY 2016,* depicts the mining progress that took place during the quarter. The locations of cemented rock fill (CRF), shotcrete, and areas of exposed capital potentially acid generating (PAG) rock in the damaged rock zone (DRZ) at the end of the first quarter are presented in Drawing 2, *Locations with Newly Placed CRF, Shotcrete, and Development Exposed PAG DRZ.*

2. SAMPLING AND ANALYSIS OF DEVELOPMENT ROCK

Development rock is managed in accordance with the DRMP and the First Addendum of the DRMP (Washington Department of Ecology and Department of Natural Resources, April 13, 2011). Samples of blasted, run-of-mine (ROM) rock are collected in accordance with the DRMP and three stages of analyses take place, as described below:

- **Drift Samples:** The Drift Sample is representative of each blast round, which amounts to approximately one sample for each 10 feet of advance. The Drift Sample is analyzed for total sulfur. Material with a total sulfur result of <0.3% is classified as General (G). Rock with a total sulfur content of >0.3 % is placed in a sample cell/stockpile for further classification.

- **Composite Samples:** The Composite Samples are analyzed at the KRO assay lab for total sulfur, sulfide sulfur, acid potential (AP), and neutralizing potential (NP). The NP:AP ratio is then used to define the DRZ areas in the mine development headings with PAG characteristics, where AP is determined from sulfide sulfur content. Composite Sample results with a NP:AP ratio of <3 are considered to have PAG characteristics and are mitigated with shotcrete to minimize the potential for acid rock drainage (ARD).
- **PAG/Conditional General (CG) Classification Composite Samples:** PAG/CG material is sampled from the test cells by collecting approximately 25 to 35 subsamples, compositing the material, and crushing. A split of the composite is analyzed for ABA parameters. Results are used to classify test cells as either PAG or CG.

3. ANALYTICAL RESULTS FROM DEVELOPMENT ROCK

3.1 Drift Sample Results

Drift sample total sulfur results are presented in *Buckhorn Mine Round Tracking* (Appendix A). A quarterly breakdown of the tonnages of each rock-type mined during Water Year 2016 is provided in Table 1.

Table 1. Quarterly Summary of Mined Rock Tonnages

	Classification	WY Q1 Oct - Dec 2015	WY Q2 Jan - Mar 2016	WY Q3 Apr - Jun 2016	WY Q4 Jul - Sep 2016	Total Water Year 2016
Tonnage of Mined Rock	Ore	93,018	94,846	111,164	135,146	434,174
	Conditional General/ PAG [1]	23,826	19,386	12,186	5,474	60,872
	General [2]	5,498	5,209	6,617	1,710	19,034
	Marble	5,742	2,061	1,397	1,743	10,943
Percentage of Mined Rock	Ore	72.62%	78.06%	84.62%	93.80%	82.70%
	Conditional General/ PAG [1]	18.60%	15.96%	9.28%	3.80%	11.59%
	General [2]	4.29%	4.29%	5.04%	1.19%	3.63%
	Marble	4.48%	1.70%	1.06%	1.21%	2.08%

(Source: All ore tonnages were extracted from the BH-Mine Footage Report worksheet; all waste tonnages are from the BH-geology Dev_Prod tracking worksheet.)

1. Conditional General / PAG rock is potentially reactive rock that has a total sulfur content of > 0.3%.
2. General rock is non-reactive rock that can be used as aggregate for CRF or placed directly underground as URF.
3. During WY2016 Q4, 6,188 tons of General rock were mined and placed directly as URF.

3.2 Composite Sample Results

Composite sample results for capital development headings are presented in *DRMP Monthly Drift Sample Composite Results (*Appendix B*).* Composite results included in the quarterly report are for capital development headings only, whereas expense heading results are additionally reported in the annual report. No capital development headings were mined in the 4th Quarter of Water Year 2016.

3.3 Backfill Quantities and Humidity Cell Testing

During the 4th Quarter of Water Year 2016, 34,812 tons of CG development rock was placed underground as CG CRF. The CG was mixed with approximately 6% cement and placed underground as Cemented Rock Fill (CG CRF). Prior to the addition of cement, the neutralization potential to acid potential (NP:AP) ratio averaged for all CG material crushed during the quarter, excluding four outliers, was 25.2. No PAG rock was placed beneath the 4,950 elevation during the quarter.

As stipulated in the First Addendum of the DRMP, one CG CRF composite sample is collected for every 20 kilotons of material that are placed underground. The CG CRF composite samples collected during the quarter were sent to a certified analytical laboratory for acid base accounting (ABA) and humidity cell tests (HCT). Ongoing ABA and HCT results are provided in *Humidity Cell Test Results for Conditional General Cemented Rock Fill* (Appendix C).

4. SHOTCRETE MITIGATION

Kinetic testing has indicated that a considerable lag time is anticipated before the onset of acid generation from PAG material, if not mitigated. PAG areas situated above the estimated post-closure water table (4,950 feet above mean sea level) are shotcreted as soon as practicable, whereas PAG areas below the 4,950 ft elevation do not require mitigation. In development headings, 670 feet of PAG DRZ are currently exposed above 4,950 feet elevation. During the WY2016 Q4, development-heading production exposed zero additional linear feet of PAG DRZ above the 4,950 feet elevation. During the quarter, 301 feet of previously-exposed PAG DRZ was shotcreted in development headings above the 4,950 feet elevation.

Drawing 1

Locations of Mine Development – Fourth Quarter WY 2016 (Plan View)

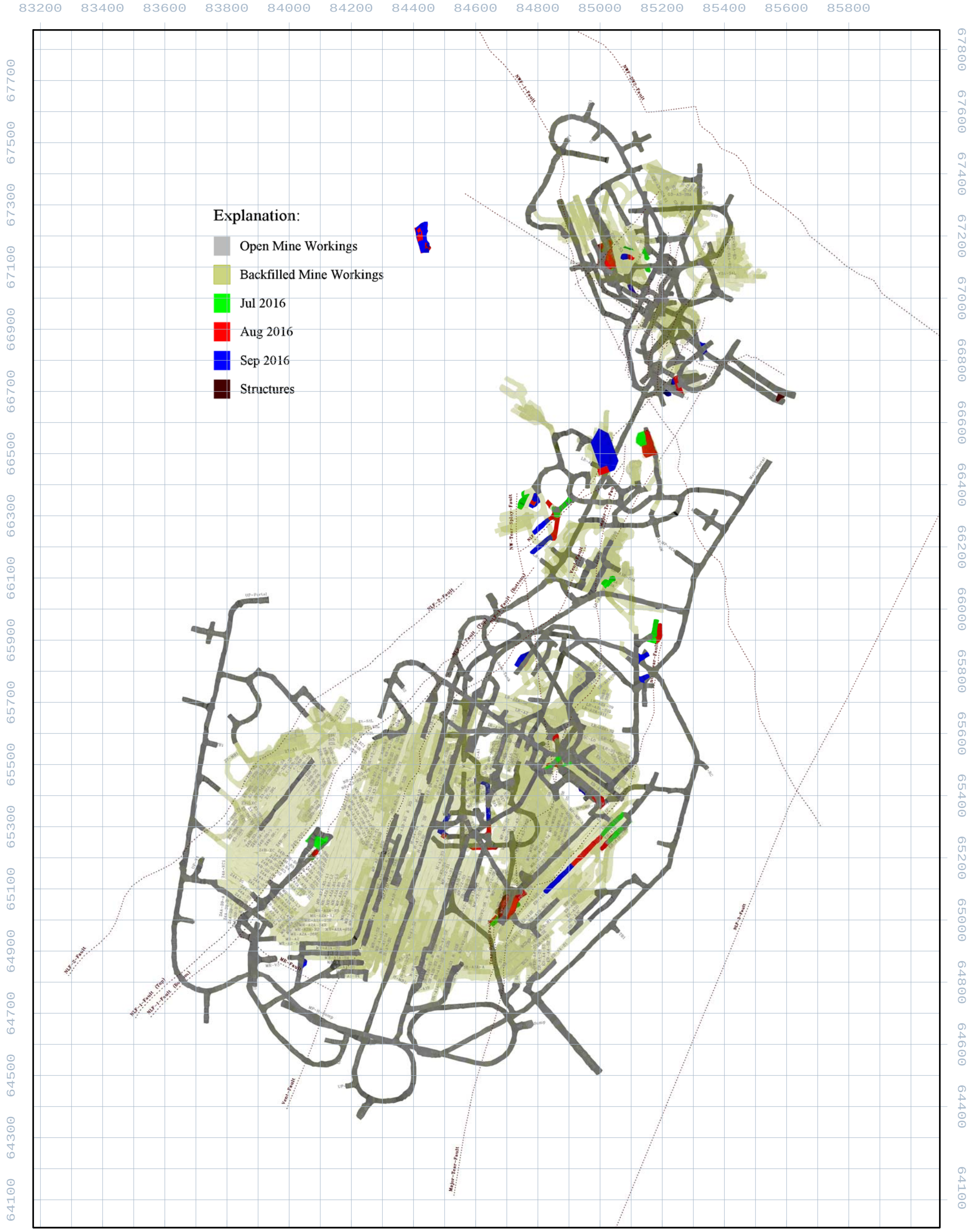

KINROSS GOLD CORPORATION
365 Fish Hatchery Road
Republic, WA 99166

KINROSS

DATE:	06-Oct-2016
DRAWN BY:	JRS
DRAWING#:	
Note 1:	
Note 2:	
Note 3:	

Buckhorn Mine

UG Mine Progress
Q4 Water Year 2016
Jul - Sep 2016

SCALE: 1"=300'

Drawing 2

Locations with newly placed CRF, Shotcrete, and Exposed PAG DRZ (Plan View)

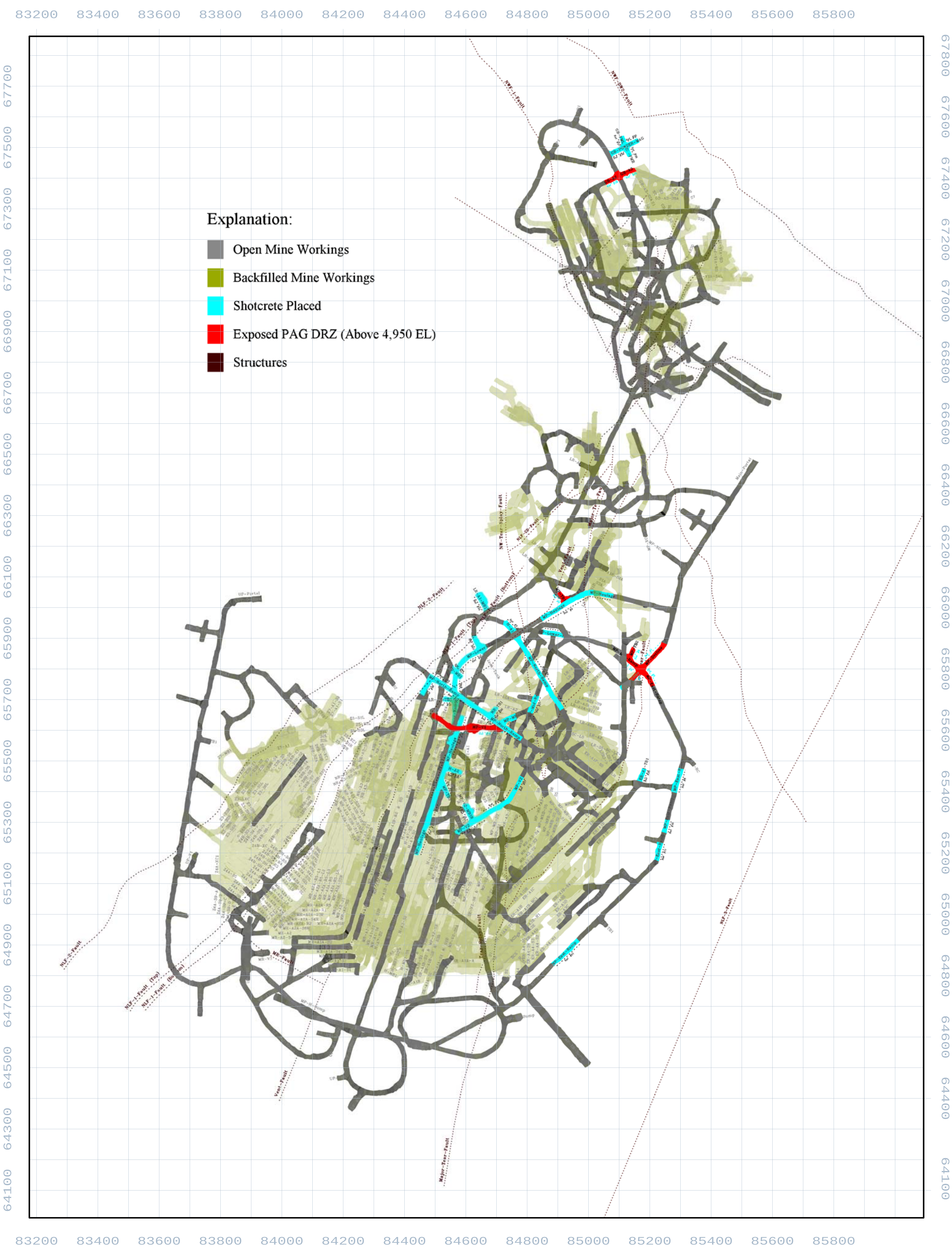

KINROSS GOLD CORPORATION
365 Fish Hatchery Road
Republic, WA 99166

N

KINROSS

DATE:	04-Oct-2016
DRAWN BY:	JRS
DRAWING#:	
Note 1:	
Note 2:	
Note 3:	

Buckhorn Mine

UG Mine Remediation
Q4 Water Year 2016
Jul - Sep 2016

SCALE: 1"=300'

200 0 100 200 300 400 500
Feet

Appendix A

Buckhorn Mine Round Tracking

Appendix A: Buckhorn Mine Round Tracking

Shot Date	Heading	Round Number	Total Sulfur (%)	WASTE CLASSIFICATION		
				Marble (tons)	General (tons)	PAG/CG (tons)
7/4/2016	NR-A1-S11B-S3	2	0.021	0	250	0
7/6/2016	NR-A1-S11B-S3	3	0.308	0	0	215
7/11/2016	MP-XCC-S1	1	0.013	324	0	0
7/13/2016	LR-A2B-SRL-S1R	3	1.149	0	0	279
7/13/2016	MP-XCC-S1	2	0.026	203	0	0
7/14/2016	MP-XCC-S1	3	0.367	185	0	0
7/16/2016	MP-XCC-S1	4	0.303	257	0	0
7/20/2016	MP-XCC-S1	6	0.096	0	314	0
7/23/2016	MP-XCC-S1	7	0.005	455	0	0
7/26/2016	MP-XCC-S1-MB	1	0.066	184	0	0
7/28/2016	5220-L	1SLA	0.000	135	0	0
7/29/2016	MP-XCC-S1L	1	0.008	0	0	0
7/30/2016	MP-XCC-S1-MB	2	0.006	0	0	0
8/2/2016	MP-XCC-S1L	2	0.048	0	0	0
8/4/2016	MP-XCC-S1L	3	2.850	0	0	0
8/5/2016	MP-XCC-S1L	4	3.480	0	0	0
8/6/2016	MP-XCC-S1L	5	3.430	0	0	210
8/8/2016	MP-XCC-S1L	6	4.460	0	0	195
8/9/2016	MP-XCC-S1L	7	6.400	0	0	0
8/10/2016	LR-A2B-CAL-S1	1	0.648	0	0	0
8/12/2016	MP-XCC-S1L	8	6.020	0	0	0
8/14/2016	MP-XCC-S1L	9	7.315	0	0	0
8/22/2016	LR-A2B-SRR-S1	3	0.689	0	0	252
8/24/2016	LR-A2B-SRR-S1	4	1.294	0	0	255
8/25/2016	MP-XCC-S1	9	0.273	0	98	0
8/29/2016	LR-A2B-SRR-S1	5	1.294	0	0	0
8/29/2016	MP-XCC-S1	10	0.002	0	117	0
8/31/2016	MP-XCC-S4	1	2.070	0	0	114
9/2/2016	LR-A2B-SRR-S1	6	1.900	0	0	214
9/3/2016	MP-XCC-S1	11	0.670	0	0	0
9/4/2016	LR-A2B-SRR-S1	7	1.900	0	0	207
9/5/2016	LR-A2B-SRR-S1	8	1.900	0	0	201
9/6/2016	MP-XCC-S1	12	0.863	0	0	126
9/8/2016	LR-A2B-SRR-S1	10	0.780	0	0	196
9/10/2016	LR-A2B-SRR-S1	11	0.711	0	0	223
9/11/2016	LR-A2B-SRR-S1	12	0.256	0	252	0
9/12/2016	MP-XCC-S1	13	0.725	0	0	117
9/13/2016	LR-A2B-SRR-S1	13	0.186	0	267	0
9/14/2016	LR-A2B-SRR-S1	14	0.314	0	0	177
9/15/2016	LR-A2B-SRR-S1	15	0.000	0	189	0
9/17/2016	LR-A2B-SRR-S1	16	0.418	0	0	200
9/18/2016	LR-A2B-SRR-S1	17	1.750	0	0	202
9/18/2016	MP-XCC-S1	15	0.211	0	0	0
9/19/2016	LR-A2B-SRR-S1	18	1.560	0	0	194
9/20/2016	MP-XCC-S1	16	0.770	0	0	221
9/21/2016	LR-A2B-SRR-S1	19	1.060	0	0	236
9/23/2016	LR-A2B-SRR-S1	20	1.900	0	0	227
9/24/2016	UP-MR-A1A	1-2BU	1.390	0	0	112
9/25/2016	UP-MR-A1A	3BU	1.390	0	0	90
9/25/2016	UP-MR-A1A	4BU	1.070	0	0	112
9/26/2016	LR-A2B-SRR-S1	21	0.160	0	223	0
9/26/2016	UP-MR-A1A	5BU	0.591	0	0	0
9/27/2016	4750-S1L	1SLA	0.229	0	0	0
9/29/2016	LR-A2B-SRR-S1	22	1.440	0	0	255
9/29/2016	4750-S1L	2SLA	0.463	0	0	346
9/30/2016	LR-A2B-SRR-S1	23	2.190	0	0	298
			Totals	**1743**	**1710**	**5474**

Appendix B

DRMP Monthly Drift Sample Composite Results

Appendix B: DRMP Monthly Drift Sample

Heading	Composite	Total Sulfur (%)	Sulfide Sulfur (%)	Acid Generation Potential (AP)	Neutralization Potential (NP)	Neutralization Potential Acid Generation Ratio (NP:AP)
No capital headings were mined in Quarter 4 of Water Year 2016						

Appendix C

Conditional General Cemented Rockfill Humidity Cell Interim Results

Crown Resources Corporation
A Kinross company
363 Fish Hatchery Road
Republic, WA, USA 99166

phone: (509) 775-3157
fax: (509) 775-3447

BUCKHORN MINE - HUMIDITY CELL TEST RESULTS FOR CONDITIONAL GENERAL CEMENTED ROCKFILL, FOURTH QUARTER WATER YEAR 2016

Introduction

The Washington Department of Ecology (Ecology) and Department of Natural Resources (DNR) issued the first addendum to the Development Rock Management Plan (DRMP) for the Buckhorn Mine to Crown Resources Corporation (Crown) on April 13, 2011 (Ecology 2011). The DRMP addendum included a new category of rock classification, referred to as Conditional General (CG), which is rock that contains greater than 0.3% sulfide sulfur and contains greater than three (3) times more Neutralization Potential (NP) than Acid Potential (AP) (i.e. NP/AP > 3).

The DRMP addendum includes a plan to batch Conditional General (CG) development rock as a component of cemented rockfill (CRF), which may be placed above an elevation of 4,950 feet in the underground workings. The DRMP addendum requires that:

> **"*A humidity cell test (HCT) will be conducted on composite samples representing each 20 kilotons of cemented rock fill (CRF) made from conditional general (CG) rock. These HCT tests will continue for a minimum of 18 months (or 72 weeks). In addition, the acid generation potential of the conditional general (CG) rock is depleted or calculated in such a way that confirms the leachate parameters, including metals such as arsenic are stable and predictable*."**

In accordance with the addendum, ongoing geochemical testing is conducted on composite samples of CG CRF representative of each 20-kiloton batch of CG CRF placed in the underground workings above an elevation of 4,950 feet. The components of this program are described in detail in the *Sampling and Analysis Plan – Geochemical Testing of Cemented Rockfill, Buckhorn Mine*. Table 1 lists the samples that were submitted for kinetic testing as of September 30, 2016, excepting those that were terminated per the DRMP Humidity Cell Test Program, Sample Completion Notification(s) dated February 10, 2015 and October 30, 2015.

Table 1. Samples Submitted for Kinetic Testing

Sample Name	Composite Interval		HCT Start Date	Current Cycle
	From	To		
CRF-120414	11/30/2013	12/4/2013	9/25/2014	105
CRF-112914	12/5/2013	12/29/2013	9/25/2014	105
CRF-011914	12/30/2013	1/19/2014	9/25/2014	105
CRF-021714	1/20/2014	2/17/2014	9/25/2014	105
CRF-031614	2/18/2014	3/16/2014	9/25/2014	105
CRF-040614	3/17/2014	4/6/2014	9/25/2014	105
CRF-050314	4/7/2014	5/3/2014	9/25/2014	105
CRF-060114	5/4/2014	6/1/2014	9/25/2014	105
CRF-061614	6/2/2014	6/16/2014	9/25/2014	105
CRF-071314	6/17/2014	7/13/2014	4/30/2015	74
CRF-080214	7/14/2014	8/2/2014	4/30/2015	74
CRF-083114	8/3/2014	8/31/2014	4/30/2015	74
CRF-092114	9/1/2014	9/21/2014	4/30/2015	74
CRF-101214	9/22/2014	10/12/2014	4/30/2015	74
CRF-110814	10/13/2014	11/8/2014	4/30/2015	74
CRF-121414	11/9/2014	12/14/2014	4/30/2015	74
CRF-010215	12/15/2014	1/2/2015	4/30/2015	74
CRF-022115	1/3/2015	2/21/2015	4/30/2015	74
CRF-032215	2/22/2015	3/22/2015	9/24/2015	53
CRF-041815	3/23/2015	4/18/2015	9/24/2015	53
CRF-052615	4/19/2015	5/26/2015	9/24/2015	53
CRF-062815	5/27/2015	6/28/2015	9/24/2015	53

Table 2 presents the available acid base accounting (ABA) results for the same sample set.

Table 2. Static Testing Results

Sample Name	Paste pH	Total Sulfur	Sulfide Sulfur	AP	NP	NNP	NPR
	pH units	%	%	t $CaCO_3$/1000 t	t $CaCO_3$/1000 t	t $CaCO_3$/1000 t	-
CRF-092113	11.76	0.22	0.03	0.9	174	173	185
CRF-101213	11.80	0.23	0.04	1.3	443	442	355
CRF-110213	11.81	0.21	0.04	1.3	393	392	315
CRF-111513	11.80	1.24	0.24	7.5	276	269	37
CRF-112913	11.41	0.935	0.36	11.3	200	188	18
CRF-120413	10.41	0.775	0.21	6.6	226	219	34
CRF-011914	11.30	0.799	0.18	5.6	159	153	28
CRF-021714	11.38	1.38	0.48	15.0	189	174	13
CRF-031614	11.28	0.427	0.08	2.5	235	233	94
CRF-040614	10.97	1.26	0.21	6.6	158	151	24
CRF-050314	11.39	0.407	0.17	5.3	160	155	30
CRF-060114	11.32	0.27	0.07	2.2	162	160	74
CRF-061614	11.12	0.478	0.12	3.8	182	178	49
CRF-071314	10.78	0.412	0.19	5.9	84	78	14
CRF-080214	11.46	0.37	0.13	4.1	130	126	32
CRF-083114	11.55	0.226	0.03	0.9	120	119	128
CRF-092114	11.86	0.276	0.08	2.5	133	130	53
CRF-101214	11.60	0.192	0.04	1.3	102	101	82
CRF-110814	11.77	0.419	0.12	3.8	165	161	44
CRF-121414	11.46	1.01	0.27	8.4	120	112	14
CRF-010215	11.81	0.434	0.07	2.2	147	145	67
CRF-022115	11.45	0.485	0.11	3.4	135	132	39

Notes:
Acid Generation Potential (AP) is calculated from sulfide sulfur
Neutralization Potential (NP)
Net Neutralization Potential (NNP = NP - AP)

Samples are submitted to SGS CEMI (SGS) (Vancouver, British Columbia) for testing. HCT Leachate is collected weekly and measured for standard parameters and sulfate. Trace metals are analyzed weeks 1 through 5 and then every 5th week through test termination.

Crown Resources Corporation
A Kinross company
363 Fish Hatchery Road
Republic, WA, USA 99166

phone: (509) 775-3157
fax: (509) 775-3447

Humidity Cell Test Results

HCTs that started prior to February 20, 2014 have run for the minimum required 18 months (72 weeks) of testing and are no longer managed under the DRMP. A complete synopsis of the kinetic testing results to date is presented:

- **General Comment** – The HCTs exhibit similar geochemical behavior and demonstrate the CG CRF material is not likely to generate acid.
- **pH and alkalinity** -- The pH of all of cells decreases from an initially alkaline pH to a circumneutral pH in the general range of 7.5 to 8.5 by week 20 (Figure 1). All samples continue to leach measurable concentrations of alkalinity (Figure 2) and maintain neutral pH, indicating the CG CRF material is well-buffered.

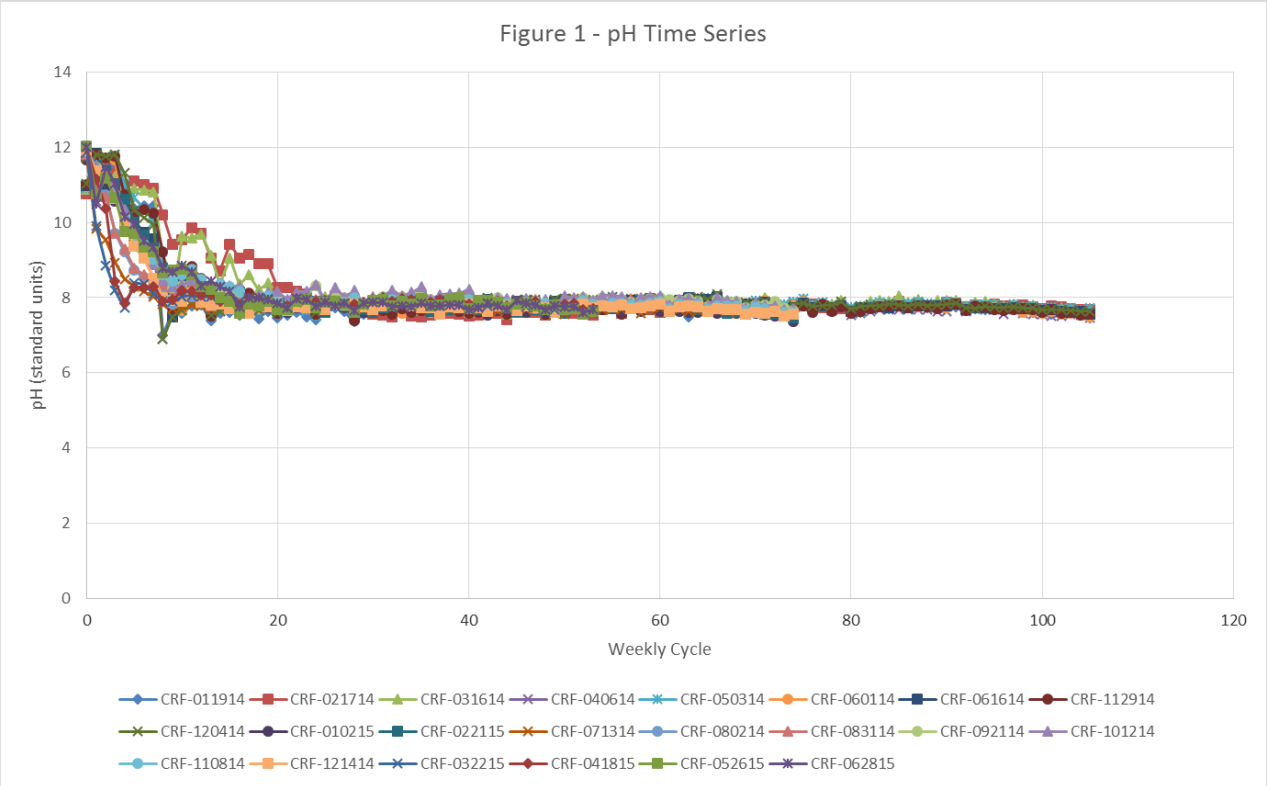

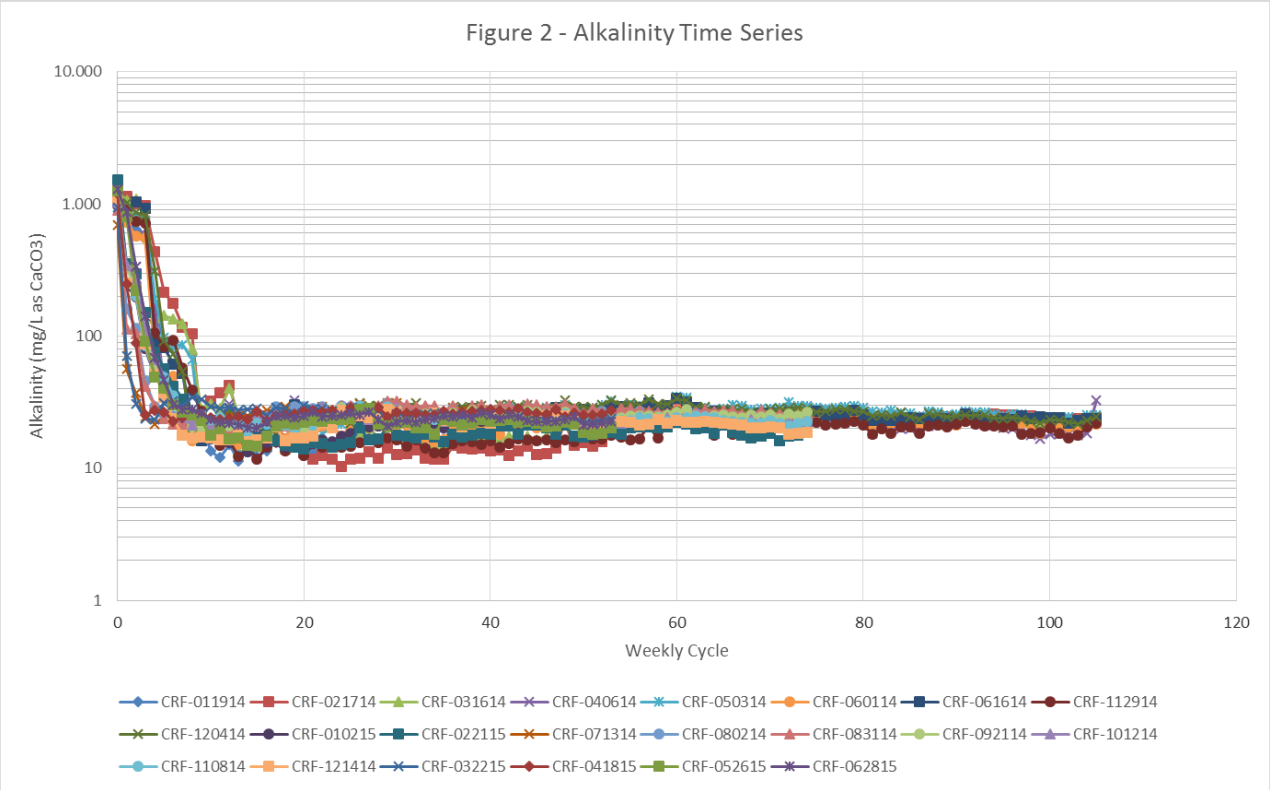

- **Sulfate** -- Sulfate concentrations increase in the early weeks of testing to a maximum of 305 mg/L and, in general, decrease to less than 50 mg/L after several months of leaching (Figure 3).

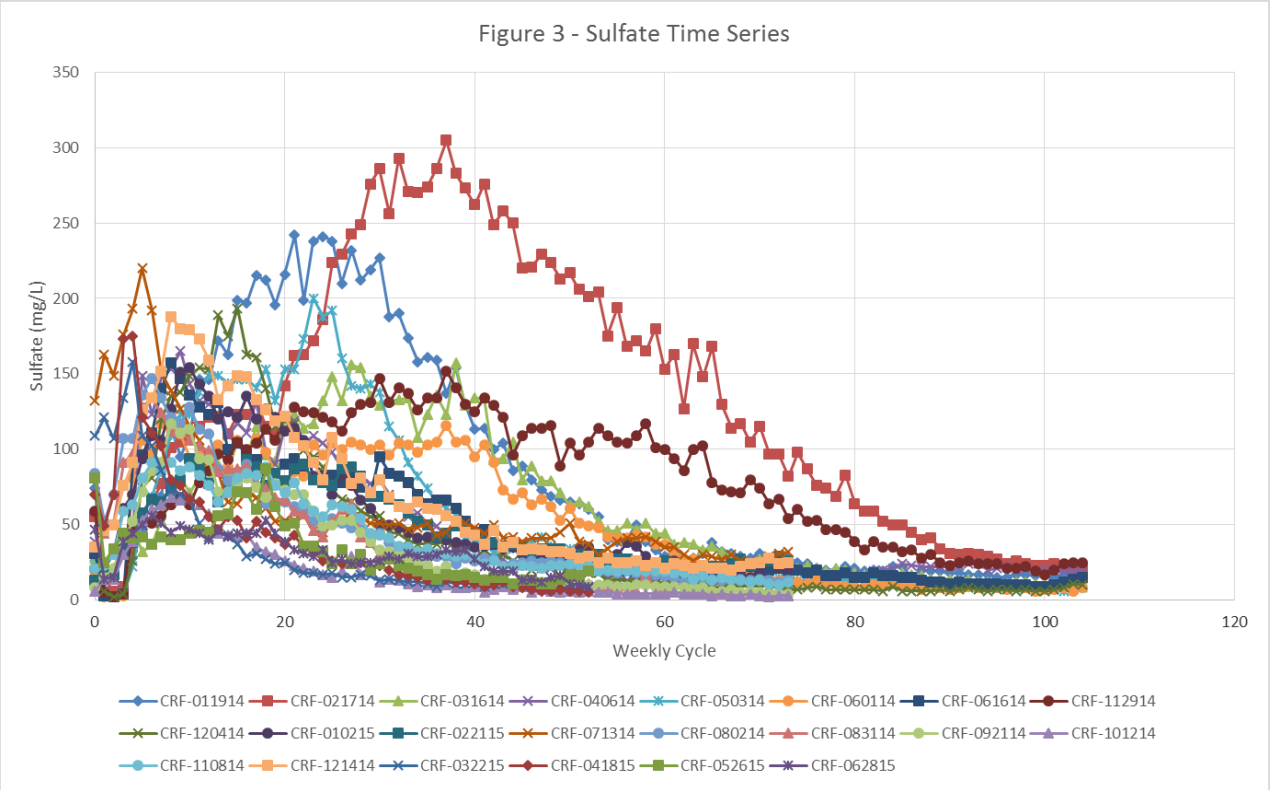

- **Metal Leaching** – CG CRF test results are representative of metal leaching under circumneutral to slightly alkaline conditions:
  - Leachate metal concentrations to date are generally low.
  - Concentrations of beryllium, cadmium, lithium, mercury, silver, zinc, and zircon have generally been near or below detectable limits over the period of testing.
  - Concentrations of iron, aluminum, antimony, barium, bismuth, calcium, chromium, cobalt, copper, lead, nickel, potassium, selenium, sodium, strontium, thallium, tin, titanium, and vanadium show brief spikes in concentration during the first flush period and rapidly decrease to stable concentrations near their respective detection limits.
  - Arsenic is generally detected in leachates at concentrations between approximately 0.001 and 0.018 mg/L (Figure 4). Arsenic concentrations exhibit

a slight increase over time in some cells but stabilize at low concentrations (around 0.015 mg/L).

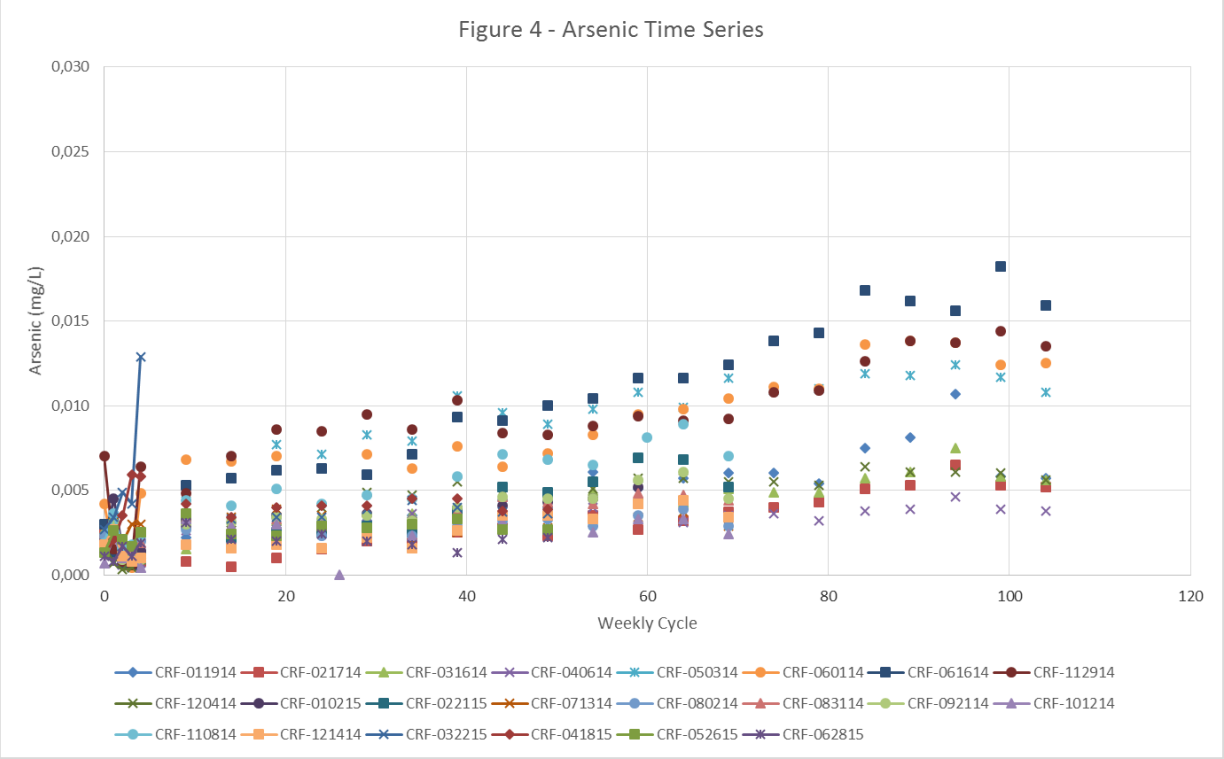

- Uranium concentrations slightly increase through time (Figure 5) and reach a steady state concentration below 0.0002 mg/L by week 55.

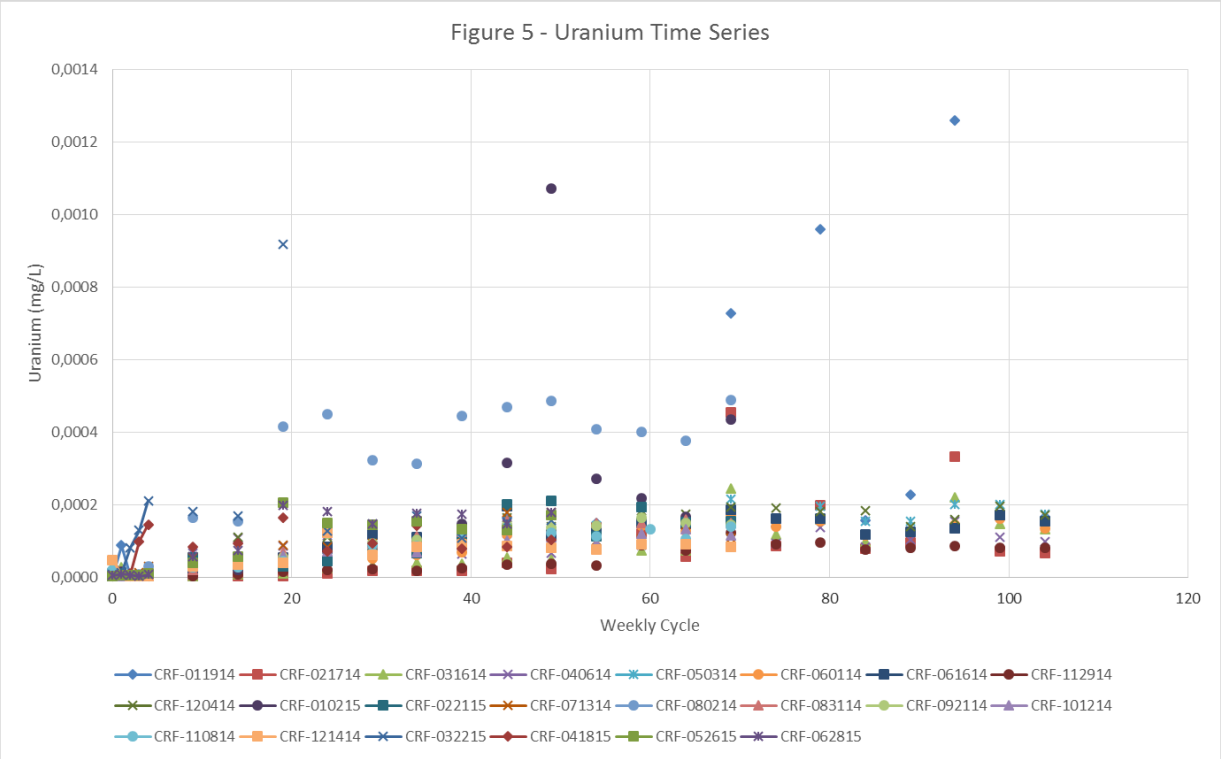

- Chromium concentrations decrease over time from upwards of 0.1 mg/L to less than 0.003 mg/L by week 50 (Figure 6). After week 50, chromium concentrations in the different cells tend to stabilize below 0.001 mg/L.

Crown Resources Corporation
A Kinross company
363 Fish Hatchery Road
Republic, WA, USA 99166

phone: (509) 775-3157
fax: (509) 775-3447

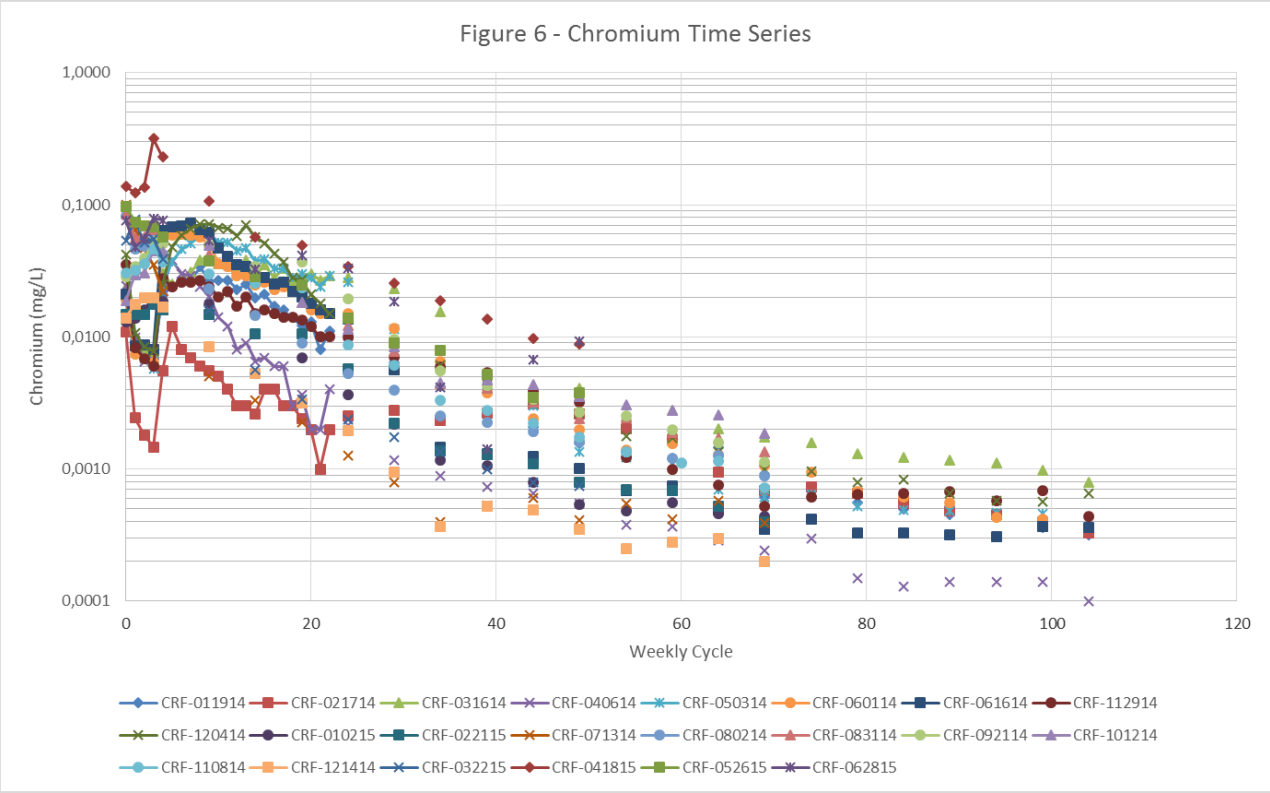

References

Ecology. 2011. First Amendment to the Development Rock Management Plan, April 13, 2011. Crown Resources Corporation (Kinross), Buckhorn Mountain Mine. Issued to Crown on April 15, 2011.

Golder Associates Inc. 2005. Buckhorn Mt. Project: Expected Mine Water Quality. August 29, 2005.

ATTACHMENT 9

MENU

International Network for Acid Prevention

Acid and Metalliferous Drainage (AMD) is one of the most serious and potentially enduring environmental problems for the mining industry. Left unchecked, it can result in such long-term water quality impacts that could well be this industry's most harmful legacy. Effectively dealing with AMD is a formidable challenge as indicated by the high liability cost carried by many mining companies.

It should be noted that AMD is also known as Acid Mine Drainage or Metal Leaching and Acid Rock Drainage (ML/ARD). It encompasses contaminant mobility under acidic or neutral/alkaline pH conditions.

Our Mission

INAP drives leading practice in acid and metalliferous drainage risk management so that mining companies can operate sustainably in their respective environments across the asset lifecycle. This is achieved through industry-led collaboration, knowledge development and sharing.

Learn More About INAP

Join INAP

INAP invites all companies concerned with risk management of sulfide mine waste and AMD mitigation to take an active role in the INAP network. Take advantage of our:

- Networking & Info-sharing
- Technology Transfer
- Gap-driven Research

Get Member Info

Global AMD Resource

In 2009, INAP published the **GARD Guide**, a best practice guide for the prevention and mitigation of Acid Rock Drainage. Since that time, the GARD Guide has rapidly become recognized as the premier global guide on AMD. The GARD Guide is free for all to use and is found on the internet.

Get the GARD Guide

INAP UPDATES

12th Virtual ICARD Proceedings

Proceedings of the 12th Virtual ICARD, September 2022 now available.
→ Download the proceedings here

ICARD 2024

Plan to attend 13th ICARD in Halifax, Nova Scotia, Canada from September 16 - 20, 2024. Download the Call for Abstracts here. For more information, please visit the event website.

INAP MEMBERS

AngloAmerican

KINROSS

NEWCREST MINING LIMITED

Newmont

ABOUT US

INAP was created in 1998 to help meet the challenge of Acid and Metalliferous Drainage. This industry-led organization fills the need for an international body to mobilize data, information, experience and resources to manage sulfide mine waste and prevent AMD.

FOLLOW US

Join our INAP LinkedIn Group

PAGES

INAP Members
Contact Us
About Us

Partners
AMD
GARD Guide
ICARD
Research
Newsletters

JOIN INAP

INAP invites all companies concerned with risk management of sulfide mine waste and AMD mitigation to take an active role in the INAP network. Click the button below to message us about further membership information.

More About Membership

Web Design by Interlinx Group

ATTACHMENT 10

Chapter 4

From GARDGuide

Click Here to Leave a Comment

4.0 Defining the Problem – Characterization

4.0 Defining the Problem – Characterization

4.1 Introduction

The generation, release, mobility, and attenuation of acid rock drainage (ARD) is a complex process governed by a combination of physical, chemical, and biological factors (see Chapter 2). Neutral mine drainage (NMD) and saline drainage (SD) are governed by similar factors but may or may not involve the oxidation of sulphides. Whether ARD, NMD, or SD enters the environment depends largely on the characteristics of the sources and pathways. Characterization of these features is therefore key to the prediction, prevention, and management of drainage impacted by the products of sulphide oxidation at mine sites.

In this chapter, the term “ARD” refers to drainage types that are affected by the products of sulphide oxidation, including acid, neutral and saline drainage.

Environmental characterization programs are designed to collect sufficient data to answer the following questions:

- Is ARD likely to occur and what are the potential sources?
- What type of chemistry is expected?
- When is likely to start and how much will be generated?
- What are the significant pathways that transport contaminants to the receiving environment and can those contaminants be attenuated along those pathways?
- What are the anticipated environmental impacts?
- What can be done to prevent or mitigate/manage ARD?

Figure 4-1 shows how the information presented in this chapter is integrated with other chapters of the GARD Guide in the development and execution of a site characterization program to address these questions.

Table 4-2: Characterization Activities by Mine Phase

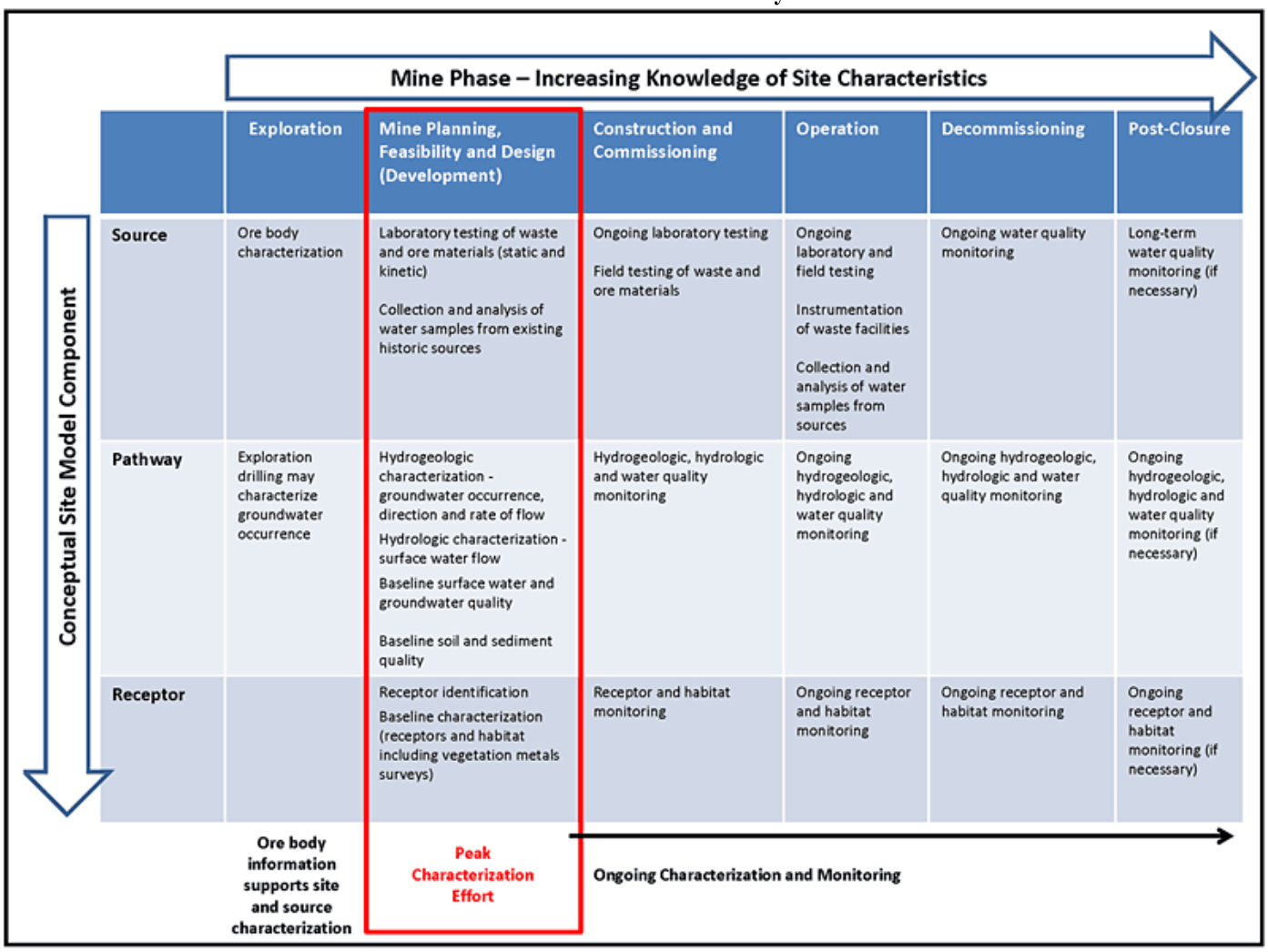

ATTACHMENT 11

ipcc

INTERGOVERNMENTAL PANEL ON climate change

CLIMATE CHANGE 2023

Synthesis Report

Summary for Policymakers

A Report of the Intergovernmental Panel on Climate Change

Introduction

This Synthesis Report (SYR) of the IPCC Sixth Assessment Report (AR6) summarises the state of knowledge of climate change, its widespread impacts and risks, and climate change mitigation and adaptation. It integrates the main findings of the Sixth Assessment Report (AR6) based on contributions from the three Working Groups[1], and the three Special Reports[2]. The summary for Policymakers (SPM) is structured in three parts: SPM.A Current Status and Trends, SPM.B Future Climate Change, Risks, and Long-Term Responses, and SPM.C Responses in the Near Term[3].

This report recognizes the interdependence of climate, ecosystems and biodiversity, and human societies; the value of diverse forms of knowledge; and the close linkages between climate change adaptation, mitigation, ecosystem health, human well-being and sustainable development, and reflects the increasing diversity of actors involved in climate action.

Based on scientific understanding, key findings can be formulated as statements of fact or associated with an assessed level of confidence using the IPCC calibrated language[4].

---

1 The three Working Group contributions to AR6 are: AR6 Climate Change 2021: The Physical Science Basis; AR6 Climate Change 2022: Impacts, Adaptation and Vulnerability; and AR6 Climate Change 2022: Mitigation of Climate Change. Their assessments cover scientific literature accepted for publication respectively by 31 January 2021, 1 September 2021 and 11 October 2021.

2 The three Special Reports are: Global Warming of 1.5°C (2018): an IPCC Special Report on the impacts of global warming of 1.5°C above pre-industrial levels and related global greenhouse gas emission pathways, in the context of strengthening the global response to the threat of climate change, sustainable development, and efforts to eradicate poverty (SR1.5); Climate Change and Land (2019): an IPCC Special Report on climate change, desertification, land degradation, sustainable land management, food security, and greenhouse gas fluxes in terrestrial ecosystems (SRCCL); and The Ocean and Cryosphere in a Changing Climate (2019) (SROCC). The Special Reports cover scientific literature accepted for publication respectively by 15 May 2018, 7 April 2019 and 15 May 2019.

3 In this report, the near term is defined as the period until 2040. The long term is defined as the period beyond 2040.

4 Each finding is grounded in an evaluation of underlying evidence and agreement. The IPCC calibrated language uses five qualifiers to express a level of confidence: very low, low, medium, high and very high, and typeset in italics, for example, *medium confidence*. The following terms are used to indicate the assessed likelihood of an outcome or a result: virtually certain 99–100% probability, very likely 90–100%, likely 66–100%, more likely than not >50–100%, about as likely as not 33–66%, unlikely 0–33%, very unlikely 0–10%, exceptionally unlikely 0–1%. Additional terms (extremely likely 95–100%; and extremely unlikely 0–5%) are also used when appropriate. Assessed likelihood is typeset in italics, e.g., *very likely*. This is consistent with AR5 and the other AR6 Reports.

A. Current Status and Trends

Observed Warming and its Causes

A.1 Human activities, principally through emissions of greenhouse gases, have unequivocally caused global warming, with global surface temperature reaching 1.1°C above 1850-1900 in 2011-2020. Global greenhouse gas emissions have continued to increase, with unequal historical and ongoing contributions arising from unsustainable energy use, land use and land-use change, lifestyles and patterns of consumption and production across regions, between and within countries, and among individuals (*high confidence*). {*2.1, Figure 2.1, Figure 2.2*}

A.1.1 Global surface temperature was 1.09 [0.95 to 1.20]°C[5] higher in 2011–2020 than 1850–1900[6], with larger increases over land (1.59 [1.34 to 1.83]°C) than over the ocean (0.88 [0.68 to 1.01]°C). Global surface temperature in the first two decades of the 21st century (2001–2020) was 0.99 [0.84 to 1.10]°C higher than 1850–1900. Global surface temperature has increased faster since 1970 than in any other 50-year period over at least the last 2000 years (*high confidence*). {*2.1.1*, *Figure 2.1*}

A.1.2 The *likely* range of total human-caused global surface temperature increase from 1850–1900 to 2010–2019[7] is 0.8°C to 1.3°C, with a best estimate of 1.07°C. Over this period, it is *likely* that well-mixed greenhouse gases (GHGs) contributed a warming of 1.0°C to 2.0°C[8], and other human drivers (principally aerosols) contributed a cooling of 0.0°C to 0.8°C, natural (solar and volcanic) drivers changed global surface temperature by –0.1°C to +0.1°C, and internal variability changed it by –0.2°C to +0.2°C. {*2.1.1*, *Figure 2.1*}

A.1.3 Observed increases in well-mixed GHG concentrations since around 1750 are unequivocally caused by GHG emissions from human activities over this period. Historical cumulative net CO_2 emissions from 1850 to 2019 were 2400 ± 240 $GtCO_2$ of which more than half (58%) occurred between 1850 and 1989, and about 42% occurred between 1990 and 2019 (*high confidence*). In 2019, atmospheric CO_2 concentrations (410 parts per million) were higher than at any time in at least 2 million years (*high confidence*), and concentrations of methane (1866 parts per billion) and nitrous oxide (332 parts per billion) were higher than at any time in at least 800,000 years (*very high confidence*). {*2.1.1*, *Figure 2.1*}

A.1.4 Global net anthropogenic GHG emissions have been estimated to be 59 ± 6.6 $GtCO_2$-eq[9] in 2019, about 12% (6.5 $GtCO_2$-eq) higher than in 2010 and 54% (21 $GtCO_2$-eq) higher than in 1990, with the largest share and growth in gross GHG emissions occurring in CO_2 from fossil fuels combustion and industrial processes (CO_2-FFI) followed by methane, whereas the highest relative growth occurred in fluorinated gases (F-gases), starting from low levels in 1990. Average annual GHG emissions during 2010–2019 were higher than in any previous decade on record, while the rate of growth between 2010 and 2019 (1.3% yr^{-1}) was lower than that between 2000 and 2009 (2.1% yr^{-1}). In 2019, approximately 79% of global GHG

---

5 Ranges given throughout the SPM represent *very likely* ranges (5–95% range) unless otherwise stated.

6 The estimated increase in global surface temperature since AR5 is principally due to further warming since 2003–2012 (0.19 [0.16 to 0.22] °C). Additionally, methodological advances and new datasets have provided a more complete spatial representation of changes in surface temperature, including in the Arctic. These and other improvements have also increased the estimate of global surface temperature change by approximately 0.1°C, but this increase does not represent additional physical warming since AR5.

7 The period distinction with A.1.1 arises because the attribution studies consider this slightly earlier period. The observed warming to 2010–2019 is 1.06 [0.88 to 1.21]°C.

8 Contributions from emissions to the 2010–2019 warming relative to 1850–1900 assessed from radiative forcing studies are: CO_2 0.8 [0.5 to 1.2]°C; methane 0.5 [0.3 to 0.8]°C; nitrous oxide 0.1 [0.0 to 0.2]°C and fluorinated gases 0.1 [0.0 to 0.2]°C. {*2.1.1*}

9 GHG emission metrics are used to express emissions of different greenhouse gases in a common unit. Aggregated GHG emissions in this report are stated in CO_2-equivalents (CO_2-eq) using the Global Warming Potential with a time horizon of 100 years (GWP100) with values based on the contribution of Working Group I to the AR6. The AR6 WGI and WGIII reports contain updated emission metric values, evaluations of different metrics with regard to mitigation objectives, and assess new approaches to aggregating gases. The choice of metric depends on the purpose of the analysis and all GHG emission metrics have limitations and uncertainties, given that they simplify the complexity of the physical climate system and its response to past and future GHG emissions. {*2.1.1*}

emissions came from the sectors of energy, industry, transport, and buildings together and 22%[10] from agriculture, forestry and other land use (AFOLU). Emissions reductions in CO_2-FFI due to improvements in energy intensity of GDP and carbon intensity of energy, have been less than emissions increases from rising global activity levels in industry, energy supply, transport, agriculture and buildings. (*high confidence*) {*2.1.1*}

A.1.5 Historical contributions of CO_2 emissions vary substantially across regions in terms of total magnitude, but also in terms of contributions to CO_2-FFI and net CO_2 emissions from land use, land-use change and forestry (CO_2-LULUCF). In 2019, around 35% of the global population live in countries emitting more than 9 tCO_2-eq per capita[11] (excluding CO_2-LULUCF) while 41% live in countries emitting less than 3 tCO_2-eq per capita; of the latter a substantial share lacks access to modern energy services. Least Developed Countries (LDCs) and Small Island Developing States (SIDS) have much lower per capita emissions (1.7 tCO_2-eq and 4.6 tCO_2-eq, respectively) than the global average (6.9 tCO_2-eq), excluding CO_2-LULUCF. The 10% of households with the highest per capita emissions contribute 34–45% of global consumption-based household GHG emissions, while the bottom 50% contribute 13–15%. (*high confidence*) {*2.1.1, Figure 2.2*}

Observed Changes and Impacts

A.2 Widespread and rapid changes in the atmosphere, ocean, cryosphere and biosphere have occurred. Human-caused climate change is already affecting many weather and climate extremes in every region across the globe. This has led to widespread adverse impacts and related losses and damages to nature and people (*high confidence*). Vulnerable communities who have historically contributed the least to current climate change are disproportionately affected (*high confidence*). {*2.1, Table 2.1, Figure 2.2, Figure 2.3*} (*Figure SPM.1*)

A.2.1 It is unequivocal that human influence has warmed the atmosphere, ocean and land. Global mean sea level increased by 0.20 [0.15 to 0.25] m between 1901 and 2018. The average rate of sea level rise was 1.3 [0.6 to 2.1] mm yr^{-1} between 1901 and 1971, increasing to 1.9 [0.8 to 2.9] mm yr^{-1} between 1971 and 2006, and further increasing to 3.7 [3.2 to 4.2] mm yr^{-1} between 2006 and 2018 (*high confidence*). Human influence was *very likely* the main driver of these increases since at least 1971. Evidence of observed changes in extremes such as heatwaves, heavy precipitation, droughts, and tropical cyclones, and, in particular, their attribution to human influence, has further strengthened since AR5. Human influence has *likely* increased the chance of compound extreme events since the 1950s, including increases in the frequency of concurrent heatwaves and droughts (*high confidence*). {*2.1.2, Table 2.1, Figure 2.3, Figure 3.4*} (*Figure SPM.1*)

A.2.2 Approximately 3.3 to 3.6 billion people live in contexts that are highly vulnerable to climate change. Human and ecosystem vulnerability are interdependent. Regions and people with considerable development constraints have high vulnerability to climatic hazards. Increasing weather and climate extreme events have exposed millions of people to acute food insecurity[12] and reduced water security, with the largest adverse impacts observed in many locations and/or communities in Africa, Asia, Central and South America, LDCs, Small Islands and the Arctic, and globally for Indigenous Peoples, small-scale food producers and low-income households. Between 2010 and 2020, human mortality from floods, droughts and storms was 15 times higher in highly vulnerable regions, compared to regions with very low vulnerability. (*high confidence*) {*2.1.2, 4.4*} (*Figure SPM.1*)

A.2.3 Climate change has caused substantial damages, and increasingly irreversible losses, in terrestrial, freshwater, cryospheric, and coastal and open ocean ecosystems (*high confidence*). Hundreds of local losses of species have been driven by increases in the magnitude of heat extremes (*high confidence*) with mass mortality events recorded on land and in the ocean (*very high confidence*). Impacts on some ecosystems are approaching irreversibility such as the impacts of hydrological changes resulting from the retreat of glaciers, or the changes in some mountain (*medium confidence*) and Arctic ecosystems driven by permafrost thaw (*high confidence*). {*2.1.2, Figure 2.3*} (*Figure SPM.1*)

[10] GHG emission levels are rounded to two significant digits; as a consequence, small differences in sums due to rounding may occur. {*2.1.1*}

[11] Territorial emissions.

[12] Acute food insecurity can occur at any time with a severity that threatens lives, livelihoods or both, regardless of the causes, context or duration, as a result of shocks risking determinants of food security and nutrition, and is used to assess the need for humanitarian action. {*2.1*}

A.2.4 Climate change has reduced food security and affected water security, hindering efforts to meet Sustainable Development Goals (*high confidence*). Although overall agricultural productivity has increased, climate change has slowed this growth over the past 50 years globally (*medium confidence*), with related negative impacts mainly in mid- and low latitude regions but positive impacts in some high latitude regions (*high confidence*). Ocean warming and ocean acidification have adversely affected food production from fisheries and shellfish aquaculture in some oceanic regions *(high confidence)*. Roughly half of the world's population currently experience severe water scarcity for at least part of the year due to a combination of climatic and non-climatic drivers (*medium confidence*). {*2.1.2, Figure 2.3*} (*Figure SPM.1*)

A.2.5 In all regions increases in extreme heat events have resulted in human mortality and morbidity (*very high confidence*). The occurrence of climate-related food-borne and water-borne diseases (*very high confidence*) and the incidence of vector-borne diseases (*high confidence*) have increased. In assessed regions, some mental health challenges are associated with increasing temperatures (*high confidence*), trauma from extreme events (*very high confidence*), and loss of livelihoods and culture (*high confidence*). Climate and weather extremes are increasingly driving displacement in Africa, Asia, North America (*high confidence*), and Central and South America (*medium confidence*), with small island states in the Caribbean and South Pacific being disproportionately affected relative to their small population size (*high confidence*). {*2.1.2, Figure 2.3*} (*Figure SPM.1*)

A.2.6 Climate change has caused widespread adverse impacts and related losses and damages[13] to nature and people that are unequally distributed across systems, regions and sectors. Economic damages from climate change have been detected in climate-exposed sectors, such as agriculture, forestry, fishery, energy, and tourism. Individual livelihoods have been affected through, for example, destruction of homes and infrastructure, and loss of property and income, human health and food security, with adverse effects on gender and social equity. (*high confidence*) {*2.1.2*} (*Figure SPM.1*)

A.2.7 In urban areas, observed climate change has caused adverse impacts on human health, livelihoods and key infrastructure. Hot extremes have intensified in cities. Urban infrastructure, including transportation, water, sanitation and energy systems have been compromised by extreme and slow-onset events[14], with resulting economic losses, disruptions of services and negative impacts to well-being. Observed adverse impacts are concentrated amongst economically and socially marginalised urban residents. (*high confidence*) {*2.1.2*}

[13] In this report, the term 'losses and damages' refers to adverse observed impacts and/or projected risks and can be economic and/or non-economic (see Annex I: Glossary).

[14] Slow-onset events are described among the climatic-impact drivers of the AR6 WGI and refer to the risks and impacts associated with e.g., increasing temperature means, desertification, decreasing precipitation, loss of biodiversity, land and forest degradation, glacial retreat and related impacts, ocean acidification, sea level rise and salinization. {*2.1.2*}

Adverse impacts from human-caused climate change will continue to intensify

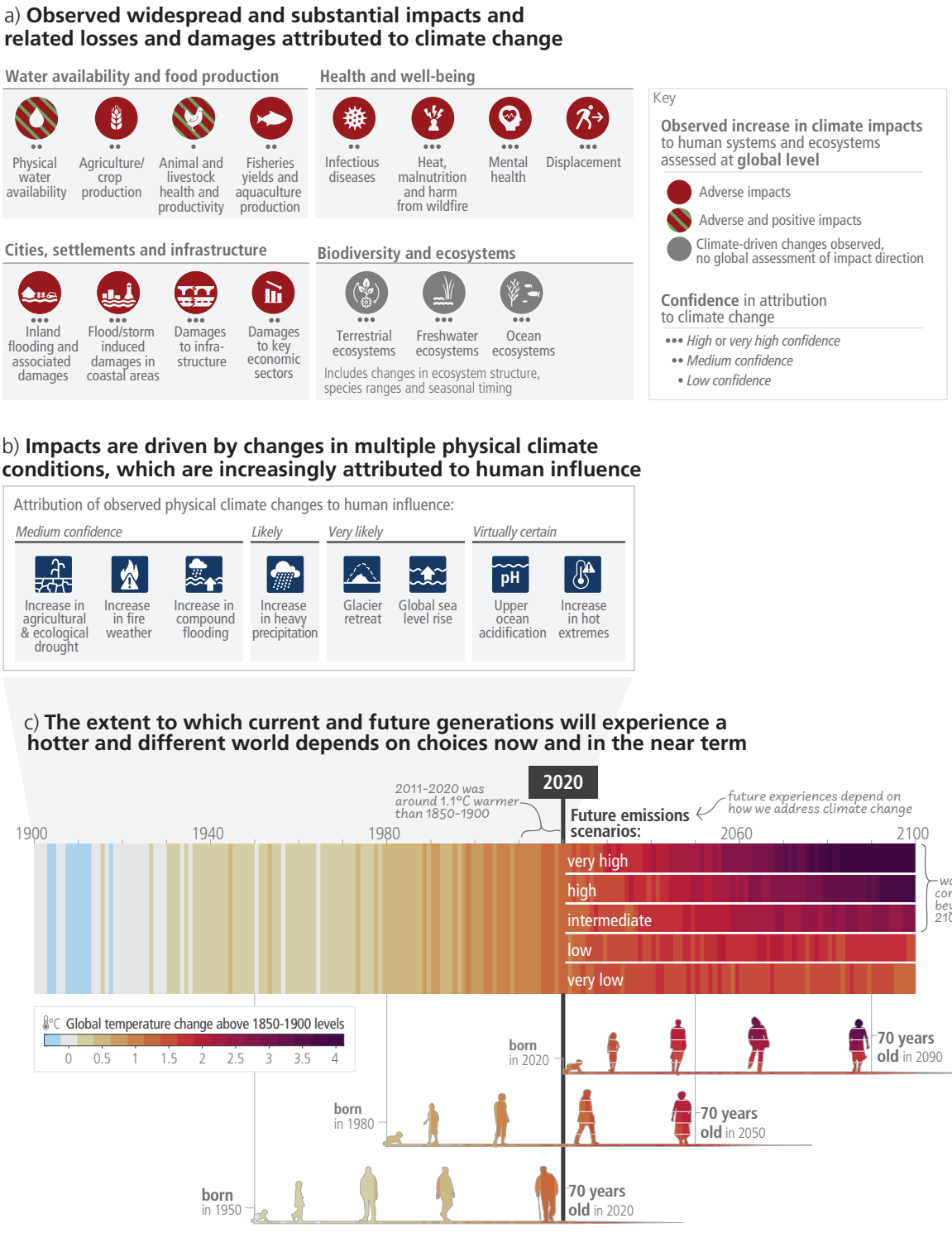

Figure SPM.1: (a) Climate change has already caused widespread impacts and related losses and damages on human systems and altered terrestrial, freshwater and ocean ecosystems worldwide. Physical water availability includes balance of water available from various sources including ground water, water quality and demand for water. Global mental health and displacement assessments reflect only assessed regions. Confidence levels reflect the assessment of attribution of the observed impact to climate change. **(b)** Observed impacts are connected to physical climate changes including many that have been attributed to human influence such as the selected climatic impact-drivers shown. Confidence and likelihood levels reflect the assessment of attribution of the observed climatic impact-driver to human influence. **(c)** Observed (1900–2020) and projected (2021–2100) changes in global surface temperature (relative to 1850-1900), which are linked to changes in climate conditions and impacts, illustrate how the climate has already changed and will change along the lifespan of three

representative generations (born in 1950, 1980 and 2020). Future projections (2021–2100) of changes in global surface temperature are shown for very low (SSP1-1.9), low (SSP1-2.6), intermediate (SSP2-4.5), high (SSP3-7.0) and very high (SSP5-8.5) GHG emissions scenarios. Changes in annual global surface temperatures are presented as 'climate stripes', with future projections showing the human-caused long-term trends and continuing modulation by natural variability (represented here using observed levels of past natural variability). Colours on the generational icons correspond to the global surface temperature stripes for each year, with segments on future icons differentiating possible future experiences. {*2.1, 2.1.2, Figure 2.1, Table 2.1, Figure 2.3, Cross-Section Box.2, 3.1, Figure 3.3, 4.1, 4.3*} (*Box SPM.1*)

Current Progress in Adaptation and Gaps and Challenges

A.3 Adaptation planning and implementation has progressed across all sectors and regions, with documented benefits and varying effectiveness. Despite progress, adaptation gaps exist, and will continue to grow at current rates of implementation. Hard and soft limits to adaptation have been reached in some ecosystems and regions. Maladaptation is happening in some sectors and regions. Current global financial flows for adaptation are insufficient for, and constrain implementation of, adaptation options, especially in developing countries (*high confidence*). {*2.2, 2.3*}

A.3.1 Progress in adaptation planning and implementation has been observed across all sectors and regions, generating multiple benefits (*very high confidence*). Growing public and political awareness of climate impacts and risks has resulted in at least 170 countries and many cities including adaptation in their climate policies and planning processes (*high confidence*). {*2.2.3*}

A.3.2 Effectiveness[15] of adaptation in reducing climate risks[16] is documented for specific contexts, sectors and regions (*high confidence*). Examples of effective adaptation options include: cultivar improvements, on-farm water management and storage, soil moisture conservation, irrigation, agroforestry, community-based adaptation, farm and landscape level diversification in agriculture, sustainable land management approaches, use of agroecological principles and practices and other approaches that work with natural processes (*high confidence*). Ecosystem-based adaptation[17] approaches such as urban greening, restoration of wetlands and upstream forest ecosystems have been effective in reducing flood risks and urban heat (*high confidence*). Combinations of non-structural measures like early warning systems and structural measures like levees have reduced loss of lives in case of inland flooding (*medium confidence*). Adaptation options such as disaster risk management, early warning systems, climate services and social safety nets have broad applicability across multiple sectors (*high confidence*). {*2.2.3*}

A.3.3 Most observed adaptation responses are fragmented, incremental[18], sector-specific and unequally distributed across regions. Despite progress, adaptation gaps exist across sectors and regions, and will continue to grow under current levels of implementation, with the largest adaptation gaps among lower income groups. (*high confidence*) {*2.3.2*}

A.3.4 There is increased evidence of maladaptation in various sectors and regions. Maladaptation especially affects marginalised and vulnerable groups adversely. (*high confidence*) {*2.3.2*}

A.3.5 Soft limits to adaptation are currently being experienced by small-scale farmers and households along some low-lying coastal areas (*medium confidence*) resulting from financial, governance, institutional and policy constraints (*high confidence*). Some tropical, coastal, polar and mountain ecosystems have reached hard adaptation limits (*high confidence*). Adaptation does not prevent all losses and damages, even with effective adaptation and before reaching soft and hard limits (*high confidence*). {*2.3.2*}

[15] Effectiveness refers here to the extent to which an adaptation option is anticipated or observed to reduce climate-related risk. {*2.2.3*}

[16] See Annex I: Glossary. {*2.2.3*}

[17] Ecosystem-based Adaptation (EbA) is recognized internationally under the Convention on Biological Diversity (CBD14/5). A related concept is Nature-based Solutions (NbS), see Annex I: Glossary.

[18] Incremental adaptations to change in climate are understood as extensions of actions and behaviours that already reduce the losses or enhance the benefits of natural variations in extreme weather/climate events. {*2.3.2*}

A.3.6 Key barriers to adaptation are limited resources, lack of private sector and citizen engagement, insufficient mobilization of finance (including for research), low climate literacy, lack of political commitment, limited research and/or slow and low uptake of adaptation science, and low sense of urgency. There are widening disparities between the estimated costs of adaptation and the finance allocated to adaptation (*high confidence*). Adaptation finance has come predominantly from public sources, and a small proportion of global tracked climate finance was targeted to adaptation and an overwhelming majority to mitigation (*very high confidence*). Although global tracked climate finance has shown an upward trend since AR5, current global financial flows for adaptation, including from public and private finance sources, are insufficient and constrain implementation of adaptation options, especially in developing countries (*high confidence*). Adverse climate impacts can reduce the availability of financial resources by incurring losses and damages and through impeding national economic growth, thereby further increasing financial constraints for adaptation, particularly for developing and least developed countries (*medium confidence*). {*2.3.2, 2.3.3*}

Box SPM.1 The use of scenarios and modelled pathways in the AR6 Synthesis Report

Modelled scenarios and pathways[19] are used to explore future emissions, climate change, related impacts and risks, and possible mitigation and adaptation strategies and are based on a range of assumptions, including socio-economic variables and mitigation options. These are quantitative projections and are neither predictions nor forecasts. Global modelled emission pathways, including those based on cost effective approaches contain regionally differentiated assumptions and outcomes, and have to be assessed with the careful recognition of these assumptions. Most do not make explicit assumptions about global equity, environmental justice or intra-regional income distribution. IPCC is neutral with regard to the assumptions underlying the scenarios in the literature assessed in this report, which do not cover all possible futures.[20] {*Cross-Section Box.2*}

WGI assessed the climate response to five illustrative scenarios based on Shared Socio-economic Pathways (SSPs)[21] that cover the range of possible future development of anthropogenic drivers of climate change found in the literature. High and very high GHG emissions scenarios (SSP3-7.0 and SSP5-8.5[22]) have CO_2 emissions that roughly double from current levels by 2100 and 2050, respectively. The intermediate GHG emissions scenario (SSP2-4.5) has CO_2 emissions remaining around current levels until the middle of the century. The very low and low GHG emissions scenarios (SSP1-1.9 and SSP1-2.6) have CO_2 emissions declining to net zero around 2050 and 2070, respectively, followed by varying levels of net negative CO_2 emissions. In addition, Representative Concentration Pathways (RCPs)[23] were used by WGI and WGII to assess regional climate changes, impacts and risks. In WGIII, a large number of global modelled emissions pathways were assessed, of which 1202 pathways were categorised based on their assessed global warming over the 21st century; categories range from pathways that limit warming to 1.5°C with more than 50% likelihood (noted >50% in this report) with no or limited overshoot (C1) to pathways that exceed 4°C (C8). {*Cross-Section Box.2*} (*Box SPM.1, Table 1*)

Global warming levels (GWLs) relative to 1850–1900 are used to integrate the assessment of climate change and related impacts and risks since patterns of changes for many variables at a given GWL are common to all scenarios considered and independent of timing when that level is reached. {*Cross-Section Box.2*}

---

19 In the literature, the terms pathways and scenarios are used interchangeably, with the former more frequently used in relation to climate goals. WGI primarily used the term scenarios and WGIII mostly used the term modelled emission and mitigation pathways. The SYR primarily uses scenarios when referring to WGI and modelled emission and mitigation pathways when referring to WGIII.

20 Around half of all modelled global emission pathways assume cost-effective approaches that rely on least-cost mitigation/abatement options globally. The other half looks at existing policies and regionally and sectorally differentiated actions.

21 SSP-based scenarios are referred to as SSPx-y, where 'SSPx' refers to the Shared Socioeconomic Pathway describing the socioeconomic trends underlying the scenarios, and 'y' refers to the level of radiative forcing (in watts per square metre, or W m^{-2}) resulting from the scenario in the year 2100. {*Cross-Section Box.2*}

22 Very high emissions scenarios have become *less likely* but cannot be ruled out. Warming levels >4°C may result from very high emissions scenarios, but can also occur from lower emission scenarios if climate sensitivity or carbon cycle feedbacks are higher than the best estimate. {*3.1.1*}

23 RCP-based scenarios are referred to as RCPy, where 'y' refers to the level of radiative forcing (in watts per square metre, or W m^{-2}) resulting from the scenario in the year 2100. The SSP scenarios cover a broader range of greenhouse gas and air pollutant futures than the RCPs. They are similar but not identical, with differences in concentration trajectories. The overall effective radiative forcing tends to be higher for the SSPs compared to the RCPs with the same label (*medium confidence*). {*Cross-Section Box.2*}

Box SPM.1, Table 1: Description and relationship of scenarios and modelled pathways considered across AR6 Working Group reports. {*Cross-Section Box.2 Figure 1*}

Category in WGIII	Category description	GHG emissions scenarios (SSPx-y*) in WGI & WGII	RCPy** in WGI & WGII
C1	limit warming to 1.5°C (>50%) with no or limited overshoot***	Very low (SSP1-1.9)	
C2	return warming to 1.5°C (>50%) after a high overshoot***		
C3	limit warming to 2°C (>67%)	Low (SSP1-2.6)	RCP2.6
C4	limit warming to 2°C (>50%)		
C5	limit warming to 2.5°C (>50%)		
C6	limit warming to 3°C (>50%)	Intermediate (SSP2-4.5)	RCP 4.5
C7	limit warming to 4°C (>50%)	High (SSP3-7.0)	
C8	exceed warming of 4°C (>50%)	Very high (SSP5-8.5)	RCP 8.5

* See footnote 21 for the SSPx-y terminology.

** See footnote 23 for the RCPy terminology.

*** Limited overshoot refers to exceeding 1.5°C global warming by up to about 0.1°C, high overshoot by 0.1°C-0.3°C, in both cases for up to several decades.

Current Mitigation Progress, Gaps and Challenges

A.4 Policies and laws addressing mitigation have consistently expanded since AR5. Global GHG emissions in 2030 implied by nationally determined contributions (NDCs) announced by October 2021 make it *likely* that warming will exceed 1.5°C during the 21st century and make it harder to limit warming below 2°C. There are gaps between projected emissions from implemented policies and those from NDCs and finance flows fall short of the levels needed to meet climate goals across all sectors and regions. (*high confidence*) {*2.2, 2.3, Figure 2.5, Table 2.2*}

A.4.1 The UNFCCC, Kyoto Protocol, and the Paris Agreement are supporting rising levels of national ambition. The Paris Agreement, adopted under the UNFCCC, with near universal participation, has led to policy development and target-setting at national and sub-national levels, in particular in relation to mitigation, as well as enhanced transparency of climate action and support (*medium confidence*). Many regulatory and economic instruments have already been deployed successfully (*high confidence*). In many countries, policies have enhanced energy efficiency, reduced rates of deforestation and accelerated technology deployment, leading to avoided and in some cases reduced or removed emissions (*high confidence*). Multiple lines of evidence suggest that mitigation policies have led to several[24] Gt CO_2-eq yr^{-1} of avoided global emissions (*medium confidence*). At least 18 countries have sustained absolute production-based GHG and consumption-based CO_2 reductions[25] for longer than 10 years. These reductions have only partly offset global emissions growth (*high confidence*). {*2.2.1, 2.2.2*}

A.4.2 Several mitigation options, notably solar energy, wind energy, electrification of urban systems, urban green infrastructure, energy efficiency, demand-side management, improved forest and crop/grassland management, and reduced food waste and loss, are technically viable, are becoming increasingly cost effective and are generally supported by the

[24] At least 1.8 $GtCO_2$-eq yr^{-1} can be accounted for by aggregating separate estimates for the effects of economic and regulatory instruments. Growing numbers of laws and executive orders have impacted global emissions and were estimated to result in 5.9 $GtCO_2$-eq yr^{-1} less emissions in 2016 than they otherwise would have been. (*medium confidence*) {*2.2.2*}

[25] Reductions were linked to energy supply decarbonisation, energy efficiency gains, and energy demand reduction, which resulted from both policies and changes in economic structure (*high confidence*). {*2.2.2*}

public. From 2010 to 2019 there have been sustained decreases in the unit costs of solar energy (85%), wind energy (55%), and lithium-ion batteries (85%), and large increases in their deployment, e.g., >10× for solar and >100× for electric vehicles (EVs), varying widely across regions. The mix of policy instruments that reduced costs and stimulated adoption includes public R&D, funding for demonstration and pilot projects, and demand-pull instruments such as deployment subsidies to attain scale. Maintaining emission-intensive systems may, in some regions and sectors, be more expensive than transitioning to low emission systems. (*high confidence*) {*2.2.2, Figure 2.4*}

A.4.3 A substantial 'emissions gap' exists between global GHG emissions in 2030 associated with the implementation of NDCs announced prior to COP26[26] and those associated with modelled mitigation pathways that limit warming to 1.5°C (>50%) with no or limited overshoot or limit warming to 2°C (>67%) assuming immediate action (*high confidence*). This would make it *likely* that warming will exceed 1.5°C during the 21st century (*high confidence*). Global modelled mitigation pathways that limit warming to 1.5°C (>50%) with no or limited overshoot or limit warming to 2°C (>67%) assuming immediate action imply deep global GHG emissions reductions this decade (*high confidence*) (see SPM Box 1, Table 1, B.6)[27]. Modelled pathways that are consistent with NDCs announced prior to COP26 until 2030 and assume no increase in ambition thereafter have higher emissions, leading to a median global warming of 2.8 [2.1 to 3.4] °C by 2100 (*medium confidence*). Many countries have signalled an intention to achieve net zero GHG or net zero CO_2 by around mid-century but pledges differ across countries in terms of scope and specificity, and limited policies are to date in place to deliver on them. {*2.3.1, Table 2.2, Figure 2.5, Table 3.1, 4.1*}

A.4.4 Policy coverage is uneven across sectors (*high confidence*). Policies implemented by the end of 2020 are projected to result in higher global GHG emissions in 2030 than emissions implied by NDCs, indicating an 'implementation gap' (*high confidence*). Without a strengthening of policies, global warming of 3.2 [2.2 to 3.5] °C is projected by 2100 (*medium confidence*). {*2.2.2, 2.3.1, 3.1.1, Figure 2.5*} (*Box SPM.1, Figure SPM.5*)

A.4.5 The adoption of low-emission technologies lags in most developing countries, particularly least developed ones, due in part to limited finance, technology development and transfer, and capacity (*medium confidence*). The magnitude of climate finance flows has increased over the last decade and financing channels have broadened but growth has slowed since 2018 (*high confidence*). Financial flows have developed heterogeneously across regions and sectors (*high confidence*). Public and private finance flows for fossil fuels are still greater than those for climate adaptation and mitigation (*high confidence*). The overwhelming majority of tracked climate finance is directed towards mitigation, but nevertheless falls short of the levels needed to limit warming to below 2°C or to 1.5°C across all sectors and regions (see C7.2) (*very high confidence*). In 2018, public and publicly mobilised private climate finance flows from developed to developing countries were below the collective goal under the UNFCCC and Paris Agreement to mobilise USD 100 billion per year by 2020 in the context of meaningful mitigation action and transparency on implementation (*medium confidence*). {*2.2.2, 2.3.1, 2.3.3*}

[26] Due to the literature cutoff date of WGIII, the additional NDCs submitted after 11 October 2021 are not assessed here. {*Footnote 32 in the Longer Report*}

[27] Projected 2030 GHG emissions are 50 (47–55) $GtCO_2$-eq if all conditional NDC elements are taken into account. Without conditional elements, the global emissions are projected to be approximately similar to modelled 2019 levels at 53 (50–57) $GtCO_2$-eq. {*2.3.1, Table 2.2*}

B. Future Climate Change, Risks, and Long-Term Responses

Future Climate Change

B.1 Continued greenhouse gas emissions will lead to increasing global warming, with the best estimate of reaching 1.5°C in the near term in considered scenarios and modelled pathways. Every increment of global warming will intensify multiple and concurrent hazards (*high confidence*). Deep, rapid, and sustained reductions in greenhouse gas emissions would lead to a discernible slowdown in global warming within around two decades, and also to discernible changes in atmospheric composition within a few years (*high confidence*). {*Cross-Section Boxes 1 and 2, 3.1, 3.3, Table 3.1, Figure 3.1, 4.3*} (*Figure SPM.2, Box SPM.1*)

B.1.1 Global warming[28] will continue to increase in the near term (2021–2040) mainly due to increased cumulative CO_2 emissions in nearly all considered scenarios and modelled pathways. In the near term, global warming *is more likely than not* to reach 1.5°C even under the very low GHG emission scenario (SSP1-1.9) and *likely* or *very likely* to exceed 1.5°C under higher emissions scenarios. In the considered scenarios and modelled pathways, the best estimates of the time when the level of global warming of 1.5°C is reached lie in the near term[29]. Global warming declines back to below 1.5°C by the end of the 21st century in some scenarios and modelled pathways (see B.7). The assessed climate response to GHG emissions scenarios results in a best estimate of warming for 2081–2100 that spans a range from 1.4°C for a very low GHG emissions scenario (SSP1-1.9) to 2.7°C for an intermediate GHG emissions scenario (SSP2-4.5) and 4.4°C for a very high GHG emissions scenario (SSP5-8.5)[30], with narrower uncertainty ranges[31] than for corresponding scenarios in AR5. {*Cross-Section Boxes 1 and 2, 3.1.1, 3.3.4, Table 3.1, 4.3*} (*Box SPM.1*)

B.1.2 Discernible differences in trends of global surface temperature between contrasting GHG emissions scenarios (SSP1-1.9 and SSP1-2.6 vs. SSP3-7.0 and SSP5-8.5) would begin to emerge from natural variability[32] within around 20 years. Under these contrasting scenarios, discernible effects would emerge within years for GHG concentrations, and sooner for air quality improvements, due to the combined targeted air pollution controls and strong and sustained methane emissions reductions. Targeted reductions of air pollutant emissions lead to more rapid improvements in air quality within years compared to reductions in GHG emissions only, but in the long term, further improvements are projected in scenarios that combine efforts to reduce air pollutants as well as GHG emissions[33]. (*high confidence*) {*3.1.1*} (*Box SPM.1*)

B.1.3 Continued emissions will further affect all major climate system components. With every additional increment of global warming, changes in extremes continue to become larger. Continued global warming is projected to further intensify the global water cycle, including its variability, global monsoon precipitation, and very wet and very dry weather and

---

[28] Global warming (see Annex I: Glossary) is here reported as running 20-year averages, unless stated otherwise, relative to 1850–1900. Global surface temperature in any single year can vary above or below the long-term human-caused trend, due to natural variability. The internal variability of global surface temperature in a single year is estimated to be about ±0.25°C (5–95% range, *high confidence*). The occurrence of individual years with global surface temperature change above a certain level does not imply that this global warming level has been reached. {*4.3, Cross-Section Box.2*}

[29] Median five-year interval at which a 1.5°C global warming level is reached (50% probability) in categories of modelled pathways considered in WGIII is 2030–2035. By 2030, global surface temperature in any individual year could exceed 1.5°C relative to 1850–1900 with a probability between 40% and 60%, across the five scenarios assessed in WGI (*medium confidence*). In all scenarios considered in WGI except the very high emissions scenario (SSP5-8.5), the midpoint of the first 20-year running average period during which the assessed average global surface temperature change reaches 1.5°C lies in the first half of the 2030s. In the very high GHG emissions scenario, the midpoint is in the late 2020s. {*3.1.1, 3.3.1, 4.3*} (*Box SPM.1*)

[30] The best estimates [and *very likely* ranges] for the different scenarios are: 1.4 [1.0 to 1.8]°C (SSP1-1.9); 1.8 [1.3 to 2.4]°C (SSP1-2.6); 2.7 [2.1 to 3.5]°C (SSP2-4.5); 3.6 [2.8 to 4.6]°C (SSP3-7.0); and 4.4 [3.3 to 5.7]°C (SSP5-8.5). {*3.1.1*} (*Box SPM.1*)

[31] Assessed future changes in global surface temperature have been constructed, for the first time, by combining multi-model projections with observational constraints and the assessed equilibrium climate sensitivity and transient climate response. The uncertainty range is narrower than in the AR5 thanks to improved knowledge of climate processes, paleoclimate evidence and model-based emergent constraints. {*3.1.1*}

[32] See Annex I: Glossary. Natural variability includes natural drivers and internal variability. The main internal variability phenomena include El Niño-Southern Oscillation, Pacific Decadal Variability and Atlantic Multi-decadal Variability. {*4.3*}

[33] Based on additional scenarios.

climate events and seasons (*high confidence*). In scenarios with increasing CO_2 emissions, natural land and ocean carbon sinks are projected to take up a decreasing proportion of these emissions (*high confidence*). Other projected changes include further reduced extents and/or volumes of almost all cryospheric elements[34] (*high confidence*), further global mean sea level rise (*virtually certain*), and increased ocean acidification (*virtually certain*) and deoxygenation (*high confidence*). {*3.1.1*, *3.3.1*, *Figure 3.4*} (*Figure SPM.2*)

B.1.4 With further warming, every region is projected to increasingly experience concurrent and multiple changes in climatic impact-drivers. Compound heatwaves and droughts are projected to become more frequent, including concurrent events across multiple locations (*high confidence*). Due to relative sea level rise, current 1-in-100 year extreme sea level events are projected to occur at least annually in more than half of all tide gauge locations by 2100 under all considered scenarios (*high confidence*). Other projected regional changes include intensification of tropical cyclones and/or extratropical storms (*medium confidence*), and increases in aridity and fire weather *(medium* to *high confidence*). {*3.1.1*, *3.1.3*}

B.1.5 Natural variability will continue to modulate human-caused climate changes, either attenuating or amplifying projected changes, with little effect on centennial-scale global warming (*high confidence*). These modulations are important to consider in adaptation planning, especially at the regional scale and in the near term. If a large explosive volcanic eruption were to occur[35], it would temporarily and partially mask human-caused climate change by reducing global surface temperature and precipitation for one to three years (*medium confidence*). {*4.3*}

[34] Permafrost, seasonal snow cover, glaciers, the Greenland and Antarctic Ice Sheets, and Arctic sea ice.

[35] Based on 2500-year reconstructions, eruptions with a radiative forcing more negative than –1 W m^{-2}, related to the radiative effect of volcanic stratospheric aerosols in the literature assessed in this report, occur on average twice per century. {*4.3*}

With every increment of global warming, regional changes in mean climate and extremes become more widespread and pronounced

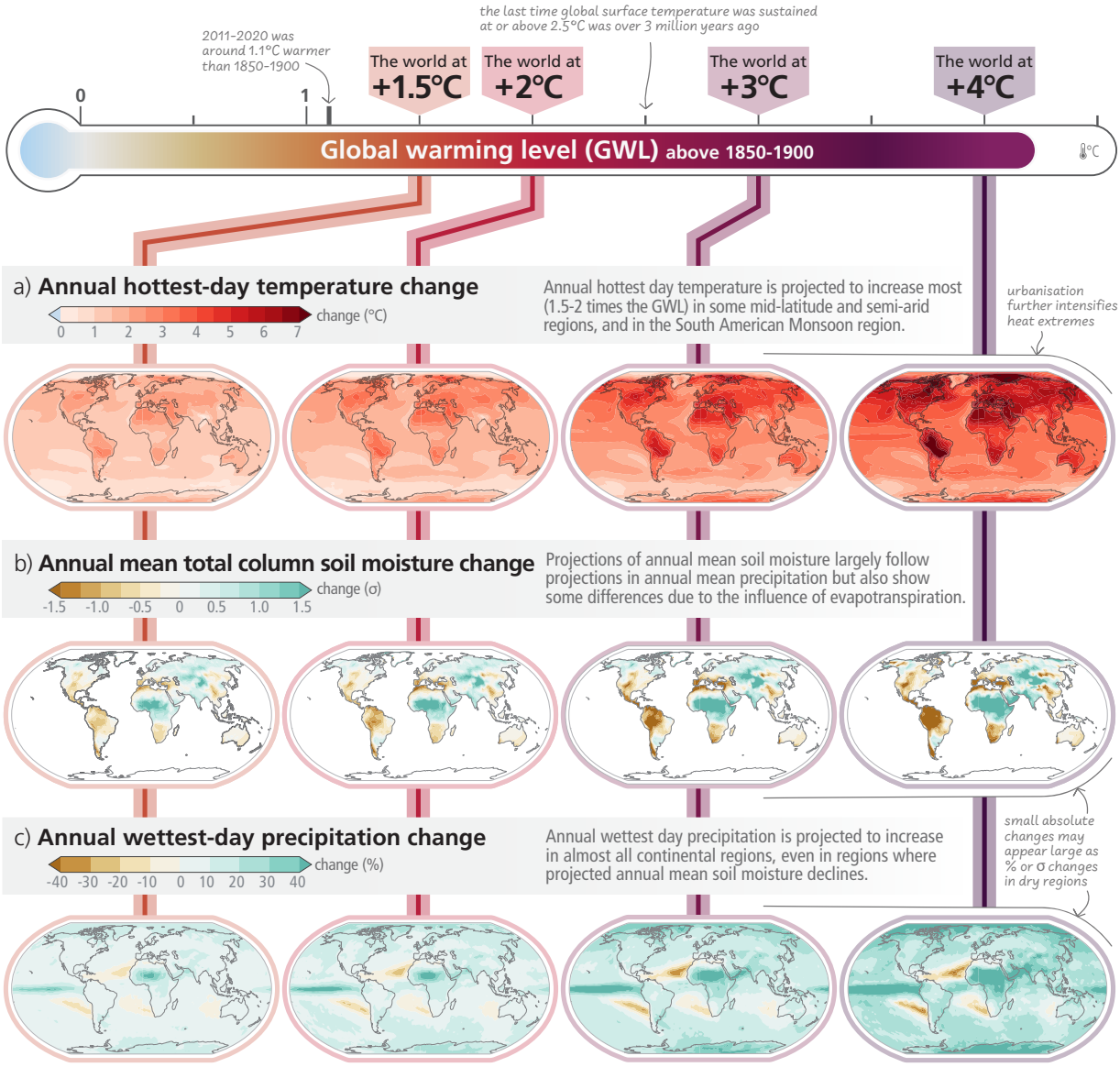

Figure SPM.2: Projected changes of annual maximum daily maximum temperature, annual mean total column soil moisture and annual maximum 1-day precipitation at global warming levels of 1.5°C, 2°C, 3°C, and 4°C relative to 1850–1900. Projected **(a)** annual maximum daily temperature change (°C), **(b)** annual mean total column soil moisture change (standard deviation), **(c)** annual maximum 1-day precipitation change (%). The panels show CMIP6 multi-model median changes. In panels (b) and (c), large positive relative changes in dry regions may correspond to small absolute changes. In panel (b), the unit is the standard deviation of interannual variability in soil moisture during 1850–1900. Standard deviation is a widely used metric in characterising drought severity. A projected reduction in mean soil moisture by one standard deviation corresponds to soil moisture conditions typical of droughts that occurred about once every six years during 1850–1900. The WGI Interactive Atlas (https://interactive-atlas.ipcc.ch/) can be used to explore additional changes in the climate system across the range of global warming levels presented in this figure. {*Figure 3.1, Cross-Section Box.2*}

Climate Change Impacts and Climate-Related Risks

B.2 **For any given future warming level, many climate-related risks are higher than assessed in AR5, and projected long-term impacts are up to multiple times higher than currently observed (*high confidence*). Risks and projected adverse impacts and related losses and damages from climate change escalate with every increment of global warming (*very high confidence*). Climatic and non-climatic risks will increasingly interact, creating compound and cascading risks that are more complex and difficult to manage (*high confidence*). {*Cross-Section Box.2, 3.1, 4.3, Figure 3.3, Figure 4.3*} (*Figure SPM.3, Figure SPM.4*)**

B.2.1 In the near term, every region in the world is projected to face further increases in climate hazards (*medium* to *high confidence*, depending on region and hazard), increasing multiple risks to ecosystems and humans (*very high confidence*). Hazards and associated risks expected in the near term include an increase in heat-related human mortality and morbidity (*high confidence*), food-borne, water-borne, and vector-borne diseases (*high confidence*), and mental health challenges[36] (*very high confidence*), flooding in coastal and other low-lying cities and regions (*high confidence*), biodiversity loss in land, freshwater and ocean ecosystems (*medium* to *very high confidence*, depending on ecosystem), and a decrease in food production in some regions (*high confidence*). Cryosphere-related changes in floods, landslides, and water availability have the potential to lead to severe consequences for people, infrastructure and the economy in most mountain regions (*high confidence*). The projected increase in frequency and intensity of heavy precipitation (*high confidence*) will increase rain-generated local flooding (*medium confidence*). {*Figure 3.2, Figure 3.3, 4.3, Figure 4.3*} (*Figure SPM.3, Figure SPM.4*)

B.2.2 Risks and projected adverse impacts and related losses and damages from climate change will escalate with every increment of global warming (*very high confidence*). They are higher for global warming of 1.5°C than at present, and even higher at 2°C (*high confidence*). Compared to the AR5, global aggregated risk levels[37] (Reasons for Concern[38]) are assessed to become high to very high at lower levels of global warming due to recent evidence of observed impacts, improved process understanding, and new knowledge on exposure and vulnerability of human and natural systems, including limits to adaptation (*high confidence*). Due to unavoidable sea level rise (see also B.3), risks for coastal ecosystems, people and infrastructure will continue to increase beyond 2100 (*high confidence*). {*3.1.2, 3.1.3, Figure 3.4, Figure 4.3*} (*Figure SPM.3, Figure SPM.4*)

B.2.3 With further warming, climate change risks will become increasingly complex and more difficult to manage. Multiple climatic and non-climatic risk drivers will interact, resulting in compounding overall risk and risks cascading across sectors and regions. Climate-driven food insecurity and supply instability, for example, are projected to increase with increasing global warming, interacting with non-climatic risk drivers such as competition for land between urban expansion and food production, pandemics and conflict. (*high confidence*) {*3.1.2, 4.3, Figure 4.3*}

B.2.4 For any given warming level, the level of risk will also depend on trends in vulnerability and exposure of humans and ecosystems. Future exposure to climatic hazards is increasing globally due to socio-economic development trends including migration, growing inequality and urbanisation. Human vulnerability will concentrate in informal settlements and rapidly growing smaller settlements. In rural areas vulnerability will be heightened by high reliance on climate-sensitive livelihoods. Vulnerability of ecosystems will be strongly influenced by past, present, and future patterns of unsustainable consumption and production, increasing demographic pressures, and persistent unsustainable use and management of land, ocean, and water. Loss of ecosystems and their services has cascading and long-term impacts on people globally, especially for Indigenous Peoples and local communities who are directly dependent on ecosystems to meet basic needs. (*high confidence*) {*Cross-Section Box.2 Figure 1c, 3.1.2, 4.3*}

[36] In all assessed regions.

[37] Undetectable risk level indicates no associated impacts are detectable and attributable to climate change; moderate risk indicates associated impacts are both detectable and attributable to climate change with at least *medium confidence*, also accounting for the other specific criteria for key risks; high risk indicates severe and widespread impacts that are judged to be high on one or more criteria for assessing key risks; and very high risk level indicates very high risk of severe impacts and the presence of significant irreversibility or the persistence of climate-related hazards, combined with limited ability to adapt due to the nature of the hazard or impacts/risks. {*3.1.2*}

[38] The Reasons for Concern (RFC) framework communicates scientific understanding about accrual of risk for five broad categories. RFC1: Unique and threatened systems: ecological and human systems that have restricted geographic ranges constrained by climate-related conditions and have high endemism or other distinctive properties. RFC2: Extreme weather events: risks/impacts to human health, livelihoods, assets and ecosystems from extreme weather events. RFC3: Distribution of impacts: risks/impacts that disproportionately affect particular groups due to uneven distribution of physical climate change hazards, exposure or vulnerability. RFC4: Global aggregate impacts: impacts to socio-ecological systems that can be aggregated globally into a single metric. RFC5: Large-scale singular events: relatively large, abrupt and sometimes irreversible changes in systems caused by global warming. See also Annex I: Glossary. {*3.1.2, Cross-Section Box.2*}

Future climate change is projected to increase the severity of impacts across natural and human systems and will increase regional differences

Examples of impacts without additional adaptation

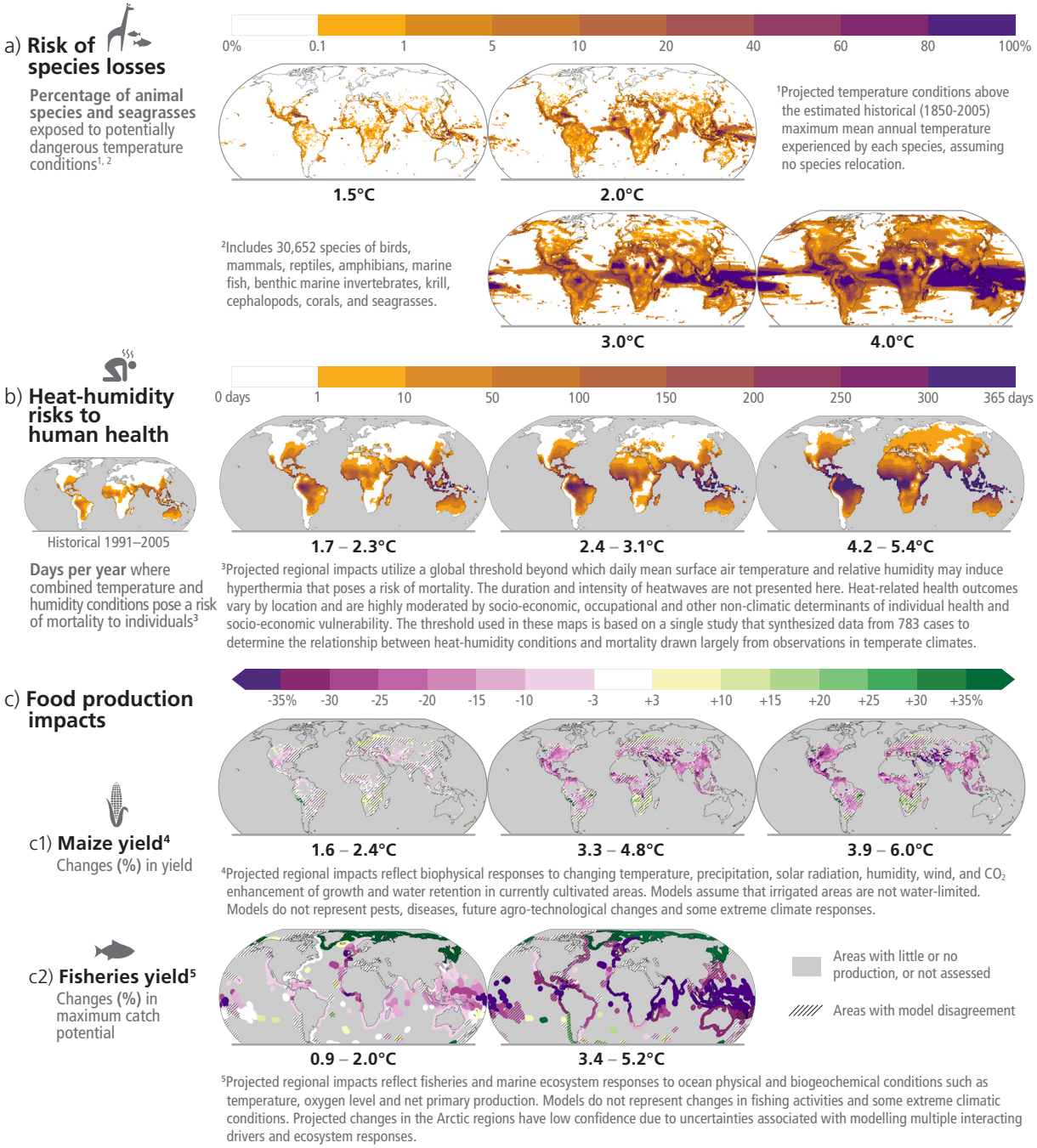

Figure SPM.3: Projected risks and impacts of climate change on natural and human systems at different global warming levels (GWLs) relative to 1850-1900 levels. Projected risks and impacts shown on the maps are based on outputs from different subsets of Earth system and impact models that were used to project each impact indicator without additional adaptation. WGII provides further assessment of the impacts on human and natural systems using these projections and additional lines of evidence. **(a)** Risks of species losses as indicated by the percentage of assessed species exposed to potentially dangerous temperature conditions, as defined by conditions beyond the estimated historical (1850–2005) maximum mean annual temperature experienced by each species, at GWLs of 1.5°C, 2°C, 3°C and 4°C. Underpinning projections of temperature are from 21 Earth system models and do not consider extreme events impacting ecosystems such as the Arctic. **(b)** Risks to human health as indicated by the days per year of population exposure to hyperthermic conditions that pose a risk of mortality from surface air temperature and humidity conditions for historical period (1991–2005) and at GWLs of 1.7°C–2.3°C (mean = 1.9°C; 13 climate models), 2.4°C–3.1°C (2.7°C; 16 climate models) and 4.2°C–5.4°C (4.7°C; 15 climate models). Interquartile ranges of GWLs by 2081–2100 under RCP2.6, RCP4.5 and RCP8.5. The presented index is consistent with common features found in many indices included within WGI and WGII assessments. **(c)** Impacts on food production: (c1) Changes in maize yield by 2080–2099 relative to 1986–2005 at projected GWLs of 1.6°C–2.4°C (2.0°C), 3.3°C–4.8°C (4.1°C) and 3.9°C–6.0°C (4.9°C). Median yield changes from an ensemble of 12 crop models, each driven by bias-adjusted outputs from 5 Earth system models, from the Agricultural Model Intercomparison and Improvement Project (AgMIP) and the Inter-Sectoral Impact Model Intercomparison Project (ISIMIP). Maps depict

2080–2099 compared to 1986–2005 for current growing regions (>10 ha), with the corresponding range of future global warming levels shown under SSP1-2.6, SSP3-7.0 and SSP5-8.5, respectively. Hatching indicates areas where <70% of the climate-crop model combinations agree on the sign of impact. (c2) Change in maximum fisheries catch potential by 2081–2099 relative to 1986–2005 at projected GWLs of 0.9°C–2.0°C (1.5°C) and 3.4°C–5.2°C (4.3°C). GWLs by 2081–2100 under RCP2.6 and RCP8.5. Hatching indicates where the two climate-fisheries models disagree in the direction of change. Large relative changes in low yielding regions may correspond to small absolute changes. Biodiversity and fisheries in Antarctica were not analysed due to data limitations. Food security is also affected by crop and fishery failures not presented here. {*3.1.2, Figure 3.2, Cross-Section Box.2*} (*Box SPM.1*)

Risks are increasing with every increment of warming

a) High risks are now assessed to occur at lower global warming levels

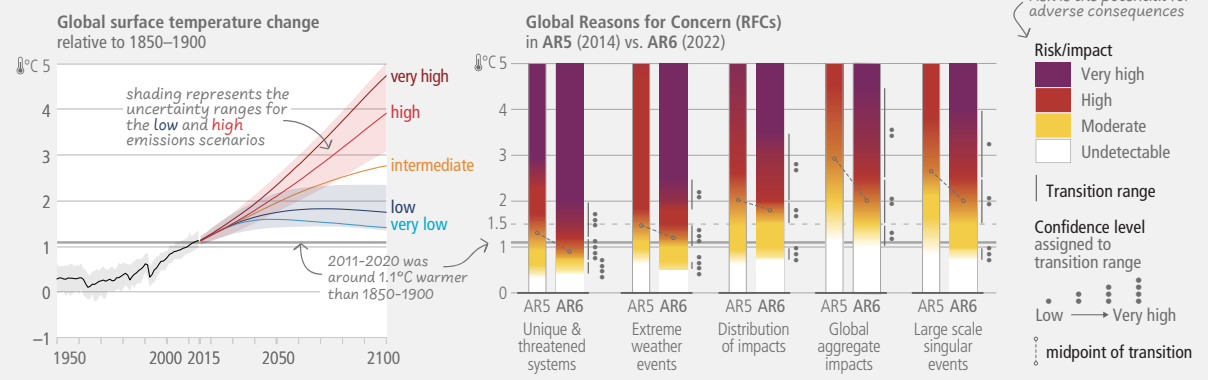

b) Risks differ by system

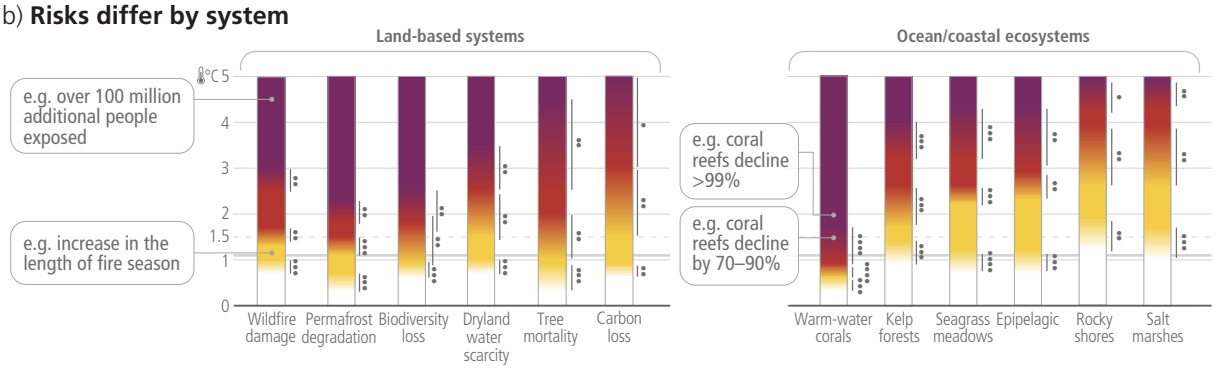

c) Risks to coastal geographies increase with sea level rise and depend on responses

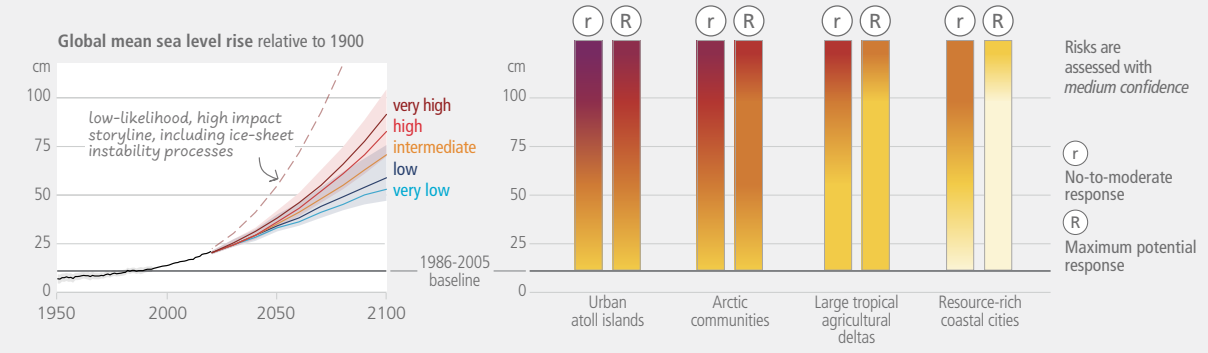

d) Adaptation and socio-economic pathways affect levels of climate related risks

Limited adaptation (failure to proactively adapt; low investment in health systems); incomplete adaptation (incomplete adaptation planning; moderate investment in health systems); proactive adaptation (proactive adaptation management; higher investment in health systems)

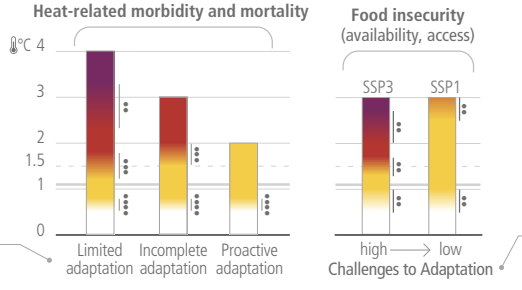

The SSP1 pathway illustrates a world with low population growth, high income, and reduced inequalities, food produced in low GHG emission systems, effective land use regulation and high adaptive capacity (i.e., low challenges to adaptation). The SSP3 pathway has the opposite trends.

Figure SPM.4: Subset of assessed climate outcomes and associated global and regional climate risks. The burning embers result from a literature based expert elicitation. **Panel (a): Left** – Global surface temperature changes in °C relative to 1850–1900. These changes were obtained by combining CMIP6 model simulations with observational constraints based on past simulated warming, as well as an updated assessment of equilibrium climate sensitivity. *Very likely* ranges are shown for the low and high GHG emissions scenarios (SSP1-2.6 and SSP3-7.0) (Cross-Section Box.2). **Right** – Global Reasons for Concern (RFC), comparing AR6 (thick embers) and AR5 (thin embers) assessments. Risk transitions have generally shifted towards lower temperatures with updated scientific understanding. Diagrams are shown for each RFC, assuming low to no adaptation. Lines connect the midpoints of the transitions from moderate to high risk across AR5 and AR6. **Panel (b)**: Selected global risks for land and ocean ecosystems, illustrating general increase of risk with global warming levels with low to no adaptation. **Panel (c): Left** - Global mean sea level change in centimetres, relative to 1900. The historical changes (black) are observed by tide gauges before 1992 and altimeters afterwards. The future changes to 2100 (coloured lines and shading) are assessed consistently with observational constraints based on emulation of CMIP, ice-sheet, and glacier models, and *likely* ranges are shown for SSP1-2.6 and SSP3-7.0. **Right** - Assessment of the combined risk of coastal flooding, erosion and salinization for four illustrative coastal geographies in 2100, due to changing mean and extreme sea levels, under two response scenarios, with respect to the SROCC baseline period (1986–2005). The assessment does not account for changes in extreme sea level beyond those directly induced by mean sea level rise; risk levels could increase if other changes in extreme sea levels were considered (e.g., due to changes in cyclone intensity). "No-to-moderate response" describes efforts as of today (i.e., no further significant action or new types of actions). "Maximum potential response" represent a combination of responses implemented to their full extent and thus significant additional efforts compared to today, assuming minimal financial, social and political barriers. (In this context, 'today' refers to 2019.) The assessment criteria include exposure and vulnerability, coastal hazards, in-situ responses and planned relocation. Planned relocation refers to managed retreat or resettlements. The term response is used here instead of adaptation because some responses, such as retreat, may or may not be considered to be adaptation. **Panel (d)**: Selected risks under different socio-economic pathways, illustrating how development strategies and challenges to adaptation influence risk. **Left** - Heat-sensitive human health outcomes under three scenarios of adaptation effectiveness. The diagrams are truncated at the nearest whole °C within the range of temperature change in 2100 under three SSP scenarios. **Right** - Risks associated with food security due to climate change and patterns of socio-economic development. Risks to food security include availability and access to food, including population at risk of hunger, food price increases and increases in disability adjusted life years attributable to childhood underweight. Risks are assessed for two contrasted socio-economic pathways (SSP1 and SSP3) excluding the effects of targeted mitigation and adaptation policies. {*Figure 3.3*} (*Box SPM.1*)

Likelihood and Risks of Unavoidable, Irreversible or Abrupt Changes

B.3 Some future changes are unavoidable and/or irreversible but can be limited by deep, rapid, and sustained global greenhouse gas emissions reduction. The likelihood of abrupt and/or irreversible changes increases with higher global warming levels. Similarly, the probability of low-likelihood outcomes associated with potentially very large adverse impacts increases with higher global warming levels. (*high confidence*) {*3.1*}

B.3.1 Limiting global surface temperature does not prevent continued changes in climate system components that have multi-decadal or longer timescales of response (*high confidence*). Sea level rise is unavoidable for centuries to millennia due to continuing deep ocean warming and ice sheet melt, and sea levels will remain elevated for thousands of years (*high confidence*). However, deep, rapid, and sustained GHG emissions reductions would limit further sea level rise acceleration and projected long-term sea level rise commitment. Relative to 1995–2014, the *likely* global mean sea level rise under the SSP1-1.9 GHG emissions scenario is 0.15–0.23 m by 2050 and 0.28–0.55 m by 2100; while for the SSP5-8.5 GHG emissions scenario it is 0.20–0.29 m by 2050 and 0.63–1.01 m by 2100 (*medium confidence*). Over the next 2000 years, global mean sea level will rise by about 2–3 m if warming is limited to 1.5°C and 2–6 m if limited to 2°C (*low confidence*). {*3.1.3, Figure 3.4*} (*Box SPM.1*)

B.3.2 The likelihood and impacts of abrupt and/or irreversible changes in the climate system, including changes triggered when tipping points are reached, increase with further global warming (*high confidence*). As warming levels increase, so do the risks of species extinction or irreversible loss of biodiversity in ecosystems including forests (*medium confidence*), coral reefs (*very high confidence*) and in Arctic regions (*high confidence*). At sustained warming levels between 2°C and 3°C, the Greenland and West Antarctic ice sheets will be lost almost completely and irreversibly over multiple millennia, causing several metres of sea level rise *(limited evidence)*. The probability and rate of ice mass loss increase with higher global surface temperatures (*high confidence*). {*3.1.2, 3.1.3*}

B.3.3 The probability of low-likelihood outcomes associated with potentially very large impacts increases with higher global warming levels (*high confidence*). Due to deep uncertainty linked to ice-sheet processes, global mean sea level rise above the *likely* range – approaching 2 m by 2100 and in excess of 15 m by 2300 under the very high GHG emissions scenario (SSP5-8.5) (*low confidence*) – cannot be excluded. There is *medium confidence* that the Atlantic Meridional Overturning Circulation will not collapse abruptly before 2100, but if it were to occur, it would *very likely* cause abrupt shifts in regional weather patterns, and large impacts on ecosystems and human activities. {*3.1.3*} (*Box SPM.1*)

ATTACHMENT 12

Acid Mine Drainage and Effects on Fish Health and Ecology: A Review

For:

U.S. Fish and Wildlife Service, Anchorage Fish and Wildlife Field Office,

Anchorage, Alaska, 99501

Prepared by:

Reclamation Research Group, LLC, Bozeman, Montana

June 2008

Suggested Citation: Jennings, S.R., Neuman, D.R. and Blicker, P.S. (2008). "Acid Mine Drainage and Effects on Fish Health and Ecology: A Review". Reclamation Research Group Publication, Bozeman, MT.

Table of Contents

Purpose

In Alaska, several large mine projects are currently proposed, ranging from open-pit, hard rock mines to strip mines for extracting coal. These large-scale projects have the potential to impact fish and wildlife resources through alteration or removal of vast areas of habitat. The U.S. Fish and Wildlife Service (Service) is responsible for managing fish and wildlife resources for the American public and in carrying out its mission, participates in pre-development activities for industrial projects. This report was commissioned to provide information to the Conservation Planning Assistance branch of the Anchorage Fish and Wildlife Field Office to aid in review of documents required as part of the permit process with the U.S. Environmental Protection Agency (EPA), U.S. Army Corps of Engineers and the State of Alaska.

Acid Mine Drainage Overview

Acid rock drainage (ARD) is produced by the oxidation of sulfide minerals, chiefly iron pyrite or iron disulfide (FeS_2). This is a natural chemical reaction which can proceed when minerals are exposed to air and water. Acidic drainage is found around the world both as a result of naturally occurring processes and activities associated with land disturbances, such as highway construction and mining where acid-forming minerals are exposed at the surface of the earth. These acidic conditions can cause metals in geologic materials to dissolve, which can lead to impairment of water quality when acidic and metal laden discharges enter waters used by terrestrial or aquatic organisms.

Chemistry of Acid Rock Drainage

The reaction of pyrite with oxygen and water produces a solution of ferrous sulfate and sulfuric acid. Ferrous iron can further be oxidized producing additional acidity. Iron and sulfur oxidizing bacteria are known to catalyze these reactions at low pH thereby increasing the rate of reaction by several orders of magnitude (Nordstrom and Southam 1997). In undisturbed natural systems, this oxidation process occurs at slow rates over geologic time periods. When pyrite is exposed to oxygen and water it is oxidized, resulting in hydrogen ion release - acidity, sulfate ions, and soluble metal ions as shown in equation 1. The acidity of water is typically expressed as pH or the logarithmic concentration of hydrogen ion concentration in water such that a pH of 6 has ten times the hydrogen ion content of neutral pH 7 water.

$$2FeS_{2\,(s)} + 7O_2 + 2H_2O \rightarrow 2Fe^{+2} + 4SO_4^{-2} + 4H^{+} \quad (1)$$

Further oxidation of Fe^{+2} (ferrous iron) to Fe^{+3} (ferric iron) occurs when sufficient oxygen is dissolved in the water or when the water is exposed to sufficient atmospheric oxygen (equation 2).

$$2Fe^{+2} + \tfrac{1}{2}\, O_2 + 2H^{+} \rightarrow 2Fe^{+3} + H_2O \quad (2)$$

Ferric iron can either precipitate as $Fe(OH)_3$, a red-orange precipitate seen in waters affected by acid rock drainage, or it can react directly with pyrite to produce more ferrous iron and acidity as shown in equations 3 and 4.

$$2Fe^{+3} + 6H_2O \leftrightarrow 2Fe(OH)_{3\,(s)} + 6H^{+} \quad (3)$$

$$14Fe^{+3} + FeS_{2\,(s)} + 8H_2O \rightarrow 2SO_4^{-2} + 15Fe^{+2} + 16H^{+} \quad (4)$$

When ferrous iron is produced (equation 4) and sufficient dissolved oxygen is present the cycle of reactions 2 and 3 is perpetuated (Younger, et al., 2002). Without dissolved oxygen equation 4 will continue to completion and water will show elevated levels of ferrous iron (Younger, et al., 2002). The rates of chemical reactions (equations 2, 3, and 4) can be significantly accelerated by bacteria, specifically *Thiobacillus ferrooxidans.* Another microbe, *Ferroplasma Acidarmanus*, has been identified in the production of acidity in mine waters (McGuire et al. 2001)

Hydrolysis reactions of many common metals also form precipitates and in doing so generate H^{+}. These reactions commonly occur where mixing of acidic waters with

substantial dissolved metals blend with cleaner waters resulting in precipitation of metal hydroxides on stream channel substrates (Equations 5 through 8).

$$Al^{+3} + 3H_2O <\!\!-\!\!> Al(OH)_{3(s)} + 3H^{+} \quad (5)$$

$$Fe^{+3} + 3H_2O <\!\!-\!\!> Fe(OH)_{3(s)} + 3H^{+} \quad (6)$$

$$Fe^{+2} + 0.25\ O_2 + 2.5\ H_2O <\!\!-\!\!> Fe(OH)_{3(s)} + 2H^{+} \quad (7)$$

$$Mn^{+2} + 0.25\ O_2 + 2.5\ H_2O <\!\!-\!\!> Mn(OH)_{3(s)} + 2H^{+} \quad (8)$$

Metal sulfide minerals in addition to pyrite may be associated with economic mineral deposits and some of these minerals may also produce acidity and SO_4^{-2}. Oxidation and hydrolysis of metal sulfide minerals pyrrhotite ($Fe_{1-x}S$), chalcopyrite ($CuFeS_2$), sphalerite ((Zn, Fe)S) and others release metals such as zinc, lead, nickel, and copper into solution in addition to acidity and SO_4^{-2} (Jennings et al., 2000; Younger et al., 2002).

Acid Mine Drainage

Acid rock drainage occurs when sulfide ores are exposed to the atmosphere, which can be enhanced through mining and milling processes where oxidation reactions are initiated. Mining increases the exposed surface area of sulfur-bearing rocks allowing for excess acid generation beyond natural buffering capabilities found in host rock and water resources. Collectively the generation of acidity from sulfide weathering is termed Acid Mine Drainage (AMD).[1] Mine tailings and waste rock, having much greater surface area than in-place geologic material due to their smaller grain size, are more prone to

[1] As this literature review is focused on mining, the term AMD will be used in the text, yet rocks found in undisturbed environments are similarly able to generate acidity (or ARD) without the anthropogenic influence of mining. The term Mine Influence Water is also synonymous.

generating AMD. Since large masses of sulfide minerals are exposed quickly during the mining and milling processes, the surrounding environment can often not attenuate the resulting low pH conditions. Metals that were once part of the host rock are solubilized and exacerbate the deleterious effect of low pH on terrestrial and aquatic receptors. Concentrations of common elements such as Cu, Zn, Al, Fe and Mn all dramatically increase in waters with low pH. Logarithmic increases in metal levels in waters from sulfide-rich mining environments are common where surface or groundwater pH is depressed by acid generation from sulfide minerals.[2] These environmental, human health, and fiscal consequences, if not mitigated, can have long-lasting effects. Acid mine drainage continues to emanate from mines in Europe established during the Roman Empire prior to 467 AD (CSS, 2002). Georgius Agricola's *De Re Metallica* (1556), the first and seminal treatise on mining exhibits detailed woodcut illustrations not only of the known mechanics of 16th Century mining, but also depictions of the devastation of streams. The cost of mitigation of environmental damage from acid mine drainage is great. The U.S. Forest Service (USFS) estimates that between 20,000 to 50,000 mines are currently generating acid on lands managed by that agency; with negative impacts from these mines affecting some 8,000 to 16,000 km of streams (USDA, Forest Service 1993). Many of these mines are small abandoned facilities located in remote areas of the western United States and originating prior to modern environmental controls. However, several large scale mines developed in the latter half of the twentieth century have declared bankruptcy and left tax payers with the responsibility of treating acid waters in perpetuity. Examples include the Zortman Landusky Mine in Montana, the Summitville Mine in Colorado, and the Brohm Mine in South Dakota. The largest and most expensive sites that EPA has listed under the Comprehensive Environmental Resource Compensation and Liability ACT (CERCLA; aka Superfund) are mining sites in the West, including Iron Mountain Mine in California, Bunker Hill in Idaho, and the Butte-Clark Fork River complex in Southwestern Montana. Human health risks and ecological injury, chiefly from elevated metals, have been identified by EPA and natural resource trustees at many of these mega-mining Superfund sites.

Acidic drainage has been identified as the largest environmental liability facing the Canadian mining industry and is estimated at $2 to $5 billion dollars (MEND 2001). In response to the challenge presented by mitigation of AMD, 200 technology-based reports were generated to evaluate sampling, prediction, prevention, treatment and monitoring of potentially acid-generating materials and locations. A 1986 estimate for Canada suggests

[2] Note: The authors recognize that AMD and elevated metal levels in water are inextricably linked, however the purpose of this report is to assess the effect of acidity on fisheries independent from elevated metals.

that acid-generating tailings cover 12,000 hectares plus an additional 350 million tons of mine waste rock were noted (MEND 2001).

Effect of Acid Mine Drainage on Aquatic Resources

Once acid drainage is created, metals are released into the surrounding environment, and become readily available to biological organisms. In water, for example, when fish are exposed directly to metals and H^+ ions through their gills, impaired respiration may result from chronic and acute toxicity. Fish are also exposed indirectly to metals through ingestion of contaminated sediments and food items. A common weathering product of sulfide oxidation is the formation of iron hydroxide ($Fe(OH)_3$), a red/orange colored precipitate found in thousands of miles of streams affected by AMD. Iron hydroxides and oxyhydroxides may physically coat the surface of stream sediments and streambeds destroying habitat, diminishing availability of clean gravels used for spawning, and reducing fish food items such as benthic macroinvertebrates. Acid mine drainage, characterized by acidic metalliferous conditions in water, is responsible for physical, chemical, and biological degradation of stream habitat.

Water contaminated by AMD, often containing elevated concentrations of metals, can be toxic to aquatic organisms, leaving receiving streams devoid of most living creatures (Kimmel 1983). Receiving waters may have pH as low as 2.0 to 4.5, levels toxic to most forms of aquatic life (Hill 1974). Data relating to specific effects of low pH on growth and reproduction (Fromm 1980) may be related to calcium metabolism and protein synthesis. Fromm (1980) suggested that a “no effects” level of pH for successful reproduction is near 6.5, while most fish species are not affected when the pH is in a range from 5.5 to 10.5. Howells et al. (1983) reported interactions of pH, calcium, and aluminum may be important to understanding the overall effects on fish survival and productivity. Several reports indicate low pH conditions alter gill membranes or change gill mucus resulting in death due to hypoxia. Hatchery raised salmonids can tolerate pH 5.0, but below this level hemeostatic electrolyte and osmotic mechanisms become impaired (Fromm 1980).

A study of the distribution of fish in Pennsylvania streams affected by acid mine drainage (Cooper and Wagner 1973) found fish severely impacted at pH 4.5 to 5.5. Ten species revealed some tolerance to the acid conditions of pH 5.5 and below; 38 species were found living in waters with pH values ranging from 5.6 to 6.4; while 68 species were found only at pH levels greater than 6.4. Further, these investigators reported complete loss of fish in 90% of streams with waters of pH 4.5 and total acidity of 15 mg/L. Healthy, unpolluted streams generally support several species and moderate abundance of

individuals; whereas impacted streams are dominated by fewer species and often low to moderate numbers of only a few organisms. Streams affected by acid mine drainage are poor in taxa richness and abundance. In older studies (Warner 1971), more species of insects and algae were found in unpolluted West Virginia streams (pH $\geq$ 4.5) compared to those streams polluted by acid (pH 2.8 to 3.8). Reductions of benthic fauna in a West Virginia stream severely affected by acid mine water were reported by Menendez (1978). In more recent studies (Farag et al. 2003), some streams in the Boulder River watershed in Montana impacted by nearly 300 abandoned metal mines are devoid of all fish near mine sources. Populations of brook trout *(Salvelinus fontinalis*), rainbow trout (*Oncorhynchus mykiss*), and cutthroat trout (*O. clarki*) were found further downstream and away from sources of acid mine drainage. In a 2003 study evaluating the effect of localized habitat degradation from a gold mine near the Yukon River (in AK?) on population structure of salmon, it was suggested that coho salmon (*O. kisutch*) may be at risk of losing genetic diversity due to localized habitat degradation (Olsen et al. 2004). The abandoned Britannia copper mine in British Columbia has been releasing acid mine drainage into local waters for many years. Investigators compared fish abundance, distribution and survival at contaminated and non-contaminated areas (Barry et al. 2000). Chum salmon (*O. keta*) fry abundance was significantly lower near the impacted waters (pH < 6 and dissolved copper > 1 mg/L) than the reference area. The investigators also reported that laboratory bioassays confirmed acid mine drainage from the Britannia Mine was toxic to juvenile chinook (*O. tshawytscha)* and chum salmon. Chinook salmon smolt transplanted to surface cages near Britannia Creek experienced 100% mortality within 2 days (Barry 2000).

The scientific literature is replete with studies designed to quantify the adverse environmental effects of acid mine drainage on aquatic resources. Most recent investigations focus on multiple bioassessments of large watersheds. These assessments include water and sediment chemistry, benthic macroinvertebrate sampling for taxa richness and abundance, laboratory acute water column evaluations, laboratory chronic sediment testing, caged fish within impacted streams, and development of models to explain and predict impacts of acid mine drainage on various aquatic species (Soucek et al. 2000, Woodward et al. 1997, Maret and MacCoy 2002, Hansen et al. 2002, Kaeser and Sharpe 2001, Baldigo and Lawrence 2000, Johnson et al. 1987, Griffith et al. 2004, Schmidt et al. 2002, Martin and Goldblatt 2007, Beltman et al. 1999, Hansen et al. 1999, Boudou et al. 2005).

Major Environmental Incidents Caused by Acid Mine Drainage

Releases of acid mine waters containing elevated metal and cyanide concentrations with resulting impacts to landscapes and waterways have been documented by several organizations (UNEP 2002). Fish kills resulting from the uncontrolled release of acid and metals from mine wastes into receiving streams have been reported from world wide areas in which hard rock mining, milling, and smelting activities have occurred. In 1998, a mine flood incident in Spain deposited some 6 million m^3 of acid water over the banks of the Guadiamar River with metal and sulfide rich sediments. The U.S. EPA described 66 incidents in which environmental injuries from mining activities are detailed (EPA 1995). Nordstrom and Alpers (1999) reported that millions, perhaps billions, of fish have been killed from mining activities in the U.S. during the past century.

In 1989, a large fish kill (> 5000 salmonids) in Montana's Clark Fork River resulted when acid, metalliferous tailings and efflorescent metal salts were flushed into the river during a thunderstorm event. Within 20 minutes, the acidity of the river water was reduced by several orders of magnitude, and copper concentrations rose dramatically. Fish gill tissue copper levels indicated acute toxicity (Munshower et al. 1997). The Sacramento River in California has experienced several fish kills due to sudden releases of acid water from upstream mine areas; more than 20 fish kills were reported since 1963, and in 1967, at least 47,000 fish died (Nordstrom et al. 1977).

Prediction of Acid Mine Drainage

Accurate prediction of acidic drainage from proposed mines is recognized by both industry and government as a critical requirement of mine permitting and long-term operation. Substantial emphasis has been placed on prediction of acid drainage associated with coal development in the Eastern U.S. (Pennsylvania DEP 1998; Skousen and Ziemkiewicz, 1996), and metal mining in the Western U.S. and in Canada (MEND 2001). The standard protocols for evaluating geologic materials for their ability to produce AMD are generally agreed upon within the scientific community, yet much uncertainty remains in the ability of scientists and engineers to predict the ultimate drainage quality years in the future, as many complex variables influence acid generation and neutralization.

The backbone of predicting acid generating potential from any geologic formation is the ability to characterize the presence and quantity of both acid-forming minerals and

neutralizing minerals in the geologic materials to be unearthed during mining operations. Typically samples are collected by drilling during exploration, analyzed and interpreted with respect to their risk of acid formation. Methods for characterizing acid-forming minerals were developed during the 1970's in areas of the eastern U.S. mined for coal (Smith et al., 1974). Ultimately, these techniques lead to a standardized EPA protocol for characterization of mine soil and overburden (Sobek et al., 1978). In these analytical approaches, the amount of sulfur present in geologic materials is measured and attributed to being either an acid-forming mineral such as pyrite (FeS_2) or non-acid-forming mineral such as gypsum ($CaSO_4 \cdot 2H_2O$). The relative amount of acid-forming minerals is then contrasted to the amount of neutralizing minerals such as calcite ($CaCO_3$) to develop a prediction of the probability of acid generation. The ratio of neutralization potential (NP) to acid potential (AP) is commonly presented in graphical interpretations with the inference that geologic materials with an abundance of NP are unlikely to generate acidic drainage. In Eastern coal mines NP:AP ratios <1 commonly produce acidic drainage, NP:AP ratios between 1 and 2 may produce either acidic or neutral drainage and NP:AP ratios >2 should produce alkaline water (Skousen et al., 2002). However, this index does not always accurately predict the resultant acid generation from a mine. Of 56 mines evaluated by Skousen and others (2002) 11% did not conform to the expected results based on NP:AP ratios, including four sites with ratios > 2: these sites eventually produced acidic drainage. Furthermore, the applicability of the experimental findings from West Virginia coal deposits hosted in sedimentary rock to metal mines developed in igneous parent material is unknown. Sedimentary sulfide mineralization is caused by diagenetic interaction between microbes, Fe and S in a low temperature saturated environment resulting in formation of poorly crystallized pyrite while igneous pyrite is formed by high temperature magmatic fluids or molten rock cooling slowly to form well developed crystalline structure. Mineralogical variation between each geologic domain causes dissimilar reactivity to weathering conditions and leads to laboratory variability in assessment. Recurrence of inaccurate interpretations between laboratory and field data has caused investigators to reexamine the adequacy of the analytical methods. Because of the challenges inherent in interpreting laboratory data and predictive models, forecasting future water quality impacts from AMD should not be considered routine and robust, rather they should be considered an area of uncertainty and on-going research.

If the rates of weathering and availability of acid-forming and neutralizing minerals are dissimilar the potential exists that acid-generation may overwhelm the pool of resident NP. Slowly reacting neutralizing minerals may lead to generation of acidic water. Sherlock and others (1995) evaluated the rates of weathering of sulfides, carbonates and silicates and determined that sulfide minerals reacted fastest and cautioned that conventional methods of prediction do not consider the specific mineralogy and reaction kinetics are at risk of erroneous interpretations and predictions.

Research has also focused on the presence of minerals which are detected by the NP analytical method, yet do not contribute to production of alkalinity. Siderite ($FeCO_3$) has been found in mining environments and while contributing to the measured NP, no actual neutralization has been observed in the field (Frisbee and Hossner, 1989). In an evaluation of 31 overburden[3] samples containing siderite, pyrite, calcite and quartz using 4 dissimilar methods for NP determination, siderite-containing samples showed wide variation in NP between three laboratories (Skousen et al., 1997). Using the standard Sobek (1978) test for NP, Weber and others (2004) showed that up to 432 hours may be required for complete hydrolysis of siderite-containing samples in laboratory testing, implying that inaccurate interpretations of NP are common for rock containing this siderite since routine laboratory tests would not be run for such a great length of time. The limitations of laboratory testing for NP without supporting mineralogical characterization can often lead to overestimation of NP (Lawrence and Scheske, 1997; Paktunc, 1999). Conventional laboratory methods for determination of NP employ wet chemical methods where the presence of carbonates in soil is made based on titration of a sample with acid followed by back titration with a base. No determination of the mineralogical source of carbonate is made by the NP test. Similarly, quantification of acid-forming minerals is challenging in a laboratory setting. Analysis of total sulfur levels is routinely accomplished using standardized laboratory equipment, however the typical Sobek method employs subsequent acid extractions to distinguish between acid-forming minerals containing sulfur and non-acid sulfur minerals. In research using pure mineral samples, Jennings and Dollhopf (1995) showed that conventional analytical methods failed to accurately characterize acid-forming minerals. Incomplete recovery of sulfur-bearing minerals has been observed using the Sobek method since a residual sulfur fraction is commonly observed in laboratory testing implying the standard method of dissolution failed to solubilize or dissolve the sulfide found in the sample. Regional variation is observed in the interpretation of residual sulfur leading to non-standardized findings. The residual sulfur component is commonly characterized as non-acid forming organic sulfur in sedimentary rock and as acid-forming sulfide in metal mining samples. Collectively, the static tests described have significant limitations in accurately predicting whether acidic drainage will form.

Kinetic[4] tests are commonly run as a companion to static[5] testing to measure the weathering behavior of geologic material when exposed to field conditions. Kinetic tests

[3] Overburden is defined as geologic material overlying a resource of interest. In surface mining overburden is typically removed as waste material.

[4] Kinetic tests of mine waste are typically accomplished by monitoring the chemical constituents in water resulting from simulated laboratory weathering or actual field site weathering of mine waste materials over a period of months to years. Water is leached through the geologic material and recovered as drainage.

may be run in a laboratory column or in the field in large containers. The quality and quantity of leachate is subsequently evaluated to offer a supporting interpretation to static testing. Six large columns each containing 1.6 tons of waste rock were evaluated over a period of 3 years showing two pH controls: 1) sulfide oxidation with calcite dissolution sustaining a neutral pH, and 2) simultaneous silicate and sulfide weathering occurring at an equilibrium pH of 3-4 (Stromberg and Banwart, 1999). During the period of investigation the columns either remained at near-neutral pH or became acidic after 0.5 to 3 years lag time. The lag time in appearance of low pH was caused by mineralogical reactions occurring in the waste rock that either neutralized the acidity formed until exhausted or rendered non-reactive, or the acid reactions required a period of time to initiate. In a companion study Stromberg and Banwart (1999) showed there was a large difference in weathering rates based on particle size. In the columns particles smaller than 0.25 mm were responsible for approximately 80% of both the sulfide oxidation and silicate dissolution. Calcite particles larger than 5-10 mm were found to react too slowly to neutralize acid produced by sulfide oxidation. Similar unique reaction kinetics has been observed at the Bingham Canyon Mine in Utah where fresh waste rock exhibits a paste pH[6] of 7.0. Within 6 years the pH of the waste rock dumps declines to 4.7 further decreasing to pH 3.7 after 50 years of weathering (Borden 2001). Scharer and others (2000) observed that NP was strongly related to particle size and particles greater than ¼ inch (6.4 mm) were only 20% consumed at the onset of acid conditions. Kinetic data on the depletion rate of NP supplemented by geochemical modeling suggests that waste rock with NP/AP ratios as high as 5 may turn acidic in the long term: this is much different than the results mentioned above by Skousen (2002) who identified 2 as the ratio below which NP/AP ratios would generally not become acidic. If neutralizing minerals are depleted or non-reactive long-term generation of acidic drainage may be initiated with potentially dire ecological consequences if untreated.

Notable uncertainty exists in the long-term predictions of acid generation from geologic materials found in mining environments. Evaluation of Environmental Impact Statements from 25 mines performed by Kuipers and others (2006) showed 15 of 25 mines (60%) exceeded surface water quality standards for metals and pH after permitting.

---

[5] Static testing is the laboratory analysis of geologic materials for chemical characteristics such as total metal levels, pH or total S. Static testing is the analysis of the bulk concentrations in rock or soil material.

[6] Paste pH or saturated paste pH is the measurement of pH in a slurry of soil or rock with deionized water after allowing time for reaction of the slurry. Paste pH is a measure of the soil solution indicative of the acidity of soil water in the context of plant growth or leaching to groundwater.

Similarly, kinetic tests performed using humidity cells[7] over a 3 to 7 year period showed that rates of acid generation have a 50% chance of stabilizing within one year while the remainder of the humidity cells fluctuated significantly throughout the test periods (Morin and Hutt, 2000).

Assessment of Acid Rock Drainage and Metals Release

Canada's Mine Environment Neutral Drainage (MEND) Program was implemented to develop and apply new technologies to prevent and control acid drainage. Recognizing acid drainage as the greatest environmental problem facing the mining industry and the regulatory agencies' responsibility to protect the environment and safeguard human health, the MEND Program was funded jointly by Natural Resources Canada and The Mining Association of Canada. In 2005, MEND released a report titled *List of Potential Information Requirements in Metal Leaching/Acid Rock Drainage Assessment (ML/ARD) and Mitigation Work* (Price 2005). The purpose of this document is to improve the assessment and mitigation of metal leaching/acid rock drainage. It achieves this goal by providing a comprehensive list of information and data necessary to assess the potential for ML/ARD, and multiple strategies for mitigation. The document is intended to be used as a general guide for the mining industry, regulators, environmental advocacy groups, and other stakeholders. The MEND program uses the term 'Acid Rock Drainage' to describe the acidic water drainage from mines.

The MEND report (Price 2005) recommends a set of informational variables and data that should be generated and developed so that informed decisions can be made with respect to the potential for acid drainage and toxic metal release. These recommendations were intended to mitigate the consequences of sulfide mineral oxidation caused by mining, milling, and other process involved in metal resource development. These information requirements are summarized in the following statements:

General site characteristics: location, access, climate, ecology, history of previous mining, waste materials, geology, hydrology, mineralogy, descriptions of all materials that will be excavated or exposed, soils, reclamation objectives, end land uses, data tables, relevant figures, and other pertinent information. This is not exhaustive and site-specific information and data will be required.

[7] Humidity cells are laboratory equipment to simulate weathering of rock in a small benchtop enclosure where soil or rock is repeatedly wetted and dried over a period of months to years to monitor changes in drainage water quality. A humidity cell is a specialized type of kinetic testing.

Specific material characterization and predictions of ML/ARD: The ability to accurately predict the potential for ML/ARD requires a careful and complete characterization of all materials and waste types under the probable weathering (oxygen, bacteria, moisture, volumes of materials, etc.) conditions. Representativeness and adequacy of samples collected, measures of variability and uncertainty, and analytical procedures selected need to be appropriate. Industry-regulatory quality assurance and quality control procedures need to be followed. To be complete, predictions and assessments are to be made pre-mining (baseline data), during the operational phase, post-mining, and long-term. The document defines specific tests to define the geological and mineralogical properties of materials.

Static and kinetic tests: Static tests require appropriate sampling intensity, sample preparation, determinations of elemental concentrations (total and water soluble), and full acid-base accounting. Kinetic tests are recommended to evaluate reaction rates and to predict and measure drainage chemistry. Humidity cell, column test and actual field verification tests should be conducted. Monitoring of site drainage (seeps, mine drainage, pit lakes, etc.) should include parameters to be evaluated and the frequency of monitoring during and post-mining.

Assessments of waste materials: Waste materials may include waste rock, tailings, treatment wastes, low grade ore and overburden materials. All media require assessments and predictions for acid drainage and releases of metals. Post-disposal weathering of waste piles, including changes in pH, carbonate content, soluble weathering products (acid water and metals). Thermal properties, pore gas composition, and oxygen concentrations may be significant parameters in the assessments of long-term water quality degradation.

The MEND document (Price 2005), also provides an approach to interpretation and display of the above characterization data. Identification of ARD generating materials is important, but toxicity from metals with neutral pH can be significant factors and are not to be overlooked. Predicting drainage chemistry is based on data and information gathered and their proper interpretation. Factors include the weathering environment and climate, data predicting ARD/ML potential, anticipated rates of leaching from mine wastes and mine workings, metal releases based on kinetic tests and geochemical modeling. Additional issues are in stream alkalinity, dilution, and natural attenuation.

Estimating environmental and ecological impacts should be based on identifying potential receptors, endangered species, sensitivity and distributions of selected species and forms of exposure. A conceptual site model can be useful in determining mechanisms of contaminant release, contaminant pathways and receptors of concern. Acute and

chronic toxicity testing of identified aquatic and terrestrial receptors and pre- and post-mining monitoring programs are recommended.

In the United States, the National Research Council (1999) took up the issue of metal mining recognizing the controversy associated with permitting and compliance of hardrock mining. The committee was well versed on the potential deleterious impacts of mining and spent most of their deliberations contemplating the weaknesses of the existing regulatory framework. Recommendations were put forward for the Federal agencies consideration suggesting greater coordination and use of the best available scientific practices. This report did not explore technical topics such as AMD in detail, rather the recommendations were policy oriented.

Water Quality and Acid Mine Drainage: Pre-mine Predictions and Post-mine Comparisons

A major and unique study (Kuipers et al. 2006) was conducted comparing predicted and actual water quality at several mines in the United States. The overall purpose of this study was to examine the reliability of pre-mining water quality predictions at hard rock mining operations. The approach included reviews of the history and accuracy of water quality predictions in Environmental Impact Statements (EISs) for major hard rock mines and then examined and compared actual water quality to the predictions postulated in the EISs. A total of 183 mines were identified, with 71 having reviewed EISs. The investigation focused on 25 mines for in-depth analysis. Nearly all of the EISs reviewed reported that they expected acceptable water quality (concentrations lower than relevant standards) after mitigation was taken into account. Data analyses in this report, in general, refuted these EIS predictions. The following are major findings of the investigation:

Surface water: Sixty percent of the case study mines (15/25) exceeded surface water quality standards due to mining-related activities. Of these, four (17%) noted a low potential to exceed standards, seven (47%) a moderate potential, two a high potential, and three had no information in their EISs for surface water quality impacts in the absence of mitigation measures. The specific water quality parameters exceeding standards varied between sites and were not specifically identified in the report.

Ground water: The majority (64% or 16/25) of the case study mines also exceeded drinking water standards in groundwater. At three of the mines, all in Nevada, the elevated concentrations of metals that did not meet the standards may be related to baseline conditions. However, due to mining activities, 52% of the case study mines

clearly exceeded standards in surface water. In terms of post-mitigation groundwater quality impacts, 77% (10/13) of the mines that predicted low groundwater quality impacts in their EISs were above the water quality standards. Most mines predicted no impacts to groundwater quality after mitigation were in place, but in the majority of case study mines, impacts have occurred.

Metals of Concern: Elements that most often exceeded standards or that had increasing concentrations in groundwater or surface water included toxic heavy metals such as copper, cadmium, lead, mercury, nickel, or zinc (12/19 or 63% of mines), arsenic and sulfate (11/19 or 58% of mines for each) and cyanide (10/19 or 53% of mines).

Acid mine drainage: The majority of the case study mines (18/25 or 72%) predicted low potential for acid drainage in one or more EISs. Of the 25 case study mines, 36% have developed acid drainage on site to date. Of these 9 mines, 8 (89%) predicted low acid drainage potential initially or had no information on acid drainage potential. The Greens Creek Mine in Alaska initially predicted moderate acid drainage potential but later predicted low potential for acid drainage for an additional waste rock disposal facility. Therefore, nearly all the mines that developed acid drainage either underestimated or ignored the potential for acid drainage in their EISs.

Factors Leading to Failures in Predicting Post-Mine Water Quality and Acid Mine Drainage

In the report comparing predicted and actual water quality at hard rock mines (Kuipers et al. 2006), the authors identified two types of characterization failures that led to differences between predicted water quality as speculated in EIS documents and the actual water quality either during or after mining began. The two characterization failure types were: 1) insufficient or inaccurate characterization of the hydrology, and 2) insufficient or inaccurate geochemical characterization of the proposed mine. Inaccurate pre-mining characterization and interpretation can, therefore, result in a failure to recognize or predict water quality impacts. The authors reported primary causes of hydrologic characterization failures as follows: overestimations of dilution, lack of hydrological characterization, overestimations of discharge volumes, and underestimations of storm size. The primary causes of geochemical characterization failures were identified as: lack of adequate geochemical characterization, in terms of sample representativeness and sample adequacy.

In the 25 case study mines, the authors identified mitigation failures with the following primary causes: mitigation measures were not identified or they were inadequate, or not

implemented; waste rock mixing and segregation was not effective, liners leaked, tailings were spilled, or embankments failed, and land application discharge was not effective. The authors provided a table summarizing these failures (Table 1) for the 25 case study mines.

Table 1. Water Quality Predictions Failure Modes, Root Causes and Examples from Case Study Mines (Kuipers et.al, 2006).

Failure Mode	**Root Cause**	**Examples**
Hydrologic Characterization	Lack of hydrologic characterization	Royal Mountain King, CA; Black Pine, MT
	Dilution overestimated	Greens Creek, AK; Jerritt Canyon, NV
	Amount of discharge underestimated	Mineral Hill, MT
	Size of storms underestimated	Zortman and Landusky, MT
Geochemical Characterization	Lack of adequate geochemical characterization	Jamestown, CA; Royal Mountain King, CA; Grouse Creek, ID; Black Pine, MT
	Sample size and/or representation	Greens Creek, AK; McLaughlin, CA; Thompson Creek, ID; Golden Sunlight, MT; Mineral Hill, MT; Zortman and Landusky, MT; Jerritt Canyon, NV
Mitigation	Mitigation not identified, inadequate, or not installed	Bagdad, AZ; Royal Mountain King, CA; Grouse Creek, ID
	Waste rock mixing and segregation not effective	Greens Creek, AK; McLaughlin, CA; Thompson Creek, ID; Jerritt Canyon, NV
	Liner leak, embankment failure or tailings spill	Jamestown, CA; Golden Sunlight, MT; Mineral Hill, MT; Stillwater, MT; Florida Canyon, NV; Jerritt Canyon, NV; Lone Tree, NV; Rochester, NV
	Land application ineffective	Beal Mountain, MT

Treatment of Acid Mine Drainage

Water treatment for elevated metal levels and acidity is a common outcome of acid mine drainage. The effectiveness and feasibility of water treatment is highly variable depending on the treatments employed and unique site characteristics. Water treatment installations may include both passive and active systems. Passive water treatment systems, typically wetlands, operate without chemical amendments and without motorized or mechanized assistance. In contrast active water treatment systems are highly engineered water treatment facilities commonly employing chemical amendment of acid mine water to achieve a water quality standard specified in a discharge permit. In-depth evaluation of AMD treatment options was not performed as part of this literature review; rather emphasis was placed on prevention of AMD formation. Active treatment systems are operational at the Berkeley Pit, Butte, Montana; Britannia Beach, British Columbia; Iron Mountain Mine, Shasta County, California; and, Idaho Springs/Clear Creek, Colorado. Passive treatment systems are most frequently employed in Appalachian coal mining regions for control of acidic drainage. Semi-passive treatment systems are also in use where alkaline amendments are added to surface water at remote sites such as the Summitville Superfund site, Colorado.

Recommendations for Acidic Drainage Minimization

Acidic drainage from mines is observed at many mine sites and the undesirable consequences of acidification are well known. Every effort should be employed to minimize the causes of acid generation. Because mineralogy and other factors (particle size, reactivity of NP and presence of oxidizers) that influence AMD formation are highly variable from one mine to another, and among different geologic materials within a proposed mine site, accurate prediction of future acid generation is difficult at best. Predicting the potential for AMD formation is costly, and of questionable reliability (Kuipers et al. 2006). In addition, concern has arisen over the lag time between waste emplacement and observation of an acid drainage problem. With acid generation, there is no general method to predict its long-term duration or to predict when acidic drainage will commence. There are historical, and now modern mining examples of long-term AMD generation requiring active treatment in perpetuity. There are two primary approaches to addressing AMD: circumvent mining sulfide rich ore deposits with high AMD potential, and implementing mitigation measures to limit potential AMD impacts. It is noted that avoiding mining of sulfide ores with the potential to form AMD may be difficult because they are most often associated with the mineral resource of interest.

Selective handling and avoidance of sulfide ore and overburden is a strategy for minimizing the risk of future acid generation (Skousen et al., 1998). In a review of selective handling of acid-forming materials in coal mining in the Eastern U.S., Perry and others (1997) found that selective handling had not eliminated acid formation due in part to the inherent difficulty in segregating benign overburden from acid-forming waste. In some mining operations acid-forming minerals can be avoided through the mine planning process or through using underground mining rather than surface mining.

Mine waste isolation and avoidance of oxidizing conditions can be performed using several methods that keep sulfides isolated from oxygen. Subaqeous disposal of tailings and waste rock below the water table is commonly practiced in Canada as a protocol for mine reclamation (Samad and Yanful, 2004). Paste backfill is a mining methodology for minimization of acid formation by backfilling mine workings using a mixture of mine tailings, Portland cement and other binders to create a waste disposal option that is both geotechnically stable and geochemically non-reactive since sufficient NP can be added to neutralize any future acidity (Benzaazoua, T.B. and B. Bussiere, 2002). Depyritization of tailings can be accomplished to remove sulfide minerals from waste products to create a benign sand fraction suitable to use as a general backfill and a companion low-volume sulfide concentrate requiring careful disposal. Most mine tailings contain small amounts of sulfide minerals that can be readily separated from non-acid forming silicate minerals using conventional mineral processing equipment to create a cleaned material with sufficient NP to ameliorate any future acidity (Benzaazoua, B. et al., 2000).

In many cases, the measures described above are most effective when used in combination and adapted to the situation at a specific site. For the most part, only limited data are available to document the long-term effectiveness of any of these controls. The Kuipers Report (2006) provides a unique view of the failure to predict the formation of AMD at many hardrock mines. There are many research investigations being conducted by university, government, and industrial entities to develop new treatment strategies for AMD. The transfer of laboratory data to site-specific conditions (climate, geology, physical properties of ores, etc.) can be problematic and significantly impact their feasibility and performance in the field.

Thorough baselines studies of the biological, hydrologic, and geochemical conditions characteristic of the unique site are required to provide a basis for long-term monitoring and provide an insight into mechanistic processes involved in AMD evolution (Edwards et al., 2000). Associated financial assurances for resource mitigation in the event of default of a mine property are also required (NRC, 1999) to ensure both short-term and long-term mitigation of AMD and the associated impacts to water quality and fisheries.

Based on review of the acid mine drainage literature it is clear that severe world-wide ecological consequences, especially for aquatic resources, have resulted from mining ore deposits with acid-forming minerals. Accurate prediction of the onset and aggressiveness of low-quality acidic water discharge is perilously difficult using the best available science. Multiple complex geochemical, biological and hydrologic factors create a daunting task for mining engineers to profitably recover mineral resources while preventing discharges of metals and acidity to surface and ground water. The deleterious effects of elevated metals levels and acidity to salmonids are clearly reported in the scientific literature. The inevitability of impacts to fisheries from AMD caused by mining is an open question and dependent on the outcome of complex geochemical reactions and human attempts to understand and mitigate their consequences. The track record of industry is replete with problems, thus little comfort is afforded by extensive pre-mine studies.

Summary

Acid mine drainage commonly forms as a result of natural geochemical processes that oxidize metal sulfides exposed at the earth's surface by mining. Oxidation of sulfur and hydrolysis of iron result in acid-sulfate waters which have been observed at thousands of historic mine sites and at operational mines where mitigation measures have failed to prevent the release of acid mine drainage to down-gradient surface waters. Resultant low pH conditions mobilize metals from waste materials resulting in degradation of water quality and impairment of aquatic health. Acid mine drainage and associated weathering products commonly result in physical, chemical and biological impairment of surface water. Pre-mine characterization of the risk of AMD formation is often inaccurate leading to notable post-mine risk to fisheries. Fisheries have been impaired world-wide by releases of AMD from mining areas. The mining industry has spent large amounts of money to prevent, mitigate, control and otherwise stop the release of AMD using the best available technologies, yet AMD remains as one the greatest environmental liabilities associated with mining, especially in pristine environments with economically and ecologically valuable natural resources. Problematic to the long-term operation of large scale metal mines is recognition that no hard rock surface mines exist today that can demonstrate that AMD can be stopped once it occurs on a large scale. Evidence from literature and field observations suggests that permitting large scale surface mining in sulfide-hosted rock with the expectation that no degradation of surface water will result due to acid generation imparts a substantial and unquantifiable risk to water quality and fisheries.

References and Literature Cited

Agricola, G. (1556). “De re metallica.” Translated 1950 by: H. C. Hoover, L.H. Hoover. Dover, NY.

Baldigo, B. P., and G. B. Lawrence (2000). "Composition of fish communities in relation to stream acidification and habitat in the Neversink River, New York." Transactions of the American Fisheries Society 129(1): 60-76.

Barry, K. L., J. A. Grout, C. D. Levings, B. H. Nidle, and G. E. Piercey (2000). "Impacts of acid mine drainage on juvenile salmonids in an estuary near Britannia Beach in Howe Sound British Columbia." Canadian Journal of Fisheries and Aquatic Sciences 57(10): 2031-2043.

Beltman, D. J., W. H. Clements, J. Lipton, and D. Cacela (1999). "Benthic invertebrate metals exposure, accumulation, and community level effects downstream from a hard rock mine site." Environmental Toxicology and Chemistry 18(2): 299-307.

Benzaazoua, B., B. Bussiere, M. Kongolo, J. McLaughlin, and P. Marion (2000). "Environmental desulphurization of four Canadian mine tailings using froth flotation." International Journal of Mineral Processing 60(1): 57-74.

Benzaazoua, B., and B. Bussiere (2002). "Chemical factors that influence the performance of mine sulphidic paste backfill." Cement and Concrete Research 32(7): 1133-1144.

Borden, R. (2001). "Geochemical evolution of sulfide-bearing waste rock soils at the Bingham Canyon Mine, Utah." Geochemistry: Exploration, Environment, and Analysis 1(1): 15-21.

Boudou, A., R. Maury-Brachet, M. Coquery, G. Durrieu, and D. Cossa (2005). "Synergic effect of gold mining and damming on mercury contamination in fish." Environmental Science & Technology 39(8): 2448-2454.

Cooper, E. L., and C. C. Wagner (1973). “The effects of acid mine drainage on fish populations.” *In*: Fish and Food Organisms in Acid Waters of Pennsylvania, US Environmental Protection. EPA-R#-73-032: 114.

CSS (2002). Center for Streamside Studies. “Environmental impacts of hardrock mining in Eastern Washington.” College of Forest Resources and Ocean and Fishery Sciences, University of Washington, Seattle, WA.

Edwards, K. J., P.L. Bond, G.K. Druschell, M.M. McGuire, R.J. Hamers, and J.F. Banfield (2000). "Geochemical and biological aspects of sulfide mineral dissolution: lessons from Iron Mountain, California." Chemical Geology 169(3-4): 383-397.

EPA (1995). “Human Health and Environmental Damages from Mining and Mineral Processing Wastes.” Washington DC, Office of Solid Waste, U.S. Environmental Protection Agency.

Farag, A. M., D.Skaar, D.A. Nimick, E. MacConnell, and C. Hogstrand (2003). "Characterizing aquatic health using salmonids mortality, physiology, and biomass estimates in streams with elevated concentrations of arsenic, cadmium, copper, lead, and zinc in the Boulder River Watershed, Montana." Transaction of the American Fisheries Society 132(3): 450-457.

Frisbee, N. M., and L.R. Hossner (1989). “Weathering of siderite (FeCO3) from lignite overburden”. Proceedings of the Symposium on Reclamation; A Global Perspective, Calgary, Alberta.

Fromm, P. O. (1980). "A review of some physiological and toxicological responses of freshwater fish to acid stress." Environmental Biology of Fishes 5(1): 79-93.

Griffith, M. B., J. M. Lazorchak, and A.T. Herlihy (2004). "Relationships among exceedances of metals criteria, the results of ambient bioassays, and community metrics in mining impacted streams." Environmental Toxicology and Chemistry 23(7): 1786-1795.

Hansen, J. A., D. F. Woodward, E. E. Little, A. J. DeLonay, and H. L. Bergman (1999). "Behavioral avoidance: possible mechanism for explaining abundance and distribution of trout in a metals-impacted river." Environmental Toxicology and Chemistry 18(2): 313- 17.

Hansen, J. A., P. G. Welsh, J. Lipton, and D. Cacela (2002). "Effects of copper exposure on growth and survival of juvenile bull trout." Transactions of the American Fisheries Society 131(4): 690-697.

Hill, R. D. (1974). “Mining impacts on trout habitat.” Proceedings of a Symposium on Trout Habitat, Research, and Management, Boone, NC, Appalachian Consortium Press.

Howells, G. D., D. J. A. Brown, K. Sadler (1983). "Effects of acidity, calcium, and aluminum on fish survival and productivity - a review." Journal of the Science of Food and Agriculture 34(6): 559-570.

Jennings, S. R., and D.J. Dollhopf (1995). "Acid-base account effectiveness for determination of mine waste potential acidity." Journal of Hazardous Materials 41(161-175).

Jennings, S. R., Dollhopf, J.D., and W.P. Inskeep (2000). "Acid production from sulfide minerals using hydrogen peroxide weathering." Applied Geochemistry 15(235-243).

Johnson, D. W., H. A. Simonin, J. R. Colquhoun, and F. M. Flack (1987). "In situ toxicity tests of fishes in acid waters." Biogeochemistry 3(1-3): 181-208.

Kaeser, A. J., and W. E. Sharpe (2001). "The influence of acidic runoff episodes on slimy sculpin reproduction in Stone Run." Transactions of the American Fisheries Society 130(6): 1106-1115.

Kimmel, W. G. (1983). “The impact of acid mine drainage on the stream ecosystem.” Pennsylvania Coal: Resources, Technology, and Utilization. Pennsylvania Academic Science Publications: 424-437.

Kuipers, J. R., A.S. Maest, K.A. MacHardy, and G. Lawson (2006). “Comparison of Predicted and Actual Water Quality at Hardrock Mines: The reliability of predictions in Environmental Impact Statements.” Kuipers & Associates, PO Box 641, Butte, MT USA 59703.

Lawrence, R. W., and M. Scheske (1997). "A method to calculate the neutralization potential of mining wastes." Environmental Geology 32(2): 100-106.

Maret, T. R., and D. E. MacCoy (2002). "Fish assemblages and environmental variables associated with hard-rock mining in the Coeur d’Alene River Basin, Idaho." Transactions of the American Fisheries Society 131(5): 865-884.

Martin, A. J., and R. Goldblatt (2007). "Speciation, behavior, and bioavailability of copper downstream of a mine-impacted lake." Environmental Toxicology and Chemistry 26(12): 2594-2603.

McGuire, M. M., K.J. Edwards, J.F. Banfield, and R.J. Hamers (2001). "Kinetics, surface chemistry, and structural evolution of microbially mediated sulfide dissolution." Geochimica et Cosmochimica Acta 65(8): 1243-1258.

MEND (2001). “List of Potential Information Requirements in Metal Leaching/ Acid Rock Drainage Assessment and Mitigation Work”. Mining Environment Neutral Drainage Program. W. A. Price, CANMET, Canada Centre for Mineral and Energy Technology.

Menendez, R. (1978). “Effects of acid water on Shavers Fork – a case history.” Surface mining and fish/wildlife needs in the Eastern United States., U.S. DOI, Fish and Wildlife Service. FWS/OBS 78/81: 160-169.

Morin, K. A., and N.M. Hutt (2000). “Lessons Learned from Long-Term and Large-Batch Humidity Cells.” Fifth International Conference on Acid Rock Drainage, Denver, CO, Society for Mining, Metallurgy and Exploration (SME).

Munshower, F. F., D.R. Neuman, S.R. Jennings and G.R. Phillips (1997). “Effects of Land Reclamation Techniques on Runoff Water Quality from the Clark Fork River Floodplain, Montana.” Washington, DC, EPA Office of Research and Development: 199-208.

Nordstrom, D. K., E.A. Jenne, and R.C. Averett (1977). “Heavy metal discharges into Shasta Lake and Keswick Reservoir on the Sacramento River, California – a reconnaissance during low flow.” U.S. Geological Survey. Open-File Report 76-49.

Nordstrom, D. K., and G. Southam (1997). "Geomicrobiology- interactions between microbes and minerals." Mineral Soc. Am 35: 261-390.

Nordstrom, D. K., and C. N. Alpers (1999). "Negative pH, efflorescent mineralogy, and consequences for environmental restoration at the Iron Mountain Superfund site, California." Proc. Natl. Acad. Sci. USA 96(7): 3455-3462.

Nordstrom, D. K., and C. N. Alpers (1999). “Negative pH, efflorescent mineralogy, and consequences for environmental restoration at the Iron Mountain Superfund site, California.” National Academy of Science. 96 (7): 3455-3462.

NRC (1999). “Hardrock Mining on Federal Lands.” National Research Council. Washington, D.C., National Academy Press.

Patunc, A. D. (1999). "Mineralogical constraints on the determination of neutralization potential and prediction of acid mine drainage." Environmental Geology 39(2): 103-112.

PDEP (1998). Pennsylvania Dept. of Environmental Protection. “Coal Mine Drainage Prediction and Pollution Prevention in Pennsylvania.” M. W. S. Brady K.B.C., and J. Schueck.

Perry, E. F., M.D. Gardner, and R.S. Evans (1997). “Effect of acid material handling and disposal on coal mine drainage quality.” Fourth International Conference on Acid Rock Drainage, Vancouver, B.C.

Price, W. A. (2005). MEND. “List of potential information requirements in metal assessment and mitigation work.” CANMET Mining and Mineral Sciences Laboratories, Natural Resources Canada. Division Report MMSL 04-040 (TR); MEND Report 5.10E.

Samad, M. A., and E.K. Yanful. (2005). "A design approach for selection the optimum water cover depth for subaqueous disposal of sulfide mine tailings." From http: pubs.nrc-cnrc.gc.ca/rp/rppdf/t04-094.pdf.

Scharer, J. M., L. Bolduc, C.M. Pettit, and B.E. Halbert (2000). “Limitations of Acid-base Accounting for Predicting Acid Rock Drainage”. Fifth International Conference on Acid Rock Drainage, Denver, CO, Society for Mining, Metallurgy and Exploration (SME).

Schmidt, T. S., D. J. Soucek, and D. S. Cherry (2002). "Modification of an ecotoxicological rating to bioassess small acid mine drainage-impacted watersheds exclusive of benthic macroinvertebrate analysis." Environmental Toxicology and Chemistry 21(5): 1091-1097.

Sherlock, E. J., R.W. Lawrence, and R. Poulin (1995). "On the neutralization of acid rock drainage by carbonate and silicate minerals." Environmental Geology 25(1): 43-54.

Skousen, J., J. Renton, H. Brown, P. Evans, B. Leavitt, K. Brady, L. Dohen, and P. Ziemkiewicz (1997). "Neutralization potential of overburden samples containing siderite." Journal of Environmental Quality 26(3): 673-681.

Skousen, J., A. Rose, G. Geidel, J. Foreman, R. Evans, and W. Hellier. (1998). "Handbook of Technologies for Avoidance and Remediation of Acid Mine Drainage Acid - Technology Initiative (ADTI)." From http: www.ott.wrcc.osmre.gov/library/hbmanual/hbtechavoid/hbtechavoid.pdf.

Skousen, J., J. Simmons, L.M. McDonald, and P. Ziemkiewicz (2002). "Acid-base accounting to predict post-mining drainage quality on surface mines." Journal of Environmental Quality 31: 2034-2044.

Skousen, J. G., and P.F. Ziemkiewicz (1996). “Acid Mine Drainage Control and Treatment.” Second Edition. Morgantown, W.V., West Virginia University and the National Mine Land Reclamation Center.

Smith, R. M., W.E. Grube, T. Arkle, and A. Sobek (1974). “Mine Spoil Potentials for Soil and Water Quality.” Cincinanati, OH, U.S. EPA. EPA-670/2-74-070: 303.

Sobek, A., W. Schuller, J.R. Freeman, and R.M. Smith (1978). “Field and Laboratory Methods Applicable to Overburdens and Minesoils.” Cincinnati, OH, U.S. EPA. EPA-600/2-78-054: 203.

Soucek, D. J., D. S. Cherry, R. J. Currie, H. A. Latimer, and G. C. Trent (2000). "Laboratory and field validation in an integrative assessment of an acid mine drainage-impacted watershed." Environmental Toxicology and Chemistry 19(4): 1036-1043.

Stromberg, B., and S. Banwart (1999). "Weathering kinetics of waste rock from the Aitik copper mine, Sweden: Scale dependent rate factors and pH controls in large column experiments." Journal of Contaminant Hydrology 39(1-2): 59-89.

UNEP (2000). “Cyanide Spill at Baia Mare Romania, Unep / Ocha Assessment Mission; Spill of Liquid and Suspended Waste at the Aurul S.A. Retreatment Plant in Baia Mare. Geneva.” UNEP /Office For The Co-Ordination Of Humanitarian Affairs. United Nations Environment Programme. Ocha Assessment Mission, Romania, Hungary, Federal Republic Of Yugoslavia.

UNEP. (2002). "Chronology of Major Tailing Dam Failures." United Nations Environmental Program, Division of Technology, Industry and Economics. From http://www.mineralresourcesforum.org/incidents/index.htm.

USDA (1993). “Acid Mine Drainage form Impact of Hard Rock Mining on the National Forests: A Management Challenge.” USDA Forest Service, Program Aid 1505: 12.

Warner, R. W. (1971). "Distribution of biota in a stream polluted by acid mine drainage." Ohio Journal of Science 71(4): 202-215.

Weber, P. A., J.E. Thomas, W.M. Skinner, and R.C. Smart (2004). " Improved acid neutralization capacity assessment of iron carbonates by titration and theoretical calculation." Applied Geochemistry 19(5): 687-694.

Woodward, D. F., J. K. Goldstein, A. M. Farag, and W. G. Brunbaugh (1997). "Cutthroat trout avoidance of metals and conditions characteristic of a mining waste site: Coeur d'Alene River, Idaho." Transactions of the American Fisheries Society 126(4): 699-706.

Younger, P. L., S.A. Banwart, and R.S. Hedin (2002). "Mine Water: Hydrology, Pollution, Remediation." NY, NY, Springer Pub.

ATTACHMENT 13

Comparison of Predicted and Actual Water Quality at Hardrock Mines

The reliability of predictions in Environmental Impact Statements

Buka Environmental

Kuipers & Associates

EXECUTIVE SUMMARY

INTRODUCTION AND APPROACH

This study reviews the history and accuracy of water quality predictions in Environmental Impact Statements (EISs) for major hardrock mines in the United States. It does so by:

- identifying major hardrock metals mines in the United States and determining which major mines had EISs
- gathering and evaluating water quality prediction information from EISs
- selecting a representative subset of mines with EISs for in-depth study
- examining actual water quality information for the case study mines, and
- comparing actual water quality to the predictions made in EISs.

Based on the results of the evaluations conducted, an analysis was performed to identify the most common causes of water quality impact and prediction failures. In addition, an analysis was conducted to determine if there were inherent risk factors at mines that may predispose an operation to having water quality problems. Conclusions are provided about the effectiveness of the underlying scientific and engineering principles used to make water quality predictions in EISs. Finally, recommendations are made for regulatory, scientific and engineering approaches that would improve the reliability of water quality predictions at hardrock mine sites.

The National Environmental Policy Act (NEPA), enacted in 1969, was the first environmental statute in the United States and forms the foundation of a comprehensive national policy for environmental decision making. NEPA requires federal agencies to take a "hard look" at the environmental impacts of each proposed project to ensure the necessary mitigation or other measures are employed to meet federal and state regulations and other applicable requirements. Under NEPA, when a new mine is permitted, agencies have a duty to disclose underlying scientific data and rationale supporting the conclusions and assumptions in an EIS.

NEPA requires federal agencies proposing major actions that may substantially affect the quality of the human environment to prepare a detailed Environmental Impact Statement (EIS). A "major action" includes actions approved by permit or other regulatory action. If the agency finds that the project *may* have a significant impact on the environment, then it must prepare an EIS. As part of the EIS process, hardrock mines operating on federal lands or otherwise subject to NEPA are required to estimate impacts to the environment, including direct impacts to water quality and indirect impacts that occur later in time but are still reasonably foreseeable. The NEPA analysis process calls for performing original research, if necessary, and reasonable scientifically supported forecasting and speculation. A wide array of scientific approaches has been used to predict water quality that could result at mine sites, and many different engineering techniques were applied to mitigate these potential impacts. The primary subject of this report is the effectiveness of water quality predictions and mitigation that were applied over the past 30 years as a part of the EIS process at hardrock mines in the United States.

IDENTIFICATION OF MAJOR AND NEPA-ELIGIBLE HARD ROCK MINES

Major Hardrock Metal Mines in the United States

Hardrock metal mines in the United States produce gold, silver, copper, molybdenum, lead, zinc and platinum group metals from open pit and underground mining operations. For the purpose of this study, "major" mines were defined as: those that have a disturbance area of over 100 acres and a financial assurance amount of over $250,000; have a financial assurance of $1,000,000 alone (regardless of acreage); or have a production history (since 1975) of greater than 100,000 ounces of gold, 100,000,000 pounds of copper or the monetary value equivalent in another metal. Using those criteria, 183 major hardrock metal mines were identified as having operated since 1975.
The major hardrock mines are located in fourteen states (Alaska, Arizona, California, Colorado, Idaho, Michigan, Montana, Nevada, New Mexico, South Carolina, South Dakota, Utah, Washington and Wisconsin), with the vast

majority (178 of 183) located in western states. Nevada has the greatest number of major mines of any state, with 74 (40%) of the total major mines. Sixty-three percent (63%) of the mines produce gold and/or silver, 16% produce copper, 4% produce copper and molybdenum, 2% produce molybdenum only, 4% produce lead and zinc, and 1% produce platinum group metals (percentages add to greater than 100 because some mines produce multiple commodities).

Seventy-two percent (72%) of the major hardrock mines in the U.S. that have operated since 1975 are open pit mines, while 15% are underground. Sixty-six percent (66%) of the major hardrock mines use cyanide heap or vat leaching, 24% use flotation or gravity processing and 12% process ore by acid dump leaching and solvent extraction/ electrowinning.

Forty-five percent (45%) of the 183 major hardrock mines in operation since 1975 are still operating, and 49% have closed. Only one new major hardrock mine is currently (as of 2005) in construction, and seven others are in various stages of permitting. After the NEPA processes were completed, development proposals were withdrawn for four of the major hardrock mines identified in this study.

Major Hardrock Metal Mines Subject to NEPA

Mines located on federal land administered by the Bureau of Land Management or the Forest Service are subject to the requirements of NEPA. Also subject to NEPA regulations are certain National Pollution Discharge Elimination System (NPDES) permits issued by the Environmental Protection Agency, certain 404 Wetlands permits from the Army Corp of Engineers, and mines located on Native American trust lands administered by the Bureau of Indian Affairs (BIA). In addition, some states (California, Montana, Washington and Wisconsin) have a state-mandated process that is equivalent to NEPA.

NEPA requires environmental analysis of federal actions. As it has evolved, an EIS is required for any "major federal action significantly affecting the quality of the human environment," and an Environmental Assessment (EA) is required for lesser actions. EAs do not require public comment; the results of an EA can determine whether the action is significant, which will trigger an EIS, but usually the EA is performed in lieu of an EIS.

Of the 183 major modern-era hardrock mines identified, 137 (75%) had federal actions that triggered NEPA analysis. Ninety-three (68%) were located on BLM land, thirty-four (25%) on Forest Service land, and nine (7%) on both BLM and Forest Service land. Disturbance of wetlands triggered NEPA analysis at five (4%) of the mines, requiring a 404 wetlands permits from the Corp of Engineers (COE); a discharge into a water of the United States was the only NEPA trigger at three (2%) mines; and NEPA analysis was triggered at two (1%) mines because they were located on Indian Lands. Twenty-three (19%) mines were located in states that have their own NEPA-equivalent statutes. In many cases, more than one federal agency may be involved in the NEPA process (e.g., Forest Service and BLM, based on location, or Forest Service and EPA, based on location and a NPDES discharge); in addition, state agencies may be responsible for carrying out their own NEPA-equivalent or alternative processes. When this occurs, a Memorandum of Understanding (MOU) is usually written among the various agencies describing their shared responsibilities in order to avoid duplication of efforts. When two or more federal and/or state agencies are involved, the agencies establish a formal agreement delineating which will act in the lead and cooperating roles. In some cases an EIS (or EA) may be developed that will satisfy both NEPA and a NEPA-equivalent state law.

The general makeup of the mines where NEPA is applicable is roughly similar to that of major mines. The NEPA-applicable mines are located in 11 states with all but one located in the western states. Nevada had the most NEPA-applicable major mines with 50% (69) of the total. Eighty-five percent (116) of the NEPA-applicable mines produced gold and/or silver, while 15% (21) produced copper. Seventy-six percent (104) of the NEPA-applicable major mines were open-pit, while 14% (19) were underground mines. Sixty-nine percent (95) used cyanide heap or vat leach, 20% (28) used flotation/gravity and 11% (15) used acid dump leach processing. Forty-seven percent (64) of the major mines subject to NEPA were still operating, 45% (61) have closed, one was in construction, six were in permitting, and five were withdrawn from consideration after undergoing the NEPA process.

EISs were performed at 82 (60%) of the 137 major mines subject to NEPA, either as part of new permitting actions or later expansions or other actions. EAs were performed at the remainder of the mines subject to NEPA. EISs and EAs were obtained by writing, e-mailing, and/or calling state and federal agencies, including the BLM, Forest Service, tribal agencies and by conducting library searches. The process of obtaining NEPA documents took approximately 16 months and involved numerous follow-up calls, and written and email contact. Of the 137 major mines subject to NEPA, 71 mines had documents that were obtained and reviewed. A total of 104 NEPA documents, either EISs or EAs, were reviewed for the 71 mines. The general characteristics of mines with reviewed EISs are similar to those of all major hard rock mines and all NEPA-eligible mines, as shown in Table ES-1.

EVALUATION OF WATER QUALITY PREDICTION INFORMATION IN NEPA DOCUMENTS

Information on the following elements related to water quantity and quality predictions was collected from the 104 NEPA documents: geology/mineralization; climate; hydrology; field and laboratory tests performed; constituents of concern identified; predictive models used; water quality impact potential; mitigation; potential water quality impacts; predicted water quality impacts; and discharge information. There are two types of water quality predictions made in EISs: "potential" water quality, which leans toward worst-case water quality that does not take mitigation into account; and "predicted" water quality, which does consider the beneficial effects of mitigation. Both types of water quality predictions were recorded and used for subsequent comparisons to actual water quality. For each type of information collected from the NEPA documents, a score was derived to characterize the element (e.g., geology/ mineralization used six scores, including one for no information provided). The scoring allowed numeric summaries (percentages) to be calculated based on the information collected from the NEPA documents. The results for the EIS information collected for each mine reviewed in detail (71 mines, 104 EISs) are contained in Section 5 of the report. Limited information on certain water quality elements is contained in Table ES-4.

A preliminary evaluation of the availability of operational water quality information was performed before selection of the case study mines. Operational and post-operational water quality information was available from EISs conducted after the new project EIS, especially for the states of Alaska, Montana and Idaho, where multiple EISs were often available. In other states, such as Arizona, California, Nevada and Wisconsin, technical reports and water quality data were available from state agencies that regulate mining activities.

SELECTION OF CASE STUDY MINES

The case study mines were selected based on:

- the ease of access to information on operational water quality
- the variability in general categories such as geographic location, commodity type, extraction and processing methods, and
- the variability in EIS elements related to water quality, such as climate, proximity to groundwater and surface water resources, acid drainage potential and contaminant leaching potential.

Case studies were developed for the twenty-five mines listed in Table ES-2.

Table ES-1. Comparison of General Categories for All Hard Rock Mines, NEPA-eligible Mines and Mines with Reviewed EISs (% of mines in sub-category)

Category	Sub-category	Major Mines (%)	NEPA-eligible Mines (%)	Mines with Reviewed EISs (%)
Location	Alaska	4.4%	5.1%	9.9%
	Arizona	10.9%	9.5%	11.3%
	California	8.2%	9.5%	11.3%
	Colorado	4.9%	0.0%	0.0%
	Idaho	7.7%	4.4%	8.5%
	Michigan	0.5%	0.0%	0.0%
	Montana	8.2%	10.9%	18.3%
	Nevada	40.4%	50.4%	32.4%
	New Mexico	3.8%	2.2%	2.8%
	South Carolina	1.6%	0.0%	0.0%
	South Dakota	2.7%	0.7%	1.4%
	Utah	3.8%	2.9%	1.4%
	Washington	2.2%	2.9%	0.0%
	Wisconsin	0.5%	0.7%	1.4%
Commodity	Primary Gold	12.6%	12.4%	19.7%
	Primary Silver	7.1%	6.6%	7.0%
	Gold and Silver	62.8%	65.7%	54.9%
	Copper	16.4%	15.3%	19.7%
	Copper and Molybdenum	4.4%	2.9%	1.4%
	Molybdenum	2.2%	0.7%	1.4%
	Lead and Zinc	3.8%	3.6%	5.6%
	Platinum Group	1.1%	1.5%	2.8%
Extraction Methods	Underground	14.8%	13.9%	18.3%
	Open Pit	72.1%	75.9%	71.8%
	Underground + Open Pit	12.0%	10.2%	9.9%
Processing Methods	Heap or Vat Leach	65.6%	69.3%	62.0%
	Flotation and Gravity	24.0%	20.4%	26.8%
	Dump Leach (SX/EW)	12.0%	10.9%	11.3%
	Heap Leach	39.3%	38.7%	25.4%
	Vat Leach	9.3%	10.2%	14.1%
	Heap Leach and Vat Leach	16.9%	20.4%	22.5%
	Smelter	3.3%	1.5%	1.4%
Operational Status	Operating	44.8%	46.7%	49.3%
	Closed	48.6%	44.5%	36.6%
	In Construction	0.5%	0.7%	1.4%
	Permitting	3.8%	4.4%	7.0%
	Withdrawn	2.2%	3.6%	5.6%
Total number of mines in category		183	137	71

Table ES-2. Case Study Mines

Mine	State	Mine	State
Greens Creek	AK	Golden Sunlight	MT
Bagdad	AZ	Mineral Hill	MT
Ray	AZ	Stillwater	MT
American Girl	CA	Zortman and Landusky	MT
Castle Mountain	CA	Florida Canyon	NV
Jamestown	CA	Jerritt Canyon	NV
McLaughlin	CA	Lone Tree	NV
Mesquite	CA	Rochester	NV
Royal Mountain King	CA	Round Mountain	NV
Grouse Creek	ID	Ruby Hill	NV
Thompson Creek	ID	Twin Creeks	NV
Beal Mountain	MT	Flambeau	WI
Black Pine	MT		

The major characteristics of the case study mines were similar to those of all mines with reviewed EISs, as shown in Table ES-3. The availability of information on operational water quality was also a major factor in the selection of case-study mines. The highest percentage of case study mines was from Nevada, and this state had the highest percentage of mines for all major mines, NEPA-eligible mines, and mines with reviewed EISs. Somewhat higher percentages of mines from California and Montana were selected for case studies because of the ease of obtaining operational water quality information from these states. Similar percentages of gold and/or silver mines were selected for the case studies as were present in all mines with reviewed EISs. However, a lower percentage of primary copper mines was selected for case study because of the difficulty in obtaining operational water quality information on these facilities. Case study mines had very similar percentages as all mines with reviewed EISs in terms of extraction and processing methods. In terms of operational status, no case study mines were in construction, in permitting, or withdrawn because operational water quality information would not be available for mines in these types of operational status.

Case study mines were also similar to all mines with reviewed EISs in terms of EIS elements related to water quality, as shown in Table ES-4. The elements listed in Table ES-4 are considered "inherent" factors that may affect water quality conditions. That is, these elements are related to conditions that either relate to climatic and hydrologic conditions at and near the mine site (in the case of climate, and proximity to water resources) or to qualities of the mined materials that may affect water quality (in the case of acid drainage and contaminant leaching potential). For a number of mines, little or no information on these elements was available in initial EISs, but subsequent NEPA documents either contained the first information or contained improved information after water quality conditions developed at the mine site during and after operation. Therefore, for acid drainage and contaminant leaching potential, the highest documented potential in any of the EISs was recorded.

Case study mines were similar to all mines with reviewed EISs in terms of climate and proximity to surface water resources. When compared to all mines with reviewed EISs, a higher percentage of case study mines had shallower depths to groundwater. However, six of the case study mines had groundwater depths greater than 50 feet below the ground surface. In terms of acid drainage potential, lower percentages of case study mines had low and high acid drainage potential, but higher percentages had moderate acid drainage potential. Therefore, the case study mines provide a somewhat more evenly distributed range of acid drainage potentials than all mines with reviewed EISs. Case study mines had nearly identical percentages of mines with low and high contaminant leaching potential, but more case study mines had moderate acid drainage potential, reflecting fewer mines in the "no information" category for case study mines.

Table ES-3. Comparison of General Categories for All Mines with Reviewed EISs and Case Study Mines (% of mines in subcategory)

Category	Subcategory	All Mines with Reviewed EISs	Case Study Mines
Location	Alaska	10%	4%
	Arizona	11%	8%
	California	11%	24%
	Colorado	0%	0%
	Idaho	9%	8%
	Michigan	0%	0%
	Montana	18%	24%
	Nevada	32%	28%
	New Mexico	3%	0%
	South Carolina	0%	0%
	South Dakota	1%	0%
	Utah	1%	0%
	Washington	0%	0%
	Wisconsin	1%	4%
Commodity	Primary Gold	20%	12%
	Primary Silver	7%	4%
	Gold and Silver	55%	64%
	Copper	20%	4%
	Copper and Molybdenum	1%	4%
	Molybdenum	1%	4%
	Lead and Zinc	6%	4%
	Platinum Group	3%	4%
Extraction Methods	Underground	18%	16%
	Open Pit	72%	76%
	Underground + Open Pit	10%	8%
Processing Methods	Heap and/or Vat Leach	62%	72%
	Flotation and Gravity	27%	28%
	Dump Leach (SX/EW)	11%	8%
	Heap Leach	25%	20%
	Vat Leach	14%	16%
	Heap Leach and Vat Leach	23%	32%
	Smelter	1%	0%
Operational Status	Operating	49%	52%
	Closed	37%	48%
	In Construction	1%	0%
	Permitting	7%	0%
	Withdrawn	6%	0%
Total number of mines		71	25

Table ES-4. Comparison of EIS Elements for All Mines with Reviewed EISs and Case Study Mines (% of mines with sub-element)

Element	Sub-element	All Mines with Reviewed EISs	Case Study Mines
Climate	Dry/Arid	20%	20%
	Dry/Semi-Arid	35%	28%
	Humid Subtropical	4%	12%
	Marine West Coast	4%	4%
	Boreal Forest	28%	32%
	Continental	3%	4%
	Sub-Arctic	4%	0%
Surface Water Proximity	No information	7%	4%
	Perennial Streams >1 mile	26%	24%
	Perennial streams <1 mile	25%	28%
	Perennial streams on site	44%	44%
Groundwater Proximity	No information	12%	4%
	Groundwater >200 ft deep	16%	8%
	Groundwater 50-200 ft deep	13%	16%
	Groundwater 0-50 ft deep/springs on site	59%	72%
Acid Drainage Potential (highest)	No information	9%	8%
	Low	58%	48%
	Moderate	6%	32%
	High	27%	12%
Contaminant Leaching Potential (highest)	No information	22%	12%
	Low	32%	32%
	Moderate	30%	40%
	High	17%	16%
Total number of mines		71	25

Overall, the case study mines display a variability in geographic location, commodity type, extraction and processing methods and in EIS elements related to water quality. Considering the additional limitation of having readily accessible operational water quality information, the case study mines reflect well the distribution of general categories and water quality-related elements that are present in the larger subsets of hard rock mines in the United States.

Case studies for each mine contain information collected from EISs and other documents, information on actual water quality, a comparison of predicted and actual water quality, and an analysis of the causes of water quality impacts and prediction errors.

COMPARISON OF PREDICTED AND ACTUAL WATER QUALITY

Operational and post-operational water quality information was collected from EISs conducted after the new project EIS for mines in Alaska, Montana and Idaho. Interviews of state agency personnel were conducted in California, Montana, Nevada and Wisconsin. Technical reports and water quality data from state agencies that regulate mining were collected for mines in Arizona, California, Nevada and Wisconsin. In some cases, the water quality data showed pre-mining and operational water quality, but baseline data were generally difficult to obtain. The information collected on actual water quality conditions was held in databases or in electronic and paper files for comparison to predicted water quality.

For this evaluation, a water quality impact is defined as increases in water quality parameters as a result of mining operations, whether or not an exceedence of water quality standards or permit levels has occurred. Information on whether groundwater, seep, or surface water concentrations exceeded standards as a result of mining activity is also included. Nearly all the EISs reviewed reported that they expected acceptable water quality (concentrations lower than relevant standards) after mitigation were taken into account. Indeed, if this prediction was not made in the EIS, the regulatory agency would not be able to approve the mine (with certain exceptions, such as pit water quality, in states where pit water is not considered a water of the state).

A comparison between potential (pre-mitigation), predicted, and actual surface water quality for the case study mines is presented in Table ES-5. Sixty percent of the case study mines (15/25) had mining-related exceedences in surface water. Of the mines with surface water quality exceedences, four (17%) noted a low potential, seven (47%) a moderate potential, two a high potential, and three had no information in their EISs for surface water quality impacts in the absence of mitigation measures. For the mines with surface water quality exceedences, only one mine, the McLaughlin Mine in California, was correct in predicting a moderate potential for surface water quality impacts with mitigation in place. However, this mine predicted low acid drainage potential, yet acid drainage has developed on site. Of the mines without surface water quality exceedences (7 or 28%), all were correct thus far in predicting no impacts to surface water with mitigation in place. Three of the seven are desert mines in California, one (Stillwater in Montana) has had increases in contaminant concentrations but no exceedences, and the other three have had no exceedences or increases in mining-related contaminant concentrations in surface water to date. Therefore, most case study mines predicted no impacts to surface water quality after mitigation are in place, but at the majority of these mines, impacts have already occurred.

A comparison between potential (pre-mitigation), predicted, and actual groundwater quality for the case study mines is presented in Table ES-6. The majority (64% or 16/25) of the case study mines had exceedences of drinking water standards in groundwater. However, exceedences at three of the mines, all in Nevada, may be related to baseline conditions; therefore, 52% of the case study mines clearly had mining-related exceedences of standards in surface water. Of the 13 mines with mining-related exceedences in groundwater, only two noted a low potential for groundwater quality impacts in the original EIS. The majority (9 or 69%) stated that there would be a moderate potential, and two stated there was a high potential for groundwater impacts in the absence of mitigation. In terms of predicted (post-mitigation) groundwater quality impacts, 77% (10/13) of the mines with exceedences predicted low groundwater quality impacts in their EISs, including mines predicting low impacts in the original EIS.

Of the mines with mining-related groundwater quality exceedences (13), only one mine – the same mine that correctly predicted that there would be surface water exceedences (McLaughlin, CA), was correct in predicting a high potential for groundwater quality impacts with mitigation in place; the others predicted a low potential (not exceeding standards) in at least one EIS. Of the mines without groundwater quality exceedences (5 or 25%), all were correct in predicting no impacts to surface water with mitigation in place. Again, three of the five are desert mines in California, one (Stillwater, MT) has had increases in contaminant concentrations but no exceedences, and the other (Greens Creek, AK) has had mining-related exceedences in seeps. Therefore, most mines predict no impacts to groundwater quality after mitigation were in place, but in the majority of case study mines, impacts have occurred.

Therefore, as with surface water, the predictions made about groundwater quality impacts without considering the effects of mitigation were somewhat more accurate than those made taking the effects of mitigation into account. Again, the ameliorating effect of mitigation on groundwater quality was overestimated in the majority of the case study mines.

A comparison between acid drainage and development for the case study mines is presented in Table ES-7a. Of the 25 case study mines, nine (36%) have developed acid drainage on site to date. Nearly all the mines (8/9) that developed acid drainage either underestimated or ignored the potential for acid drainage in their EISs.

Table ES-5. Summary of Predicted and Actual Impacts to Surface Water Resources at Case Study Mines

Element	Number/Total	Percentage
Mines with mining-related surface water exceedences	15/25	60%
Mines with surface water exceedences that predicted low impacts without mitigation	4/15	27%
Mines with surface water exceedences that predicted low impacts with mitigation	11/15	73%

Table ES-6. Summary of Predicted and Actual Impacts to Groundwater Resources at Case Study Mines

Element	Number/Total	Percentage
Mines with mining-related groundwater exceedences	13/25	52%
Mines with groundwater exceedences predicting low impacts without mitigation	2/13	15%
Mines with groundwater exceedences predicting low impacts with mitigation	10/13	77%

Table ES-7a. Summary of Acid Drainage Potential Predictions and Results for Case Study Mines

Element	Number/Total	Percentage
Mines predicting low acid drainage potential	18/25	72%
Mines that have developed acid drainage	9/25	36%
Mines with acid drainage that predicted low acid drainage potential	8/9	89%

The majority of the case study mines (18/25 or 72%) predicted low potential for acid drainage in one or more EISs. Of the 25 case study mines, 36% have developed acid drainage on site to date. Of these 9 mines, 8 (89%) predicted low acid drainage potential initially or had no information on acid drainage potential. The Greens Creek Mine in Alaska initially predicted moderate acid drainage potential but later predicted low potential for acid drainage for an additional waste rock disposal facility. Therefore, nearly all the mines that developed acid drainage either underestimated or ignored the potential for acid drainage in their EISs.

Of the 25 case study mines, 19 (76%) had mining-related exceedences in surface water or groundwater. However, nearly half of the mines with exceedences (8/19 or 42%) predicted low contaminant leaching potential in their EISs. The constituents that most often exceeded standards or that had increasing concentrations in groundwater or surface water included toxic heavy metals such as copper, cadmium, lead, mercury, nickel, or zinc (12/19 or 63% of mines), arsenic and sulfate (11/19 or 58% of mines for each) and cyanide (10/19 or 53% of mines).

Eight case study mines predicted low contaminant leaching potential (Table ES-7b). Of these eight mines, five (63%) had exceedences of standards in either surface water or groundwater or both after mining began. The three mines that predicted low contaminant leaching potential and had no exceedences of water quality standards were the three California desert mines: American Girl, Castle Mountain, and Mesquite.

Table ES-7b. Summary of Contaminant Leaching Potential Predictions and Results for Case Study Mines (percentages)

Element	Number/Total	Percentage
Mines predicting low contaminant leaching potential	8/25	32%
Mines with mining-related exceedences in surface water or groundwater	19/25	76%
Mines with exceedences that predicted low contaminant leaching potential	8/19	42%
Mines with exceedences that predicted moderate contaminant leaching potential	8/19	42%
Mines with exceedences that predicted high contaminant leaching potential	3/19	16%

Stated another way, 21 of the 25 case study mines (84%) had exceedences of water quality standards in either surface water or groundwater or both. The exceedences at two of these mines may be related to baseline conditions. Therefore, 76% of the case study mines had mining related exceedences in surface water or groundwater (Table ES-7b). Of the remaining 19 mines, 42% (eight) predicted low contaminant leaching potential (or had no information), 42% (eight) predicted moderate contaminant leaching potential, and only three (16%) predicted high contaminant leaching potential. Therefore, nearly half of the mines that had exceedences of water quality standards underestimated or ignored the potential for contaminant leaching potential in EISs. The constituents that most often exceeded standards or that had increasing concentrations in groundwater or surface water included toxic heavy metals such as copper, cadmium, lead, mercury, nickel, or zinc (12/19 or 63% of mines), arsenic and sulfate (11/19 or 58% of mines for each), and cyanide (10/19 or 53% of mines).

CAUSES OF WATER QUALITY IMPACTS AND PREDICTION ERRORS

Inherent Factors Affecting Water Quality at Mine Sites

This study attempts to determine if there are certain factors that make a mine more or less likely to cause water quality problems and more or less likely to accurately predict future water quality. Such factors could include inherent characteristics of the mined materials and the mine, management approaches to handling mined materials and water, and the type and number of geochemical tests that are performed on mined materials. The inherent factors evaluated include: geology and mineralization; proximity to water resources and climatic conditions; and geochemical characteristics of mined materials, such as acid drainage and contaminant leaching potential.

The relationship between inherent hydrologic and geochemical characteristics and water quality impacts shows that mines with close proximity to surface water or groundwater resources and with a moderate to high acid drainage or contaminant leaching potential have an increased risk of impacting water quality.

Surface water impacts for the mines with close proximity to surface water and high acid drainage or contaminant leaching potential are compared to surface water impacts for all the case study mines in Table ES-8. Overall, for the 13 mines with close proximity to surface water and high acid drainage or contaminant leaching potential, 12 (92%) have had some impact to surface water as a result of mining activity. For all case study mines, only 64% had some surface water quality impact. Eleven of the 13 (85%) have had exceedences of standards or permit limits in surface water as a result of mining activity.

Table ES-8. Surface Water Quality Impacts for Mines with Close Proximity to Surface Water and Elevated Acid Drainage Potential Compared to Surface Water Impacts for All Case Study Mines

	# Mines	Percent (%) with Impact to Surface Water	Percent (%) with Exceedences of Standards in Surface Water	Percent (%) with Exceedences that Predicted No Exceedences
Mines with close proximity to surface water and elevated acid drainage and contaminant leaching potential	13	92 (12/13)	85 (11/13)	91 10/11)
All case study mines	25	64 (16/25)	60 (15/25)	73 (11/15)

Of the 11 mines with surface water exceedences, ten (91%) predicted that surface water standards would not be exceeded. Considering the two mines that accurately predicted no surface water exceedences (Stillwater and Flambeau) and the one that accurately predicted exceedences (McLaughlin), 77% of mines with close proximity to surface water or direct discharges to surface water and moderate to high acid drainage or contaminant leaching potential underestimated actual impacts to surface water. For all case study mines, 73% of the mines with surface water quality exceedences predicted that there would be no exceedences. Compared to all case study mines, higher percentages of mines with close proximity to surface water and elevated acid drainage or contaminant leaching potential had surface water quality impacts and exceedences. EIS water quality predictions made before the ameliorating effects of mitigation were considered ("potential" water quality impacts) were more accurate at predicting operational water quality than predictions based on assumed improvements from mitigation.

Groundwater impacts for the mines with close proximity to groundwater and high acid drainage or contaminant leaching potential are compared to groundwater impacts for all the case study mines in Table ES-9. Of the 15 mines with close proximity to groundwater and high acid drainage or contaminant leaching potential, all but one (93%) have had mining-related impacts to groundwater, seeps, springs or admit water. For all case study mines, only 56% had mining-related impacts to groundwater. For the 15 mines with close proximity to groundwater and elevated acid drainage or contaminant leaching potential, 13 or 87% had mining-related exceedences in groundwater. For all case study mines, only 52% had exceedences in groundwater.

Table ES-9. Groundwater Quality Impacts for Mines with Close Proximity to Groundwater and Elevated Acid Drainage Potential Compared to Groundwater Impacts for All Case Study Mines

	# Mines	Percent (%) with Impact to Groundwater or Seeps	Percent (%) with Exceedences of Standards in Groundwater or Seeps	Percent (%) with Exceedences that Predicted No Exceedences
Mines with close proximity to groundwater and elevated acid drainage and contaminant leaching potential	15	93 (14/15)	93 (14/15)	86 (12/14)
All case study mines	25	68 (17/25)	68 (17/25)	52 (13/25)

These results, although not comprehensive, suggest that the combination of proximity to water resources (including discharges) and moderate to high acid drainage or contaminant leaching potential does increase the risk of water quality impacts and is a good indicator of future adverse water quality impacts. Although this finding makes intuitive sense from a risk perspective, a comprehensive study of cause and effect has never been conducted. Mines with these inherent factors are the most likely to require perpetual treatment to reduce or eliminate the long-term adverse impacts to surface water resources. Although all mines must rely on well executed mitigation measures to ensure the integrity of water resources during and after mining, mines with the inherent factors identified in this study must have mitigation measures that are even more carefully designed to avoid water quality impacts.

FAILURE MODES AND ROOT CAUSES OF WATER QUALITY IMPACTS

This section identifies the underlying causes of water quality impacts at the case study mines. It uses information gathered from the case studies and conducts a "failure modes" and "root cause" analysis. A failure is an outcome that is different than intended or predicted. A failure mode is the general type of failure that occurred or is predicted to occur (e.g., prediction failure, mitigation failure), while a root cause is the underlying, more specific, reason for the failure. The objective of the analysis presented in this section is to identify the most common types and causes of failures in protecting water quality at existing mines so that the failures can be prevented in the future. Results from this analysis can be used to make recommendations for improving both the policy and the scientific and engineering underpinnings of EISs.

Methodology and Approach

The approach uses existing ("historical") information from the 25 case study mines with EISs to identify the causes of water quality impacts that occurred during mining operations. In contrast, most similar risk analyses are conducted before operations begin and focus on generating predictions from engineering design information (e.g., likelihood of failure based on factor of safety calculations). Because our approach is retrospective rather than prospective, we know unequivocally whether a prediction has failed or a water quality failure has occurred. Therefore, the focus of this analysis is to determine what caused the failure to occur. The information used to determine how failure occurred is contained in the case studies, which summarize and compare water quality predictions in EISs with actual water quality conditions during mining operations.

Types of Characterization Failures

There are two types of characterization failures identified in the case studies: hydrologic and geochemical. Inaccuracies in hydrologic and geochemical characterization can lead to a failure to recognize or predict water quality impacts. The primary root causes of hydrologic characterization failures identified in this study are:

- dilution overestimated
- lack of hydrological characterization
- amount of discharge overestimated
- size of storms underestimated.

The primary root causes of geochemical characterization failures identified are:

- lack of adequate geochemical characterization
- sample size and/or representativeness.

The other failure mode identified in the case studies is mitigation failure in which the primary root causes are:

- mitigation not identified, inadequate or not installed
- waste rock mixing and segregation not effective
- liner leak, embankment failure or tailings spill
- land application discharge not effective.

Table ES-10 shows the various failures modes, root causes and identifies various mines that serve as examples of the failure modes. The results are summarized in Table ES-11 and are as described below.

Six of 25 mines exhibited inadequacies in hydrologic characterization.

- At two of the mines, dilution was overestimated.
- At two of the mines, a lack of hydrologic characterization was noted.
- At one of the mines, the amount of discharge generated was underestimated.
- At one of the mines, the size of storms was underestimated.

Eleven of 25 mines exhibited inadequacies in geochemical characterization. Geochemical failures resulted from:

- assumptions made about the geochemical nature of ore deposits and surrounding areas (e.g., mining will only be done in oxidized area)
- site analogs inappropriately applied to a new proposal (e.g., historic underground mine workings do not produce water or did not indicate acid generation)
- inadequate sampling (e.g., geochemical characterization did not indicate potential due to composite samples or samples not being representative of actual mining)
- failure to conduct and have results for long-term contaminant leaching and acid drainage testing procedures before mining begins
- failure to conduct the proper tests, or to improperly interpret test results, or to apply the proper models.

Sixteen of 25 mines exhibited failures in mitigation measures.

- At three of the mines mitigation was not identified, inadequate, or not installed.
- At four of the mines waste rock mixing and segregation was not effective.
- At nine of the mines liner leaks, embankment failures or tailings spills caused impacts to water resources.
- At one mine, land application disposal resulted in impacts to water resources.

Table ES-10. Water Quality Predictions Failure Modes, Root Causes and Examples from Case Study Mines

Failure Mode	Root Cause	Examples
Hydrologic Characterization	Lack of hydrologic characterization	Royal Mountain King, CA; Black Pine, MT
	Dilution overestimated	Greens Creek, AK; Jerritt Canyon, NV
	Amount of discharge underestimated	Mineral Hill, MT
	Size of storms underestimated	Zortman and Landusky, MT
Geochemical Characterization	Lack of adequate geochemical characterization	Jamestown, CA; Royal Mountain King, CA; Grouse Creek, ID; Black Pine, MT
	Sample size and/or representation	Greens Creek, AK; McLaughlin, CA; Thompson Creek, ID; Golden Sunlight, MT; Mineral Hill, MT; Zortman and Landusky, MT; Jerritt Canyon, NV
Mitigation	Mitigation not identified, inadequate, or not installed	Bagdad, AZ; Royal Mountain King, CA; Grouse Creek, ID
	Waste rock mixing and segregation not effective	Greens Creek, AK; McLaughlin, CA; Thompson Creek, ID; Jerritt Canyon, NV
	Liner leak, embankment failure or tailings spill	Jamestown, CA; Golden Sunlight, MT; Mineral Hill, MT; Stillwater, MT; Florida Canyon, NV; Jerritt Canyon, NV; Lone Tree, NV; Rochester, NV; Twin Creeks, NV
	Land application discharge not effective	Beal Mountain, MT

Table ES-11. Summary of Failure Modes for Case Study Mines

Failure Mode	Number of Case Study Mines Showing Failure Mode	Percent of Case Study Mines Showing Failure Mode
Hydrologic Characterization	6	24%
Geochemical Characterization	11	44%
Mitigation	16	64%

CONCLUSIONS AND RECOMMENDATIONS

Identification of Risk and Prevention of Impacts

- Actual water quality impacts are closer to potential (pre-mitigation) rather than predicted (post-mitigation) impacts in EISs; therefore, the threshold for significance determinations, and thus EIS (rather than EA) analysis, should be potential rather than predicted impacts.

- Cyanide is not specifically identified as a contaminant of concern often enough; whenever cyanide is being used in heap or vat leaching or flotation, it should be listed as a potential contaminant of concern.

- A minimum and relatively consistent set of geochemical tests should be required by federal and state mining agencies. See the companion report (*Predicting Water Quality at Hardrock Mines: Methods and Models, Uncertainties, and State- of-the-Art*) for recommendations for minimum required geochemical testing.

- Mines with close proximity or discharges to water resources, moderate to high acid drainage and/or contaminant leaching potential should undergo more scrutiny by agencies in the permitting process than mines with low inherent water quality impact factors.

- Hydrologic characterization failures are most often caused by over-estimation of dilution, failure to recognize hydrologic features and underestimation of water production quantities. They can be addressed by requiring adequate hydrologic characterizations and making environmentally conservative assumptions about water quality and quantity.

- Lack of adequate geochemical characterization is the single-most identifiable root cause of water quality prediction failures. Improvements in geochemical characterization can provide the greatest contribution to ensuring accurate water quality predictions at hardrock mine sites. As noted in the companion report, the same geochemical test units should be used for testing of all sources and parameters used to predict water quality impacts. In addition, more extensive information on mineralogy and mineralization should be included in EISs, and more attention should be paid to uncertainties in geochemical and hydrologic characterization.

- Mixing and segregation mitigation failures occur at a moderate frequency and are typically caused by using too little neutralizing material and not effectively isolating acid generating material from nearby water resources. This can be addressed by requiring adequate geochemical and hydrologic characterization and minimizing transport along hydrologic pathways.

- Mitigation frequently fails to perform according to plan. It is important to consider the likelihood and consequences of mitigation failure in EISs and identify additional mitigation measures that can be installed if failure occurs. Multiple mitigation measures (e.g., installation of liner and leachate collection system or pump-back system) should be required in most cases and planned for in the design phase.

- Improvements are needed in the prediction of appropriate mitigation measures. Preventive mitigation measures are more cost effective and environmentally protective than remediation after impacts have occurred.

- EISs for new mines should include comprehensive baseline water quality, hydrologic, and geochemical evaluations and careful and supportable identification of mitigation measures, including an evaluation of potential mitigation failures.

Data and Data Quality Issues

- Operational and post-operational water quality information for hard rock mine sites should be readily accessible to the public in a user-friendly web-based format.

- Information provided to the public should include: maps clearly showing the location of mine units, streams, and surface water and groundwater sampling locations; identification of facilities/source areas associated (upgradient) with wells and other sampling points; pre-mining and baseline/background water quality and quantity information; well depths; groundwater elevations in monitoring wells; and water quality data for all monitoring locations.

- In many cases existing conditions were explained by baseline water quality conditions with limited baseline water quality information. An independent review of baseline water quality data for hard rock mines should be conducted to verify those claims.

- With the cooperation of industry and regulators, a more systematic and complete effort should be undertaken to compare water quality predictions against actual water quality impacts as a follow-up to this study.

ATTACHMENT 14

Predicting Water Quality at Hardrock Mines

Methods and Models, Uncertainties, and State-of-the-Art

Buka Environmental

Kuipers & Associates

Predicting Water Quality at Hardrock Mines

Methods and Models, Uncertainties, and State-of-the-Art

Ann S. Maest
Buka Environmental
Boulder, Colorado

James R. Kuipers
Kuipers & Associates
Butte, Montana

Contributing Authors:

Constance L. Travers
and
David A. Atkins
Stratus Consulting, Inc.
Boulder, Colorado

effects were most pronounced in samples with sulfur content <0.5% and total organic carbon contents >7%, which would be rare in most hardrock mines. The precipitation of gypsum (mostly in kinetic tests) can underestimate the AGP because there will be lower concentrations of sulfate in the effluent after gypsum precipitates. However, Morin and Hutt (1998) found this was rare in kinetic results from the International Kinetic Database (IKD, version 98.3, MDAG Publishing, 1998).

Recommendation: Mineralogy should be thoroughly examined as part of the environmental characterization process, with special attention paid to identifying the types of metal sulfides, silicates, and carbonates in mined materials and the surface area of these minerals available for reaction. In many cases, this will involve mineralogical examination that is more detailed and sophisticated than simple bulk powder X-ray diffraction. If siderite is a dominant carbonate, the NP tests should be modified to ensure that siderite is not included in NP. As a check on NP, use mineralogic NP (based on the amount of calcium and magnesium carbonates present) for samples of lithologies of interest. Use of total sulfur for AGP may result in slight overestimations of AGP, but using total S would result in more protective and supportable management decisions. However, if there is a substantial amount of non-acid producing sulfates or organic sulfur, they should be subtracted from the total sulfur value.

Estimating NP and AP in low-S, low NP wastes.

Problem Statement: Rocks with low sulfur content can produce acid, and rocks with low NP can buffer acid, yet standard ABA tests may not predict these results.

Background: Rocks with low sulfur content can produce acid, and rocks with low neutralization potential can produce neutralizing ability. For example, Lapakko and Antonson (1994) observed that samples from the Duluth Complex in northeastern Minnesota (a large copper/nickel resource with elevated levels of platinum group metals) with %S values from 0.41 to 0.71% produced pH values from 4.8 to 5.3, and samples with %S values from 1.12 to 1.64% produced pH values of 4.3 to 4.9 after 150 weeks. Also, as noted above, a number of researchers have found that certain feldspars can effectively neutralize acid at low %S values.

Li (2000) presents a method for predicting the acid drainage potential for wastes in this category. He defines low-sulfide, low-neutralization potential waste as those with sulfur contents <1% and neutralizing potential <20 kg $CaCO_3$ equivalents per ton (eq/t). Li notes that there are many documented cases of acid generation by mine waste with a sulfide-sulfur content of 0.1 to 1.0% S. At these low S contents, the addition of neutralizing potential by silicates becomes more important, and the procedure includes using mineralogic and kinetic information to evaluate the importance of silicate buffering. If the silicate dissolution rate is greater than the sulfate production rate, the material may be buffered initially but eventually form acid, although the common silicates do not yield alkalinity at appreciable rates until the pH falls to <3 (Stumm, 1997). In this case, the relative availability of acid-producing and -neutralizing material is evaluated to determine whether or not the waste is expected to generate acid. Scharer et al. (2000a) note that wastes with neutral drainage (such as some in the low-S, low-NP category) will have slower sulfide oxidation rates (because sulfides oxidize more slowly at neutral pH values) but can produce elevated concentrations of sulfate, base cations, and metals.

Recommendation: For rocks with low S content and/or low NP, standard ABA testing must be supplemented early in the mining process with additional information on mineralogy, availability of acid-producing and neutralizing material, and kinetic tests to determine the relative weathering rates of sulfides and neutralizing minerals.

Interpretation of static testing results using NP/AP ratios.

Problem Statement: NP/AP ratios are routinely used to predict the likelihood of acid generation at a mine site. Depending on the amount and availability of neutralizing material, material with even "safe" ratios (e.g., >3:1) may produce acid in the longer-term.

Background: The results of static ABA tests are usually presented as either NNP (NP – AP) or NP/AP. Use of the NP/AP ratio is preferred because it allows comparison of acid generation and neutralization potentials over a wide range of results (Tremblay and Hogan, 2000). Practitioners of ABA methods have used various NP/AP ratios to define acid-generating, uncertain, and non-acid-generating screening criteria for mined materials, with suggested non-acid-generating ratios ranging from 1:1 to 4:1 (White et al.,

ATTACHMENT 15

Summer 8-13-2021

Geology and Lithogeochemistry of the Pickett Mountain Volcanogenic Massive Sulfide Deposit, Northern Maine

Michael J. McCormick
University of Maine, michael.j.mccormick@maine.edu

1.2.1. Classification of VMS Deposits

A useful practice in VMS study and exploration is to classify each deposit according to a number of different parameters that have been developed. VMS deposit are grouped according to three parameters: (1) content of base metals (Franklin et al., 1981; Large, 1992; Franklin et al., 2005), (2) content of precious metal gold (Au) (Hannington et al., 1995; Poulsen and Hannington, 1995; Sillitoe et al., 1996), and (3) lithology of host rocks (Barrie and Hannington, 1999; Franklin et al., 2005). The most common grouping is based on the base metals, where deposits are divided into Zn-Pb-Cu, Zn-Cu, and Cu-Zn groups (based on contained ratios of Zn, Pb, and Cu metal) (Galley et al., 2007). Classification by Au content (ppm) versus Zn+Pb+Cu (wt.%) simply divides VMS deposits into Au-rich and normal deposits (Galley et al., 2007). The third classification scheme, which is growing in popularity and application in economic geology, is the lithology of deposit host rocks. Based on host rock lithology, there are six deposit types: (1) mafic-backarc, (2) bimodal-mafic, (3) bimodal-felsic, (4) felsic-siliciclastic, (5) pelitic-mafic, and (6) hybrid bimodal-felsic (Barrie and Hannington, 1999; Franklin et al., 2005). These classification groups have been developed as more information has been discovered and collected on VMS deposits with time.

1.2.2. VMS Research History

VMS deposits were initially thought to be epigenetic to volcanism. In the 1960's they were reinterpreted as syngenetic deposits after the discovery of the Brunswick No. 6 deposit in the BMC (McCutcheon, 2003; McCutcheon et al., 2005a; Shanks and Thurston, 2012). The acceptance and application of the plate tectonics theory replaced the geosynclinal theory in the 1960's and 1070's, and VMS deposits of the BMC were interpreted as comparable to the Kuroko deposits in Japan (Goodfellow et al., 1974; Ishihara, 1974; McCutcheon, 2003). Technological advances and application of stream/soil geochemical surveys, ground/airborne geophysical surveys, diamond core drilling, and lithogeochemistry have all greatly improved knowledge regarding the genesis, classification, and exploration of VMS deposits.

(collectively called the Bathurst Supergroup), is the sedimentary Miramichi Group (van Staal, 1994; van Staal et al., 2003; McCutcheon et al., 2005b; Goodfellow, 2007).

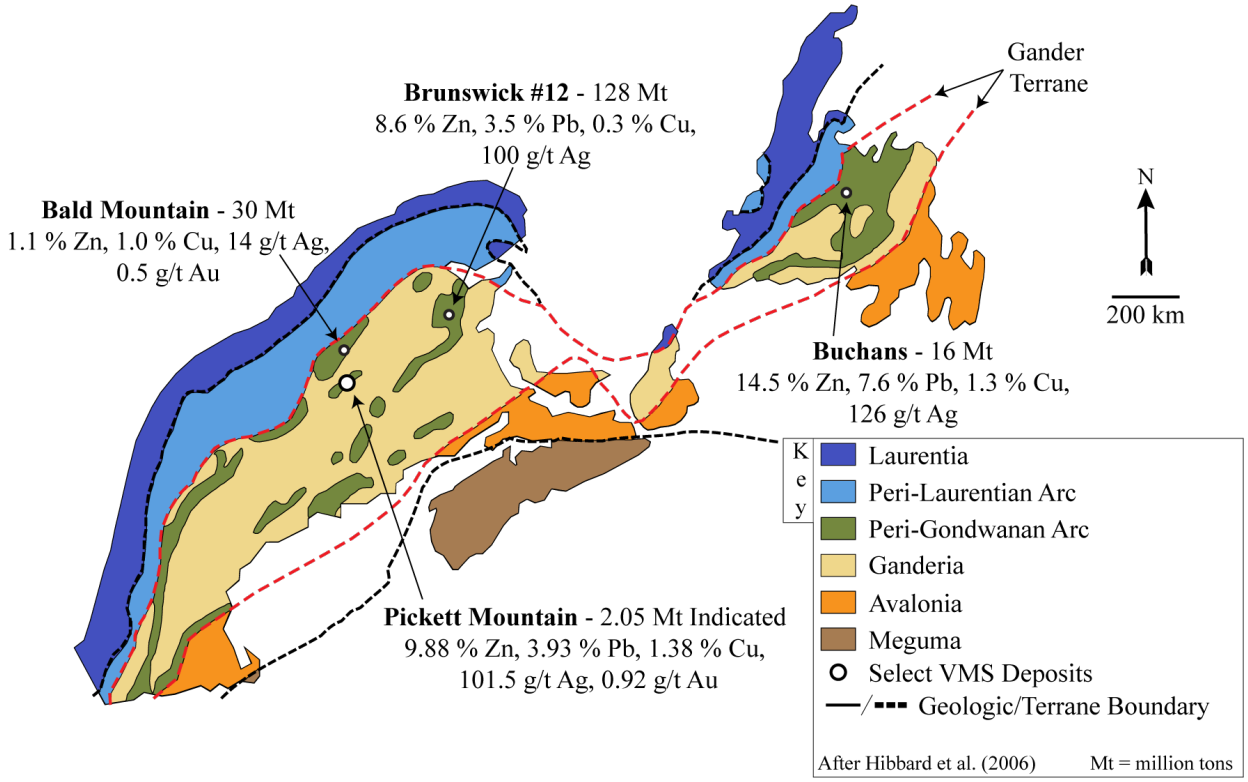

Figure 2.1. Generalized lithotectonic map of the Gander Terrane extending through Newfoundland, New Brunswick, and Maine. Within the Gander Terrane, there are Ordovician Peri-Gondwanan, arc/back-arc volcanics. Included are the names, sizes, and ore grades of a few of the major VMS deposits within the Gander Terrane.

The many VMS deposits of the BMC are found within the Cambro-Ordovician volcanics of the Tetagouche-Exploits back-arc basin, within the larger Gander terrane. The VMS deposits of Maine are found in Cambro-Ordovician arc-back-arc volcanic "inliers" (i.e., the Munsungun-Winterville, Castle Hill, Lobster Mountain, and Weeksboro-Lunksoos Lake Belt (WLLB) inliers) that are genetically linked to those of the BMC, in the Gander terrane (Figure 2.2). These inliers are collectively called the Northern Maine Volcanic Belt (NMVB) (Berry IV and Osberg, 1989; Winchester and van Staal, 1994; Ludman et al., 2017), which stretches from the southwest border with New Hampshire through Winterville, Maine, and have been interpreted to have occurred in settings that directly correlate to the Ordovician volcanics

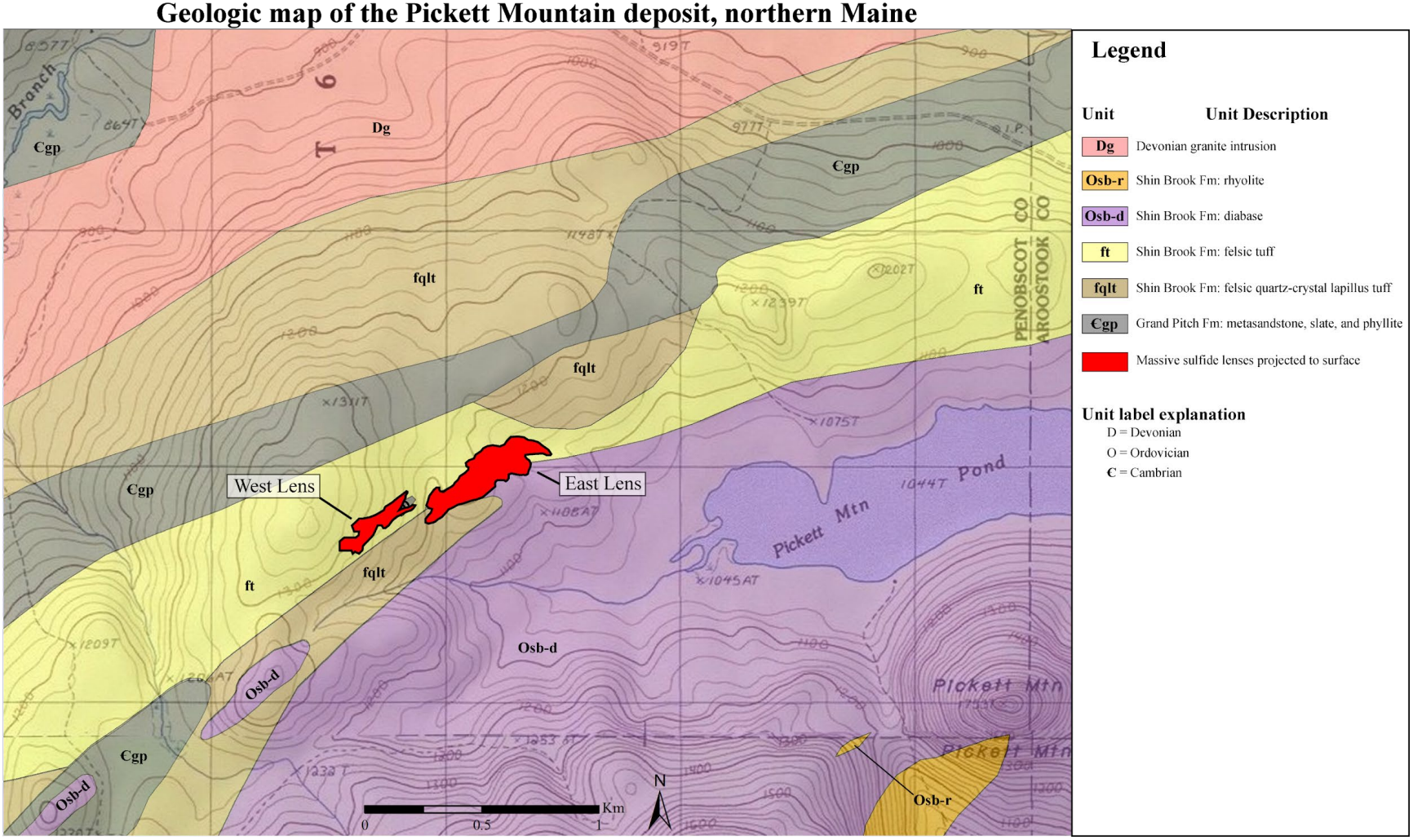

Figure 2.5. Revised deposit-scale bedrock geologic map of the Pickett Mountain deposit, northern Maine, in this study.

ATTACHMENT 16

Chapter 6

GEOCHEMISTRY OF ACID MINE WATERS

D. Kirk Nordstrom[1] and C.N. Alpers[2]

[1]*U.S. Geological Survey, 3215 Marine Street, Boulder, CO 80303-1066*

[2]*U.S. Geological Survey, Placer Hall, 6000 J Street, Sacramento, CA 95879-6129*

INTRODUCTION

There are about a dozen major hydrogeochemical processes that can account for the chemical composition of most natural waters. One of these is the oxidation of pyrite, a process at least as important a source of sulfate in natural waters as seawater and sea spray, gypsum dissolution, and atmospheric emissions. The natural process of pyrite oxidation is fundamental to the supergene alteration of ore deposits, the formation of acid-sulfate soils, and the development of acidity and metal mobilization in natural waters. As mineral deposits continue to be mined, and inactive or abandoned mines with their associated waste-rock and tailings piles continue to be exposed to weathering, large concentrations of sulfate and heavy metals will continue to be found in both surface waters and ground waters. Nearly 5×10^{10} tons of mining and mineral processing wastes had been generated in the United States as of 1985 and about 10^9 tons continue to be generated each year (U.S. Environmental Protection Agency, 1985). A more recent estimate indicates that there may be more than 500,000 inactive or abandoned mine sites in the U.S. (Lyon et al., 1993). Hazardous mine sites in serious need of remediation are probably much fewer but may still range in the thousands. Inventories of mineral resources, mine sites, and their associated environmental hazards are being assembled at various scales by federal and state agencies to better assess the magnitude of the problem.

The water-quality hazard produced by pyrite oxidation is known as "acid rock drainage," or if from a mined area, "acid mine drainage." We use the terms "acid mine drainage" and "acid mine water" synonymously, reflecting popular usage. These waters drain from waste rock, tailings, open pits, and underground mines into surface streams, rivers, and lakes. Acid mine waters typically have pH values in the range of 2–4 and high concentrations of metals known to be toxic to living organisms (Ash et al., 1951; Martin and Mills, 1976; Nordstrom and Ball, 1985). Natural waters acidified by mine drainage have killed enormous numbers of fish and benthic organisms, harmed livestock, and destroyed crops and have made many rivers, streams, and lakes turbid, colored, and unfit for most beneficial purposes. In the United States, 10^7 fish were reported killed during 1961–1975 from the effects of mining activities (Biernacki, 1978), and this number can safely be considered a gross underestimate. For example, the eighth annual report of the Federal Water Pollution Control Administration (1968) states that of the 11.59×10^6 fish reported killed in 1967 from all types of pollution only 16,413 were reported killed from the state of California. The California Department of Fish and Game (Nordstrom et al., 1977), however, recorded 47,100 fish killed from mine drainage at one site during a 7-day period in January of 1967. Many other mining-related fish kills may not be adequately recorded in federal or state archives.

Kleinmann (1989) has estimated that about 19,300 km of rivers and streams and more than 180,000 acres of lakes and reservoirs in the continental U.S. have been seriously damaged by acid mine drainage. Although a quantitative assessment of environmental damage from mining activities may be difficult or impossible, the volume of water bodies affected by acid mine drainage could be comparable to that affected by acid rain or other industrial sources of acidification.

It is important to note that pyrite oxidation also occurs in the absence of mining and there are numerous localities world-wide where naturally acidic waters containing high concentrations of metals are known (Runnells et al., 1992). The geochemical processes of weathering may be very similar in terms of mineral oxidation and dissolution but the hydrologic regime, the rates of reaction, and the environmental consequences can be quite different. Geochemical reactions in mined areas are more rapid because of:

1) greater accessibility of air through mine workings, wastes, and tailings,
2) greater surface areas for sulfides in mine workings, wastes, and especially tailings, and
3) different compositions of tailings as a result of mineral processing.

The presence of flues and flue dust piles (typically high in arsenic, zinc, and cadmium), slag piles, and soils and rocks contaminated by smelter fumes can be particularly detrimental to flora and fauna. Erosion of these materials by both aeolian and fluvial transport can contaminate drainage systems for very long distances (Moore and Luoma, 1990). The slower weathering of unmined mineral deposits occurs over longer time frames and tends to lead to more stable and insoluble mineral phases than those at mined deposits.

As an example of the extremes to which mine waters can develop acidity and high metal concentrations, the analyses of four of the most acidic mine waters ever reported are shown in Table 6.1. These waters were found in the Richmond mine workings at Iron Mountain, California (Nordstrom et al., 1991). Note that all samples have negative pH values and metal concentrations in grams per liter. These concentrations are some of the highest recorded metal and sulfate concentrations and the lowest pH values known. A survey of the literature indicates that only one known determination for copper, one for zinc, and one for arsenic have been found to be higher than those from the Richmond mine

waters (Table 6.1). Although these extreme values are rare, they do indicate the dramatic changes in water quality caused by natural processes and enhanced by mining activities.

TABLE 6.1—Comparison of four of the most acidic mine waters at Iron Mountain, California with the most acidic and metal-rich mine waters reported in the world (pH values in standard units, concentrations in grams per liter, Nordstrom et al., 1991; Nordstrom and Alpers, 1999).

	Iron Mountain				Other sites	References
pH	-0.7	-2.5	-2.6	-3.6	0.67	Goleva et al. (1970)
Cu	2.3	4.8	3.2	n.d.	48	Clarke (1916)
Zn	7.7	23.5	20	n.d.	50	Braeuning (1977)
Cd	0.048	0.21	0.17	n.d.	0.041	Lindgren (1928)
As	0.15	0.34	0.22	n.d.	0.40	Goleva (1977)
Fe (total)	86.2	111	101	16.3	48	Blowes et al. (1991)
Fe (II)	79.7	34.5	34.9	9.8	48	Blowes et al. (1991)
SO_4	360	760	650	n.d.	209	Lindgren (1928)

The chemical reaction responsible for the formation of acid mine waters requires three basic ingredients: pyrite, oxygen, and water. The overall reaction is often written as:

$$FeS_{2(aq)_3} + 15/4\ O_{2(g)} + 7/2\ H_2O_{(l)} \rightarrow Fe(OH)_{3(s)} + 2\ H_2SO_{4(aq)} \quad [1]$$

where one mole of ferric hydroxide and 2 moles of sulfuric acid are produced for every mole of pyrite oxidized. For each mole of pyrite oxidized in equation [1], 1 electron is lost by oxidation of iron, 14 electrons are lost by oxidation of disulfide, and 15 electrons are gained by reduction of oxygen. Iron is also hydrolyzed and precipitated. All of these reactions cannot take place in a single step. Electron transfer reactions take place generally with only one or two electrons at a time (Basolo and Pearson, 1967). Hence, there could be 15 or more reactions with as many possible rate-determining steps to consider. To further complicate matters, several other oxidizing agents besides oxygen have been implicated in pyrite oxidation, e.g., ferric iron. Fortunately, all the intermediate reactions need not be determined to delineate the rate-controlling mechanisms involved with pyrite oxidation.

This chapter reviews the abiotic and microbial rates and mechanisms for sulfide mineral oxidation, the secondary minerals formed as a result of sulfide oxidation, and the major environmental factors that control the quality and quantity of acid water produced from mining activities.

HISTORICAL BACKGROUND

The history of mining and its environmental consequences, like technology in general, goes back several thousands of years, well before recorded history. Theophrastus (*ca.* 315 B.C.) mentions the degradation of pyrite to acid and salts (see Agricola, 1556). By the time of Pliny (23–79 A.D.), it was already well known that oil of vitriol (sulfuric acid), vitriol (ferrous sulfate), and alum (aluminum sulfates) were produced by the natural lixiviation (leaching) of pyritiferous rocks. Oil of vitriol was used to make other acids and compounds, vitriol was primarily used to blacken leather, and alum was used to tan hides. The acid waters and their associated efflorescent (or flowering) salts produced from pyrite oxidation were also known to be highly toxic. Georgius Agricola (1546) wrote "When moisture corrodes cupriferous and friable pyrite it produces an acid juice from which *atramentum sutorium* forms and also liquid alum.... Experiments show that when porous, friable pyrite is attacked by moisture such an acid juice is produced." *De Re Metallica* (Agricola, 1556), considered to be the first systematic book on mining and mineralogy, contains the following passage, "Since I have explained the nature of vitriol and its relatives which are attained from cupriferous pyrites I will next speak of an acrid solidified juice...; it is hard and white and so acrid that it kills mice, crickets and every kind of animal." The "solidified juice" was later identified (by Herbert Hoover, translator) as goslarite, a hydrated zinc sulfate that likely contained some cadmium. With the dawn of the industrial revolution, acid mine drainage became a major source of water pollution on a large scale.

In the United States, occasional effort was directed towards the problem of acid mine drainage in the Appalachian coal mining region before 1900 (Vranesh, 1979). The State of Indiana has had a land reclamation act for coal-stripping since 1942 and a history of concern with the adverse effects of strip mining that can be traced back to 1917 (Wilber, 1969). Western mines were originally exempt from regulations on mine drainage or other environmental hazards because of the interest in attracting businesses and people to the West. Mining and metallurgical engineers occasionally investigated the problem (e.g., Burke and Downs, 1938), but primarily with an aim to alleviate coal mine drainage problems. From the 1920s through the 1940s, government agencies and the mining industry investigated acid mine drainage produced in the Appalachians from coal mines (Ash et al., 1951). Twenty years later the Appalachian Regional Commission reviewed the coal mine drainage problems (Appalachian Regional Commission, 1969). From the late 1960s through the late 1970s the National Coal Association and Bituminous Coal Research, Inc. sponsored a series of Coal Mine Drainage Research Symposia that resulted in several useful publications on the problem. About the same time, considerable research was supported by the Federal Water Pollution Control Federation and, later, the Environmental Protection Agency (EPA) on both the causes of acid mine drainage and its remediation. Even more attention has been given to the problem with the advent of the Comprehensive Environmental Response, Compensation and Liability Act (CERCLA or Superfund) in 1980. Several mining sites around the country were put on EPA's National Priority List for Superfund investigation and remediation.

FORMATION OF ACID MINE WATERS

The general description of the weathering of pyrite will now be examined in more detail. Equation [1], the overall reaction for the breakdown of pyrite to ferric hydroxide and sulfuric acid, is a gross oversimplification. It gives the correct picture in that oxygen is the ultimate driving force for the oxidation of pyrite and the final products are an insoluble form of oxidized iron and an aqueous sulfuric acid solution. Some problems with equation [1] are that it does not explain geochemical mechanisms or rates, it does not explain that ferric hydroxide is a fictitious, idealized phase, and it does not reflect the slow oxidation of aqueous ferrous iron in acid solutions that often results in high ferrous iron concentrations in

acid mine waters. Furthermore, factors such as microbial catalysis, neutralization reactions, sorption reactions, and climatic effects have an important influence on pyrite weathering, but are not considered explicitly in equation [1].

Mine operators as well as reclamation and remediation teams would like to know the potential or actual production of acid waters from a mine or from waste materials at a mine or a mineral processing facility. There is no simple, single test to assess metal and acid mobility in these settings because of the numerous variables that affect contaminant transport. The problem is multifaceted and we must emphasize that acid mine drainage forms within a complex environmental system where several factors need to be considered within the five general categories as shown in Table 6.2. These five categories are traditional scientific disciplines that must be integrated to characterize a field site.

TABLE 6.2—Environmental factors affecting acid mine water formation.

	Traditional Scientific Disciplines				
	Inorganic chemistry	Organic chemistry	Geology/ mineralogy	Hydrology	Microbiology
Sulfide oxidation	✔	✔	✔	✔	✔
$Fe^{(II)}_{(aq)} \rightarrow Fe^{(III)}_{(aq)}$	✔	✔		✔	✔
pH	✔	✔	✔	✔	✔
Temperature	✔		✔	✔	✔
Gangue dissolution	✔		✔	✔	
Rock type/structure	✔		✔	✔	
Porosity			✔	✔	
Permeability			✔	✔	
Flow paths (recharge/discharge)	✔		✔	✔	
Climate	✔			✔	
Evapoconcentration/ efflorescent salt formation	✔		✔	✔	
Efflorescent salt dissolution	✔		✔	✔	
Photochemistry	✔	✔		✔	✔

Stoichiometry and kinetics of abiotic pyrite oxidation

The voluminous literature on pyrite oxidation has been reviewed by Lowson (1982) with regard to abiotic chemical oxidation and by Nordstrom (1982a) with regard to biotic and abiotic geochemical oxidation. More recent contributions can be found in Goldhaber (1983), McKibben and Barnes (1986), Moses et al. (1987), Moses and Herman (1991), and Evangelou (1995). When pyrite oxidizes there are two species that can oxidize, the ferrous iron and the sulfidic sulfur. In studies on acid mine waters and pyrite oxidation, it has long been recognized that iron easily leaches out of pyrite but tends to stay in the ferrous state in acid solutions. Ancient history records the production of vitriol and oil of vitriol from washing pyritiferous ores and shales. During the last two centuries this vitriol was determined to be a mixture of ferrous sulfate and sulfuric acid. Hence, another common representation of the pyrite oxidation reaction is:

$$FeS_{2(s)} + 7/2O_{2(g)} + H_2O_{(l)} \rightarrow Fe^{2+}_{(aq)} + 2SO^{2-}_{4(aq)} + 2H^{+}_{(aq)} \quad [2]$$

The sulfur moiety in pyrite oxidizes more quickly than the iron, but it must transfer a large number of electrons (14 times as many as iron per mole of pyrite). Consequently, there are several possible side reactions and sulfur intermediates that may occur during oxidation.

One side reaction is the formation of elemental sulfur during oxidation (Stokes, 1901; Bergholm, 1955; Clark, 1966). The yield is low and increases with higher temperatures, up to a maximum at about 100–150°C (Lowson, 1982). The lowest yield is at ambient temperatures but increases with increasing acidity. Field observations without laboratory identification are not reliable sources of information on elemental sulfur forming from pyrite oxidation because other minerals such as copiapite and jarosite may commonly be misidentified as elemental sulfur. Positive identification of elemental sulfur has been made at numerous inactive tailings impoundments (Blowes, 1995, written commun.). When acid waters react with minerals such as pyrrhotite and sphalerite they will produce H_2S, which readily oxidizes to elemental sulfur. Elemental sulfur is found commonly in nature where sulfur-rich, near-surface, hydrothermal solutions with temperatures around 100–150°C have oxidized or where H_2S-rich spring waters have oxidized on exposure to air.

Another side reaction, or group of reactions, is the formation of intermediate sulfoxyanions of lower oxidation state than that found in sulfate: i.e., thiosulfate ($S_2O_3^{2-}$), polythionates ($S_nO_6^{2-}$), and sulfite (SO_3^{2-}). Steger and Desjardins (1978) reported a thiosulfate compound on the surface of oxidizing pyrite but their method did not distinguish between thiosulfate, polythionate, and sulfite. Goldhaber (1983) measured rates of reaction and reaction products for the pH range 6–9 and found that polythionates, thiosulfate, sulfite, and sulfate formed but only at high stirring rates. The proportions of intermediate sulfoxyanions were sensitive to pH in Goldhaber's (1983) experiments. Polythionates were found to be dominant at low pH and thiosulfate was dominant at high pH, with some sulfite formed at the highest pH values. Some ambiguity exists in his determination of polythionates and thiosulfate. He used the colorimetric method of Nor and Tabatai (1976), which assumes tetrathionate is the dominant polythionate and does not completely distinguish between thiosulfate and polythionate. The pyrite and sphalerite oxidation experiments of Moses et al. (1987) included more direct determination of sulfate, sulfite, polythionates, and thiosulfate by ion chromatography (Moses et al., 1984). Their results were similar to those of Goldhaber (1983) except that additional experiments carried out in the presence of $Fe^{3+}_{(aq)}$ did not produce any detectable intermediate sulfoxyanions. These results are also similar to those of aqueous H_2S oxidation with oxygen (Chen and Morris, 1971, 1972; Zhang and Millero, 1994; Vairavamurthy et al., 1994).

Experiments documenting the formation of intermediate sulfoxyanions during pyrite oxidation should not be taken as evidence that the same oxyanions are to be found in natural waters during sulfide weathering. In experimental systems, these compounds can only be detected in solution when the aqueous layer next to the mineral surface is strongly sheared by high stirring rates so that these metastable products can not back-react by further electron exchange with the solid. Such strong shearing is not found generally in ground-water systems and even rapidly-moving surface waters rarely exhibit such shearing at the mineral surface. Luther (1987, 1990) has pointed out that species such as thiosul-

fate and sulfite would not be detected in solutions containing $Fe^{3+}_{(aq)}$ because they oxidize so rapidly; experiments by Williamson and Rimstidt (1993) and references therein confirmed that this reaction is rapid. Furthermore, intermediate sulfoxyanions are an excellent source of energy for chemoautotrophic bacteria of the *Thiobacillus* genus and may be quickly biodegraded before detectable concentrations can accumulate (Gould et al., 1994).

The experiments of Granger and Warren (1969) are often cited as evidence for the formation of sulfoxyanions from pyrite oxidation and the role of sulfoxyanions in the genesis of ore deposits. However, these authors admitted that the thiosulfate they found in their column experiments may have been formed by the oxidation of residual aqueous Na_2S solution. They had first added H_2O_2 solution in an effort to sterilize the column and then added Na_2S solution to reduce the iron oxide stains that had formed from the peroxide treatment. After such a traumatic chemical treatment, significant quantities of thiosulfate would have formed from the aqueous sulfide solution and would have been difficult to remove completely from the column. The thiosulfate thus formed may have had nothing to do with pyrite oxidation.

It has long been known that ferric iron rapidly oxidizes pyrite (Stokes, 1901). Experiments carried out by Garrels and Thompson (1960) and McKibben and Barnes (1986) have confirmed the balanced reaction stoichiometry:

$$FeS_{2(s)} + 14Fe^{3+}_{(aq)} + 8H_2O_{(l)} \rightarrow 15Fe^{2+}_{(aq)} + 2SO^{2-}_{4(aq)} + 16H^{+}_{(aq)} \quad [3]$$

for the oxidation of pyrite by aqueous ferric ions. This reaction is considerably faster than the reaction with oxygen as the oxidant, but significant concentrations of oxidized iron only occur at low pH values because of the low solubility of hydrolyzed ferric iron at circumneutral pH values. Hence, it is thought that pyrite oxidation is initiated by oxygen at circumneutral pH (equation [2]) but as pH values reduce to about 4, the rate of oxidation becomes governed by equation [3]. Oxygen is still required to replenish the supply of ferric iron according to

$$Fe^{2+}_{(aq)} + 1/4O_{2_{(g)}} + H^{+}_{(aq)} \rightarrow Fe^{3+}_{(aq)} + 1/2H_2O_{(l)} \quad [4]$$

but the oxygen does not have to diffuse all the way to the pyrite surfaces. It is quite possible for pyrite to oxidize in the absence of dissolved oxygen. Nevertheless, the overall rate of pyrite oxidation in a tailings pile, in a mine, or in a waste rock pile will largely be determined by the overall rate of oxygen transport (advection and diffusion).

Considerable speculation can be found in the literature on the question of the initiation and propagation of pyrite oxidation. Undoubtedly, during the initiation of pyrite oxidation, there are complex chemical and microbiological processes occurring in microenvironments (Williams et al., 1982), i.e., within a few tens of nanometers of the surface of a sulfide grain. These regions are inaccessible to normal sampling techniques and are not represented by the bulk aqueous phase. For example, when oxygen initially adsorbs to a pyrite surface and transfers electrons, an accumulation of protons will form at or near the surface. Acidophilic iron-oxidizing bacteria will begin to colonize and a film of acidic water will cover the mineral grain without affecting the bulk aqueous phase. Even before some acidic water develops, neutrophilic *Thiobacilli* will catalyze the initial stage of pyrite oxidation (Blowes et al., 1995; Gould et al., 1994). The extent to which these microenvironmental gradients affect the bulk properties are dependent on many factors, not the least of which is the pyrite concentration in the rock, soil, or waste material. The existence and importance of these microenvironments is well illustrated by the formation of jarosite, a mineral that can only form under acid conditions and has been found in soil waters of circumneutral pH (Carson et al., 1982).

The oxidation of at least 18 different sulfide minerals has been investigated (Table 6.3). Most of these have been studied with and without microbial catalysis by *Thiobacillus ferrooxidans*. The microbial oxidation rate is usually greater than the abiotic rate, all other conditions being equal. Unfortunately, most of the microbial studies were done without measurement of surface area and without a consistent procedure for removing small particles or otherwise cleaning the samples before the experiment. The lack of these characteristics prevents any direct comparison of microbial oxidation rates except in a qualitative manner. The results for abiotic and biotic oxidation of pyrite, however, are of considerably better quality than for other sulfide minerals and some quantitative comparisons are possible.

It should be noted that arsenic-rich minerals such as arsenopyrite and orpiment are also subject to bacterially catalyzed oxidation (Ehrlich, 1963a, 1964). Indeed, the occurrence of arsenite-oxidizing bacteria in acid mine waters has been reported by Wakao et al. (1988) and one of the first reports of arsenite oxidation by heterotrophic bacteria was that of Turner (1949).

There are now numerous reports on the oxidation rates of pyrite and marcasite by oxygen (Bergholm, 1955; McKay and Halpern, 1958; Smith and Shumate, 1970; Mathews and Robins, 1974; Goldhaber, 1983; McKibben and Barnes, 1986; Moses et al., 1987; Nicholson et al., 1988; Moses and Herman, 1991), by ferric iron (Bergholm, 1955; Garrels and Thompson, 1960; Smith and Shumate, 1970; Mathews and Robins, 1972; Wiersma and Rimstidt, 1984; McKibben and Barnes, 1986; Moses et al., 1987; Brown and Jurinak, 1989; Moses and Herman, 1991), and by hydrogen peroxide (McKibben and Barnes, 1986). The oxidation rates of pyrrhotite in the presence of oxygen (Nicholson and Scharer, 1994) and marcasite, covellite, galena, sphalerite, chalcopyrite, and arsenopyrite in the presence of ferric iron (Rimstidt et al., 1994) have been measured. Pyrite oxidation rates from different studies are generally comparable, but differences in experimental design, initial pH values, temperatures, grain size, mineral preparation, method for data reduction and rate law expression make a quantitative comparison difficult. For this paper, we use the results of McKibben and Barnes (1986) on pyrite to compare with the biotic rates in the next section. Table 6.4 summarizes the reaction rates from several studies cited above for a pH close to 2, $m_{Fe(III)} = 10^{-3}$, temperatures close to 25°C, and oxygen in equilibrium with the atmosphere.

The rates in Table 6.4 show that the oxidation of pyrite by ferric iron (according to the reaction stoichiometries given in equations [2] and [3]) can be about 2–3 orders of magnitude faster than by oxygen, that some minerals oxidize more rapidly than pyrite and some more slowly, and that oxidation rates can range over three orders of magnitude. These rates are demonstrably faster than the dissolution rates for aluminosilicate minerals (White and Brantley, 1995) by one to several orders of magnitude.

TABLE 6.3—Sulfide oxidation studies (more references can be found in Nordstrom and Southam, 1997).

Mineral	Formula	Oxidant	pH	Reference
Pyrite	FeS_2	O_2, Fe^{3+}, H_2O_2	0-10	See references in next sections
Marcasite	FeS_2	O_2, Fe^{3+}	2–3	Wiersma and Rimstidt (1984); Silverman et al. (1961)
Pyrrhotite	$Fe_{1-x}S$	O_2	2–6	Nicholson and Scharer (1994)
Sphalerite	(Zn, Fe)S	O_2, Fe^{3+}	2–7	Rimstidt et al. (1994); Torma et al. (1972); Khalid and Ralph (1977)
Galena	PbS	O_2, Fe^{3+}	2	Rimstidt et al. (1994); Torma and Subramanian (1974)
Chalcopyrite	$CuFeS_2$	O_2, Fe^{3+}	1.2–2.5	Rimstidt et al. (1994); Torma et al. (1976)
Arsenopyrite	FeAsS	O_2, Fe^{3+}	2	Rimstidt et al. (1994); Ehrlich (1964)
Covellite	CuS	O_2, Fe^{3+}	2	Walsh and Rimstidt (1986); Rickard and Vanselow (1978)
Chalcocite	Cu_2S	O_2	2–4.8	Beck (1977); Sakaguchi et al. (1976)
Greenockite	CdS	O_2	2.3	Torma et al. (1974)
Millerite	NiS	O_2	2.3	Torma et al. (1974)
Cobalt sulfide	CoS	O_2	2.3	Torma et al. (1974)
Klockmannite	CuSe	O_2	2.3	Torma and Habashi (1972)
Cinnabar	HgS	Fe^{3+}	2	Burkstaller et al. (1975)
Enargite	Cu_3AsS_4	O_2	3	Ehrlich (1964)
Orpiment	As_2S_3	O_2		Ehrlich (1963a)
Bornite	Cu_5FeS_4	O_2		Landesman et al. (1966)
Molybdenite	MoS_2	O_2	2.5	Brierley and Murr (1973)
Tetrahedrite	$(Cu,Fe)_{12}Sb_4S_{13}$	O_2		Yakhontova et al. (1980)
Stibnite	Sb_2S_3	O_2		Torma et al. (1974)
Pentlandite	$(Fe, Ni)_9S_8$	O_2		Brierley and Le Roux (1977)

TABLE 6.4—Abiotic reaction rates (mol m^{-2} s^{-1}) for sulfide mineral oxidation.

Mineral/Oxidant	MB86[1]	BJ89[2]	R94[3,7]	N94[4]	NS94[5]
Pyrite/O_2	3.1×10^{-10}			5.3×10^{-10}	1.1×10^{-10}
Pyrite/Fe^{3+}	9.6×10^{-9}	1.8×10^{-8}	1.9×10^{-8}		
Pyrrhotite/O_2				1.4×10^{-8}	
Marcasite/Fe^{3+}			1.5×10^{-7}		
Arsenopyrite/Fe^{3+}			1.7×10^{-6}		
Galena/Fe^{3+}			1.6×10^{-6}		
Sphalerite/Fe^{3+}			7.0×10^{-8}		
Blau. covellite[6]/Fe^{3+}			7.1×10^{-8}		
Chalcopyrite/Fe^{3+}			9.6×10^{-9}		
Covellite/Fe^{3+}			9.1×10^{-9}		

[1] McKibben and Barnes (1986); because there appears to be an error in the stated value for pyrite oxidation by oxygen we have used the corrected value from Nicholson (1994).
[2] Brown and Jurinak (1989); average from oxidation rates measured in different electrolytes.
[3] Rimstidt et al. (1994).
[4] Nicholson (1994); the value for pyrite is an average from four studies covering a pH range of 1-8.
[5] Nicholson and Scharer (1994) and Tervari and Campbell (1976).
[6] "blau. covellite" is blaubleibender or "blue-remaining" covellite having slightly different optical and X-ray properties than ordinary covellite.
[7] The values listed for R94 are all given in terms of the amount of Fe(III) reduced except for pyrite. All values for pyrite are given in the same units, per mole of pyrite oxidized, for purposes of direct comparison.

Galvanic protection does occur during oxidative dissolution of coexisting sulfide minerals. This phenomenon is the same as that for galvanized iron. The more electroconductive metal sulfide (the one with the higher standard electrode reduction potential, see Sato, 1992) will oxidize at a slower rate and the less electroconductive sulfide will oxidize at a faster rate than either one would when not in contact. Sveshnikov and Dobychin (1956) reported that rates of metal release from different sulfides are related to their electrode potentials and that a mixture of sulfide minerals in contact releases more metals into solution and decreases the pH more than monomineralic samples. Sveshnikov and Ryss (1964) postulated that these electronic properties of co-existing conductive sulfides are important during the weathering of sulfide mineral deposits. Sato (1992) has used electrochemical data on metal sulfides, typical of heavy metal sulfide deposits, to explain the mineral assemblage that is found during supergene enrichment.

Nicholson and Scharer (1994) mixed pyrrhotite and pyrite in different proportions to see if there was any evidence for galvanic protection, but could not detect any such effect in their study. Kwong (1995) has done laboratory experiments to show the effect of galvanic protection during dissolution of multi-sulfide mineral assemblages. The relative rates of mineral dissolution follow the sequence indicated by standard electrode potentials as outlined by Sato (1992).

Because the oxidation rate for pyrite by $Fe^{3+}_{(aq)}$ is faster than that by oxygen, it is important to know the oxidation rate for ferrous to ferric iron according to equation [4]. Numerous studies on the ferrous iron oxidation rate show that, under acid conditions, the rate becomes very slow and independent of pH. Singer and Stumm (1968) reported an abiotic rate of 2.7×10^{-12} mol L^{-1} s^{-1} at pH values below 4. Similar rates have been reported elsewhere. Such rates are considerably slower than the rate of oxidation of pyrite by $Fe^{3+}_{(aq)}$; hence, equation [4] would be the rate-limiting step were it not for the catalytic effect of bacteria.

Microbial oxidation: Historical perspective

Microorganisms are abundant in natural waters containing acid mine drainage; indeed, they are often the *only* form of life under such conditions. Powell and Parr (1919) and later Carpentor and Herndon (1933) suggested that pyrite oxidation and the consequent acid mine drainage from coal deposits may be catalyzed by bacteria. Lackey (1938) observed flagellates, rhizopods, ciliates, and green algae in 62 West Virginia streams. Joseph (1953) found gram-positive and gram-negative bacilli and cocci, fungi, green algae, diatoms, and actinomyces in acidified surface waters and soils in West Virginia and Pennsylvania. Acid mine waters from a copper mine in the southwestern U.S. were found to contain yeasts, flagellates, protozoa, and amoebae (Ehrlich, 1963b). "Acid slime streamers" have often been observed in acid mine waters (Dugan et al., 1970; Dugan, 1972).

As long ago as 1888 it was recognized by S.N. Winogradsky that certain microbes could oxidize reduced inorganic compounds, such as sulfur, to gain energy for the reduction of carbon dioxide for metabolism and growth (see Sokolova and Karavaiko, 1968). Microorganisms that utilize reduced inorganic substances are known as chemolithotrophic (see Mills, 1999). Nathansohn (1902) first isolated a *Thiobacillus* species and the acidophilic bacterium, *Thiobacillus thiooxidans*, was isolated and identified by Waksman and Jåffe (1921, 1922) from soils containing free sulfur and phosphate. Colmer and Hinkle (1947), Colmer et al. (1950), Temple and Colmer (1951), and Temple and Delchamps (1953) isolated a new chemoautotrophic and acidophilic bacterium, *Thiobacillus ferrooxidans*, and showed that microbial degradation of pyrite was an important factor in the production of acid mine waters.

The nutritional requirements for *T. ferrooxidans* are ubiquitous. Nitrogen and carbon dioxide are available in the atmosphere. Sulfur is readily available in mined environments, and only small amounts of phosphorous are needed. *Thiobacilli* have several adaptive techniques that permit them to tolerate low pH and high metal concentrations (Tuovinen et al., 1971; Kushner, 1978). Some studies have shown that *T. ferrooxidans* can tolerate g/l concentrations of Zn, Ni, Cu, Co, Mn, and Al (Tuovinen et al., 1971). Scala et al. (1982) found consistent and roughly equal concentrations of *T. thiooxidans* and *T. ferrooxidans* in mine effluents of different compositions from quite different mines, in different geological and climatological environments, in different parts of the country (from California to Virginia). The diversity of microorganisms and their populations in mineral deposit and mine waste environments is complex and not well understood. Further investigations on the microbial ecology of mines and mine wastes are certainly needed.

T. thiooxidans oxidizes elemental sulfur but not iron, *T. ferrooxidans* oxidizes both iron and sulfur compounds, and a third species, *Leptospirillum ferrooxidans*, behaves metabolically like *T. ferrooxidans* but has a helical-rod morphology first described by Markosyan (1972). *L. ferrooxidans* is now thought to be equally important as the other two bacilli (Sand et al., 1992). Mixed cultures oxidize reduced iron and sulfur compounds faster than single-species cultures (Kelly et al., 1979; Wakao et al., 1982). Apparently, bacteria are preconditioned by the medium in which they are cultured and may have a synergistic association with other species. For example, *T. ferrooxidans* grown in ferrous-containing solutions exhibited different surface chemistry than those grown on minerals such as pyrite, elemental sulfur, and chalcopyrite (Devasia et al., 1993) as exhibited by hydrophobicity and electrophoretic mobility measurements. The bacilli grown on mineral sulfides developed a proteinaceous cell surface appendage that adhered to the solid surface whereas the cells grown in ferrous iron solutions contained no such characteristic. The importance of these features bears on the mechanism of microbial oxidation. Free-floating bacteria can catalyze the oxidation of iron from ferrous to ferric in aqueous solution, and then the ferric iron directly oxidizes the pyrite. Silverman (1967) calls this the indirect mechanism. The direct contact mechanism works by direct adhesion of the bacteria to the pyrite surface. There has been a long-standing debate over whether the direct or indirect mechanism is dominant. We contend that the indirect mechanism is the dominant one, but there is some evidence for enhancement of the pyrite oxidation rate by direct microbial contact. Surface-etch patterns may result from bacterial attachment (Bennett and Tributsch, 1978), and direct microbial growth on pyrite surfaces has been observed (Konishi et al., 1990).

Microbial oxidation: Kinetics

The catalytic effect of *T. ferrooxidans* on the aqueous oxidation of ferrous to ferric iron is well-established. Singer and Stumm (1968, 1970a, b) found that bacteria increased the ferrous iron oxidation rate by 10^5 over the abiotic rate, from about 3×10^{-12} mol L^{-1} s^{-1} to about 3×10^{-7} mol L^{-1} s^{-1}. Silverman and Lundgren (1959), Lundgren et al. (1964), and Lacey and Lawson (1977) grew *T. ferrooxidans* on culture media and typically measured oxidation rates of $2.8–8.3 \times 10^{-7}$ mol L^{-1} s^{-1}. Wakao et al. (1977) measured field oxidation rates of ferrous iron oxidation in acid mine drainage and estimated 3×10^{-6} mol L^{-1} s^{-1} but the stream velocity was not measured. Nordstrom (1985) measured stream velocities and iron oxidation rates of 2 to 8×10^{-7} mol L^{-1} s^{-1} in a mountainous stream drainage containing acid mine waters, where the range of values depended on climatic conditions. From these studies we have chosen an average microbial oxidation rate for ferrous iron of 5×10^{-7} mol L^{-1} s^{-1} for the purpose of comparison with the abiotic rates.

Table 6.5 summarizes abiotic and microbial rates of oxidation for ferrous iron and pyrite under roughly comparable conditions (except for the field rates cited here and discussed later). The

microbial oxidation rate of pyrite by oxygen is very similar to the abiotic oxidation rates of pyrite by either oxygen or ferric iron. Studies by Wakao et al. (1984) showed that adsorption of bacterial cells on pyrite surfaces actually inhibited pyrite oxidation and that it was the growth of free-floating ferrous-iron-oxidizing bacteria that contributed to pyrite oxidation. These results help to clarify the reaction mechanism. Pyrite oxidation is primarily accomplished by microbial catalysis by the indirect mechanism, as defined earlier.

Estimates of field oxidation rates of pyritiferous waste rock or tailings cover a wide range of values, from three orders of magnitude less than the microbial rate to two orders of magnitude greater (Table 6.5). The field rates are primarily based on flux rates of oxygen depletion upon reaction with pyrite in waste rock or tailings. There may be complications with the assumptions made in translating temperature and oxygen profiles into flux rates. The relation between flux rates and actual *in situ* rates of pyrite oxidation may be more difficult to quantify than previously realized. The main problem is estimating the reactive surface area of the sulfides. Other problems may include the consumption of oxygen by processes other than pyrite oxidation, the dependence of temperature profiles on the moisture content, the salinity of the moisture, the temperature dependence of the oxygen consumption rate, climatic variability in pressure and temperature, site heterogeneities, and variations in thermal conductivities of the various waste materials. Averaging hydrologic properties over spatial and temporal intervals may cause inaccurate estimations of flux rates and oxidation rates at some sites.

A direct comparison of the rates of microbial oxidation of aqueous ferrous iron with rates of microbial oxidation of pyrite would be helpful in discerning the rate-controlling step of these processes, but it is difficult to accomplish. Aqueous iron oxidation is expressed as a molar concentration change with respect to time (mol L^{-1} s^{-1}), whereas pyrite oxidation is a function of surface area and the ratio of pyrite mass to solution volume or porosity (mol m^{-2} s^{-1}). Two investigations make such a comparison possible: Southham and Beveridge (1992) described bacterial cell densities on pyrite surfaces and Olson (1991) conducted an interlaboratory comparison of pyrite bioleaching rates. Neither study reported pyrite surface area but both reported grain size, so that surface areas may be estimated from the relationship between surface area and grain size for sulfide minerals.

Figure 6.1 depicts the dependence of surface area (in cm^2 g^{-1}) on grain size for pyrite and other sulfide minerals. The solid line represents the diameter-to-surface-area relationship for an ideal sphere or cube of pyrite with a density of 5.0 g cm^{-3} (see Parks, 1990; Nicholson, 1994). The dashed line is a best fit for cleaned quartz grains from Parks (1990). Two suggestions are evident from Figure 6.1. More recent determinations demonstrate the effect of more carefully sized and cleaned pyrite grains (compare museum pyrite of Braley, 1954, with any of the more recent non-diagenetic pyrite). Secondly, the diagenetic or framboidal pyrite has much more surface area for a given mass than coarse-grained pyrite. Several of the data points on Figure 6.1 lie close to the best fit of Parks (1990), which will be used as a lower limit and as an estimate of the relationship of surface area to grain diameter.

Southam and Beveridge (1992) determined values of 10^7 to 10^9 cells g^{-1} for *Thiobacilli* on surfaces of Lemoine tailings at Chibougamau, Quebec, Canada, by the most probable number method. Their tailings samples were in the size range of 200 mesh and higher, hence about 50 micrometers (μm) in diameter or about 500 cm^2 g^{-1} in surface area. A cell count of 10^8 cells g^{-1} for a surface area of 500 cm^2 g^{-1} works out to 2 x 10^5 cells cm^{-2} or 2 x 10^9 cells m^{-2} on pyrite surfaces. For a tailings aquifer with 30% porosity and assuming only pure pyrite in the solids, the cell concentration in the slurry becomes (1 - porosity)(pyrite density)(cell count) = (0.7) x (5 g ml^{-1}) x (10^8 cells g^{-1}) = 3.5 x 10^8 cells ml^{-1}, which is the same concentration of cells in solution that would oxidize aqueous ferrous iron optimally at 5 x 10^{-7} mol L^{-1} s^{-1} (Silverman and Lundgren, 1959). It is also in the same range of cell concentration found in acid mine waters in the environment (Scala et al., 1982). Therefore, it appears that the observed concentration of *Thiobacilli* on pyrite surfaces would produce aqueous Fe^{III} concentrations of the same order of magnitude as those formed by microbial oxidation of ferrous iron in aqueous solution by free-floating bacteria.

A preferable method of estimating the microbial rate of pyrite oxidation can be obtained from the interlaboratory comparison of pyrite bioleaching rates coordinated by the National Institute of Science and Technology (Olson, 1991). Eight laboratories participated in tests using a standardized method with 1 gram of pyrite from the same source. The pyrite was cleaned and sterilized after sizing to -165/+250 mesh (58 to 91 μm). Then sample was inoculated with a standard culture of *Thiobacillus ferrooxidans*. From Figure 6.1, the surface area would have been about 350 cm^2 g^{-1}. The reported oxidation rate (12.4 mg Fe L^{-1} h^{-1} or about 6 x 10^{-8} mol L^{-1} s^{-1}) is about an order of magnitude lower than the microbial oxidation rate of aqueous ferrous iron (Table 6.5). Olson

TABLE 6.5—Comparison of abiotic, microbial, and field oxidation rates (pH ≈ 2, T ≈ 25°C).

Reaction or Process (references)	Abiotic rate	Microbial rate	Field rate
Oxidation of aqueous ferrous iron (Singer and Stumm, 1968; Lacey and Lawson, 1977; Nordstrom, 1985)	3 x 10^{-12} mol L^{-1} s^{-1}	5 x 10^{-7} mol L^{-1} s^{-1}	5 x 10^{-7} mol L^{-1} s^{-1}
Oxidation of pyrite by ferric iron (McKibben and Barnes, 1986; Rimstidt et al., 1994)	1 to 2 x 10^{-8} mol m^{-2} s^{-1}		
Oxidation of pyrite by oxygen (McKibben and Barnes, 1986; Olson, 1991)	0.3 to 3 x 10^{-9} mol m^{-2} s^{-1}	8.8 x 10^{-8} mol m^{-2} s^{-1}	
Oxidation of waste dump (Ritchie, 1994a, b)			0.03 x 10^{-8} mol m^{-2} s^{-1}
Oxidation of tailings (Elberling et al., 1993)			20 to 60 x 10^{-8} mol m^{-2} s^{-1}

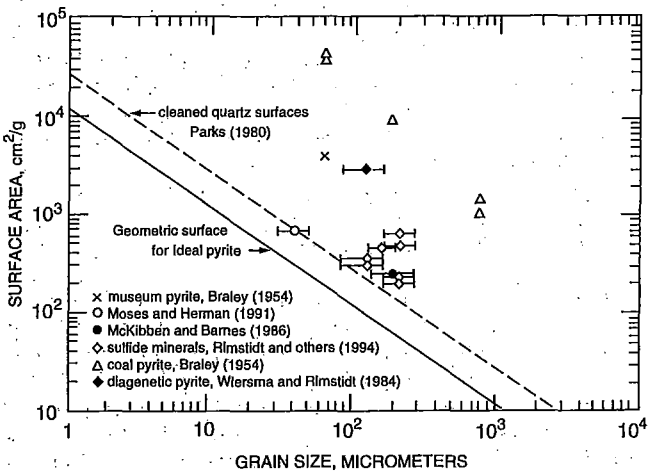

FIGURE 6.1—Surface area versus grain size for pyrite and other sulfide minerals.

(1991) used 1 g of pyrite in 50 ml of solution, so we can calculate the microbial oxidation rate of pyrite as

$$R = \frac{12.4 \text{ mg Fe } L^{-1}h^{-1}}{56 \text{ mg Fe mmol}^{-1}} \frac{50 \text{ ml}}{(1\text{g})\,(350 \text{ cm}^2\text{g}^{-1})}$$

$$\frac{1 \text{ mol}}{10^3 \text{ mmol}} \frac{1 \text{ L}}{10^3 \text{ ml}} \frac{10^4 \text{ cm}^2}{\text{m}^2} \frac{1 \text{ h}}{3{,}600 \text{ s}}$$

$$= 8.8 \times 10^{-8} \text{ mol m}^{-2} \text{ s}^{-1} \qquad [5]$$

This rate falls squarely between the abiotic oxidation of pyrite by ferric iron and the microbial oxidation of ferrous iron, i.e., within the uncertainty of the data, there is little difference between the oxidation rate of pyrite by ferric iron and the oxidation rate of ferrous iron by *T. ferrooxidans*. The lower rate of microbial pyrite oxidation compared to the oxidation rate of ferrous iron by *T. ferrooxidans* suggests that the heterogeneous reaction is the rate-determining step. We would suggest, however, that the uncertainties on the rates are large enough and the natural variation in the ferrous iron oxidation rate is large enough that there is not a significant difference. Hence, the rate of pyrite oxidation proceeds about as fast as the aqueous ferric iron can be produced from ferrous iron through microbial catalysis.

Field oxidation rates

What are the actual oxidation rates of pyritic mine waste in the field? What governs oxidation rates at field sites? Singer and Stumm (1970a) conceived of rates in the conventional sense of chemical kinetics. They described the abiotic oxidation of aqueous ferrous to ferric iron as the "rate-determining step" for the production of acid mine drainage because it is orders of magnitude slower than the oxidation of pyrite by ferric iron. This abiotic iron oxidation rate, however, has limited relevance because iron- and sulfur-oxidizing bacteria are ubiquitous in ground and surface waters, catalyzing aqueous iron and pyrite oxidation by orders of magnitude. Singer and Stumm (1970a, b) recognized that microbial catalysis greatly speeds up the oxidation of aqueous ferrous iron and that either the complete elimination of oxygen or the use of bactericides would be necessary to eliminate microbial activity. The microbial oxidation of aqueous ferrous iron, under optimal conditions of temperature, oxygen supply, and nutrient availability, is the fastest rate known in the system. This rate provides an upper limit to the pyrite oxidation rate. The lower limit is zero (or negative if sulfate reduction is considered) in the absence of oxygen and water. These extremes of rate cover a wide range over which actual rates may occur in the field.

The effects of sulfide surface area, degree of crystallinity, and purity cannot be overstated. One has only to compare the spontaneous oxidation of "framboidal," "microcrystalline," or "cryptocrystalline" pyrite (see Pabst, 1940; Caruccio, 1970) with untarnished, large, euhedral pyrite cubes that have survived in museums for several centuries to notice the difference in oxidation rates. The signatures of kings, queens, and other dignitaries over the last century can still be seen clearly on an exposed surface of massive chalcopyrite in the Falun mine in Sweden. Caruccio (1970) and Caruccio et al. (1976) pointed out that the grain size and surface area of pyrite in coal deposits has a considerable influence on the production rate of acid mine drainage, with framboidal pyrite being the most reactive. Normalizing reaction rates to unit surface area is now routinely done when reporting dissolution rates of minerals but differences in degree of crystallinity and purity (solid solution substitutions) may also affect reaction rates. Furthermore, the "reactive surface area" may be significantly less than the total measured surface area as measured by standard techniques (Dzombak and Morel, 1990). Reactive surface area refers to those sites on the surface that are actively available to adsorb and chemically bond with aqueous species, and can be reduced by intergranular contact or inclusion within other minerals. Another complication in the field is that not all exposed surface sites are in the flow path of the water, thereby reducing further the reactive surface area.

Field oxidation rates for pyrite are complicated by air and water transport processes, microbial growth kinetics, microbial ecology, organic compounds, temperature gradients, secondary mineral formation, neutralization reactions, climatic patterns, and the site-specific design of mine workings, waste dumps, and tailings. The production rate of acid mine drainage is governed by rates of transport and attenuation processes, which tend to be slower than rates of pyrite oxidation. Some confusion exists in the literature because the distinction between oxidation rates and transport/attenuation rates has not been made clear. In this sense, an obvious parallel or analogy can be made with silicate mineral weathering rates and discrepancies between laboratory and field studies (see Alpers and Nordstrom, 1999, and White and Brantley, 1995).

Ritchie (1994a, b) has reviewed and analyzed the physical factors that pertain to the acid production rate from waste piles. He has shown that the limiting factor is the transport and reaction of oxygen in the waste. Three main processes are dominant in these systems: convection of oxygen, diffusion of oxygen, and the intrinsic oxidation rate which he has calculated for two sites and compared with results compiled from other sites. Ritchie (1994 a, b) described the "global oxidation rate" as the overall flux rate of acid mine drainage from a waste dump and the "intrinsic oxidation rate" as the oxygen consumption rate, measured from oxygen profiles in units of mol kg^{-1} s^{-1} or mol m^{-3} s^{-1}. Several assumptions are involved in making these computations, including a stoichio-

metric relationship between oxygen consumed and pyrite oxidized (i.e., that oxygen is consumed only by pyrite).

The oxidation of pyrite is a highly exothermic reaction, which can cause thermal air convection in waste dumps and underground mines (Zverev et al., 1983). Air temperatures of 50 to 65°C are commonly achieved in waste-rock piles and copper heap-leach dumps (Cathles and Apps, 1975; Harries and Ritchie, 1981; Cathles, 1994; Ritchie, 1994a) and a water temperature of 47°C was reported from the Richmond Mine at Iron Mountain, California (Alpers and Nordstrom, 1991). Temperature and density gradients resulting from heat generation cause convective air transport, which can be a significant oxygen-supply mechanism (Ritchie, 1994a). Cathles (1994) indicated that convective gas flux driven by thermal gradients was dominant in the well-instrumented Midas Test Dump and other larger dumps at Kennecott's Bingham Canyon Mine (Cathles and Apps, 1975). However, Ritchie (1994a) asserted that the convective flux in a large dump generally applies over a much smaller area than the diffusive oxygen flux.

The relative importance of diffusion vs. convection depends primarily upon the range of air permeability. Ritchie (1994a) suggested a cutoff permeability value of 10^{-9} m^2. Above this value, convection should dominate and below this value, diffusion should dominate. Ritchie (1994a) also pointed out that he has found the global oxidation rate to be insensitive to changes in the intrinsic oxidation rate. Hence, for unsaturated waste rock, the dominant rate-limiting process should be oxygen diffusion, especially in a newly built waste-rock dump (Ritchie, 1994a). Parts of waste rock piles, usually located near the center, are typically dominated by diffusion whereas the outer edges may be dominated by convection. With time, convective gas transport will penetrate further into the dump as it ages (Ritchie 1994a).

Other factors that affect the ultimate release of acid drainage include the climate, hydrologic variables, mineralogy of the waste materials, physical structure of the waste and geological structure and setting of the mine site, historical evolution of mineral-processing practices, materials used and discarded in mineral processing, geomorphology of the terrain, and vegetation. Discussion of these subjects is beyond the scope of this chapter and can be found in other chapters of this volume or in other review papers. For example, Moore and Luoma (1990) have outlined the sources, transport mechanisms, and sinks for mining and mineral-processing wastes. They use the categories "primary," "secondary," and "tertiary" according to how many times the mining waste has been retransported. A comprehensive overview of tailings problems and their management has been published by Ritcey (1989).

REDOX CHEMISTRY AND MINERAL SOLUBILITIES

Eh-pH diagrams and redox chemistry

The traditional graphical method of delineating the stabilities of reduction-oxidation (or redox) species in geochemical systems (and in corrosion systems) has been through the use of Eh-pH (or pε-pH) diagrams. These are a type of master variable diagram where the independent or master variable is pH. Originally developed by Pourbaix (1945, 1966; also see Pourbaix and Pourbaix, 1992; Sato, 1992) to portray equilibrium relationships in metal corrosion systems, they were introduced and championed in the geochemical literature by Krumbein and Garrels (1952), Garrels (1954) and Garrels and Christ (1965). Hem (1961, 1985), Krauskopf (1967), Krauskopf and Bird (1995) and many others have used the concepts of Eh and pH as a convenient means of representing redox relationships for ions and minerals. The reader is referred to these sources as well as discussions by Stumm and Morgan (1981) and Nordstrom and Munoz (1994) for an introduction to the construction of these diagrams from thermodynamic data.

A pε-pH diagram for the Fe-S-K-O_2-H_2O system is shown on Figure 6.2 with the thermodynamic stability fields of several major ions and minerals of iron. The formation and occurrence of jarosite, goethite, and other secondary iron minerals are discussed in the next section. The stability boundary between goethite and jarosite can vary over several units of pH depending on the crystallinity and particle size of these minerals. Metastable phases such as ferrihydrite may form more readily than the thermodynamically stable phase in some conditions, and thus can play an important role in controlling aqueous metal concentrations.

Figure 6.2 indicates that goethite is stable under mildly acidic to basic oxidizing conditions, jarosite is stable under acidic oxidizing conditions, and pyrite is stable under a large range of strongly reducing conditions. Acidity tends to promote dissolution of minerals under a range of redox conditions. Additional iron minerals can be shown on diagrams similar to Figure 6.2, if additional components such as carbonate, silica, phosphate, and uranium are included, but such multi-component diagrams can become very cluttered and most of these additional minerals are not particularly relevant to acid mine waters.

These pε-pH diagrams can be very useful in showing the general stability relations among redox-sensitive ions and minerals but their limitations must be clearly understood:

1) The redox chemistry of a solution or a natural water cannot be measured by a simple "Eh" parameter. There is no such thing as a single representative redox potential or an Eh of a water. A measurement of electromotive force (EMF) with a platinum

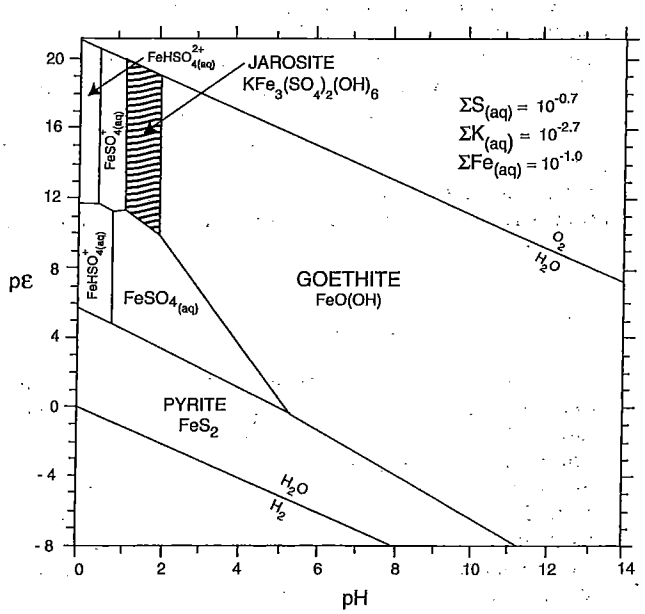

FIGURE 6.2—pε-pH diagram, showing stable solid phases in Fe-S-K-O-H system at 25°C (modified from Alpers et al., 1989).

electrode (converted to Eh by subtracting the reference electrode half-cell potential) for a water sample may or may not reflect an equilibrium potential for a single redox couple but there is no single Eh that represents the water (Thorstenson, 1984; Hostetler, 1984). Hence, Eh measurements may be quantitatively correlated to a specific redox couple such as Fe(II/III) but otherwise they are of little use.

2) Redox couples of different elements rarely, if ever, reach equilibrium at temperatures below 100°C. This fact is one of the reasons why a single Eh cannot be assigned to a water sample. Redox disequilibrium is the rule, not the exception. Lindberg and Runnells (1984) showed that when different redox couples are measured in the same water sample, none of them appear to be in equilibrium. The reasons for this are largely kinetic. Electrons transfer much more readily between redox-sensitive ions and surfaces such as electroconductive minerals (most sulfides) and bacteria than with other ions in solution.
3) Redox potential measurements respond to electroactive aqueous ions. To be electroactive an ion must have a sufficiently high exchange current density (Bricker, 1982) so that there is no kinetic hindrance to the transfer of electrons. This criterion requires both sufficiently high concentrations of the redox-sensitive ions as well as the lack of kinetic barriers to electron transfer. Only two common elements clearly meet this requirement: iron (II/III) and sulfur (sulfide). All other elements and ions found in natural waters (with the possible exception of uranium and cobalt under unusual circumstances) do not.
4) The redox conditions of a water sample are best characterized analytically by determining the concentrations of multiple redox species for each redox-active element in the sample. Acid mine waters are easily analyzed for Fe(II) and Fe(total) (with Fe(III) computed by difference or by direct determination, To et al., 1999) by visible spectrophotometry using a ferroin reagent such as bipyridine, orthophenanthroline, or ferrozine. The more precise and sensitive nature of methods using a colorimetric reagent such as ferrozine make them preferable to atomic absorption or inductively-coupled plasma atomic-emission spectroscopy (Ball and Nordstrom, 1994). Once the concentrations of redox species have been determined then the classification of Berner (1981) can be used to describe the redox chemistry. Berner suggests a practical lower limit of detection as 10^{-6} molar for oxygen, iron, sulfide, and methane. The presence of oxygen classifies a water as "oxic," the absence of oxygen and presence of ferrous iron classifies it as "post-oxic," the presence of sulfide classifies it as "sulfidic," and the presence of methane classifies it as "methanic." This general classification works well for the typical ground water evolving into more reducing conditions with time and depth, but not for acid mine waters. Acid mine waters and other types of surface waters are usually of a mixed redox chemistry and only be determining relevant redox species can you interpret the redox chemistry of the water.

Nordstrom et al. (1979) showed that acid mine waters typically have sufficient iron concentrations to give an equilibrium potential at the platinum electrode for the Fe (II/III) redox couple but that the O_2/H_2O redox couple was far from equilibrium with respect to the iron couple. Careful analyses of acid mine waters from the Leviathan/Bryant Creek system demonstrate the limits of redox measurements for mine waters even more clearly (Ball and Nordstrom, 1989, 1994). Figures 6.3a and 6.3b compare platinum electrode Eh measurements with Eh values calculated from Fe (II/III) determinations and speciated with the WATEQ4F code (Ball and Nordstrom, 1991; see Alpers and Nordstrom, 1999). The comparison of measured and calculated Eh on Figures 6.3a and 6.3b shows an excellent correlation for samples with total iron concentrations greater than 10^{-5} m. Most of the deviations are found at the lowest Eh values where the iron concentrations are so low (less than 10^{-6} m) that iron is no longer electroactive. Furthermore, these waters are saturated with atmospheric oxygen so that a mixed potential results from the oxygen competing with the low concentrations of iron. Poor comparisons of calculated and measured Eh are occasionally found at very high iron concentrations and low pH values because of inherent problems with the chemical model under these conditions (see Alpers and Nordstrom, 1999).

Iron photoreduction

Iron (II) concentrations in oxygenated surface waters have not only been detected but have been found to vary from night to day. The concentrations of Fe (II) reach a peak during midday, at the peak of insolation. The solar radiation reduces both dissolved Fe (III) and colloidal ferric hydroxide in natural waters (Waite and

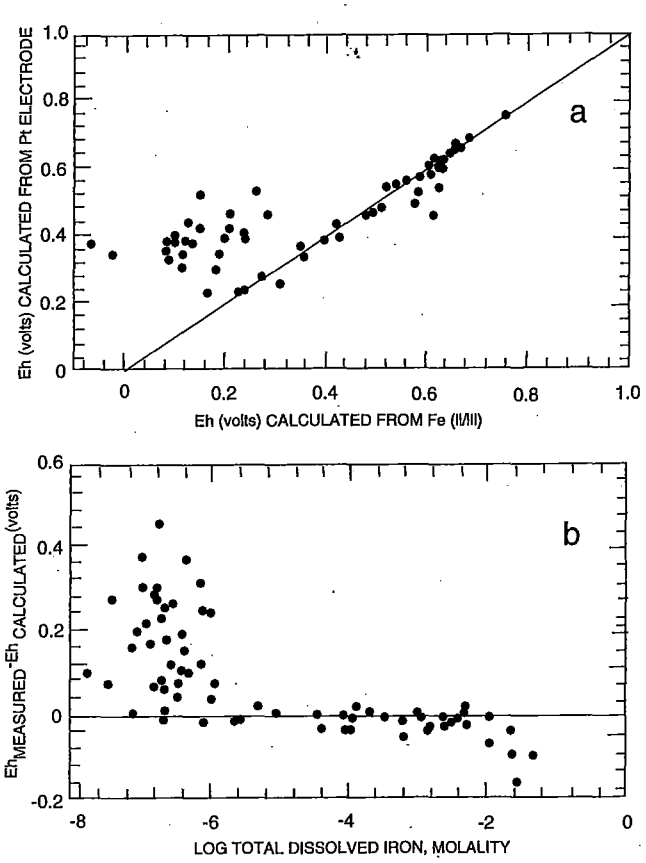

FIGURE 6.3—(a) Comparison of Eh calculated from the Fe (II/III) redox couple to Eh measured with a platinum electrode. (b) Difference between calculated and measured Eh plotted as function of total dissolved iron concentrations in molal units. Data from Leviathan/Bryant Creek watershed, California and Nevada (Ball and Nordstrom, 1989; 1994).

Morel, 1984). The same effect has been found for acid mine waters that have dissolved iron <5 mg/l (McKnight et al., 1988; McKnight and Bencala, 1988). McKnight et al. (1988) found the daytime production of Fe(II) to be nearly 4 times faster than the nighttime oxidation of Fe(II). These results might also be enhanced by light inhibition of iron- and sulfur-oxidizing bacteria (Le Roux and Marshall, 1977). The continual exposure of acid mine waters to the sun promotes recycling of the iron between dissolved and particulate phases and may have important consequences on the sorption of metals. Solar radiation could lead to Ostwald ripening of iron colloids which would increase the iron hydroxide particle size and decrease the reactive surface area. Alternatively, recycling of iron hydroxides and recreation of fresh colloidal surfaces would promote surface area and the opportunity for increased adsorption of metals (McKnight and Bencala, 1989). These effects, however, may only be detectable in streams with relatively small concentrations of iron. Acid mine waters with more typical iron concentrations of 20–1000 mg/l may not show this effect. In wetlands, an opposite effect has been observed, where Fe (II) concentrations reach a minimum during daylight hours; this effect has been attributed to daytime oxygenation by algae (Wieder, 1994).

Saturation indices (SI) and mineral solubilities

When complete water analyses for the major ions are available, a speciation computation can be done to determine the state of saturation with respect to any particular minerals for which thermodynamic data are available (see Alpers and Nordstrom, 1999). Numerous acid mine waters and tailings pore waters have been subject to these calculations to achieve more quantitative interpretations on the control of metal concentrations by mineral solubilities. Some brief examples of the usefulness of this approach are shown here.

Acid mine waters are characterized by low pH, high iron and aluminum concentrations, high metal concentrations, and high sulfate concentrations. Minerals that might be stable under these conditions should be hydrolyzed iron- and aluminum-sulfate minerals and insoluble metal-sulfate minerals. Prime candidates include jarosite, alunite, barite, anglesite, gypsum, and a suite of ferric- and aluminum-hydroxysulfate compounds. Figures 6.4a-d show two examples of SI values for barite, one for alunite, and one for anglesite. If equilibrium solubility is achieved and if it exerts the dominant control on the concentration of one or more elements, then the SI values should show a linear and horizontal trend close to zero. Such a pattern signifies that the water chemistry reflects the stoichiometry of the given mineral and may have reached equilibrium saturation. As expected, the values tend to plateau with the appropriate stoichiometry of the mineral but generally in the region of supersaturation. This effect might be explained by the particle size effect on solubility because the solubility product constant usually refers to a coarse-grained, well-crystallized material and it might also be due to solid solution substitution of trace components. Some of the apparent supersaturation could also be due to inadequacies in the chemical model, especially in the activity coefficient and stability constant expressions.

The behavior of aluminum and iron as reflected in saturation indices can be seen on Figures 6.5a-d. On Figure 6.5a, a plateau in the SI values for $Al(OH)_3$ is seen at pH values above about 4.5. At pH values above 4.5, solubility equilibrium is apparently reached with respect to microcrystalline or amorphous $Al(OH)_3$ and seems to be maintained at all higher pH values. This phenomenon was pointed out by Nordstrom and Ball (1986) and can be more clearly seen on Figure 6.5b in which the activity of the free aluminum ion is plotted against pH. The rate of aluminum leaching from common minerals at low pH is not generally fast enough relative to the flow rate of surface and ground waters to reach equilibrium with gibbsite. Furthermore, gibbsite solubility is so high at very low pH that it becomes an unstable or metastable phase with respect to other aluminous minerals, especially in the presence of high sulfate concentrations (Nordstrom, 1982b).

When acid mine drainage is diluted by neutral surface waters, the pH and aluminum concentrations eventually reach the gibbsite solubility curve and aluminum concentrations become controlled by one of 3 possibilities: (1) solubility of a solid phase (such as gibbsite), (2) a surface coating control with a stoichiometry similar to gibbsite, or (3) a common aluminosilicate mineral with an exchange ratio of Al^{3+} to H^+ of 1:3. A pH of 5 is also equal to the pK_1, the negative logarithm of the first hydrolysis constant for aluminum, and without hydrolysis the precipitation of hydrolyzed aluminum would not be possible. Hem and Roberson (1990) have shown that the rate of aluminum hydrolysis increases as pH values rise to about 5 so that the hydrolysis kinetics for dissolved aluminum favors the tendency toward equilibrium. Nordstrom et al. (1984) have shown that, when rapid mixing causes precipitation of aluminum in acid mine waters, the solid produced is an amorphous aluminum-hydroxysulfate material that might best be described as an amorphous basaluminite.

Comparable diagrams for iron are shown on Figures 6.5c-d. Apparent supersaturation with respect to ferric hydroxide or ferrihydrite occurs at pH values above about 4. The supersaturation might be explained by substitution of sulfate for hydroxide ions in the ferrihydrite and the formation of a schwertmannite-like phase. Schwertmannite [$Fe_8O_8(OH)_6(SO_4)$] was described by Bigham et al. (1990) and Bigham (1994) and is discussed in more detail in a later section of this chapter. The apparent supersaturation with respect to ferric hydroxide might also be explained by the formation of colloidal iron particles that cannot be filtered out by 0.1 micrometer pore size membranes. This apparent supersaturation behavior for ferric hydroxide is commonly seen for both surface waters and ground waters.

In general, the stoichiometry of a phase controlling the solubility of an aqueous constituent can be derived from an appropriately-selected ion-activity plot. For example, if pure ferric hydroxide were controlling the solubility of ferric iron, the reaction

$$Fe(OH)_3 + 3\ H^+ \rightleftharpoons Fe^{3+} + 3\ H_2O \qquad [6a]$$

and its log equilibrium constant expression

$$\log K = \log a_{Fe^{3+}} - 3\ \log a_{H^+} + 3\ \log a_{H_2O} \qquad [6b]$$

would indicate that a plot of Fe^{3+} activity versus pH (= $-\log a_{H^+}$) should have a slope of -3.

The observed slope of -2.4 on Figure 6.5d is clearly inconsistent with solubility control by pure ferric hydroxide having a molar Fe:OH ratio of 1:3 (Nordstrom, 1991). Similar results (a

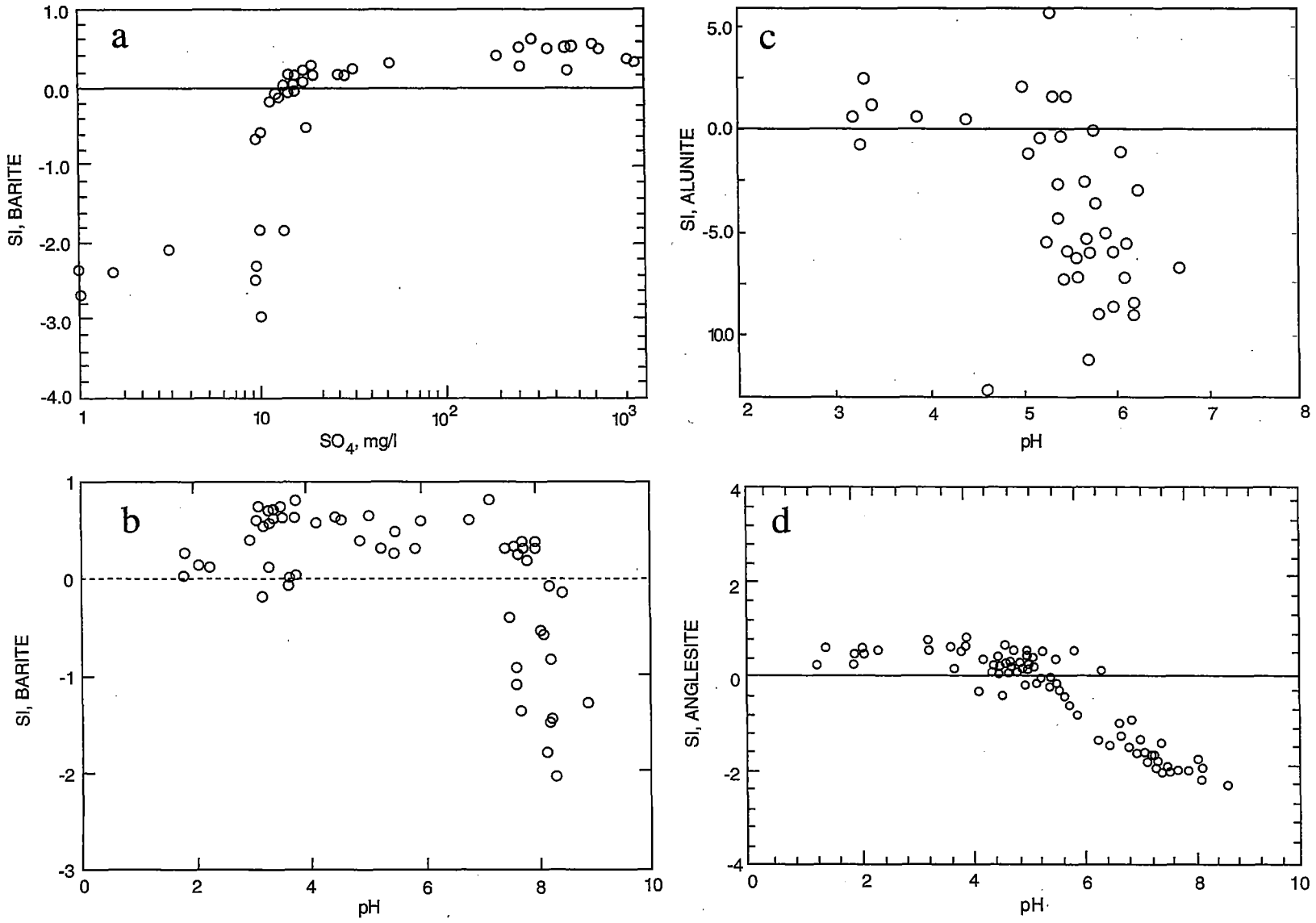

FIGURE 6.4—(a) Saturation indices for barite plotted as a function of sulfate concentration for data from the Osamu Utsumi mine site (Nordstrom et al., 1992). (b) Saturation indices for barite plotted as a function of pH for data from the Leviathan mine site (Ball and Nordstrom, 1989, 1994). (c) Saturation indices for alunite plotted as a function of pH for data from the Osamu Utsumi mine site (Nordstrom et al., 1992). (d) Saturation indices for anglesite plotted as function of pH for mine tailings based on data from Blowes (1990).

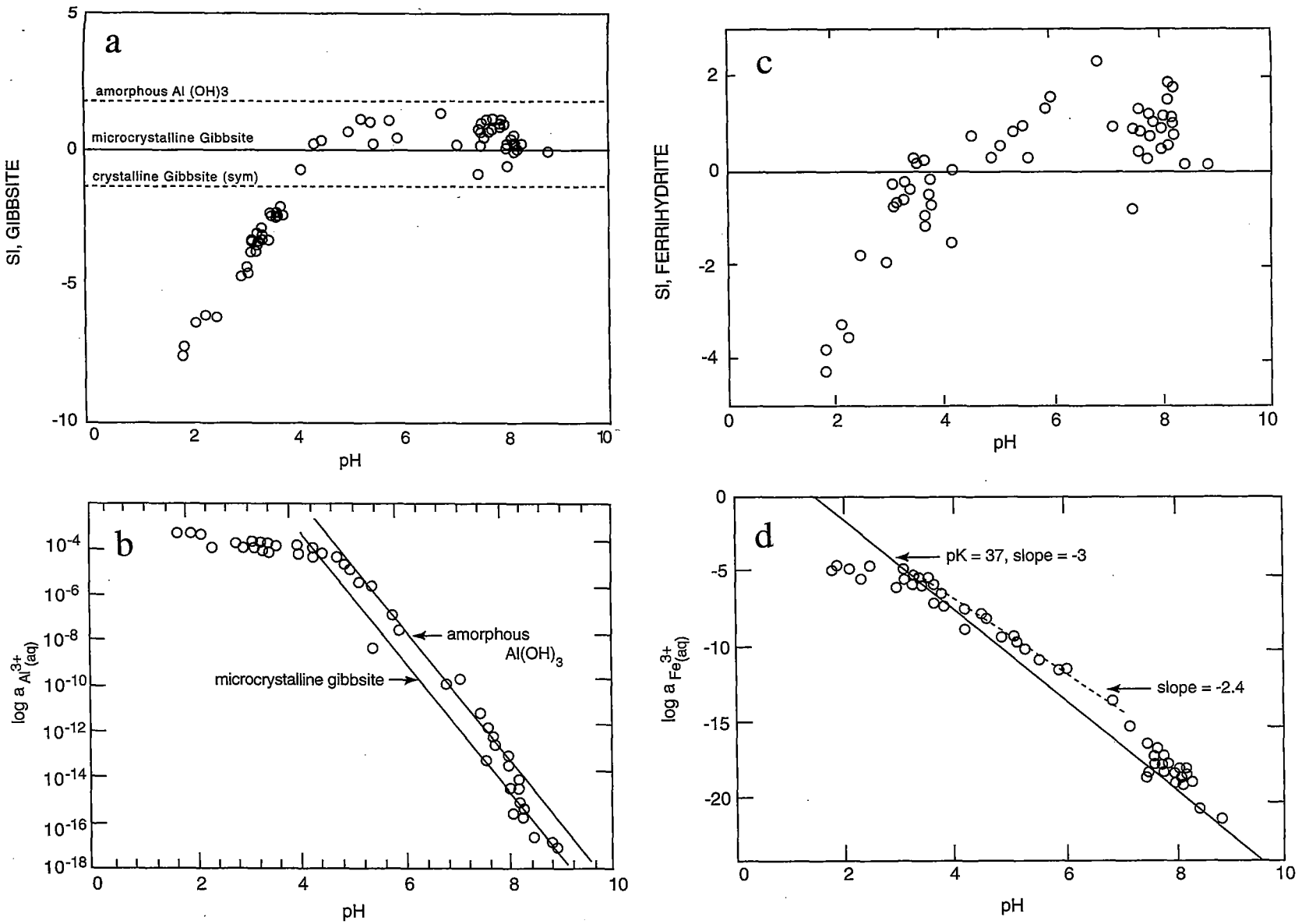

FIGURE 6.5—(a) Saturation indices for gibbsite as a function of pH for data from the Leviathan mine site (Ball and Nordstrom, 1989, 1994). (b) Logarithm of the activity of the aluminum ion plotted against pH with the equilibrium solubility lines for amorphous $Al(OH)_3$ and microcrystalline gibbsite shown (for 25°C). (c) Saturation indices for ferrihydrite ($\equiv Fe(OH)_3$) as a function of pH for data from the Leviathan mine site (Ball and Nordstrom, 1989, 1994). (d) Logarithm of the activity of the ferric ion plotted against pH with the equilibrium solubility for freshly precipitated ferrihydrite at 25°C shown as a solid line and the best fit for data in the pH range of 3.5 to 7 shown as a dashed line (Nordstrom, 1991). The higher slope from the fitted line suggests non-stoichiometric substitution of sulfate for hydroxide in the precipitating ferric phase.

slope of -2.35) in other surface-water environments and in laboratory experiments were interpreted by Fox (1988) to represent a ferric hydroxide in which nitrate has partially substituted for hydroxide, i.e., $Fe(OH)_{2.35}(NO_3)_{0.65}$. Kimball et al. (1994) found a regressed slope of -2.23 from iron data on the acid mine waters of St. Kevin Gulch, Colorado during a neutralization experiment.

The relation on Figure 6.5d could be caused by a reaction involving a hypothetical sulfate-substituted ferric hydroxide such as

$$Fe(OH)_{2.4}(SO_4)_{0.3} + 2.4\,H^+ \rightleftharpoons Fe^{3+} + 0.3\,SO_4^{2-} + 2.4\,H_2O \quad [7a]$$

with its log equilibrium constant expression

$$\log K = \log a_{Fe^{3+}} - 2.4 \log a_{H^+} + 0.3 \log a_{SO_4^{2-}} + 2.4 \log a_{H_2O} \quad [7b]$$

The data on Figure 6.5d do not indicate solubility with schwertmannite of the composition reported by Bigham (1994). The expected slope on a plot of a_{Fe3+} vs. pH showing schwertmannite solubility equilibrium would be -2.75, based on the reaction

$$FeO(OH)_{0.75}(SO_4)_{0.125} + 2.75H^+ \rightleftharpoons Fe^{3+} + 0.125\,SO_4^{2-} + 1.75\,H_2O \quad [8a]$$

and its log equilibrium constant expression

$$\log K = \log a_{Fe^{3+}} - 2.75 \log a_{H^+} + 0.125 \log a_{SO_4^{2-}} + 1.75 \log a_{H_2O} \quad [8b]$$

Bigham (1994) reported that schwertmannite is associated with mine drainage ranging in pH from about 2.5 to 6, and is most commonly associated with "typical" mine effluents with pH from 3 to 4. Bigham (1994) also noted that ferrihydrite is associated with mine drainage in the pH range of about 5 to 8. The data on Figure 6.5d with slope of -2.4 span from pH of about 4 to about 7. This suggests that the apparent stoichiometry is more likely to represent a sulfate-substituted ferrihydrite, schwertmannite, or other hydrous ferric oxide with a molar Fe:OH ratio of 1:2.4. It is also possible that mixtures of different iron mineral phases are precipitating from these waters over this pH range and the slope is not clearly resolvable into a particular reaction. This complex chemistry needs more detailed work to quantitatively relate water chemistry to iron colloids and other precipitates.

In his thesis work (Blowes, 1990) and in subsequent papers (Blowes and Jambor, 1990; Blowes et al., 1991; Blowes and Ptacek, 1994; Ptacek and Blowes, 1994), Dr. Blowes and his colleagues have mapped the saturation indices for siderite, calcite, goethite, ferrihydrite, gypsum, melanterite, and anglesite with depth in tailings piles at Heath Steele, New Brunswick, and Waite Amulet, Quebec. Similar detailed hydrogeochemical studies are being completed at Kidd Creek and Copper Cliff, Ontario. In some of these studies, two aqueous models are compared: the ion association model and the specific ion interaction (Pitzer) model. For some minerals, the comparisons of saturation indices computed by both models are nearly identical, but for others the Pitzer model gives SI values that are more consistently at equilibrium. The mineralogy at these sites has also been studied in detail and it fully supports the interpretations based on the Pitzer model saturation index computations, which are more appropriate for solutions of high ionic strength. The strengths and limitations of these aqueous models as applied to acid mine waters are discussed by Alpers and Nordstrom (1999).

SECONDARY MINERALS

Acid mine waters are highly reactive solutions that can dissolve most primary minerals and form a wide variety of secondary minerals. The understanding of secondary mineral formation has important consequences for environmental management of mining wastes. Insoluble secondary minerals with large surface areas can effectively immobilize many of the major contaminants in acid mine waters, providing an important attenuation and detoxifying mechanism. Soluble secondary minerals also slow down toxic metal mobility but only temporarily until the next rainstorm or snowmelt event. Hence, the occurrence and properties of these minerals are equal in importance to the water chemistry and pyrite oxidation rates for the interpretation of chemical processes occurring in mine waste environments.

For the purpose of this discussion, secondary minerals are defined as those that form during weathering. A further distinction can be made between secondary minerals formed by natural processes prior to human disturbance and those formed after the commencement of mining, exploration, or other human activity. In this chapter we refer to these effects as pre-mining and post-mining.

There are clear similarities in the geochemistry of pre- and post-mining weathering processes, as well as in the nature of the associated aqueous solutions and secondary minerals; however, there are also some important differences. Mining tends to cause a dramatic increase in the rate of sulfide oxidation reactions because of rapid exposure of large volumes of reactive material to atmospheric oxygen. Blasting and crushing of ores and waste material leads to a considerable increase in the available surface area of reactive minerals. Hydrologic changes caused by mine dewatering in both underground and open-pit mines may expose large volumes of rock to atmospheric oxygen.

The type of secondary mineral formed depends on the composition of the water, the type and composition of the primary minerals, the temperature, and the moisture content. The initial minerals that precipitate in certain environments tend to be poorly crystalline, metastable phases that may transform to more stable phases over time. Therefore, those secondary minerals that are preserved in the geologic record in leached cappings, gossans, and zones of secondary enrichment may be quite different in their mineralogy compared with the secondary minerals that form over shorter time frames in mine drainage settings.

Four important processes lead to the formation of secondary minerals from acid mine waters: (1) iron oxidation and hydrolysis, (2) reaction of acid solutions with sulfides, gangue minerals, and country rock, (3) mixing of acid mine waters with more dilute waters, and (4) evaporation of acid mine waters.

A suite of Fe(III) minerals can form from iron oxidation and hydrolysis. Many of these phases have very low solubility, fall in the colloidal size range (less than 1.0 micrometer), and can adsorb or coprecipitate significant quantities of trace elements. Reaction of acid mine waters with country rock and some gangue minerals, such as calcite and dolomite, will cause neutralization and precip-

itation of metals. Evaporation concentrates the acid, sulfate, and metals found in acid mine waters until they reach mineral saturation, forming efflorescent sulfate salts, a common feature associated with oxidizing sulfide-bearing mine wastes.

This section describes five categories of secondary minerals: (1) metal oxides, hydroxides, and hydroxysulfates, (2) soluble sulfates, (3) less-soluble sulfates, (4) carbonates, and (5) secondary sulfides. For each category, one or more lists of mineral formulas are provided (Tables 6.6–6.13). These lists are intended to include the more common secondary minerals in each category, but it should not be inferred that all minerals on the lists have been demonstrated to control metal concentrations in acid mine waters on a large scale. A discussion of the secondary minerals that are likely to control metal concentrations in acid mine waters is included as the final part of this section.

Metal oxides, hydroxides, and hydroxysulfates

Most divalent and trivalent metals exhibit amphoterism, i.e., they produce a solubility minimum at circum-neutral pH values with enhanced solubilities under both acidic and basic conditions. Figure 6.6 shows both the amphoteric solubilities of ferrihydrite, gibbsite, and the hydroxides of Cu, Zn, Fe(II), and Cd at 25°C, as well as the importance of pH in controlling the dissolved concentration of these metals. Different metals reach their minimum solubility at different pH values. This phenomenon provides the basis for the removal of metals during rapid neutralization of acid mine drainage by alkaline treatment (lime, limestone, or sodium hydroxide). The pH-specific solubility minimum varies for each metal, causing a different efficiency of metal removal for neutralization to a given pH (Barton, 1978). At metal concentrations greater than 10^{-6} molar, metal hydroxides should precipitate in the following sequence with increasing pH: Fe(III), Pb, Al, Cu, Zn, Fe(II), and Cd. This sequence is also very closely followed by the pH-dependent sequence of adsorption of metals on hydrated ferric oxide surfaces (Dzombak and Morel, 1990).

Iron—The minerals discussed in this section are ferrous (Fe^{II}) and ferric (Fe^{III}) oxides, hydroxides, and hydroxysulfates. The list of minerals in Table 6.6 includes some that are not observed to form readily during weathering, but are included for completeness and for analogy with other metals, especially aluminum (Table 6.7; discussed in a later subsection).

Ferrous hydroxide is considerably more soluble than its ferric equivalent at a given pH (Fig. 6.6) and the former appears only rarely in nature. $Fe(OH)_2$, when slightly oxidized, takes on a green appearance and is also known as "green rust." It occurs when Fe^{II}-rich solutions are mixed with a highly alkaline solution and allowed to oxidize slightly. This material has been prepared in the laboratory and Ponnamperuma et al. (1967) have argued effectively for its occurrence in nature, but it is not credited as a mineral because it is unstable and poorly characterized.

Ferrihydrite is a poorly crystalline form of hydrous ferric oxide/hydroxide that seems to be the first phase to form upon neutralization of Fe(III)-bearing solutions at low temperature, surficial conditions. For many years, this phase was considered to be "amorphous $Fe^{III}(OH)_3$." However, careful examination by X-ray diffraction (XRD) and Mössbauer spectroscopy (e.g., Schwertmann, 1985a) has revealed that this material is commonly a poorly crystalline substance with a range of structural order, yielding an XRD pattern with two to six peaks (Carlson and Schwertmann, 1981). Ferrihydrite formed in mining environments tends to have two to four XRD peaks, and is associated with waters having pH values of 5 to 8 (Bigham, 1994). The "two-line" ferrihydrite is also referred to as "proto-ferrihydrite" (Chukhrov et al., 1973), although this is not an approved mineral name. At least two formulas for ferrihydrite have been reported: $Fe_5HO_8 \cdot 4H_2O$ (Towe and Bradley, 1967) and $Fe_2O_3 \cdot 2FeO(OH) \cdot 2.6H_2O$, a structural formula based on infrared spectroscopy (Russell, 1979). The latter formula can also be expressed as $Fe_2O_3 \cdot 1.8H_2O$.

Hematite (Fe_2O_3) and goethite [FeO(OH)] are the most common and most stable forms of ferric oxide and oxyhydroxide, respectively. The solubility and stability of hematite and goethite are sufficiently close that grain size and surface Gibbs free energy have important influence on the phase relations. With regard to coarse-grained minerals, goethite appears to be stable relative to hematite at temperatures below about 80°C (Langmuir, 1969, 1971, 1972). However, fresh goethite nearly always occurs in a particle size less than 0.1 micrometers in soils and sediments, so it is unstable relative to coarser-grained hematite under the geologic conditions that form sedimentary rocks. This conclusion is supported by both laboratory (Berner, 1969, 1971) and field evidence (Walker, 1967, 1974, 1976). Both goethite and hematite have slow growth kinetics at surficial temperatures, so the initial solid products from the hydrolysis of $Fe^{3+}_{(aq)}$ are poorly crystalline, metastable phases such as microcrystalline goethite or ferrihydrite. Thus, kinetic factors play an important role in determining the nature of the ferric precipitate(s) that may form as a result of ferrous iron oxidation and hydrolysis. Some progress has been made in understanding these factors and how they influence the distribution of hematite and goethite in soil profiles (Kämpf and Schwertmann, 1982; Schwertmann, 1985a, b). Ferrihydrite is known to convert to hematite if conditions are maintained between pH 5 and 9. Outside of this range, most of the ferrihydrite dissolves and reprecipitates as goethite (Schwertmann and Murad, 1983). Other factors may influence the formation of these phases, such as humidity, Al-content (Tardy and Nahon, 1985), grain size, and the presence of trace elements (Torrent and Guzman, 1982; Thornber, 1975). The preparation and characterization of iron oxides has been reviewed by Schwertmann and Cornell (1991).

Relatively little work has been done to understand the factors that influence the distribution of hematite and goethite in the weathered zone of mineral deposits. Leached cappings and gossans represent the *in situ* oxidized equivalents of porphyry copper and massive sulfide deposits, respectively. The mineralogy of iron in the oxidized zones of these deposits is dominated by hematite, goethite, and jarosite [$(K,Na,H_3O)Fe^{III}_3(SO_4)_2(OH)_6$]. The early literature (e.g., Locke, 1926; Tunell, 1930) documented the observation that "deep maroon to seal brown" hematitic iron oxide tends to remain in rocks after oxidation of supergene chalcocite-bearing ores, which form as the enrichment product of copper-iron sulfide protores. Increasing amounts of goethite and jarosite relative to hematite correlate with progressively higher ratios of pyrite to chalcocite at depth (Loghry, 1972; Alpers and Brimhall, 1989). The texture of the iron oxides (or "limonites") also reflects a systematic change from indigenous (in original sulfide cavities) to transported (outside sulfide cavities and in fractures) with increasing relative pyrite content prior to oxidation (Blanchard, 1968; Loghry, 1972).

Aluminum has been observed to substitute into goethite and

TABLE 6.6—Iron oxide, hydroxide, and hydroxysulfate minerals.

Mineral	Formula
Hematite	α-Fe_2O_3
Maghemite	γ-Fe_2O_3
Magnetite	$FeO{\cdot}Fe_2O_3$
Goethite	α-FeO(OH)
Akaganéite	β-FeO(OH,Cl)
Lepidocrocite	γ-FeO(OH)
Feroxyhyte	δ'-FeO(OH)
Ferrihydrite	$Fe_5HO_8{\cdot}4H_2O$ or $Fe_2O_3{\cdot}2FeO(OH){\cdot}2.6H_2O$
Schwertmannite	$Fe^{III}_8O_8(SO_4)(OH)_6$
Fibroferrite	$Fe^{III}(SO_4)(OH){\cdot}5H_2O$
Amarantite	$Fe^{III}(SO_4)(OH){\cdot}3H_2O$
Jarosite	$KFe^{III}_3(SO_4)_2(OH)_6$
Natrojarosite	$NaFe^{III}_3(SO_4)_2(OH)_6$
Hydronium Jarosite	$(H_3O)Fe^{III}_3(SO_4)_2(OH)_6$
Ammonium Jarosite	$(NH_4)Fe^{III}_3(SO_4)_2(OH)_6$
Argentojarosite	$AgFe^{III}_3(SO_4)_2(OH)_6$
Plumbojarosite	$Pb_{0.5}Fe^{III}_3(SO_4)_2(OH)_6$
Beaverite	$PbCuFe^{III}_2(SO_4)_2(OH)_6$
Chromate jarosite	$KFe^{III}_3(CrO_4)_2(OH)_6$

TABLE 6.7—Aluminum oxide, hydroxide, and hydroxysulfate minerals.

Mineral	Formula
Corundum	α-Al_2O_3
[γ-Alumina][1]	γ-Al_2O_3
Diaspore	α-AlO(OH)
Boehmite	γ-AlO(OH)
Gibbsite	γ-$Al(OH)_3$
Bayerite	α-$Al(OH)_3$
Doyleite	$Al(OH)_3$
Nordstrandite	$Al(OH)_3$
Alunite	$KAl_3(SO_4)_2(OH)_6$
Natroalunite	$NaAl_3(SO_4)_2(OH)_6$
[Hydronium Alunite][2]	$(H_3O)Al_3(SO_4)_2(OH)_6$
Ammonium Alunite	$(NH_4)Al_3(SO_4)_2(OH)_6$
Osarizawaite	$PbCuAl_2(SO_4)_2(OH)_6$
Jurbanite	$Al(SO_4)(OH){\cdot}5H_2O$
Basaluminite	$Al_4(SO_4)(OH)_{10}{\cdot}5H_2O$
Hydro-basaluminite	$Al_4(SO_4)(OH)_{10}{\cdot}12\text{-}36H_2O$

[1] γ-Alumina is a synthetic compound, used as a catalyst in industry. Surface properties are reviewed by Goldberg et al. (1995).
[2] Hydronium alunite has not been found in nature and therefore is not considered a mineral.

TABLE 6.8—Some other oxide and hydroxide minerals and native metals.

Mineral	Formula
Pyrolusite	MnO_2
Hausmannite	Mn_3O_4
Manganite	γ-MnO(OH)
Pyrochroite	$Mn(OH)_2$
Todorokite	$(Mn^{II},Ca,Mg)Mn^{IV}_3O_7{\cdot}H_2O$
Takanelite	$(Mn^{II},Ca)Mn^{IV}_4O_9{\cdot}H_2O$
Rancieite	$(Ca,Mn^{II})Mn^{IV}_4O_9{\cdot}3H_2O$
Native copper	Cu
Tenorite	CuO
Cuprite	Cu_2O
Delafossite	$CuFeO_2$
Bunsenite	NiO
Theophrastite	$Ni(OH)_2$
Jamborite	$(Ni^{II},Ni^{III},Fe)(OH)^2(OH,S,H_2O)$
Native silver	Ag
Native gold	Au
Native mercury	Hg
Montroydite	HgO
Massicot litharge	PbO
Plattnerite	PbO_2

TABLE 6.9—Selected soluble iron-sulfate minerals.

Mineral	Formula
Melanterite	$Fe^{II}SO_4{\cdot}7H_2O$
Siderotil	$Fe^{II}SO_4{\cdot}5H_2O$
Rozenite	$Fe^{II}SO_4{\cdot}4H_2O$
Szomolnokite	$Fe^{II}SO_4{\cdot}H_2O$
Halotrichite	$Fe^{II}Al_2(SO_4)_4{\cdot}22H_2O$
Roemerite	$Fe^{II}Fe^{III}_2(SO_4)_4{\cdot}14H_2O$
Coquimbite	$Fe^{III}_2(SO_4)_3{\cdot}9H_2O$
Kornelite	$Fe^{III}_2(SO_4)_3{\cdot}7H_2O$
Rhomboclase	$(H_3O)Fe^{III}(SO_4)_2{\cdot}3H_2O$
Ferricopiapite	$Fe^{III}_5(SO_4)_6O(OH){\cdot}20H_2O$
Copiapite	$Fe^{II}Fe^{III}_4(SO_4)_6(OH)_2{\cdot}20H_2O$
Voltaite	$K_2Fe^{II}_5Fe^{III}_4(SO_4)_{12}{\cdot}18H_2O$

TABLE 6.10—Some other soluble sulfate minerals.

Mineral	Formula
Epsomite	$MgSO_4 \cdot 7H_2O$
Hexahydrite	$MgSO_4 \cdot 6H_2O$
Goslarite	$ZnSO_4 \cdot 7H_2O$
Bianchite	$ZnSO_4 \cdot 6H_2O$
Gunningite	$ZnSO_4 \cdot H_2O$
Zincosite	$ZnSO_4$
Gypsum	$CaSO_4 \cdot 2H_2O$
Anhydrite	$CaSO_4$
Morenosite	$NiSO_4 \cdot 7H_2O$
Retgersite	$NiSO_4 \cdot 6H_2O$
Boothite	$CuSO_4 \cdot 7H_2O$
Chalcanthite	$CuSO_4 \cdot 5H_2O$
Chalcocyanite	$CuSO_4$
Alunogen	$Al_2(SO_4)_3 \cdot 17H_2O$
Mirabilite	$Na_2SO_4 \cdot 10H_2O$
Thenardite	Na_2SO_4

TABLE 6.11—Some less-soluble sulfate and hydroxysulfate minerals.

Mineral	Formula
Celestite	$SrSO_4$
Anglesite	$PbSO_4$
Barite	$BaSO_4$
Radium sulfate	$RaSO_4$
Antlerite	$Cu_3(SO_4)(OH)_4$
Brochantite	$Cu_4(SO_4)(OH)_6$
Langite, Wroewolfeite	$Cu_4(SO_4)(OH)_6 \cdot 2H_2O$
Posnjakite	$Cu_4(SO_4)(OH)_6 \cdot H_2O$

TABLE 6.12—Some carbonate minerals.

Mineral	Formula
Rhombohedral	
Calcite	$CaCO_3$
Magnesite	$MgCO_3$
Siderite	$FeIICO_3$
Rhodochrosite	$MnCO_3$
Smithsonite	$ZnCO_3$
Otavite	$CdCO_3$
Gaspéite	$NiCO_3$
Sphaerocobaltite	$CoCO_3$
Orthorhombic	
Aragonite	$CaCO_3$
Strontianite	$SrCO_3$
Witherite	$BaCO_3$
Cerrusite	$PbCO_3$
Double	
Dolomite	$CaMg(CO_3)_2$
Kutnahorite	$Ca(Mn,Mg)(CO_3)_2$
Ankerite	$Ca(Fe^{II},Mg,Mn)(CO_3)_2$
Minrecordite	$CaZn(CO_3)_2$
Hydroxyl	
Malachite	$Cu_2(CO_3)(OH)_2$
Azurite	$Cu_3(CO_3)_2(OH)_2$
Hydrocerussite	$Pb_3(CO_3)_2(OH)_2$
Hydrozincite	$Zn_5(CO_3)_2(OH)_6$
Aurichalcite	$(Zn,Cu)_5(CO_3)_2(OH)_6$

TABLE 6.13—Supergene and diagenetic sulfide minerals.

Mineral	Formula
Supergene sulfide minerals	
Chalcocite	Cu_2S
Djurleite-I	$Cu_{1.965}S$
Djurleite-II	$Cu_{1.934}S$
Digenite	$(Cu,Fe)_9S_5$
Anilite	Cu_7S_4
Geerite	Cu_8S_5
Spionkopite	$Cu_{39}S_{28}$
Yarrowite	Cu_9S_8
Blue-remaining covellite	$Cu_{(1+x)}S$
Covellite	CuS
Violarite	Ni_2FeS_4
Millerite	NiS
Diagenetic sulfide minerals	
Amorphous FeS	FeS with coprecipitated Zn, Cd, Mn, Cu, Ni, As)
Mackinawite	$(Fe,Ni)_9S_8$
Smythite	$(Fe,Ni)_9S_{11}$
Greigite	$Fe^{II}Fe^{III}{}_2S_4$
Pyrite, marcasite	FeS_2

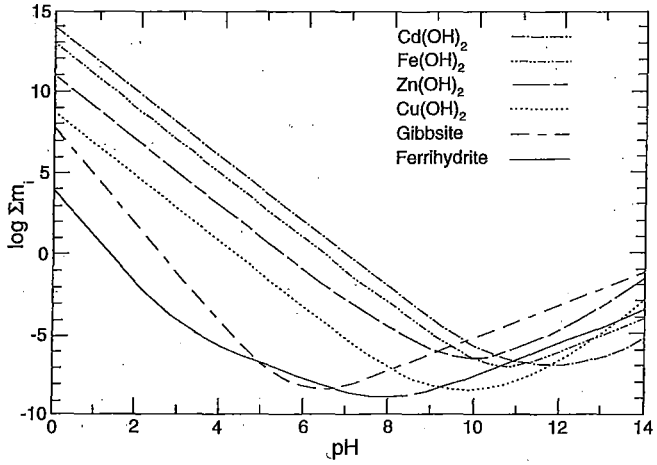

FIGURE 6.6—Solubility curves for gibbsite, ferrihydrite, and the hydroxides of Cu, Zn, Fe (II), and Cd shown as a function of pH.

hematite in certain soils, to maximum concentrations of 33 mole % AlO(OH) and 14 mole % Al_2O_3, respectively (Yapp, 1983; Tardy and Nahon, 1985; Schwertmann, 1985a). Although both iron and aluminum are highly soluble in acid mine waters, we are unaware of any data showing significant aluminum substitution in iron oxide minerals formed in mine drainage settings. Adsorption and precipitation of hydrolyzable metal ions tends to take place at pH values near the first hydrolysis pK for that metal. The first pK of hydrolysis for Fe^{III} is 2.2, and for Al is 5.0, so the coprecipitation of Al in hydrous Fe^{III} oxides formed at pH values less than about 4.5 is unlikely. This fundamental difference between iron and aluminum chemistry leads to spatial and temporal separation of precipitating phases of hydrolyzed iron and aluminum in oxidizing mineral deposits and mine waters.

Schwertmannite is a poorly crystalline iron-hydroxysulfate mineral that has recently been discovered to be a fairly common phase in ochres formed in mine drainage environments (Bigham et al., 1990; Bigham, 1994; Murad et al., 1994). The structure of schwertmannite appears to be related to that of akaganéite, an iron oxyhydroxide with essential chloride (Bigham, 1994; Murad et al., 1994). A combination of powder XRD and Mössbauer spectroscopy is necessary for definitive identification of schwertmannite (Murad et al., 1994). Schwertmannite or other sulfate-substituted, hydrous ferric oxides are most likely to control ferric iron solubility in acid mine drainage, as discussed previously (Fig. 6.5d).

Jarosite-alunite—The jarosite-alunite group of minerals shares a common crystal structure and stoichiometry, with many possible compositional substitutions. The general jarosite-alunite formula is $AB_3(SO_4)_2(OH)_6$ where the B sites are occupied by Fe^{III} to form jarosites and by Al to form alunites. Endmember formulas for some of the more common jarosite group minerals are given in Table 6.6, and the more common alunite endmember formulas in Table 6.7. The A site is occupied either by a monovalent cation or by a divalent cation alternating with a vacancy to maintain charge balance. The most common occupants of the A site in order of abundance in natural alunites and jarosites are $K^+ > Na^+ > H_3O^+$ (Kubisz, 1960, 1961, 1964; Brophy and Sheridan, 1965; Scott, 1987). The pure potassium-iron endmember is jarosite and the pure potassium-aluminum endmember is alunite. Pure endmembers are rare; jarosites and alunites formed during weathering and those synthesized at temperatures below 100°C tend to contain considerable hydronium ion in the A site (Dutrizac and Kaiman, 1976; Dutrizac, 1983; Alpers et al., 1989, 1992; Stoffregen and Alpers, 1992). Hydronium jarosite has been reported as a naturally occurring mineral (Kubisz, 1970), whereas hydronium alunite has not yet been found in nature. The hydronium endmembers can be synthesized readily (Ripmeester et al., 1986). Solid solutions between alunite and jarosite have also been synthesized (Parker, 1962; Brophy et al., 1962), but thermodynamic relations for iron-aluminum substitution have not been established and mineral compositions intermediate to alunite and jarosite are not commonly observed. This effect is probably caused by the different first hydrolysis constants for Fe^{III} (pK_1 = 2.2) and Al (pK_1 = 5.0), as discussed earlier regarding hematite and goethite. Further summaries on substitutional properties of the alunite-jarosite group were presented by Scott (1987), Stoffregen and Alpers (1987, 1992), and Alpers et al. (1989). Information on the relation between the crystallographic, chemical, and isotopic properties of alunite and jarosite was reported by Alpers et al. (1992) and by Stoffregen and Alpers (1992).

Aluminum—A list of some aluminum oxide, hydroxide, and hydroxysulfate minerals and their formulas is provided in Table 6.7. Thermodynamic properties of aluminous minerals have been reviewed, evaluated, and tabulated by Hemingway and Sposito (1996). Properties of aqueous aluminum ions and polymers have been reviewed and evaluated by Nordstrom and May (1996) and Bertsch and Parker (1996), respectively.

Solubility and stability relations among gibbsite, alunite, basaluminite, jurbanite, and alunogen were delineated by Nordstrom (1982b). In acid mine waters, aluminum-sulfate and -hydroxysulfate minerals become more stable than common soil minerals such as gibbsite and kaolinite. At pH values less than about 5.5 (depending on sulfate and potassium activities) gibbsite becomes unstable relative to alunite (Nordstrom, 1982b). Below pH values of about 4, jurbanite becomes most stable. Alunogen becomes stable only at pH values below 0 (i.e., hydrogen ion activities greater than 1.0). Some of these stability relationships need to be revised in light of the work by Reardon (1988), who applied the Pitzer approach to aluminum-sulfate solutions, and the recent revisions on thermodynamic properties of aluminum minerals and aqueous species (Hemingway and Sposito, 1996; Nordstrom and May, 1996). Despite its apparent thermodynamic stability, jurbanite tends to occur only rarely as a post-mining efflorescence (Anthony and MacLean, 1976), and has not been found commonly as a mineral precipitate from acid mine waters. We suspect that jurbanite has little significance as a solubility control in spite of the near-zero SI values commonly found, for three reasons:

1) recalculation of the solubility field is needed, based on revised thermodynamic properties for auxiliary species that may show the stability field of jurbanite to be at lower pH values,
2) jurbanite appears to be an efflorescent salt and most efflorescent salts in mine wastes form at pH values much less than 4,
3) other factors seem to govern aluminum and sulfate concentrations in acid mine waters (Nordstrom and Ball, 1986).

The behavior of aluminum in acid mine waters (and stream waters affected by acid rain) has been described by Nordstrom and Ball (1986). For waters with pH values less than 4.5 to 5.0, dissolved aluminum tends to behave as a conservative ion in surface waters, whereas for waters with pH values above 5.0, solubility control of dissolved aluminum by microcrystalline to amorphous

$Al(OH)_3$ is apparent, as described previously (Figs. 6.5a and 6.5b). Such control may be caused by equilibrium solubility or by a surface reaction involving the exchange of Al^{3+} for $3H^+$ on an aluminous surface. May and Nordstrom (1991) showed that a characteristic change of behavior for aluminum from conservative to non-conservative is common for a wide variety of sulfate-acidified waters. When the pH in an acid mine water increases to 5 or higher because of rapid mixing with circumneutral, dilute water, an aluminum-hydroxysulfate compound precipitates immediately. This precipitate is usually white, and is most commonly amorphous to XRD, electron diffraction, transmission electron microscopy, and scanning electron microscopy (Nordstrom et al., 1984). It seems to be of fairly constant composition, similar to the amorphous basaluminite reported by Adams and Rawajfih (1977). It has been observed many times by people working on acid mine waters and mine wastes. The occurrence of the white, aluminous precipitate at pH values of 5 or above is so consistent that one can frequently use its presence to predict the pH of the water when a pH electrode and meter are unavailable. A classic example is the caved portal at the Gem Mine (often called the Paradise portal), in the San Juan Mountains of southwestern Colorado, which has been discharging mine water continuously with a pH of 5.5 ± 0.3 for more than 30 years. This site has a striking white precipitate, affectionately known as "white death," that consists primarily of aluminum, sulfate, and water (Nordstrom et al., 1984); anomalous concentrations of lanthanide elements have been found in this precipitate (Carlson-Foscz, 1991; Nordstrom et al., 1995).

As with the iron minerals, thermodynamic stability relations among the aluminum minerals and their kinetic rates of formation can vary greatly, depending upon sulfate concentration, salinity, pH, particle size, and temperature. Precipitation rates for some of these aluminous minerals may be sluggish so that the equilibrium conditions are not often reached in surface waters. In soil and ground waters, longer residence times favor solubility control by mineral-solution equilibria.

Other metals—Native metals, oxides, and hydroxides of several other metals such as copper, nickel, manganese, silver, gold, and mercury may occur from the weathering and oxidation of primary sulfide minerals (Table 6.8). These minerals tend to occur as residual products in oxidized zones (gossans and leached cappings), where many pore volumes of water have reacted with the formerly mineralized rocks. It is unlikely that these phases exert solubility control on large volumes of water, but rather they are likely to form during dry periods when isolated microenvironments may reach saturation with a given native metal, oxide or hydroxide. The absence of discrete trace-metal-bearing oxides and hydroxides in most oxidized mine wastes suggests that other mechanisms, such as adsorption or coprecipitation with hydrous iron oxides, limit the concentrations of dissolved trace metals in mining environments (see Smith, 1999).

The behavior of nickel in tailings impoundments and acid-mine-drainage precipitates illustrates that the fate of trace metals in mine drainage settings is generally tied to that of the major elements, particularly iron. Mineralogical analysis and microanalysis by Jambor and co-workers as part of a study on the Copper Cliff tailings area at Sudbury, Ontario, has indicated that nickel tends to occur dispersed in hydrous iron oxides forming alteration rims on pentlandite and nickeliferous pyrrhotite, rather than as discreet nickel oxide or hydroxide phases (Alpers et al., 1994b). Overall, the bulk of the nickel liberated by oxidation of these sulfides ends up in goethite, a part of the nickel remains in solution and is transported from the site of oxidation, a small amount is taken up by vermiculite and associated mixed-layer silicates that replace biotite, and some may occur as secondary violarite (see Supergene and Diagenetic Sulfides section, below), which is expected to occur but has not yet been found in the Copper Cliff tailings (Alpers et al., 1994b).

Copper oxides, particularly tenorite and cuprite, are known to form in the oxidized zone of sulfide deposits and are indicative of low pyrite content and(or) a high wallrock neutralization capacity (Loghry, 1972; Anderson, 1982). The behavior of copper in tailings impoundments and waste-rock piles is similar to that of nickel in that discrete secondary copper oxides are rarely formed; rather the copper is either transported away from the oxidized zone in solution, is fixed in other secondary phases such as sulfates, carbonates, or silicates, or is coprecipitated and(or) adsorbed to hydrous iron oxides.

Manganese oxides and hydroxides are known to form from acid mine drainage, often at considerable distance from the source(s) of sulfide oxidation and acid formation. Krauskopf (1957) pointed out that the redox and hydrolysis properties of iron and manganese are such that they sometimes behave differently under changing conditions of oxidation and reduction. Hem (1978, 1980) considered the effects of manganese oxidation and disproportionation on the coprecipitation of other trace metals with manganese oxides. He demonstrated the effect of manganese on the coprecipitation of CoO(OH) (Hem et al., 1985) and on the precipitation of zinc as hetaerolite, $ZnMn_2O_4$, at 25°C (Hem et al., 1987). He further discussed the possibility that low-temperature "ferrite" compounds may be responsible for the low concentrations of trace metals found in uncontaminated natural waters. Hem also made many other significant contributions to our understanding of the hydrolysis and precipitation of trace metals (Hem, 1985).

Manganese oxides are actively precipitating at Pinal Creek, Arizona, in the Globe-Miami mining district, and so provide an opportunity for study of geochemical processes controlling manganese solubility in a mine drainage setting. At Pinal Creek, an alluvial ground-water aquifer was contaminated by acidic recharge (pH about 2.7) from copper mining and smelting activities (Eychaner, 1991). After neutralization by interaction with the alluvial material, the contaminated ground-water emerges at near-neutral pH in a perennial reach of Pinal Creek, about 15 km downgradient from the acid source, at which point manganese-rich crusts have developed in the streambed. Chemical and XRD analyses (Lind, 1991) suggest that the manganese occurs as a mixture of two related hydrous oxides, takanelite and rancieite (see Table 6.8), plus an Mn-bearing carbonate, probably kutnohorite (see Table 6.12). The overall oxidation state of the manganese in the less-than-75 micrometer size fraction of the Pinal Creek precipitates was 3.65 (Lind, 1991). To test the hypothesis that neutralization of acidic Mn-bearing water would lead to formation of similar Mn-bearing minerals, titrations were made of Mn-rich ground waters from the Pinal Creek area with a 0.1 molar NaOH solution with and without CO_2 present; these experiments yielded hausmannite (which aged to manganite), kutnohorite, and a mixed Ca-Mn species similar to todorokite (Hem and Lind, 1993).

Soluble sulfates

Soluble sulfate minerals, often occurring as efflorescent salts, are common in mines, on mine tailings and waste rock, and on sulfide mineralization exposed to the air. These phases store metals and sulfate during dry periods and dissolve readily during flushing events, a process that has an important influence on temporal variations of metals in surface waters affected by mine wastes.

Iron sulfates—The most common efflorescent minerals are hydrated iron sulfate salts (Table 6.9). Based both on laboratory experiments of evaporating acid mine waters as well as field observations, the hydrated iron sulfate minerals seem to follow a paragenetic sequence as shown below (Buurman, 1975; Nordstrom, 1982a; C. Maenz, written commun., 1995).

melanterite (rozenite, szomolnokite)
↘
copiapite
↘
roemerite, coquimbite, kornelite
↘
rhomboclase
↘
voltaite, halotrichite

The formation of melanterite as the first phase to precipitate from the evaporation of many acid mine waters is consistent with the preponderance of aqueous ferrous iron in these waters. Reactions (2) and (3) indicate that aqueous ferrous iron and sulfate are the initial products of pyrite oxidation, and it is these ions that combine to form melanterite. The remaining iron sulfates in the generalized paragenetic sequence form as the solutions evaporate and the ferrous iron oxidizes to ferric; however, a simple progression from ferrous to ferric salts is not observed because of differences in solubility among the various salts and the influence of other major elements which substitute to a variable degree for divalent and trivalent iron, such as copper and zinc for ferrous iron and aluminum for ferric iron.

Copper tends to partition into melanterite in preference to zinc (Alpers et al., 1994a). The result of this partitioning is a tendency toward higher ratios of zinc/copper in residual solutions as melanterite and related phases form in the dry season, and then lower ratios of zinc/copper as the salts are flushed in the wet season (Alpers et al., 1994a).

Another important role of the soluble iron sulfates is to store acidity and oxidation potential in the form of hydronium and ferric ions. The mineral rhomboclase is essentially a solid form of sulfuric acid plus ferric sulfate. Although generally considered rare, large quantities of rhomboclase and other iron sulfate salts were found at Iron Mountain, California, in inactive underground mine workings within a volcanogenic massive sulfide deposit (Alpers and Nordstrom, 1991). The salts were observed to be actively forming from waters with pH values from 1 to less than -3 (Nordstrom et al., 1991; Alpers et al., 1991; Nordstrom and Alpers, 1999). Rhomboclase may be present in trace amounts in other settings where acid waters evaporate to dryness, providing a storage mechanism for hydronium ions. Other ferric-sulfate and mixed ferrous-ferric-sulfate salts have been found associated with mine wastes and spoils in numerous localities including coal and metal mines (e.g., Zodrov and McCandlish, 1978a, b; Zodrov et al., 1979; Cravotta, 1994; Plumlee et al., 1995).

Dissolution of these salts can create large quantities of very acid mine waters. Flooding of underground mines and mine wastes as a remedial measure may not result in short-term improvements in water quality because the ferric salts will dissolve and the ferric iron will hydrolyze (if pH is above 2.2), providing an oxidant that will cause continued sulfide oxidation (e.g., Cravotta, 1994).

Other metal sulfates—There are a large number of additional metal sulfates that occur as efflorescent minerals in weathered mineral deposits and mining environments. Some of the more common ones are listed in Table 6.10. One of the important aspects of these salts is that they are a solid form of acid mine drainage that is stored until the next rainstorm event when the salts can quickly dissolve and be transported to a drainage system. Dagenhart (1980) demonstrated that the concentrations of copper, zinc, iron, and aluminum increase sharply during the rising limb of the discharge as rain dissolves and flushes efflorescent salts from oxidizing tailings into a receiving stream. This phenomenon is probably common at mined sites and may be an important factor in the association of fish kills during periods of high runoff, especially after a significant dry period.

Less-soluble sulfates

Although there are a great many metal sulfate minerals of low solubility known to occur, the most common ones are barite, celestite, and anglesite (Table 6.11). These are likely to provide solubility controls for the concentrations of barium, strontium, and lead (see previous section on mineral solubilities, Fig. 6.4). Their low solubilities tend to immobilize these elements in the environment and make them less bioavailable than many of the other hazardous metals at mine sites. In particular, lead concentrations in acid mine drainage and tailings pore waters appear to be controlled at relatively low levels by anglesite solubility (e.g., Blowes and Jambor, 1990).

Carbonates

Many carbonate minerals occur as either primary or secondary minerals in mine wastes. Examples are given in Table 6.12. Carbonates may originate as an accessory gangue mineral that accompanies the mineral deposit and mine waste (mine working residuum, waste piles, tailings), as an amended material for neutralization, or as a secondary product from weathering of wastes or amendments. Carbonate minerals are important as neutralizers of acid in mine drainage (Blowes and Ptacek, 1994). Siderite forms as a secondary phase in tailings impoundments where calcite reacts with Fe(II)-rich solutions (Ptacek and Blowes, 1994). The hydroxyl-bearing carbonates in Table 6.13 form as secondary minerals in the oxidation of Zn-Cu-Pb ores and related mine wastes.

Supergene and diagenetic sulfides

The supergene enrichment process that affects primary sulfide ores may also be a factor in redistribution of metals in mine waste environments, particularly tailings impoundments. Supergene alteration of copper- and nickel-sulfide deposits has resulted in

enrichment of ore grades by oxidation and leaching of metals in the unsaturated zone above the water table followed by transport of metals to a zone of more reducing conditions where secondary sulfide minerals are formed (Anderson, 1982; Alpers and Brimhall, 1989). A list of some supergene copper and nickel minerals is given in Table 6.13. The two compositions for djurleite are based on the investigation by Potter (1977). An example of active supergene enrichment in a tailings impoundment is the presence of secondary covellite near the depth of active oxidation at Waite Amulet, Ontario (Blowes and Jambor, 1990).

Diagenetic processes affect mine drainage geochemistry in areas where reducing conditions can lead to sulfate reduction and the formation of secondary sulfides. The sulfides are generally insoluble, so this represents a plausible geochemical mechanism for metal fixation in mine workings, anoxic wetlands, and lake bottoms, if reducing conditions are maintained. Iron is commonly the most abundant transition metal and therefore is the most likely metal to combine with H_2S to produce secondary sulfides in environments affected by mine drainage. Other divalent metals present will also tend to form secondary sulfides, as indicated in Table 6.13. The relative solubility of metal sulfides, starting from the most soluble, is: MnS > FeS > NiS ~ ZnS > CdS ~ PbS > CuS > HgS (DiToro et al., 1991).

A summary of mineralogic controls on metal concentrations

As a guide to the aqueous geochemistry for acid mine waters, we have compiled a list of minerals in Table 6.14 that might be important in governing metal concentrations. This list is drawn from our experience in modeling and interpreting mine water chemistry and is meant as a guide rather than a strict protocol. The two columns in Table 6.14 show those minerals most likely to have a solubility control and those less likely but possible.

SUMMARY

Physical, chemical, and biological processes all play important roles in the production, release, mobility, and attenuation of contaminants in acid mine waters. Physical aspects include the geology (geomorphology, structure, petrology, geophysical features), the hydrology (water budget, porosity, permeability, flow direction, flow rate, dispersion, mixing, surface transport characteristics), and the effects of mining and mineral processing. The specific processes that have been studied and found to contribute to the overall phenomenon of acid mine water geochemistry are:

1) pyrite oxidation
2) oxidation of other sulfides
3) oxidation and hydrolysis of aqueous iron and other elements
4) neutralizing capacity of gangue minerals and country rock
5) neutralizing capacity of bicarbonate-buffered waters
6) oxygen transport
7) fluid transport of water and water vapor
8) form and location of permeable zones relative to flow paths
9) climatic variations (diel, storm events, seasonal)
10) evaporation, efflorescence, redissolution
11) heating by conduction and radiation (due to a variety of exothermic reactions including pyrite oxidation, dissolution of soluble salts, and dilution of concentrated acid)
12) temperature
13) microbial catalysis of reaction rates
14) microbial sorption and uptake of metals
15) mineral precipitation and dissolution during transport
16) adsorption and desorption of metals during transport
17) photoreduction of iron
18) organic complexing
19) microenvironmental processes (surface films, microbial films, mineral coatings)

TABLE 6.14—Minerals whose solubilities might control metal concentrations in mine waters.

Solubility equilibrium likely	Solubility equilibrium difficult but possible
alunogen	alunite
anglesite	ankerite
barite	antlerite
basaluminite (amorphous)	atacamite, paratacamite
calcite	azurite
cerussite	bronchantite
chalcanthite	chrysocolla
epsomite	goethite
ferrihydrite	hemimorphite
gibbsite (amorphous to microcrystalline)	hematite
goslarite	hydrozincite
gypsum	jarosite
halotrichite-pickeringite	kaolinite
manganese oxides	kutnohorite
melanterite	malachite
otavite	natroalunite
rhodochrosite	natrojarosite
schwertmannite	plumbojarosite
scorodite	
siderite	
silica (microcrystalline)	
smithsonite	
witherite	

Many of these processes are represented schematically on Figure 6.7. Perhaps the most important factors affecting the production of acid mine waters are the amount, concentration, grain size, and distribution of pyrite present in a mine, tailings, or waste pile. The rate of oxidation can vary depending on the accessibility of air, moisture, and microbes to the pyrite surfaces and the neutralizing capacity of available buffering materials. These complex geochemical processes can be modeled with either equilibrium or kinetic principles to estimate the result of pyrite oxidation, carbonate buffering, and silicate hydrolysis (see Chapter 14 on geochemical modeling). Modeling calculations of this type have been done for pyritic rocks and waters of different initial compositions (e.g., Lichtner, 1994). Modeling calculations, however, are well-educated guesses. There will always be inadequate data and contentious ambiguities in the conclusions. The advantage of modeling is that it can take into account some of the complex interactions between hydrology, geochemistry, geology, and other site characteristics as well as performing database management. This advantage is a major step beyond various acid-base accounting, static, and kinetic tests for which comparison, evaluation, and agreement is lacking (White and Jeffers, 1994).

The geochemistry of acid mine waters is a complex subject that draws upon many technical disciplines. Although considerable

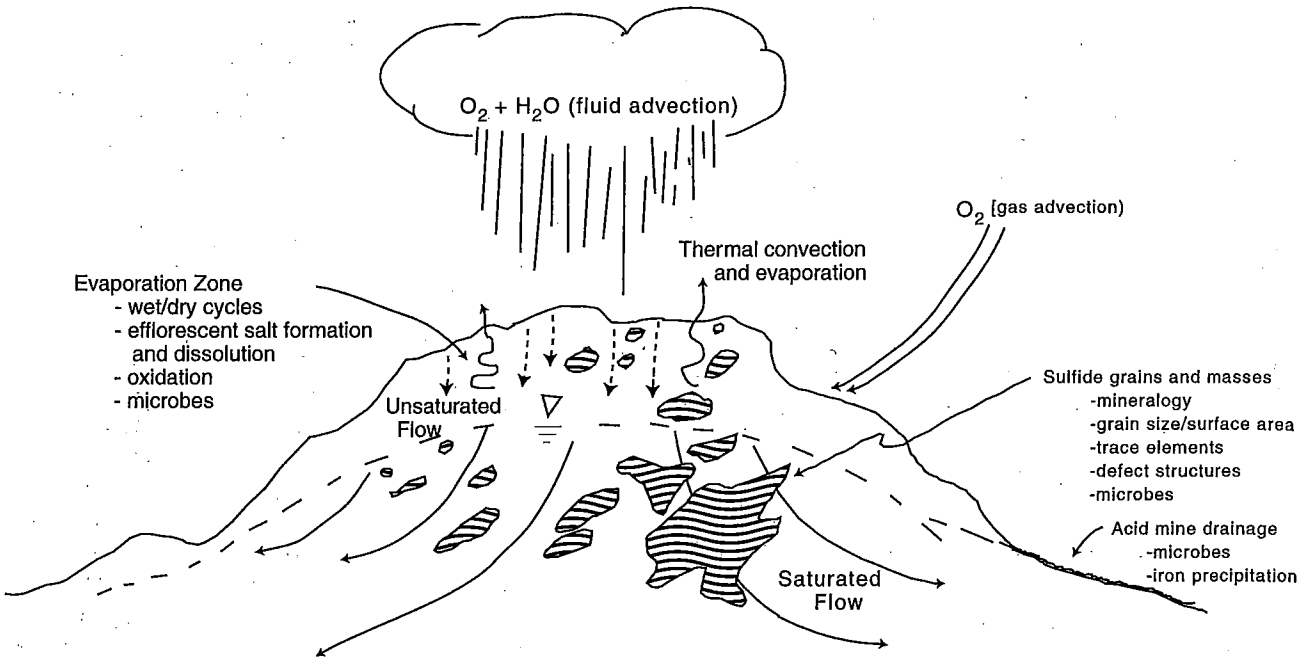

FIGURE 6.7—Schematic diagram depicting a hypothetical tailings or waste pile or mineralized site, showing the various materials and processes involving reaction and flow.

research has been accomplished on this subject, surprises and new challenges continue to appear. Inadequate recognition of the importance of the multi-disciplinary nature of the subject can result in inappropriate or even dangerous remediation measures. In this arena, as with many other environmental problems, the quick fixes are rare; complexity and heterogeneity of this environment along with high-cost, high-risk options are the rule. A cautious, phased, and iterative approach to both site characterization and remediation would seem most warranted.

ACKNOWLEDGMENTS—We are deeply indebted to Geoff Plumlee and the Society of Economic Geologists for inviting us to participate in this short course and for showing enormous patience with our unanticipated delays. The reviewers, David Blowes, Briant Kimball, Geoff Plumlee, Teresa Rogers, and Katie Walton-Day were most helpful in catching errors and mistakes and in asking for important points of clarification. Their comments led to significant improvements in the manuscript. Finally, we would like to acknowledge all the students and colleagues with whom we have shared both sweat and joy in attempting to demystify some of the secrets of mine water geochemistry.

REFERENCES

Adams, F. and Rawajfih, Z., 1977, Basaluminite and alunite—A possible cause of sulfate retention by acid soils: Soil Science Society of America Journal, v. 41, pp. 686–692.

Agricola, G., 1546, De Natura Fossilium (Textbook of Mineralogy), translated by Bandy, M.C., and Bandy, J.A., 1955: Geological Society of America Spec. Pub. No. 63, 240 pp.

Agricola, G., 1556, De Re Metallica, translated by Hoover, H.C., and Hoover, L.H., 1950: Dover Publications, New York, 638 pp.

Alpers, C.N., and Brimhall, G.H., 1989, Paleohydrologic evolution and geochemical dynamics of cumulative supergene metal enrichment at La Escondida, Atacama Desert, northern Chile: Economic Geology, v. 84, pp. 229–255.

Alpers, C.N., and Nordstrom, D.K., 1991, Geochemical evolution of extremely acid mine waters at Iron Mountain, California—Are there any lower limits to pH?; *in* Proceedings, 2nd Internl Conference on the Abatement of Acidic Drainage, Montreal, Quebec, Canada: CANMET, Ottawa, Sept. 16–18, 1991, v. 2, pp. 324–342.

Alpers, C.N., and Nordstrom, D.K., 1999, Geochemical modeling of water-rock interactions in mining environments; *in* Plumlee, G.S., and Logsdon, M.J. (eds.), The Environmental Geochemistry of Mineral Deposits, Part A. Processes, Techniques, and Health Issues: Society of Economic Geologists, Reviews in Economic Geology, v. 6A, pp. 289–323.

Alpers, C.N., Nordstrom, D.K., and Ball, J.W., 1989, Solubility of jarosite solid solutions precipitated from acid mine waters, Iron Mountain, California, U.S.A.: Sciences Géologiques Bulletín, v. 42, pp. 281–298.

Alpers, C.N., Meinz, C., Nordstrom, D.K., Erd, R.C., and Thompson, J.M., 1991, Storage of metals and acidity by iron-sulfate minerals associated with extremely acidic mine waters from Iron Mountain, California [abs.]: Geological Society of America Annual Meeting, Abstracts with Programs, v. 23, no. 5, p. A383.

Alpers, C.N., Rye, R.O., Nordstrom, D.K., White, L.D., and King, B.-S., 1992, Chemical, crystallographic, and isotopic properties of alunite and jarosite from acid hypersaline Australian lakes: Chemical Geology, v. 96, pp. 203–226.

Alpers, C.N., Nordstrom, D.K., and Thompson, J.M., 1994a, Seasonal variations of Zn/Cu ratios in acid mine waters from Iron Mountain, California; *in* Alpers, C.N., and Blowes, D.W. (eds.), Environmental Geochemistry of Sulfide Oxidation: American Chemistry Society Symposium Series 550, Washington, D.C., pp. 324–344.

Alpers, C.N., Blowes, D.W., Nordstrom, D.K., and Jambor, J.L., 1994b, Secondary minerals and acid mine-water chemistry; *in* Jambor, J.L., and Blowes, D.W. (eds.), The Environmental Geochemistry of Sulfide Mine-Wastes: Mineralogical Association of Canada, Nepean, Ontario, Short Course Handbook, v. 22, pp. 247–270.

Anderson, J.A., 1982, Characteristics of leached capping and techniques of appraisal; *in* Titley, S.R. (ed.), Advances in Geology of the Porphyry Copper Deposits, Southwestern North America, Tucson: University of Arizona Press, Tucson, pp. 275–295.

Anthony, J.W., and MacLean, W.J., 1976, Jurbanite, a new post-mine aluminum sulfate mineral from San Manuel, Arizona: American Mineralogist, v. 61, pp. 1–4.

Appalachian Regional Commission, 1969, Acid mine drainage in Appalachia: Report to the President, 126 pp.

Ash, S.H., Felegy, E.W., Kennedy, D.O., and Miller, P.S., 1951, Acid mine drainage problems—Anthracite region of Pennsylvania: U.S. Bureau of Mines Bulletin 508, 72 pp.

Ball, J.W., and Nordstrom, D.K., 1989, Final revised analyses of major and trace elements from acid mine waters in the Leviathan mine drainage basin, California and Nevada—October 1981 to October 1982: U. S. Geological Survey Water-Resources Investigations Report 89–4138, 46 pp.

Ball, J.W., and Nordstrom, D.K., 1991, User's manual for WATEQ4F, with revised thermodynamic data base and test cases for calculating speciation of major, trace, and redox elements in natural waters: U.S. Geological Survey Open-File Report 91–183, 189 pp., plus diskette.

Ball, J.W., and Nordstrom, D.K., 1994, A comparison of simultaneous plasma, atomic absorption, and iron colorimetric determinations of major and trace constituents in acid mine waters: U.S. Geological Survey Water-Resources Investigations Report 93–4122, 151 pp.

Barton, P., 1978, The acid mine drainage; *in* Nriagu, J.O. (ed.), Sulfur in the Environment, Part II. Ecological Impacts: John Wiley and Sons, New York, pp. 313–358.

Basolo, F., and Pearson, R.G., 1967, Mechanisms of inorganic reactions—A study of metal complexes in solution, 2nd ed.: John Wiley and Sons, New York, 701 pp.

Beck, J.V., 1977, Chalcocite oxidation by concentrated cell suspensions of *Thiobacillus ferrooxidans*; *in* Schwartz, W. (ed.), Conference Bacterial Leaching 1977: GBF, Verlag Chemie, Weinheim, pp. 119–128.

Bennett, J.C., and Tributsch, H., 1978, Bacteria leaching patterns on pyrite crystal surface: Journal of Bacteriology, v. 134, pp. 310–326.

Bergholm, A., 1955, Oxidation of pyrite: Jernkontorets Annallen, v. 139, pp. 531–549.

Berner, R.A., 1969, Goethite stability and the origin of red beds: Geochimica et Cosmochimica Acta, v. 33, pp. 267–273.

Berner, R.A., 1971, Principles of chemical sedimentology: McGraw-Hill Book Company, New York, 240 pp.

Berner, R.A., 1981, A new geochemical classification of sedimentary environments: Journal of Sedimentary Petrology, v. 51, pp. 359–365.

Bertsch, P.M. and Parker, D.R., 1996, Aqueous polynuclear aluminum species; *in* Sposito, G., (ed.), The Environmental Chemistry of Aluminum, 2nd ed.: CRC Press/Lewis Publishers, Boca Raton, Fla., pp. 117–168.

Biernacki, A., 1978, Fish kills caused by pollution—Fifteen year summary 1961–1975: U.S. Environmental Protection Agency Report EPA-440/4–78–011, 78 pp.

Bigham, J.M., 1994, Mineralogy of ochre deposits formed by sulfide oxidation; *in* Jambor J.L., and Blowes, D.W., (eds.), The Environmental Geochemistry of Sulfide Mine-Wastes: Mineralogical Association of Canada, Nepean, Ontario, Short Course Handbook, v. 22, pp. 103–132.

Bigham, J.M., Schwertmann, U., Carlson, L., and Murad, E., 1990, A poorly crystallized oxyhydroxysulfate of iron formed by bacterial oxidation of Fe(II) in acid mine waters: Geochimica et Cosmochimica Acta, v. 54, pp. 2743–2758.

Blanchard, R., 1968, Interpretation of leached outcrops: Nevada Bureau of Mines Bulletin, v. 66, 196 pp.

Blowes, D.W., 1990, The geochemistry, hydrogeology, and mineralogy of decommissioned sulfide tailings—A comparative study: Unpub. Ph.D. thesis, Univ. of Waterloo, Ontario, Canada, 635 pp.

Blowes, D.W., and Jambor, J.L., 1990, The pore-water geochemistry and the mineralogy of the vadose zone of sulfide tailings, Waite Amulet, Quebec, Canada: Applied Geochemistry, v. 5, pp. 327–346.

Blowes, D.W., and Ptacek, C.J., 1994, Acid-neutralization mechanisms in inactive mine tailings; *in* Jambor, J.L., and Blowes, D.W., (eds.), The Environmental Geochemistry of Sulfide Mine-Wastes: Mineralogical Association of Canada, Nepean, Ontario, Short Course Handbook, v. 22, pp. 271–292.

Blowes, D.W., Reardon, E.J., Jambor, J.L, and Cherry, J.A., 1991, The formation and potential importance of cemented layers in inactive sulfide mine tailings: Geochimica et Cosmochimica Acta, v. 55, pp. 965–978.

Blowes, D.W., Al, T., Lortie, L., Gould, W.D., and Jambor, J.L., 1995, Microbiological, chemical, and mineralogical characterization of the Kidd Creek mine tailings impoundment, Timmins area, Ontario: Geomicrobiology Journal, v. 13, pp. 13–31.

Braeuning, E., 1977, Mine water development in the lead and zinc deposits of Bawdwin, Burma; *in* 2nd Internl Symposium on Water-Rock Interaction: Strasbourg, France, pp. 1237–1245.

Braley, S.A., 1954, Summary of report of Commonwealth of Pennsylvania, No. 326–B: Department of Health, Industrial Fellowship, Mellon Institute, 279 pp.

Bricker, O.P., 1982, Redox potential—Its measurement and importance in water systems; *in* Minear, R.A., and Keith, L H. (eds.), Water Analysis, v. 1, Inorganic Species, Part 1: Academic Press, New York, pp. 55–83.

Brierley, C.L., and Murr, L.E., 1973, Leaching—Use of a thermophilic and chemoautotrophic microbe: Science, v. 179, pp. 488–489.

Brierley, J.A., and Le Roux, N.W., 1977, A facultative thermophilic *Thiobacillus*-like bacterium—Oxidation of iron and pyrite; *in* Schwartz, W. (ed.), Conference Bacterial Leaching 1977: GBF, Verlag Chemie, Weinheim, pp. 55–66.

Brophy, G.P., and Sheridan, M.E., 1965, Sulfate studies IV. The jarosite-natrojarosite-hydronium jarosite solid solution series: American Mineralogist, v. 50, pp. 1595–1607.

Brophy, G.P., Scott, E.S., and Snellgrove, R.A., 1962, Sulfate studies II. Solid solution between alunite and jarosite: American Mineralogist, v. 47, pp. 112–126.

Brown, A.D., and Jurinak, J.J., 1989, Mechanisms of pyrite oxidation in aqueous mixtures: Journal of Environmental Quality, v. 18, pp. 545–550.

Bryner, L.C., Beck, J.F., Davis, D.B., and Wilson, D.G., 1954, Microorganisms in leaching sulfide minerals: Industrial and Engineering Chemistry, v. 46, pp. 2587–2592.

Burke, S.P., and Downs, W.R., 1938, Oxidation of pyrite sulfur in coal mines: American Institute of Mining, Metallurgical, and Petroleum Engineering, v. 130, pp. 425–444.

Buurman, P., 1975, *In vitro* weathering products of pyrite: Geologie en Mijnvouw, v. 54, pp. 101–105.

Burkstaller, J.E., McCarty, P., and Parks, G.A., 1975, Oxidation of cinnabar by Fe(III) in acid mine waters: Environmental Science and Technology, v. 9, p. 676–678.

Carlson, L., and Schwertmann, U., 1981, Natural ferrihydrites in surface deposits from Finland and their association with silica: Geochimica et Cosmochimica Acta, v. 4, pp. 421–429.

Carlson-Foscz, V., 1991, Rare earth element mobility in acid mine drainage, Ophir region, San Juan Mountains, Colorado: Unpub. M.S. thesis, Dartmouth College, Dartmouth, N.H., 71 pp.

Carpentor, L.V., and Herndon, L.K., 1933, Acid mine drainage from bituminous coal mines: West Virginia University Engineering Exploration Station Research Bulletin No. 19, 38 pp.

Carrucio, F.T., 1970, The quantification of reactive pyrite by grain size distribution—3rd Symposium on Coal Mine Drainage Research: National Coal Association/Bituminous Coal Research, pp. 123–131.

Carrucio, F.T., Geidel, G., and Sewell, J. M., 1976, The character of drainage as a function of the occurrence of framboidal pyrite and ground water quality in eastern Kentucky—6th Symposium on Coal Mine Drainage Research: National Coal Association/Bituminous Coal Research, pp. 1–16.

Carson, C.D., Fanning, D.S., and Dixon, J.B., 1982, Alfisols and ultisols with acid sulfate weathering features in Texas; *in* Kittrick, J.A., Fanning, D.S., and Hossner, L.R. (eds.), Acid Sulfate Weathering: Soil Science Society of America Spec. Pub. No. 10, Madison, Wis., pp. 127–146.

Cathles, L.M., 1994, Attempts to model the industrial-scale leaching of copper-bearing mine waste; *in* Alpers, C.N., and Blowes, D.W. (eds.), Environmental Geochemistry of Sulfide Oxidation: American Chemical Society Symposium Series 550, Washington, D.C., pp. 123–131.

Cathles, L.M., and Apps, J.A., 1975, A model of the dump leaching process that incorporates oxygen balance, heat balance, and air convection: Metallurgical Transactions B, v. 6B, p. 617–624.

Chen, K.Y., and Morris, J.C., 1971, Oxidation of aqueous sulfide by O_2, 1. General characteristics and catalytic influences: Proceedings of the 5th Internatl Water Pollution Research Conference, III–32, pp. 1–17.

Chen, K.Y., and Morris, J.C., 1972, Kinetics of oxidation of aqueous sulfide by O_2: Environmental Science and Technology, v. 6, pp. 529–537.

Chukhrov, F., Zvijagin, B.B., Gorshkov, A.I., Erilova, L.P., and Balashova, V.V., 1973, Ferrihydrite: Izvetzia Akadamik Nauklady SSSR Series Geology, v. 4, pp. 23–33.

Clark, C.S., 1966, Oxidation of coal mine pyrite: Journal of Sanitary Engineering Division, Proceedings of American Society of Civil Engineers, v. 92, pp. 127–145.

Clarke, F.W., 1916, The data of geochemistry, 3rd ed.: U.S. Geological Survey Bulletin 616, 821 pp.

Colmer, A.R., and Hinkle, M.E., 1947, The role of microorganisms in acid mine drainage: Science, v. 106, pp. 253–256.

Colmer, A.R., Temple, K.L., and Hinkle, M.E., 1950, An iron-oxidizing bacterium from the acid drainage of some bituminous coal mines: Journal of Bacteriology, v. 59, pp. 317–328.

Cravotta, C.A. III, 1994, Secondary iron-sulfate minerals as sources of sulfate and acidity; *in* Alpers, C.N., and Blowes, D.W. (eds.), Environmental Geochemistry of Sulfide Oxidation: American Chemical Society Symposium Series 550, Washington, D.C., pp. 345–364.

Dagenhart, T.V., Jr., 1980, The acid mine drainage of Contrary Creek, Louisa County, Virginia: Factors causing variations in stream water chemistry: Unpub. M.S. thesis, Univ. of Virginia, 215 pp.

Devasia, P., Natarajan, K.A., Sathayanarayana, D.N., and Rao, G.R., 1993, Surface chemistry of *Thiobacillus ferrooxidans* relevant to adhesion on mineral surfaces: Applied and Environmental Microbiology, v. 59, pp. 4051–4055.

DiToro, D.M., Mahony, J.D., Hanson, D.J., Scott, K.J., Hicks, M.B., Mayr, S.M., and Redmond, M.S., 1991, Toxicity of cadmium in sediments: The role of acid volatile sulfide: Environmental and Toxicological Chemistry, v. 9, pp. 1487–1502.

Dugan, P.R., 1972, Biochemistry of acid mine drainage; *in* Biochemical Ecology of Water Pollution: Plenum Press, New York, pp. 123–137.

Dugan, P.R., MacMillan, C.B., and Pfister, R.M., 1970, Aerobic heterotrophic bacteria indigenous to pH 2.8 acid mine water, I. Microscopic examination of acid streamers, II. Predominant slime-producing bacteria in acid streamers: Journal of Bacteriology, v. 101, p. 973–988.

Dutrizac, J.E., 1983, Factors affecting alkali jarosite precipitation: Metallurgical Transactions B, v. 14B, p. 531–539.

Dutrizac, J.E., and Kaiman, S., 1976, Synthesis and properties of jarosite-type compounds: Canadian Mineralogist, v. 14, pp. 151–158.

Dzombak, D.A., and Morel, F.F., 1990, Surface complexation modeling—Hydrous ferric oxide: John Wiley and Sons, New York, 545 pp.

Ehrlich, H.L., 1963a, Bacterial action on orpiment: Economic Geology, v. 58, pp. 991–994.

Ehrlich, H.L., 1963b, Microorganisms in acid drainage from a copper mine: Journal of Bacteriology, v. 86, pp. 350–352.

Ehrlich, H.L., 1964, Bacterial oxidation of arsenopyrite and enargite: Economic Geology, v. 59, p. 1306–1308.

Elberling, B., Nicholson, R.V., and David, D., 1993, Field evaluation of sulfide oxidation rates: Nordic Hydrology, v. 24, p. 323–338.

Evangelou, V.P. (Bill), 1995, Pyrite oxidation and its control: CRC Press, Boca Raton, Fla., 285 pp.

Eychaner, J.H., 1991, The Globe, Arizona research site—Contaminants related to copper mining in a hydrologically integrated environment; *in* Mallard, G.E., and Aronson, D.A., (eds.), Proceedings, U.S. Geological Survey Toxic Substances Hydrology Program: U.S. Geological Survey Water-Resources Investigations Report 91–4034, pp. 439–447.

Federal Water Pollution Control Administration, 1968, Pollution caused fish kills—1967: 8th Annual Report, Washington, D.C., 16 pp.

Fox, L.E., 1988, The solubility of colloidal ferric hydroxide and its relevance to iron concentrations in river water: Geochimica et Cosmochimica Acta, v. 52, pp. 771–777.

Garrels, R.M., 1954, Mineral species as functions of pH and oxidation potentials with special reference to the zone of oxidation and secondary enrichment of sulfide ore deposits: Geochimica et Cosmochimica Acta, v. 5, pp. 153–168.

Garrels, R.M., and Christ, C.M., 1965, Solutions, minerals, and equilibria: Freeman and Cooper, New York, 450 pp.

Garrels, R.M., and Thompson, M.E., 1960, Oxidation of pyrite by iron sulfate solutions: American Journal of Science, v. 258A, pp. 57–67.

Goldberg, S., Davis, J.A., and Hem, J.D., 1995, The surface chemistry of aluminum oxides and hydroxides; *in* Sposito, G., (ed.), The Environmental Chemistry of Aluminum, 2nd ed.: CRC Press/Lewis Publishers, Boca Raton, Fla., pp. 271–332.

Goldhaber, M.B., 1983, Experimental study of metastable sulfur oxyanion formation during pyrite oxidation at pH 6–9 and 30°C: American Journal of Science, v. 283, pp. 193–217.

Goleva, G.A., 1977, Hydrogeochemistry of ore elements: Nedra, Moscow, 215 pp.

Goleva, G.A., Polyakov, V.A., and Nechayeva, T.P., 1970, Distribution and migration of lead in ground waters: Geochemistry International, v. 7, pp. 256–268.

Gould, W.D., Béchard, G., and Lortie, L., 1994, The nature and role of microorganisms in the tailings environment; *in* Jambor, J.L., and Blowes, D.W. (eds.), The Environmental Geochemistry of Sulfide Mine-Wastes: Mineralogical Association of Canada, Short Course Handbook, v. 22, pp. 185–200.

Granger, H.C., and Warren, C.G., 1969, Unstable sulfur compounds and the origin of roll-type uranium deposits: Economic Geology, v. 64, pp. 160–171.

Harries, J.R., and Ritchie, A.I.M., 1981, The use of temperature profiles to estimate the pyritic oxidation rate in a waste rock dump from an open-cut mine: Water, Air, and Soil Pollution, v. 15, pp. 405–423.

Hem, J.D., 1961, Stability field diagrams as aids in iron chemistry studies: Journal American Water Works Association, Feb., 1961, pp. 211–232.

Hem, J.D., 1978, Redox processes at surfaces of manganese oxide and their effects on aqueous metal ions: Chemical Geology, v. 21, pp. 199–218.

Hem, J.D., 1980, Redox coprecipitation mechanisms of manganese oxide; *in* Kavanaugh, M.C., and Leckie, J.O. (eds.), Particulates in Water: Advances in Chemistry Series 189, American Chemical Society, Washington, D.C., pp. 45–72.

Hem, J.D., 1985, Study and interpretation of the chemical characteristics of natural water, 3rd ed.: U.S. Geological Survey Water-Supply Paper 2254, 264 pp.

Hem, J.D., and Lind, C., 1993, Chemical processes in manganese oxide and carbonate precipitation in Pinal Creek, Arizona; *in* Morganwalp, D.W., and Aronson, D.A., (eds.), U.S. Geological Survey Toxic Substances Hydrology Program with Abstracts: U.S. Geological Survey Open-File Report 93–454, pp. 163.

Hem, J.D., and Roberson, C.E., 1990, Aluminum hydrolysis reaction and products in mildly acidic aqueous systems; *in* Melchior, D.C., and Bassett, R.L. (eds.), Chemical Modeling of Aqueous Systems II: American Chemical Society Symposium Series 416, Washington, D.C., pp. 430–446.

Hem, J.D., Roberson, C.E., and Lind, C.E., 1985, Thermodynamic stability of CoOOH and its coprecipitation with manganese: Geochimica et Cosmochimica Acta, v. 49, pp. 801–810.

Hem, J.D., Roberson, C.E., and Lind, C.E., 1987, Synthesis and stability of hetaerolite, $ZnMn_2O_4$, at 25°C: Geochimica et Cosmochimica Acta, v. 51, pp. 1539–1547.

Hemingway, B.S., and Sposito, G., 1996, Inorganic aluminum-bearing solid phases; *in* Sposito, G. (ed.), The Environmental Chemistry of

Aluminum, 2nd ed.: CRC Press/Lewis Publishers, Boca Raton, Fla., pp. 81–116.
Hostetler, J.D., 1984, Electrode electrons, aqueous electrons, and redox potentials in natural waters: American Journal of Science, v. 294, pp. 734–759.
Joseph, J.M., 1953, Microbiological study of acid mine waters—Preliminary report: Ohio Journal of Science, v. 53, pp. 123–127.
Kämpf, N., and Schwertmann, U., 1982, Goethite and hematite in a clino-sequence in southern Brazil and their application in classification of kaolinitic soils: Geoderma, v. 29, pp. 27–39.
Kelly, D.P., Norris, P.R., and Brierly, C.L., 1979, Microbiological methods for extractions and recovery of metals: Symposium on Microbial Technology, Society of General Microbiology, v. 29, pp. 263–308.
Khalid, A.M., and Ralph, B.J., 1977, The leaching behavior of various zinc sulphide minerals with three *Thiobacillus* species; *in* Schwartz, W. (ed.), Conference Bacterial Leaching 1977: GBF, Verlag Chemie, Weinheim, p. 165–173.
Kimball, B.A., Broshears, R.A., McKnight, D.M., and Bencala, K.E., 1994, Effects of instream pH modification on transport of sulfide-oxidation products; *in* Alpers, C.N., and Blowes, D.W. (eds.), Environmental Geochemistry of Sulfide Oxidation: American Chemical Society Symposium Series 550, Washington, D.C., pp. 224–243.
Kleinmann, R.L.P., 1989, Acid mine drainage in the United States—Controlling the impact on streams and rivers: 4th World Congress on the Conservation of the Built and Natural Environments, Univ. of Toronto, pp. 1–10.
Konishi, Y., Asai, S., and Sakai, H.K., 1990, Bacterial dissolution of pyrite by *Thiobacillus ferrooxidans*: Bioprocess Engineering, v. 5, pp. 5–17.
Krauskopf, K.B., 1957, Separation of iron and manganese in sedimentary processes: Geochimica et Cosmochimica Acta, v. 12, pp. 61–84.
Krauskopf, K.B., 1967, Introduction to geochemistry, 1st ed.: McGraw-Hill Book Company, New York, 617 pp.
Krauskopf, K.B. and Bird, D.K., 1995, Introduction to geochemistry, 3rd ed.: McGraw-Hill Book Company, New York, 647 pp.
Krumbein, W.C., and Garrels, R.M., 1952, Origin and classification of chemical sediments in terms of pH and oxidation-reduction potentials: Journal of Geology, v. 60, pp. 1–33.
Kubisz, J., 1960, Hydronium jarosite—$(H_3O)Fe_3(SO_4)_2(OH)_6$: Bulletin Academia Polonia, Science, Series Science Geology and Geography, v. 8, no. 2, pp. 95–99.
Kubisz, J., 1961, Natural hydronium jarosites: Bulletin Academia Polonia, Science, Series Science Geology and Geography, v. 9, no. 4, pp. 195–200.
Kubisz, J., 1964, Minerals of the alunite-jarosite group: Polonia Academia Nauk, Prace Geologia, v. 22, pp. 1–93 (in Polish).
Kubisz, J., 1970, Studies on synthetic alkali-hydronium jarosites, I. Synthesis of jarosite and natrojarosite: Mineralogia Polonia, v. 1, pp. 45–57.
Kushner, D.J. (ed.), 1978, Microbial life in extreme environments: Academic Press, New York, 465 pp.
Kwong, Y.T.J., 1995, Influence of galvanic sulfide oxidation on mine water chemistry; *in* Hynes, T.P., and Blanchette, M.C. (eds.), Proceedings of Sudbury '95—Mining and the Environment, v. 2, May 28–June 1, Sudbury, Ontario: CANMET, Ottawa, pp. 477–484.
Lacey, D.T., and Lawson, F., 1977, Kinetics of the liquid-phase oxidation of acid ferrous sulfate by the bacterium *Thiobacillus ferrooxidans*: Biotechnology and Bioengineering, v. 12, pp. 29–50.
Lackey, J.B., 1938, The flora and fauna of surface waters polluted by acid mine drainage: Public Health Report 53, pp. 1499–1507.
Landesman, J., Duncan, D.W., and Walden, C.C., 1966, Oxidation of inorganic sulfur compounds by washed cell suspensions of *Thiobacillus ferrooxidans*: Canadian Journal of Microbiology, v. 12, pp. 957–964.
Langmuir, D., 1969, The Gibbs free energies of substances in the system $Fe–O_2–H_2O–CO_2$: U.S. Geological Survey Professional Paper 650–B, pp. 180–184.
Langmuir, D., 1971, Particle size effect on the reaction goethite = hematite + water: American Journal of Science, v. 271, pp. 147–156.
Langmuir, D., 1972, Correction—Particle size effect on the reaction goethite = hematite + water: American Journal of Science, v. 272, pp. 972.
Le Roux, N.W., and Marshall, V.M., 1977, Effect of light on *Thiobacilli*; *in* Schwartz, W., (ed.), Conference Bacterial Leaching 1977: GBF, Verlag Chemie, Weinheim, pp. 21–35.
Lichtner, P.C., 1994, Time-space continuum formulation of supergene enrichment and weathering of sulfide-bearing ore deposits; *in* Alpers, C.N., and Blowes, D.W. (eds.), Environmental Geochemistry of Sulfide Oxidation: American Chemical Society Symposium Series 550, Washington, D.C., pp. 153–170.
Lind, C., 1991, Manganese minerals and associated fine particulates in the Pinal Creek streambed; *in* Mallard, G.E., and Aronson, D.A. (eds.), Proceedings, U.S. Geological Survey Toxic Substances Hydrology Program: U.S. Geological Survey Water-Resources Investigations Report 91–4034, pp. 486–491.
Lindberg, R.D., and Runnells, D.D., 1984, Ground water redox reactions—An analysis of equilibrium state applied to Eh measurements and geochemical modeling: Science, v. 225, pp. 925–927.
Lindgren, W., 1928, Mineral deposits, 3rd ed.: McGraw-Hill, New York, 1049 pp.
Locke, A., 1926, Leached outcrops as guides to copper ores: Williams and Wilkins Co., Baltimore, Md, 166 pp.
Loghry, J.D., 1972, Characteristics of favorable cappings from several southwestern porphyry copper deposits: Unpub. M.S. thesis, Univ. of Arizona, Tucson, 112 pp.
Lowson, R.T., 1982, Aqueous oxidation of pyrite by molecular oxygen: Chemical Reviews, v. 82, pp. 461–497.
Lundgren, D.G., Anderson, K.J., Remson, C.C., and Mahoney, R.P., 1964, Culture, structure and physiology of the chemoautotroph *Ferrobacillus ferrooxidans*: Developments in Industrial Microbiology, v. 6, pp. 250–259.
Luther, G.W., II, 1987, Pyrite oxidation and reduction—Molecular orbital theory considerations: Geochimica et Cosmochimica Acta, v. 51, pp. 3193–3199.
Luther, G.W., II, 1990, The frontier-molecular-orbital theory approach in geotechnical processes; *in* Stumm, W., (ed.), Aquatic Chemical Kinetics: John Wiley and Sons, Inc., New York, pp. 173–198.
Lyon, J.S., Hilliard, T.J., and Bethell, T.N., 1993, Burden of gilt: Mineral Policy Center, Washington, D.C., 68 pp.
Markosyan, G.E., 1972, A new iron-oxidizing bacterium *Leptospirillum ferrooxidans*: gen. et sp. nov. Biol. Zh. Arm. v. 25, p. 26 (in Russian).
Martin, H.W., and Mills, W.R., Jr, 1976, Water pollution caused by inactive ore and mineral mines: USEPA Contract Report 68–03–2212, 184 pp.
Mathews, C.T., and Robins, R.G., 1972, The oxidation of ferrous disulfide by ferric sulfate: Australian Chemical Engineering, v. 47, pp. 21–25.
Mathews, C.T., and Robins, R.G., 1974, Aqueous oxidation of iron disulfide by molecular oxygen: Australian Chemical Engineering, v. 15, pp. 19–24.
May, H.M., and Nordstrom, D.K., 1991, Assessing the solubilities and reactions kinetics of aluminous minerals in soils; *in* Ulrich, B., and Sumner, M.E. (eds.), Soil Acidity: Springer-Verlag, pp. 125–148.
McKay, D.R., and Halpern, J., 1958, A kinetic study of the oxidation of pyrite in aqueous suspension: Transactions of the Metallurgical Society AIME, v. 121, pp. 301–309.
McKibben, M.A., and Barnes, H.L., 1986, Oxidation of pyrite in low temperature acidic solutions—Rate laws and surface textures: Geochimica et Cosmochimica Acta, v. 50, pp. 1509–1520.
McKnight, D., and Bencala, K.E., 1988, Diel variations in iron chemistry in an acidic stream in the Colorado Rocky Mountains, U.S.A.: Arctic and Alpine Research, v. 20, pp. 492–500.
McKnight, D.M., and Bencala, K.E., 1989, Reactive iron transport in an acidic mountain stream in Summit County, Colorado—A hydrologic perspective: Geochimica et Cosmochimica Acta, v. 53, pp. 2225–2234.
McKnight, D.M., Kimball, B.A., and Bencala, K.E., 1988, Iron photoreduction and oxidation in an acidic mountain stream: Science, v. 240, pp. 637–640.

Mills, A.L., 1999, The role of bacteria in environmental geochemistry; *in* Plumlee, G.S., and Logsdon, M.J. (eds.), The Environmental Geochemistry of Mineral Deposits, Part A. Processes, Techniques, and Health Issues: Society of Economic Geologists, Reviews in Economic Geology, v. 6A, pp. 125–132.

Moore, J.N., and Luoma, S.N., 1990, Hazardous wastes from large-scale metal extraction: Environmental Science and Technology, v. 24, p. 1278–1285.

Moses, C.O., and Herman, J.S., 1991, Pyrite oxidation at circumneutral pH: Geochimica et Cosmochimica Acta, v. 55, pp. 471–482.

Moses, C.O., Nordstrom, D.K., and Mills, A.L., 1984, Sampling and analyzing mixtures of sulphate, sulphite, thiosulfate, and polythionate: Talanta, v. 31, pp. 331–339.

Moses, C.O., Nordstrom, D.K., Herman, J.S. and Mills, A.L., 1987, Aqueous pyrite oxidation by dissolved oxygen and by ferric iron: Geochimica et Cosmochimica Acta, v. 51, pp. 1561–1571.

Murad, E., Schwertmann, U., Bigham, J.M., and Carlson, L., 1994, Mineralogical characteristics of poorly crystallized precipitates formed by oxidation of Fe^{2+} in acid mine sulfate waters; *in* Alpers, C.N., and Blowes, D.W. (eds.), Environmental Geochemistry of Sulfide Oxidation: American Chemical Society Symposium Series 550, Washington, D.C., pp. 190–200.

Nathansohn, A., 1902, Über eine neue Gruppe von Schwefelbakterien und ihren Stoffwechsel: Mitt. Zool. Staatsmus. Neapel, v. 15, pp. 655–680.

Nicholson, R.V., 1994, Iron-sulfide oxidation mechanisms—Laboratory studies; *in* Jambor, J.L., and Blowes, D.W. (eds.), The Environmental Geochemistry of Sulfide Mine-Wastes: Mineralogical Association of Canada, Short Course Handbook, v. 22, pp. 163–183.

Nicholson, R.V., and Scharer, J.M., 1994, Laboratory studies of pyrrhotite oxidation kinetics; *in* Alpers, C.N., and Blowes, D.W. (eds.), Environmental Geochemistry of Sulfide Oxidation: American Chemical Society Symposium Series 550, Washington, D.C., pp. 14–30.

Nicholson, R.V., Gillham, R.W., and Reardon, E.J., 1988, Pyrite oxidation in carbonate-buffered solutions, 1. Experimental kinetics: Geochimica et Cosmochimica Acta, v. 52, pp. 1077–1085.

Nor, Y.M., and Tabatai, M.A., 1976, Oxidation of elemental sulfur in soils: Soil Science Society of America Journal, v. 41, pp. 736–741.

Nordstrom, D.K., 1982a, Aqueous pyrite oxidation and the consequent formation of secondary iron minerals; *in* Kittrick, J.A., Fanning, D.S., and Hossner, L.R., (eds.), Acid Sulfate Weathering: Soil Science Society of America Spec. Pub. No. 10, pp. 37–56.

Nordstrom, D.K., 1982b, The effects of sulfate on aluminum concentrations in natural waters—Some stability relations in the system Al_2O_3–SO_3–H_2O at 298 K: Geochimica et Cosmochimica Acta, v. 46, pp. 681–692.

Nordstrom, D.K., 1985, The rate of ferrous iron oxidation in a stream receiving acid mine effluent; *in* Selected Papers in the Hydrological Sciences: U.S. Geological Survey Water-Supply Paper 2270, pp. 113–119.

Nordstrom, D.K., 1991, Chemical modeling of acid mine waters in the western United States; *in* Mallard, G.E., and Aronson, D.A. (eds.), Proceedings, U.S. Geological Survey Toxic Substances Hydrology Program: U.S. Geological Survey Water-Resources Investigations Report 91–4034, pp. 534–538.

Nordstrom, D.K., and Alpers, C.N., 1999, Negative pH, efflorescent mineralogy, and consequences for environmental restoration at the Iron Mountain Superfund site, California: Proceedings of the National Academy of Sciences, v. 96, pp. 3455–3462.

Nordstrom, D.K., and Ball, J.W., 1985, Toxic element composition of acid mine waters from sulfide ore deposits: 2nd Internatl Mine Water Symposium, Granada, Spain, pp. 749–758.

Nordstrom, D.K., and Ball, J.W., 1986, The geochemical behavior of aluminum in acidified surface waters: Science, v. 232, pp. 54–56.

Nordstrom, D.K., and May, H.M., 1996, Aqueous equilibrium data for mononuclear aluminum species; *in* Sposito, G. (ed.), The Environmental Chemistry of Aluminum, 2nd ed.: CRC Press/Lewis Publishers, Boca Raton, Fla., pp. 39–80.

Nordstrom, D.K., and Munoz, J.L., 1994, Geochemical thermodynamics, 2nd ed.: Blackwell Science, 493 pp.

Nordstrom, D.K., and Southam, G., 1997, Geomicrobiology of sulfide mineral oxidation; *in* Banfield, J.F., and Nealson, K.H. (eds.), Geomicrobiology—Interactions Between Microbes and Minerals: Reviews in Mineralogy, Mineralogical Society of America, Washington, D.C., v. 35, pp. 361–390.

Nordstrom, D.K., Jenne, E.A., and Averett, R.C., 1977, Heavy metal discharges into Shasta Lake and Keswick Reservoir on the Upper Sacramento River, California—A reconnaissance during low flow: U.S. Geological Survey Open-File Report 76–49, pp. 25.

Nordstrom, D.K., Jenne, E.A., and Ball, J.W., 1979, Redox equilibria of iron in acid mine waters; *in* Jenne, E.A., (ed.), Chemical Modeling in Aqueous Systems: American Chemical Society Symposium Series 93, Washington, D.C., pp. 51–80.

Nordstrom, D.K., Ball, J.W., Roberson, C.E., and Hanshaw, B.B., 1984, The effect of sulfate on aluminum concentrations in natural waters, II. Field occurrences and identification of aluminum hydroxysulfate precipitates [abs.]: Geological Society of America Abstracts with Programs, v. 16, no. 6, pp. 611.

Nordstrom, D.K., Alpers, C.N., and Ball, J.W., 1991, Measurement of negative pH and extremely high metal concentrations in acid mine water from Iron Mountain, California [abs.]: Geological Society of America Annual Meeting, Abstract with Programs, v. 23, no. 5, pp. A383.

Nordstrom, D.K., McNutt, R.H., Puigdomènech, I., Smellie, J.A.T., and Wolf, M., 1992, Ground water chemistry and geochemical modeling of water-rock interactions at the Osamu Utsumi mine and Morro do Ferro analogue study sites, Poços de Caldas, Minas Gerais, Brazil: Journal of Geochemical Exploration, v. 45, pp. 249–287.

Nordstrom, D.K., Carlson-Foscz, V., and Oreskes, N., 1995, Rare earth element (REE) fractionation during acidic weathering of San Juan tuff, Colorado [abs.]: Geological Society of America Annual Meeting, Abstracts with Programs, v. 27, no. 6, p. A–199.

Olson, G.J., 1991, Rate of pyrite bioleaching by *Thiobacillus ferrooxidans*—Results of an interlaboratory comparison: Applied and Environmental Microbiology, v. 57, pp. 642–644.

Pabst, A., 1940, Cryptocrystalline pyrite from Alpine County, California: American Mineralogist, v. 25, pp. 425–431.

Parker, R.L, 1962, Isomorphous substitution in natural and synthetic alunite: American Mineralogist, v. 47, pp. 127–136.

Parks, G.A., 1990, Surface energy and adsorption at mineral/water interfaces—An introduction; *in* Hochella, M.F., Jr., and White, A.F. (eds.), Mineral-Water Interface Geochemistry: Reviews in Mineralogy, Mineralogical Society of America, Washington, D.C., v. 23, pp. 133–175.

Plumlee, G.S., Smith, K.S., Mosier, E.L., Ficklin, W.H., Montour, M., Briggs, P.H., and Meier, A.L., 1995, Geochemical processes controlling acid-drainage generation and cyanide degradation at Summitville; *in* Posey, H.H., Pendleton, J.A., and Van Zyl, D., (eds.), Summitville Forum Proceedings: Colorado Geological Survey Spec. Pub. No. 38, pp. 23–34.

Ponnamperuma, F.N, Tianco, E.M., and Loy, T., 1967, Redox equilibria in flooded soils, I. The iron hydroxide systems: Soil Science, v. 103, pp. 374–382.

Potter, R.W., II, 1977, An electrochemical investigation of the system copper-sulfur: Economic Geology, v. 72, pp. 1524–1542.

Pourbaix, M., 1945, Thermodynamique des solutions aqueuses diluee—Representation graphique du pH et du potentiel: Ph.D. thesis, Delft, Beranger, Paris and Liege.

Pourbaix, M., 1966, Atlas of electrochemical equilibria in aqueous solutions: Pergamon Press, New York, 670 pp.

Pourbaix, M., and Pourbaix, A., 1992, Potential-pH equilibrium diagrams for the system S-H_2O from 25 to 150°C—Influence of access of oxygen in sulfide solutions: Geochimica et Cosmochimica Acta, v. 56, pp. 3157–3178.

Powell, A.R., and Parr, S.W., 1919, Forms in which sulfur occurs in coal: Bulletin of the American Institute of Mining and Metallurgical Engineering, pp. 2041–2049.

Ptacek, C.J., and Blowes, D.W., 1994, Influence of siderite on the geochemistry of inactive mine tailings impoundment; *in* Alpers, C.N., and Blowes, D.W. (eds.), Environmental Geochemistry of Sulfide Oxidation: American Chemical Society Symposium Series 550, Washington, D.C., pp. 172–189.

Reardon, E.J., 1988, Ion interaction parameters for Al–SO_4 and application to the prediction of metal sulfate solubility in binary salt systems: Journal of Physical Chemistry, v. 42, pp. 6426–6431.

Rickard, P.A., and Vanselow, D.G., 1978, Investigations into the kinetics and stoichiometry of bacterial oxidation of covellite (CuS) using a polarographic probe: Canadian Journal of Microbiology, v. 24, pp. 998–1003.

Rimstidt, J.D., Chermak, J.A., and Gagen, P.M., 1994, Rates of reaction of galena, sphalerite, chalcopyrite, and arsenopyrite with Fe(III) in acidic solutions; *in* Alpers, C.N., and Blowes, D.W. (eds.), Environmental Geochemistry of Sulfide Oxidation: American Chemical Society Symposium Series 550, Washington, D.C., pp. 2–13.

Ripmeester, J.A., Ratcliffe, C.I., Dutrizac, J.E. and Jambor, J.L., 1986, Hydronium ion in the alunite-jarosite group: Canadian Mineralogist, v. 24, pp. 435–447.

Ritcey, G.M., 1989, Tailings management, problems and solutions in the mining industry: Elsevier Science Publishing Co. Inc., Amsterdam, 970 pp.

Ritchie, A.I.M., 1994a, Sulfide oxidation mechanisms—Control and rates of oxygen transport; *in* Jambor, J.L., and Blowes, D.W. (eds.), The Environmental Geochemistry of Sulfide Mine-Wastes: Mineralogical Association of Canada, Short Course Handbook, v. 22, pp. 201–245.

Ritchie, A.I.M., 1994b, Rates of mechanisms that govern pollutant generation from pyritic wastes; *in* Alpers, C.N., and Blowes, D.W. (eds.), Environmental Geochemistry of Sulfide Oxidation: American Chemical Society Symposium Series 550, Washington, D.C., pp. 108–122.

Runnells, D.D., Shepard, T.A., and Angino, E.E., 1992, Metals in water—Determining natural background concentrations in mineralized areas: Environmental Science and Technology, v. 26, pp. 2316–2322.

Russell, J.D., 1979, Infrared spectroscopy of ferrihydrite—Evidence for the presence of structural hydroxyl groups: Clay Minerals, v. 14, pp. 109–113.

Sakaguchi, H., Torma, A.E., and Silver, M., 1976, Microbiological oxidation of synthetic chalcocite and covellite by *Thiobacillus ferrooxidans*: Applied and Environmental Microbiology, v. 31, pp. 7–10.

Sand, W., Rhode, K., and Zenneck, C., 1992, Evaluation of *Leptospirillum ferrooxidans* for leaching: Applied and Environmental Microbiology, v. 58, pp. 85–92.

Sato, M., 1992, Persistency-field Eh-pH diagrams for sulfides and their application to supergene oxidation and enrichment of sulfide ore bodies: Geochimica et Cosmochimica Acta, v. 56, pp. 3133–3156.

Scala, G., Mills, A.L., Moses, C.O., and Nordstrom, D.K., 1982, Distribution of autotrophic Fe and sulfur-oxidizing bacteria in mine drainage from sulfide deposits measured with the FAINT assay [abs.]: American Society of Microbiology Annual Meeting.

Schwertmann, U., 1985a, The effect of pedogenic environments on iron oxide minerals, *in* Stewart, B.A. (ed.), Advances in Soil Science, v. 1: Springer-Verlag, New York, pp. 171–200.

Schwertmann, U., 1985b, Occurrence and formation of iron oxides in various pedoenvironments; *in* Stucki, F.W., Goodman, B.A. and Schwertmann, U. (eds.), Iron in Soils and Clay Minerals: D. Reidel Pub. Co., Boston, Mass., NATO Advanced Study Institute Series C, v. 217, pp. 267–308.

Schwertmann, U., and Cornell, R.M, 1991, Iron oxides in the laboratory—Preparation and characterization: Verlag Chemie, Weinheim, Germany, 137 pp.

Schwertmann, U., and Murad, E., 1983, The effect of pH on the formation of goethite and hematite from ferrihydrite: Clays and Clay Minerals, v. 31, pp. 277–284.

Scott, K.D., 1987, Solid solution in, and classification of, gossan-derived members of the alunite-jarosite family, Northwest Queensland, Australia: American Mineralogist, v. 72, pp. 178–187.

Silverman, M.P., 1967, Mechanism of bacterial pyrite oxidation: Journal of Bacteriology, v. 94, pp. 1046–1051.

Silverman, M.P., and Lundgren, D.G., 1959, Studies on the chemoautotrophic iron bacterium *Ferrobacillus ferrooxidans*, I. An improved medium and a harvesting procedure for securing high cell yields: Journal of Bacteriology, v. 77, pp. 642–647.

Silverman, M.P., Rogoff, M.H., and Wender, I., 1961, Bacterial oxidation of pyritic materials in coal: Applied and Environmental Microbiology, v. 9, pp. 491–496.

Singer, P.C., and Stumm, W., 1968, Kinetics of the oxidation of ferrous iron, 2nd Symposium on Coal Mine Drainage Research: National Coal Association/Bituminous Coal Research, pp. 12–34.

Singer, P.C., and Stumm, W., 1970a, Acid mine drainage—The rate-determining step: Science, v. 167, pp. 1121–1123.

Singer, P.C., and Stumm, W., 1970b, Oxygenation of ferrous iron: Federal Water Quality Administration Report 14010–06/69, 198 pp.

Smith, E.E., and Shumate, K.S., 1970, Sulfide to sulfate reaction mechanism: Federal Water Pollution Control Federation Report, 115 pp.

Smith, K.S., 1999, Metal sorption on mineral surfaces—An overview with examples relating to mineral deposits; *in* Plumlee, G.S., and Logsdon, M.J. (eds.), The Environmental Geochemistry of Mineral Deposits, Part A. Processes, Techniques, and Health Issues: Society of Economic Geologists, Reviews in Economic Geology, v. 6A, pp. 161–182.

Sokolova, G.A., and Karavaiko, G.I., 1968, Physiology and geochemical activity of *Thiobacilli*: Izdatelstvo "Nauka," Moscow, 283 pp.

Southam, G., and Beveridge, T.J., 1992, Enumeration of *Thiobacilli* within pH-neutral and acidic mine tailings and their role in the development of secondary mineral soil: Applied and Environmental Microbiology, v. 58, pp. 1904–1912.

Steger, H.F., and Desjardins, L.E., 1978, Oxidation of sulfide minerals, IV. Pyrite, chalcopyrite, and pyrrhotite: Chemical Geology, v. 23, pp. 225–237.

Stoffregen, R.E., and Alpers, C.N., 1987, Woodhouseite and svanbergite in hydrothermal ore deposits—Products of apatite destruction during advanced argillic alteration: Canadian Mineralogist, v. 45, pp. 201–211.

Stoffregen, R.E., and Alpers, C.N., 1992, Observations on the unit-cell dimensions, H_2O contents, and δD values of natural and synthetic alunite: American Mineralogist, v. 77, pp. 1092–1998.

Stokes, H.N., 1901, On pyrite and marcasite: U.S. Geological Survey Bulletin 186, 50 pp.

Stumm, W., and Morgan, J.J., 1981, Aquatic chemistry, 2nd ed.: Wiley-Interscience, New York, 770 pp.

Sveshnikov, G.B., and Dobychin, S.L., 1956, Electrochemical solution of sulfides and dispersion aureoles of heavy metals: Geokhimiya, no. 4, pp. 413–419.

Sveshnikov, G.B., and Ryss, Yu.S., 1964, Electrochemical processes in sulfide deposits and their geochemical significance: Geokhimya, v. 3, pp. 208–218.

Tardy, Y., and Nahon, D., 1985, Geochemistry of laterites, stability of Al-goethite, Al-hematite, and Fe^{3+}-kaolinite in bauxites and ferricretes: American Journal of Science, v. 285, pp. 865–903.

Temple, K.L., and Colmer, A.R., 1951, The autotrophic oxidation of iron by a new bacterium—*Thiobacillus ferrooxidans*: Journal of Bacteriology, v. 62, pp. 605–611.

Temple, K.L., and Delchamps, E.W., 1953, Autotrophic bacteria and the formation of acid in bituminous coal mines: Applied Microbiology, v. 1, pp. 255–258.

Tervari, P.H., and Campbell, A.B., 1976, Dissolution of iron sulfide (troilite) in aqueous sulfuric acid: Journal of Physical Chemistry, v. 80, pp. 1844–1848.

Thornber, M.R., 1975, Supergene alteration of sulfides, II. A chemical study of the Kambalda nickel deposits: Chemical Geology, v. 15, pp. 117–144.

Thorstensen, D.C., 1984, The concept of electron activity and its relation to redox potentials in aqueous geochemical systems: U.S. Geological Survey Open-File Report 84–072, 45 pp.

To, B.T., Nordstrom, D.K., Cunningham, K.M., Ball, J.W., and

McCleskey, R.B., 1999, New method for the direct determination of dissolved Fe(III) concentration in acid mine waters: Environmental Science and Technology, v. 33, pp. 807–813.

Torma, A.E., and Habashi, F., 1972, Oxidation of copper (II) selenide by *Thiobacillus ferrooxidans*: Canadian Journal of Microbiology, v. 18, pp. 1780–1781.

Torma, A.E., and Subramanian, K.N., 1974, Selective bacterial leaching of a lead sulphide concentrate: International Journal of Mineral Processing, v. 1, pp. 125–134.

Torma, A.E., Walden, C.C., Duncan, D.W., and Branion, R.M., 1972, The effect of carbon dioxide and particle surface area on the microbiological leaching of a zinc sulfide concentrate: Biotechnology and Bioengineering, v. 15, pp. 777–786.

Torma, A.E., Legault, G., Kougiomoutzakis, D., and Ouellet, R., 1974, Kinetics of bio-oxidation of metal sulfides: Canadian Journal of Chemical Engineering, v. 52, pp. 515–517.

Torma, A.E., Gabra, G.G., Guay, R., and Silver, M., 1976, Effects of surface active agents on the oxidation of chalcopyrite by *Thiobacillus ferrooxidans*: Hydrometallurgy, v. 1, pp. 301–309.

Torrent, J., and Guzman, R., 1982, Crystallization of Fe(III)-oxides from ferrihydrite in salt solutions—Osmotic and specific ion effects: Clays and Clay Minerals, v. 17, pp. 463–469.

Towe, K.M., and Bradley, W.F., 1967, Mineralogical constituents of colloidal "hydrous ferric oxides": Journal of Colloid and Interface Science, v. 24, pp. 384–392.

Tunell, G., 1930, The oxidation of disseminated copper ores in altered porphyry: Unpub. Ph.D. thesis, Harvard Univ., 104 pp.

Tuovinen, O.H., Niemela, S.I., and Gyllenberg, H.G., 1971, Tolerance of *Thiobacillus ferrooxidans* to some metals: Antonie van Leeuwenhoek, v. 37, pp. 489–496.

Turner, A.W., 1949, Bacterial oxidation of arsenite: Nature, v. 164, pp. 76–77.

U.S. Environmental Protection Agency, 1985, Wastes from the extraction and beneficiation of metallic ores, phosphate rock, asbestos, overburden from uranium mining, and oil shale: Report to Congress, EPA/530–SW–85–033.

Vairavamurthy, A., Manowitz, B., Zhou, W., and Jeon, Y., 1994, Determination of hydrogen sulfide oxidation products by sulfur K-edge X-ray absorption near-edge structure spectroscopy; *in* Alpers, C.N., and Blowes, D.W. (eds.), Environmental Geochemistry of Sulfide Oxidation: American Chemical Society Symposium Series 550, Washington, D.C., pp. 412–430.

Vranesh, G., 1979, Mine drainage—The common enemy; *in* Argal, G.O., Jr., and Brawner, C.O. (eds.), Proceedings, 1st Internatl Mine Drainage Symposium: Miller Freeman Publications, pp. 54–97.

Waite, T.D., and Morel, F.M.M., 1984, Photoreductive dissolution of colloidal iron oxides in natural waters: Environmental Science and Technology, v. 18, pp. 860–868.

Wakao, N., Sakurai, Y., and Shiota, H., 1977, Microbial oxidation of ferrous iron in acid mine water at sulfur and iron-sulfide mine: Soil Science and Plant Nutrition, v. 23, pp. 207–216.

Wakao, N., Mishina, M., Sakurai, Y., and Shiota, H., 1982, Bacterial pyrite oxidation, I. The effect of pure and mixed cultures of *Thiobacillus ferrooxidans* and *Thiobacillus thiooxidans* on release of iron: Journal of General and Applied Microbiology, v. 28, pp. 331–343.

Wakao, N., Mishina, M., Sakurai, Y., and Shiota, H., 1984, Bacterial pyrite oxidation, III. Adsorption of *Thiobacillus ferrooxidans* cells on solid surfaces and its effect on iron release from pyrite: Journal of General and Applied Microbiology, v. 30, pp. 63–77.

Wakao, N., Koyatsu, H., Komai, Y., Shimokawara, H., Sakurai, Y., and Shiota, H., 1988, Microbial oxidation of arsenite and occurrence of arsenite-oxidizing bacteria in acid mine water from a sulfur-pyrite mine: Geomicrobiology Journal, v. 6, pp. 11–24.

Waksman, S.A., and Jåffe, J.S., 1921, Acid production by a new sulfur-oxidizing bacterium: Science, v. 53, pp. 216.

Waksman, S.A., and Jåffe, J.S., 1922, Microorganisms concerned in the oxidation of sulphur in the soil, II. *Thiobacillus thiooxidans*, a new sulphur-oxidizing organism isolated from the soil: Journal of Bacteriology, v. 7, pp. 239–256.

Walker, T.R., 1967, Formation of red beds in modern and ancient deserts: Geological Society of America Bulletin, v. 78, pp. 353–368.

Walker, T.R., 1974, Formation of red beds in moist tropical climates—A hypothesis: Geological Society of America Bulletin, v. 84, pp. 633–638.

Walker, T.R., 1976, Diagenetic origin of continental red beds; *in* Falke, H. (ed.), The Continental Permian in Central, West, and South Europe: D. Reidel Publishing Co., pp. 241–282.

Walsh, A.W., and Rimstidt, J.D., 1986, Rates of reaction of covellite and blaubleibender covellite with ferric iron at pH 2.0: Canadian Mineralogist, v. 24, pp. 35–44.

White, A.F., and Brantley, S.L., 1995, Chemical weathering rates of silicate minerals: Reviews in Mineralogy, Mineralogical Society of America, Washington, D.C., v. 31, 583 pp.

White, W.W., III, and Jeffers, T.H., 1994, Chemical predictive modeling of acid mine drainage from metallic sulfide-bearing waste rock; *in* Alpers, C.N., and Blowes, D.W. (eds.), Environmental Geochemistry of Sulfide Oxidation: American Chemical Society Symposium Series 550, Washington, D.C., pp. 608–630.

Wieder, R.K., 1994, Diel changes in iron(III)/iron(II) in effluent from constructed acid mine drainage treatment wetlands: Journal of Environmental Quality, v. 23, no. 4, pp. 730–738.

Wiersma, C.L., and Rimstidt, J.D., 1984, Rates of reactions of pyrite and marcasite with ferric iron at pH 2: Geochimica et Cosmochimica Acta, v. 48, pp. 85–92.

Wilber, C.G., 1969, The biological aspects of water pollution: C.C. Thomas, New York, 296 pp.

Williams, E.G., Rose, A.W., Parizek, R.R., and Waters, S.A., 1982, Factors controlling the generation of acid mine drainage: Pennsylvania State University Report to the U.S. Bureau of Mines, 265 pp.

Williamson, M.A., and Rimstidt, J.D., 1993, The rate of decomposition of the ferric-thiosulfate complex in acidic aqueous solutions: Geochimica et Cosmochimica Acta, v. 57, pp. 3555–3561.

Yakhontova, L. K., Zeman, I., and Nesterovich, L.G., 1980, Oxidation of tetrahedrite: Doklady, Earth Sciences Section, Akademia Nauk SSSR, v. 253, pp. 461–464.

Yapp, C.J., 1983, Stable hydrogen isotopes in iron oxides—Isotope effects associated with the dehydration of a natural goethite: Geochimica et Cosmochimica Acta, v. 47, pp. 1277–1287.

Zhang, J., and Millero, F.J., 1994, Kinetics of oxidation of hydrogen sulfide in natural waters; *in* Alpers, C.N., and Blowes, D.W. (eds.), Environmental Geochemistry of Sulfide Oxidation: American Chemical Society Symposium Series 550, Washington, D.C., pp. 393–409.

Zodrov, E.L., and McCandlish, K., 1978a, Hydrated sulphates in the Sydney Coalfield, Cape Breton, Nova Scotia: Canadian Mineralogist, v. 16, pp. 17–22.

Zodrov, E.L., and McCandlish, K., 1978b, Roof weakness—Fossilization and (cyclic) regenerative hydrated sulphates, Discussion: Canadian Institute of Mining and Metallurgy Bulletin, v. 71, pp. 90–91.

Zodrov, E.L., Wiltshire, J., and McCandlish, E., 1979, Hydrated sulphates in the Sydney Coalfield, Cape Breton, Nova Scotia, II. Pyrite and its alteration products: Canadian Mineralogist, v. 17, pp. 63–70.

Zverev, V.P., Dol'nikov, V.A., Khutorskoy, M.D., Dobrovol'skiy, Ye.V., Lyal'ko, V.I., Mitnik, M.M. and Fotogdinov, R.A., 1983, Sulfide oxidation kinetics and heat effects: Geochemistry International, v. 20, pp. 82–90.

REVIEWS IN ECONOMIC GEOLOGY

(ISSN 0741–0123)

Published by the
SOCIETY OF ECONOMIC GEOLOGISTS, INC.
Completed by Barbara Ramsey, Visual Information Specialist, USGS
Printed by BookCrafters, Inc., 613 E. Industrial Drive, Chelsea, Michigan 48118

Additional copies of this volume may be obtained from:
Society of Economic Geologists, Inc.
5808 South Rapp St., Suite 209
Littleton, CO 80120 USA
Tel. 1.303.797.0332
Fax 1.303.797.0417
e-mail: socecongeol@csn.net

Vol. 1:	FLUID-MINERAL EQUILIBRIA IN HYDROTHERMAL SYSTEMS	(1984)	ISBN 0–9613074–0–4
Vol. 2:	GEOLOGY AND GEOCHEMISTRY OF EPITHERMAL SYSTEMS	(1985)	ISBN 0–9613074–1–2
Vol. 3:	EXPLORATION GEOCHEMISTRY: DESIGN AND INTERPRETATION OF SOIL SURVEYS	(1986)	ISBN 0–9613074–2–0
Vol. 4:	ORE DEPOSITION ASSOCIATED WITH MAGMAS	(1989)	ISBN 0–9613074–3–9
Vol. 5:	SEDIMENTARY AND DIAGENETIC MINERAL DEPOSITS: A BASIN ANALYSIS APPROACH TO EXPLORATION	(1991)	ISBN 0–9613074–4–7
Vol. 6:	THE ENVIRONMENTAL GEOCHEMISTRY OF MINERAL DEPOSITS (A and B)	(1999)	ISBN 1–887483–50–0
Vol. 7:	APPLICATIONS OF MICROANALYTICAL TECHNIQUES TO UNDERSTANDING MINERALIZING PROCESSES	(1998)	ISBN 1–887483–51–9
Vol. 8:	VOLCANIC-ASSOCIATED MASSIVE SULFIDE DEPOSITS: PROCESSES AND EXAMPLES IN MODERN AND ANCIENT SETTINGS	(1999) (in press)	ISBN 1–887483–52–7 ISBN
Vol. 9:	ORE GENESIS AND EXPLORATION: THE ROLES OF ORGANIC MATTER	(in press)	ISBN
Vol. 10:	TECHNIQUES IN HYDROTHERMAL ORE DEPOSITS GEOLOGY	(1998)	ISBN 1–887483–54–3

Reviews in Economic Geology is a publication of the Society of Economic Geologists designed to accompany the Society's Short Course series. Like the Short Courses, each volume provides comprehensive updates on various applied and academic topics for practicing economic geologists and geochemists in exploration, development, research, and teaching. Volumes are produced in conjunction with each new Short Course, first serving as a textbook for that course, and subsequently made available to SEG members and others at modest cost.

REVIEWS IN ECONOMIC GEOLOGY

(ISSN 0741-0123) Volume 6A

THE ENVIRONMENTAL GEOCHEMISTRY OF MINERAL DEPOSITS

Part A: Processes, Techniques, and Health Issues

ISBN 1–887483–50–0

Volume Editors

G.S. PLUMLEE
U.S. Geological Survey
MS964 Denver Federal Center
Denver, CO 80225
gplumlee@usgs.gov

M.J. LOGSDON
Geochimica, Inc.
206 North Signal Street, Suite M
Ojai, CA 93023
mark.logsdon@worldnet.att.net

SOCIETY OF ECONOMIC GEOLOGISTS, INC.

ATTACHMENT 17

Journal of Geochemical Exploration 114 (2012) 57–69

Contents lists available at SciVerse ScienceDirect

Journal of Geochemical Exploration

journal homepage: www.elsevier.com/locate/jgeoexp

Static tests response on 5 Canadian hard rock mine tailings with low net acid-generating potentials

B. Plante *, B. Bussière, M. Benzaazoua [1]

Université du Québec en Abitibi-Témiscamingue (UQAT), 445 boul. de l'Université, Rouyn-Noranda, Québec, Canada J9X 5E4

ARTICLE INFO

Article history:
Received 29 November 2010
Accepted 27 December 2011
Available online 8 January 2012

Keywords:
Acid mine drainage prediction
Static tests
Acid–base accounting
Mineralogical considerations

ABSTRACT

It is crucial for mining operators to predict the acid-generating potential of their mine wastes as early as possible in a mine development project, because of the high remediation costs of acid-generating tailings and the risks of environmental issues associated with an incorrect classification of the wastes. However, many tailings having low net acid-generating potentials fall into the uncertainty zone of the static test. Different chemical and mineralogical static test results are compared in this paper for 5 Canadian hard rock mine tailings having low net acid-generating potential, in order to help determine which method is more appropriate for such tailings. Static test methods showed significant result variations (NNP or NP/AP) for each tailings tested, demonstrating the need to develop tools to identify the most appropriate technique for a given mine waste. Thus, static test selection guidelines were developed based on mineralogical considerations for each test. A modification to the Lawrence and Scheske method based on the Paktunc CNP method is proposed in order to improve its accuracy, which enables to account for the presence of oxidizable cations (such as iron and manganese) within the minerals.

1. Introduction

Mine drainage arises as a result of water percolating through various components of a mining complex, such as tailings impoundments and waste rock piles. Acid-mine drainage (AMD) occurs when mine drainage comes into contact with sulfide minerals that have oxidized due to exposure to water and oxygen. The generation of AMD is known to be catalyzed by bacteria under acidic conditions (e.g. Blowes et al., 2003; Johnson and Hallberg, 2003; Nordstrom, 2000). AMD appears when the neutralization capacities of the carbonate and silicate minerals contained in the mine waste cannot counterbalance the acidity produced by sulfide oxidation. AMD is typically characterized by high acidity, low pH and high concentrations of heavy metals and sulfates (e.g. Blowes et al., 2003; Nordstrom and Alpers, 1999).

Once mine tailings have been identified as acid generating a remediation strategy must be implemented at the mine in order to prevent sulfide oxidation within the tailings, and to facilitate effluent treatment. Typical costs for the reclamation of an acid-generating mine tailings impoundment in Canada are between 100 000 $ and 250 000 $ per hectare, while they are generally between 2000 $ and 20 000 $ per hectare for tailings that are not generating contaminated drainage (Aubertin et al., 2002). Because of the high remediation costs of potentially acid-generating tailings, it is crucial for mining operators to accurately predict the acid-generating potential of their mine wastes as early as possible in the mine development project. This allows for the early selection of an appropriate waste management and remediation method. Many prediction techniques are available, generally classified as static or kinetic depending on the time scale of the experimental procedure (Blowes et al., 2003; Morin and Hutt, 1997). The static tests generally take less than a week to perform, while the kinetic procedures can last from a few weeks to years. The first tests used to characterize the acid-generating potential of a given mine waste are usually the static tests, which are relatively quick and inexpensive; the present study focuses on these tests.

Many static prediction techniques are available to evaluate the acid-generating potential of mine tailings (Adam et al., 1997; Day, 1991; Duncan and Bruynesteyn, 1979; Lapakko, 1994a; Lawrence and Wang, 1996, 1997; Lawrence et al., 1989; Skousen et al., 2002; Sobek et al., 1978; Weber et al., 2004, 2005). These procedures generally estimate the global acid-generating (AP) and acid-neutralizing (NP) potentials and are often called acid–base accounting (ABA) tests (Lawrence and Wang, 1996). Static test procedures can be separated in two distinct classes; chemical methods and mineralogical methods. Chemical methods require experimentation and testing in a chemistry lab, while mineralogical methods are mainly based on the mineralogical composition of the tailings.

The acid-generating potential (AP) and neutralizing potential (NP) are defined separately in the different static test procedures

* Corresponding author at: Stavibel, 25 rue Gamble Ouest, Rouyn-Noranda, Québec, Canada J9X 3B6. Tel.: +1 819 764 5181#257; fax: +1 819 764 3118.
E-mail addresses: benoit.plante@uqat.ca (B. Plante), bruno.bussiere@uqat.ca (B. Bussière), mostafa.benzaazoua@insa-lyon.fr (M. Benzaazoua).
[1] Current address: Laboratoire de Génie Civil et Ingénierie Environnementale (LGCIE), Institut National des Sciences Appliquées (INSA), Bat. 404 - Sadi Carnot, 9 rue de la Physique, 69621 Villeurbanne, France.

0375-6742/$ – see front matter © 2012 Elsevier B.V. All rights reserved.
doi:10.1016/j.gexplo.2011.12.003

considered in this study. The difference between the two parameters is known as the net acid-neutralizing potential (NNP = NP–AP); the NP/AP ratio is also used to interpret the results of static test. Tailings with low net acid-generation potential may generate contaminants from sulfide oxidation nonetheless and have a significant environmental impact, with acidic conditions or with near-neutral conditions (contaminated neutral drainage; e.g. Nicholson, 2004; Plante et al., 2011). Although the extent of their environmental impact may not always be as important as for highly acidic tailings, their management may call for the implementation of control and remediation measures comparable to those of highly acidic tailings.

In recent years, research related to static tests has focused (amongst other issues) on silicate mineral contributions to the NP (e.g. Jambor et al., 2002, 2007; Li, 2000; Sherlock et al., 1995), the effect of iron-bearing carbonates on NP determination and methods to account for the presence of iron within neutralizing minerals (Bennett et al., 2000; Frostad et al., 2003; Jambor et al., 2003; Lapakko, 1994b; Malmström et al., 2000; Paktunc, 1999a; 1999b; Weber et al., 2004). Additionally there has been considerable interest in static test result extrapolation from the lab to the field (Bethum et al., 1997; Feasby et al., 2001; Frostad et al., 2000; Lapakko, 1994b; Liao et al., 2007; Miller et al., 2003). Several studies have compared various static NP determination methods (Kwong and Ferguson, 1997; Lawrence and Wang, 1996; Paktunc, 1999b). These comparisons highlight some important considerations which need to be addressed in the choice of an appropriate NP determination method. These considerations include sample mineralogy, such as silicate vs carbonate neutralization, iron content (or other oxidizable/hydrolysable elements) of neutralising minerals, previous oxidation of the sulfides, and the sulfide content of the sample.

This paper compares the results of a number of different chemical and mineralogical NP determination procedures for 5 Canadian hard rock mine tailings with low net acid-generating potential. The limitations of static test procedures for these particular tailings located near or within the uncertainty zone are highlighted. These comparisons will help determine which method would be more appropriate for a given low net acid-generating potential tailings. Given the the economic and environmental impact of a misclassification of the acid-generating potential, this research aims to develop practical selection tools for mine operators.

2. Materials and methods

Several characterization techniques were used to assess the static test responses on the different tailings studied. These tailings samples were chosen for their low net acid-generating potentials, close to or within the uncertainty zone. The following presents a brief description of the methods used to characterize the samples and the main characterization results.

2.1. Static tests

This section describes the different chemical and mineralogical procedures considered in this research to evaluate the NP and AP. Tables 1 and 2 compare the chemical and mineralogical NP and AP determination procedures, including details about their calculation and main characteristics.

2.1.1. Chemical NP procedures

Some of the NP procedures are defined as chemical because they involve some level of chemical reaction. The method proposed by Sobek et al. (1978) (original Sobek test) was the most popular NP determination approach for many years. In this test, excess acid is added according to different fizz ratings representing different neutralizing potentials. The aqueous suspension of the sample is allowed to react with neutralizing minerals while heating for 1–2 h.

Table 1
The different Sobek procedures examined in this study.

Parameter	Sobek et al., 1978	Modified Sobek I (Lawrence et al., 1989)	Modified Sobek II (Lawrence and Wang, 1996, 1997)
Temperature/ test duration	Near 100 °C/1–2 h	Room temp/24 h	Room temp/24 h
HCl volume and normality	No fizz: 20 mL of 0.1 N HCl Weak fizz: 40 mL of 0,1 N HCl Medium fizz: 40 mL of 0.5 N HCl Strong fizz: 80 mL of 0.5 N HCl		2 to 5 mL of 1.0 N HCl, depending on the fizz rating; acid added in two steps, at the test startup and after 2 h
Titration end-point	pH 7.0	pH 8.3	pH 8.3
AP calculation	Total sulfur	Sulfide sulfur	Sulfide sulfur

The residual acid is then back-titrated to a defined end-point of pH 7. Different modifications of the original Sobek test have been proposed in order to try to better reflect the real conditions in which AMD occurs (see Table 1 for a comparison of the modified procedures to the original test). The modified Sobek I method (proposed by Lawrence et al., 1989) eliminates boiling from the procedure and works at room temperature for longer times (24 h instead of 1–2 h in the original Sobek) and suggests a titration end-point pH of 8.3. Lawrence and Wang (1996, 1997) (Modified Sobek II, in Table 1) suggested a different set of hydrochloric acid volumes and normality prescribed by the fizz ratings, and proposed modifications in the manner by which the acid is added. The different Sobek test versions use Eq. (1) for NP calculation. The AP calculation according to the Modified Sobek I and II methods is carried out using the $S_{sulfide}$ content (Eq. (2), in Table 2), while the original Sobek test uses the S_{total} content in the calculation. Lawrence and Wang (1996) provided evidence that the original Sobek procedure is generally more aggressive than the modified Sobek II procedure; consequently, the original Sobek results are generally higher than the modified Sobek II results. The authors explain that the original Sobek procedure generally overestimates the NP because of the high temperatures involved (near 100 °C, Table 1) even if reaction times are lower (1–2 h in the original Sobek vs 24 h in the modified II Sobek). The Sobek II modified procedure (Lawrence and Wang, 1996) was selected for the analysis of the tailings samples in this study for these reasons.

The standard carbonate NP method (CNP; e.g. Frostad et al., 2003) consists of measuring the total inorganic carbon and converting the value into equivalent $CaCO_3$ (see Eqs. (3) and (4) in Table 2). Lawrence and Wang (1996, 1997) showed that the modified Sobek II procedure usually gives slightly higher NP results than the CNP because of the silicates contribution to the NP in the modified Sobek II procedure, which is not accounted for in the CNP method. The validity of this method is limited also by the contribution of carbonates other than calcite, such as dolomite, magnesite, siderite and ankerite. Since siderite ($FeCO_3$) is considered as a non neutralizing carbonate mineral (Coastec Research Inc., 1991; Skousen et al., 1997), it may become necessary to take its presence into account when calculating the CNP. The corrected CNP (CCNP) is determined using the standard CNP along with the siderite content (%$FeCO_3$, in wt.%, evaluated by XRD in the present study) according to Eqs. (5) and (6) presented in Table 2. The validity of this correction method is limited by the accuracy and precision of the siderite contents measurements. A similar NP correction was reported by Frostad et al. (2003), where the Fe molar ratio is considered when calculating the contribution of Ca and Mg carbonates from quantitative XRD mineralogy.

2.1.2. Mineralogical NP approaches

The mineralogical approaches of NP evaluation are rarely employed in practice, mainly because of limited quantification capabilities. However, the latest advances in mineralogical quantification, such as Rietveld fitting of XRD data (Rietveld, 1993; Taylor and Hinczak,

Table 2
NP methods considered in this study.

Method	Formulations	Definitions	Characteristics
Modified Sobek procedure (Lawrence and Wang, 1996)	$NP = \frac{50a[x-y(b/a)]}{c}$ [eq.1] $AP = 31.25 \cdot \%S_{sulfide}$ [eq.2]	NP: kg $CaCO_3$/t 50:conversion factor a: HCl normality (mol/L) b: NaOH normality (mol/L) x: HCl volume (mL) y: NaOH volume (mL) c: sample mass (g)	– Not as aggressive as the Standard Sobek method (no boiling); – Underestimates the NP with dolomitic minerals; – Widely used in North America, particularly in Canada.
Inorganic carbon (e.g. Frostad et al., 2003; Lawrence and Wang, 1996)	$CNP = \%C \cdot \frac{M_{CaCO_3}}{M_C} \cdot \frac{1000kg/t}{100\%}$ [eq.3] $CNP = \%C_{inorg} \cdot 83,33$ [eq.4]	CNP: kg $CaCO_3$/t %C: carbon weight content (%) M_{CaCO3}: calcite molar mass (100.09 g/mol) M_C: carbon molar mass (12.011 g/mol)	– Simple and effective when carbonates are the main neutralizing minerals; – Does not take into account the non-oxidizable cations such as iron, which diminishes the NP when released.
Corrected Carbonate NP	$CCNP = CNP - \frac{\%FeCO_3}{100\%} \cdot \frac{M_{CaCO_3}}{M_{FeCO_3}} \cdot 1000\frac{kg}{t}$ [eq.5] $CCNP = CNP - 8.64 \cdot \%FeCO_3$ [eq.6]	CCNP, CNP: kg $CaCO_3$/t %$FeCO_3$: siderite weight content M_{CaCO3}: calcite molar mass (100.09 g/mol) M_{FeCO3}: siderite molar mass (115.86 g/mol)	– Takes only carbonates into account; – Correction for siderite carbonate content
Lawrence and Scheske (1997)	$NP = 1000\ kg/t \cdot M_{CaCO_3} \cdot \sum_{i=1}^{n} \frac{C_{Mi}R_i}{M_{Mi}}$ [eq.7]	NP: kg $CaCO_3$/t M_{CaCO3}: calcite molar mass (100.09 g/mol) M_{Mi}: "i" molar mass (g/mol) C_{Mi}: "i" weight content (wt.%) R_i: "i" reactivity factor (unitless)	– Takes neutralizing silicates into account, based on relative reactivity; – Does not take into account the iron content of neutralizing minerals, which diminishes the NP when released.
Paktunc (1999b) carbonates	$NP = \sum_{i=1}^{k} \frac{10X_i\omega_a c_i}{n_{M,i}\omega_i}$ [eq.8] $AP = \sum_{i=1}^{k} \frac{10n_{M,a}X_i\omega_a}{\omega_i}$ [eq.9]	10: conversion factor (1 000 kg.t^{-1}/100%) NP, AP: kg H_2SO_4/t X_i: "i" mineral content (wt.%) ω_a and ω_i: H_2SO_4 and "i" mineral molar mass (g/mol) c_i: sum of stoichiometric coefficients of non-oxidizable cations $n_{M,i}$ and $n_{M,a}$: stoichiometric factors of acid generation and neutralization, respectively	– Takes only carbonates into account; – Takes into account the content of non-oxidizable cations such as iron, which diminishes the NP when released.

2001), or the ModAn program (Paktunc, 1998, 2001), enable sufficient mineralogical precision for the successful use of mineralogical NP determinations. Two mineralogical approaches are compared in this study: the Lawrence and Scheske (1997) and the Paktunc (1999b) carbonate NP.

The Paktunc (1999b) method calculates the mineralogical AP based on the sulfide minerals content while the Lawrence and Scheske (1997) method uses the $S_{sulfide}$ content. The Lawrence and Scheske (1997) mineralogical method (based on previous work from Kwong, 1993 and Sverdrup, 1990) calculates the NP from the sum of the individual contribution of the neutralizing minerals composing the material, based on their proportions and relative reactivity (see Eq. (7) in Table 2).

The Paktunc carbonate NP (or Paktunc CNP) sums the individual contributions of carbonates to the NP based on their concentration and composition. The Paktunc CNP method accounts for the presence of iron (or other oxidizable cations such as manganese) and its subsequent oxidation and hydrolysis reactions, an acid-generating process which ultimately decreases the overall NP of the host mineral (see Eqs. ((8) and (9) in Table 2).

2.2. Physical, mineralogical and chemical characterization methods

The tailings volumetric particle size distribution was determined by laser diffraction (e.g. Merkus, 2009; Xu, 2000) for sizes between 0.05 and 879 μm using a Malvern Instruments Mastersizer S analyzer. The tailings specific gravity (G_s) was determined using a Micromeritics AccuPyc 1330 pycnometer (Allen, 1990), while the specific surface (S_s) was determined with a Micromeritics Gemini surface analyzer using the nitrogen BET adsorption isotherm (Brunauer et al., 1938).

The tailings chemical composition was determined by ICP-AES following an acid digestion using concentrated nitric (HNO_3), hydrofluoric (HF) and hydrochloric (HCl) acids, as well as liquid bromide (Br_2). Sulfate (SO_4^{2-}) content was determined using a 40% HCl extraction followed by ICP-AES determination of the extracted sulfur (modified from Sobek et al., 1978). Silicon content was determined by a sodium peroxide/sodium hydroxide (Na_2O_2/NaOH) fusion using a Claisse Peroxide Fluxer followed by dissolution in diluted HCl and ICP-AES measurement of silicon. The inorganic carbon content (C_{inorg}) was determined using a LECO furnace with a ±0.05 to 0.1 wt.% precision.

The tailings mineralogy was determined with a Bruker A.X.S. Advance D8 XRD using a cobalt X-ray source. Mineral quantification was performed using the Rietveld quantification method (Rietveld, 1993; Taylor and Hinczak, 2001) with a 0.5 to 1% absolute error on tailings samples pulverized to approximately 90%<10 μm with a McCrone Micronizing mill. A Savitzky–Golay smoothing filter (Savitzky and Golay, 1964) was applied on the raw XRD data in order to accentuate the signal-to-noise ratio in XRD data. Acquisition runs were performed at 0.005°/s from 5 to 70° (2Θ) for regular scanning, and at 0.001°/s for higher resolution runs. Only well crystallized phases are detected with this technique because only crystalline phases effectively diffract X-rays. Therefore, the mineralogical quantification from XRD data does not take into consideration the amorphous phases that may be present within the tailings. Many secondary minerals formed in acid-mine drainage conditions are amorphous and therefore not detected by XRD (e.g. Cravotta, 1994; Hakkou et al., 2008).

Estimation of the calcium, iron, magnesium, and manganese content of ankerite minerals was done on polished sections of the tailings samples using a Hitachi S-3500N Scanning Electron Microscope (SEM) coupled with an Oxford Instruments EDS (Energy Dispersive X-ray Spectroscopy) probe. The analyses were performed using 20 kV, 120–130 μA, a 25 Pa vacuum, a working distance of 15 mm and a detector dead time of approximately 25–40%. The ankerite composition was determined by analyzing between 6 and 10 ankerite particles from each tailings site by EDS (since MAT-M1 and MAT-M2 were generated from the same tailings material, their ankerite composition are assumed to be the same). The proportions of calcium, magnesium, manganese and iron were deducted from these analyses, with the oxygen dosed stoichiometrically. The ankerite compositions were obtained with approximately 10% accuracy on the stoichiometric coefficient using this method.

2.3. Materials

2.3.1. Tailings sample preparation

All five tailings come from the Abitibi-Témiscamingue region of Québec, Canada. Sample UQ-8 was sampled in a tailings impoundment and weathered in a laboratory kinetic test (Villeneuve, 2004) prior to the present study, while samples GRE-M1, LAR-M3, MAT-M1 and MAT-M2 were processed via desulfurization (froth flotation using xanthates and MIBC frother; see Benzaazoua et al., 2000 for more details) in order to obtain acid-generation properties close to or within the uncertainty zone of static tests interpretation.

2.3.2. Physical properties

The D_{10}, D_{50} and D_{90} values taken from the grain size distributions are presented in Table 3 along with specific gravity (G_s) and specific surface areas (S_s). The grain size distributions of the studied tailings are typical of fine tailings from hard rock mines (Bussière, 2007; Vick, 1983), with D_{10} values ranging approximately from 1 to 4 μm and 80 to 95% passing 80 μm. G_s values are between 2.7 and 3.1 for all tailings studied. S_s values are similar for tailings LAR-M3, MAT-M1 and MAT-M2, from 1.5 to 1.9 m^2/g, while GRE-M1 and UQ-8 tailings have significantly higher S_s values with 3.24 and 5.89 m^2/g respectively. The higher S_s value of UQ-8 is related to a significant proportion of secondary oxides generated by sulfide oxidation prior to sampling.

2.3.3. Chemical and mineralogical properties

Table 3 presents the chemical composition of the tailings studied. All five tailings studied have relatively low sulfide contents, with the highest value at 5.72 wt.% (for UQ-8). The low sulfate contents are consistent with fresh tailings (less than 0.57 wt.% $S_{sulfate}$), except for sample UQ-8 which was partly oxidized (1.37 wt.% $S_{sulfate}$). The inorganic carbon (C_{inorg}) content of the tailings reflect the levels of carbonate minerals in the different tailings and ranges from 0.21 to 3.06 wt.%.

Table 4 presents the mineralogical composition of the tailings samples. Sample UQ-8 is composed of around 50 wt.% quartz and albite, with approximately equal amounts of pyrite, dolomite, ankerite

Table 3
Chemical composition and physical properties of the tailings studied (element concentrations in wt.%).

Element (wt.%)	UQ-8	GRE-M1	LAR-M3	MAT-M1	MAT-M2
Al	3.81	7.51	5.87	3.16	2.99
C_{inorg}	2.79	1.39	0.21	3.06	2.75
Ca	3.43	2.89	1.68	3.79	3.60
Cu	0.012	0.030	0.023	0.026	0.028
Fe	17.1	11.5	2.83	16.6	17.9
Mg	1.65	2.87	0.73	3.15	2.94
Mn	0.456	0.196	0.043	0.434	0.409
Na	1.80	1.36	1.37	1.01	1.01
Ni	0.005	0.017	0.008	0.007	0.007
Pb	0.008	0.034	0.046	0.028	0.028
S_{total}	7.09	1.09	0.816	1.90	2.85
$S_{sulfate}$	1.37	0.202	0.15	0.57	0.234
$S_{sulfide}$	5.72	0.89	0.666	1.33	2.62
Si	n/a	53.09	68.81	53.29	46.82
Zn	0.007	0.159	0.108	0.234	0.276
Ca + Mg + Mn	5.54	5.96	2.45	7.37	6.95
G_s	3.04	2.90	2.78	3.03	3.07
S_s (m^2/g)	5.89	3.24	1.54	1.90	1.49
% under 80 μm (%)	94.6	94.0	89.2	90.3	83.6
D_{10} (μm)	1.08	3.92	3.46	2.04	2.35
D_{50} (μm)	11.88	20.38	22.43	15.68	22.78
D_{90} (μm)	54.8	63.84	83.27	78.45	104.5

Table 4
Mineralogical composition of the tailings studied.

Mineral (wt.%)	UQ-8	GRE-M1	LAR-M3	MAT-M1	MAT-M2
Quartz	23.2	37.4	55.0	43.6	43.0
Albite	26.2	13.1	17.9	5.8	5.1
Chlorite	6.1	18.0	4.8	13.9	10.8
Muscovite	5.3	15.8	11.3		
Paragonite		6.9	6.6		
Phlogopite mica				4.1	4.2
Hornblende	3.8				
Calcite	2.9	2.8	1.0	4.0	3.6
Ankerite	6.1	4.6	1.8	8.9	8.3
Dolomite	7.7				
Pyrite	7.5	1.5	1.6	2.6	5.1
Magnetite				5.9	8.0
Siderite	7.5			11.2	11.8
Gypsum	3.7				
Total	100.0	100.1	100.0	100.0	99.9

and siderite (between 6.1 and 7.7 wt.%), and 2.9 wt.% calcite. The presence of gypsum (3.7 wt.%) results from the previous oxidation of this material in the field. Sample GRE-M1 is mainly composed of quartz, chlorite, muscovite and albite (for more than 80 wt.%), with minor amounts of ankerite (4.6 wt.%) and calcite (2.8 wt.%) and trace amounts of pyrite (1.5 wt.%). Approximately 55 wt.% of the LAR-M3 sample is composed of quartz, with albite and muscovite accounting for nearly 30 wt.% together; trace amounts of ankerite (1.8 wt.%), calcite (1.0 wt.%) and pyrite (1.6 wt.%) were also detected. Since samples MAT-M1 and MAT-M2 were obtained by desulfurization of the same material at two different levels, their global mineralogy are similar; the pyrite content of MAT-M1 (2.6 wt.%) is about half the pyrite content of MAT-M2 (5.1 wt.%). The balance of these samples is mostly composed of quartz (more than 43 wt.%) and chlorite (10 to 14 wt.%), with minor amounts of ankerite (between 8 and 9 wt.%) and calcite (between 3.6 and 4 wt.%).

The ankerite compositions in Table 5 show significant variations between mine sites, with stoichiometric coefficients varying from 0.25 to 0.37 for Mg and from 0.57 to 0.68 for iron, while Mn composition show little difference, varying from 0.06 to 0.08 in the samples studied. No ankerite composition analysis was performed on the LAR-M3 sample because of its low concentration (1.8 wt.%). As a result using a hypothetical ankerite composition for the LAR-M3 sample will not significantly affect the results.

3. Results and interpretation

3.1. Static test results

The chemical and mineralogical static test results are presented in Tables 6 and 7. Table 6 presents the mineralogical NP calculations from the Lawrence–Scheske and Lawrence–Scheske–Paktunc methods. Table 7 shows the static test results from all methods considered in this study.

The mineralogical results in Table 6 suggest that 72 to 95% of the NP is provided by carbonate minerals for the samples studied, depending on the method considered. Therefore, 5 to 28% of the NP is provided by silicate minerals. Sample UQ-8 has the highest NP contribution from carbonates (94–95%) while sample LAR-M3 has the lowest (72–76%). The main carbonate NP sources are ankerite (12.2–86.6 kg $CaCO_3$/t) and calcite (10.0–40.0 kg $CaCO_3$/t) for all tailings, in addition to dolomite (83.6 kg $CaCO_3$/t) for the UQ-8 sample. The main silicate NP source is chlorite (3.2–12.1 kg $CaCO_3$/t) for all studied samples.

Different criteria were proposed to evaluate the acid-generating potential based on NNP values. SRK (1989) and Miller et al. (1991) suggested the following ABA interpretations: acid generation is uncertain for NNP values between −20 and 20 kg $CaCO_3$/t, acid generation is likely for NNP values below −20 kg $CaCO_3$/t, and acid generation is unlikely for NNP values above 20 kg $CaCO_3$/t. Another useful tool to evaluate the AMD production potential using static tests is the NP to AP ratio (Price, 2005). Typically, the material may be considered non acid-generating if NP/AP > 2, uncertain if 2 > NP/AP > 1 and acid generating if NP/AP < 1 (Price, 2009).

The NP results in Table 7 vary significantly for a given sample depending on the method employed. On the other hand, AP results are similar for both the chemical and the Paktunc AP methods for all tailings studied, except for UQ-8 where the difference is more significant.

3.2. Static test comparisons

The different NP results are compared with each other in Fig. 1. The 1:1 line is shown for each comparison plot.

3.2.1. CCNP vs modified Sobek II NP

The CCNP results are higher than the modified Sobek II results for all tailings studied (Fig. 1a), except for LAR-M3 for which the results are very similar. Discrepancies between these methods may arise as a result of incorrect siderite quantification for CCNP calculation and the oxidation/hydrolysis of iron released during the modified Sobek II procedure. In addition, it can be seen that the results from the oxidized UQ-8 sample show the greatest deviation from the 1:1 relationship, probably because dissolution of acidic salts (hydroxides and sulfates) during the test diminishes the modified Sobek II NP results (Weber et al., 2004), and because dolomite in UQ-8 sample may not dissolve completely (Kwong and Ferguson, 1997). Therefore, the dolomite contribution to the overall UQ-8 NP is not fully taken into account in the modified Sobek II method.

Table 5
Ankerite composition in the tailings samples.

Element	UQ-8	GRE-M1	MAT-M1 and MAT-M2
	n = 10	n = 6	n = 10
Mg (coeff. a)			
Mean	0.25	0.37	0.33
Standard deviation	0.14	0.11	0.09
Mn (coeff. b)			
Mean	0.08	0.06	0.07
Standard deviation	0.02	0.02	0.03
Fe (coeff. c)			
Mean	0.68	0.57	0.60
Standard deviation	0.14	0.13	0.08
Composition	$Ca(Mg_{0.25}Mn_{0.08}Fe_{0.68})(CO_3)_2$	$Ca(Mg_{0.37}Mn_{0.06}Fe_{0.57})(CO_3)_2$	$Ca(Mg_{0.33}Mn_{0.07}Fe_{0.60})(CO_3)_2$
Molar mass	208.86	203.98	205.23

Table 6
individual contributions to the NP for mineralogical methods taking all minerals into account.

Mineral	Lawrence–Scheske NP (kg $CaCO_3$/t)					Lawrence–Scheske–Paktunc NP (kg $CaCO_3$/t)				
	UQ-8	GRE-M1	LAR-M3	MAT-M1	MAT-M2	UQ-8	GRE-M1	LAR-M3	MAT-M1	MAT-M2
Quartz	1.5	2.5	3.7	2.9	2.9	1.5	2.5	3.7	2.9	2.9
Albite	2.0	1.0	1.4	0.4	0.4	2.0	1.0	1.4	0.4	0.4
Chlorite	4.1	12.1	3.2	9.3	7.3	4.1	12.1	3.2	9.3	7.3
Muscovite	0.1	0.4	0.3	0.0	0.0	0.1	0.4	0.3	0.0	0.0
Phlogopite mica	0.0	0.0	0.0	3.9	4.0	0.0	0.0	0.0	3.9	4.0
Paragonite	0.0	0.2	0.2	0.0	0.0	0.0	0.2	0.2	0.0	0.0
Hornblende	1.9	0.0	0.0	0.0	0.0	1.9	0.0	0.0	0.0	0.0
Calcite	29.0	28.0	10.0	40.0	36.0	29.0	28.0	10.0	40.0	36.0
Ankérite	58.6	45.0	16.9	86.6	80.7	38.7	32.0	12.2	60.6	56.5
Dolomite	83.6	0.0	0.0	0.0	0.0	83.6	0.0	0.0	0.0	0.0
total NP	180.8	89.2	35.6	143.1	131.2	160.9	76.1	30.9	117.2	107.0
NP carbonates	171.2	73.0	26.9	126.5	116.7	151.3	60.0	22.2	100.6	92.5
NP other	9.6	16.2	8.7	16.6	14.5	9.6	16.2	8.7	16.6	14.5
% NP carbonates	95%	82%	76%	88%	89%	94%	79%	72%	86%	86%
% NP other	5%	18%	24%	12%	11%	6%	21%	28%	14%	14%

3.2.2. Paktunc CNP vs modified Sobek II NP

The modified Sobek II NP results are close to the Paktunc CNP results that take into account the presence of oxidizable cations for all tailings, except for UQ-8 (Fig. 1b) where the modified Sobek II NP is significantly lower than the Paktunc CNP. This difference is again mainly due to (1) the presence of soluble acidic salts (Weber et al., 2004) and (2) the possible incomplete dissolution of dolomite during the modified Sobek II procedure. The modified Sobek II NP results are slightly higher than the Paktunc CNP for the GRE-M1, MAT-M1 and MAT-M2 tailings, probably because the silicates contribution to the NP is only accounted for in the modified Sobek II method.

3.2.3. CCNP vs Paktunc CNP

The Paktunc CNP results are lower than the CCNP results for all tailings except LAR-M3, for which the results are similar (Fig. 1c). These results are explained by the ankerite iron deduction from the NP in the Paktunc CNP method. The difference between the CCNP and the Paktunc CNP results increases with ankerite content.

Table 7
static test results from different methods on the 5 studied tailings samples.

Parameter	UQ-8	GRE-M1	LAR-M3	MAT-M1	MAT-M2
Modified Sobek II NP	64.2	71.7	13.6	93.9	91.0
Paktunc CNP	143.5	53.6	19.8	88.5	81.2
Lawrence–Scheske NP	180.8	89.2	35.6	143.1	131.2
CNP	232.5	115.8	17.5	255.0	229.2
CCNP	167.7	115.8	17.5	158.2	127.3
L–S–P NP	160.9	76.1	30.9	117.2	107.0
AP	199.4	27.7	24.5	54.5	81.8
Paktunc AP	125.1	25.0	26.7	43.4	85.1
Modified Sobek II NP–chemical AP					
NNP	−135.2	44.0	−10.9	39.4	9.2
NP/AP	0.3	2.6	0.6	1.7	1.1
Paktunc CNP–Paktunc AP					
NNP	18.4	28.5	−6.9	45.1	−3.9
NP/AP	0.7	1.9	0.8	1.6	1.0
Lawrence–Scheske NP–chemical AP					
NNP	−18.6	61.5	11.1	88.6	49.4
NP/AP	0.9	3.2	1.5	2.6	1.6
CCNP–chemical AP					
NNP	−31.7	88.1	−7.0	103.7	45.5
NP/AP	0.8	4.2	0.7	2.9	1.6
Lawrence–Scheske–Paktunc NP–chemical AP					
NNP	−38.5	48.4	6.4	62.7	25.2
NP/AP	0.8	2.7	1.3	2.2	1.3

3.2.4. Paktunc CNP vs Lawrence–Scheske NP

The Lawrence–Scheske NP results are systematically higher than the Paktunc CNP results for the tailings studied (Fig. 1d), mainly because the iron content is not accounted for in the Lawrence–Scheske method, and because the silicates contribution to the NP is taken into account in the Lawrence–Scheske NP.

3.2.5. Lawrence–Scheske NP vs modified Sobek II NP

All of the studied samples have a Lawrence and Scheske NP higher than the modified Sobek NP (Fig. 1e). All studied samples contain ankerite, which partially explains the higher NP results from the Lawrence–Scheske method than from the modified Sobek II procedure.

The Lawrence–Scheske method can be modified in order to take the iron content of neutralizing minerals into account, by incorporating the "c_i" parameter from the Paktunc CNP method. This modified Lawrence–Scheske–Paktunc method (Eq. (7)) combines the characteristics of both methods, accounting for the silicates contribution to the overall NP and the non-oxidizable cations content of the minerals:

$$NP = 1000\ kg/t \cdot M_{CaCO_3} \cdot \sum_{i=1}^{n} \frac{C_{Mi} R_i c_i}{M_{Mi}} \quad (7)$$

In Eq. (7), NP stands for neutralization potential (kg $CaCO_3$/t), M_{CaCO3} is the calcite molar mass (100.09 g/mol), M_{Mi}, C_{Mi} and R_i are respectively the molar mass (g/mol), the weight content (wt.%) and the reactivity factor (unitless), and the c_i is the sum of the stoichiometric coefficients of non-oxidizable cations in the carbonate. The results from the Lawrence–Scheske–Paktunc method are shown in Fig. 1e. It appears that the NP results obtained by this method are closer to the modified Sobek II results than for the original Lawrence–Scheske version.

Sample UQ-8 still shows a greater modified Sobek NP than the Lawrence–Scheske NP, despite the correction for the iron content of the carbonate minerals. As mentioned previously, discrepancy can be explained by incomplete dolomite dissolution (Kwong and Ferguson, 1997) and the presence of acid salts (Weber et al., 2004) that both lower the modified Sobek II NP result. An unweathered UQ-8 sample (Villeneuve, 2004; Villeneuve et al., 2003, 2009) gave a Sobek II NP result of 180 kg $CaCO_3$/t, which is closer to the NP estimated by the mineralogical methods (143.5 to 180.8 kg $CaCO_3$/t). Since the XRD mineralogical quantification of the fresh UQ-8 sample is close to that of the weathered UQ-8 sample (aside from the presence of gypsum), one can assume that the lower modified Sobek NP result

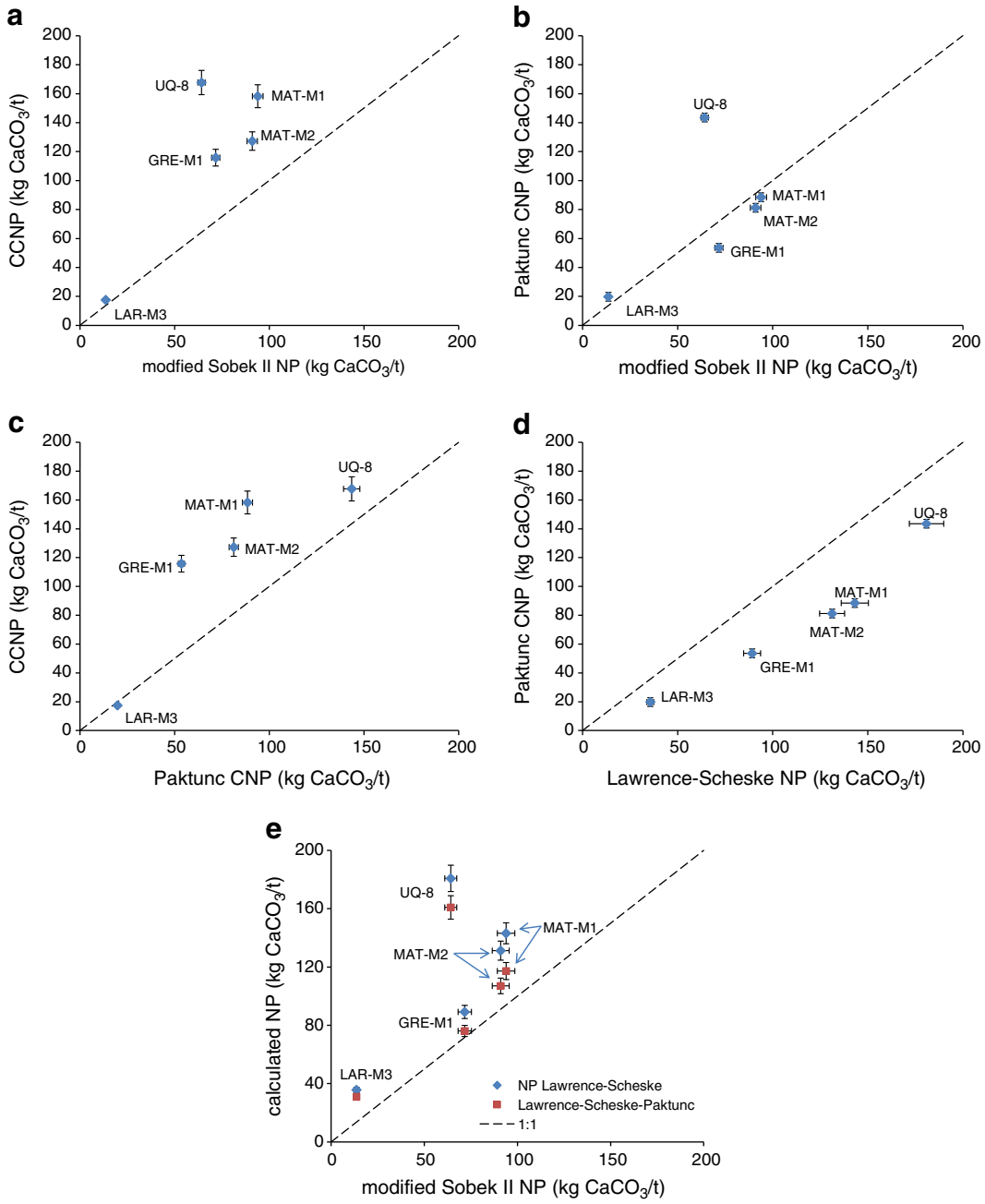

Fig. 1. Comparison of NP results from different methods on the studied samples: a) CCNP vs modified Sobek II NP, b) Paktunc CNP vs modified Sobek II NP, c) CCNP vs Paktunc CNP, d) Paktunc CNP vs Lawrence–Scheske NP and e) calculated NP for Lawrence–Scheske NP and Lawrence–Scheske–Paktunc NP vs modified Sobek II.

on the weathered UQ-8 sample is mainly attributed to the presence of soluble acidic oxidation product salts rather than to incomplete dolomite dissolution. The absence of such acidic salts from the XRD data collected from the UQ-8 sample suggests that these salts are amorphous (e.g. Cravotta, 1994; Hakkou et al., 2008) and/or at concentrations under the detection level. Dolomite dissolution during the modified Sobek II procedure is verified in Section 4.1.

4. Discussion

4.1. Mineralogical evolution during modified Sobek II test

As seen in the previous section, subtle changes in a static test method or interpretation may lead to a significant change in the acid-generating nature prediction statement, particularly for low acid-generating tailings. To obtain an accurate acid-generating potential classification, some hypotheses related to the modified Sobek II procedure must be validated:

1. Dolomite dissolves only partially during the modified Sobek II test;
2. Siderite does not contribute to the NP determination during the modified Sobek II test;
3. Ankerite and calcite are completely dissolved during the modified Sobek II test;
4. Neutralizing silicates contribute at least partially to NP in the modified Sobek II test.

The mineralogical composition of the samples after submission to the modified Sobek II test procedure was evaluated by XRD. The comparison of XRD diffraction patterns of the samples before and after submission to a modified Sobek II procedure enable a better

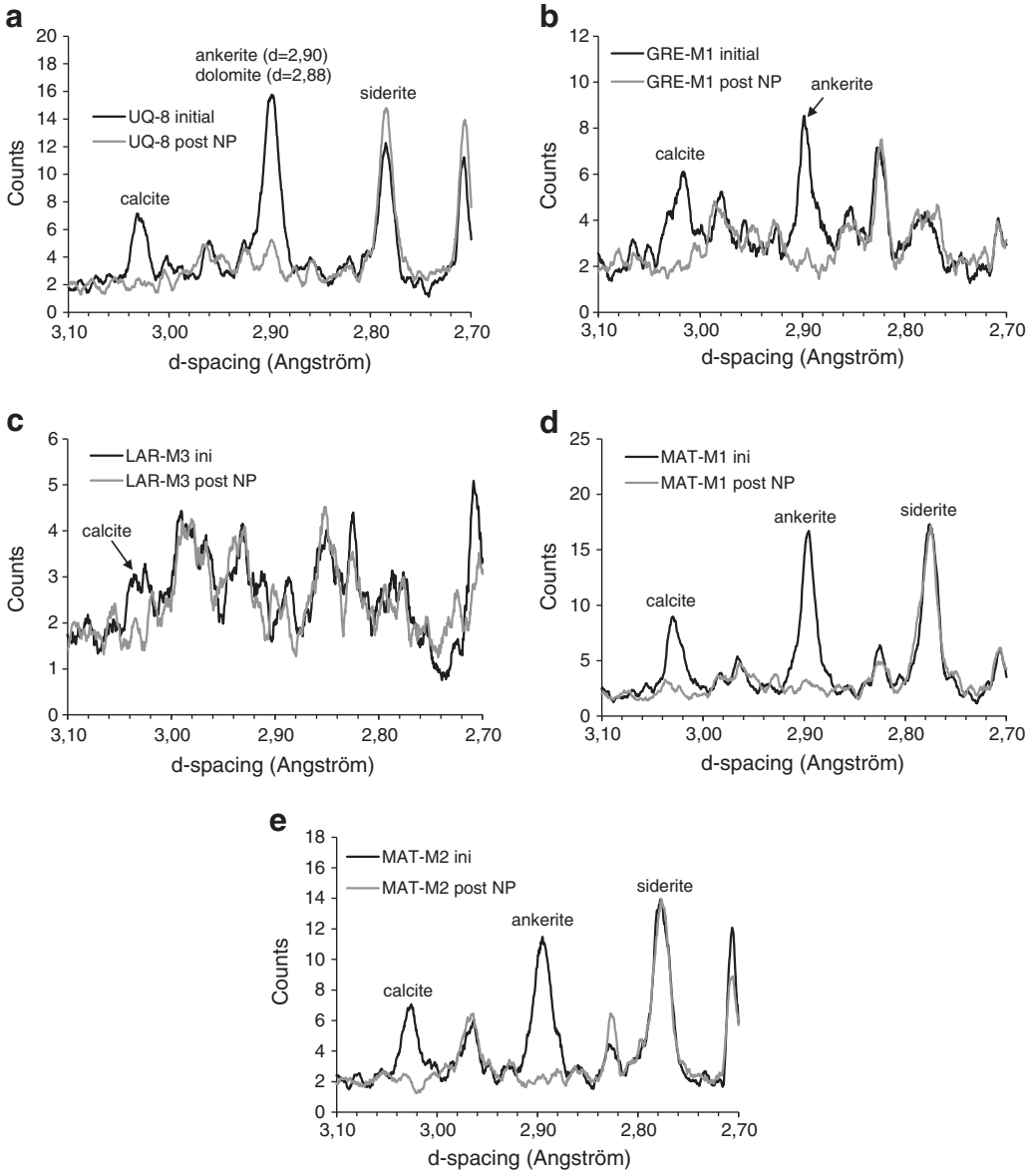

Fig. 2. XRD evidence of carbonates fate during the modified Sobek II procedure (d-spacing between 2.70 and 3.10 Å for a) UQ-8, b)GRE-M1, c)LAR-M3, d) MAT-M1 and e) MAT-M2).

appreciation of the mineral dissolution during the modified Sobek II test, particularly for carbonates. Fig. 2a–e shows XRD data of major carbonate peaks (d-spacing ranging from 2.70 to 3.10 Å) from samples before and after the modified Sobek procedure. The major calcite peak (d = 3.035 Å) disappears after the modified Sobek II procedure, indicating complete calcite dissolution in all samples studied (Fig. 2a–e). The ankerite and dolomite major peaks (respectively 2.89 and 2.88 Å) disappear after the procedure, except for the UQ-8 sample (Fig. 2a). While both ankerite and dolomite are detected by XRD in this sample, the GRE-M1, MAT-M1 and MAT-M2 samples only contain XRD-detectable ankerite (Fig. 2b, d and e respectively). Observation of ankerite and dolomite secondary peaks is necessary to appreciate the dissolution level of these minerals because their peaks are overlapped. The secondary ankerite and dolomite XRD peaks of the UQ-8 tailings are shown in Fig. 3. A significant decrease in the ankerite secondary peaks can be seen at d = 2.199 and 1.812 Å on Fig. 3a and b respectively. The decrease in dolomite secondary peaks at d = 2.191 and 1.785 Å is not as significant. The remaining secondary dolomite peaks suggest incomplete dolomite consumption during the modified Sobek procedure.

The XRD data shown in Figs. 2 and 3 were acquired with a single acquisition run at 0.005°/s steps. A higher definition XRD pattern using two acquisition runs at 0.001°/s was undertaken on the UQ-8 sample after the modified Sobek II procedure (see Fig. 4a–c) in order to clarify the interpretations regarding dolomite dissolution. The major dolomite and ankerite peaks are overlapped and still present after the modified Sobek II digestion procedure (2.88 and 2.90 Å respectively, Fig. 4a). The secondary dolomite peaks are detected (2.191 and 1.785 Å, shown respectively on Fig. 4b and c), but the presence of the secondary ankerite peaks is questionable (2.199 Å and 1.812 Å, shown respectively on Fig. 4b and c). Thus, the ankerite is most likely dissolved while dolomite is still present, which means that the peak at 2.88–2.90 Å (Fig. 4a) is attributable mainly to dolomite.

The major siderite peaks shown in Fig. 2 are practically unaltered during the modified Sobek II procedure for samples UQ-8, MAT-M1 and MAT-M2. Thus, it appears that siderite does not seem to dissolve in the conditions of the modified Sobek II procedure. On the other hand, Siderite is believed to be consumed during the original Sobek procedure without enough time for iron to oxidize and hydrolize,

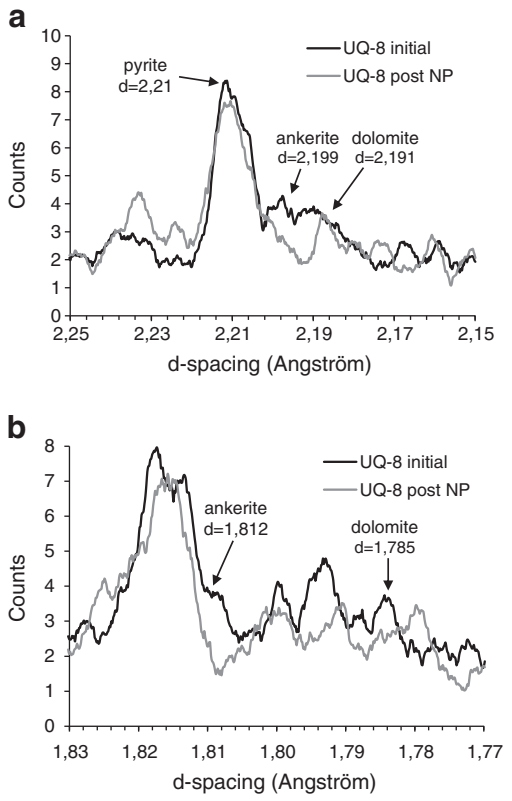

Fig. 3. XRD data showing secondary ankerite and dolomite peaks before and after the modified Sobek II procedure on tailings UQ-8 sample (d-spacing for a) 2.15–2.25 Å and b) 1.77–1.83 Å).

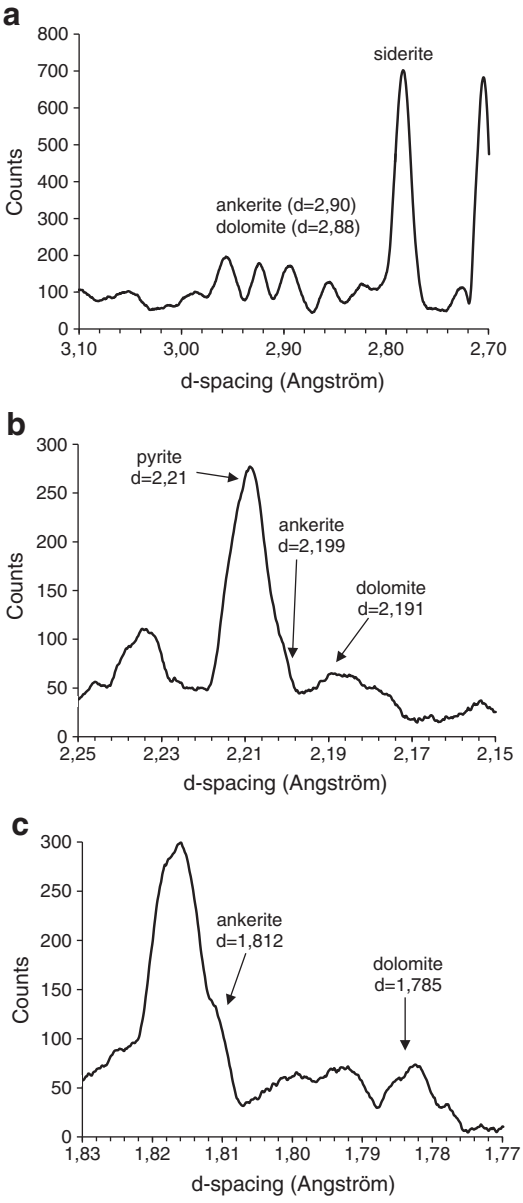

Fig. 4. XRD data showing the main and secondary ankerite/dolomite peaks with multiple data acquisition runs on tailings UQ-8 after the modified Sobek II procedure (d-spacing for a) 2.70–3.10 Å, b) 2.15–2.25 Å and c) 1.77–1.83 Å).

therefore overestimating the NP obtained by the original Sobek procedure when siderite is present (Jambor et al., 2003). To this regard, the modified SObek II method is best suited for siderite-containing samples.

The main silicates found in the studied tailings are presented in Table 4. The neutralizing silicates identified by Jambor et al. (2002, 2007) that are also found in the studied samples are chlorite (approx. 6 kg $CaCO_3$/t when pure), mica/phlogopite (approx. 8 kg $CaCO_3$/t when pure), and mica/muscovite (approx. 1 kg $CaCO_3$/t when pure). These proposed mineral NP should only be considered as indicators of the most reactive minerals to acid digestion, because they were determined using the original Sobek procedure. The neutralizing silicate minerals within in the studied tailings do not appear to be significantly altered during the modified Sobek procedure, as suggested by XRD data. No muscovite peak decrease is observed for the studied tailings, except for LAR-M3 (Fig. 5a). A slight chlorite peak alteration is observed for all tailings except MAT-M2 suggesting that chlorite is slightly altered by the procedure, as illustrated by the GRE-M1 sample in Fig. 5b. The major phlogopite peak is not significantly different in shape and size before and after the modified Sobek II procedure, as illustrated in Fig. 5c for the MAT-M2 sample. However, it is possible that the silicates alteration in the static test become negligible to the bulk of the particle after it is micronized for XRD analysis. Therefore, it is possible that silicate alteration is greater than what can be deduced from XRD data as interpreted in the present study.

In summary, the following hypotheses were verified by the XRD data obtained in this study:

1. Dolomite only partially dissolves during the modified Sobek II test, while calcite and ankerite seem to be completely dissolved; however, this needs to be verified further on more samples because only one sample contained dolomite.
2. XRD data interpretation does not detect significant alteration of siderite during the modified Sobek II procedure, unlike in the original Sobek procedure test, where siderite is dissolved (Jambor et al., 2003), probably due to the higher digestion temperature;
3. Calcite and ankerite are completely dissolved during the Sobek II procedure;
4. Slight chlorite and muscovite alteration were caused by the modified Sobek II procedure. Therefore, neutralizing silicates partially contribute to the NP as determined by this method.

4.2. Static test selection

Mineralogical investigations are necessary for an appropriate static test selection and in the results interpretation. Methods only taking carbonates into account (such as CNP, Paktunc CNP) should be avoided when silicate minerals provide a significant proportion of a material's NP. The silicates contribution to the NP can be crucial: Heikkinen and Räisänen (2008) observed a particular case in which

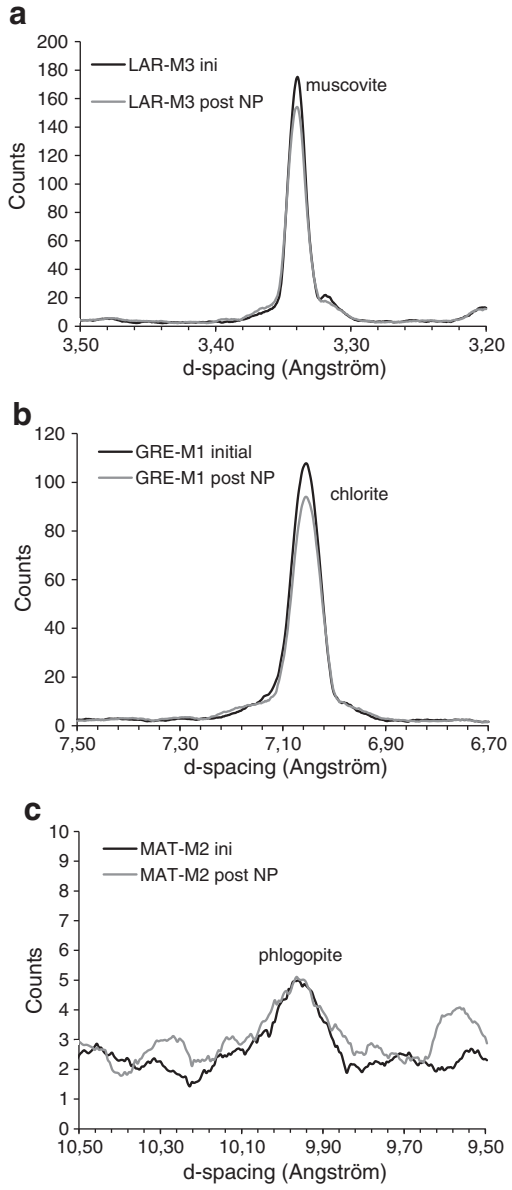

Fig. 5. XRD evidence of neutralizing silicate minerals fate during the modified Sobek II procedure (d-spacing for a) 3.20–3.50 Å, b) 6.70–7.50 Å and c) 9.50–10.50 Å).

the CNP procedure suggests that the tailings are likely acid-generating, while the Lawrence and Scheske (1997) method suggests that they are not. When iron-bearing neutralizing minerals provide a significant proportion of a material's NP, methods not accounting for the released iron oxidation and hydrolysis from neutralizing minerals should also be avoided. Particular attention should be given to the presence of acidic salts resulting from sulfide oxidation, which may decrease the apparent NP in Sobek-like methods. Weber et al. (2004) argued that sulfide-rich materials (particularly when containing framboïdal pyrite) and materials containing secondary acidic salts resulting from previous sulfide oxidation decrease the apparent NP of samples subjected to a Sobek-like procedure because of the acidity and iron released by the oxidation products. Paste pH measurement provides a qualitative idea of the presence of acidity within the sample.

Finally, particular care must be observed for tailings with significant dolomite content, as Sobek-like methods appear to incompletely dissolve this mineral. These precautions become even more important for samples close to or within the uncertainty zone of static test interpretation, as is often the case for low net acid-generating materials.

Guidelines for an appropriate NP method selection for low net acid-generating tailings may be drawn from comparisons between NP results from the studied samples and the literature. These guidelines are summarized in the flowchart shown in Fig. 6. The following presents the static test results interpretation with regards to the flowchart in Fig. 6.

4.2.1. UQ-8

The NNP values for the UQ-8 tailings vary between −135 kg $CaCO_3$/t (modified Sobek II NP–chemical AP) and 18.4 kg $CaCO_3$/t (Paktunc CNP and AP), while the NP/AP ratio varies from 0.3 to 1.7. The UQ-8 tailings may be classified as likely AMD generating or within the uncertainty zone, depending on the methods employed in the static test interpretation.

Since UQ-8 contains a significant amount of dolomite, the Sobek II procedure should be avoided. In addition, methods not accounting for the ankerite and siderite content of the UQ-8 tailings should be avoided. Therefore, the Lawrence–Scheske, CNP and the CCNP (which only take siderite into account) methods should not be used for the UQ-8 tailings. Finally, methods not taking the silicates into account are acceptable for the UQ-8 tailings because the neutralizing silicates are expected to contribute 5–6% of the overall NP (see Table 6). Thus, two approaches are more appropriate to evaluate the net acid-generating potential of UQ-8 using the guidelines:

1. The Paktunc CNP–Paktunc AP couple, which classifies the sample in the uncertainty zone with the NNP (18.4 kg $CaCO_3$/t) but acid-generating with the NP/AP ratio (0.7).
2. The Lawrence–Scheske–Paktunc NP–chemical AP couple classifies the sample as potentially acid-generating with the NNP (−38.5 kg $CaCO_3$/t) and the NP/AP ratio (0.8).

Hence, it is expected that the true NNP value would be between these two boundaries.

4.2.2. GRE-M1

All methods considered in this study classify the GRE-M1 sample as non acid-generating based on NNP values between 28.5 and 88.1 kg $CaCO_3$/t. The NP/AP values correspond to uncertain and to non-acid generating with values between 1.9 and 4.2. The GRE-M1 sample contains ankerite and a contribution of 18–21% from neutralizing silicates (mainly from chlorite; see Table 6). The CCNP, the Paktunc CNP and the Lawrence–Scheske NP methods could be considered for the GRE-M1 tailings because of the low contributions from silicates compared to other minerals, while the significant contribution of ankerite to the NP favours the use of methods considering the iron content of minerals.

The remaining approaches (Sobek II–chemical AP, Paktunc CNP–Paktunc AP and Lawrence–Scheske–Paktunc–chemical AP methods) classify the GRE-M1 material as non acid-generating with the NNP criteria with values between 28.5 and 48.4 kg $CaCO_3$/t. The NP/AP ratio of the Sobek II–chemical AP and Lawrence–Scheske–Paktunc NP–chemical AP methods (2.6 and 2.7 respectively) consider the GRE-M1 tailings non-acid generating. The Paktunc CNP–Paktunc AP NP/AP ratio (1.9) falls just at the limit of the uncertainty zone but does not account for the silicates contribution to the NP. Thus, this material may be considered as non-acid generating.

4.2.3. LAR-M3

The LAR-M3 tailings are classified in the NNP uncertainty zone for all methods considered with values between −10.9 and 11.1 kg $CaCO_3$/t. However, they fall between the acid-generating and uncertainty zones with the NP/AP ratio (0.6–1.5). The LAR-M3 tailings are mainly composed of silicates with less than 3 wt.% calcite and ankerite which provide 72–76% of the NP (Table 6), while the silicates are believed to contribute for approximately 24 to 28% of the overall NP (Table 6). Therefore, methods not accounting for the presence of

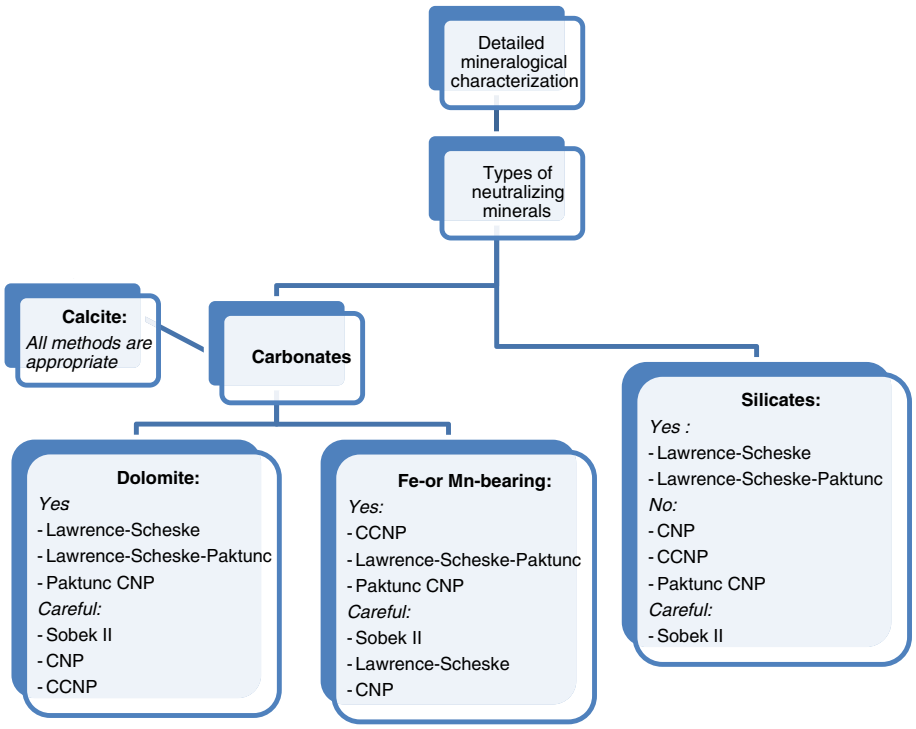

Fig. 6. Static test selection flowchart for low-NP, low-AP mine tailings.

iron or silicate contributions should be avoided for these tailings. Thus, the preferred methods for the LAR-M3 tailings are the Sobek II–chemical AP and Lawrence–Scheske–Paktunc–chemical AP methods that give NNP values and NP/AP ratios within the uncertainty zones. Despite the use of the flowchart, the static test assessment of the LAR-M3 tailings is still uncertain.

4.2.4. MAT-M1

The MAT-M1 tailings are considered non acid-generating with the NNP values of all methods considered in this study, with values between 39.4 and 103.7 kg $CaCO_3$/t. The NP/AP ratios for this sample range from 1.6 to 2.9. The MAT-M1 tailings contain calcite, ankerite and siderite, as well as neutralizing silicates providing between 12 and 14% of the overall NP (Table 6). Therefore, methods not considering the iron content of minerals (Lawrence–Scheske NP, CNP, CCNP) must not be used for these tailings, but methods not taking silicates into account (Paktunc CNP, CNP, CCNP) may still be used. This leaves the Sobek II–chemical AP, Paktunc CNP–Paktunc AP and the Lawrence–Scheske–Paktunc NP–chemical AP methods that classify the MAT-M1 tailings as non acid-generating with the NNP criteria (respectively 39.4, 45.1 and 62.7 kg $CaCO_3$/t). The NP/AP ratios of these methods (respectively 1.7, 1.6 and 2.6) consider the MAT-M1 tailings to lie between the uncertainty and non acid-generating zones.

4.2.5. MAT-M2

According to NNP criteria, the MAT-M2 material is considered either non acid-generating (Lawrence–Scheske NP–chemical AP, CCNP–chemical AP, Lawrence–Scheske–Paktunc NP–chemical AP) or within the uncertainty zone (modified Sobek II–chemical AP, Paktunc CNP–Paktunc AP). The NP/AP ratio considers this tailings sample within the uncertainty zone (1.0–1.6 NP/AP ratios).The MAT-M2 tailings contain the same minerals as MAT-M1 but in different amounts: calcite, ankerite and siderite, with neutralizing silicates providing between 11 and 14% of the overall NP (Table 6). AS for MAT-M1, methods not accounting for the iron content of minerals (Lawrence–Scheske NP, CCNP) should be avoided, while methods not taking silicates into account (Paktunc CNP, CNP, CCNP) may still be used. The Paktunc CNP–Paktunc AP and Sobek II–chemical AP methods classify the MAT-M2 tailings as uncertain with the NNP value (−3.9 and 9.2 kg $CaCO_3$/t respectively), while the Lawrence–Scheske–Paktunc NP–chemical AP couple classifies the MAT-M2 tailings just above the uncertainty zone with the NNP value (25.2 kg $CaCO_3$/t).

In summary, it has been demonstrated that proper method selection and interpretation based on mineralogical data can reduce the range of static test results and refine their interpretation for tailings having low net acid-generating potentials. However, one method alone rarely is perfectly suited for a material as methods rarely account for all characteristics of a given mineralogy.

5. Conclusion

Static tests are an important tool in the optimization of mine waste management at the mine site. A misclassification of the AMD generation potential for a given waste can have important economical and environmental impacts. In this study, different static tests were used to assess the NP of mine wastes and were compared for 5 Canadian hard rock mine tailings with low net acid-generation potentials. Significant differences in NP results were obtained for the tailings studied depending on the method used, demonstrating the need to develop tools for appropriate method selection. Results suggested that dolomite does not completely dissolve during a modified Sobek II test, while ankerite and calcite do dissolve. It was also demonstrated that siderite is not dissolved by the modified Sobek II test and that the main neutralizing silicates appear to be only slightly altered by the test. A modification to the Lawrence and Scheske method (called the Lawrence–Scheske–Paktunc method), which takes into account the presence of oxidizable cations such as iron and manganese in the minerals, was also suggested to improve the precision of this method.

Guidelines were issued in order to improve static tests selection for low net acid-generating tailings. The tool is based on the mineralogy of the tailings and on the characteristics of each static test. However, it is recommended to perform kinetic tests (ex. humidity cells or column tests; see Morin and Hutt, 1997, and Demers et al., 2010, for more

details) to better define the AMD generating potential for results located within or close to the uncertainty zone.

Acknowledgements

The authors would like to acknowledge the financial contribution of The Polytechnique-UQAT-NSERC Chair on Environment and Mine Waste Management. The URSTM staff is thanked for their help in the laboratory work.

References

Adam, K., Kourtis, A., Gazea, B., Kontopoulos, A., 1997. Evaluation of static tests used to predict the potential for acid drainage generation at sulfide mine sites. Transactions of the Institution of Mining and Metallurgy, section A, mining industry 106, A1–A8.

Allen, T., 1990. Particle Size Measurement. Chapman and Hall, New York.

Aubertin, M., Bussière, B., Bernier, L., 2002. Environnement et gestion des résidus miniers. Presses Internationales Polytechnique, Corporation de l'École Polytechnique de Montréal, Montréal.

Bennett, J.W., Comarmond, M.J., Jeffrey, J., 2000. Comparison of sulfidic oxidation rates measured in the laboratory and the field. Proceedings from the 5th International Conference on Acid Rock Drainage (ICARD), Denver, 1, pp. 171–180.

Benzaazoua, M., Bussiere, B., Kongolo, M., McLaughlin, J., Marion, P., 2000. Environmental desulphurization of four Canadian mine tailings using froth flotation. International Journal of Mineral Processing 60, 57–74.

Bethum, K.J., Lockington, D.A., Williams, D.J., 1997. Acid mine drainage: comparison of laboratory testing to mine site conditions. 4th ICARD, Vancouver, BC, pp. 305–318.

Blowes, D.W., Ptacek, C.J., Jambor, J.L., Weisener, C.G., 2003. The geochemistry of acid mine drainage. In: Holland, H.D., Turekian, K.K. (Eds.), Chapter 9.05 of the Treatise on geochemistry. Elsevier. ISBN: 0-08-043751-6, pp. 149–204 (Elsevier Ltd.).

Brunauer, S., Emmett, P.H., Teller, E., 1938. Adsorption of gases in multimolecular layers. Journal of the American Chemical Society 60, 309.

Bussière, B., 2007. Colloquium 2004: hydro-geotechnical properties of hard rock tailings from metal mines and emerging geo-environmental disposal approaches. Canadian Geotechnical Journal 44 (9), 1019–1052.

Coastec Research Inc., 1991. Acid rock drainage prediction manual. MEND report 1.16.1b, MEND, Ottawa, Ontario.

Cravotta, C.A., 1994. Secondary iron-sulphate minerais as sources of sulphate and acidity. Environmental Geochemistry of Sulfide Oxidation: American Chemical Soc Washington DC, pp. 335–364.

Day, S.J., 1991. New methods for determination of key mineral species in acid generation prediction by acid base accounting. MEND report 1.16.1c. MEND, Ottawa, Ontario.

Demers, I., Bussière, B., Aachib, M., Aubertin, M., 2010. Repeatability evaluation of instrumented column tests in cover efficiency evaluation for the prevention of acid mine drainage. Water, Air, and Soil Pollution 1–16. doi:10.1007/s11270-010-0692-6.

Duncan, D.W., Bruynesteyn, A., 1979. Determination of Acid Production Potential of Waste Materials. Metallurgy Society AIME, paper A79-29. (10p.).

Feasby, D.G., Liu, L., Graham, B., Elliott, L., 2001. Selection of test procedures to evaluate potential for acid rock drainage and metal leaching from mine tailings and waste rock. Proceedings from the Securing the Future International Conference on Mining and the Environment, June 25–July 1, Skellefteå, Sweden, pp. 1–10.

Frostad, S., Klein, B., Lawrence, R.W., 2000. Kinetic Testing 2. Scaling up laboratory data to predict field rates of weathering: Proceedings from the 5th International Conference on Acid Rock Drainage (ICARD), Denver, CO, 1, pp. 651–659.

Frostad, S.R., Price, W.A., Bent, H., 2003. Operational NP determination — accounting for iron manganese carbonates and developing a site-specific fizz rating. In: Spiers, G., Beckett, P., Conroy, H. (Eds.), Mining and the environment, Sudbury 2003. Laurentian University, Sudbury, Ontario, pp. 231–237.

Hakkou, R., Benzaazoua, M., Bussière, B., 2008. Acid mine drainage at the abandoned kettara mine (Morocco): 1. Environmental characterization. Mine Water and the Environment 27, 145–159.

Heikkinen, P.M., Räisänen, M.L., 2008. Mineralogical and geochemical alteration of Hitura sulfide mine tailings with emphasis on nickel mobility and retention. Journal of Geochemical Exploration 97 (1), 1–20.

Jambor, J.L., Dutrizac, J.E., Groat, L.A., Raudsepp, M., 2002. Static tests of neutralization potentials of silicate and aluminosilicate minerals. Environmental Geology 43, 1–17.

Jambor, J.L., Dutrizac, J.E., Raudsepp, M., Groat, L.A., 2003. Effect of peroxide on neutralization-potential values of siderite and other carbonate minerals. Journal of Environmental Quality 32, 2373–2378.

Jambor, J.L., Dutrizac, J.E., Raudsepp, M., 2007. Measured and computed neutralization potentials from static tests of diverse rock types. Environmental Geology 52, 1019–1031.

Johnson, D.B., Hallberg, K.B., 2003. The microbiology of acidic mine waters. Research in Microbiology 154, 466–473.

Kwong, Y.T.J., 1993. Prediction and prevention of acid rock drainage from a geological and mineralogical perspective. MEND Report 1.32.1. CANMET, Ottawa. (47p.).

Kwong, Y.T.J., Ferguson, K.T., 1997. Mineralogical changes during NP determinations and their implications. Proc. 4th International Conference on Acid Rock Drainage (ICARD), Vancouver, Canada, pp. 435–447.

Lapakko, K.A., 1994a. Evaluation of neutralization potential determinations for metal mine waste and a proposed alternative. Proc. International Land reclamation and Mine Drainage Conference, Pittsburg, USBM SP 06A-94, pp. 129–137.

Lapakko, K.A., 1994b. Comparison of Duluth complex rock dissolution in the laboratory and field. International Land Reclamation and Mine Drainage Conference and Third International Conference on the Abatement of Acidic Drainage, Pittsburgh, P.A., V.1, pp. 419–428.

Lawrence, R.W., Scheske, M., 1997. A method to calculate the neutralization potential of mining wastes. Environmental Geology 32 (2), 100–106.

Lawrence, R.W., Wang, Y., 1996. Determination of neutralizing potential for acid rock drainage prediction. MEND/NEDEM report 1.16.3, Canadian Centre for Mineral and Energy Technology, Ottawa, Canada.

Lawrence, R.W., Wang, Y., 1997. Determination of neutralization potential in the prediction of acid rock drainage. Proc. 4th ICARD, Vancouver, BC, pp. 449–464.

Lawrence, R.W., Poling, G.W., Marchant, P.B., 1989. Investigation of predictive techniques for acid mine drainage. MEND/NEDEM report 1.16.1a, Canadian Centre for Mineral and Energy Technology, Ottawa, Canada.

Li, M.G., 2000. Acid acid rock drainage prediction for low-sulfide. Low-Neutralization Potential Mine Wastes: 5th International Conference on Acid Rock Drainage (ICARD), Denver, USA, pp. 567–580.

Liao, B., Huang, L.N., Ye, Z.H., Lan, C.Y., Shu, W.S., 2007. Cut-off net acid generation pH in predicting acid-forming potential in mine spoils. Journal of Environmental Quality 36, 887–891.

Malmström, M.E., Destouni, G., Banwart, S.A., Stromberg, B.H.E., 2000. Resolving the scale-dependence of mineral weathering rates. Environmental Science and Technology 34 (7), 1375–1378.

Merkus, H.G., 2009. Particle size measurements: fundamentals, practice, quality. Particle technology series. Springer Science+Business Media B.V.

Miller, S.D., Jeffery, J.J., Wong, J.W.C., 1991. Use and misuse of the acid–base account for AMD prediction. Proc. of the 2nd International Conference on the Abatement of Acidic Drainage, Montreal, Canada, 3, pp. 489–506.

Miller, S., Andrina, J., Richards, D., 2003. Overburden geochemistry and acid rock drainage scale-up investigations at the Grasberg Mine, Papua Province, Indonesia. 6th International Conference on Acid Rock Drainage (ICARD), Cairns, North Queensland, Australia, pp. 111–121.

Morin, K.A., Hutt, N.M., 1997. Environmental Geochemistry of Minesite Drainage: Practical Theory and Case Studies. MDAG Publishing, Vancouver.

Nicholson, R.V., 2004. Overview of near neutral pH drainage and its mitigation: results of a MEND study. MEND Ontario workshop, Sudbury, Canada, May. 2004.

Nordstrom, D.K., 2000. Advances in the hydrogeochemistry and microbiology of acid mine waters. International Geology Review 42, 499–515.

Nordstrom, K.D., Alpers, C.N., 1999. Geochemistry of acid mine waters. In: Plumlee, G.S., Logsdon, M.J. (Eds.), The environmental geochemistry of mineral deposits, Part A: processes, techniques, and health issues: Reviews in Economic Geology, 6A, pp. 133–160.

Paktunc, A.D., 1998. ModAn: an interactive computer program for estimating mineral quantities based on bulk composition. Computers & Geosciences 24 (5), 425–431.

Paktunc, A.D., 1999a. Discussion of "A method to calculate the neutralization potential of mining wastes" by Lawrence and Scheske. Environmental Geology 38 (1), 82–84.

Paktunc, A.D., 1999b. Mineralogical constraints on the determination of neutralization potential and prediction of acid mine drainage. Environmental Geology 39 (2), 103–112.

Paktunc, A.D., 2001. ModAn — a computer program for estimating mineral quantities based on bulk composition: windows version. Computers & Geosciences 27, 883–886.

Plante, B., Benzaazoua, M., Bussière, B., 2011. Kinetic testing and sorption studies by modified weathering cells to characterize the potential to generate contaminated neutral drainage. Mine Water and the Environment 30, 22–37.

Price, W.A., 2005. List of potential information requirements in metal leaching/acid rock drainage assessment and mitigation work. MEND Report 5.10E. MEND, Smithers, British Columbia.

Price, W.A., 2009. Prediction manual for drainage chemistry from sulphidic geologic materials. MEND Report 1.20.1. MEND, Smithers, British Columbia.

Rietveld, H.M., 1993. The Rietveld Method. In: Young, R.A. (Ed.), Oxford University Press.

Savitzky, A., Golay, M.J.E., 1964. Smoothing and differentiation of data by simplified least squares procedures. Analytical Chemistry 36, 1627–1639.

Sherlock, E.J., Lawrence, R.W., Poulin, R., 1995. On the neutralization of acid rock drainage by carbonate and silicate minerals. Environmental Geology 25, 43–54.

Skousen, J., Renton, J., Brown, H., Evans, P., Leavitt, B., Brady, K., Cohen, L., Ziemkiewicz, P., 1997. Neutralization potential of overburden samples containing siderite. Journal of Environmental Quality 26, 673–681.

Skousen, J., Simmons, J., McDonald, L.M., Ziemkiewicz, P., 2002. Acid–base accounting to predict post-mining drainage quality on surface mines. Journal of Environmental Quality 31, 2034–2044.

Sobek, A.A., Schuller, W.A., Freeman, J.R., Smith, R.M., 1978. Field and laboratory methods applicable to overburdens and minesoil. EPA report no. EPA-600/2-78-054, pp. 47–50.

SRK, 1989. Draft acid rock drainage technical guide, vol. 1, prepared for the British Columbia Acid Mine Drainage Task Force. Steffens, Robertson and Kirsten (SRK), Inc. (B.C.), in association with Norecol Environment Consultants and Gormely Process Engineering, Vancouver, B.C.

Sverdrup, H., 1990. The kinetics of base cation release due to chemical weathering. Lund University Press, Lund.

Taylor, J.C., Hinczak, I., 2001. Rietveld made easy: a practical guide to the understanding of the method and successful phase quantifications. Sietronics Pty Ltd.
Vick, S.G., 1983. Planning, Design, and Analysis of Tailings Dams. John Wiley and Sons.
Villeneuve, M., 2004. Évaluation du comportement géochimique à long terme de rejets miniers à faible potentiel de génération d'acide à l'aide d'essais cinétiques. Mémoire de maîtrise, École Polytechnique de Montréal, Canada.
Villeneuve, M., Bussière, B., Benzaazoua, M., Aubertin, M., Monroy, M., 2003. The influence of kinetic test type on the geochemical response low acid generating potential tailings. Proc. of the 10th international conference on Tailings and Mine Waste 2003, Vail, Colorado, USA.
Villeneuve, M., Bussière, B., Benzaazoua, M., Aubertin, M., 2009. Assessment of interpretation methods for kinetic tests performed on tailings having a low acid generating potential. Paper presented at Securing the Future and 8th International Conference on Acid Rock Drainage (ICARD), June 23–26, 2009, Skellefteå, Sweden.
Weber, P.A., Thomas, J.E., Skinner, W.M., Smart, R.S.C., 2004. Improved acid neutralisation capacity assessment of iron carbonates by titration and theoretical calculation. Applied Geochemistry 19, 687–694.
Weber, P.A., Thomas, J.E., Skinner, W.M., Smart, R., St, C., 2005. A methodology to determine the acid-neutralization capacity of rock samples. The Canadian Mineralogist 43, 1183–1192.
Xu, R., 2000. Particle characterization: light scattering methods. Kluwer Academic.

ATTACHMENT 18

Chapter 19

Geologic Controls on the Composition of Natural Waters and Mine Waters Draining Diverse Mineral-Deposit Types

G.S. Plumlee,[1] K.S. Smith,[1] M.R. Montour,[1] W.H. Ficklin,[2] and E.L. Mosier[3]
[1]*U.S. Geological Survey, Box 25046, MS 973, Federal Center, Denver, CO 80225-0046*
[2]*Deceased;* [3]*Retired*

INTRODUCTION

Sulfide-bearing mineral deposits formed in reduced conditions out of contact with an oxygenated atmosphere. When sulfides in the deposits are exposed by natural erosion or by mining to atmospheric oxygen and water, weathering of the sulfides can produce natural or mining-related acid-rock drainage. The prediction of water quality that results from mining and mineral processing activities has therefore become a high priority in the permitting of mining activities worldwide, in order to prevent the formation of or mitigate the environmental effects of deleterious drainage waters. In addition, estimating the compositions of natural waters that drained mineral deposits prior to mining is crucial to establish appropriate baseline environmental standards at mine sites.

There are a variety of techniques currently in use to predict the acidity or metal content of mine-drainage waters, most common of which are static and kinetic testing procedures. In static procedures such as acid-base accounting (White et al., 1997, 1999), the contents of acid-generating sulfide minerals from ores and wastes from a proposed mine are measured and balanced against the measured contents of acid-consuming minerals such as carbonates; based on this balance, the materials are determined to be acid generating or non-acid-generating. In kinetic tests such as column or humidity-cell tests (ASTM, 1996), samples of ores and wastes are allowed to react over a period of time under laboratory conditions with oxidized waters or moist air, and the pH and metal contents of the resulting leachates are then measured.

Although both static and kinetic methods are widely used to help predict the compositions of mine waters, they have several potential limitations. Most important of these are (1) whether the samples used in the tests adequately represent the range of mineralogic characteristics commonly present in complex mineral deposits, (2) whether the time scale and laboratory conditions of kinetic tests adequately reproduce the time scales and physical, geochemical, and biological conditions actually present in the mine, mine dump, or tailings impoundment environment, and (3) whether kinetic test leachate compositions accurately reproduce actual drainage quality.

Another approach to mine-drainage prediction that can be used to supplement the static and kinetic engineering tests is one in which the compositions of existing mine waters draining geologically similar deposit types in similar climates are measured empirically and then interpreted in a geologic and geochemical context. By evaluating the compositions of waters draining geologically comparable deposits in comparable climates, it is possible to place constraints on the potential ranges in composition of waters that might result from the development of a particular ore deposit. Such empirical examinations of existing drainage waters help overcome the issues of sample representation, adequacy of time scales, and accuracy of reproduction of natural conditions by laboratory experiments—the waters already are draining larger, more representative volumes of rock, and they are generated under field conditions and time scales.

Past studies that demonstrated the importance of geologic controls on mine-drainage compositions include those of Wildeman et al. (1974) in the Central City mining district, Colorado, and those of Wai et al. (1980) in the Bunker Hill mine, Coeur d'Alene district, Idaho. Results of both these studies showed that drainage compositions vary predictably within a mine (Wai et al., 1980) and across a district (Wildeman et al., 1974) as a function of deposit geology. However, in the time since these studies were carried out and prior to the early 1990s, a systematic examination of mine-drainage compositions across a spectrum of mineral deposit types, and within different ore types of given deposit types was generally lacking. Since the early 1990s, a number of studies have begun to examine both natural- and mine-drainage water compositions in the context of mineral-deposit geology (Ficklin et al., 1992; Plumlee et al., 1992, 1993a, b; Runnells et al., 1992; Smith et al., 1994; Price et al., 1995; studies in du Bray, 1995; Goldfarb et al., 1996, 1997; Eppinger et al., 1997; Kelley and Taylor, 1997).

This paper summarizes results to date of an ongoing empirical study examining the composition of mine waters and natural waters draining a broad spectrum of mineral deposit types, mineralogic zones within deposit types, and geologically similar mineral deposit types in different climates (Ficklin et al., 1992; Plumlee et al., 1992, 1993a; Smith et al., 1994). We include in this study data that we have collected and data compiled from the literature.

The results to date of this empirical study illustrate the many fundamental controls that mineral-deposit geology exerts, in combination with geochemical processes and biogeochemical processes, on the compositions of mine-drainage waters and natural waters draining unmined mineral deposits. Other important controls, such as climate, mining method used, and mineral processing method used, modify the effects mandated by deposit geology, geochemical, and biogeochemical processes. Our results show that, by interpreting empirical drainage data in a geologic context, it is possible to constrain the potential ranges in pH and ranges in metal concentrations of mine- and natural-drainage waters that may develop within different mineralogic zones, ore types, or alteration types in a given mineral deposit. Our results are not sufficiently precise that they can be used to quantitatively predict

373

pyrite or base-metal sulfides (such as chalcopyrite and sphalerite) also led to greater dissolved base-metal contents in waters draining deposits with generally similar acid-neutralizing capacities.

Concentrations of individual elements in the drainage waters in part reflect the elements' abundances in the deposits drained by the waters. Due to the abundance of sphalerite in many metal deposits, zinc is the predominant metal (other than Fe, Al, and Mn) in most drainage waters; however, copper-rich, sphalerite-poor deposits tend to have copper-dominant drainage waters, arsenic-rich deposits have arsenic-rich waters, and so on. Due to its limited tendency to sorb onto particulates, zinc is generally the predominant metal in drainage waters with near-neutral pH values. The greatest dissolved zinc values we have measured in near-neutral drainage waters occur in waters draining pyrite- and sphalerite-rich ores with abundant carbonate minerals to buffer pH, but that have limited dissolved oxygen (which prevents the formation of iron particulates that would otherwise sorb more of the dissolved zinc).

For natural waters that drain unmined mineral deposits, the content of dissolved base metals increases at a given pH with increasing base-metal sulfide content of the deposit. In addition, deposits with base-metal sulfides exposed at the ground surface by rapid erosion or glaciation (the natural analogs to the exposure of fresh sulfides by mining activity) commonly have natural-drainage waters with similar pH values but greater dissolved base-metal concentrations than natural waters draining deposits with no sulfides exposed at the ground surface.

A number of mines that are currently in production are developed in mineral deposits that have undergone extensive to complete oxidation during weathering prior to mining. Especially common in dry climates where water tables are deep, this oxidation removes the acid-generating sulfide minerals and leaves behind non-acid-generating oxides, hydroxides, and carbonates. Thus, all deposit types, regardless of their original sulfide content, that have been completely oxidized during pre-mining weathering will most likely generate non-acidic waters with generally low concentrations of metals. However, even small pockets of sulfide-rich, carbonate-poor rocks that remain after weathering can be sufficient to generate acid-mine waters in an otherwise oxidized deposit.

Climate and mining method controls

As can be seen from the Appendix, and as will be shown in the following discussions, climate and the methods used during mining and mineral processing can affect drainage compositions, though mostly within the compositional ranges mandated by geologic characteristics. For example, waters draining mine dumps and those that form in open pits tend to have somewhat more acidic and metalliferous compositions than those draining mine workings, due to the increased surface area of sulfides exposed to weathering and increased opportunities for (a) atmospheric oxygen access to the sulfides and (b) evaporative concentration. Waters draining sulfide-rich tailings impoundments can be quite acidic and metal-bearing even in deposit types with high carbonate contents (see Fig. 19.6, acidic waters draining pyrite- and carbonate-rich deposits). The milling and tailings disposal process can concentrate the pyrite sufficiently that acid generated by sulfide oxidation overwhelms the acid-neutralizing capacity of carbonates in the tailings; for example, physical sorting of dense sulfides from less dense carbonates may create sulfide-rich zones in the tailings that have high acid-generating potential. Similarly, storm waters draining sulfide-rich, carbonate-bearing mine waste dumps may potentially be acidic, if the acid waters formed by the dissolution of soluble salts growing on sulfide surfaces flush so rapidly from the dumps as to not have time to react with carbonate minerals in the dumps.

Mineral deposits commonly generate less drainage in arid and semi-arid climates than in wet climates. For example, in arid climates, many mines are developed above deep water tables, and many mine dumps may not drain except for short periods after storms. The data in the Appendix indicate that, for acid-generating deposit types, those drainage waters that do occur in arid climates tend to be more acidic and metalliferous than those in wetter climates due to the effects of increased evaporation and the decreased potential to be diluted by non-mineralized ground and surface waters.

MINE- AND NATURAL-DRAINAGE SIGNATURES OF DIVERSE MINERAL-DEPOSIT TYPES

Although mineral deposits can be typed according to overall similarities in their geologic characteristics, geologic setting, and mode of formation, they typically have complex variations in mineralogy, alteration, and (or) wallrock within a given deposit. Thus, the grouping of mine- and natural-drainage waters based on similar geologic characteristics alone (Fig. 19.6) is insufficient to characterize the possible range of drainage compositions that can occur within a geologically complex deposit type. Instead, drainage compositions must be measured and summarized for each ore type, mineralogic zone, alteration type, and (or) host rock type for a given mineral deposit type. In the following discussion, we will use Ficklin plots to show how drainage compositions vary as a predictable function of deposit type and location within a deposit type. We will start our discussion with the deposit types having geologic characteristics in their main ore zones that are favorable for the generation of the most acidic waters, and shift progressively to those deposits having ores that are likely to generate less acidic and metal-bearing waters. However, even in the deposit types most likely to generate highly acidic waters, we will show that a variety of drainage compositions, including those that are less acidic and metalliferous, can occur within different parts of the deposits.

Volcanogenic massive sulfide (VMS) deposits

Syngenetic VMS deposits result from the discharge of hydrothermal mineralizing fluids onto the ocean floor, a process analogous to that observed today where sub-oceanic hot spring systems, known as "black smokers," form chimneys and other sulfide deposits on the ocean floor. For summaries of the geologic characteristics of this type, the reader is referred to reviews such as Franklin (1993), Slack (1993), Taylor et al. (1995), Evans et al. (1995), and references contained therein.

The deposits form in or near areas of subaqueous volcanism, which provides the heat source for the hydrothermal systems, and are commonly associated with volcanic or metamorphosed volcanic rocks. Volcanic-hosted VMS deposits include Cyprus-type, which occur in basaltic volcanic rocks, and Kuroko-type, which occur in andesitic to rhyolitic volcanic rocks (Franklin, 1993). In contrast, Besshi-type VMS deposits occur in sequences of pre-

dominantly sedimentary rocks such as turbidites and black shales (or their metamorphosed equivalents, graphitic schists), with some interbedded volcanic rocks such as basalts or intrusive rocks such as diabase sills.

Variations in metal contents permit further differentiation of VMS deposits. Franklin (1993) differentiates copper-zinc (Cu > Zn content) and zinc-lead-copper (Zn > Pb > Cu content) subtypes. Deposits of the zinc-lead-copper subtype are associated with silicic volcanic rocks. Blackbird-type deposits (named after the Blackbird mining district, Idaho) are cobalt- and arsenic-rich Besshi-type deposits.

VMS deposits are typically zoned, with pyrite, pyrrhotite, and chalcopyrite forming in the hotter, sub-seafloor and near-vent portions of the deposits. These "yellow ores" grade upward and outward into sphalerite- and (in the case of the zinc-lead-copper-subtype deposits) galena-rich ores ("black ores") that were deposited on the ocean floor. As implied by their name, VMS deposits can consist of massive ore lenses that are predominantly to nearly entirely composed of sulfides. The wallrocks present around the sub-seafloor feeder zones of the deposits are typically altered to chlorite-sericite-pyrite or chlorite-rich assemblages. Some carbonate minerals may be present in the surrounding host rocks, especially in sediment-hosted Besshi-type deposits.

Drainage-water compositions

Geologic controls on the composition of mine drainage waters from VMS deposits are summarized by Taylor et al. (1995) and Goldfarb et al. (1996). As shown on Figure 19.7A, mine-drainage compositions measured in VMS deposits span a large range in pH and metal contents, reflecting geologic controls, the effects of evaporation, and climate. Mine waters from the Iron Mountain, California, Kuroko-type deposit are the most acidic and metalliferous ever measured (Alpers and Nordstrom, 1991; Nordstrom and Alpers, 1999), with field pH values as low as -3.5 and dissolved contents of Fe, Al, Zn, and Cu as high as tens of grams per liter. These extreme compositions most likely reflect several factors. First, the mine waters likely flow through the massive sulfide lenses and do not interact with any potentially acid-consuming wallrock minerals. Second, the temperatures in the mine stopes are very hot (possibly as high as 60–70°C) and water temperatures reach as high as 46–47°C (D.K. Nordstrom, written commun., 1998), due to heat generated by exothermic pyrite oxidation. Thus evaporative concentration of the mine waters is likely to be important (Alpers and Nordstrom, 1991). Third, the climate at the West Shasta district is relatively dry, but with a distinct annual wet-dry

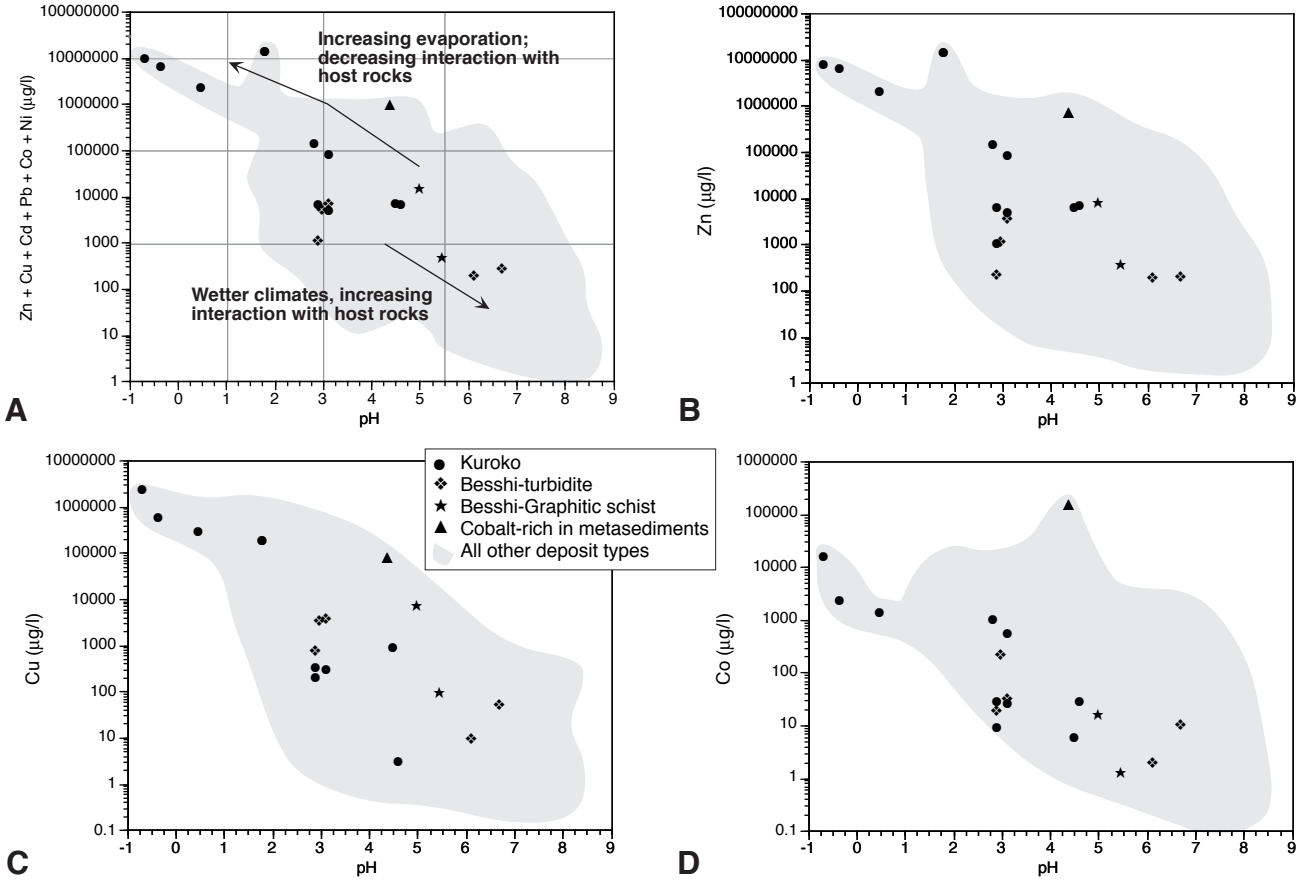

FIGURE 19.7—Plots of mine-drainage compositions for volcanogenic massive sulfide (VMS) deposits: A. Ficklin diagram; B. Zinc; C. Copper. D. Cobalt. Note differences in scale of the concentration axis between the plots. Shaded areas enclose all data points on corresponding Figures 19.1, 19.2.

cycle, which also enhances periodic evaporative concentration of the mine waters.

Mine-water compositions measured in some portions of Iron Mountain (C.N. Alpers, oral commun., 1994), as well as in other Kuroko-type VMS deposits such as Holden, Washington (Kilburn and Sutley, 1997) are typically quite acidic and metalliferous, although less so than the extremely acid waters at Iron Mountain (Appendix). The waters with less extreme acid pH values likely reflect buffering by reactions with aluminosilicate minerals in the deposit host rocks. The Holden mine site is also located in a wetter climate than Iron Mountain, which may lead to greater recharge of ground waters into the mine workings, and may preclude high amounts of evaporation that would lead to extreme concentrations of acid and metals in solution.

Although we have not included in our summary mine-drainage data for Cyprus-type VMS deposits, it is likely that the water compositions are generally similar to those of Kuroko-type VMS deposits. Waters that interact with the intermediate to basaltic-composition rocks hosting Cyprus deposits may be somewhat less acidic than those draining Kuroko-type deposits, due to the increased reactivity and acid-buffering capacity of the basaltic host rocks.

The limited data we have collected on waters draining Besshi-type deposits hosted by graphitic schists in the Great Smoky Mountains of Tennessee indicate a somewhat higher pH and lower overall metal content than for waters draining Kuroko-type deposits. This may result from both the partly disseminated nature of the ore within the graphitic schists and the wetter climate. The data collected by Goldfarb et al. (1996) for turbidite-hosted, Besshi-type VMS deposits in Prince William Sound, Alaska, show a trend to significantly higher pH values and lower metal contents than for waters draining the Kuroko-type VMS deposits. Goldfarb et al. (1996) attributed the higher pH and lower metal contents to the significantly wetter and lower-temperature climate of the area.

Another factor that may affect drainage pH in some VMS deposits is the presence of carbonate minerals in the deposit host rocks. In such deposits, mine waters that interacted significantly with carbonate-bearing host rocks might be expected to have near-neutral pH values but elevated levels of zinc, copper, and cadmium (see for example the distribution of data points marked by triangles on Figure 19.6, which depict drainage compositions of pyrite-rich, base metal-rich and carbonate-rich deposit types).

The relative abundances of metals such as Zn and Cu in the VMS drainage waters in part reflect (1) the overall chemical composition and mineralogy of the deposits, (2) the mineralogic zones within the deposits, and (or) (3) seasonal variations stemming from flushing of salts from the mine workings. For example, the Co- and Cu-rich massive sulfides of the Blackbird mine, Idaho (data summarized by Evans et al., 1995, and McHugh et al., 1987), have exceptionally high levels of Co in the drainage waters (Fig. 19.7D). Copper-rich stockwork feeder zones of VMS deposits generate drainage waters that are enriched in Cu relative to Zn, whereas waters that drain the overlying sphalerite-rich ore zones of the deposits likely have enrichments of Zn over Cu in the waters. Alpers et al. (1994) have shown that seasonal flushing of soluble salts from the mine workings at Iron Mountain results in significant decreases in Zn/Cu due to the selective dissolution of copper-bearing melanterite during the flush.

High sulfidation epithermal (quartz alunite epithermal) deposits

High-sulfidation epithermal, or quartz-alunite epithermal, deposits are Au-Cu-Ag deposits that form in close spatial and temporal association with shallow (within the upper several km of the Earth's crust) silicic volcanic or intrusive centers (Fig. 19.8). At Summitville, Colorado, for example, the deposits are hosted by a 22 Ma quartz latite volcanic dome, and were formed during the late stages of the dome-forming cycle of volcanism. Other examples include Red Mountain Pass, Colorado; Goldfield and Paradise Peak, Nevada; Mount Macintosh, British Columbia, Canada; and Julcani, Peru (see references to studies of these deposits contained in Plumlee et al., 1995c). The deposits are characterized by intense acid leaching and alteration of the deposit host rocks that were generated by magmatic gas condensates prior to ore-stage mineralization. In general, the cores of the deposits are characterized by intersecting zones of silica alteration (where all constituents of the host rock except silica were removed by the leaching), flanked by thin zones of quartz-alunite-pyrite and quartz-kaolinite alteration. In some of these deposits such as Summitville, the silica alteration is vuggy, due to the complete acid leaching of original feldspar phenocrysts from the volcanic host rock. The core of intensely altered rock is surrounded proximally by large volumes of argillically altered rock (the rock is altered to clays and pyrite), and a distal zone of propylitically altered rock (altered to contain epidote, chlorite, some pyrite, and calcite) (Fig. 19.8). Subsequent to the intense acid alteration, hydrothermal fluids, whose flow was focused primarily along the higher-permeability vuggy silica zones, deposited sulfide-rich assemblages containing pyrite, native sulfur, enargite (a copper-arsenic sulfosalt), chalcocite and covellite (copper sulfides), and native gold in the central portions of the deposits, grading upward and outward into sphalerite-, galena-, and barite-rich assemblages in some deposits. At depth beneath the acid-altered rocks, the hydrothermal fluids typically deposited chalcopyrite (a copper-iron sulfide) and tennantite-tetrahedrite (copper-arsenic sulfosalts) in rocks altered to quartz sericite-pyrite assemblages.

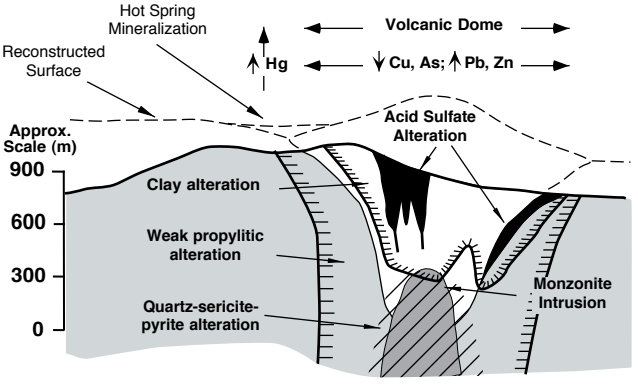

FIGURE 19.8—Generalized cross-section of a high-sulfidation deposit, based primarily on zoning relationships observed at Summitville, Colorado, and Julcani, Peru. Figure from Plumlee et al. (1995c), based on references contained therein.

APPENDIX

This appendix is a compilation of dissolved compositions of mine waters and natural waters draining diverse mineral deposit types. Most mine, mine-dump, and tailings data were collected from past producing sites. The data included were either collected during this study, or were compiled from data published in the literature. The data are grouped according to deposit type and, for a given deposit type, further grouped according to ore zone, alteration zone, or mineralogic zone within the deposit.

Abbreviations for water type are as follows: a-adit; mg-groundwater from underground mine; d-mine dump; ms-seep affected by mining activity; t-tailings water; ts-seep affected by tailings waters; op-pond or lake in open pit; os-seep affected by open-pit waters; og-ground water affected by open-pit mining; mst-stream affected by mine drainage waters; ns-natural seep; nst-stream affected by natural drainage waters. Sites we know to be currently under remediation are noted by "r". Tailings water compositions listed here do not include measured concentrations of cyanide and organic chemicals.

The data contained in this compilation were determined by a variety of analytical methods, which we have indicated whenever possible using different type styles. Anions were determined using ion chromatography. Major cations and trace metals were determined by a variety of techniques, including flame or graphite furnace AA (shown in plain type), ICP-AES (bold type), or ICP-MS (italic type). In a few data sets compiled from the literature, no analytical methods were documented; in these cases, plain type was used for all elements listed. Negative concentration values indicate that the species or element was present in the sample, but in concentrations below the analytical detection limit. Samples marked with an asterisk have metal concentrations measured in mg/l or µg/l units; those without asterisks were measured in generally equivalent ppm or ppb units. These and other sources of uncertainty in the data and interpretations are discussed in the Summary of Data and Methods section.

Deposit type *Ore / alteration type* Sample	Description	Water Type	Reference
Volcanogenic massive sulfide (VMS)			
Kuroko-type, hosted by volcanic rocks			
*Rich-90WA103	Richmond Mine, Iron Mtn., California	a, r	Alpers and Nordstrom (1991)
*Rich-90WA108	Richmond Mine, Iron Mtn., California	a, r	Alpers and Nordstrom (1991)
*Rich-90WA109	Richmond Mine, Iron Mtn., California	a, r	Alpers and Nordstrom (1991)
*Rich-90WA110A	Richmond Mine, Iron Mtn., California	a, r	Alpers and Nordstrom (1991)
*LMG	Les Mines Gallen, Rouyn Noranda, Quebec	ms	Rao et al. (1994)
Hol-511	Holden, Washington, USA	t	Kilburn and Sutley (1997)
Hol-528	Holden, Washington, USA	t	Kilburn and Sutley (1997)
Hol-529	Holden, Washington, USA	t	Kilburn and Sutley (1997)
Hol-534	Holden, Washington, USA	a	Kilburn and Sutley (1997)
Hol-548	Holden, Washington, USA	d	Kilburn and Sutley (1997)
Hol-549A	Holden, Washington, USA	t	Kilburn and Sutley (1997)
Hol-549B	Holden, Washington, USA	t	Kilburn and Sutley (1997)
Besshi-type, hosted by sedimentary and intermediate submarine volcanic host rocks			
Duch-1	Duchess Mine, Latouche Island, Alaska	a	Goldfarb et al. (1996)
Duch-2	Duchess Mine, Latouche Island, Alaska	t	Goldfarb et al. (1996)
Black-18A	Blackbird Mine, Latouche Island, Alaska	t	Goldfarb et al. (1996)
Beat-16	Beatson Mine, Latouche Island, Alaska	t	Goldfarb et al. (1996)
V-Ely-1	Creek downstream from Ely Mine, Vermont	mst	This study
Besshi-type, hosted by graphitic schists			
FC-3	Adit, Fontana Creek, Tennessee	a	This study
SUG-1 0.2	Sugar Mine, Tennessee	a	This study
Cobalt-rich, hosted by metamorphosed sediments			
*BB25	Cobalt, Idaho	os, r	McHugh et al. (1987)
High sulfidation (quartz alunite epithermal)			
Acid-sulfate alteration			
AD-3	Reynolds Adit, Summitville, Colorado	a, r	This study; Plumlee et al. (1995b)
AD-3	Reynolds Adit, Summitville, Colorado	a, r	This study; Plumlee et al. (1995b)
AD-3	Reynolds Adit, Summitville, Colorado	a, r	This study; Plumlee et al. (1995b)
AD-3	Reynolds Adit, Summitville, Colorado	a, r	This study; Plumlee et al. (1995b)
AD-3	Reynolds Adit, Summitville, Colorado	a, r	This study; Plumlee et al. (1995b)
AD-1435C	Reynolds Adit, Summitville, Colorado	a, r	This study; Plumlee et al. (1995b)

Deposit type *Ore / alteration type* Sample	Temp. °C	Spec. Cond. µS/cm	Alk. mg/l $CaCO_3$	pH	Diss. O_2 ppm	SO_4 mg/l	F mg/l	Cl mg/l	Al mg/l	As µg/l
Volcanogenic massive sulfide (VMS)										
Kuroko-type, hosted by volcanic rocks										
*Rich-90WA103	35			0.48		118000			**2210**	**56400**
*Rich-90WA108	42			-0.35		420000			**4710**	**169000**
*Rich-90WA109	32			-0.7		360000			**6680**	**154000**
*Rich-90WA110A	42			-1		760000			**1420**	**340000**
*LMG				1.8					3520	50000
Hol-511	15	4420		2.9		1400	1		*8.4*	*-1*
Hol-528	8	5600		2.9		1700	2	2	*>10*	*-1*
Hol-529	5	2680		3.1		860		1	*>10*	*-1*
Hol-534	4.5	840		4.5		340	0.6	3	*2.4*	*-1*
Hol-548	3	960		4.6		340	0.7	1.7	*2.2*	*1*
Hol-549A	16	16000		3.1		12000	7		*>10*	*1*
Hol-549B	18	37500		2.8		39700	60		*>10*	*1*
Besshi-type, hosted by sedimentary and intermediate submarine volcanic host rock										
Duch-1	7	320	20	6.1	9.5	166	0.07	3.8	0.015	
Duch-2	12	790		2.9	9	197	0.07	4	>3	
Black-18A	10	822	-10	3.1	8	311	0.4	3.7	>3	
Beat-16	7	146	38	6.7	5	31	0.07	3.4	0.004	
V-Ely-1	21.5	1046		2.98	9	352	0.16	0.51	**14**	
Besshi-type, hosted by graphitic schist										
FC-3	14	73.2		5.45	6.5	23	0.06	0.48	-0.5	*-1*
SUG-1 0.2	13	286		4.98	6	103	0.16	0.55	**1.8**	*-1*
Cobalt-rich, hosted by metamorphosed sediments										
*BB25				4.38		2400	2.4	21	54	39
High sulfidation (quartz alunite epithermal)										
Acid sulfate alteration										
AD-3	4	2100		3.16		2200			**112**	360
AD-3	4.5	3200		2.94	10	1920		4.7	**130**	**400**
AD-3	4	5400		2.72	10	4530			**290**	*2900*
AD-3						4510	-0.5	2.2	**230**	*790*
AD-3	4	1800		3.23	10	**1650**	**0.67**	**6.5**	**150**	*130*
AD-1435C	4	10		3.25	-	2133			**160**	*460*
Chand-1	4	7110		2.37	10	15000	3.7	1.0	**430**	*3900*
Chand-1	6	5530		2.77	12	**6250**	**0.99**	**1.5**	**340**	*1500*
Chand-1	4	5820		2.92	12	**12600**	**1.6**	**1.3**	**310**	*2500*
Dike 2	6	10300		2.31	10	23000		26	**2350**	*5700*
550D-R	13.5	7650		2.52	10	8370			**890**	*190*
North Dump						3800	1.7	2	**260**	*-40*
N Dump S Seep	7.5	7500		2.41	10	**11300**	**3.3**	**2.5**	**710**	*160*
SC12	14.5	4100		2.9	10	3360			**200**	*110*
Blackstrap	~14	38000		1.75		125800		240	**5380**	**15000**
SOB-1 Seep	18	19500		1.71	10	29850			**2100**	*28000*
IOWA-1	5	2800		2.79	10	1900	-0.5	2.0	**190**	*18*
SPIT-1 Pond	19	3300		2.48	10	2320	0.70	1.3	**140**	*690*
SPIT-2 Pond	19	4600		2.41	10	7890	-0.25	2.2	**290**	*3400*
NPIT-1 Pond	14	2510		2.73		2140	1.1	0.59	**180**	*110*
Ch Seep	3	3670		3.01	10	**5000**	**-0.5**	**0.51**	**280**	*82*
Missionary East	5	1450		3.84	4.5	**1540**	**0.51**	**1.1**	**120**	*200*
Sh-1	8	5090		3.41	6	**7310**	**1.2**	**27**	**210**	*-20*

Deposit type	Ca	Cd	Ce	Co	Cu	Fe tot	Fe^{++}	Mg	Mn	Ni
Ore /alteration type	mg/l	µg/l	µg/l	µg/l	µg/l	mg/l	mg/l	mg/l	µg/l	µg/l
Sample										
Volcanogenic massive sulfide (VMS)										
Kuroko-type, hosted by volcanic rocks										
*Rich-90WA103	**183**	**15900**		**1300**	**290000**	**20300**	18100	**821**	**17100**	**660**
*Rich-90WA108	**424**	**43000**		**2200**	**578000**	**55600**	50800	**1380**	**41800**	**2800**
*Rich-90WA109	**330**	**48300**		**15500**	**2340000**	**86200**	79700	**1450**	**42100**	**2900**
*Rich-90WA110A	**279**	**211000**		**5300**	**4760000**	**111000**	34500	**437**	**22900**	**3700**
*LMG	5	45300			191000	29800	16700	2790	146000	
Hol-511	*130*	*5.9*	*27*	*9*	*200*	*270*		*27*	*2100*	*11*
Hol-528	*130*	*22*	*48*	*27*	*330*	*390*		*44*	*2700*	*28*
Hol-529	*84*	*28*	*24*	*25*	*300*	*110*		*28*	*1500*	*23*
Hol-534	*94*	*29*	*2*	*5.6*	*900*	*0.94*		*8.8*	*320*	*7.2*
Hol-548	*78*	*62*	*4.2*	*27*	*3*	*-0.2*		*9.6*	*320*	*78*
Hol-549A	*160*	*1500*	*110*	*510*	*>40000*	*440*		*>100*	*>6000*	*150*
Hol-549B	*130*	*2300*	*170*	*970*	*>40000*	*>500*		*>100*	*>6000*	*180*
Besshi-type, hosted by sedimentary and intermediate submarine volcanic host rocks										
Duch-1	42	0.8		1.8	9.5	0.13		4	200	-6
Duch-2	18	0.9		18	760	7.1		5.7	200	7
Black-18A	10	9.6		30	3600	21		36	750	10
Beat-16	12	-0.7		10	52	4.5		2.9	390	8
V-Ely-1	**42**	**-10**		**210**	**3500**	**17**		**14**	**1300**	**52**
Besshi-type, hosted by graphitic schists										
FC-3	**6.9**	*0.7*	*0.2*	*1.2*	**97**	*0.047*		**2.4**	**150**	*1.0*
SUG-1 0.2	**9.9**	*18*	*54*	*15*	**7200**	**0.55**		**7.1**	**940**	7.4
Cobalt-rich, hosted by metamorphosed sediments										
*BB25	140			150000	78000	0.15		115	14000	
High sulfidation (quartz alunite epithermal)										
Acid sulfate alteration										
AD-3	**80**	**180**	**84**	**670**	**93000**	260		**25**	14	**760**
AD-3	**93**	**200**	**80**	**700**	**120000**	**310**		**34**	**18000**	**800**
AD-3	**120**	**330**	*80*	**1600**	**234000**	**920**		**51**	**31000**	**1900**
AD-3	**110**	**300**	*180*	**950**	**230000**	**570**		**45**	**23000**	**1200**
AD-3	**69**	**72**	*130*	**420**	**70000**	**190**	**177**	**20**	**12000**	**550**
AD-1435C	**48**	**70**	*20*	**540**	**84000**	**250**		**18**	**10000**	**640**
Chand-1	**150**	**440**	*450*	**2000**	**400000**	**1400**	**196**	**87**	**40000**	**2600**
Chand-1	**160**	**380**	*390*	**1400**	**290000**	**910**	**985**	**71**	**34000**	**1800**
Chand-1	**160**	**430**	*380*	**1400**	**260000**	**880**	**760**	**65**	**35000**	**1700**
Dike 2	**360**	**1000**	**2000**	**7000**	**220000**	**5010**		**380**	**180000**	**10000**
550D-R	**220**	**360**	*200*	**3000**	**56000**	**1100**		**150**	**92000**	**3600**
North Dump	**130**	**140**	*70*	**1000**	**39000**	**320**		**46**	**40000**	**1100**
N Dump S Seep	**310**	**400**	*1000*	**2400**	**100000**	**1200**	**635**	**100**	**65000**	**2600**
SC12	**250**	**180**	*150*	**1700**	**100000**	**540**		**58**	**77000**	**1400**
Blackstrap	**380**	**3000**	**6000**	**16000**	**460000**	**27900**		**840**	**370000**	28000
SOB-1 Seep	**480**	**460**	*780*	**7700**	**706000**	**12000**		**190**	**> 100000**	**11000**
IOWA-1	**82**	**81**	*300*	**460**	**19000**	**170**		**29**	**19000**	**580**
SPIT-1 Pond	**15**	**73**	*78*	**670**	**42000**	**470**		**9**	**4200**	**860**
SPIT-2 Pond	**30**	**110**	*220*	**1100**	**120000**	**840**		**23**	**19000**	**1300**
NPIT-1 Pond	**60**	**120**	*200*	**630**	**37000**	**280**	**79**	**29**	**15000**	**830**
Ch Seep	**69**	**220**	*260*	**950**	**270000**	**540**	**338**	**31**	**28000**	**1200**
Missionary East	**59**	**50**	*94*	**260**	**58000**	**150**	**169**	**15**	**5800**	**350**
Sh-1	**560**	**130**	*1100*	**1300**	**32000**	**600**	**223**	**140**	**100000**	**1300**

Deposit type *Ore / alteration type* Sample	Pb µg/l	Si mg/l	U µg/l	Zn µg/l	Zn+Cu+Cd+ Co+Ni+Pb µg/l
Volcanogenic massive sulfide (VMS)					
Kuroko-type, hosted by volcanic rocks					
*Rich-90WA103	**3600**			**2010000**	2321460
*Rich-90WA108	**4300**			**6150000**	6780300
*Rich-90WA109	**3800**			**7650000**	10060500
*Rich-90WA110A	**11900**			**23500000**	28491900
*LMG	1800			13800000	14038100
Hol-511	*-0.3*		*3.2*	*1000*	1226
Hol-528	*-0.3*		*2.9*	*6000*	6407
Hol-529	*-0.3*		*2.2*	*4800*	5176
Hol-534	*22*		*2.5*	*6000*	6964
Hol-548	*0.6*		*0.7*	*6500*	6671
Hol-549A	*26*		*210*	*81000*	83246
Hol-549B	*23*		*600*	*140000*	143533
Besshi-type, hosted by sedimentary and intermediate submarine volcanic host rocks					
Duch-1	0.9			180	194
Duch-2	74			200	1060
Black-18A	220			3300	7170
Beat-16	-0.5			190	260
V-Ely-1	**-50**	**24**		**1100**	4868
Besshi-type, hosted by graphitic schists					
FC-3	*-0.6*	**5.8**	*-0.1*	**350**	450
SUG-1 0.2	**230**	**7.4**	*0.6*	**7400**	14870
Cobalt-rich, hosted by metamorphosed sediments					
*BB25			0.1	700000	928000
High sulfidation (quartz alunite epithermal)					
Acid sulfate alteration					
AD-3	**370**	**30**	31	**18000**	112980
AD-3	*320*	**31**	*410*	**20000**	142020
AD-3	**230**	**30**	*140*	**47000**	285060
AD-3	*320*	**32**	*38*	**31000**	263770
AD-3	*75*	**27**	*15*	**12000**	83117
AD-1435C	**92**	**28**	*40*	**11000**	96342
Chand-1	***220***	**37**	*170*	**57000**	462260
Chand-1	*310*	**39**	*170*	**47000**	340890
Chand-1	*220*	**42**	*100*	**49000**	312750
Dike 2	**12**	**83**	1000	**170000**	408012
550D-R	*0.2*	**43**	*310*	**61000**	123960
North Dump	*6.3*	**30**	*60*	**23000**	64246
N Dump S Seep	*0.4*	**60**	*210*	**55000**	160400
SC12	*5*	**27**	*60*	**28000**	131285
Blackstrap	*-200*	**84**	*36000*	**610000**	1117020
SOB-1 Seep	*-2*	**110**	*300*	**82000**	807160
IOWA-1	*-0.1*	**35**	*44*	**11000**	31121
SPIT-1 Pond	*0.1*	**1**	*42*	**11000**	54603
SPIT-2 Pond	*1.0*	**1**	*90*	**20000**	142511
NPIT-1 Pond	*1.3*	**11**	*150*	**15000**	53581
Ch Seep	*180*	**27**	*72*	**29000**	301550
Missionary East	*210*	**19**	*29*	**6800**	65670

ATTACHMENT 19

Chapter 3

THE ENVIRONMENTAL GEOLOGY OF MINERAL DEPOSITS

G.S. Plumlee
U.S. Geological Survey, Box 25046, MS 964, Federal Center, Denver, CO 80225-0046

INTRODUCTION

Mineral deposits are concentrations of metallic or other mineral commodities in the Earth's crust that result from a variety of complex geologic processes. The natural weathering and erosion of a mineral deposit at the Earth's surface disperses its constituents into the waters, soils, and sediments of its surrounding environment. There, the constituents may be taken up by plants and (or) organisms. The concentrations and chemical, mineralogical, or biological forms of metals and other constituents from a mineral deposit prior to mining in soils, waters, sediments, plants, and organisms are defined here to be the natural environmental signatures of the deposit.

Modern mining and mineral processing activities employ a wide variety of methods to prevent or minimize adverse environmental impacts (Ripley et al., 1996; Plumlee and Logsdon, 1999; references therein). However, if not carried out with appropriate mitigation and prevention practices (as was common in most historical operations), or as a result of accidental releases, mining and mineral processing can disperse potentially deleterious metals, other deposit constituents, and mineral processing chemicals or byproducts into the environment. Mining-related environmental signatures are defined here as the concentrations and chemical, mineralogical, or biological forms of these metals and chemicals *prior to mitigation or remediation* in mining and milling wastes, mine waters, mineral processing solutions and byproducts, and smelter emissions and byproducts.

The geologic characteristics of mineral deposits exert important and predictable controls on the natural environmental signatures of mineralized areas prior to mining, and on the environmental signatures that could result from mining and mineral processing if appropriate preventive and mitigative practices were not followed. A good understanding of the environmental geology of mineral deposits is therefore crucial to the development of effective mining-environmental prediction, mitigation, and remediation practices.

This chapter summarizes the important geologic characteristics of mineral deposits that influence their environmental signatures, how climate and mining and mineral processing methods modify the environmental signatures mandated by deposit geology, and how climate and geology influence the effects of the deposits on the surrounding environment. In addition, the chapter will show how mineral deposit types with similar geologic characteristics have generally similar and predictable environmental signatures, and will discuss the development of empirical geoenvironmental models of various mineral deposit types.

Mineral deposits and mineral deposit types

"Mineral deposits" as considered here include metallic, or hard-rock, deposits (those in which metals such as Au, Ag, Cu, Pb, Zn, Ni, or Co are the dominant commodity), energy mineral deposits (including coal and uranium deposits), and industrial mineral deposits (those which contain mineral commodities such as sand, gravel, zeolites, phosphates, etc.).

"Mineral deposit types" are groups of mineral deposits having similar geologic characteristics, geologic environments of occurrence, and geologic processes of formation (Guilbert and Park, 1986; Cox and Singer, 1986; Bliss, 1992). Different categories of metallic mineral deposit types can be identified based on their mode of formation. Magmatic deposits are those that form directly from magmas, such as Ni-sulfide deposits hosted by layered mafic intrusions. Magmatic hydrothermal deposit types form from fluids expelled from crystallizing magmas, and include types such as porphyry, skarn, and polymetallic replacement deposits. Hydrothermal deposit types form from heated waters circulating in the Earth's crust; common hydrothermal types include volcanogenic massive sulfide, epithermal, polymetallic vein, and Carlin-type sediment-hosted Au deposits. Supergene deposits form from surface and ground waters that weather and redeposit metals from an existing mineral deposit. Residual deposits are formed by the natural weathering of rocks, which removes most of the rock constituents and results in the residual enrichment of economic constituents in the highly weathered rock remnants; these include deposit types such as bauxite Al and laterite Ni. Placer deposits form by sedimentary accumulation of dense minerals eroded from rocks or mineral deposits, and include placer Au and beach-sand Ti deposits.

Industrial mineral deposit types have a broad spectrum of origins, including: chemical (those that form by chemical precipitation from water, such as phosphate and evaporite deposits); sedimentary (those that form by sedimentary processes, such as sand and gravel deposits); metamorphic (those that form by metamorphic processes, such as some garnet deposits); weathering (those that form by weathering of existing rocks, such as some clay deposits); igneous (those that form by igneous processes, such as deposits of perlite in volcanic domes); and hydrothermal (those that form by hydrothermal processes, such as hydrothermal clay deposits).

This discussion will focus primarily on the environmental geology of metallic deposits, but will also include some discussion of the environmental geology of uranium and industrial mineral deposits.

Other sources of geologic information

As part of this discussion, only some of the basic terms and concepts of economic geology will be discussed; for further details the interested reader is referred to general economic geology textbooks such as Guilbert and Park (1986). Holland and Petersen (1995) present an overview of the geologic, economic, and environmental issues related to mineral-resource development. For detailed geologic discussions of particular mineral deposits, mining districts, or mineral deposit types, see general journals such as *Economic Geology* or *Mineralium Deposita*, papers by national geological surveys (for example, U.S. Geological Survey Professional Papers or Bulletins are available for a number of historic U.S. mining districts), and special publications by professional associations such as the Society of Economic Geologists or the Geological Association of Canada (e.g., Kirkham et al., 1993).

There are also a number of journals and volumes available with papers that discuss the environmental aspects of mining from a geologic standpoint, including the journals *Environmental Geology, Applied Geochemistry*, *Journal of Geochemical Exploration*, and *Environmental Geochemistry and Health,* and volumes such as Jambor and Blowes (1994), Kwong (1993), Alpers and Blowes (1994), Pasava et al. (1995), and Ripley et al. (1996). Conceptual models that describe the important geoenvironmental characteristics of a number of mineral-deposit types are presented in du Bray (1995). Many of the papers included in this two-part volume also discuss environmental processes in a geologic context.

ENVIRONMENTAL GEOLOGY CHARACTERISTICS OF MINERAL DEPOSITS

In general, the geologic characteristics of mineral deposits that control their environmental signatures (their environmental-geology characteristics) influence either the chemical or physical response of the deposits to weathering and environmental processes (Table 3.1). Geologic features such as the acid-generating or acid-consuming minerals in the deposit, host rocks, and wallrock alteration are examples of characteristics that influence the chemical response of the deposits to weathering. Other characteristics such as mineral textures, the presence of faults or joints, and the porosity and hydraulic conductivity of the deposit and associated host rocks, ultimately control the access of weathering agents into the deposit and the speed with which the deposit is weathered and dispersed into the environment. Some geologic characteristics such as the mineralogy and trace element content of minerals can affect both the chemical and physical response of the deposit to weathering and environmental dispersion.

Primary mineralogy

Primary minerals are defined as those that form during the original formation of the deposit. The primary ore (economically valuable) and gangue (non-economic) minerals present in a mineral deposit play a key role in determining how readily the deposit's constituents are dispersed into the environment (Tables 3.2–3.5, Figs. 3.1–3.3).

TABLE 3.1—Geologic characteristics of mineral deposits that affect their environmental signatures.

Characteristic	Controls	Remarks
Iron sulfide content	Chemical	Oxidation generates acid; also supplies ferric iron, which is an aggressive oxidant.
Content of other sulfides	Chemical	Many (but not all) may generate acid during oxidation.
Content of carbonates, aluminosilicates and other nonsulfide minerals	Chemical	Many of these minerals can consume acid; iron and manganese carbonates may generate acid under some conditions.
Mineral resistance to weathering	Physical	Function of the mineral (different minerals weather at different rates) and the texture and trace-element content of the mineral.
Secondary mineralogy	Chemical and physical	Soluble secondary minerals can store acid and metals, to be released when the minerals dissolve. Insoluble secondary minerals can armor reactive minerals, thereby restricting access of weathering agents.
Extent of pre-mining or pre-erosion weathering and oxidation	Chemical	Pre-mining oxidation greatly reduces potential for sulfide deposits to generate acid.
Host rock lithology	Chemical and physical	May consume or generate acid. Physical characteristics (porosity, permeability) control access of weathering agents.
Wallrock alteration	Chemical and physical	May increase or decrease the host rock's ability to consume acid. May increase or decrease host rock's ability to transmit ground waters. May also increase or decrease resistance to erosion.
Major-, trace-elements in deposit and host rocks	Chemical	Elemental composition of deposit and host rocks are typically reflected in environmental signatures.
Physical nature of ore body (vein, disseminated, massive)	Physical	Controls access of weathering agents.
Porosity, hydraulic conductivity of host rocks	Physical	Control access of weathering agents.
Presence and openness of faults, joints	Physical	Control access of weathering agents.
Deposit grade, size	Physical and chemical	Controls magnitude of natural, mining impacts on surroundings.

TABLE 3.2—Examples of sulfide oxidation reactions and other mineral dissolution reactions that may generate acid. The reactions depicted are idealized, and likely do not represent the appropriate reaction products for the entire range of ambient chemical conditions in nature. However, they illustrate the range of acid amounts that can be generated (moles acid >0) or consumed (moles acid <0) depending on the mineral, the oxidant (oxygen versus ferric iron) and the reaction products (oxidation state, chemical species, and minerals) produced.

Mineral	Formula	Acid generation/consumption reaction	Moles acid
Pyrite	FeS_2	$FeS_2 + 3.5\ O_2 + H_2O = Fe^{2+} + 2\ SO_4^{=} + 2\ H^+$	2
		$FeS_2 + 3.75\ O_2 + 0.5\ H_2O = Fe^{3+} + H^+ + 2\ SO_4^{=}$	1
		$FeS_2 + 3.75\ O_2 + 3.5\ H_2O = 2\ SO_4^{=} + 4\ H^+ + Fe(OH)_{3\ (s)}$	4
		$FeS_2 + 14\ Fe^{3+} + 8\ H_2O = 15\ Fe^{2+} + 2\ SO_4^{=} + 16\ H^+$	16
Pyrrhotite	$Fe_{1-x}S$	x = 0.1: $Fe_{0.9}S + 1.95\ O_2 + 0.1\ H_2O = 0.9\ Fe^{2+} + SO_4^{=} + 0.2\ H^+$	0.2
		x = 0.1: $Fe_{0.9}S + 2.175\ O_2 + 0.7\ H^+ = 0.9\ Fe^{3+} + SO_4^{=} + 0.35\ H_2O$	-0.7
		x = 0.1: $Fe_{0.9}S + 2.175\ O_2 + 2.35\ H_2O = SO_4^{=} + 2\ H^+ + 0.9\ Fe(OH)_{3\ (s)}$	2
		x = 0.1: $Fe_{0.9}S + 7.8\ Fe^{3+} + 4\ H_2O = 8.7\ Fe^{2+} + SO_4^{=} + 8\ H^+$	8
Sphalerite,	ZnS, CuS, PbS	$MS + 2\ O_2 = M^{2+} + SO_4^{=}$ (M = Zn, Cu, Pb)	0
Covellite,		$MS + 8\ Fe^{3+} + 4\ H_2O = M^{2+} + 8\ Fe^{2+} + SO_4^{=} + 8\ H^+$	8
Galena	PbS	$PbS + 2\ O_2 = PbSO_4$ (anglesite)	0
		$PbS + 0.5\ O_2 + 2\ H^+ = Pb^{2+} + H_2O + S°$ (native sulfur)	-2
Chalcopyrite	$CuFeS_2$	$CuFeS_2 + 4\ O_2 = Cu^{2+} + Fe^{2+} + 2\ SO_4^{=}$	0
		$CuFeS_2 + 16\ Fe^{3+} + 8\ H_2O = Cu^{2+} + 17\ Fe^{2+} + 2\ SO_4^{=} + 16\ H^+$	16
Enargite	Cu_3AsS_4	$Cu_3AsS_4 + 8.75\ O_2 + 2.5\ H_2O = 3\ Cu^{2+} + HAsO_4^{=} + 4\ SO_4^{=} + 4\ H^+$	4
		$Cu_3AsS_4 + 35\ Fe^{3+} + 20\ H_2O = 3\ Cu^{2+} + 35\ Fe^{2+} + HAsO_4^{=} + 4\ SO_4^{=} + 39\ H^+$	39
Arsenopyrite	FeAsS	$FeAsS + 3.25\ O_2 + 1.5\ H_2O = Fe^{2+} + HAsO_4^{=} + SO_4^{=} + 2\ H^+$	2
		$FeAsS + 3.5\ O_2 + H_2O = Fe^{3+} + HAsO_4^{=} + SO_4^{=} + H^+$	1
		$FeAsS + 13\ Fe^{3+} + 8\ H_2O = 14\ Fe^{2+} + HAsO_4^{=} + SO_4^{=} + 15\ H^+$	15
		$FeAsS + 3.5\ O_2 + 3\ H_2O = SO_4^{=} + 2\ H^+ + FeAsO_4 \cdot 2H_2O$ (scorodite)	2
Native sulfur	S°	$S° + H_2O + 1.5\ O_2 = 2\ H^+ + SO_4^{=}$	2
Realgar	AsS	$AsS + 2.75\ O_2 + 2.5\ H_2O = HAsO_4^{=} + SO_4^{=} + 4\ H^+$	4
		$AsS + 11\ Fe^{3+} + 8\ H_2O = 11\ Fe^{2+} + HAsO_4^{=} + SO_4^{=} + 15\ H^+$	15
Siderite	$FeCO_3$	$FeCO_3 + H^+ = Fe^{2+} + HCO_3^-$	-1
		$FeCO_3 + 2\ H^+ + 0.25\ O_2 = Fe^{3+} + 0.5\ H_2O + HCO_3^-$	-2
		$FeCO_3 + 0.25\ O_2 + 2.5\ H_2O = Fe(OH)_3 + H^+ + HCO_3^-$	1
Alunite	$KAl_3(SO_4)_2(OH)_6$	$KAl_3(SO_4)_2(OH)_6 + 6\ H^+ = K^+ + 3Al^{3+} + 2\ SO_4^{=} + 6\ H_2O$	-6
		$KAl_3(SO_4)_2(OH)_6 + 3\ H_2O = K^+ + 3Al(OH)_3 + 2\ SO_4^{=} + 3\ H^+$	3

Acid-generating minerals

Many metallic mineral deposits that form beneath the Earth's surface contain sulfide minerals, a consequence of their formation under relatively reduced conditions out of contact with atmospheric oxygen. Sulfide minerals that are exposed by erosion or mining are unstable in the presence of atmospheric oxygen or oxygenated ground waters. Bacterially catalyzed oxidation of sulfides by oxygenated ground and surface waters is well known as the cause of acid-rock drainage (Nordstrom and Alpers, 1999). However, the amount of acid generated (Tables 3.2 and 3.3) is a complex function of the sulfide minerals present in an ore body, their resistance to weathering (see discussion below and Table 3.4), whether the sulfides contain iron, whether oxidized or reduced metal species are produced by the oxidation, whether other elements such as arsenic are major constituents of the sulfides, whether oxygen or aqueous ferric iron is the oxidant, and whether hydrous metal oxides or other minerals precipitate as a result of the oxidation process. Iron sulfides (pyrite, FeS_2; marcasite, FeS_2; pyrrhotite, $Fe_{1-x}S$), sulfides with metal/sulfur ratios <1, and sulfosalts such as enargite (Cu_3AsS_4), generate acid when they react with oxygen and water. Other sulfides with metal/sulfur ratios = 1, such as sphalerite (ZnS), galena (PbS), and chalcopyrite ($CuFeS_2$) tend not to produce acid when oxygen is the oxidant. However, aqueous ferric iron is a very aggressive oxidant that, when it reacts with sulfides, generates significantly greater quantities of acid than are generated by oxygen-driven oxidation alone (Nordstrom and Alpers, 1999; Tables 3.2, 3.3). Sulfide oxidation by ferric iron also occurs more rapidly than by oxygen alone (Nordstrom and Alpers, 1999). Thus, because of their role in producing aqueous ferric iron, the amounts of iron sulfides present in a mineral assemblage play a crucial role in determining whether acid will be generated during weathering. In general, sulfide-rich mineral assemblages with high percentages of iron sulfides or sulfides having iron as

TABLE 3.3—Common sulfides known or inferred to generate acid when oxidized. Sulfides listed as inferred to generate acid are postulated on the basis of idealized chemical reactions such as those listed in Table 3.2.

Mineral	Formula
Common sulfides known (*inferred*) to generate acid with oxygen as the oxidant:	
Pyrite, marcasite	FeS_2
Pyrrhotite	$Fe_{1-x}S$
Bornite	Cu_5FeS_4
Arsenopyrite	FeAsS
Enargite/famatinite	Cu_3AsS_4/Cu_3SbS_4
Tennantite/tetrahedrite	$(Cu,Fe,Zn)_{12}As_4S_{13}$/ $(Cu,Fe,Zn)_{12}Sb_4S_{13}$
Realgar	AsS
Orpiment	As_2S_3
Stibnite	Sb_2S_3
Common sulfides that may generate acid with ferric iron as the oxidant:	
All of the above, plus:	
Sphalerite	ZnS
Galena	PbS
Chalcopyrite	$CuFeS_2$
Covellite	CuS
Cinnabar	HgS
Millerite	NiS
Pentlandite	$(Fe,Ni)_9S_8$
Greenockite	CdS
Common minerals that may generate acid if hydrous oxides are formed:	
Siderite	$FeCO_3$
Rhodochrosite	$MnCO_3$
Alunite	$KAl_3(SO_4)_2(OH)_6$

TABLE 3.4—Factors affecting resistance of sulfide minerals to oxidation, listed in order of increasing resistance from top to bottom of table. The mineral resistance ranking by Brock (1979), is modified to include arsenopyrite (Jambor, 1994) and other sulfides based on the authors' field observations. This ranking is only one of a number of published rankings that are in general agreement, but differ in a variety of specifics. Grain size, texture, and trace element content can substantially shift the relative resistance of the different sulfide minerals; for example, trace element-rich botryoidal pyrite and marcasite generally oxidize much more rapidly than coarse, euhedral sphalerite.

Mineralogy (Brock, 1979; Jambor, 1994)	Grain size	Texture	Trace element content	Resistance to oxidation
Pyrrhotite Chalcocite Galena Sphalerite Arsenopyrite[1]	Fine	Framboidal Colloform Botryoidal	High	Low
Pyrite, Enargite Marcasite Bornite[2] Chalcopyrite Argentite[2] Cinnabar	Medium	 Massive		Medium
Molybdenite	Coarse	Euhedral	Low	High

[1]Based on the observations of Jambor (1994).
[2]Based on the author's observations.

TABLE 3.5—Relative reactivities of common rock-forming and deposit-forming minerals, listed in order of decreasing reactivity. Originally produced by Sverdrup (1990) for soils, and modified by Kwong (1993) and the author (author modifications shown in italics) to include more minerals based on observations of weathering rates observed in mineral deposits. Dissolving minerals are those whose components are taken completely into solution. Weathering minerals are those whose components are partially removed into solution and partially converted to other minerals. For mineral formulas, the reader is referred to standard mineralogic texts such as Deer et al. (1978). Calc-silicates common in skarn deposits (garnet, diopside, wollastonite) are included in the intermediate-weathering group rather than the fast weathering group (as originally classified by Kwong and Sverdrup); the low pH of mine waters that drain some skarn deposits where these minerals are abundant indicate that these minerals do not react readily with acid waters (see Plumlee et al., 1999).

Mineral Group	Typical minerals
Readily dissolving	cerussite, calcite, aragonite, *strontianite*
Less readily dissolving	*rhodochrosite, siderite, dolomite, ankerite, magnesite, brucite, fluorite (?)*
Fast weathering	anorthite, nepheline, olivine, jadeite, leucite, spodumene, *volcanic glass*
Intermediate-weathering	epidote, zoisite, enstatite, hypersthene, augite, hedenbergite, hornblende, glaucophane, tremolite, actinolite, anthophyllite, serpentine, chrysotile, talc, chlorite, biotite, *diopside (?), wollastonite (?), garnet (?), rhodonite (?), hematite (?)*
Slow weathering	albite, oligoclase, labradorite, vermiculite, montmorillonite, gibbsite, kaolinite, magnetite
Very slow weathering	potassium feldspar, muscovite
Inert	quartz, rutile, zircon

a constituent (such as chalcopyrite or iron-rich sphalerite) will generate significantly more acidic waters than sphalerite- and galena-rich assemblages without iron sulfides.

Precipitation of hydrous oxides during the sulfide oxidation process can also lead to the formation of acid (Table 3.2). In fact, some non-sulfide minerals such as siderite ($FeCO_3$) and alunite ($KAl_3(SO_4)_2(OH)_6$) can also generate acid during weathering if hydrous iron or aluminum oxides precipitate.

Acid-consuming minerals

In most mineral deposits, acid-generating sulfide minerals are either intergrown with or occur in close proximity to a variety of carbonate and aluminosilicate minerals that can react with and consume acid generated during sulfide oxidation. However, like the sulfides, the ease and rapidity with which these minerals can react with acid varies substantially (Table 3.5).

Alkaline earth carbonates such as calcite ($CaCO_3$), dolomite [$(Ca, Mg)(CO_3)_2$], and magnesite ($MgCO_3$) typically react with acid according to reactions such as:

$$MCO_{3(S)} + H^+ = M^{2+} + HCO_3^- \quad [1]$$

As discussed previously, if hydrous iron or manganese oxides form as a result of the dissolution of their respective carbonates (siderite and rhodochrosite), then a net generation of acid results;

ATTACHMENT 20

Prediction Manual for Drainage Chemistry from Sulphidic Geologic Materials

MEND Report 1.20.1

This work was done on behalf of MEND and sponsored by:

The Mining Association of Canada (MAC)
Natural Resources Canada (NRCan)
British Columbia Ministry of Energy, Mines and Petroleum Resources/
British Columbia Technical Research Committee on Reclamation
International Network for Acid Prevention (INAP)
Ontario Ministry of Northern Development, Mines and Forestry and
Yukon Mining and Petroleum Environment Research Group

December 2009

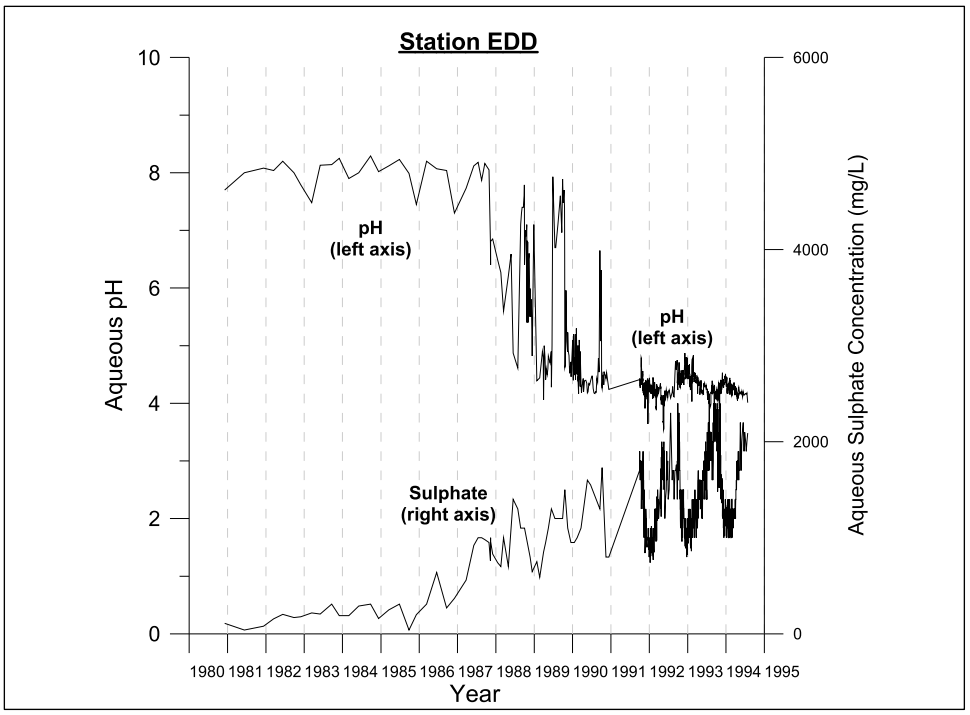

Figure 3.4b The onset of acidic drainage 17 years after dump monitoring started.

3.9 Predict Drainage Chemistry throughout the Life of a Project

It would be important to predict drainage chemistry at all stages of a project, including: exploration, project planning, construction, mining and processing, closure and post-closure (see Chapter 4). The prediction questions, information requirements and prediction materials and methods may change with each stage. Prediction of future drainage chemistry should be part of mine planning to ensure the necessary mitigation measures are included in the advanced exploration, operating and closure plans. Verification of those predictions and additional studies to resolve uncertainties in the closure plan should occur during construction, mining, processing and after the mine closes. It is recommended that prediction continue after mine closure, as long as properties potentially influencing weathering and leaching are in flux and there is significant uncertainty regarding drainage chemistry.

It is recommended that prediction continue after mine closure, as long as properties potentially influencing weathering and leaching are in flux, and there is significant uncertainty regarding drainage chemistry.

Predictions regarding future drainage chemistry should be updated whenever there are major changes to the project or site conditions to ensure that the understanding, mitigation plans and financial and human resources remain sufficient to protect the environment. Major changes to the project include modifications to the mine or the mine plans that may significantly alter the drainage chemistry. Changes to site conditions include significant changes in weathering, drainage conditions and drainage chemistry.

4.2 Step 2 – Measure Existing Drainage Chemistry, If any, and Predict Potential Future Drainage Chemistry

The main questions that should be asked regarding the characteristics of the drainage chemistry are whether the drainage will meet water quality objectives, if the drainage will not meet water quality objectives, what parameters will not be met and how large will their exceedance be, what will be the spatial extent of the problem and when will the exceedance(s) occur?

The answer to these questions will depend on the:

- initial composition of the excavated and exposed materials;
- changes in physical and geochemical properties due to weathering;
- drainage conditions (hydrogeology and hydrology);
- transportation of contaminants; and
- the sensitivity of valued components of the environment and the drainage chemistry required to have a significant environmental impact.

Drainage chemistry prediction should be made for each different combination of geologic material, form(s) of exposure (e.g. waste rock, tailings and mine walls) and post-mining condition(s) (e.g. deposited aerially or underwater). Prediction of drainage chemistry is typically done first for individual samples, then for whole geologic strata or waste units and finally for project components and the project as a whole. If there is, or potentially will be, a drainage chemistry problem, the existing prediction information is then used to decide what additional prediction is required and how to mitigate and/or modify excavation and materials handling to prevent significant environmental impacts (see Chapter 2).

While Step 2 comprises much of any prediction program, practitioners are cautioned not to ignore the other steps. Step 1 is important in selecting samples and test work and interpreting the results. Step 3 will be required to address gaps and uncertainty in the initial prediction. An important objective of Step 2 is to identify gaps and uncertainty and indicate what follow-up work is required (e.g. operational material characterization), which parameters should be measured and the sampling procedure and frequency.

4.2.1 Properties and Processes Potentially Affecting Drainage Chemistry

The prediction of drainage chemistry from sulphidic geologic materials may require site specific measurement or estimation of the following properties and processes.

- The total solid phase concentration of different elements and the potential acid generation potential and acid neutralization potential.
- The aqueous concentrations of soluble elements, acidity and alkalinity and the resulting pore water pH.
- The minerals in which potentially deleterious elements and potential acidity and neutralization occur. The extent to which potentially deleterious elements and potential acidity and neutralization occur in relatively reactive minerals. For example, will acid generation and elemental release result almost entirely from sulphide oxidation or will there be significant contributions from other sources?

- differences between materials and conditions in pre-development laboratory tests and the actual materials and weathering conditions at the site;
- changes to the project plans alter the materials or weathering conditions;
- uncertainty about future site conditions such as the composition of waste rock fines, ultimate pit walls or the height of the water table; and
- a lack of samples from the perimeter of the project (e.g. waste rock far from the ore zone) prior to development.

There is often great value in continuing to run laboratory kinetic tests during subsequent stages of project development and setting up field test pads and study sites on project components to improve the understanding of weathering. Properties that are difficult to predict prior to project development include the composition of waste rock fines and materials segregated during tailings deposition and changes during ore processing. Additional weathering studies may be needed once the composition of these materials and the location of final walls are determined. Changes to the mine plan will likely require additional prediction studies and changes in the operational material characterization and monitoring of weathering and drainage (Section 3.14).

4.4 Prediction During Different Stages of Project Development

The stage of the project, along with gaps in the existing prediction data and proposed new developments, will determine the information required, when it will be required and potential sources of test materials and test sites. From the perspective of prediction, the main stages of the project include:

- exploration;
- feasibility studies and project planning;
- construction;
- mining and processing;
- closure; and
- post-closure.

Although the materials and methods may change depending on the stage of project development, it is important that prediction be conducted throughout the life of a project with closure planning starting at the mine planning and mine development stage. One objective in conducting prediction at each stage is to demonstrate that the project has the necessary facilities, plans, understanding, site capacity, resources and intent to sustain the mitigation needed for environmental protection (Section 3.5). This includes identification and contingency plans to deal with significant gaps in the prediction of drainage chemistry. Another common consideration at every stage of the project is that sampling, analysis, test work and the interpretation of prediction results should be completed in time to meet the proactive, decision making needs of a project.

It is important that prediction be conducted throughout the life of a project. This includes all major stages of a project: exploration, mine planning, construction, mining and processing, closure, and post-closure.

4.4.1 Minimum Mass of Material Requiring Prediction

Prediction is required if the material is capable of producing a significant environmental impact. The lowest or minimum mass capable of producing a significant impact may decrease with:

- increases in sulphide and trace element content;
- increases in particle surface area (e.g. smaller particle size);
- increases in drainage volume;
- increases in mineral reactivity and contaminant solubility (e.g. acidic weathering conditions and drainage pH); and
- reductions in dilution and/or attenuation prior to a sensitive receptor.

For example, the surface area and drainage inputs of drill cores are typically too low to be a concern.

For exploration, the British Columbia Ministry of Energy, Mines and Petroleum Resources typically use a criterion of 1,000 tonnes of sulphidic material before any prediction is required. A small sized pile (i.e. less than 1,000 tonnes) typically has limited drainage inputs and a low particle surface area. Criteria of this sort should not substitute for common sense. The minimum tonnage for conducting prediction may need to be reduced where:

- the sulphidic material is highly reactive;
- the sulphidic material has high concentrations of soluble contaminants;
- there is significant drainage through the pile; or
- there is very little attenuation or dilution between the discharge source and the sensitive environment.

Sensitivity analyses can be conducted to predict the minimum mass capable of producing a significant environmental impact using project site data and/or assumptions regarding the site and project conditions. A simple example of a sensitivity analysis showing the required watershed area for dilution by background drainage, to prevent exceedance of downstream water quality objectives by hypothetical dump drainage, is provided in Table 4.1. The calculations in Table 4.1 assume dilution is permissible, a 3 m dump height is in place and no geochemical interactions occur, such as precipitation/dissolution or adsorption/desorption.

Table 4.1 Required area for dilution to prevent hypothetical drainage from small rock dumps from exceeding downstream water quality objectives.

		Neutral pH with Zinc	Acidic pH with Copper
Downstream Objective	mg/L	0.03	0.004
Background Concentration	mg/L	0.005	0.001
Dump Drainage Concentration	mg/L	2	20
Dump Mass	tonnes	1000	100
Bulk Density	t/m^3	1.5	1.5
Dump Volume	m^3	670	67
Dump Height	m	3	3
Dump Area	m^2	220	22
Required Area for Dilution	m^2	18,000	150,000
	ha	1.8	15

Assumptions:
1) Flows per unit area from the waste rock dump are the same (same timing, lag, and rate) as from the rest of the watershed.
2) The only source of dump drainage is incident precipitation. Drainage from upstream does not flow through the waste rock pile.
3) The watershed for dilution is the catchment area above the mixing point with the waste rock drainage.
4) There are no geochemical interactions in the receiving environment, such as precipitation/dissolution or adsorption/desorption, that would reduce the contaminant load.

4.4.2 Exploration

Exploration includes a wide range of activities and the prediction requirements depend on the degree of exposure or disturbance of sulphidic geologic material. Exploration activities such as collecting rock chips and soil sampling disturb relatively little sulphidic overburden or bedrock and drainage chemistry prediction is usually not required. Diamond drilling and trenching expose or disturb more sulphidic overburden or bedrock and the drill core and overburden should be placed in locations with relatively little leaching and away from sensitive resources. Drainage chemistry prediction will only be required if the amount of drilling and trenching is extremely large.

Exploration activities that may result in the excavation or movement of large masses of sulphidic bedrock or overburden and where drainage chemistry prediction may be required include:

- excavation of an exploration adit;
- removal of a bulk bedrock sample for processing; and
- construction of large rock cuts for a road or drill pad.

The excavation or movement of sulphidic bedrock or overburden by these activities may rival a small mine.

One reason for conducting prediction testing during advanced exploration is for environmental protection. In addition, starting the prediction of drainage chemistry as soon as possible, assuming that there is adequate knowledge of the deposit and material to test, will increase the time available for a cost-effective, phased prediction program and any time intensive kinetic test work. This will minimize delays during mine development if further data collection is needed to address unacceptable uncertainty regarding some aspect of the future drainage chemistry (Sections 3.13 and 3.20).

Starting the prediction of drainage chemistry as soon as possible during exploration will increase the time available for a cost-effective, phased prediction program and any time intensive kinetic test work.

Creation of a data base of prediction materials, methods, results and relevant properties of the project and site should accompany the initiation of drainage chemistry prediction (Section 3.24).

4.4.3 Feasibility Studies and Project Planning

The objectives of prediction during feasibility studies and project planning prior to excavation and processing are to:

- predict the potential future drainage chemistry, determine the magnitude and spatial variability in influential properties and processes, and predict the timing of significant changes; and
- determine what excavation, waste handling, disposal, mitigation, financial resources, monitoring, operational material characterization and supplemental prediction is required.

Prediction during project planning consists of Steps 1 and 2 from Sections 4.1 and 4.2. Typically this requires a:

- review of the general properties of the project and the site; and
- prediction of both the most probable drainage chemistry and the potential for any unacceptable conditions or performance.

Prediction of drainage chemistry should be done for all materials that will be excavated or exposed for construction and during mining. This work should reduce the uncertainty regarding drainage chemistry to a level at which effective impact prevention strategies can be selected and the potential liability determined.

Because of the site specific nature of the problem and large potential environmental impacts and costs, even for conceptual planning and approval, a comprehensive prediction of future drainage chemistry may be required to indicate what, where and when mining, processing, mitigation and closure measures are required to protect the environment.

An important part of pre-mining prediction is indicating what operational material characterization and supplemental prediction studies should be performed. In the development of plans for operational material characterization, thought should be given to the purpose, the time available to obtain results, what parameters are to be measured, materials to be samples and the sampling procedure and frequency of operational material characterization. Materials and

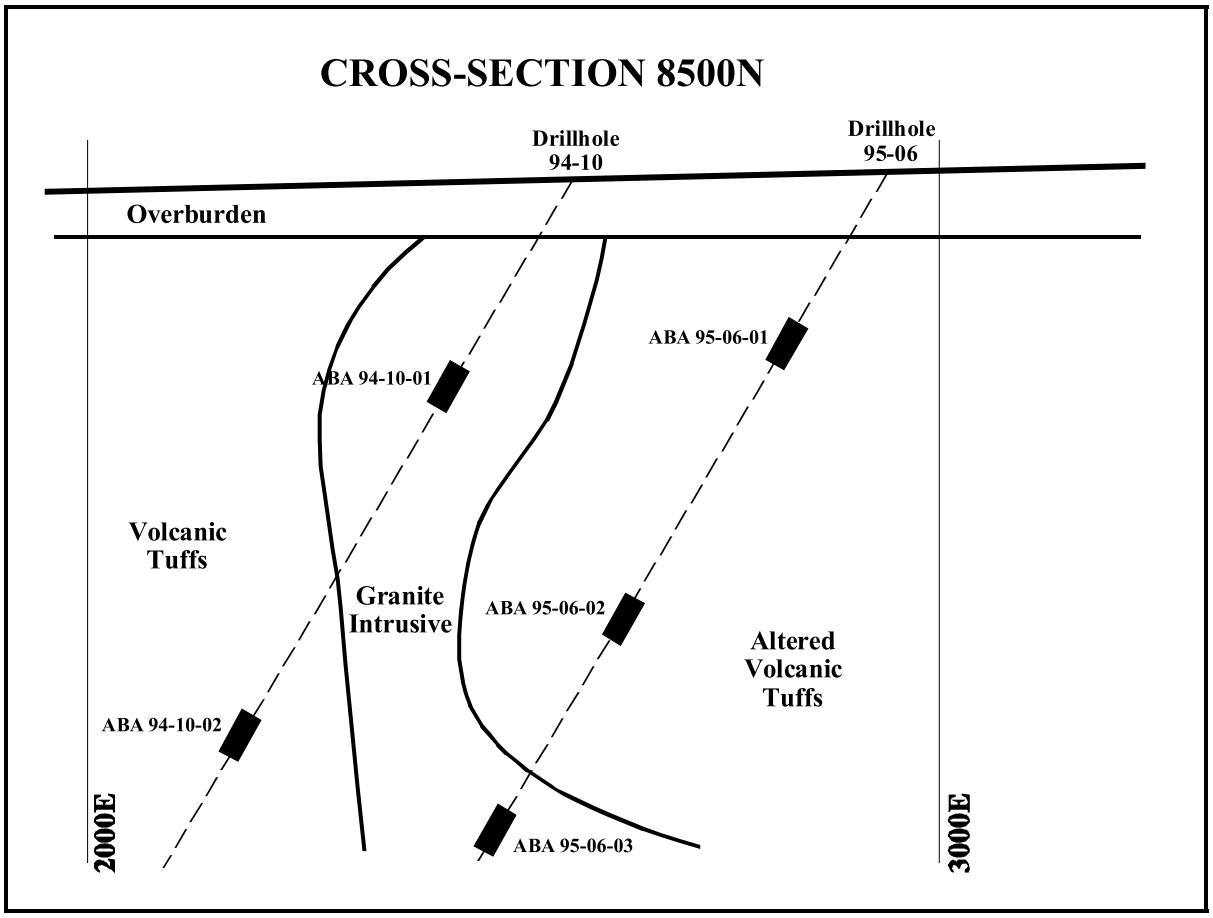

Figure 8.1 Example of required geologic cross sections showing the location of core samples.

Sampling sites for pre-mine drill core, blast hole cuttings and post-blast waste rock should be recorded in block models (Figures 6.6 and 6.7) and shown on cross sections and plan view maps (Figure 8.1). If possible, cross sections and maps should also show the location of:

Sampling sites for pre-mine drill core, blast hole cuttings and post-blast waste rock should be recorded in block models and shown on cross sections and plan view maps.

- drill holes;
- discrete geologic units and other more diffuse forms of alteration such as mineralization, hydrothermal alteration, weathering or leaching;
- proposed project components, such as open pits or underground excavations; and
- existing disturbances.

The large number of potentially influential physical, mineralogical, geochemical, weathering and leaching properties and processes can make sampling geologic materials, waste materials and walls an onerous undertaking. Commonly, the most cost-effective way to characterize geologic materials, waste materials and walls will be an iterative phased process of sampling and analysis,

similar to that used to determine other geologic characteristics such as ore reserves. Ideally, there will be several phases to ensure that sampling:

- focuses on the materials of greatest concern;
- minimizes work on materials with no significant uncertainty;
- uses the most appropriate materials and methods; and
- makes timely refinements in response to unforeseen conditions.

Sufficient numbers of samples should be taken to accurately characterize the variability and central tendency (e.g. average, median and 10th and 90th percentiles) of the different waste materials, project components and geologic units. This includes characterization of localized areas of material with differences in physical, geochemical, mineralogical, weathering and leaching conditions that alter drainage chemistry. The required sampling frequency will depend on the phase of the project, mass of material, variability of critical parameters, the questions being asked and the degree of accuracy required for each project component.

Sufficient samples should be taken to accurately characterize the variability and central tendency, like the average, median and 10th and 90th percentiles.

The sampling frequency should be based on a review of:

- results of previous prediction sampling and analysis;
- descriptions of the materials exposed on surfaces and intercepted by excavations or drilling (Sections 6.6.4, 6.6.5 and 6.6.6);
- sampling frequency required to characterize other geologic properties such as the geotechnical properties or ore grades; and
- results of any previous analyses of other geologic properties.

Sensitivity and gap analyses should be conducted after every phase of sampling to:

- check whether the proposed sample selection, storage and preparation will still answer prediction questions; and
- identify information gaps and evaluate their impact on the overall environmental risk and liability.

Each phase of sampling should be informed by the previous campaigns. Sampling needs will become more clearly defined with project development and improvements in the understanding of the geologic materials and site conditions. Procedures that should be used to check whether sampling frequencies are adequate are:

- regular comparison of geologic descriptions and analytical results of samples from within supposedly homogeneous materials;
- periodic nested sampling in between regular sample intervals; and
- periodic random sampling in addition to regular sample intervals.

Descriptions of the sample geology should also be compared with geologic descriptions of the materials the samples are supposed to represent. Analytical results for nested and random

10.0 WHOLE-ROCK AND NEAR-TOTAL SOLID PHASE ELEMENTAL ANALYSIS

Some Important Points in this Chapter

The analyses discussed provides the total or near-total amounts of selected chemical elements in a solid phase sample. This is accomplished in two major steps. First, most or all of a sample is digested in a hot chemical flux or strong acid combination. Second, the digested sample is analyzed by one of several techniques, such as X-ray Fluorescence (XRF) or Inductively Coupled Plasma (ICP). It is important to be aware of the strengths and weaknesses of each method of digestion and analysis because it may affect predictions of drainage chemistry from sulphidic materials. For example, whole-rock analyses may be reported as oxide equivalents, such as CaO and Al_2O_3, which require mathematical conversions to obtain pure element concentrations. These analyses do not reveal the forms in which an element occurs, such as in one or more minerals, although this can sometimes be estimated using a few assumptions. Also, solid phase levels, whether high or low are not on their own measures of the potential aqueous concentrations in drainage or of the threat to the environment. However, tests in other chapters are combined with these solid phase results for drainage predictions, such as the length of time until elements are fully leached from a sample.

10.1 Introduction

Whole-rock or near-total solid phase elemental analysis is used to quantify elemental concentrations in rock materials that may be exposed through mining activities. Information regarding solid phase elemental abundance represents a key component of mine waste geochemical characterization and accordingly, such analyses should be conducted on all geologic materials impacted by a mine or project. The initial solid phase elemental data often comes from sampling and analyses conducted as part of geochemical exploration. More comprehensive sampling and analysis is usually conducted as part of pre-mine planning, with regular operational characterization used for verification and filling data gaps.

These analyses should be conducted on all geologic materials impacted by a mine or project.

10.2 Objectives

The primary objective of whole rock or near-total solid phase elemental analysis is to determine the concentration of elements that are drainage chemistry concerns (e.g. metals and metalloids). Other uses for the results include the following:

- check whether trace elements of potential concern occur in elevated concentrations compared with concentrations normally found in rock and soil at the site or more universally;
- estimate trace element depletion times;

- determine the maximum potential contribution of acid insoluble sulphate minerals (barite [$BaSO_4$], anglesite [$PbSO_4$] and celestite [$SrSO_4$]) to the estimates of sulphide-S and AP (Chapter 12);
- determine the maximum potential contribution of less acid generating sulphide minerals than pyrite to compare to the estimates of sulphide-S and AP (Chapter 12);
- identify samples with elemental levels indicative of anomalous geochemical conditions;
- verify the predicted lithological classification and mineralogical composition; and
- estimate the concentrations of constituents that may control important properties of the drainage chemistry (e.g. neutralizing minerals).

10.2.1 Limitations

Whole rock and near-total solid phase elemental analysis provides limited information about the form (e.g. mineral) in which the elements exist and on its own is not a measure of the potential concentrations in drainage or the threat to the environment. There are a large number of properties and processes that determine whether solid phase elements will report to drainage. These include:

- the elemental forms present (i.e. mineralogical associations) and whether the forms are relatively soluble or will become more soluble through processes such as oxidation;
- environmental conditions (e.g. sub-aerial versus saturated storage conditions, climate, etc.); and
- volume, chemistry and flow rate of the drainage.

Information on the mineralogy (Chapter 17), geochemical conditions and rates of weathering (Chapters 18 and 19), secondary mineral solubility (Chapters 19 and 20) and the resulting drainage chemistry are required to interpret the environmental significance of solid phase elemental analysis results.

Relatively high elemental concentrations will not result in elevated aqueous concentrations in drainage, if their mineral form is relatively insoluble or unalterable, or if the weathering conditions are not conducive to elemental mobility. An example of this is the relative stability of copper that is often observed in weathered rock materials (e.g. zones of supergene enrichment) given the sparingly soluble nature of such materials under specific conditions. Conversely, if the element is in a form that is very soluble or will become more soluble due to weathering, normal or relatively low solid phase elemental concentrations may result in high concentrations in mine drainage. An example of a relatively rapid weathering reaction that increases solubility is sulphide oxidation under aerobic, low pH weathering conditions.

Relatively high solid phase elemental concentrations will not result in elevated aqueous concentrations in drainage.

10.2.2 Overview of the Methods

There are a large number of possible methods for measuring the whole rock or near-total solid phase elemental concentration. Some methods measure the concentration of a single element. Other methods simultaneously measure the concentration of a large number of elements. Multi-element methods are most commonly used due to their cost-effectiveness. Methods that measure

the concentration of a single element are generally used when the equipment for multi-element analysis is unavailable or the element is not amenable to multi-element techniques.

Most methods for measuring the whole rock or near-total solid phase elemental concentration typically have two stages: 1) digestion of the sample in acid to release the elements into a measurable form; and 2) analysis of the concentrations of the elements in the resulting digestion. More than one method for the multi-element analysis can generally be used with each method of digestion and vice versa. For example, X-ray Fluorescence Spectroscopy (XRF), Inductively Coupled Plasma (ICP) or Atomic Absorption Spectroscopy (AAS) can all be used to measure the elemental concentration after digestion by Lithium Borate fusion. ICP or AAS can also be used for analysis after wet digestion by a strong acid method, such as four acid (HF-HNO_3-$HClO_4$-HCl) or aqua regia (HCl-HNO_3) digestions. There are two common ICP options for analysis, Atomic Emission Spectroscopy (AES) or Mass Spectroscopy (MS). Non destructive methods for trace element analysis (i.e. those not requiring digestion) include XRF which is conducted using pressed powders.

Most methods for measuring the whole rock or near-total solid phase elemental concentration typically have two stages: 1) digestion of the sample in acid to release the elements into a measurable form; and 2) analysis of the concentrations of the elements in the resulting digestion.

10.3 Methods of Sample Digestion

The purpose of sample digestion is to release elements from the mineral phase into a phase in which they can be analyzed (e.g. liquid solution or glass disk). Digestion methods vary in their ability to digest different minerals and therefore the proportion of the sample they are able to digest. Digestion methods also vary in their susceptibility to interference by sample properties such as sulphide content. The best detection method will depend on the degree of digestion required, sample mineralogy and the intended use for the results. Lithium borate fusion completely digests most samples, providing whole rock elemental results. Lithium borate is the recommended procedure if the objective is to measure the total concentration of major mineral forming cations. Sodium peroxide fusion can be used as a replacement for lithium borate fusion to measure the total concentration of major mineral forming cations when the sulphide mineral concentration is > 5%.

The two most common wet acid digestions are the four acid and aqua regia procedures. The four acid digestion (hydrofluoric, perchloric, nitric and hydrochloric acids) produces near-total solid phase elemental results. Aqua regia (hydrofluoric and nitric acids) is weaker and produces partially digested solid phase elemental results. The lithium borate fusion, and the four acid and aqua regia procedures all digest sulphides, carbonates, sulphates and oxides and therefore provide a good measure of the total concentration of solid phase trace elements in the most reactive minerals. Silicate minerals, which are typically not as environmentally significant, are not wholly digested with aqua regia. Limitations in the degree of digestion should be indicated when using and communicating solid phase elemental results.

The more complete the digestion, the higher the concentration of total dissolved solutes and the greater the dilution required in the subsequent analysis, resulting in higher minimum detection limits. Consequently, aqua regia has a slightly lower minimum detection limit than the four acid digestion for some trace elements, and both aqua regia and four acid digestion have lower minimum detection limits than lithium borate fusion.

An assessment of the sulphur content, ideally a total-S analysis by the specialty Leco Furnace (Chapter 12), which is part of ABA, should be conducted in advance of solid phase elemental analysis to detect samples where elevated sulphide may interfere with the analysis.

10.3.1 Lithium Borate Fusion

In lithium borate fusion, a finely ground sample is mixed with lithium borate flux to lower the melting point. The mixture is then fused (i.e. heated until molten) in a furnace. The flux is usually lithium tetraborate ($Li_2B_4O_7$), lithium metaborate ($LiBO_2$) or a mixture of the two. The temperature in fusion with lithium tetraborate ($Li_2B_4O_7$), which has a melting point of 920ºC, is approximately 1100°C. The temperature in fusion with lithium metaborate, which has a melting point of 845°C, is approximately 1000°C. Fusion produces a glass disc.

Analysis of the fused glass disc is traditionally done directly by XRF (Section 10.4.1). The minimum detection limit for trace elements can be lowered by dissolving the fused disc in a known volume of 4-5% nitric acid and analyzing the resulting solution with an ICP technique (Section 10.4.3).

Lithium borate fusion is very effective in dissolving cations bonded with oxygen (e.g. oxides, carbonates, silicates and sulphates) and unlike wet acid digestion methods is able to completely digest major rock forming minerals. Lithium borate fusion is therefore used to measure the total concentration of common major mineral forming cations: Al, Ba, Ca, Cr, Fe, K, Mg, Mn, Na, P, Si, and Ti. The results are referred to as whole rock analysis and are often reported as oxide equivalents (e.g. MgO, Fe_2O_3).

The high temperature of fusion techniques results in the loss of volatile species (e.g. CO_2 from carbonates and water from phyllosilicates and/or hydrated minerals). Measurement of loss of weight on ignition (LOI) should be conducted along with fusion techniques as a check on the mass of these species and whether the sum of the oxide equivalents approaches 100%.

Other considerations to take into account include:

- fused sample disks can be stored indefinitely if additional analyses are required;
- sample fusion enhances XRF analysis by minimizing particle size effects;
- samples with elevated sulphide mineral concentrations do not fuse well with lithium borate and the sample may dissolve slowly, preventing a clean disk from being produced and causing signal interference that prevents optimum detection limits from being achieved in the subsequent XRF analysis. Lithium borate fusion and analysis by XRF is not recommended for samples with ≥ 5% sulphide minerals. If samples have elevated sulphide and/or metal contents, the proponent should discuss the nature of the samples and the digestion and analysis procedures with analytical personnel. One option for samples with

≥ 5% sulphide minerals is to use sodium peroxide fusion (Section 10.3.2), instead of the more common borate fusion. Another option is analysis by an ICP technique; and

- high concentrations of metals such as Cu and Zn can damage the crucibles used for lithium borate fusion.

10.3.2 Sodium Peroxide Fusion

Sodium peroxide (Na_2O_2) flux is an aggressive flux used to digest samples with ≥ 5% sulphide minerals or other refractory or resistant minerals. In the sodium peroxide fusion method, sodium peroxide and sodium hydroxide are added to the sample, which is heated to 550°C. Diluted nitric acid is used to dissolve the digested residue and the resulting solution is analyzed by an ICP or other wet analysis method.

Since sodium peroxide fusion results in complete sample dissolution, the analyte solution has a high salt content and typically needs to be diluted prior to analysis, increasing the detection limits for trace elements.

10.3.3 Four Acid Method

The four acid method uses hydrofluoric acid, perchloric acid, nitric acid and hydrochloric acid. First a mixture of hydrofluoric acid, perchloric acid and nitric acid are added to a finely ground sample. The acid mixture is then taken to near dryness to allow the reaction to go to completion. Lastly, the nearly dry cake is leached with hydrochloric acid to further the digestion and dissolve the residue. The resulting solution can be analyzed by an ICP or another wet analysis method.

Wet acid digestions are classified as "near total" or "partial" depending whether they are capable of fully dissolving the element(s) of interest. The four acid method is the most powerful wet acid dissolution procedure in common use and is considered a near total digestion. Although the lower digestion temperature makes it less able to digest silicates than fusion methods, the four acid method is capable of dissolving most metal salts, carbonates, sulphides, silicates and almost all sulphates and oxides. The addition of hydrofluoric acid makes the four acid method procedure significantly more effective at breaking down silicate minerals than the aqua regia digestion.

Wet acid digestions are classified as "near total" or "partial" depending whether they are capable of fully dissolving the element(s) of interest.

Elements whose concentrations may be underestimated due to incomplete digestion by the four acid digestion include rare earths and Ba, Sn, Ta, Ti, W, and Zr. The four acid method is also only able to partially digest massive sulphide samples and large amounts of sulphide will result in the formation of sulphate, which may precipitate if combined with barium and lead.

Care must be taken during the drying step of the four acid method not to continue beyond near dryness as this could result in a loss of elements by volatilization (e.g. Au, As, Cr, and Sb). There have also been reports of volatilization causing a loss of sulphur (as hydrogen sulphide) in samples containing pyrrhotite.

10.3.4 Three Acid Method

The three acid digestion differs from the four acid digestion by not using hydrofluoric acid, which makes the digestion of silicates less complete. This strong acid digestion is capable of dissolving most metal salts and carbonates.

10.3.5 Aqua Regia

In the aqua regia digestion, the sample is digested in a heated water bath with a 3:1 mixture of hydrochloric and nitric acids (aqua regia). Nitric acid destroys organic matter, oxidizes sulphide material and reacts with concentrated hydrochloric acid to generate aqua regia according to the following reaction: $3\ HCl + HNO_3 = 2\ H_2O + NOCl + Cl_2$. After cooling, the digest solution is diluted with distilled water and analyzed.

Aqua regia is an effective solvent for most base metal sulphates, sulphides, oxides and carbonates, but provides only a partial digestion for most rock forming elements and elements of a refractory nature. It is typically less expensive and does not provide as complete a digestion as the four acid method. Elements commonly occurring in minerals that are not digested by aqua regia and whose concentrations may be underestimated due to incomplete digestion include: Al, B, Ba, Be, Ca, Ce, Cr, Cs, Ga, Ge, Hf, In, K, La, Li, Mg, Na, Nb, Rb, Re, S, Sb, Sc, Sn, Sr, Ta, Te, Th, Ti, Tl, W, Y and Zr.

Aqua regia is an effective solvent for most base metal sulphates, sulphides, oxides and carbonates, but provides only a partial digestion for most rock forming elements and elements of a refractory nature.

10.4 Methods of Analysis

Methods of analysis vary in the type of sample that can be analyzed, instrumentation, detection methods, elements measured, detection limits and susceptibility to interference by other sample components (e.g. sulphide content). Elemental analysis by XRF is done on glass disks and solid, undigested samples (e.g. pressed pellets). More commonly, elemental analysis is conducted on liquid samples created by digesting and dissolving the sample with strong acids.

10.4.1 X-ray Fluorescence Spectroscopy (XRF)

In XRF analysis, a beam of primary X-rays irradiate the sample. Constituent elements emit fluorescent (secondary) X-rays when a primary X-ray of sufficient energy strikes an atom in the sample, dislodging an electron from one of the atom's inner orbital shells (lower quantum energy states). The atom regains stability by filling the vacancy in the inner orbital shell with an electron from one of the higher quantum energy orbital shells. The electron drops to the lower energy state by releasing a fluorescent X-ray. Each element emits a unique fluorescent X-ray energy spectrum (energies and wavelengths) that can be used to identify the elemental source because the quantum state of each electron orbital shell in each atom is different.

Diffraction crystals are used to disperse and sort the emitted fluorescent X-rays by wavelength. The dispersed fluorescent X-rays strike a detector causing a small electrical impulse. The element concentration in the sample is then determined by comparing the electrical impulse of the characteristic wavelengths to that of standard reference materials.

The most common use of XRF is to measure the concentrations of major elements (e.g. Al, Ba, Ca, Cr, Fe, K, Mg, Mn, Na, P, Si, and Ti) in a lithium borate fused disk. XRF can also be used to measure the concentrations of trace elements, such as: As, Ba, Ce, Cu, La, Nb, Ni, Rb, Sn, Sr, Ta, Th, U, W, Y, Zn, and Zr in an undigested pressed pellet. The pellet is created with a bonding agent under high pressure to ensure sample integrity under the vacuum and a consistent surface to receive the X-rays.

Reduced accuracy of XRF measurements may result from:

- geometric effects caused by the sample's shape, surface texture, thickness and density;
- spectroscopic interferences and other sample matrix effects; and
- absorption of fluorescent X-rays by other elements in the sample, and secondary and tertiary X-ray excitation by other elements in the sample.

Certain metals can interfere with the analysis of other metals. For example, iron tends to absorb copper X-rays and enhances the emission of X-rays from chromium. Modern XRF instruments have software that mathematically corrects for these types of interferences.

Other points to consider are:

- if the composition of the sample cannot be matched closely to the calibration standards, empirical correction factors have to be applied;
- XRF is not suitable for measuring lighter elements, like lithium, which produce lower energy XRF emissions with lower penetrating power, ICP is better suited to the detection of lighter elements; and
- XRF has relatively high minimum detection limits and other analysis techniques such as ICP or AAS are recommended for measuring trace element concentrations (i.e. < 100 ppm).

10.4.2 Field Portable and Hand Held XRF Instruments

Field portable and hand held Energy Dispersive X-ray Fluorescence (EDXRF) analyzers are relatively inexpensive and able to provide real time data and may be a cost-effective analytical solution where qualitative or semi-qualitative data is sufficient and there is little time available for analytical feedback (Guerin et al., 2006). The main disadvantages of field portable and hand held XRF are the low precision and accuracy resulting from sample heterogeneity, the small field of view, sample matrix effects, the difficulty in maintaining consistent distances between the instrument and the sample, limitations of the instruments in the resolution for some elements and limited calibration.

The main disadvantages of field portable and hand held XRF are the low precision and accuracy resulting from sample heterogeneity, the small field of view, sample matrix effects, the difficulty in maintaining the distance to the sample, limitations of the instruments in the resolution for some elements, and limited calibration.

Field portable XRF instruments measure the composition over a surface area of approximately one square centimeter and to a depth of approximately 2 millimeters. The small width and depth of view make it possible to measure the spatial variability and the composition of discrete areas such as veins or surface coatings. Measurements at a number of different locations and removal of surface coatings will be required to determine the overall composition of rock samples.

Unconsolidated samples should be homogenized prior to analysis if the objective is to determine the overall composition.

Sieving can be used to create a more uniform particle size. Soil moisture contents above 20 percent that can interfere with the analysis can be minimized by drying, preferably in a convection or toaster oven. The effect of moisture on XRF results will depend on the composition of the sample and drying may not be required.

The strength of the X-ray signal decreases as the distance from the radioactive source increases and it is important to maintain a consistent distance between the window and the sample. For best results, the window of the probe should be in direct contact with the sample.

Resolution may be a problem in analyzing some elements with field portable XRF instruments. For example, concentrations of arsenic often cannot be measured accurately for samples that have lead to arsenic ratios of 10 to 1 or more because the lead peak masks the arsenic peak.

10.4.3 Inductively Coupled Plasma

In Inductively Coupled Plasma (ICP) analysis, liquid samples are nebulized and the resulting aerosol is transported by argon gas into a plasma torch. Radio frequencies in the torch create extremely high temperatures within the plasma of partly ionized argon gas, removing any remaining solvent and causing the samples to atomize and the analyte species to become thermally excited. The mass of the ions (Mass Spectroscopy - ICP-MS, Section 10.4.5) or the intensity of characteristic radiation (Emission Spectroscopy - ICP-AES, Section 10.4.4) produced by the thermally excited analyte species are used to measure elemental concentrations in the sample.

ICP procedures have the capability to measure the concentration of many elements simultaneously (up to 70 in theory and commonly over 40 in practice), many more elements than can be determined with XRF analysis. Like Atomic Absorption Spectroscopy (AAS), ICP-AES and ICP–MS also benefit from high sensitivity and accordingly low detection limits.

Other comments include:

- ICP instruments are highly automated, enhancing analysis speed, accuracy and precision;
- highly skilled staff are required to operate, repair and maintain these complex instruments; and
- high concentrations of sulphide minerals and iron may cause signal interference, preventing optimum detection limits from being achieved. The concentrations of sulphide minerals and iron and the impact on the detection limits will depend on the laboratory procedures and equipment.

10.4.4 Inductively Coupled Plasma Atomic Emission Spectroscopy (ICP-AES)

In Inductively Coupled Plasma Atomic Emission Spectroscopy (ICP-AES), light emitted by the thermally excited atoms is collected by a spectrometer. In the spectrometer, the light, which is characteristic of the elements in the sample, is passed through a diffraction grating that separates it into a spectrum of its constituent wavelengths. Each wavelength of diffracted light is collected

and amplified to yield an intensity measurement, which is converted to an elemental concentration using calibration standards.

Other comments include the following:

- the emission spectra are complex and inter-element interferences are possible (e.g. one phosphorus wavelength has both copper and aluminum interference; and
- rigid control of the temperature and humidity must be maintained for stable performance of the spectrometer.

10.4.5 Inductively Coupled Plasma Mass Spectroscopy (ICP-MS)

In Inductively Coupled Plasma Mass Spectroscopy (ICP-MS), the mass of the ions produced by the thermally excited analyte species in the plasma are introduced into a mass spectrometer. The mass spectrometer separates and collects the ions according to their mass to charge ratios and quantifies them with a channel electron multiplier. The concentration of each element in the sample is determined by comparing the intensity of the electron signal to that of known standards. There are several different types of mass analyzers which can be employed to separate isotopes based on their mass to charge ratio.

ICP-MS is capable of very low detection limits for a wide range of elements with detection limits lower than those of ICP-AES and Graphite Furnace Atomic Absorption Spectroscopy (Section 10.4.6). ICP-MS is also a good alternative measurement technique for elements not easily measured by ICP-AES or Atomic Absorption Spectroscopy and is capable of discriminating between the mass of the various isotopes where more than one stable isotope of an element occurs.

ICP-MS is capable of very low detection limits for a wide range of elements, detection limits lower than those of ICP-AES and graphite furnace atomic absorption spectroscopy.

Other comments include the following:

- ICP-MS is used if ultra-trace geochemical analysis is required (e.g. after sequential extraction or selective leaches) because of its high sensitivity and low detection limits. The ultra-pure acids required for sample digestion prior to ultra-trace geochemical analysis can increase the costs;
- instrument performance is reduced if the total dissolved solute concentration of the sample solution is too high. Dilution of the sample solution required to lower the total dissolved solute concentration can result in higher detection limits for some elements;
- interference from some common matrix elements and other molecular species can affect the measurement accuracy for some base metals (e.g. chloride can interfere with a number of elements and ArCl has the same mass as arsenic). However, the advent of high resolution detectors now permits separation of species with similar mass to charge ratios, thus minimizing the effects associated with such spectral interferences; and.
- some doubly charged ionic species create difficulties.

10.4.6 Atomic Absorption Spectroscopy (AAS)

In Atomic Absorption Spectroscopy (AAS), liquid or solid samples are converted into the gas phase (vaporized) by the high temperature of a flame, a graphite furnace or chemical reaction (hydride generation). The vaporized atoms are then introduced into a beam of ultraviolet or visible light with the same wavelength as the element of interest. The vaporized atoms absorb the light and make transitions to higher electronic energy levels. The concentration of the element in the sample is determined by comparing the amount of light absorption with that of standards with known concentrations.

Advantages of AAS are that it is well established, the equipment is relatively easy to use and inexpensive and the technology is straightforward and well understood. AAS can measure a wide range of concentrations for most elements and has relatively few interferences. The main disadvantage is that AAS only analyses one element at a time. The technique becomes uneconomic if analysis of a large number of elements is required. Although relatively rare, interference by other elements or chemical species can reduce the sensitivity.

10.4.7 Neutron Activation

Neutron Activation Gamma Spectroscopy analysis is a non-dissolution method and often the method used for Br, Cl, I and U analysis. Neutron activation is also used in exploration as it has a low detection limit for gold and gold related trace elements. Due to the lower detection limits compared to most other analysis procedures, neutron activation analysis can be used to check results from other procedures. A disadvantage of this procedure is the possibility of matrix interference by mineralized samples.

10.5 Other Analytical Methods

There are a number of other digestion and analytical methods that can be used to quantify the solid phase concentrations of specific elements. They include: Leco furnace methods, gravimetric and volumetric (titrimetric) procedures and ion specific electrodes. Many of these methods have a long history of use. The Leco furnace is the most common method for total carbon and sulphur analysis (Chapters 12 and 13). Gravimetric and volumetric (titrimetric) procedures are used instead of multi-element procedures when the element concentration exceeds the maximum detection limit and to measure a particular elemental species, such as non-sulphide copper or zinc.

In gravimetric methods, the element of interest is precipitated as an insoluble compound, which can be separated and weighed. The weight of the compound is used to calculate the concentration of constituent elements. One of the more common gravimetric analyses is the precipitation of the highly insoluble compound barium sulphate, which is used to calculate the concentration of barium.

In volumetric or titrimetric methods, the concentration of the element in a solution of the digested sample is calculated from the amount of reacting species that must be added to completely react with the element of interest. The amount of the reacting species is calculated by determining the volume that was added of a standard solution with a known concentration. A chemical or electronic indicator is used to signal completion of the reaction between the element of interest and the reacting species.

Specific ion electrodes measure the potential difference between a standard ion electrode and a solution of the same ion. Examples include the specific ion electrodes used to determine the concentration of fluoride or chloride.

10.6 Reporting of Results as Oxide Equivalents

Whole-rock fusion technique results for major cations are usually reported as oxide equivalents with the cation balanced with oxygen (e.g. Al_2O_3 and MgO). This does not mean that the cations in the sample necessarily occur in these oxide forms - in many cases, they do not. Elemental concentrations can be derived from the oxide concentration from the atomic weight ratios.

Whole-rock fusion technique results for major cations are usually reported as oxide equivalents, but often the elements do not occur as these oxide minerals.

The sum of a whole-rock analysis as oxide equivalents, including Loss On Ignition (LOI), will typically be close to 100%, hence the term "whole-rock". LOI reflects volatilized elements not included in the analysis, like sulphur (SO_2), carbon (CO_2) and water of crystallization (H_2O). A significant deviation from 100% can indicate an analytical error or the presence of anomalous levels of sulphides, carbonates, phyllosilicates and/or hydrated minerals.

10.7 Use of the Results

10.7.1 Compare with Concentrations in Non-Mineralized Rock and Soil

One use of solid phase element data is to identify trace elements that may be of potential concern in mine drainage. This can be achieved through comparison of the sample concentrations with the upper concentrations found in non-mineralized rock and soil. Where the trace elements occur in relatively reactive minerals (e.g. sulphides and carbonates), this comparison is useful in identifying which elements are more likely to be a concern.

10.7.2 Calculate Depletion Times and Duration of Leaching

Another potential use for solid phase total element data is in conjunction with the release rates measured in kinetic tests to calculate mass depletion times. For example, solid phase total zinc concentrations coupled with humidity cell measurements of the zinc release rates can be used to calculate the time to deplete zinc in the solid phase sample.

Some of the many factors that influence depletion rate and that warrant consideration in the calculation and use of depletion times include:

- differences between the kinetic test and the mine component in properties that control release rates, such as mineral exposure, rate of leaching per unit surface area or mass and the temperature; and
- future changes in geochemical conditions or the depletion of one of several mineral sources for the element that may change the depletion rate.

The larger mass and scale of full-scale mine components compared to a humidity cell often increase solute concentrations above solubility limits resulting in the precipitation of secondary minerals and the lowering of bulk depletion rates. Trace elements may occur in a number of different minerals that weather at different rates. For example, zinc may occur as major structural components or trace constituents in sphalerite, tennantite, tetrahedrite, various oxide and carbonate minerals, and pyrite. The relative release rates from different minerals may fluctuate with changes in the geochemical conditions. Microprobe or other mineralogical information is required to determine potential mineral sources for an element.

10.7.3 Estimate the Concentrations of Different Minerals

Total solid phase elemental data can be used to estimate maximum potential concentrations of certain minerals. For example, the maximum amount of sphalerite can be calculated by assuming all measured zinc occurs as this one mineral. This amount can then be subtracted from measured sulphur to determine the minimum amount of other sulphur bearing minerals. Thus, calculations of mineral concentrations in this way are based on assumptions about the mineral sources for the elements. These calculations can be verified using mineralogical tests (Chapter 17).

Total solid phase elemental data can be used to estimate maximum potential concentrations of certain minerals.

Software exists to calculate mineralogy from total element data. However, the large and heterogeneous mixtures of minerals found at many sites, especially after weathering and oxidation begin, cannot often be calculated reliably.

10.7.4 Estimate Maximum Potential Concentration of Acid Insoluble Sulphate

As part of Acid Base Accounting (ABA) (Chapter 14) and sulphur species determination (Chapter 12), potentially acid generating sulphide can be calculated by subtracting measured acid soluble sulphate from measured total sulphur. However, this approach leads to relatively acid insoluble sulphate minerals, like barite, to be considered sulphide. Total solid phase elemental concentrations can be used to determine whether the maximum potential contribution of acid insoluble sulphate to the calculated sulphide is significant and requires corrections.

Total concentrations of barium and lead can be used to calculate the maximum potential concentration of the primary acid insoluble sulphate minerals barite [$BaSO_4$] and anglesite [$PbSO_4$], based on the ratio of their molecular weight to that of sulphur and the assumption that these minerals are the only source for these elements:

1. % Ba x (32.07/137.3) = % Barite-S
2. % Pb x (32.07/207.2) = % Anglesite-S

Further assessment of the % barite-S and anglesite-S will be required if their maximum potential amounts are a significant portion of the calculated % sulphide-S. This will only occur if the % sulphide-S is low or the concentrations of total barium and lead are high. More accurate estimates of the % barite and anglesite may require the use of sub-microscopic techniques, such as Electron Microprobe, to determine the proportions of total barium and lead that occur as acid insoluble sulphate compared to other minerals. Lead may occur in galena and barium may occur in various silicates, oxides and carbonates. A more detailed assessment of the contribution of %

acid insoluble sulphate-S to the % sulphide-S is the work done by the Kemess mine, and described in Section 12.6.9.2.

10.7.5 Estimate the Type and Concentration of Non-Iron Sulphide Minerals

Another use of total solid phase elemental data is to estimate the type and maximum concentration of non-iron sulphide minerals and, as a result, the degree to which all sulphide could be more or less acid generating compared to iron sulphide (e.g. pyrite and pyrrhotite). In the calculation of the acid potential in Acid Base Accounting, it is assumed that all the sulphide-S will produce the same amount of acidity as the oxidation of iron sulphide close to near-neutral pH (Chapter 12). Iron sulphide minerals are generally present in much higher concentrations than other sulphide minerals and therefore this assumption is generally true. However, it is important to check whether a significant portion of the sulphide is in the form of non-iron minerals capable of increasing or decreasing the acidity per unit of S.

A coarse estimate of the levels of non-iron sulphide minerals can be made by assuming the total concentration of the corresponding elements occur as sulphides. In reality, the identity of the sulphide minerals will ideally come from the mineralogical data (Chapter 17).

Some sample calculations for converting elemental concentrations to the concentration of sulphide-S, assuming the entire concentration is in that sulphide mineral, is provided below. Note that these calculations assume ideal mineral formulas, which do not apply fully to most mine sites.

Covellite and Cu Sulphide Fraction of Chalcopyrite (1 Cu : 1 S):
% Cu x 32.07/63.54 = % Cu-S
Cu in Chalcocite (Cu_2S):
% Cu x 32.07/(2 x 63.54) = % Cu-S
Molybdenite: % Mo x (2 x 32.07)/95.94 = % Mo-S
Pentlandite: % Ni x 32.07/58.7 = % Ni-S
Galena: % Pb x 32.07/207.2 = % Pb-S
Sphalerite: % Zn x 32.07/65.38 = % Zn-S

When the approximate estimate indicates that potentially more or less acid generating sulphide-S may significantly alter the magnitude of the Acid Potential and NPR, a more detailed assessment should be conducted of the sulphide minerals, the proportion of the trace elements in non-sulphide minerals and acid generation by the reaction products.

10.7.6 Identification of Anomalous Geochemical Conditions

Total solid phase elemental data can be used to identify materials with an anomalous geochemical composition that may impact drainage chemistry. For example, low concentrations of Ca and Mg may indicate materials with very low levels of neutralizing capacity (Chapter 13), a situation where even very low sulphide concentrations may result in acidic drainage and higher sulphide concentrations may result in the rapid onset of acidic drainage. Low concentrations or anomalous ratios between nutrients (e.g. Mg > Ca) may indicate challenges for plant growth.

10.8 Detection Limits

Table 10.1 provides current examples of the elements measured, the minimum and maximum detection limits and the current costs for different total, near total and partial solid phase elemental methods. Detection limits differ for different elements. The detection limits and the elements may vary over time and between laboratories due to differences in the techniques, the standards used to calibrate individual instruments and the statistical method used to calculate the detection limit. Detection limits may also vary between samples and sample sets due to differences in composition. For example, dilution required as a result of high concentrations of some elements may increase the minimum detection limits for other elements. The detection limits may also vary due to interferences in the sample.

Methods may vary slightly between laboratories due to differences in the instruments and differences in sample preparation, analysis and QA/QC procedures which have been developed over years of performing the analyses. For example, one manufacturer may suggest operational methods and sample preparation techniques which are different from another instrument manufacturer. As with all analyses, accuracy requires careful calibration with a range of appropriate standards. Likewise, analytical precision requires that the techniques used are consistent between samples and between laboratory personnel.

10.9 Recommended Methods

When selecting a method, it is important to consider the purpose of the data and limitations of the technique and ensure the selected method or methods provides the required elemental analyses and accuracy and is compatible with the materials being investigated. Discussions with the testing laboratory should be conducted to ensure an appropriate method is selected based on these considerations. The methods of digestion and analysis should always be reported when using and communicating results, so reviewers are aware of the potential limitations of the information.

It is important when selecting a method to consider the purpose for the data and limitations of the technique and ensure the selected method or methods provides the required elemental analyses and accuracy, and is compatible with the materials being investigated.

Due to cost and ability to provide the necessary level of accuracy and detection limits, the most commonly used methods are wet acid digestion, such as four acid and aqua regia, followed by ICP-AES. Four acid digestion is slightly more expensive to conduct than aqua regia but provides a more complete sample digestion. In most situations, the objective is to identify anomalously high elemental concentrations and thus the lower minimum detection limits provided by ICP-MS are often not required.

Where the objective is to determine the concentration of major mineral forming cations or the total elemental composition of the whole rock, digestion by lithium borate fusion with analysis by XRF or ICP-AES is recommended. Sodium peroxide fusion rather than lithium borate fusion is recommended when the sulphide mineral concentration is > 5%.

Table 10.1 Examples of detection limits and costs for total solid phase elemental analysis.

Digest Anal-ysis	Lithium Borate XRF/ ICPAES	Na H_2O_2 ICPAES	Lithium Borate ICP/MS	Pellet XRF	Aqua Regia		Four Acids	
					ICPMS/AES	ICP/AES	ICPMS/AES	ICP/AES
	%	%	ppm	ppm	ppm	ppm	ppm	ppm
Ag			1 - 1000		0.01 - 100	0.2 - 100	0.01 - 100	0.5 - 100
Al	0.01-100	0.01 - 30			0.01 - 15%	0.01 - 15%	0.01 - 25%	0.01 - 25%
As		0.01 - 10		5-5000	0.1 - 10,000	2 - 10,000	0.2 - 10,000	5 - 10,000
B					10 - 10,000	10 - 10,000		
Ba	0.01-100		0.5 - 10,000	10 - 10,000	10 - 10,000	10 - 10,000	10 - 10,000	10 - 10,000
Ca	0.01-100	0.01 - 30			0.01 - 15%	0.01 - 15%	0.01 - 25%	0.01 - 25%
Cd					0.01 - 500	0.5 - 500	0.02 - 500	0.5 - 500)
Co		0.002 - 30	0.5 - 10,000		0.1 - 10,000	1 – 10,000	0.1 - 10,000	1 - 10,000
Cr	0.01-100	0.01 - 30	10 - 10,000		1 - 10,000	1 – 10,000	1 - 10,000	1 - 10,000
Cu		0.005 - 30	5 - 10,000	10 - 10,000	0.2- 10,000	1 – 10,000	0-2 - 10,000	1 - 10,000
Fe	0.01-100	0.05 - 60			0.01 - 15%	0.01 - 15%	0.01 - 25%	0.01 - 25%
Hg					0.01 - 10,000	1 - 10,000		
K	0.01-100	0.1 - 30			0.01 - 10%	0.01 - 10%	0.01 - 10%	0.01 - 10%
Mg	0.01-100	0.01 - 30			0.01 - 15%	0.01 - 15%	0.01 - 15%	0.01 - 15%
Mn	0.01-100	0.01 - 30			5 - 10,000	5 - 10,000	5 - 10,000	5 - 10,000
Mo			2 - 10,000		0.05 - 10,000	1 - 10,000	0.05 - 10, 000	1 - 10, 000
Na	0.01-100				0.01 - 10%	0.01 - 10%	0.01 - 10%	0.01 - 10%
Ni		0.005 - 30	5 - 10,000	10 - 15,000	0.2 - 10,000	1 - 10,000	0.2 - 10,000	1 - 10,000
P	0.01-100				10 - 10,000	10 - 10,000	10 - 10,000	10 - 10,000
Pb		0.01 - 30	5 - 10,000)		0.2 - 10,000	2 - 10,000	0.5 - 10,000	2 - 10,000
S		0.01 - 60			0.01 - 10%	0.01 - 10%	0.01 - 10%	0.01 - 10%
Sb					0.05 - 10,000	2 - 10,000	0.05 - 1000	5 - 10,000
Se					0.2 - 1,000)		1 - 1000	
Si		0.01 - 30						
Sn			1 - 10,000	5 - 10,000	0.2 - 500		0.2 - 500	
Sr	0.01-100		0.1 - 10,000	2 - 10,000	0.2 - 10,000	1 - 10,000	0.2 - 10,000	1 - 10,000
Ti	0.01-100	0.01 - 50			0.005 - 10%	0.01 - 10%	0.005 - 10%	0.01 - 10%
U			0.5 - 1000	4 - 10,000	0.05 - 10,000	10 - 10,000	0.1 - 500	
W			1 - 10,000	10 - 10,000	0.05 - 10,000	10 - 10,000	0.1 - 10,000	10 - 10,000
Zn		0.01 - 30	5 - 10,000	10 - 10,000	2 - 10,000	2 - 10,000	2 - 10,000	2 - 10,000
Zr		0.01 - 30	0.5 - 10,000	2 - 10,000	0.5 - 500		0.5 - 500	
Cost $	32.00	25.00	27.50	27.50	18.75	9.00	22.50	12.00

10.10 Recipes

10.10.1 Elemental Analysis

1. Use matrix matched calibration standards to correct for inter-element interference (both major and trace elements).
2. The instrument should be calibrated according to internal laboratory QA/QC procedures and the instrument Operator's Manual supplied by the manufacturer.

10.10.2 Lithium Tetraborate Fusion Digestion / XRF or ICP Analysis

1. A finely ground sample is mixed with lithium tetraborate flux (to lower the melting point of the mixture) and fused (heated until molten) in a furnace at approximately 1100°C.
2. The resulting melt is cooled and a thin glass disk is prepared.
3. Elemental Analysis

3a. Glass disk is analyzed by XRF spectrometry.

3b. Glass disk is dissolved in a known volume of 4-5% nitric acid and the resulting solution is analyzed by ICP-MS or ICP–AES.

4. Oxide concentrations are calculated from the resulting elemental concentrations so results can be reported in an oxide format.
5. To determine Loss On Ignition (LOI), approximately 1 g of sample is placed in a dry porcelain crucible, weighed, and ashed at 1000°C for about 1 hour. The sample and crucible are then cooled in a desiccator, re-weighed and the LOI calculated.

10.10.3 Pressed Pellet / XRF Analysis

1. A finely ground sample of about 2 g is combined with a liquid binder, compressed on a boric acid backing in an aluminum mold and dried.
2. The concentrations of trace elements in the pressed pellet are analyzed by XRF spectrometry.

10.10.4 Four Acid Digestion / ICP Analysis

1. A finely ground (pulped) sample is digested with a mixture of hydrofluoric, perchloric, and nitric acids.
2. The digestion is taken to near dryness.
3. A small amount of hydrochloric acid is added to further the digestion and dissolve the residue.
4. The sample is then made up to a final volume in a volumetric flask with hydrochloric acid and homogenized.
5. An exact aliquot of the sample is transferred to a clean auto sampler tube.
6. The concentrations of trace elements are analyzed by ICP-MS or ICP–AES.

10.10.5 Aqua Regia Digestion / ICP Analysis

1. A finely ground sample is mixed with a small known volume of aqua regia solution (concentrated HCl:HNO_3 - 3:1).
2. Test tubes are placed in racks in a hot water bath making sure that the water level in the pan is above the level of the sample solution. Digest at approximately 95°C for 2 hours.

3. The sample is cooled and brought up to a known volume in a volumetric flask with demineralized/deionized water. The samples are then capped, shaken and centrifuged.
4. Using a macro pipettor, an exact aliquot of the sample solution is taken and transferred to a clean autosampler tube, adding a known additional volume of demineralized/deionized water, if necessary, and shaken to mix it.
5. The concentrations of trace elements are analyzed by ICP-MS or ICP–AES.

10.11 Summary of Key Considerations

- Whole rock or near-total solid phase elemental analysis would be useful to perform on sulphidic geologic materials impacted by a mine.
- Whole rock and near-total solid phase elemental analysis provides limited information about the form (e.g. mineral) in which the elements exist and on its own is not a measure of the potential concentrations in drainage or the threat to the environment.
- Information on the mineralogy, geochemical conditions, rate of weathering, secondary mineral solubility and the resulting drainage chemistry would be useful to interpret the environmental significance of solid phase elemental analysis results.
- Digestion methods vary in their ability to dissolve different minerals and their susceptibility to interference by features such as the sulphide content.
    - Whole Rock Digestion → Lithium borate fusion.
    - Whole Rock Digestion, sulphide > 5% → Sodium peroxide fusion.
    - Near Total Digestion Whole Rock Digestion → Four acid.
    - Reactive Mineral Digestion → Aqua regia.
- An assessment of the sulphur content, ideally a sulphide-S analysis, would be useful to conduct in advance of solid phase elemental analysis to detect samples where elevated sulphide may interfere with the analysis.
- Report methods of digestion and analysis and detection limits, when using and communicating results, so others are aware of the potential limitations of the data.

10.12 References

Guerin, F., S. Wilson and R. Nicholson. 2006. Optimizing In-Pit Disposal of Problematic Waste Rock Using Leaching Tests, Portable XRF, Block and Mass Transport Models. In: Proceedings of 13th British Columbia - MEND Metal Leaching/Acid Rock Drainage Workshop, Challenges with Open Pits and Underground Workings. Vancouver, British Columbia, November 29-30.

ATTACHMENT 21

Received: 12 October 2020 | Revised: 25 April 2021 | Accepted: 27 April 2021

DOI: 10.1002/hyp.14199

RESEARCH AND OBSERVATORY CATCHMENTS: THE LEGACY AND THE FUTURE

WILEY

How realistic are water-balance closure assumptions? A demonstration from the southern sierra critical zone observatory and kings river experimental watersheds

Mohammad Safeeq[1,2] | Ryan R. Bart[3] | Norman F. Pelak[3] | Chandan K. Singh[3] | David N. Dralle[4] | Peter Hartsough[5] | Joseph W. Wagenbrenner[6]

[1]Division of Agriculture and Natural Resources, University of California, Davis, California

[2]Civil and Environmental Engineering, University of California, Merced, California

[3]Sierra Nevada Research Institute, University of California, Merced, California

[4]USDA Forest Service, Pacific Southwest Research Station, Davis, California

[5]Department of Land, Air and Water Resources, University of California, Davis, California

[6]USDA Forest Service, Pacific Southwest Research Station, Arcata, California

Correspondence
Mohammad Safeeq, Civil and Environmental Engineering, University of California, Merced, CA 95343.
Email: msafeeq@ucmerced.edu

Funding information
Division of Earth Sciences, National Science Foundation, Grant/Award Numbers: EAR-0619947, EAR-0725097, EAR-1239521, EAR-1331939; National Institute of Food and Agriculture, Grant/Award Number: 2018-67004-27405

Abstract

The water balance is an essential tool for hydrologic studies and quantifying water-balance components is the focus of many research catchments. A fundamental question remains regarding the appropriateness of water-balance closure assumptions when not all components are available. In this study, we leverage in-situ measurements of water fluxes and storage from the Southern Sierra Critical Zone Observatory (SSCZO) and the Kings River Experimental Watersheds (KREW) to investigate annual water-balance closure errors across large (1016–5389 km^2) river basins and small (0.5–5 km^2) headwater-catchment scales in the southern Sierra Nevada. The results showed that while long-term water balance in river basins can be closed within 10% of precipitation, in the smaller headwater catchments as much as a quarter of precipitation remained unaccounted for. A detailed diagnosis of this water-balance closure error using distributed soil moisture measurements in the top 1 m suggests an unaccounted deeper storage and a net groundwater export from the headwater catchments. This imbalance was also found to be very sensitive to the timescales over which water-balance closures were attempted. While some of the closure errors in the simple water balance can be attributed to measurement uncertainties, we argue for a broader consideration of groundwater exchange when evaluating hydrological processes at headwater scales, as the assumption of negligible net groundwater exchange may lead to an overestimation of fluxes derived from the water balance method.

1 | INTRODUCTION

Many hydrologic problems, such as understanding effects of wildfire (Roche et al., 2020), climate change (Gleick, 1987), and drought-related tree mortality (Bales et al., 2018; Goulden & Bales, 2019), involve quantifying or predicting changes in hydrologic stores and fluxes. However, since there is generally incomplete knowledge of one or more of the variables of interest at the scale of analysis, hydrologists frequently use a water mass balance to back-calculate less well-defined variables from more well-defined ones. This process, which often imposes assumptions and biases in the application of the water balance, can increase uncertainties in answering the hydrologic problem.

A standard catchment water balance with no human withdrawal or input of water can be described as:

$$P - ET - Q - G_n - \frac{dS}{dt} = 0, \quad (1)$$

where P is precipitation, ET is evapotranspiration, Q is runoff, G_n is net subsurface or groundwater exchange relative to the catchment with positive values indicating net output and negative values suggesting input originating outside of the drainage area, and dS/dt is the change in the terrestrial water storage S over time t with positive values suggesting an increase in storage and negative values indicating loss. There are two primary challenges with the application of this water balance. First, multiple components of the water balance are often not readily measured. Second, forcing water-balance closure can be problematic even when measurements of all the water-balance components are available due to biases in the measurements.

Of the water-balance components, measurements of G_n and dS/dt are infrequent and sparse. Thus, not surprisingly, these same components are often approximated to be negligible quantities. The assumption that $dS/dt = 0$ at annual and smaller timescales is known to be problematic (Istanbulluoglu et al., 2012; Rice & Emanuel, 2019; Wang et al., 2015; Wang, Huang, et al., 2014). Similarly, net groundwater exchange is common and occurs via a number of mechanisms (Markovich et al., 2019; Meixner et al., 2016; Sophocleous, 2002; Tonina & Buffington, 2009). Headwater catchments, with relatively high topographic positions, are more likely to lose water to regional aquifers while lower elevation catchments are more likely to gain additional water (Winter et al., 1998). Catchments that are small relative to a regional aquifer are also more likely to experience net groundwater exchange (Fan, 2019). In the absence of a regional aquifer, losses may also occur due to bypass flow around or beneath a stream gauge (Boano et al., 2014; Payn et al., 2009), especially in alluvial streams.

Measurements of water-balance components are often biased due to a variety of reasons, including instrument accuracy, varying environmental conditions, and uneven distribution of gauges (Kampf et al., 2020; Wang, Huang, et al., 2014; Wang, McKenney, et al., 2014). As a consequence, achieving perfect water-balance closure, where inputs equal outputs, seems unlikely unless the biases coincidently cancel each other out. Kampf et al. (2020) highlighted multiple issues and challenges with closing the water balance. In a closed water balance, errors in measured fluxes and assumptions in unmeasured fluxes propagate uncertainty (Kampf et al., 2020). In other words, assuming water-balance closure and estimating one of the unknown fluxes (often G_n or dS/dt) as a residual will contain uncertainties, as the biases associated with the measured variables will be reallocated to the inferred variables (Fekete et al., 2004; Wang, Huang, et al., 2014; Wang, McKenney, et al., 2014). Kampf et al. (2020) instead advocate for an open water balance, in which the known fluxes are compared to elucidate information about the characteristics of the watershed, but in which unknown water-balance fluxes are not imposed by a strict relationship with the rest of the water balance. Yet practical considerations, such as a lack of information on difficult-to-measure fluxes or an inability to quantify the uncertainty of measured fluxes, will necessitate the continued use of water balance equations to infer unknown terms, making it absolutely critical to evaluate underlying water-balance-closure assumptions.

Independently quantifying each term in the water-balance equation along with associated uncertainty has proven to be, and will likely continue to be, extremely challenging (Flerchinger & Cooley, 2000; Mazur et al., 2011; Pan et al., 2017; Scott & Biederman, 2019). However, research catchments and observatories, where multiple components of the water balance are often measured, provide an opportunity to test the assumptions that underpin the water balance. The Southern Sierra Critical Zone Observatory (SSCZO) and the Kings River Experimental Watersheds (KREW) are co-located in the southern Sierra Nevada of California, a region that is a primary water source for agriculture, urban areas, and the environment in the San Joaquin Valley. Runoff from the southern Sierra Nevada is overallocated for downstream uses, thus making estimates of water-balance components, such as mountain-block recharge, very important (Hanak et al., 2017). In this paper we examine how realistic water balance assumptions are in the southern Sierra Nevada, with the aim of determining the scale(s) over which the water-balance closure assumptions are valid. Specifically, our objective was to assess water-balance closure at two scales, the river-basin scale (1016–5389 km^2) and the headwater-catchment scale (0.5–5 km^2). We took advantage of the multiple gauged catchments in the KREW along with evapotranspiration and detailed soil moisture measurements provided by the SSCZO to produce a quasi-replicate experiment at the headwater catchment and river-basin scales to understand closure patterns within and between watersheds.

2 | MATERIALS AND METHODS

2.1 | Study area

2.1.1 | River basins

Southern Sierra Nevada basins (1016–5389 km^2) of the Merced, San Joaquin, Kings, Kaweah, Tule, and Kern Rivers were selected to investigate the water balance at larger scales (Table 1). The average elevation ranges from 1638 m for the Merced to 2328 m for the Kings (Figure 1). The underlying geology is granitic with scattered metamorphic sedimentary and volcanic rocks (Jennings & Gutierrez, 2010) throughout the study area (Figure 1). Except in the Merced, Mesozoic granodiorite dominates the rock type, covering over 75% of the basin area. In the Merced, Mesozoic granodiorite occupies 45% of the basin followed by 25% Ordovician to Triassic argillite, 10% Jurassic mafic volcanic rocks, and 5% Triassic to late Jurassic slate. All of the selected basins have glacial history (Clark et al., 2003; Matthes & Fryxell, 1965; Warhaftig & Birman, 1965) and as a result rock and rock materials of glacial origin occupy as much as 8% of the basin surface area. Matthes and Fryxell (1965) documented evidence of mild glaciation in headwaters of the Tule River, but the percentage of glacial drift is negligible (Jennings & Gutierrez, 2010). Entisol (45%), Inceptisol

TABLE 1 River basin characteristics and long-term mean water balance components

River basin	Area (km^2)	Elevation (m)			$\bar{P}$ (mm/year)	$\bar{Q}$ (mm/year)	$\overline{ET}$ (mm/year)	$\bar{G}_n$ (mm/year)	ET_o (mm/year)	Aridity (–)
		Min	Max	Mean						
Merced	2760	95	3944	1647	972	428	475	69	1734	0.497
San Joaquin	4353	92	4228	2111	939	484	342	113	1702	0.439
Kings	4008	171	4300	2332	923	500	369	54	1684	0.430
Kaweah	1456	189	3818	1725	848	350	476	22	1852	0.385
Tule	1016	165	3100	1218	677	154	464	59	2028	0.290
Kern	5389	748	4405	2201	555	151	287	117	1843	0.323

Note: $\bar{P}$ = mean annual (1981–2019) precipitation from PRISM AN81m (Daly et al., 2008, 2015). $\bar{Q}$ = mean annual (1985–2019) full natural flow from the California Department of Water Resources (online at: https://cdec.water.ca.gov/). $\overline{ET}$ = mean annual (1985–2019) evapotranspiration using Goulden and Bales (2019). $\bar{G}_n$ = net groundwater exchange, calculated using Equation (5a). ET_o = mean annual (1970–2000) reference evapotranspiration (Trabucco & Zomer, 2018). Aridity = mean aridity-wetness index using mean annual (1970–2000) precipitation from WorldClim2 Global Climate (Fick & Hijmans, 2017) and mean annual (1970–2000) ET_o from Trabucco and Zomer (2018).

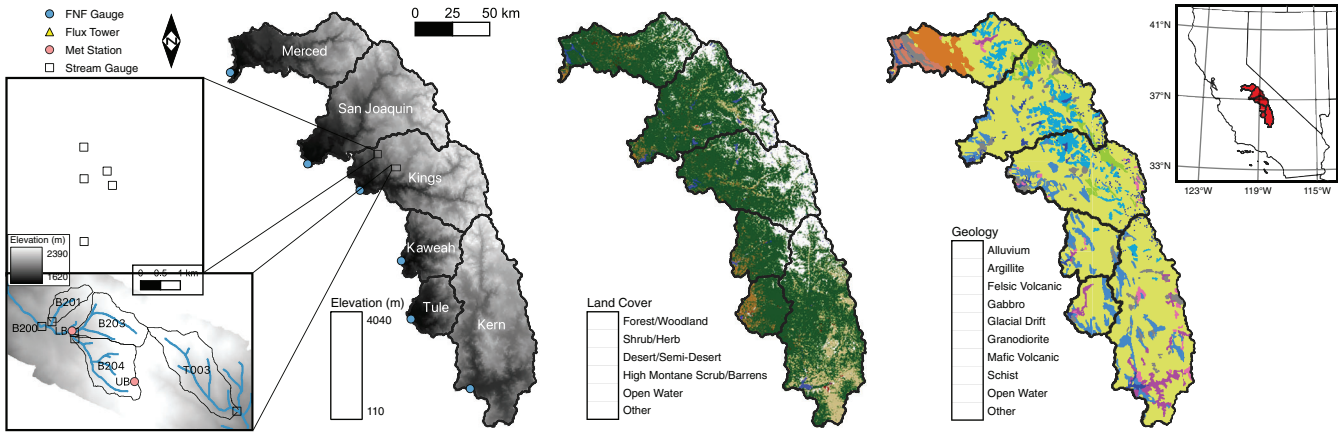

FIGURE 1 Study area showing the river basins and their elevation (left), land cover (center), and geology (right). The inset figures (far left) show the Providence (top) and Bull (bottom) headwater catchments, while the inset figure (far right) shows the location of the river basins within the state of California. FNF is full natural flow. LP, UP, LB, and UB are meteorological stations for lower Providence, upper Providence, lower Bull, and upper Bull, respectively

(25%), Alfisol (18%), and Mollisol (8%) soil orders, largely Dystric Xeropsamments (28%), Dystric Xeropchrepts (14%), Ultic Haploxeralfs (10%), and Typic Cryorthents (8%) dominate the study area (40%). The main land covers (Comer et al., 2003) are forest and woodland (68%), high montane scrub and barrens (18%), and desert or semi-desert (9%) (Figure 1). The vegetation is dominated by California dry-mesic and mesic mixed-conifer forest and woodland (18%), followed by subalpine lodgepole pine forest and woodland (9%), lower montane blue-oak-foothill pine woodland and savanna (7%), montane Jeffrey pine (7%), red fir (7%), and mixed oak woodland (6%). Nearly one-sixth (17%) of the study area is classified as alpine bedrock and scree, particularly above 3200 m of elevation (Rundel, 2011).

The climate of the river basins can be characterized as arid near the foothills of the Tule and Kern and mostly semi-arid and dry sub-humid at the higher elevations. Because of the latitudinal climate gradient in California, the proportion of the basin area with a dry sub-humid climate increases between the Kern and Merced river basins. The average annual basin precipitation increases from south to north with the Merced receiving ~43% more precipitation than the Kern. The Kings is the coldest basin with a 7°C average annual mean daily air temperature followed by the San Joaquin and the Kern (8°C), the Merced (10°C), the Kaweah (11°C), and the Tule (13°C). The percentage of the total annual precipitation falling as snow ranges from as little as 30% in the Tule to as much as 75% in the Kings (Safeeq et al., 2016).

2.1.2 | Headwater catchments

Our 10 headwater catchments (0.5–5 km^2) are part of the KREW and SSCZO networks and drain into the Kings River near the tail end of the Pine Flat Reservoir (Table 2). These catchments are clustered into two groups, the lower elevation (mean elevation 1859 m) Providence and the higher elevation (mean elevation 2308 m) Bull catchments. Three catchments in each group are nested within the larger P300 and B200 catchments, respectively (Figure 1). The underlying rock is largely Mesozoic granodiorite in Providence and early Proterozoic to

TABLE 2 Headwater catchment characteristics and long-term mean water balance components

Catchment	Area (ha)	Elevation (m)			$\bar{P}$ (mm/year)	$\bar{Q}$ (mm/year)	$\overline{ET}$ (mm/year)	$\bar{G}_n$ (mm/year)	ET_o (mm)	Aridity (–)
		Min	Max	Mean						
B201	53	2151	2382	2256	1366	534	539	293	1680	0.531
B203	138	2182	2490	2372	1422	712	469	241	1672	0.522
B204	167	2194	2489	2362	1394	619	477	298	1684	0.517
T003	228	2040	2470	2285	1436	571	605	260	1688	0.521
B200[a]	474	2120	2490	2319	1335	516	507	312	1724	0.531
P301	99	1793	2108	1974	1309	454	652	203	1772	0.551
P303	132	1722	2025	1898	1309	321	706	282	1762	0.548
P304	49	1765	1976	1895	1322	423	704	195	1769	0.543
D102	121	1476	1980	1774	1322	337	666	319	1775	0.544
P300[a]	461	1679	2107	1881	1248	359	682	207	1724	0.532

Note: $\bar{P}$ = mean annual (2004–2019) precipitation from KREW. $\bar{Q}$ = mean annual (2004–2019) runoff from KREW. $\overline{ET}$ = mean annual (2004–2019) evapotranspiration (Goulden & Bales, 2019). $\bar{G}_n$ = net groundwater exchange, calculated using Equation (5a). ET_o and Aridity = same as Table 1.
[a]No data for 2004–2006.

Cretaceous schist in Bull. Soils are predominantly Inceptisols and Entosols in Providence and Bull, respectively. Shaver series (coarse loamy, mixed, superactive, mesic Humic Dystroxerepts) are present at lower (1750–1900 m) elevations and Gerle (coarse-loamy, mixed, superactive, frigid Humic Dystroxerepts) and Cagwin (mixed, frigid Dystric Xeropsamments) series dominate at higher (1800–2400 m) elevations (Bales et al., 2011; Hunsaker et al., 2012). Cagwin series soils have high permeability and are classified into soil hydrologic group A. Gerle and Shaver series soils have moderate permeability and are classified into soil hydrologic group B. The land cover is 40–60 m tall mature mixed conifer forest, largely white fir (*Abies concolor*), ponderosa pine (*Pinus ponderosa*), Jeffrey pine (*Pinus jeffreyi*), sugar pine (*Pinus lambertiana*), and incense cedar (*Calocedrus decurrens*). As compared to Providence, mixed conifer vegetation in Bull contains a higher percentage of red fir (*Abies magnifica*) and is sparse, with 1%–4% rock outcrop or bare ground (Safeeq & Hunsaker, 2016).

The catchments have a Mediterranean climate, with wet, cold winters and dry, hot summers. Average annual precipitation varies between 1314 mm/year at Providence and 1400 mm/year at Bull. Over 90% of the annual precipitation at the KREW catchments falls between October and April. The mean average daily temperature, over water years 2002–2019, ranged between 10°C in Providence and 7.5°C in Bull. Lower temperatures in Bull relative to Providence cause a higher proportion of precipitation to fall as snow than rain. However, none of these catchments are above the rain-snow transition elevation (>2500 m), and so the type of precipitation shifts between rain and snow depending on the storm's temperature. Atmospheric rivers play a major role in the precipitation regime with as much as 30%–40% of snow accumulation (Guan et al., 2010) and 30%–45% of all precipitation (Dettinger et al., 2011), often contributed by just one or two events each year. Based on the aridity, defined as the ratio of mean annual precipitation to mean annual reference evapotranspiration (Trabucco & Zomer, 2018), all KREW catchments are classified as dry sub-humid.

2.2 | Datasets

2.2.1 | Precipitation

Daily precipitation in the KREW catchments was measured using weighing gauges at four locations (Safeeq & Hunsaker, 2016). These gauges are located at upper and lower elevations in each catchment group, Providence and Bull, to better capture the elevational patterns of precipitation (Figure 1). For the catchment average precipitation over the water year, defined as October 1–September 30, daily precipitation values from the two gauges in each catchment group were averaged, aggregated on a water year basis, and scaled using the ratio of PRISM (Daly et al., 2008, 2015) long-term (1981–2010) precipitation over the catchment to the precipitation of the grid cell underneath the gauge. These scaling factors ranged from 0.98 in B201 to 1.03 in T003, suggesting a marginal difference between catchment average precipitation and point precipitation at the gauge locations. This is not surprising considering the weak elevation control on precipitation at this elevation range in the Kings (Safeeq & Hunsaker, 2016). Water year precipitation for the six river basins was based on monthly PRISM (Daly et al., 2008, 2015) precipitation, version AN81m, available in Google Earth Engine (Gorelick et al., 2017).

2.2.2 | Discharge

Discharge at the headwater catchment outlets was measured at 15-min intervals using a combination of nested Parshall-Montana flumes, weirs, and manual stage-discharge rating curves (Safeeq & Hunsaker, 2016). Volumetric [L^3/T] 15-min catchment discharge values were aggregated to daily and water year timescales and normalized by catchment drainage area for converting into unit runoff [L/T]. Discharge for each of the river basins is regulated by hydroelectric and other multi-purpose dams. As a result, monthly full natural or

unimpaired flow data (FNF) for each basin were obtained from the California Department of Water Resources (https://cdec.water.ca.gov/), aggregated to a water year basis, and normalized by the drainage area for converting into unit runoff. The accuracies of these unimpaired runoff values are known to be comparable to the accuracy of the U.S. Geological Survey streamflow gauges (Gleick, 1987; U.S. Department of the Interior, 1976).

2.2.3 | Evapotranspiration

Evapotranspiration (*ET*) was measured using the eddy covariance method at the US-CZ3 site within catchment P301 at 30-min intervals starting in 2008 (Goulden et al., 2012). ET data was gap-filled using energy balance closure and aggregated to the daily timescale (Rungee et al., 2019). Water year catchment and river basin ET values were derived in Google Earth Engine (Gorelick et al., 2017) using a linear regression (*ET* (mm) = 117.16*exp(2.8025**NDVI*), $R^2 = 0.84$) between ground-based ET from 10 California eddy covariance flux towers and Normalized Difference Vegetation Index (*NDVI*) from Landsat 5, 7, and 8 for the 9 nearest upwind pixels (Goulden & Bales, 2019). In an earlier study, Goulden and Bales (2014) validated this *NDVI* based *ET* model by comparing average (2003–2012) annual estimated ET against the long-term (1980–2010) mean *P*-*Q* as a proxy for measured basin-wide *ET*. This validation was performed in 11 major river basins on the western slope of the Sierra Nevada, including five of the six river basins from this study. More recently, Roche et al. (2020) performed a more robust independent cross-validation on *NDVI*-based *ET* estimates using the leave-one-out approach and reported a ± 5% prediction uncertainty, mostly in high *NDVI* regions where saturation of surface reflectance is an issue.

2.2.4 | Soil water storage

Measurements of hourly soil moisture (2009–2016) at depths of 10, 30, 60, and 90 cm below the soil surface were obtained from the SSCZO wireless sensor network data (O'Geen et al., 2018). This network included two clusters of 10 and 17 nodes located near the lower and upper Providence precipitation gauge, respectively. These sensor nodes were strategically placed to sample soil moisture variations across aspect and tree canopy conditions. First, hourly volumetric soil moisture readings, m^3/m^3, from each node were converted into mean daily measurements. We then multiplied each measurement by their respective zone of influence and calculated sum total volumetric water content, *S*(*t*), in the top 1 m soil profile at time step *t* as follows:

$$S(t) = \theta_{10}(t) \times 0.2 + \theta_{30}(t) \times 0.25 + \theta_{60}(t) \times 0.3 + \theta_{90}(t) \times 0.25, \quad (2)$$

where θ is the volumetric water content and the subscript represents the depth of measurement (cm). For effective soil depth, gaps between two adjacent sensors were split in half. Second, the volumetric water content values, *S*(*t*), were multiplied by 1000 to convert the unit from volumetric (m^3/m^3) to depth of water (mm) in the one-meter profile. Finally, the depth equivalent water storage values were averaged across the 27 nodes to derive water storage for the entire P300 catchment.

2.3 | Water balance

Accounting for the measurement uncertainties in the components of the water balance, we can rewrite Equation (1) using an error term:

$$P - ET - Q - G_n - \frac{dS}{dt} = \varepsilon, \quad (3)$$

where the term ε is the residual error in the water balance. Using Equation (3) as a baseline, we derive annual and multi-year variations of the water balance to investigate different water-balance closure assumptions at different scales.

2.3.1 | Long-term water-balance closure

Over multiple-year timescales, water-balance closure assumptions are commonly made that allow the water balance to be simplified. The mean annual water balance for a period of *N* years can be described using the equation:

$$\bar{P} - \overline{ET} - \bar{Q} - \bar{G_n} - \frac{\overline{dS}}{dt} = \bar{\varepsilon}. \quad (4)$$

For a sufficiently large *N*, both mean residual error $\bar{\varepsilon}$ and mean change in the terrestrial water storage $\overline{dS}/dt$ are often approximated as zero, assuming that the basin is at a steady state with no net change in terrestrial water storage and residual error $\bar{\varepsilon}$ is normally distributed. Equation (4) then becomes

$$\bar{P} - \overline{ET} - \bar{Q} - \bar{G_n} = 0, \quad (5a)$$

or

$$\bar{G_n}(N) = \frac{\sum_{i=1}^{N} P_i}{N} - \frac{\sum_{i=1}^{N} ET_i}{N} - \frac{\sum_{i=1}^{N} Q_i}{N}. \quad (5b)$$

These long-term water-balance equations allowed us to investigate the magnitude and spatial patterns of $\bar{G_n}$ with varying number of *N* years (2, 3, 4, …30) over which $\bar{G_n}$ converges asymptotically to zero. For each value of *N*, *N*-years of annual *P*, *ET*, and *Q* were randomly drawn from the observed reccord for estimating $\bar{G_n}$ (*N*) using Equation (5b). This sampling was repeated 1000 times and the mean, standard deviation, and coefficient of variation (CV) were estimated from the 1000 values of $\bar{G_n}(N)$ for comparison between the sites.

2.3.2 | Simplified annual water-balance closure

For many water mass balance analyses at an annual time-step, measurements of G_n and dS/dt are not available and generally assumed to be zero. Similarly, since the error associated with P, ET, and Q is often unquantified, it is assumed to be negligible, which reduces the water balance Equation (3) to just three terms:

$$P - ET - Q = 0. \quad (6)$$

This simplified form of the annual water balance allows researchers to solve for one of the unknowns, often ET or Q. However, in order to use Equation (6), it is important that the assumptions used to simplify from Equation (3) to (6) be valid. In this study, detailed measurements of all three components, P, Q, and ET, allow us to test the spatial and temporal scales where the closure assumptions apply.

We first estimated the water-balance closure imbalance as:

$$\Delta = P - ET - Q, \quad (7)$$

If the assumption of a complete water-balance closure in Equation (6) holds true, then Δwill be homoscedastic, independent of P, Q, and ET, and follow a normal distribution (Xu, 2001). The homoscedasticity of the residuals was tested by plotting Δ against P, Q, and ET.

In catchment P300, soil moisture storage was available for the top 1 m (Section 2.2.4). This additional information allowed us to simplify Equation (3) without the assumption that $dS/dt \approx 0$, such that

$$P - ET - Q - \frac{dS}{dt} = 0. \quad (8a)$$

Equation (8a) was used to examine the assumption that G_n is negligible in catchment P300. It is worth noting that the simplification associated with soil moisture storage measurements limited to the top 1 m of the soil in most cases does not completely describe the S term. Past studies have reported deep water drawdown by vegetation (Fellows & Goulden, 2017; Klos et al., 2018; O'Geen et al., 2018), especially during prolonged droughts (Bales et al., 2018; Goulden & Bales, 2019). Fellows and Goulden (2017) estimated conifer forest rooting depth to be at least 3.6 m with weathered saprolite or saprock reaching up to 20 m beneath the surface (Holbrook et al., 2014; Klos et al., 2018). Moreover, our assumption of uniform soil thickness throughout the catchment is an oversimplification considering the variation in soil depth or regolith thickness within a catchment (O'Geen et al., 2018). The use of soil moisture storage measured in the top 1 m to infer overall catchment dS/dt will likely lead to an underestimation of the total terrestrial storage and an overestimation of G_n. For this reason, we further divided total terrestrial catchment water storage between shallow (top 1 m) S_s and deep (from 1 m below the surface to bedrock) S_d zone storages as follows:

$$P - ET - Q - \left(\frac{dS_s}{dt} + \frac{dS_d}{dt}\right) = 0, \quad (8b)$$

Catchment scale measurements to characterize dS_d/dt are limited. Our focus here is to investigate the $G_n \approx 0$ assumption while acknowledging the fact that changes in dS_d/dt during prolonged droughts, as shown in earlier studies, can be significant.

The precipitation-decorrelation technique of Trask et al. (2017) provides an alternative way to examine Equation (3) by resolving the $(G_n + dS/dt)$ from the random residual error ε. The Trask et al. (2017) approach provides a middle ground between a fully closed water balance and an open water balance (Kampf et al., 2020). The technique allows the water balance for one of the unknown terms to be solved without making assumptions regarding the accuracy of known terms or forcing the net water-balance error ε to zero. The statistical basis of this technique is the fact that interannual variation in $G_n + dS/dt$ will closely follow the variation in P and can be approximated using a linear model with assumptions that the covariance of P and Δ is statistically significant and the covariance of P and $\varepsilon \approx 0$. This method can be applied using univariate, for example, $\Delta = f(P)$, or multivariate, for example, $\Delta = f(P, ET)$, statistical techniques. Following Trask et al. (2017), we estimated annual $G_n + dS/dt$ using the equation:

$$G_n(t) + \frac{dS}{dt}(t) = \overline{\Delta} + \beta_1[P_N(t) - 1] + \beta_2[ET_N(t) - 1], \quad (9)$$

where P_N is normalized $[P(t)/\bar{P}]$ precipitation for year t, ET_N is normalized $[ET(t)/\overline{ET}]$ evapotranspiration, and $\beta_1$and β_2 are coefficients determined using the least-squares fit between $\Delta(t)$ as a dependent variable and $P_N(t) - 1$ and $ET_N(t) - 1$ as explanatory variables. The -1 terms in brackets in Equation (9) serve to subtract $\beta_1$and β_2 and ensure that the covariance between the water balance components (ET and P) and ε is close to zero and water balance remains closed (Trask et al., 2017). In catchments B201, B203, and B204, $ET_N(t) - 1$ showed no explanatory power and was replaced with normalized discharge ($[Q_N(t) - 1]$, where $Q_N = Q(t)/\bar{Q}$). This anomaly may have been driven by the fact that ET in these high elevation catchments is energy limited with small interannual variations. We also explored 1- and 2-year lagged precipitation as additional explanatory variables in the least squares fit model to account for memory effects but neither was statistically significant.

3 | RESULTS

3.1 | Long-term water-balance closure

Long-term average net groundwater exchange $\bar{G}_n$ (Equation (5)) from the six river basins ranged between 22 mm/year in the Kaweah to 117 mm/year in the Kern (Table 1). On average across the river basins, $\bar{G}_n$ was equivalent to 9% of $\bar{P}$,18% of $\overline{ET}$, and 21% of $\bar{Q}$. At the extreme end, in the Kern river basin $\bar{G}_n$ was equivalent to 21% of $\bar{P}$,41% of $\overline{ET}$, and 77% of $\bar{Q}$ (Figure 2). At the headwater-catchment scale, $\bar{G}_n$ ranged between 195 mm/year in P304 to as much as 319 mm/year in D102 (Table 2). In P303 and D102, $\bar{G}_n$ was very close to being equal to $\bar{Q}$. On average across the 10 catchments, $\bar{G}_n$ was

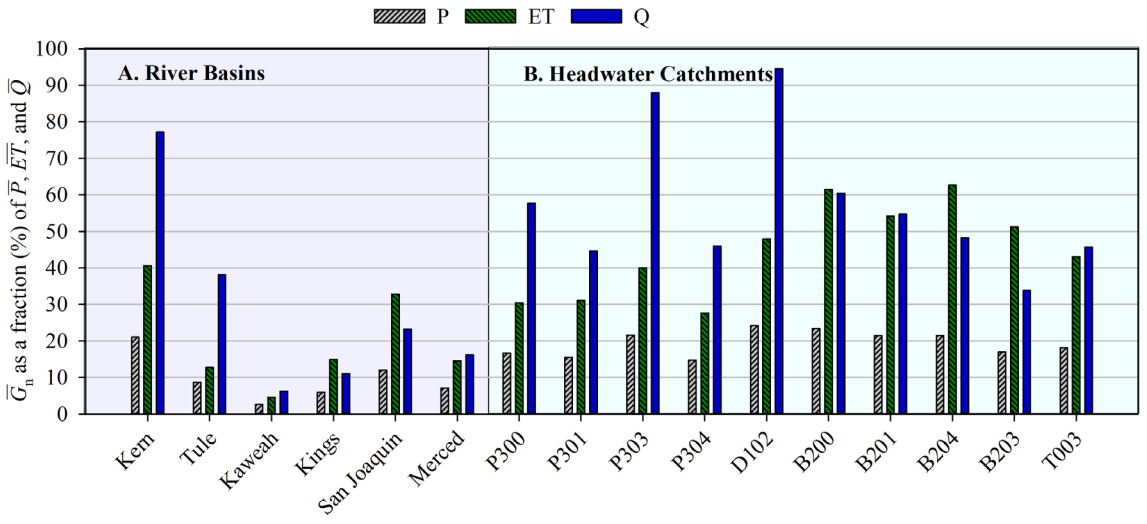

FIGURE 2 Long-term average net groundwater exchange ($\bar{G}_n$) across the different (a) river basins and (b) headwater catchments. Please note that the differences in the period of analysis between the river basins (1985–2019) and catchments (2004–2019). The river basin $\bar{G}_n$ as a percentage of precipitation, evapotranspiration, and runoff during 2004–2019 is almost half of those during 1985–2019

equivalent to 20% of $\bar{P}$,43% of $\overline{ET}$, and 54% of $\bar{Q}$. Despite the fact that P301, P303 and P304 are nested inside P300 and B201, B203, and B204 are nested inside B200, there was no evidence of lowering of $\bar{G}_n$ with increasing scale or stream order (consistent with Liu et al., 2013). Overall, $\bar{G}_n$ was highly correlated with $\bar{P}$ ($R^2 = 0.71$, $p < 0.01$) but showed weak or no association with $\overline{ET}$ ($R^2 = 0.3$, $p = 0.02$) or $\bar{Q}$ ($R^2 = 0.18$, $p = 0.10$). The relationship between $\bar{G}_n$ and elevation was also statistically insignificant ($p = 0.10$). Because of the differences in scale, relationships between $\bar{G}_n$, drainage area, and relief were explored separately for river basins and catchments, and only river basin drainage area showed moderate predictive power for $\bar{G}_n$ ($R^2 = 0.47$, $p = 0.003$).

Estimated mean $\bar{G}_n$ using different base years ($N > 1$, 1000 N-years combinations) are shown in Figure 3. The mean $\bar{G}_n$ in the six river basins and 10 headwater catchments remained relatively constant across the different base periods (Figure 3(a, b)). However, the pattern in the CV was highly variable between and within scales (i.e., river basins vs. catchments). While the decline in CV with increasing N is statistically expected due to regression toward the mean with longer time-series, the rate at which CV declines with increasing N points to differences in the sites and hydrologic memory. Large river basins have a much higher memory effect on $\bar{G}_n$ than the headwater catchments. It is also worth pointing out the differences within the river basins and headwater catchments. The Kaweah, and to some extent P304, show much higher CV in $\bar{G}_n$ for the same N. These two sites have the lowest mean $\bar{G}_n$ (Tables 1 and 2), making them more sensitive to interannual variation. These results suggest that $\bar{G}_n$ is highly sensitive to N and the definition of long-term must be carefully evaluated. For example, in river basins, 25 years may seem like a reasonable length for assuming $\bar{G}_n$ to be independent of N since the CV is below 0.25 for most basins. The time-scale for headwater catchments to fall below the 0.25 CV threshold is only 10 years. It is worth highlighting that while overlapping years and non-sequential years were used in this analysis due to the limited record, a less robust analysis of non-overlapping samples showed similar results (data not shown), suggesting that the role of overlapping years may not be substantial.

3.2 | Simplified annual water-balance closure

Annual (WY) water-balance closure error (i.e., Δ) for the river basins ranged between −188 mm/year (2014) in the Kaweah and 344 mm/year (1998) in the Kern. In the headwater catchments this error was even higher, ranging between −283 mm/year (2014) in P304 and 914 mm/year (2017) in B200. Water-balance closure error was largely positive with 71% and 82% of the years having $\Delta > 0$ in river basins and catchments, respectively. In relative terms, the absolute magnitude of Δ in any given year during the study period was as much as 46% of the annual precipitation in headwater catchments and 48% of the annual precipitation in river basins. As expected, the cumulative plots indicate a strong interannual variation in Δ (Figure 4). In particular, during the droughts Δ declined as vegetation started drawing water from the storage to meet the transpiration demand (Bales et al., 2018). The 2012–2016 drought was relatively hotter and drier than the 1987–1992 drought (Goulden & Bales, 2019), causing a larger net decline in Δ. Interestingly, none of the river basins or catchments showed a return of Δ to zero over the period of record (Figure 4), implying that all of the river basins and headwater catchments are net exporters of groundwater as dS/dt over this time-scale was approximately zero (see below). This result is consistent with the occurrence of mountain-block recharge in these basins (Markovich et al., 2019). The Kaweah looks to be a potential exception, with a significant decline in Δ during 2004–2011, just before the start of 2012–2016 drought, when compared with 1985–2003 (Figure 4(a)). Other catchments also showed similar declines, but they were

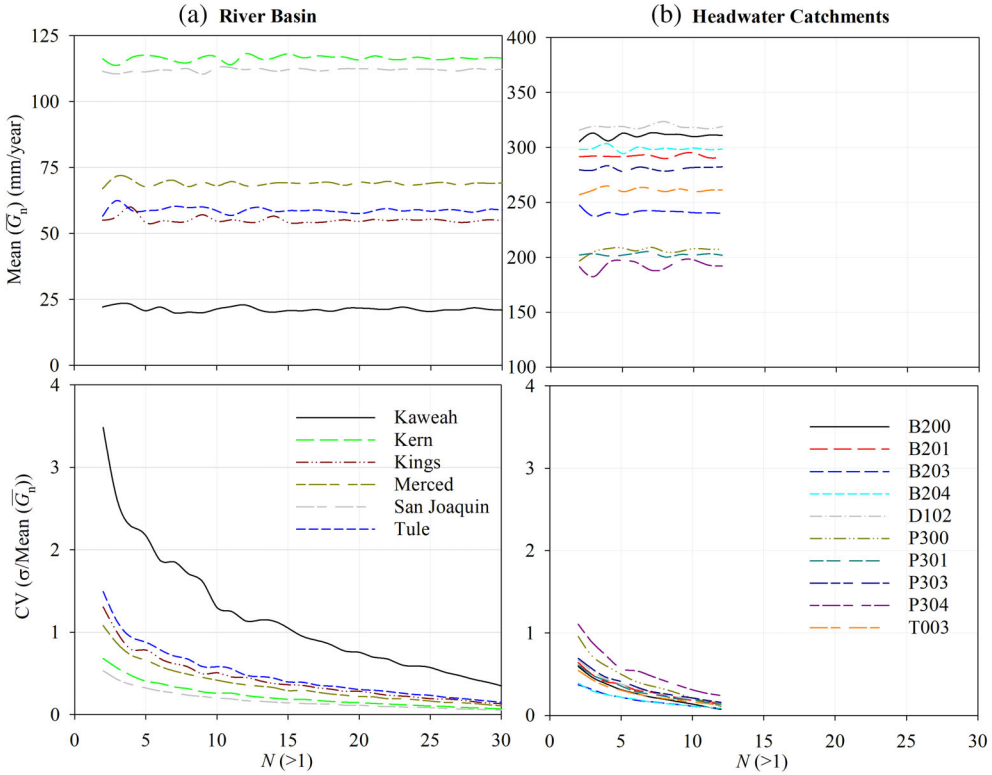

FIGURE 3 Mean of the average groundwater exchange over N-years ($\bar{G}_n$), and corresponding coefficient of variation (CV) estimated over multiple base periods (N) of 2 years and longer for (a) river basins and (b) headwater catchments. Note the different range of the y-axis in the top panel

statistically insignificant. This decline in Δ may have been driven by the canopy expansion, or structural overshoot of above ground biomass due to periods of favourable climatic and management conditions that facilitated abundant tree growth between 2009 and 2012 (Goulden & Bales, 2019; Jump et al., 2017). Overall, the Kaweah, along with the Tule, had the highest percentages (50% and 51%, respectively) of forest within the highly productive mid-elevation range of 1000–2500 m (Goulden & Bales, 2019), followed by the Merced (46%), the Kern (42%), the San Joaquin (39%), and the Kings (33%).

To examine the assumption of negligible G_n, we looked at the daily variations in water input (rain plus snowmelt), ET, Q, dS_s/dt, and the water-balance remainder (i.e., $dS_d/dt + G_n + \varepsilon$) between different years in P300 (Figure 5). The average dS_s/dt between 2009 and 2016 was 0.5 ± 12 mm (Table 3), suggesting that at annual and longer timescales dS_s/dt is negligible. Shallow soil water storage deficit from ET gets replenished from the rain and snowmelt within a year with no large carryover storage. At a daily timescale, maximum cumulative dS_s/dt varied marginally (standard deviation = 37 mm) among years compared to the variations in total annual P (standard deviation = 527 mm) and Q (standard deviation = 338 mm). The maximum cumulative dS_s/dt ranged between 190 mm in 2014 and 298 mm in 2011 (Table 3). Water year 2011 was one of the wettest, receiving 2152 mm precipitation compared to 555 mm in 2015 (Table 3). The cumulative water balance remainder, $dS_d/dt + G_n + \varepsilon$, remained largely negative or near zero during the first 2 months of the water year (Figure 5(e)), which are generally dry. We found $dS_d/dt + G_n + \varepsilon$ most significantly correlated with recharge or water input (rain plus snowmelt) with a lag of zero (cross-correlation = 0.63, $p < 0.05$).The cross-correlation between water-balance remainder and water input at a lag of one-day (cross-correlation = 0.38, $p < 0.05$) suggested an additional delayed recharge of soil moisture, especially in the snow free season when the ground is largely unsaturated. Overall, the negative $dS_d/dt + G_n + \varepsilon$ values of water-balance remainder near the beginning of the water year (suggesting$dS_s/dt > P - ET - Q$) were tied to an increase in shallow storage ($r = 0.93$, $p < 0.05$) with larger negative values (Figure 5(e)) coinciding within a day following an input (Figure 5(a)). However, at the daily time-step we did notice instances where increases in soil moisture storage did not match the recharge input, suggesting measurement error. As the water year progressed, the cumulative water balance remainder peaked at the end of the snowmelt season (March to May) before declining during the summer months. The net annual total water-balance closure error between different years ranged between −23.4 mm in 2015, the driest water year in the record, and 467 mm in 2016, which had slightly below average precipitation. As water-balance remainder was positively correlated with precipitation, the unusual behaviour for water year 2016 was in part due to 2016 being a relatively warm water year (+1.5°C warmer) and followed an extremely dry year with only 555 mm precipitation in 2015 (Figure 5). The large water-balance imbalance in 2016 may reflect, in part, the refilling of the deeper storage deficit from the drought.

The cumulative increase of Δ (Figure 4) suggests the presence of a systematic component. At longer timescales, when dS/dt is zero, there are two possible end-member sources and explanations for the systematic component of Δ variation: it is entirely made of net deep

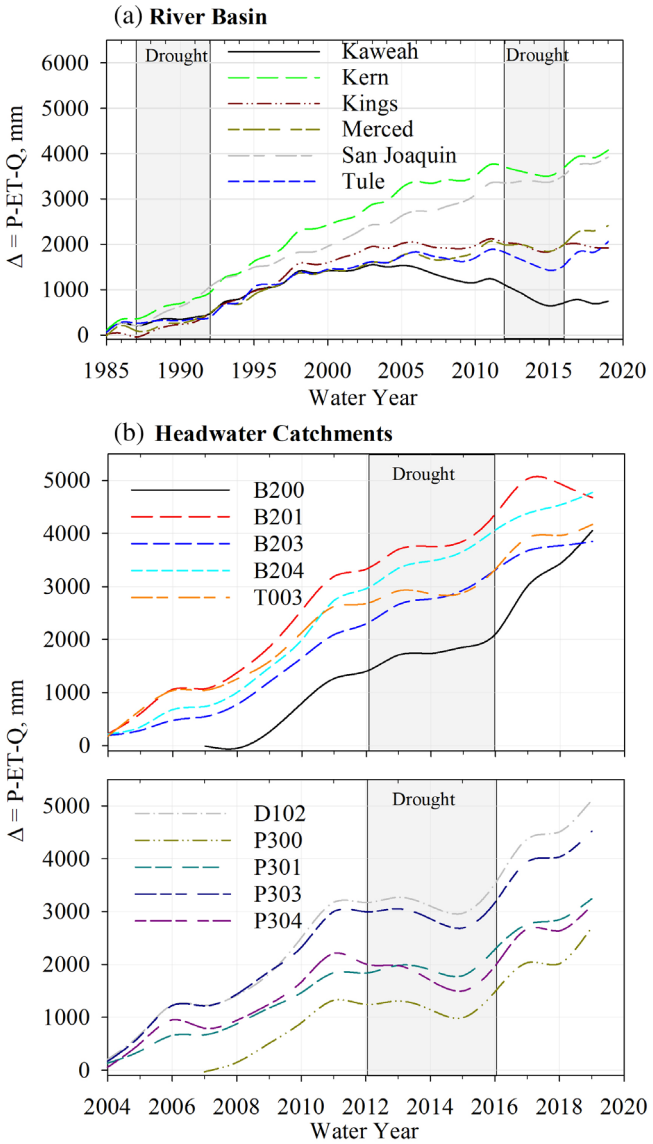

FIGURE 4 Cumulative plots of water balance closure error, $\Delta = P - ET - Q$, over time for (a) river basins and (b) headwater catchments

subsurface flows through the regolith or groundwater exchange (G_n) or it is entirely made of systematic errors associated with the measurements of *P*, *ET* and *Q*. In reality, it is likely neither one nor the other but rather a combination of G_n and systematic measurement errors. The relationships between annual Δand *P*, *ET*, and *Q* (Figure 6) revealed that Δ is biased and largely heteroscedastic for *P* and *Q* (Kruskal Wallis test, $\chi^2 > 5.991$ for 2 degrees of freedom) with a positive slope, and unbiased and homoscedastic for *ET* (Kruskal-Wallis test, $\chi^2 < 4.412$ for 2 degrees of freedom). Plotting Δagainst *P*, *ET*, and *Q* for P300 at a daily timestep revealed similar patterns, suggesting no systematic association between Δ and *ET*. These results are in line with the fact that temporal variation in forest *ET* under the Mediterranean climate of the Sierra Nevada is rather insignificant compared to variations in *P* and *Q* (Bales et al., 2018).

The components of the water balance contain both systematic and random errors. While the propagation of systematic error in the water balance is beyond the scope of this manuscript, we separated the random error from Δ using the precipitation-decorrelation method described earlier. The coefficient of determination (i.e., R^2) from the least-squares fit, developed to derive $\beta_1$and $\beta_2$in Equation (9) ranged between 0.56 for the Kings and 0.95 for P303. Eleven out of the 16 sites had R^2 values over 0.85, suggesting that the precipitation-decorrelation technique can be used to infer poorly resolved water balance terms, that is, $G_n + dS/dt$ and ε from the total mass balance closure error Δ.

The annual water-balance component estimates (Equation (3)) for the six river basins from 1985 to 2019 and 10 headwater catchments from 2004 to 2019 are shown in Figures 7 and 8, respectively. Overall, the resulting random residuals ε were homoscedastic (Kruskal-Wallis test, $\chi^2 < 2.469$ for 2 degrees of freedom) and showed no correlation ($p > 0.11$) with *P*, *ET*, or *Q*, thus satisfying the statistical criteria for being random. However, at the individual basin and catchment levels, ε was significantly correlated with *P* in B201 ($R^2 = 0.58$, $p < 0.001$) and B204 ($R^2 = 0.25$, $p < 0.02$), with *Q* in the Kern ($R^2 = 0.15$, $p = 0.01$) and the Tule ($R^2 = 0.12$, $p = 0.03$), and with *ET* in the Kaweah ($R^2 = 0.36$, $p < 0.001$), the Kern ($R^2 = 0.12$, $p = 0.03$), the Kings ($R^2 = 0.20$, $p < 0.001$), and the San Joaquin ($R^2 = 0.16$, $p = 0.01$). The strength of most of these correlations can be categorized as weak.

For river basins, the magnitude of $G_n + dS/dt$ ranged between −125 mm (WY 2014) in the Kaweah to as high as 344 (WY 1998) mm in the Kern (Figure 7). In contrast, the random residual ε ranged between −163 mm in the Kings (WY 2017) to as high as 171 mm in the San Joaquin (WY 1992). For the headwater catchments, the magnitude of $G_n + dS/dt$ ranged between −227 mm (WY 2014) in P304 to 946 mm (WY 2017) in D102 (Figure 8). The random residual ε ranged between −257 mm in B200 (WY 2008) to as high as 301 mm in P301 (WY 2016). These suggest that the absolute magnitudes of random residuals at annual time-scales are comparable to $G_n + dS/dt$ in river basins and smaller in the headwater catchments. At the headwater-catchment scale, the interannual variation in terms of standard deviation in annual $G_n + dS/dt$ can be explained by the mean catchment elevation ($R^2 = 0.77$) with standard deviation decreasing with increasing elevation. However, at the river-basin scale, this interannual variation in $G_n + dS/dt$ showed better agreement with mean basin runoff ($R^2 = 0.82$) and potential evapotranspiration ($R^2 = 0.69$). The standard deviation for annual $G_n + dS/dt$ declined with increasing mean river basin runoff and increased with increasing potential evapotranspiration.

Looking at the time-series, both the magnitude and interannual variations in $G_n + dS/dt$ were comparable to *Q* for the Tule and Kern river basins and the P303 and D102 headwater catchments (Figures 7 and 8). In terms of the magnitude, annual $G_n + dS/dt$ exceeded annual *Q* in 7% of the years for river basins (max. 66 mm) and 25% of the years for headwater catchments (max. 243 mm). Annual $G_n + dS/dt$ was negative in only 55 out of 210 site years in the river basins, suggesting these river basins are a net annual exporter of

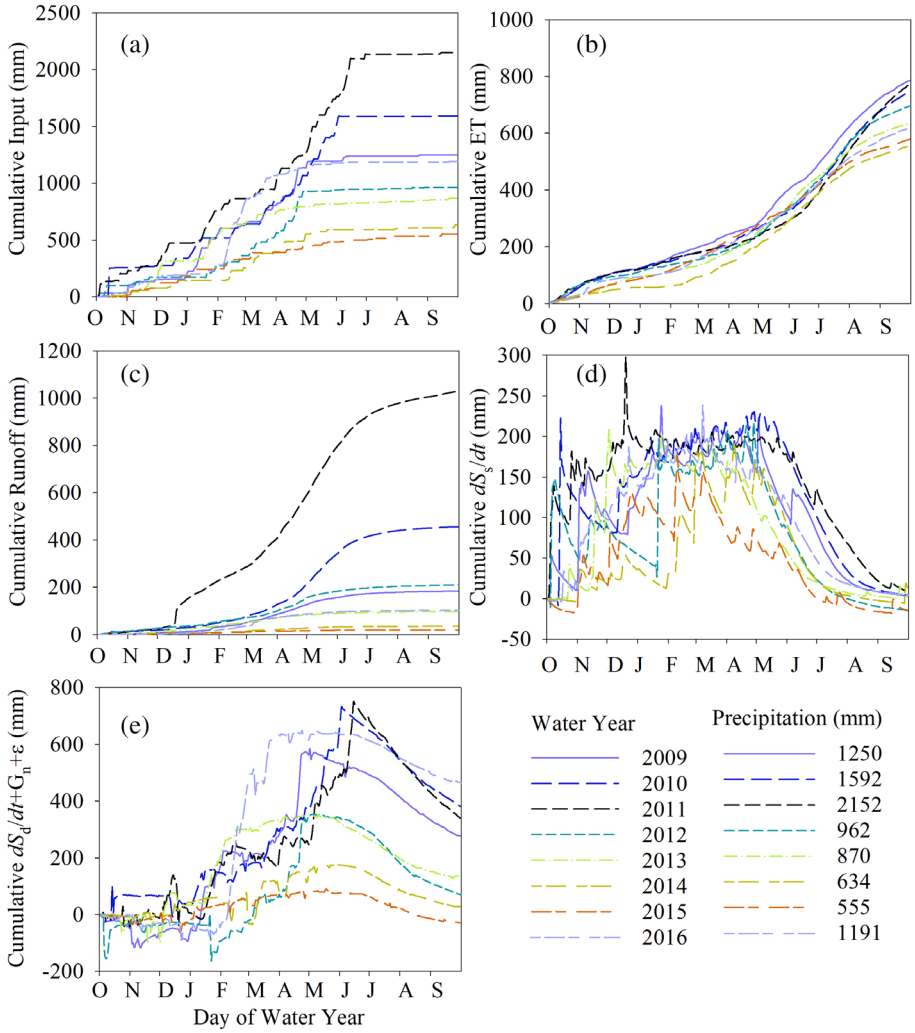

FIGURE 5 Cumulative water-balance components across water years for catchment P300: (a) input estimated as the sum of rain and snowmelt, (b) evapotranspiration (*ET*), (c) runoff, (d) change in shallow storage (dS_s/dt), and (e) water balance remainder ($dS_d/dt + G_n + \varepsilon = P - ET - Q - dS_s/dt$)

TABLE 3 Measured annual water-balance components for catchment P300

Water year	*P* (mm)	*Q* (mm)	*ET*[a] (mm)	Peak cumulative change in storage (mm)	Shallow storage change[b] (mm)	Water balance remainder[c] (mm)
2009	1250	184	785	238	2.1	279.1
2010	1592	456	750	230	5.5	380.8
2011	2152	1030	774	298	4.8	343.2
2012	962	210	698	214	−12.2	66.8
2013	870	98	634	208	4.5	133.5
2014	634	36	556	190	19.0	23.4
2015	555	20	579	178	−20.6	−23.4
2016	1191	103	620	242	1.6	466.6
Mean	1151	267	675	225	0.59	208.8
Standard deviation	527	338	90	37	12.0	182.5

[a]Measured *ET* at the P301 flux tower prior to scaling.
[b]Shallow Storage Change = dS_s/dt.
[c]Water Balance Remainder = $dS_d/dt + G_n + \varepsilon$.

groundwater. This pattern was even stronger at the headwater-catchment scale with only 12 out of 154 site years having negative $G_n + dS/dt$. The majority (67%) of these negative $G_n + dS/dt$ values, occurred in years during the 1987–1992 and 2012–2016 droughts, suggesting a water balance deficit. The cumulative water budget deficit during the 2012–2016 drought, which was more extreme than the

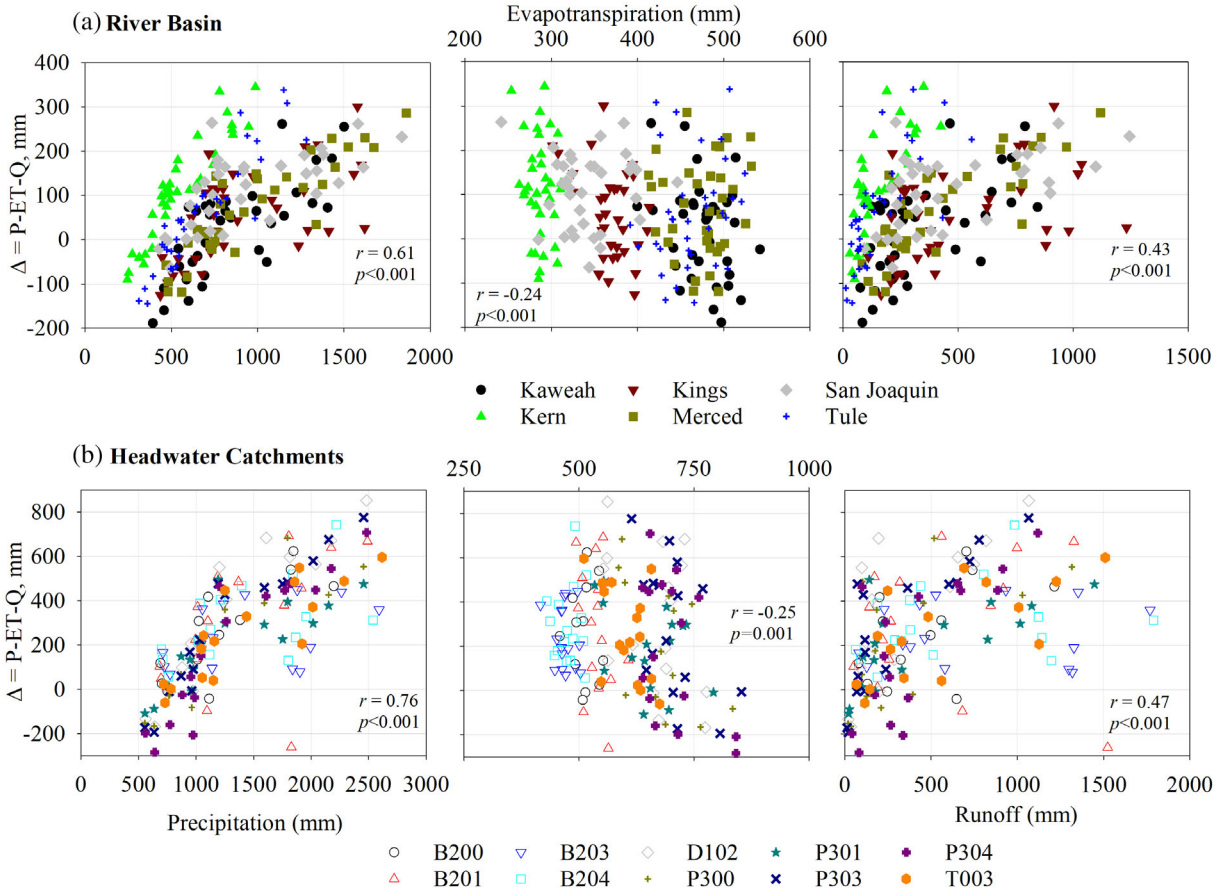

FIGURE 6 Variation in $\Delta = P - ET - Q$ with respect to precipitation (P), evapotranspiration (*ET*), and runoff (q) between the (a) river basins and (b) headwater catchments

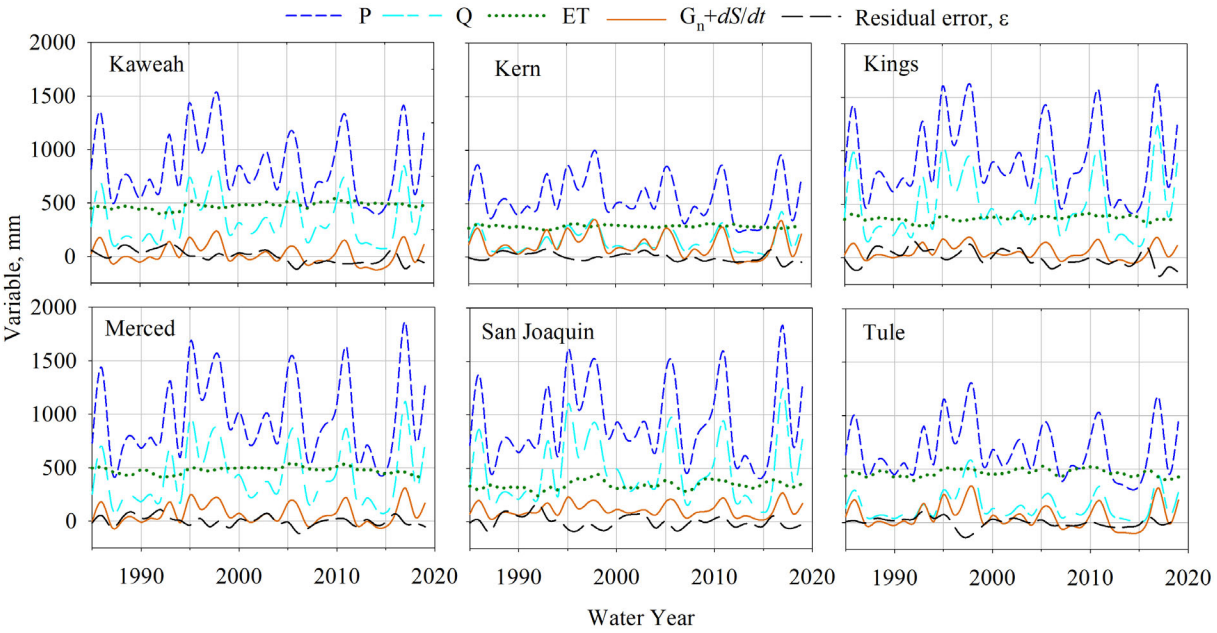

FIGURE 7 Annual water-balance components and residual error for the six studied river basins

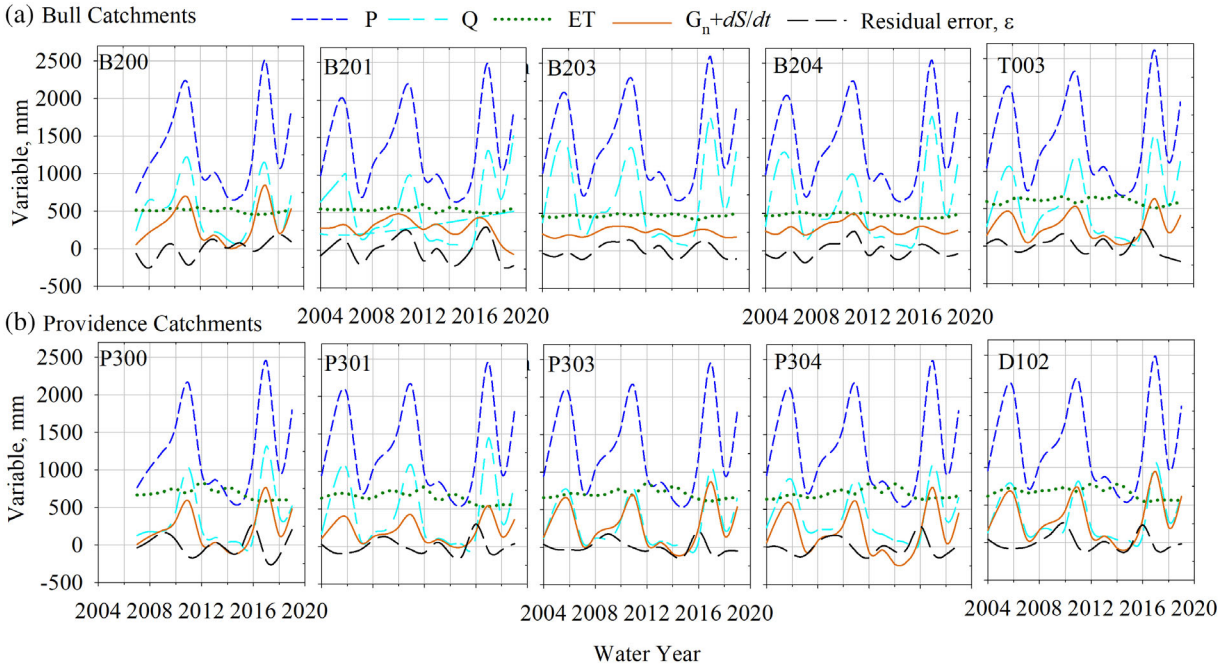

FIGURE 8 Annual water-balance components and residual error for the 10 studied headwater catchments (a) Bull and (b) Providence

1987–1992 drought, ranged from 0 mm in the San Joaquin to −405 mm in the Kaweah. These values are well within the range of multi-year deep soil drying reported earlier (Bales et al., 2018; Goulden & Bales, 2019; Roche et al., 2020). At the headwater scale, only Providence catchments P300, P303, P304, and D102 experienced overdraft (negative $G_n + dS/dt$ values) (Figure 8) with cumulative total values of −182, −166, −516, and −136 mm, respectively. These overdraft values do not concur with the shallow soil moisture measurements discussed earlier nor with deeper soil moisture measurements discussed in Section 4 below, indicating that the drying of catchments was well below the depth of our measurements, there were errors in measurements and scaling, or some combination of the two mechanisms. P304 is a groundwater driven catchment with deeper flow paths (Ackerer et al., 2020; Safeeq & Hunsaker, 2016), so a larger overdraft as reported by Goulden and Bales (2019) and Roche et al. (2020) is quite possible and may point toward limitations in soil moisture measurements.

4 | DISCUSSION AND IMPLICATIONS

We have utilized a rich dataset from the SSCZO and KREW to test water-balance closure assumptions and errors at various spatial and temporal scales. Our water-balance closure errors (i.e., $\bar{G}_n$ and Δ) were within the range of values reported in earlier studies (Bales et al., 2018; Gao et al., 2010; Saksa et al., 2017; Wang et al., 2015; Wang, Huang, et al., 2014; Wang, McKenney, et al., 2014). Gao et al. (2010) reported a 20% water-balance closure error using remotely sensed *P*, *ET* and *dS*/*dt* for the combined San Joaquin and Sacramento River basins. Wang, Huang, et al. (2014); Wang, McKenney, et al. (2014); Wang et al. (2015) reported water-balance closure errors between −50% and 25% of *P* with the majority of the watershed within a closure error of <20%. Also consistent with other studies (Abera et al., 2017; Engeland et al., 2005; Tardif et al., 2015; Wang, McKenney, et al., 2014), our results show that a high proportion of the closure error term can be attributed to the magnitude of *P* and *Q* (Figure 6).

While the reported magnitudes of water-balance closure in this study are comparable to those in the literature, differences in the scale and the various water-balance closure assumptions that were tested point to different factors and processes driving non-closure. At the river-basin scale, long-term water-balance closure in the form of $\bar{G}_n$ was well within the inherent measurement biases that are commonly used to explain non-closure, including a reported 5%–25% negative bias in measured and gridded *P* (Adam & Lettenmaier, 2003; Daly et al., 2017; Groisman & Legates, 1994), 5%–10% (mostly negative) bias in naturalized and measured *Q* (U.S. Department of the Interior, 1976; Hirsch & Costa, 2004), and ∼10% bias in ET (Wang et al., 2015). However, inherent measurement bias was not sufficient to explain the magnitude of Δ or $G_n + dS/dt$ at annual timescales and at the smaller spatial scales of the headwater catchments. Among *P*, *Q*, and *ET* in the water balance equation, *P* is the largest water flux. On average, annual *P* is 2.4 times *Q* and twice as much as *ET* in the river basins. This difference is even larger in the headwater catchments with *P* being 2.8 times *Q* and 2.3 times as much as *ET*. Hence an unbiased *P* will likely result in even larger magnitude of Δ or $G_n + dS/dt$.

The results presented here help quantify the spatial and temporal scales at which the water-balance closure assumption may be valid. At the annual timescales, it was not possible to resolve the components of Δ, but Figure 4(a) makes it clear that there was a systematic bias in Δ, due to some combination of G_n, dS/dt, and ε. Therefore, at the annual timescale, even for the larger river basins, the assumption of a

closed water balance should be used with caution. However, as shown in Section 3.2, the precipitation-decorrelation technique can be used to separate the error term ε from the combined $G_n + dS/dt$ term, and at longer timescales, dS/dt can be approximated to 0. This allows for a direct estimation of $G_n + dS/dt$ at an annual timescale and $\bar{G}_n$ at timescales longer than 1 year, rather than assuming them to be negligible as is often done to achieve water-balance closure when *P*, *Q*, and *ET* are known. Annual $G_n + dS/dt$ and $\bar{G}_n$ can then be compared to the other fluxes to evaluate the relative influence of these processes in the watershed (Figures 7 and 8). In the river basins, $\bar{G}_n$ was a relatively low percentage of the overall water balance (only 9% of average *P*) and within the margin of error of the other flux measurements (Kampf et al., 2020). Therefore, over longer periods at this scale, it may be acceptable to close the water balance.

At the headwater-catchment scale, the story is similar to the river-basin scale for short periods. The positive bias in Figure 4(b) again showed that the assumptions of negligible G_n or $G_n + dS_d/dt$ are not valid at the annual timescale. While the net change in shallow storage was relatively small over the annual timescale (0.5 $+/-$12 mm/year), the magnitude of the water balance remainder was quite large (Table 3). O'Geen et al. (2018) measured deeper (up to 10 m) soil moisture storage changes near the flux tower in P301 (Figure 1) using a neutron probe. The estimated changes in deeper storage from this dataset ranged from a 35 mm increase to a 42 mm depletion during the peak of the drought (2013–2015). While this measurement does not extend to full regolith thickness at the SSCZO (Holbrook et al., 2014), plants are less able to access storage at increasing depths (Klos et al., 2018; O'Geen et al., 2018). Additionally, the plant-available water holding capacity for the weathered granitic bedrock is very small, less than 10%, compared to 20% in the overlying soil (Hubbert et al., 2001; Jones & Graham, 1993). While the role of measurement and scaling uncertainties in soil moisture and other water balance components on the estimated water balance cannot be ignored, the magnitude of water-balance closure error (i.e., Δ) points to additional, much larger, uncounted storage affecting the water balance. At the daily timescale there was much larger variation in cumulative $dS_d/dt + G_n + \varepsilon$, which was typically negative or near zero at the beginning of the water year before peaking with snowmelt, demonstrating that even with measurements of *P*, *ET*, *Q*, and dS_s/dt, the water balance at a sub-annual timescale could not be considered closed (Figure 5). The higher mean G_n relative to *P* in the catchments was greater than the bias in *P* and *ET* reported above. However, even at longer timescales, G_n made up a larger proportion of the overall water balance for the catchments (20% of *P* on average) than for the river basins (Figure 2). Predictions for annual $G_n + dS/dt$ using the statistical precipitation-decorrelation technique compared to measurements of $G_n + dS/dt$ (solving Equation (3) with measurements of *P*, *ET*, *Q*, and dS/dt assuming $\varepsilon = 0$) were biased (Table 3), suggesting that the residual error term ε cannot be considered negligible. Taken together, the evidence from P300 suggests that at the headwater-catchment scale, even for longer timescales and rich datasets, the assumptions that are required to close the water balance may not be valid. The general trend is that the larger the spatial or temporal scale, the more acceptable the water-balance closure assumptions become.

The error in water-balance closure associated with the assumption of $G_n = 0$ has further implications for understanding critical zone processes and mass balance. From terrestrial storage, mixing, and fluxes (Dralle et al., 2018; Sprenger et al., 2018; Wlostowski et al., 2020), hyporheic flow and transport processes (Ackerer et al., 2020; Boano et al., 2014), to streamflow generation (Liu et al., 2013), inferring critical zone processes using water-balance closure without accurate knowledge of G_n can be misleading. As an example, future projections of increased impacts from extreme drought and wildfires in California (Dettinger et al., 2018) have stoked interest in understanding the effects of land management on processes such as streamflow, forest mortality, and evaporation (Bart et al., 2021; Roche et al., 2020). Setting $G_n = 0$ and neglecting changes in terrestrial storage to infer *ET* (as *P* - *Q*) or *Q* (as *P* - *ET*) could result in an overestimation of the impact of forest thinning or prescribed burns on catchment water yield by assuming that treatment-related decreases in ET directly result in corresponding increases in *Q*, rather than a more complex combination of changes in *ET*, subsurface storage, and groundwater fluxes. Furthermore, the subsurface structure of the critical zone has been identified as the biggest knowledge gap in the effort to incorporate hillslope-scale hydrological processes into Earth System Models (Fan et al., 2019), which are crucial tools for predicting the response of the critical zone to global change. Net groundwater exchange G_n is an essential component of the interaction of the subsurface with the aboveground parts of the critical zone, and so failing to accurately account for it also hampers our ability to improve models. Future studies exploring the nature and mechanisms behind the $G_n$flux out of the river basins and catchments can provide necessary insights on the actual magnitude of subsurface inflow of groundwater to lowland aquifers.

Fan et al. (2019) reviewed evidence for "leaky" watersheds, and found them to be widespread, and that "small catchment size, positioned at either the high or low end of a steep regional topographic and climatic gradient, underlain by deep permeable substrates that extend beyond the study catchment, and in drier climate or dry seasons and droughts" were factors making a watershed more likely to be leaky. The Providence and Bull headwater catchments examined in this study meet all of these criteria, underscoring the need to better characterize deeper flowpaths and quantify the net groundwater exchange (Frisbee et al., 2011). While flumes and weirs are often considered to have high measurement accuracy, they are often not anchored to bedrock. Morphologic changes such as lateral fluvial erosion, sediment deposition, and scour can also cause water to flow around the gauge. Indeed, some of the authors observed these effects firsthand while repairing the P300 weir in the summers of 2018 and 2019. Interestingly, the estimated long-term net groundwater exchange in P300 (207 mm) was on the low end of G_n values among the headwater catchments, suggesting that subsurface flow paths underneath the gauge may be common in the headwater catchments. Catchments may also be leaky at river-basin scales. Güler and Thyne (2006) used geochemical tracers to show that water originating in the Kern could be found in a different river basin on the eastern side of the Sierra Nevada. As a fraction of the overall water balance, this amount is likely to be smaller for river basins than for catchments.

The mechanism and magnitude of large-scale interbasin net groundwater exchange remain unclear (Markovich et al., 2019).

Due to the measurements available through the SSCZO and KREW programs, the analysis of water balance closure in headwater catchments was relatively rigorous. However, the role of biased data in water-balance closure cannot be ignored for larger river basins with complex topography. The in-situ measurement network for *P* is sparse for large basins, particularly in high-altitude regions. The measurement of precipitation using a sparse network can reduce the accuracy of gridded-precipitation datasets regardless of the methods used. Uncertainty in *NDVI*-based *ET* estimates may range between ±10% and 15% or less (Goulden et al., 2012). Regression-based approaches, like *NDVI*~*ET*, are not suitable in ecosystems where meteorological conditions and plant phenology play major roles or in areas where evaporation is dominant (Goulden & Bales, 2019).

5 | CONCLUSIONS

This study investigated water-balance closure assumptions over multiple spatial and temporal scales in the southern Sierra Nevada. The study was carried out on six river basins (>1000 km^2) and 10 headwater catchments (0.5–5 km^2) during the years 1985 to 2019 and 2004 to 2019, respectively. We leveraged data collected by the SSCZO and KREW to quantify the various stores and fluxes for calculating the water balance. Our results suggest that the water balance cannot be closed by current measurements without explicitly accounting for deeper storage and groundwater exchange fluxes. We found the net groundwater exchange to be much higher than the typical amount of measurement bias observed in the measurements of precipitation, streamflow, and evapotranspiration. Thus, we argue for greater consideration of groundwater exchange when evaluating and modelling hydrological processes. Long-term water balance closure at the river basin scale can be achieved but temporal scales over which the negligible net groundwater exchange assumption can be enforced must be carefully evaluated.

ACKNOWLEDGEMENTS

This work is supported by INFEWS grant (grant no. 2018-67004-27405) from the USDA National Institute of Food and Agriculture. Funding for the Kings River Experimental Watersheds (KREW) project was provided by the USDA Forest Service, the USDI and USDA Forest Service Joint Fire Science Program, from California's State Water Resources Control Board, through Proposition 50 (Water Security Clean Drinking Water, Coastal, and Beach Protection Act of 2002), the California Department of Forestry and Fire Protection, and the Sierra Resource Conservation District. SSCZO research infrastructure was supported by NSF EAR-0619947, EAR-0725097, EAR-1239521, and EAR-1331939. We thank the Sierra National Forest for their partnership and cooperation.

DATA AVAILABILITY STATEMENT

The data that support the findings of this study are openly available in the USFS data archive at https://doi.org/10.2737/RDS-2018-0028 and https://doi.org/10.2737/RDS-2017-0037 or with the original references/web link provided in the manuscript.

ORCID

Mohammad Safeeq https://orcid.org/0000-0003-0529-3925
Ryan R. Bart https://orcid.org/0000-0002-7235-8007
Norman F. Pelak https://orcid.org/0000-0002-1069-8217
Chandan K. Singh https://orcid.org/0000-0002-1802-5658
David N. Dralle https://orcid.org/0000-0002-1944-2103
Peter Hartsough https://orcid.org/0000-0001-7888-8028
Joseph W. Wagenbrenner https://orcid.org/0000-0003-3317-5141

REFERENCES

Abera, W., Formetta, G., Borga, M., & Rigon, R. (2017). Estimating the water budget components and their variability in a pre-alpine basin with JGrass-NewAGE. *Advances in Water Resources*, *104*, 37–54. https://doi.org/10.1016/j.advwatres.2017.03.010

Ackerer, J., Steefel, C., Liu, F., Bart, R., Safeeq, M., O'Geen, A., Hunsaker, C., & Bales, R. (2020). Determining how critical zone structure constrains Hydrogeochemical behavior of watersheds: Learning from an elevation gradient in California's Sierra Nevada. *Frontiers in Water*, *2*, 23. https://doi.org/10.3389/frwa.2020.00023

Adam, J. C., & Lettenmaier, D. P. (2003). Adjustment of global gridded precipitation for systematic bias. *Journal of Geophysical Research-Atmospheres*, *108*(D9), 4257. https://doi.org/10.1029/2002JD002499

Bales, R. C., Goulden, M. L., Hunsaker, C. T., Conklin, M. H., Hartsough, P. C., O'Geen, A. T., Hopmans, J. W., & Safeeq, M. (2018). Mechanisms controlling the impact of multi-year drought on mountain hydrology. *Scientific Reports*, *8*(1), 690. https://doi.org/10.1038/s41598-017-19007-0

Bales, R. C., Hopmans, J. W., O'Geen, A. T., Meadows, M., Hartsough, P. C., Kirchner, P., Hunsaker, C. T., & Beaudette, D. (2011). Soil moisture response to snowmelt and rainfall in a Sierra Nevada mixed-conifer forest. *Vadose Zone Journal*, *10*, 786–799. https://doi.org/10.2136/vzj2011.0001

Bart, R. R., Safeeq, M., Wagenbrenner, J. W., & Hunsaker, C. T. (2021). Do fuel treatments decrease forest mortality or increase streamflow? A case study from the Sierra Nevada (USA). *Ecohydrology*, *14*(1), e2254. https://doi.org/10.1002/eco.2254

Boano, F., Harvey, J. W., Marion, A., Packman, A. I., Revelli, R., Ridolfi, L., & Wörman, A. (2014). Hyporheic flow and transport processes: Mechanisms, models, and biogeochemical implications. *Reviews of Geophysics*, *52*(4), 603–679. https://doi.org/10.1002/2012RG000417

Clark, D. H., Gillespie, A. R., Clark, M. M., & Burke, R. (2003). Mountain glaciations of the Sierra Nevada. In D. Easterling (Ed.), *Quaternary geology of the United States: INQUA 2003 field guide volume* (pp. 287–310). Reno The Desert Research Institute.

Comer, P., Faber-Langendoen, D., Evans, R., Gawler, S., Josse, C., Kittel, G., Menard, S., Pyne, M., Reid, M., Schulz, K., & Snow, K., 2003. Ecological systems of the United States: A working classification of US terrestrial systems. NatureServe, Arlington, VA, 75.

Daly, C., Halbleib, M., Smith, J. I., Gibson, W. P., Doggett, M. K., Taylor, G. H., Curtis, J., & Pasteris, P. P. (2008). Physiographically sensitive mapping of climatological temperature and precipitation across the conterminous United States. *International Journal of Climatology*, *28*(15), 2031–2064. https://doi.org/10.1002/joc.1688

Daly, C., Slater, M. E., Roberti, J. A., Laseter, S. H., & Swift, L. W. (2017). High-resolution precipitation mapping in a mountainous watershed: Ground truth for evaluating uncertainty in a national precipitation dataset. *International Journal of Climatology*, *37*(S1), 124–137. https://doi.org/10.1002/joc.4986

Daly, C., Smith, J. I., & Olson, K. V. (2015). Mapping atmospheric moisture climatologies across the conterminous United States. *PLoS One*, *10* (10), e0141140. https://doi.org/10.1371/journal.pone.0141140

Dettinger, M. D., Alpert, H., Battles, J. J., Kusel, J., Safford, H., Fougeres, D., Knight, C., Miller, L., & Sawyer, S.. (2018). Sierra Nevada summary report. California's fourth climate change assessment (no. SUM-CCCA4-2018-004). California Energy Commission/Natural Resources Agency.

Dettinger, M. D., Ralph, F. M., Das, T., Neiman, P. J., & Cayan, D. R. (2011). Atmospheric rivers, floods and the water resources of California. *Water*, *3*(2), 445–478. https://doi.org/10.3390/w3020445

Dralle, D. N., Hahm, W. J., Rempe, D. M., Karst, N. J., Thompson, S. E., & Dietrich, W. E. (2018). Quantification of the seasonal hillslope water storage that does not drive streamflow. *Hydrological Processes*, *32*(13), 1978–1992. https://doi.org/10.1002/hyp.11627

Engeland, K., Xu, C.-Y., & Gottschalk, L. (2005). Assessing uncertainties in a conceptual water balance model using Bayesian methodology/estimation bayésienne des incertitudes au sein d'une modélisation conceptuelle de bilan hydrologique. *Hydrological Sciences Journal*, *50*(1), 9. https://doi.org/10.1623/hysj.50.1.45.56334

Fan, Y. (2019). Are catchments leaky? *WIREs Water*, *6*(6), e1386. https://doi.org/10.1002/wat2.1386

Fan, Y., Clark, M., Lawrence, D. M., Swenson, S., Band, L. E., Brantley, S. L., Brooks, P. D., Dietrich, W. E., Flores, A., Grant, G., Kirchner, J. W., Mackay, D. S., McDonnell, J. J., Milly, P. C. D., Sullivan, P. L., Tague, C., Ajami, H., Chaney, N., Hartmann, A., … Kirchner, J. W. (2019). Hillslope hydrology in global change research and earth system modeling. *Water Resources Research*, *55*(2), 1737–1772.

Fekete, B. M., Vörösmarty, C. J., Roads, J. O., & Willmott, C. J. (2004). Uncertainties in precipitation and their impacts on runoff estimates. *Journal of Climate*, *17*(2), 294–304. https://doi.org/10.1175/1520-0442(2004)017<0294:UIPATI>2.0.CO;2

Fellows, A. W., & Goulden, M. L. (2017). Mapping and understanding dry season soil water drawdown by California montane vegetation. *Ecohydrology*, *10*(1), e1772. https://doi.org/10.1002/eco.1772

Fick, S. E., & Hijmans, R. J. (2017). WorldClim 2: New 1-km spatial resolution climate surfaces for global land areas. *International Journal of Climatology*, *37*(12), 4302–4315. https://doi.org/10.1002/joc.5086

Flerchinger, G. N., & Cooley, K. R. (2000). A ten-year water balance of a mountainous semi-arid watershed. *Journal of Hydrology*, *237*(1), 86–99. https://doi.org/10.1016/S0022-1694(00)00299-7

Frisbee, M. D., Phillips, F. M., Campbell, A. R., Liu, F., & Sanchez, S. A. (2011). Streamflow generation in a large, alpine watershed in the southern Rocky Mountains of Colorado: Is streamflow generation simply the aggregation of hillslope runoff responses? *Water Resources Research*, *47*(6), W06512. https://doi.org/10.1029/2010WR009391.

Gao, H., Tang, Q., Ferguson, C. R., Wood, E. F., & Lettenmaier, D. P. (2010). Estimating the water budget of major US river basins via remote sensing. *International Journal of Remote Sensing*, *31*(14), 3955–3978. https://doi.org/10.1080/01431161.2010.483488

Gleick, P. H. (1987). The development and testing of a water balance model for climate impact assessment: Modeling the Sacramento Basin. *Water Resources Research*, *23*(6), 1049–1061. https://doi.org/10.1029/WR023i006p01049

Gorelick, N., Hancher, M., Dixon, M., Ilyushchenko, S., Thau, D., & Moore, R. (2017). Google earth engine: Planetary-scale geospatial analysis for everyone. *Remote Sensing of Environment*, *202*, 18–27. https://doi.org/10.1016/j.rse.2017.06.031

Goulden, M. L., Anderson, R. G., Bales, R. C., Kelly, A. E., Meadows, M., & Winston, G. C. (2012). Evapotranspiration along an elevation gradient in California's Sierra Nevada. *Journal of Geophysical Research – Biogeosciences*, *117*(G3), G03028. https://doi.org/10.1029/2012JG002027

Goulden, M. L., & Bales, R. C. (2014). Mountain runoff vulnerability to increased evapotranspiration with vegetation expansion. *Proceedings of the National Academy of Sciences*, *111*(39), 14071–14075. https://doi.org/10.1073/pnas.1319316111

Goulden, M. L., & Bales, R. C. (2019). California forest die-off linked to multi-year deep soil drying in 2012–2015 drought. *Nature Geoscience*, *12*(8), 632–637. https://doi.org/10.1038/s41561-019-0388-5

Groisman, P. Y., & Legates, D. R. (1994). The accuracy of United States precipitation data. *Bulletin of the American Meteorological Society*, *75* (2), 215–228. https://doi.org/10.1175/1520-0477(1994)075<0215:TAOUSP>2.0.CO;2

Guan, B., Molotch, N. P., Waliser, D. E., Fetzer, E. J., & Neiman, P. J. (2010). Extreme snowfall events linked to atmospheric rivers and surface air temperature via satellite measurements. *Geophysical Research Letters*, *37*(20), L20401. https://doi.org/10.1029/2010GL044696

Güler, C., & Thyne, G. D. (2006). Statistical clustering of major solutes: Use as a tracer for evaluating Interbasin groundwater flow into Indian Wells Valley, California. *Environmental and Engineering Geoscience*, *12* (1), 53–65. https://doi.org/10.2113/12.1.53

Hanak, E., Lund, J., Arnold, B., Escriva-Bou, A., Gray, B., Green, S., Harter, T., Howitt, R., MacEwan, D., Medellín-Azuara, J., Moyle, P., & Seavy, N. (2017). Water stress and a changing San Joaquin Valley (p. 50). Public policy Institute of California. Retrieved from http://www.ppic.org/main/publication.asp?i=1224

Hirsch, R. M., & Costa, J. E. (2004). U.S. stream flow measurement and data dissemination improve. *Eos, Transactions American Geophysical Union*, *85*(20), 197–203. https://doi.org/10.1029/2004EO200002

Holbrook, W. S., Riebe, C. S., Elwaseif, M., Hayes, J. L., Basler-Reeder, K., Harry, D. L., Malazian, A., Dosseto, A., Hartsough, P. C., & Hopmans, J. W. (2014). Geophysical constraints on deep weathering and water storage potential in the southern sierra critical zone observatory. *Earth Surface Processes and Landforms*, *39*(3), 366–380. https://doi.org/10.1002/esp.3502

Hubbert, K. R., Beyers, J. L., & Graham, R. C. (2001). Roles of weathered bedrock and soil in seasonal water relations of Pinus jeffreyi and *Arctostaphylos patula*. *Canadian Journal of Forest Research*, *31*(11), 1947–1957.

Hunsaker, C. T., Whitaker, T. W., & Bales, R. C. (2012). Snowmelt runoff and water yield along elevation and temperature gradients in California's southern sierra Nevada1. *JAWRA Journal of the American Water Resources Association*, *48*(4), 667–678. https://doi.org/10.1111/j.1752-1688.2012.00641.x

Istanbulluoglu, E., Wang, T., Wright, O. M., & Lenters, J. D. (2012). Interpretation of hydrologic trends from a water balance perspective: The role of groundwater storage in the Budyko hypothesis. *Water Resources Research*, *48*(3), W00H16. https://doi.org/10.1029/2010WR010100

Jennings, C. W., & Gutierrez, C. I. (2010). *2010 geologic map of California; California department of conservation*. California Geological Survey.

Jones, D. P., & Graham, R. C. (1993). Water-holding characteristics of weathered granitic rock in chaparral and forest ecosystems. *Soil Science Society of America Journal*, *57*, 256–261.

Jump, A. S., Ruiz-Benito, P., Greenwood, S., Allen, C. D., Kitzberger, T., Fensham, R., Martínez-Vilalta, J., & Lloret, F. (2017). Structural overshoot of tree growth with climate variability and the global spectrum of drought-induced forest dieback. *Global Change Biology*, *23*(9), 3742–3757.

Kampf, S. K., Burges, S. J., Hammond, J. C., Bhaskar, A., Covino, T. P., Eurich, A., Harrison, H., Lefsky, M., Martin, C., McGrath, D., Puntenney-Desmond, K., & Willi, K. (2020). The case for an open water balance: Re-envisioning network design and data analysis for a complex, uncertain world. *Water Resources Research*, *56*(6), e2019WR026699. https://doi.org/10.1029/2019WR026699

Klos, P. Z., Goulden, M. L., Riebe, C. S., Tague, C. L., O'Geen, A. T., Flinchum, B. A., Safeeq, M., Conklin, M. H., Hart, S. C., Berhe, A. A., Hartsough, P. C., Holbrook, W. S., & Bales, R. C. (2018). Subsurface plant-accessible water in mountain ecosystems with a Mediterranean climate. *WIREs Water*, *5*(3), e1277. https://doi.org/10.1002/wat2.1277

Liu, F., Hunsaker, C., & Bales, R. C. (2013). Controls of streamflow generation in small catchments across the snow–rain transition in the

southern Sierra Nevada, California. *Hydrological Processes*, *27*(14), 1959–1972. https://doi.org/10.1002/hyp.9304

Markovich, K. H., Manning, A. H., Condon, L. E., & McIntosh, J. C. (2019). Mountain-block recharge: A review of current understanding. *Water Resources Research*, *55*(11), 8278–8304.

Matthes, F., & Fryxell, F. (1965). Glacial reconnaissance of Sequoia National Park California; characteristics and distribution of the ancient glaciers in the most southerly national park of the Sierra Nevada,. U.S. Govt. Print. Off.

Mazur, K., Schoenheinz, D., Biemelt, D., Schaaf, W., & Grünewald, U. (2011). Observation of hydrological processes and structures in the artificial Chicken Creek catchment. *Physics and Chemistry of the Earth, Parts A/B/C*, *36*(1), 74–86. https://doi.org/10.1016/j.pce.2010.10.001

Meixner, T., Manning, A. H., Stonestrom, D. A., Allen, D. M., Ajami, H., Blasch, K. W., Brookfield, A. E., Castro, C. L., Clark, J. F., Gochis, D. J., Flint, A. L., Neff, K. L., Niraula, R., Rodell, M., Scanlon, B. R., Singha, K., & Walvoord, M. A. (2016). Implications of projected climate change for groundwater recharge in the western United States. *Journal of Hydrology*, *534*, 124–138. https://doi.org/10.1016/j.jhydrol.2015.12.027

O'Geen, A. (. T.)., Safeeq, M., Wagenbrenner, J., Stacy, E., Hartsough, P., Devine, S., Tian, Z., Ferrell, R., Goulden, M., Hopmans, J. W., & Bales, R. (2018). Southern sierra critical zone observatory and kings river experimental watersheds: A synthesis of measurements, new insights, and future directions. *Vadose Zone Journal*, *17*(1), 180081. https://doi.org/10.2136/vzj2018.04.0081

Pan, X., Helgason, W., Ireson, A., & Wheater, H. (2017). Field-scale water balance closure in seasonally frozen conditions. *Hydrology and Earth System Sciences*, *21*(11), 5401–5413. https://doi.org/10.5194/hess-21-5401-2017

Payn, R. A., Gooseff, M. N., McGlynn, B. L., Bencala, K. E., & Wondzell, S. M. (2009). Channel water balance and exchange with subsurface flow along a mountain headwater stream in Montana, United States. *Water Resources Research*, *45*(11), W11427. https://doi.org/10.1029/2008WR007644

Rice, J. S., & Emanuel, R. E. (2019). Ecohydrology of interannual changes in watershed storage. *Water Resources Research*, *55*(10), 8238–8251. https://doi.org/10.1029/2019WR025164

Roche, J. W., Ma, Q., Rungee, J., & Bales, R. C. (2020). Evapotranspiration mapping for Forest Management in California's Sierra Nevada. https://doi.org/10.3389/ffgc.2020.00069

Rundel, P. W. (2011). The diversity and biogeography of the alpine Flora of the Sierra Nevada, California. *Madrono*, *58*(3), 153–184. https://doi.org/10.3120/0024-9637-58.3.153

Rungee, J., Bales, R., & Goulden, M. (2019). Evapotranspiration response to multiyear dry periods in the semiarid western United States. *Hydrological Processes*, *33*(2), 182–194. https://doi.org/10.1002/hyp.13322

Safeeq, M., & Hunsaker, C. T. (2016). Characterizing runoff and water yield for headwater catchments in the southern Sierra Nevada. *Journal of the American Water Resources Association (JAWRA)*, *52*, 1327–1346. https://doi.org/10.1111/1752-1688.12457

Safeeq, M., Shukla, S., Arismendi, I., Grant, G. E., Lewis, S. L., & Nolin, A. (2016). Influence of winter season climate variability on snow–precipitation ratio in the western United States. *International Journal of Climatology*, *36*(9), 3175–3190. https://doi.org/10.1002/joc.4545

Saksa, P., Safeeq, M., & Dymond, S. (2017). Recent patterns in climate, vegetation, and forest water use in California montane watersheds. *Forests*, *8*(8), 278. https://doi.org/10.3390/f8080278

Scott, R. L., & Biederman, J. A. (2019). Critical zone water balance over 13 years in a semiarid savanna. *Water Resources Research*, *55*(1), 574–588. https://doi.org/10.1029/2018WR023477

Sophocleous, M. (2002). Interactions between groundwater and surface water: The state of the science. *Hydrogeology Journal*, *10*(1), 52–67. https://doi.org/10.1007/s10040-001-0170-8

Sprenger, M., Tetzlaff, D., Buttle, J., Carey, S. K., McNamara, J. P., Laudon, H., Shatilla, N. J., & Soulsby, C. (2018). Storage, mixing, and fluxes of water in the critical zone across northern environments inferred by stable isotopes of soil water. *Hydrological Processes*, *32*(12), 1720–1737. https://doi.org/10.1002/hyp.13135

Tardif, S., St-Hilaire, A., Roy, R., Bernier, M., & Payette, S. (2015). Water budget analysis of small forested boreal watersheds: Comparison of Sphagnum bog, patterned fen and lake dominated downstream areas in the La Grande River region, Québec. *Hydrology Research*, *46*(1), 106–120. https://doi.org/10.2166/nh.2014.219

Tonina, D., & Buffington, J. M. (2009). Hyporheic exchange in mountain rivers I: Mechanics and environmental effects. *Geography Compass*, *3*(3), 1063–1086 1063–1086.

Trabucco, A., & Zomer, R.J. (2018). Global Aridity Index and Potential Evapo-Transpiration (ET0) Climate Database v2. CGIAR Consortium for Spatial Information (CGIAR-CSI). Published online, Retrieved from the CGIAR-CSI GeoPortal at https://cgiarcsi.community

Trask, J. C., Fogg, G. E., & Puente, C. E. (2017). Resolving hydrologic water balances through a novel error analysis approach, with application to the Tahoe basin. *Journal of Hydrology*, *546*, 326–340. https://doi.org/10.1016/j.jhydrol.2016.12.029

U.S. Department of the Interior (1976). Surface water supply of the United States, 1966–1970, Part II, Pacific slope basins in California, vol. 4, northern California Valley Basins, U.S. Geol. Surv. Water-Supply Pap., 2131. 747.

Wang, S., Huang, J., Li, J., Rivera, A., McKenney, D. W., & Sheffield, J. (2014). Assessment of water budget for sixteen large drainage basins in Canada. *Journal of Hydrology*, *512*, 1–15. https://doi.org/10.1016/j.jhydrol.2014.02.058

Wang, S., McKenney, D. W., Shang, J., & Li, J. (2014). A national-scale assessment of long-term water budget closures for Canada's watersheds. *Journal of Geophysical Research-Atmospheres*, *119*(14), 8712–8725. https://doi.org/10.1002/2014JD021951

Wang, S., Pan, M., Mu, Q., Shi, X., Mao, J., Brümmer, C., Jassal, R. S., Krishnan, P., Li, J., & Black, T. A. (2015). Comparing evapotranspiration from Eddy covariance measurements, water budgets, remote sensing, and land surface models over Canada. *Journal of Hydrometeorology*, *16*(4), 1540–1560. https://doi.org/10.1175/JHM-D-14-0189.1

Warhaftig, C., & Birman, J. H. (1965). The quaternary of the Pacific mountain system in California. In H. E. Wright & D. G. Frey (Eds.), *The quaternary of the United States* (pp. 299–340). New Jersey Princeton University Press.

Winter, T. C., Harvey, J. W., Franke, O. L., & Alley, W. M. (1998). Ground water and surface water: A single resource (report no. 1139; Circular). USGS Publications Warehouse. https://doi.org/10.3133/cir1139

Wlostowski, N. A., Molotch, N., Anderson, P. S., Brantley, S., Chorover, J., Dralle, D., Kumar, P., Li, L., Lohse, K., Mallard, M. J., McIntosh, C. J., Murphy, F. S., Parrish, E., Safeeq, M., Seyfried, M., Shi, Y., & Harman, C. (2020). Signatures of hydrologic function across the critical zone observatory network. *Water Resources Research*, *57*, WRCR24937. https://doi.org/10.1029/2019WR026635

Xu, C. (2001). Statistical analysis of parameters and residuals of a conceptual water balance model – Methodology and case study. *Water Resources Management*, *15*(2), 75–92. https://doi.org/10.1023/A:1012559608269

How to cite this article: Safeeq, M., Bart, R. R., Pelak, N. F., Singh, C. K., Dralle, D. N., Hartsough, P., & Wagenbrenner, J. W. (2021). How realistic are water-balance closure assumptions? A demonstration from the southern sierra critical zone observatory and kings river experimental watersheds. *Hydrological Processes*, *35*: e14199. https://doi.org/10.1002/hyp.14199

ATTACHMENT 22

Spring 1989

Geology and petrochemistry of the Mount Chase massive sulfide prospect, Penobscot County, Maine

Michael V. Scully

Department:

sericite with minor chlorite, calcite, and fine opaque carbonaceous material. In the black shales, the carbonaceous material becomes a dominant component, and graphite is commonly seen on cleavage surfaces. The large cubic pyrites and spherulitic calcite masses are also locally abundant in the gray and black shales.

B. STRUCTURE

According to the mapping of Neuman (1967),and Ekren and Frischknecht (1967) the Mount Chase massive sulfide deposit lies within the southeast limb of the northeast-southwest trending Weeksboro-Lunksoos Lake Anticlinorium. They describe tight complex folding and a folded early cleavage in the Cambrian Grand Pitch sediments in the core of the structure, and simple homoclinal folding and a single vertical cleavage in the younger units on the flanks of the structure. They have identified only a few major faults which tend to be steeply dipping and parallel to the regional strike. One of these faults is shown passing through the Mount Chase prospect area.

In general, the limited structural observations made in this study agree well with those summarized above. The Mount Chase deposit host units show an average strike of N66E and dips ranging from vertical to 65SE. With the exception of the Sgp unit, which is correlated here with the Grand Pitch Formation, the host rocks occur as relatively simple, steeply dipping beds on the flanks of

major anticlinal structure whose axial plane is to the northwest of the prospect area. Little evidence for any well developed minor folding in the units has been found. All but the dense rhyolite and greenstone units exhibit a strong slaty cleavage which dips vertically and strikes N10-25E. This tectonic foliation is also often expressed as a slip cleavage in the bedded units where 3 mm to 1 cm displacements offset individual laminations. Ekren and Frischknecht (1967) propose that this regional foliation is slightly younger than the major folds, and was develloped after a minor change in the applied direction of the tectonic forces.

The Sgp unit of interbedded shale, silstone, and quartzite is structurally more complex than the other units in the prospect area. Minor folds have been exposed in pavement outcrops along the main access road through the prospect area (Figure 6), and small scale kink bands have been identified in thin sections of shaley portions of the unit (Figure 7). Although the presence of these features does not necessarily indicate polydeformation, the Sgp unit does appear to be more complexly deformed than overlying beds.

The major, steeply dipping fault which Ekren and Frischknecht (1967) propose strikes through the Mount Chase Prospect area, does appear to be a real structural feature. The fault has been intercepted several times in project drill holes in approximately the same location as

indicated by their regional mapping. As discussed in the previous section, the contact between the hanging wall shales and the upper greenstone complex is defined by a two to ten foot fault gouge zone. The relative movement on the fault is not known, but it does appear to be an important regional scale structural feature. The same fault has been drilled in holes more than a mile along strike to the northeast of the main drilling site. The structure may be, at least in part, responsible for the thinning and eventual dissapearance of the massive sulfide host units in that direction.

The four north-south trending cross-strike faults shown on Plate I are somewhat conjectural features which are indicated by abrupt offsets of the geologic units along strike. The parallel structures dip 80-90 NE and have an apparent strike-slip sense of offset. Since most of the project drill holes have been drilled roughly parallel to the proposed faults, the structures have not been closely defined by the drilling. However, a few fault gouge intercepts do correlate well with the proposed fault traces, and their locations are fixed between relatively close-spaced drill hole paths. The faults are also indicated by distinct offsets in the patterns of several ground geophysical surveys including magnetics, Max-Min, and Mise-A-La-Masse. These faults are considered to be later than the northeast-southwest trending fault described in the previous paragraph.

ATTACHMENT 23

January 18, 2023
File: 195602317

Attention: Tim Carr
Land Use Planning Commission
Department of Agriculture, Conservation, and Forestry
Harlow Building
18 Elkins Lane
Augusta, ME 04333

Dear Mr. Carr,

Reference: Wolfden Mount Chase LLC Application for Zone Change

On behalf of Wolfden Mount Chase LLC., Stantec Consulting Services is pleased to submit the attached Application for Zone Change for consideration of rezoning of approximately 374 acres in T6R6 WELS from General Management (M-GN) to Planned Development (D-PD). If rezoned and then ultimately approved by the Department of Environmental Protection under Maine's *Metallic Mineral Exploration, Advanced Exploration and Mining* regulations the rezone area would be used for development of an underground mining operation and associated structures. The purpose of the operation is to extract metallic ore that is rich in copper, lead, zinc, silver and gold. The proposed rezone area does not include facilities for ore concentration or tailings.

The document has been produced in a format that addresses the Land Use Planning Commission (LUPC) Chapter 10 and Chapter 12 regulations, including 27 Exhibits designed to provide the information that is required to support the proposed rezoning. In Table 2-2 of the Application, we have provided a matrix linking the applicable regulatory requirements to the relevant Application Exhibits.

Three hard copies are being submitted by hand delivery to your attention at Elkins Lane in Augusta. Please advise on how best to transmit an electronic copy compatible with State security and file size restrictions. In addition, hard copies are being posted via FedEx as follows:

- LUPC East Millinocket office – 1 copy;
- LUPC Ashland office – 2 copies; and
- Aroostook and Penobscot County Commissioners offices – 1 copy to each.

By separate transmittal Wolfden Mount Chase LLC is today submitting the Application fee ($14,350) and the Extraordinary Project Processing fee ($79,387.28).

Thank you for your attention to this submission. We look forward to working with the LUPC staff and Commission as you all undertake your review of these materials.

Respectfully yours,

Stantec Consulting Services Inc.

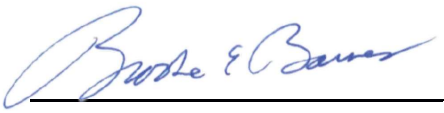

Brooke Barnes
Principal
Phone: 207 406 5461
Fax: 207 729 2715
brooke.barnes@stantec.com

Attachment: Application for Zone Change

c. Jeremy Ouellette, Wolfden Mount Chase LLC

EXHIBIT 10.0 SURROUNDING USES AND ANTICIPATED IMPACTS

10.1 INTRODUCTION

To characterize surrounding uses and anticipated impacts, LUPC guidelines for a zone change application specific to metallic mineral mining (Chapter 12) and the general guidelines for a LUPC zone change application (Chapter 10) require:

- A detailed list of existing uses and features in the area including the number and type of residences, the type and scale of commercial enterprises, and other relevant details. Examples of uses and features include, but are not limited to: homes, businesses, commercial forest land, farmland, recreational resources, natural features, cultural features, etc. (Chapter 10);
- A description of both potential positive and negative impacts the proposed development may have on the community or area. If describing economic benefits, distinguish between short-term and long-term benefits (Chapter 10);
- A description of what measures will be taken to assure no undue adverse impact of the proposed new or expanded land use to wildlife habitat. Special consideration should be given to areas near waterbodies (Chapter 10);
- If the proposed development is on or near a mapped and zoned high yield sand and gravel or bedrock aquifer, explain how the new or expanded land use will result in no undue adverse impact to the aquifer (Chapter 10);
- For recreational resources, explain why the proposed development will result in no undue adverse impact to these features AND how the values of recreational resources will be maintained (Chapter 10);
- A description of general measures that may be undertaken to assure that mining in the specified location will not have undue adverse impacts on existing uses and resources and measures that a permittee may take to avoid, minimize or mitigate any adverse impacts of existing uses and features (Chapter 12); and
- A description of socioeconomic impacts, both positive and negative, of the proposed metallic mineral mining or level C mineral exploration activities upon the immediate area and communities within and adjacent to the Commission's jurisdiction likely to be affected by the proposed activities, as well as to the county and state. Distinguish between short-term and long-term benefits (Chapter 12).

The LUPC guidelines also require the preparation of supporting figures to understand the existing surrounding uses and anticipated impacts associated with the proposed development. These figures include:

- A map and or description of the location of public, private and industrial water supplies as well as mapped aquifers located within a three-mile radius of the mining area or exploration site (Chapter 12);
- A map identifying significant natural resources and sensitive natural areas located within a three-mile radius of the mining area or exploration site including protected water bodies, significant wildlife and plant areas, fragile mountain areas, historic sites, scenic resources, public lands, registered critical areas, and Commission subdistricts (Chapter 12); and
- A map and description of existing uses, such as recreational uses, within a three-mile radius of the mining area or exploration site (Chapter 12).

Consistent with these requirements, this exhibit provides a summary of surrounding uses and potential anticipated impacts from the Project. Where appropriate, direction is provided to other Exhibits for more specific details on the analysis and methods used to inform these summaries.

10.2 RESIDENCES

There are no residences within the Project Area. There are six seasonal residences (camps) around Pleasant Lake approximately 1 mile to the north of the Project Area. Two of these residences are located approximately 675 feet from the southern lake shore, and four are located along the northern shoreline. These residences are depicted in **Exhibit 16, Figure 16-1**. Beyond these 6 seasonal residences, there are approximately 20 residences located along the eastern shore of Upper Shin Pond, located approximately three miles from the Project Area.

A 3-mile viewshed analysis was completed for areas within 3-miles of the Project Area and is presented in **Exhibit 16 – Harmonious Fit and Natural Character**. This exhibit also presents a supporting line-of-sight analysis from the Pleasant Lake seasonal camps as **Attachment 16-A Pleasant Lake Sight-Line Analysis**. Methodology for these analyses is discussed in more detail in **Exhibit 16.** The tallest point in the Project Area (top of the headframe) may be visible from the camps on the north shore of Pleasant Lake. However, when viewed from Pleasant Lake, Mount Chase (elevation 2,440 feet) will be located behind the headframe and partially mask this structure from the horizon. These analyses also indicate that existing vegetation and the Project's maintenance of a tree line surrounding proposed site infrastructure is expected to minimize visual impacts to Pleasant Lake. The proposed solar array is expected to be completely shielded by the tree line and vegetation. Residences along the shore of Upper Shin Pond are not expected to experience any visual impacts from the Project based on these analyses.

WSP (formerly John Wood Group, PLC) has completed a sound assessment (**Exhibit 16, Attachment 16-B Noise Assessment Report**) to model the potential for sound impacts from Project operations. Three points of reception (POR) locations were selected to represent the seasonal camps located along both shores of Pleasant Lake, with the closest one located approximately 4,000 feet away from the Project Area. Predicted daytime and nighttime operations sound levels at these PORs were modeled to

be well below MDEP noise guidelines. Residences along the shore of Upper Shin Pond are also not expected to experience any acoustic impacts from the Project given their distance from operations. WSP's sound assessment included a POR at the western edge of Wolfden's property, approximately 9,000 feet (1.75 miles) east of Upper Shin Pond. Similar to what was modeled for Pleasant Lake, predicted daytime and nighttime operations sound levels at this location were modeled to be well below MDEP noise guidelines.

10.3 COMMERCIAL ENTERPRISES/BUSINESSES

Herbert C. Haynes Inc (H.C. Haynes), a local forest management company based out of Winn, Maine, currently owns and manages several parcels located within 3 miles of the Project Area. These parcels are actively managed for timber production and other land-based resources (e.g., wildlife habitat, recreation, and hunting). H.C Haynes has granted a permanent easement to Wolfden allowing full and commercial access their property and the Project Area. Except for these commercial forestry activities, there are no businesses within 3 miles of the Project Area. The impact of the Project on businesses in the larger region are discussed in **Attachment 10-A**.

10.4 PUBLIC LANDS

There are no existing public lands within 3 miles.

10.5 NATURAL RESOURCES

10.5.1 Physical Setting and Soils

The Pickett Mountain Mineral Deposit contained within the Project Area is situated beneath and on an approximate 2.7-mile-long ridge with moderate elevations ranging from 1,360 to 1,140 feet (west to east). This ridge is bordered to the south by Pickett Mountain Pond, to the east by Tote Road Pond and Grass Pond, and to the north by Pleasant Lake and Mud Lake. In general, the area beyond the Project Area within 3 miles of the proposed rezone boundary is surrounded by commercial forests. The Project Area is generally forested and was logged over the last 10 years. The Wolfden parcel outside of the proposed rezone boundary will continue to be managed for timber harvesting and forest management. **Section 6.1.9 in Exhibit 6 – Structures, Features, and Uses** provides more details and figures detailing the local geological conditions. Soils in the Project Area are generally Plaisted, Dixmont, Thorndike, and Rockland soil series. **Exhibit 23 – Soil Suitability** further describes soil conditions and an assessment of soil suitability for the Project Area.

10.5.1.1 Soils

General soil conditions and their suitability for development within the Project Area were evaluated in the field by a Maine Certified Soil Scientist in September and October 2020. Over 30 test pits and observations were completed. In addition to field data collection, other information used to evaluate soils included a desktop review of the US Department of Agriculture's Natural Resources Conservation Service soil surveys, LiDAR topography, and geotechnical drilling data from past explorations. Results found that generally suitable soils or soils with limited suitability for development dominate the Project Area. Generally suitable soils are typically located on better drained, deeper soils. Soil limitations observed in

the field include shallow bedrock conditions and areas with a seasonal high-water table. These soil limitations can be addressed through careful siting of Project infrastructure and use of site-appropriate engineering design and construction approaches. Further evaluation of soil conditions and the design of the Project's infrastructure will be part of the MDEP Chapter 200 permitting efforts. **Exhibit 23, Attachment 23-A Soil Suitability Evaluation for the Wolfden-Pickett Mountain Mine Rezoning Petition** further describes the analysis and results of desktop and field investigations. As noted in **Section 10.5.4**, during construction and operations phases of the Project, an Erosion Prevention and Sediment Control Plan will be utilized to control soil erosion and sedimentation. Through adherence to this Plan and consideration of the existing soil limitations, the Project does not anticipate any adverse impacts to soils.

10.5.1.2 Acid Rock Drainage

When mineralized rock is mined and processed, the surface area of exposed sulfide mineral increases along with the potential for acid generation. Undisturbed sulfide mineral deposits have limited exposed surfaces and, therefore, pose little threat to groundwater under natural, oxygen-limited conditions. Acid rock drainage occurs as a result of the oxidation and dissolution of sulfide bearing minerals and may generate low pH contact water. The Research Productivity Council Report (**Attachment 10-B)** details the results of analyzed rock samples from the Project Area and an assessment of the potential for existing rock to influence acid rock drainage from Project operations. Generally, non-mineralized rock outside of the Pickett Mountain mineral deposit (i.e., rock excavated during development) is non-acid generating and carries some neutralizing potential. Each sample collected greater than approximately 100 feet away from the mineral deposit had "Non-Acid Generating" results. Most of the infrastructure and mine development is planned in this area further than 100 feet from the mineral deposit for geotechnical considerations and this will significantly reduce the potential for acid rock drainage in contact waters. Three of the samples closest to the mineral deposit (bearing some sulfide minerals) were found to be potentially acid rock drainage producing, as expected.

Since the process leading to acid rock drainage requires the presence of both oxygen and water, as well as time, Wolfden will implement effective strategies to prevent acid generation into the design and operation of the mine. Within the Project Area, the potential sources of acid rock drainage are limited to mineralize rock from underground being temporarily stored on the surface. Although the mineral surface area remains small for broken rock material and the exposure of the rock material to water is short in duration before being removed from the mining site, the rock storage pads are designed within a water collection area. Rock pads will be lined to collect contact water from the material and then pumped to a storage pond and treated before being discharged (detailed further in **Section 10.5.2)**. This approach will remove potentially acid generating material and thereby remove the risk related to acid rock drainage.

10.5.2 Hydrology and Water Quality

The Project Area is characterized by relatively thin glacial deposits and overlying bedrock based on subsurface drilling conducted during Wolfden's mineral exploration activities. Except for the occasional rock outcrop or rock ridge, the entire Project Area is forested. Groundwater and surface water divides are expected to be controlled by topography and groundwater flow direction should mimic topography. **Figure**

10-1 depicts anticipated groundwater and surface water divides and indicates anticipated groundwater flow directions. **Figure 10-2** details the proposed watershed conditions of the Project.

Based on studies of similar geologic and geographic settings[5] and historically averaged precipitation data,[6] the site is anticipated to receive approximately 45 inches of total annual precipitation (see **Figure 10-3**). Recharge to groundwater (i.e., net precipitation minus evapotranspiration) will result in overburden groundwater and shallow bedrock groundwater recharge and groundwater flow and discharge toward surface water bodies including lakes, ponds, and streams.

The majority of shallow groundwater recharge will occur in spring and fall when temperatures are above freezing, evapotranspiration rates are lowest, and precipitation is highest**.** On average it is expected that approximately 42% of precipitation is lost to evapotranspiration and surface run-off.[6] The majority of recharge is expected to infiltrate to shallow (possibly perched) and deeper saturated overburden groundwater where present. Additionally, a smaller amount of recharge is expected to reach bedrock groundwater (typically in the range of 5-10%[6]). This deeper groundwater, including overburden and bedrock, will form the base flow of groundwater discharge to nearby surface water bodies such as Pickett Mountain Pond and Pleasant Lake.

The perched shallow groundwater that occurs in the shallow developed soil horizon is important for the infiltration of precipitation and movement of shallow groundwater that supports wetlands and baseflow of intermittent and perennial streams. This component of subsurface flow is distinct from the deeper saturated groundwater conditions, where present, in the denser, silty glacial tills. Investigation of the soil suitability at the Project Area conducted by Atlantic Resource Co. LLC and Wood (see **Exhibit 23, Attachment 23-A**) provided soil classifications of this shallow soil located above restrictive layers that included bedrock, the water table or till. The seasonal high-water table is generally greater than 15” and bedrock, where present is dominated by smooth shield type ledge that is located below a mantle of glacial till, rather than rock outcrops. Bedrock was observed generally greater than 20” below the ground surface (see **Exhibit 23, Attachment 23-A**). Based on published soil vertical soil hydraulic conductivity values for these soil types, the mean expected horizontal saturated hydraulic conductivity is estimated to be in the range of 1.98 feet/day for these shallow soils.[7] The ratio of horizontal to vertical hydraulic conductivity is typically assumed to be 10:1.[7]

A divide in surface water and groundwater occurs along the ridge separating surface water and groundwater flow to Pickett Mountain Pond and Pleasant Lake. The watershed surrounding and contributing to Pickett Mountain Pond is approximately 2,095 acres. In comparison, the watershed surrounding Pleasant Lake and Mud Lake is approximately 8,389 acres. Pickett Mountain Pond outlet flows eventually to Mud Lake and the combined watershed has a drainage area of approximately 10,485 acres. The precipitation runoff collection area of the project is 28.4 acres where water will be collected, treated and returned within the watershed. This area is approximately 1.4% of the Pickett Mountain Pond watershed and approximately 0.3% of the combined watershed area. The water balance equation, or how precipitation is eventually distributed, takes many forms but is often generally defined as $P= INT+EVT+INF+\Delta S$, where P is precipitation, INT is interception (direct run-off into streams, water bodies),

[5] Gerber and Hebson, Groundwater Recharge Rates for Maine Soils and Bedrock, Geological Society of Maine Bulletin 4. 1996
[6] http://www.nrcc.cornell.edu/wxstation/pet/pet.html
[7] United States Geological Survey, 2010. Simulation of Groundwater Mounding Beneath Hypotehical Stormwater Inflitration Basins. USGS Scientific Investigation Report 2010-5102.

EVT is evapotranspiration and INF is interflow or groundwater flow and ∆S is change in storage. Net recharge is defined as P-INT, or the water available for infiltration that will eventually become groundwater minus losses due to evapotranspiration during the growing season. An estimated water balance for the sub-basins is provided in **Table 10-1**. Most of the overburden groundwater would be expected to discharge locally within the local drainage basin (>95%), with the exclusion of recharge to bedrock. Some shallow bedrock groundwater would also be expected to discharge locally to streams in upland mountain areas and deeper sections of ponds, where present. The net change in storage is typically represented by bedrock groundwater lost to the regional groundwater system, and changes in water table storage. In general, the Project area occupies a very small area compared to the size of the watersheds.

10.5.2.1 Water Treatment and Management Approach

The Project's water treatment approach is designed to capture, treat, and return mine water and contact water while maintaining existing hydrology and water quality to the Project area's wetlands, streams, and surrounding natural environment. Generally, water will be collected and treated and discharged in accordance with precipitation patterns. For example, more precipitation generally occurs in the spring and fall and, therefore, more water will be collected, treated, and discharged in the spring and fall than summer. While each of the Project's treatment elements are briefly summarized here, further discussion and details on each of these elements is provided in:

- **Attachment 10-C – Stormwater Collection Technical Memorandum** (completed by WSP [formerly John Wood Group, PLC])
- **Attachment 10-D – Water Treatment Scoping Study** (completed by Mine Water Service, Inc)
- **Attachment 10-E –** Water Management at the Pickett Mountain Mine Site Technical Memorandum (completed by Sevee and Maher Engineers Inc.)

Table 10-1: Estimated Hydrologic Budget

Area	Size (acres)	Interception Direct Runoff (acre/ft/yr)	Net Precipitation (acre/ft/yr)	Evapo-transpiration (acre/ft/yr)	Groundwater Recharge (acre/ft/yr)	Overburden Recharge (acre/ft/yr)	Bedrock Recharge (acre/ft/yr)	Net Precipitation (gallons/yr)	Interception Direct Runoff (gallons/yr)	Evapo-transpiration (gallons/yr)	Groundwater Recharge (gallons/yr)	Overburden Recharge (gallons/yr)	Bedrock Recharge (gallons/yr)
Pleasant Pond/ Mud Lake Sub Watershed	8389	1259	30221	12693	16320	14,808	1,511	9,846,987,465	410,291,144	4,135,734,735	5,317,373,231	4,825,023,858	492,349,373
Pickett Mountain Pond Sub Watershed	2095	315	7549	3170	4076	3,699	377	2,459,571,966	102,482,165	1,033,020,226	1,328,168,862	1,205,190,264	122,978,598
Green Mountain Pickett Mountain Watershed	10485	1574	37770	15863	20396	18,507	1,889	12,306,559,431	512,773,310	5,168,754,961	6,645,542,093	6,030,214,121	615,327,972
Developed Mine Area	28.4		106.5					34,711,674					
Developed Mine Area % of Pickett Mountain Sub Watershed	1.4%												
Pre-Development Mine Area % of Green-Pickett Mountain Sub Watershed	0.3%												

Total Annual Precipitation	45.03	inches		
Annual Interception	4%			
Annual Interception	1.80	inches		
Annual Net Precipitation	43.23	inches		
Total Available for Recharge	3.60	feet		
Bedrock Net Recharge	5%		2.16	inches
Overburden Net Recharge	49%		21.18	inches
EVT Rate & Run-off	42%		18.16	inches
Total RCH and EVT	96%			
Developed Mine Area	28.39	acres		
Mine Dewatering	30	gpm	15,768,000	gallons/yr
	0.24%	of Total Watershed Groundwater Recharge		
	0.30%	of Pleasant Pond Mud Lake Sub Watershed Groundwater Recharge		
	1.19%	of Pickett Mountain Pond Sub Watershed Groundwater Recharge		
	2.56%	of Total Watershed Bedrock Groundwater Recharge		

Key: EVT = Evapotranspiration; ft = feet; gpm = gallons per minute; RCH = Recharge; yr = year

The stormwater analysis completed by Wood (**Attachment 10-C**) has modeled anticipated seasonal volumes of precipitation in the Project Area that will need to be collected and stored in a Pre-Treatment Water Storage Pond (Pond). Water in contact with mineralized rock (ore, low grade ore, and waste rock) stored on lined pads will be collected in the Pond prior to treatment. The stormwater analysis also incorporates the need for additional collection and storage of 30 gallons per minute (gpm) of mine water (from mine dewatering) into the Pond. Pond sizing includes a contingency for increased runoff volume during a 500-year, 24-hour storm event in accordance with 06-096 Chapter 200: Metallic Mineral Exploration, Advanced Exploration and Mining. Based on current precipitation estimates and consideration for a 500-year storm event, the Pond volume was modeled to have a required capacity of approximately 6.87 million gallons with a minimum 2-foot freeboard. The conceptual location of the Pond and its approximate footprint of 3.25 acres is depicted on site plan drawings in **Exhibit 2 – Project Description.** Collected stormwater and mine water will be subsequently treated and tested at the Project's water treatment facility. Collected water will not be allowed to return to the natural environment prior to treatment.

Collected stormwater and mine water will be fed to the onsite water treatment plant at a calculated maximum rate of 200gpm and treated using a multistage approach. First, pre-treatment via ultrafiltration (UF) will occur to remove suspended solids and other particles down to 0.1 micron in size. Second, reverse osmosis (RO) membranes will be employed to remove remaining chemical constituents down to their atomic radii in size. RO can effectively remove contaminants from water and can produce pure water containing only water molecules. The use of UF and RO is well-established and used across multiple industries. Treatment plant reject water (i.e., water not meeting quality standards) will either be returned to the treatment plant for another round of UF and RO of or used by mine operations as a concrete mix for backfilling areas of completed excavation as a physically and chemically stable mixture. Untreated or contaminated water will not be allowed to return to the natural environment. Through this approach, the Project will satisfy Maine Chapter 200 and Title 38, Chapter 3 wastewater discharge requirements. The Water Treatment Scoping Study (**Attachment 10-D)** provides more background and literature on how UF and RO technology works along with details on the conceptual design of the treatment system presenting the various steps and anticipated treatment volumes.

After water has been treated by UF and RO and tested, WRAs will allow for treated and tested water infiltration back into the natural environment. The WRAs will be positioned upgradient of both wetlands and streams so that existing hydrology (replenishment of shallow or perched groundwater) is maintained (see **Attachment 10-E**). Based on the current available information, a combination of spray irrigation and snowmaking (WRSs) placed over the WRAs will provide suitable conditions to return treated water at the Project Area while maintaining wetland and stream hydrology at the site. Using these technologies, and application rates typical of similar projects at similar sites, it is currently estimated that the Project will require between 15 and 29 acres of land required for recharge. There are at least 60 acres of available area for WRAs that could be utilized for treated water disposition within the 374 acres proposed for rezoning. For the purposes of visualization, the Conceptual Site Plan displays an example footprint of 22 acres (the mean anticipated required area). The final size and locations of WRAs will be determined once detailed soil studies have been completed.

Human sewage generated from the underground mine operations will be contained to Portable Toilets (Porta Potties). These will be on contract basis and managed through replacement of filled facilities with clean facilities by the supplier. Grey and black waters generated from the surface facilities will drain to a typical state approved septic system located on the site down gradient of the building infrastructure and potable water supply. Sewage management is further discussed in **Exhibit 24 – Sewage Water/Wastewater Disposal**. No adverse impacts to hydrology and water quality are anticipated from the management of the Project's wastewater.

10.5.3 Aquifers

The Project Area is not located near a high yield sand and gravel aquifer nor a high yield bedrock aquifer. A medium yield sand and gravel aquifer has been mapped along the north shore of Pleasant Lake (approximately 1.5 miles from the Project Area) with indicated yields >/= 10 gpm. The yield of the residential well on the south side of Pleasant Lake is reported as >/= 8 gpm. It is assumed that all seasonal residencies have private water supplies (wells), though this has not been confirmed. There are no other known private or public water supplies within a 3-mile radius of the site. **Figure 10-4** depicts these features in addition to inferred surface water divides and groundwater flow direction in the vicinity of the Project Area.

The Project's water treatment approach (see **Section 10.5.2.1**) is designed to treat mine process and stormwater and remove chemicals to meet background levels prior to its return to the natural environment. Treatment of water will occur through a combination of ultrafiltration and reverse osmosis. Additionally, the control of volume and location of these water releases will be designed to maintain existing rates of flow and percolation through the Project area's existing soils. As a result, the Project does not anticipate any adverse impacts to the quantity or quality of water received by local aquifers.

10.5.4 Wetlands/Streams/Waterbodies

Within 3 miles of the Project Area, the U.S. Fish and Wildlife Service (USFWS) has mapped wetlands in T6R6 WELS as a part of the National Wetlands Inventory dataset. LUPC Land Use Guidance Maps have incorporated National Wetlands Inventory mapped wetlands and are displayed in **Exhibit 6, Figure 6-1**. Within the Project Area, a formal delineation of wetlands, streams, and potential vernal pools (PVPs) in the Project Area was completed in June 2022 to supplement previous delineation efforts. Twenty-nine wetlands, 27 watercourses, and PVPs were identified during these surveys. Further information on the delineated wetlands, PVPs, vernal pools previously delineated, and representative photographs are in **Exhibit 6, Attachment 6-A Wetland and Watercourse Delineation and Potential Vernal Pool Survey Report**. The eastern shoreline of Upper Shin Pond, Pleasant Lake, Mud Lake, Huntley Duck Pond, Pickett Mountain Pond, Grass Pond, Tote Road Pond, Bear Mountain Pond, Hale Pond, and Green Pond are located within 3 miles of the Project Area (**Figure 10-1).**

Mine infrastructure in the Project Area will be sited at least 75 feet away from delineated wetlands, streams, PVPs, and vernal pools to avoid direct impacts to these resources during construction and mine operations. An Erosion Prevention and Sediment Control Plan will be developed for the Project to provide a strategy for controlling soil erosion and sedimentation during and after construction. This plan will incorporate the standards and specifications for erosion prevention for development projects contained in

the Maine Erosion and Sediment Control Handbook for Construction: Best Management Practices. This strategy will not allow the introduction of sediment-laden runoff to enter any nearby waterways. To accomplish this strategy, temporary erosion and sediment control measures will be used during construction and will stay in effect until the Project Area has been stabilized permanently.

As previously noted, the Project's water treatment approach will return clean, treated water back to the environment using WRAs. The siting and release of water from these WRAs is designed to maintain current hydrology to wetlands, streams, PVPs, and vernal pools. At the completion of the mining project, the site will be reclaimed removing all buildings and structures. As a result of these actions, the Project does not anticipate any adverse impacts to these resources.

10.6 NATURAL COMMUNITIES/FISH AND WILDLIFE HABITAT

As noted in **Exhibit 6: Attachment 6-A Wetland and Watercourse Delineation and Potential Vernal Pool Survey Report**, the Project Area is generally dominated by forested uplands with several large, forested wetland complexes and smaller isolated wetlands throughout. A large hill is in the southwestern portion of the Project Area with topography sloping up to the north and to the east. The crest and side slopes of the hill are characterized by moderately shallow soils. Tree species in the upland forested areas include American beech, eastern hemlock, red maple, gray birch, paper birch, eastern white pine, sugar maple, and balsam fir. The upland sapling and shrub layer is dominated by regenerating species present in the forest canopy, as well as striped maple and hobblebush. The upland herbaceous layer is dominated by evergreen wood fern, Canada mayflower, and Canadian bunchberry. The upland forested communities are best characterized as a low-elevation beech-birch-maple forest, a matrix-level and widespread hardwood forest of the northern Maine landscape. The Project is planned to operate for 10-15 years after which the impacted area would revert to forest. It is anticipated that a similar forest structure to what is currently seen would return after mine operations cease and site reclamation and restoration activities are completed.

Correspondence with MDIFW and MNAP indicated their information notes no presence of significant natural communities in the Project Area. MDIFW-mapped Inland Waterfowl and Wading Bird Habitat (IWWH) is located on the inlet at the western end of Pickett Mountain Pond, approximately 0.25 miles from the Project Area. The Project does not have any anticipated impacts on this IWWH.

Critical habitat for the federally threatened Canada lynx (*Lynx canadensis*) and federally endangered Atlantic salmon (*Salmo salar*) overlaps with the Project Area and both the USFWS and MDIFW identified the potential for occurrence by listed bat species.

- Portions of the Project Area also likely support lynx movements through the region but the amount of potential habitat impacted through development is minimal versus what is available in the surrounding landscape. Pockets of coniferous or mixed coniferous communities, where snowshoe hare (primary prey source for lynx) may be present, are generally limited to the margins of wetlands and streams. Through adherence to 75-foot buffers around these areas, direct habitat impacts will be minimized. The Project will also propose a speed limit for all-Project related traffic between dusk and dawn when operating within the Project Area and along the access road to Route 11 to minimize vehicle collisions with wildlife.

- Delineated streams in the Project Area are generally intermittent in nature and unlikely to provide suitable habitat for Atlantic salmon. Regardless, the Project proposes no instream work and adherence to 75-foot buffers around wetlands and surface waters to minimize potential impacts to aquatic habitats. The Project's water management approach will maintain water quality standards to further avoid Project impacts to aquatic habitats in the immediate area that may support Atlantic salmon.

- Surveys for bat hibernacula will be required as part of the MDEP Chapter 200 permitting process and this will include inspections of all areas of talus and rock features per MDIFW recommendations noted below. In addition, the Project will limit required tree clearing to between November 1 and April 14 to avoid periods when trees may be used for reproduction and habitat for young who are unable to fly.

Other, more focused botanical and wildlife field investigations will be completed as part of the MDEP Chapter 200 permitting process. Results from these studies, and ongoing consultations with resource agencies, will inform specific design considerations to address any concerns. Through these measures, the Project anticipates no adverse impacts to natural communities, wildlife habitat, or rare and endangered species. Details on correspondence with USFWS, MDIFW, MDEP, and the MNAP, and a further discussion of potential fish and wildlife habitat in the Project Area, is provided in **Exhibit 26 – Rare or Special Plant Communities and Wildlife Habitat**.

10.7 FOREST RESOURCES

As previously described in this application, Wolfden currently owns a single parcel totaling ±7,135 acres located in the southeastern corner of T6 R6 WELS (**Exhibit 5 – Land Division History)** with the Project Area entirely contained within this parcel. Wolfden's full parcel is undeveloped and forested, except for the six privately owned seasonal residences on parcels along Pleasant Lake and the presence of logging roads. The Project and surrounding areas are predominantly commercial forests that were logged within the last 10 years and are generally in vegetative regrowth. Outside of Wolfden's parcel, but within the 3-mile radius of the Project Area, local forest management companies own and actively maintain several tracts of commercial forest. The area proposed for rezoning is approximately 374 acres, which includes approximately 129 acres of land that would be cleared for construction (**Exhibit 7 – Site Plans)**. The Project is planned to operate for 10 to 15 years after which the impacted area would be restored to forest and returned to active timber management. During mine operations, there would be no restrictions on current and future timber operations on the remaining 6,761 acres (94.8%) of the Wolfden parcel. Access to other tracts of commercially viable forest resources along the proposed access route to the Project would not be restricted. Road access conditions for logging trucks will be improved as a result of upgrades to meet the needs of loaded ore haul tracks leaving the Project. As a result, the Project does not anticipate any adverse impacts to forest resources and the local timber industry.

10.8 RECREATIONAL RESOURCES

10.8.1 Lakes and Ponds

Pleasant Lake, Mud Lake, and Grass Pond are all designated as Heritage Fish Waters by the MDIFW. Maine Heritage Fish Waters are native and wild brook trout lakes and ponds that represent unique ecological and valuable angling resources. Through discussion with local residents and users, there are various levels of use of the identified lakes and ponds within the 3-mile radius of the Project Area. Pleasant Lake has a higher level of use due the presence of six seasonal residences near or along its southern and northern shoreline as well as an unimproved boat launch along the southern shoreline. It has an average depth between 6 to 10 feet. Pickett Mountain Pond is accessible by foot, has no improved boat launch, and is very shallow (averaging 2 to 3 feet deep). The use of these ponds for recreation will not be restricted as part of the proposed Project. Some additional use of the boat launch on Pleasant Lake is anticipated due to increased traffic to the area by employees of the Project during operations. Correspondence from local residents on existing levels of use on Pleasant Lake and Pickett Mountain Pond are provided as **Attachment 10-F**.

Direct visual impacts of the top of the headframe may be experienced at Pickett Mountain Pond, the north side of Pleasant Lake, Mud Lake, Tote Road Pond, and Huntley Pond. Seasonal residences located along the north side of Pleasant Lake make may have visual line of sight to the top of the headframe. The headframe is 120 feet tall and could rise above the tree line approximately 80 feet. However, when viewed from Pleasant Lake, Mount Chase (elevation 2,440 feet) will be located behind the headframe and partially mask this structure from the horizon. In addition, most of the Project infrastructure will be well below 40 feet in total height and Wolfden intends to maintain a tree line surrounding the Project. When forest cover is incorporated into the visual analysis, the headframe is only visible from the north shore of Pleasant Lake and Pickett Mountain Pond. Sight-line analysis of the proposed solar array indicates that vegetation will completely screen views of the proposed solar panels from the Pleasant Lake and shoreline camps. The eastern shore of Upper Shin Pond is within the 3-mile radius as depicted in **Figure 10-1**; however, the Project Area is not visible from this location. See **Exhibit 16 – Harmonious Fit and Natural Character** for additional details on visual analyses.

Previous MDIFW surveys (1953, 1958) indicate both Pleasant Lake and adjoining Mud Lake are shallow mud bottom ponds with warm temperatures at all depths in summer months. However, inlet and outlet streams (i.e., West Branch of the Mattawamkeag River, Pickett Mountain Stream and Spring Brook) provided spawning and nursing areas for brook trout and landlocked salmon. The ponds did not have conditions supportive of cold-water fish species at the time of these older surveys. In 2019, MDIFW surveys suggested Pleasant Lake could support a landlocked salmon and brook trout fishery as they identified the presence of cold-water springs in the lake, ideal dissolved oxygen levels from across of the water column for this fishery, and excellent brook trout growth. A similar MDIFW survey of Pickett Mountain Pond from 1958 noted a maximum depth of seven feet and limited trout production. MDIFW noted that competition with other fish species, marginal water quality, and limited areas for reproduction reduced Pickett Mountain Pond's value as a brook trout fishery. Given the capture, collection, and treatment of impacted water to background level quality, the Project will not adversely impact surrounding water resources.

Attachment 10-B: Research Productivity Council Report

CONFIDENTIAL

Final Report

Static Acid Rock Drainage (ARD) Testing; Wolfden Resources Corp.

Reference No.: MIS-J10082

Prepared for:

Mr. Jeremy Ouellette
Wolfden Resources Corp.
1100 Russel Street
Thunder Bay, ON P7B 5N2

April 16, 2021

Prepared by:

Neri Botha, P.Eng.
Extractive Metallurgist
Minerals & Industrial Services

Reviewed by:

Leo Cheung, P.Eng.
Department Head
Minerals & Industrial Services

INTRODUCTION

Wolfden Resources Corp. initiated a study at RPC to conduct static Acid Rock Drainage (ARD) test work. The Pickett Mountain property is being investigated by Wolfden Resources Corp. to look at ways of expanding current operations.

RPC was thus contacted to conduct static testing as follows:

- Acid Base Accounting (ABA by Modified Sobek method)
- Multi-Element Assay of Solids
- Sulphur and Carbon Speciation

This report serves to summarize the findings as well as recommendations for the way forward.

PROGRAM RESULTS

Sample Preparation

Seven samples were received in preparation for the static testing and are listed in Table 1. Each of the samples were dried, crushed to 80 % passing 5 mm and split into sub-samples for ABA, multi-element assay and sulfur and carbon speciation analyses.

Table 1
Wolfden Samples Received

Sample ID	Mass (kg)
ABA - 001	2.10
ABA - 002	2.95
ABA - 003	2.20
ABA - 004	2.30
ABA - 005	2.25
ABA - 006	2.85
ABA - 007	2.90

Acid Rock Drainage (ARD) Static Analyses and Sulphur and Carbon Speciation Results

The results from sulfur and carbon speciation analyses and acid-base accounting (utilizing the Modified Sobek method) on the 7 samples (see Table 1) are given in Table 2.

Table 2
Acid Base Accounting Results on Wolfden Samples

Sample ID	Paste pH	Total Sulfur	Sulfate† (as S)	Sulfide	Carbon Total Inorganic	Carbon Total	Acid Production Potential	Neutralizing Potential pH 8.3	Net NP pH 8.3	NP/AP
		%	%	%	%	%	Kg $CaCO_3$/tonne			
ABA-001	9.5	0.124	0.009	0.114	0.15	0.21	3.8	17.4	13.6	4.6
ABA-002	9.4	0.021	0.005	0.016	< 0.01	< 0.01	0.5	5.5	5.0	11.0
ABA-003	8.3	2.70	0.008	2.69	< 0.01	< 0.01	84.1	1.7	-82.4	0.0
ABA-004	9.7	0.262	0.002	0.260	< 0.01	0.02	8.1	3.7	-4.4	0.5
ABA-005	9.7	0.085	0.002	0.083	0.05	0.07	2.6	8.5	5.9	3.3
ABA-006	8.9	0.926	0.003	0.923	0.05	0.08	28.8	7.7	-21.2	0.3
ABA-007	9.3	0.005	0.003	0.002	0.01	0.04	0.1	8.2	8.1	131

† Acid soluble, non-volatile sulfur species (sulfate (as S)).
Sulfide was determined as the difference between Total Sulfur and Sulfate (as S).

The Total Inorganic Carbon analyses seen in Table 2 indicated that the inorganic carbon content was low over all 7 samples (ranging from <0.01 % to 0.15 % in the Wolfden samples). In addition, the Total Sulfur contents of the 7 samples were also relatively low (see Table 2), ranging from 0.005 % to 2.70 % in the ABA-003 sample.

As seen from Table 2, four of the Wolfden samples obtained positive Net Neutralizing Potential values with NP/AP ratio values (ratio between Neutralizing Potential and Acid Production Potential) above 2.0. This indicated that these specific samples were not net acid producers. On three of the Wolfden samples the Net Neutralizing Potential values were negative, and the NP/AP ratio was less than 1.0, indicating that these were potentially acid producing. These samples were as follows:

- ABA-003
- ABA-004
- ABA-006

It is recommended that a specialized consultant be contacted for the full MEND Report 1.20.1 analysis and interpretation prior to follow up with the regulatory agent.

Multi-Element Assay of Solids Results

Whole rock analyses as well as ICP multi-element analyses were conducted with the results reported in Table 3 to Table 4.

Table 3
ICP Multi-Element Analyses Results on Wolfden Samples

Sample ID:			ABA-001	ABA-002	ABA-003	ABA-004	ABA-005	ABA-006	ABA-007
Analytes	Units	RL							
Aluminium	mg/kg	1	80900	96200	37300	58700	74800	61800	75900
Antimony	mg/kg	0.1	2.4	2.7	11.5	7.5	4.7	8.4	3.6
Arsenic	mg/kg	1	2	10	32	5	2	7	10
Barium	mg/kg	1	1995	283	980	190	730	901	112
Beryllium	mg/kg	0.1	2.5	1.2	1.3	1.4	2.3	2.0	0.6
Bismuth	mg/kg	1	< 1	< 1	< 1	< 1	< 1	< 1	< 1
Boron	mg/kg	1	17	12	10	4	10	11	6
Cadmium	mg/kg	0.01	1.67	1.00	3.45	0.69	0.20	4.75	0.20
Calcium	mg/kg	50	8150	11400	1030	5730	3430	3220	56800
Chromium	mg/kg	1	30	18	45	91	44	39	35
Cobalt	mg/kg	0.1	0.9	26.5	3.2	1.1	0.6	0.7	40.2
Copper	mg/kg	1	7	6	17	5	3	19	9
Iron	mg/kg	20	10250	60600	27300	9220	9470	21900	84400
Lead	mg/kg	0.1	37.8	5.3	658.	15.3	18.0	1270	7.4
Lithium	mg/kg	0.1	23.4	52.4	6.2	13.6	14.6	5.0	12.1
Magnesium	mg/kg	10	14750	39300	2740	5580	16900	2900	30000
Manganese	mg/kg	1	196	1010	257	166	238	460	2220
Mercury	mg/kg	0.01	0.45	0.15	0.32	0.14	0.04	0.17	0.03
Molybdenum	mg/kg	0.1	0.9	0.2	3.4	2.0	1.5	2.2	0.5
Nickel	mg/kg	1	1	6	3	3	1	< 1	18
Potassium	mg/kg	20	30500	16600	18300	3240	24000	28100	290
Rubidium	mg/kg	0.1	152	68.9	88.6	16.8	109.	160.	1.1
Selenium	mg/kg	1	1	< 1	< 1	< 1	1	< 1	1
Silver	mg/kg	0.1	0.3	< 0.1	1.3	0.2	< 0.1	0.8	< 0.1
Sodium	mg/kg	50	7965	21500	210	32600	13900	290	32400
Strontium	mg/kg	1	67	64	5	133	40	17	219
Tellurium	mg/kg	0.1	< 0.1	< 0.1	< 0.1	< 0.1	< 0.1	< 0.1	< 0.1
Thallium	mg/kg	0.1	10.6	1.6	2.9	0.9	3.7	3.7	< 0.1
Tin	mg/kg	0.1	3.7	1.2	1.2	2.0	3.2	2.3	1.5
Uranium	mg/kg	0.1	3.8	0.6	1.5	2.6	3.5	3.0	0.2
Vanadium	mg/kg	1	4	401	23	4	2	3	361
Zinc	mg/kg	1	571	384	1760	222	128	2190	124

Table 4
Wolfden Samples Whole Rock Analyses Results

Sample	Wt. %															
	Al_2O_3	BaO	CaO	Fe_2O_3	K_2O	MgO	MnO	Na_2O	P_2O_5	SiO_2	SrO	TiO_2	V_2O_5	ZrO_2	LOI 1000°C	Total
ABA-001	13.78	0.20	1.05	1.69	3.92	2.41	0.02	1.09	0.03	72.42	<0.01	0.12	<0.01	0.01	2.71	99.80
ABA-002	16.66	0.03	1.57	10.28	2.17	6.72	0.14	2.97	0.09	53.65	<0.01	1.66	0.07	0.02	3.75	99.85
ABA-003	6.25	0.10	0.21	3.78	2.40	0.46	0.03	0.06	0.07	77.94	<0.01	0.19	<0.01	0.01	2.41	99.91
ABA-004	10.46	0.03	0.77	1.40	0.49	0.91	0.02	4.54	0.02	79.53	0.01	0.08	<0.01	0.01	0.73	99.85
ABA-005	12.83	0.08	0.47	1.35	3.26	2.71	0.03	1.85	0.03	74.69	<0.01	0.09	<0.01	0.01	2.23	99.89
ABA-006	10.49	0.09	0.45	3.16	3.63	0.56	0.07	0.06	0.03	76.69	<0.01	0.09	<0.01	0.01	2.02	99.85
ABA-007	13.66	0.02	8.49	12.83	0.06	5.29	0.29	4.46	0.16	50.93	0.02	1.75	0.06	0.02	1.74	99.84

CONCLUSIONS AND RECOMMENDATIONS

Note that all results were only as representative as the sample received. All data obtained were in good agreement with each other and showed that:

- Of the 7 Wolfden samples subjected to static Acid Rock Drainage (ARD) testing, 3 were found to be potentially acid producing and 4 were found to be not potentially acid producing.
- It was recommended that a specialized consultant be contacted for the full MEND Report 1.20.1 analysis and interpretation prior to follow up with the regulatory agent.

Attachment 10-D: Water Treatment Scoping Study

October 25, 2022

Jeremy Ouellette, P. Eng.
Wolfden Resources, Pickett Mountain Project

Dear Jeremy:

Enclosed please find the completed water treatment study report for Wolfden Resources Pickett Mountain property. Please let me know if you require have any questions or require any clarification.

Sincerely,

Brian Danyliw

Principle, Mine Water Service

Mine Water Service Inc., 83 Digby;s Side Road
Mindemoya, Ontario, Canada P0P 1S0
705-618-6729
brian@minewaterservice.com

Wolfden Resources, Pickett Mountain Project, Mine Water Treatment Scoping Study

Introduction

Mine Water Service Inc. (MWS) was retained by Wolfden Resources to identify and examine various options to provide a water treatment process to allow treatment on surface contact water and underground mine produced water. This treatment process is required to provide effluent water of a quality that meets or exceeds identified existing water quality at the Pickett Mountain Site.

Mine Water Service is a consultancy operated by Brian Danyliw, a mining industry water treatment professional with over 40 years of experience. In addition to a thorough understanding of all aspects of water treatment relating to mining operations, Brian also has extensive process knowledge of underground mining as well as mineral processing of ore bodies similar to Pickett Mountain. In addition to Brian, the team assembled for this project included Kevin Gotschalk, Princlple with Oracle Water Services, a water treatment expert with over 40 years of water treatment experience and Dr. Paul Thoen, Chief Technology Officer with Shelton Associates, a company with extensive experience in designing, installing and operating membrane treatment facilities at mining operations throughout the world.

The scope of experience of MWS includes site and technical support on water treatment issues at over 80 mining operations around the world.

Project Report Objectives

The overall objective of this report is to provide a comprehensive and detailed plan for water treatment at the Pickett Mountain site that meets the requirements of the Land Use Planning Commission (LUPC) that treated water will meet existing site water quality. Existing site water quality is based on a set of ten (10) samples collected September 23, 2021 and analyzed by Maine Environmental Laboratory[1]. Detailed analysis reports from these ten samples can be found in Appendix 1 of this report. Water volumes and flow rates are based on the technical memorandum “Proposed Pickett Mountain Mine Project Precipitation Runoff Collection Areas - Mine Only Option” dated May 23, 2022 and revised August 25, 2022, prepared by Wood PLC Engineering consultants.”[2] discussed in detail within this report.

Included in the report is information and background on the water treatment technologies proposed to demonstrate the ability of these technologies to produce the required quality of treated water. This report details the types of treatment that will be employed, the plant process, basis of plant sizing, mass and water

[1] Maine Environmental Laboratory, One Main Street, Yarmouth, ME 04096
Report Information: Batch ID: ONE 10624, Report ID: 10624-211027-1313, Date of Issue: October 27, 2021

[2] Peters, M. (2022, May 23, Revised August 25). TECHNICAL MEMORANDUM, Proposed Pickett Mountain Mine Project Precipitation Runoff Collection Areas - Mine Only Option

balances, treatment efficacy based on computer modeling as well as relevant experience of the authors. The anticipated final treated water quality was developed utilizing input water quality data from a relevant operating mine example (Half Mile Mine- owned by Trevali Mining Corporation located West of Miramichi, New Brunswick, Canada.).

Design Criteria

Daily Identified Water Treatment Requirement:	152.1 USGPM[3]
Flow Contingency:	30%
Design Permeate (final treated effluent) Rate:	200 USGPM
Design Plant Influent Rate:	205 USGPM
Duty:	Continuous, 24 hrs/7/365
Input Water Quality:	Provided by Wolfden – Appendix 1
Background (target) Water Quality:	Provided by Wolfden – Appendix 1

Treatment Approach

The approach to water treatment for the Wolfden Resources, Pickett Mountain Project (Project) is to employ best available technologies to ensure effluent water meets Maine Chapter 200[4] and Title 38, Chapter 3 wastewater discharge requirements[5]. Proposed water treatment technologies for this Project are multistage and scalable. First, membrane filtration utilizing ultrafiltration (UF), which removes particles down to 0.1 micron in size, is a pretreatment stage to remove suspended solids. Second, reverse osmosis (RO) membranes which remove constituents down to atomic radii in size. Through this combination of proven membrane filtration techniques, water quality to meet regulatory requirements can be achieved. RO can effectively remove all contaminants from water, except for some dissolved gases (such as carbon dioxide and oxygen, which are nonhazardous normal constituents of water) and can produce pure water containing only water molecules.

Membrane filtration technologies date back to the late 1950's and were initially developed to allow for the generation of potable water from sea water. Over the years, continued development and refinement of the technology and extensive adoption of the technology across multiple industries and applications has resulted in improved efficacy and reduced costs. In the past decade, membrane filtration water treatment, and in particular some combination of microfiltration (MF), UF, nanofiltration (NF) and RO, has become the industry standard for water and wastewater treatment across multiple industries, including mining and mineral processing. The US Food and Drug Administration (USFDA) guidelines state that "An RO water purification system with several modules connected in series can produce water containing less than 0.1 ppm Total

[3] Permeate flow

[4] 06-096 CMR 200

[5] Title 38, Chapter 3: Protection and improvement of Waters. (n.d.). Retrieved July 21, 2022, from https://www.mainelegislature.org/legis/statutes/38/title38ch3sec0.html

Dissolved Solids (TDS;(resistivity about 1 megohm-cm)."[6] This level of purity is essentially pure water, containing only water molecules, without any elements, metals, or contaminants present.
Many examples of utilization of membrane filtration systems to treat mining and mineral processing influenced waters throughout the world are available. As per the US Environmental Protection Agency (USEPA) Reference Guide for Treatment Technologies for Mine-Influenced Water "[RO] Can remove 90 to 98 percent of TDS. A TDS removal efficiency of 98.5 percent was observed during pilot testing of the membranes tested."[7]

The approach taken for the Pickett Mountain Project is to design a water treatment system which will accomplish the following,

1. Treatment of surface contact water and underground produced water with the ability to produce effluent which meets or exceeds site-specific existing water chemistry (quality).
2. Treatment plant design to accommodate peak flow expectation with additional contingency flow capacity.
3. Minimization of treatment plant concentrate wastewater flow.

How Membrane Water Treatment Works

Ultrafiltration

The first step employed in the Pickett Mountain water treatment process is ultrafiltration (UF). It is designed to remove particles down to approximately 0.1 micron in size. Membranes manufactured for UF can be polymeric or ceramic and we will employ ceramic UF membranes because of their robust nature and ability to treat a wide range of influent characteristics. Ceramic UF membranes are essentially hollow tubes constructed of sintered metal (such as aluminum oxide) which results in a porous structure (Figure 1). This porous structure allows the ceramic tubes to act as filters while the sintered metal construction provides abrasion resistance, the ability to withstand a wide range of operating conditions (such as temperature extremes), and long life.

Influent water is forced under pressure through the hollow ceramic tubes. Filtrate (clean water) then passes through the pore structure of the tube walls and exits the membrane system.

[6] https://www.fda.gov/inspections-compliance-enforcement-and-criminal-investigations/inspection-technical-guides/reverse-osmosis
[7] U.S. Environmental Protection Agency, Office of Superfund Remediation and Technology Innovation, REFERENCE GUIDE to Treatment Technologies for Mining-Influenced Water, March 2014 EPA 542-R-14-001

Figure 1. Ceramic UF Membrane
Image Credit | Wikiwayman [CC BY-SA]

Reverse Osmosis Overview

Reverse osmosis (RO) represents state-of-the-art technology in water treatment. RO was developed in the late 1950's as a method of desalinating sea water. Today, RO has earned its name as the most convenient and thorough method to filter water. It is used by most water bottling plants, and by many industries that require ultra-refined water in manufacturing, such as microelectronics and pharmaceuticals, as well as high quality water to meet strict environmental discharge requirements. This advanced technology is also available for hiking enthusiasts and to homes and offices for drinking water filtration.

The RO system is dependent upon, and built around, individual membranes. Each membrane consists of a spiral wound sheet of semi-permeable material. Multiple layers of membrane and supporting material (outer wrap, spacers and permeate collection material) are formed into a tube surrounding a perforated central tube (Figure 2). Multiple layers of membrane allow the system to overcome the relatively low flow per unit area through the semi-permeable RO membranes. Feed water enters one end of the RO tube and as it passes down the length of the tube pure water passes through the RO membranes and reaches the perforated central tube. Water containing contaminants (as contaminants don’t pass through the membranes) continues along the length of the tube and exists as concentrate (wastewater). Pure water that passes through the membranes is collected in the central perforated tube and exists the system as permeate.

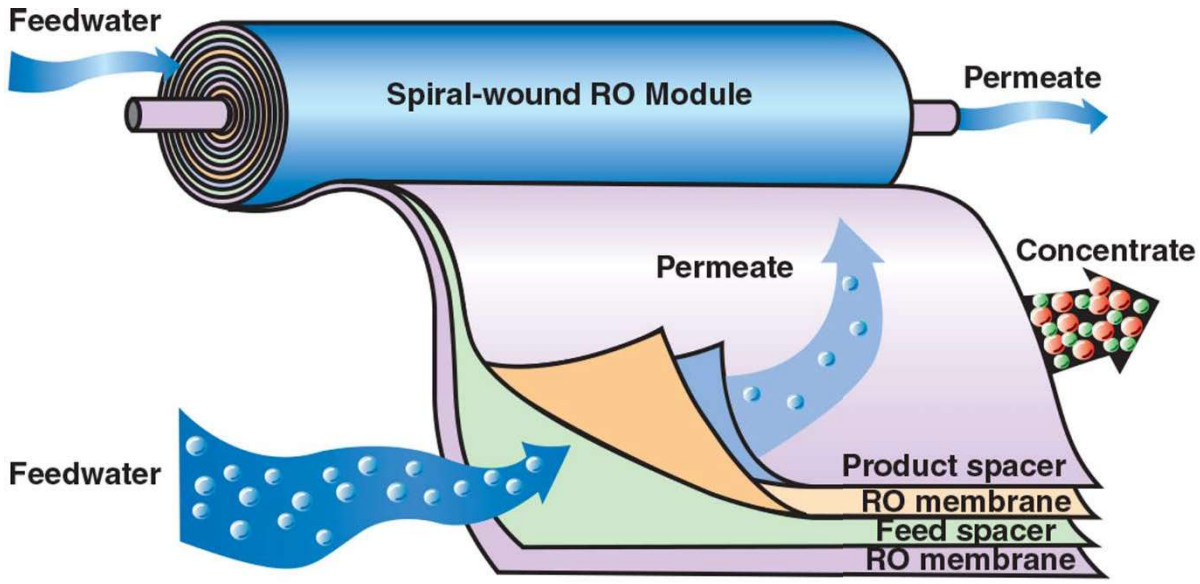

Source: Ionics Inc.
NF—nanofiltration, RO—reverse osmosis

Density of dots: highest density—concentrate, medium density—feedwater, lowest density—permeate

Figure 2. Spiral Wound RO Membrane

How RO Works

To understand "reverse osmosis," it is best to start with an understanding of normal osmosis. According to Merriam-Webster's Collegiate Dictionary, osmosis can be explained as the "movement of a water through a semipermeable membrane (as of a living cell) into a solution of higher solute concentration that tends to equalize the concentrations of solute on the two sides of the membrane". A semipermeable membrane is a membrane that will pass some atoms or molecules but not others. Saran™ wrap is a membrane, but it is impermeable to almost everything. An interesting example of a semipermeable membrane is the eggshell. Egg shells have pores large enough to allow oxygen and water vapor through, but small enough to prevent bacteria and dust from entering.

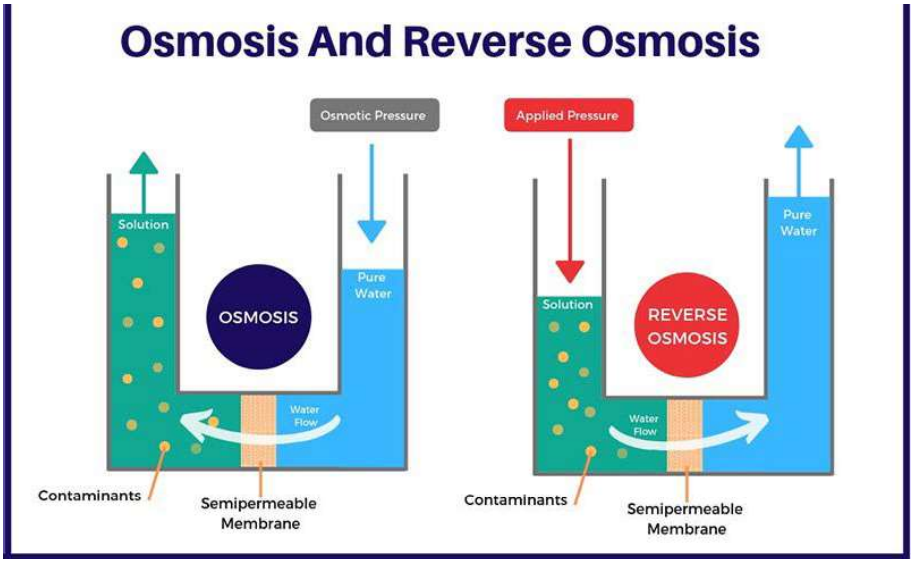

Figure 3, Osmosis and Reverse Osmosis[8]

In Figure 3 above, in the case of osmosis, the membrane allows passage of water molecules but not impurities such as organic molecules, salts or heavy metals. One way to understand osmotic pressure would be to think of the water molecules on both sides of the membrane. They are in constant motion. On the raw water side, some of the pores get plugged with contaminants, but on the pure-water side that does not happen. Therefore, more water passes from the pure-water side to the contaminated water side, as there are more pores on the pure-water side for the water molecules to pass through. The water on the contaminated side rises until one of two things occurs:

- The contaminant concentration becomes the same on both sides of the membrane (which isn't going to happen in this case since there is pure water on one side and contaminated water on the other).
- The water pressure rises as the height of the column of contaminated water rises, until it is equal to the osmotic pressure. At that point, osmosis will stop.

Osmosis is why drinking salty water (like ocean water) will kill you. When you put salty water in your stomach, osmotic pressure begins drawing water out of your body to try to dilute the salt in your stomach. Eventually, you dehydrate and die.

[8] Membracon. (2019, November 26). *Reverse osmosis systems in industrial processes*. Smart Water Magazine. Retrieved August 16, 2022, from https://smartwatermagazine.com/news/membracon/reverse-osmosis-systems-industrial-processes

In RO, the idea is to use the membrane to act like an extremely fine filter to create pure water from salty or contaminated water. The contaminated water is put on one side of the membrane and pressure is applied to stop, and then reverse, the osmotic process. It is fairly slow, but it works effectively for water purification (Figure 4).

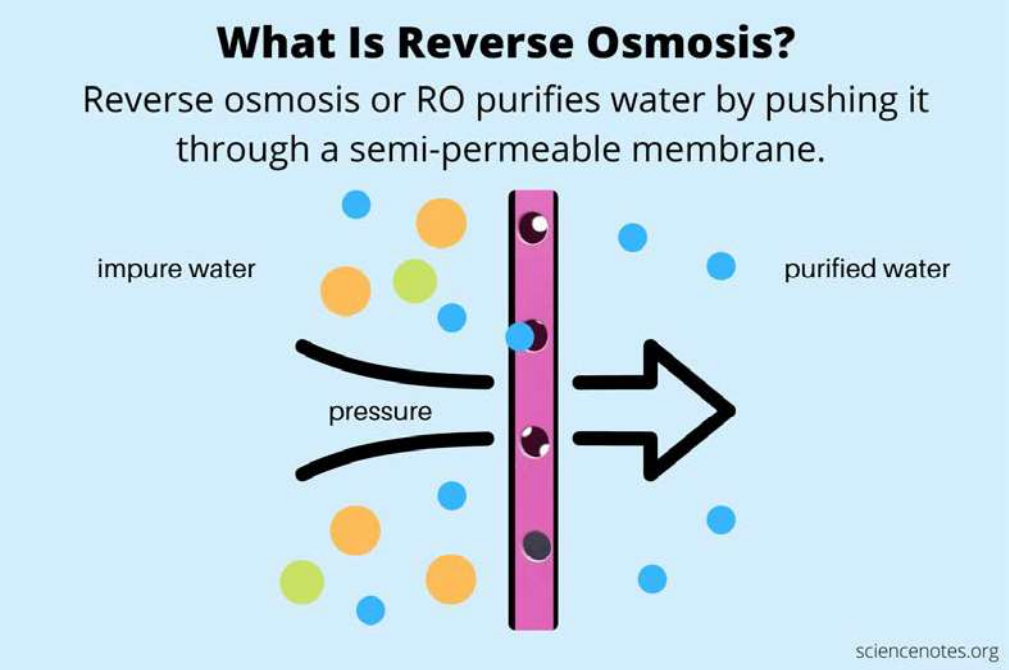

Figure 4. Reverse Osmosis[9]

Contaminant Removal

Reverse osmosis is an extremely effective technology in removing contaminants from water. The following chart (Figure 5) outlines some of RO's capabilities regarding specific contaminants compared to other filtration methods.

[9] Helmenstine, A. (2022, February 21). *What is reverse osmosis?* Science Notes and Projects. Retrieved August 16, 2022, from https://sciencenotes.org/what-is-reverse-osmosis/

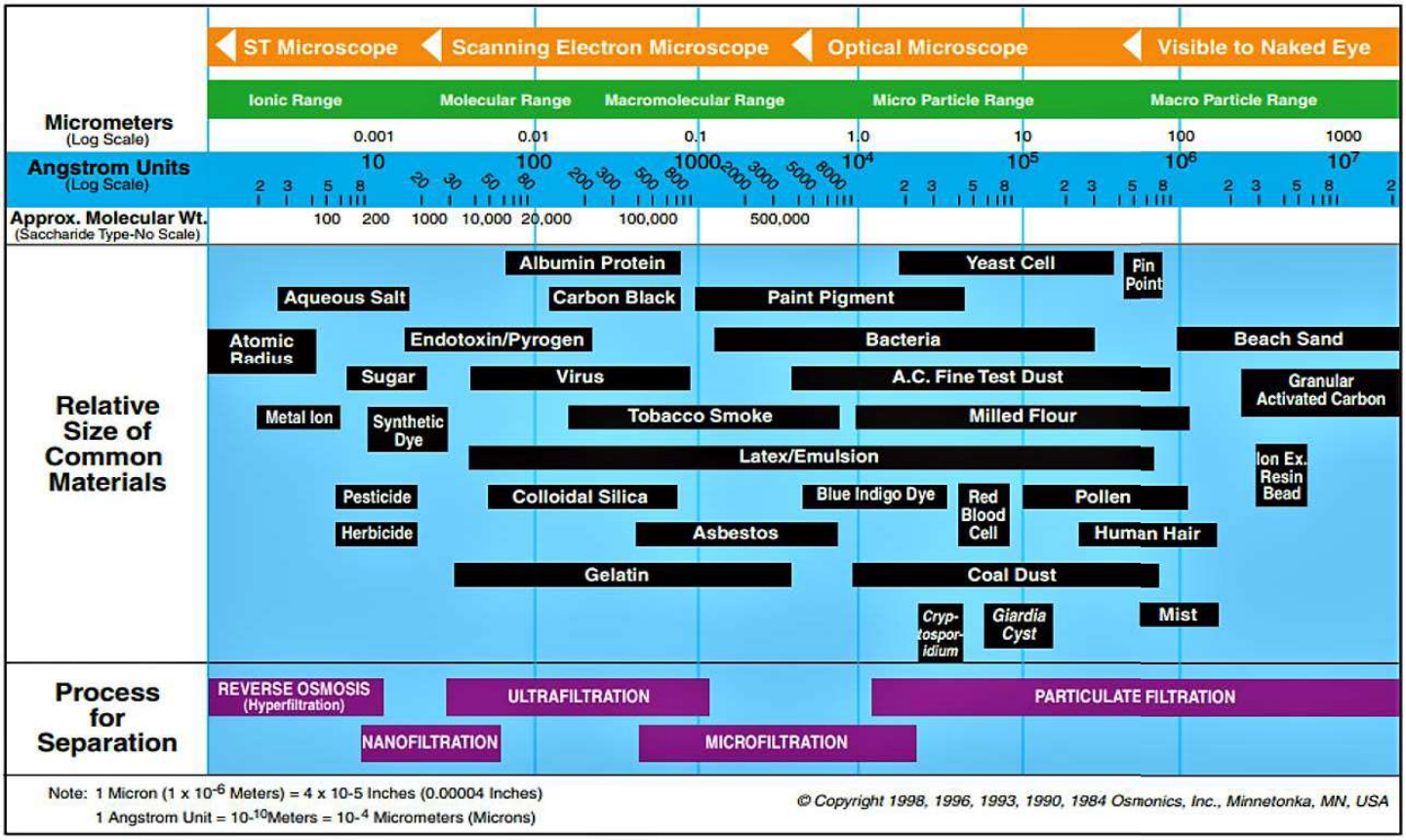

Figure 5, Membrane Filtration Removal Sizes[10]

In the case of heavy metal and other contaminant removal from wastewater, RO can separate all contaminants except for some dissolved gases such as oxygen and carbon dioxide (it should be noted that dissolved gasses are naturally present in all water and are not hazardous). The typical separation efficacy of common ions is listed in the Table 6 below. These rejection efficiencies have been established through a vast number of actual RO system operations and specific documentation for various rejection efficiencies can be found through review of a variety of technical publications. It should be noted that these separation efficiencies are for a single pass through a typical RO membrane of the same type chosen for the Pickett Mountain water treatment plant. Sequential treatment, through a second RO membrane, will result in an additional separation efficacy equal to that listed below. This means, as an example, aluminum separation through two passes would result in 96% - 98% removal in the first pass and an additional 96% - 98% removal of any residual in the second pass for a total removal efficacy of 99.8% - 99.96%. A third pass would therefore result in 99.992% - 99.999% removal.

[10] WP-Content. (2004, August 15). *Home*. WCP Online. Retrieved July 21, 2022, from https://wcponline.com/wp-content/uploads/2004/08/Figure-1-3.png

Ion	% Rejection*
Calcium	93-99
Sodium	92-98
Magnesium	93-98
Potassium	92-96
Manganese	96-98
Iron	96-98
Aluminum	96-98
Copper	96-99
Nickel	96-99
Cadmium	93-97
Silver	93-96
Zinc	96-98
Mercury	94-97
Hardness Ca&Mg	93-97
Radioactivity	93-97
Chloride	92-98
Ammonium	80-90

Ion	% Rejection*
Bromide	90-95
Phosphate	95-98
Cyanide	90-97
Sulfate	96-99
Thiosulfate	96-98
Silicate	92-95
Silica	90-98
Nitrate	90-95
Boron	50-70
Borate	30-50
Fluoride	92-95
Polyphosphate	96-98
Orthophosphate	96-98
Chromate	85-95
Bacteria	99+
Lead	95-98
Arsenic	50-90

Figure 6. Typical Rejection Rates for Thin Film Composite RO Membranes

**Nominal rejection characteristics of thin film composite reverse osmosis membranes*. Membrane Rejection Levels. (n.d.). Retrieved July 21, 2022, from https://www.watertreatmentguide.com/Membrane_Rejection.htm#Thin%20Film%20Composite

Membrane Water Treatment in Mining

Multiple examples of utilization of UF and RO to treat mining influenced waters are available throughout North America and worldwide. These mining operations include examples of treatment of site contact water, underground mine water effluent and tailings facility (TMF) decant water, from both mine only and mine/mill operations, for direct discharge to the environment.

Input and Target Water Volume and Quality

While no actual produced water from the Pickett Mountain operations is available for analysis, the choice of UF and RO for the water treatment plant will allow successful removal of any metals or other contaminants present once further analysis is conducted as part of the Chapter 200 process and the mine is in operation. For the purposes of this study and to facilitate process design and computer modeling, input water quality is based on water chemistry data supplied by Half Mile Mine. Input water is based on the highest value (worst case) from Half Mile Mine samples which were collected throughout the lifecycle of the mine from construction through operation and maintenance. Sampling at Half Mile was completed by the mine site environmental team and samples were collected using lab provided sampling guidelines and analysis

performed by RPC Science and Engineering (Research and Productivity Council). RPC is a certified laboratory based in Fredericton, New Brunswick. Sampling and analysis took place from 2011 through 2019.

While variations in water quality are expected due to variations in site-specific mineral deposits, based on the MWS's experience with multiple polymetallic massive sulfide mining operations, the Half Mile Mine water quality data is similar to other mine only operations and provides an appropriate comparison to water quality data expected from Pickett Mountain.

Produced contact water volumes are based on peak monthly volumes as described in the technical memorandum "Proposed Pickett Mountain Mine Project Precipitation Runoff Collection Areas - Mine Only Option"[11] dated May 23, 2022 and revised August 25, 2022, prepared by Wood PLC Engineering consultants.

Target effluent quality is based on water sampling results from the Pickett Mountain Site collected during groundwater sampling efforts in September 2021 and is the current data set available to evaluate background conditions (Table 1). The average target effluent water quality used in this report is the average of the target analytes from the 10 samples and includes the method detection limit (MDL) value for any samples reported by the lab as non-detect. The highest single value effluent water quality is the highest detected value and does not include the MDL for non-detects. Water analysis data is included in Appendix 1.

[11] Peters, M. (2022, May 23, Revised August 25). TECHNICAL MEMORANDUM, Proposed Pickett Mountain Mine Project Precipitation Runoff Collection Areas - Mine Only Option

Table 1. Input and Target Effluent Water Quality

Analyte	Units	Method Detection Limit	Target Effluent Quality Average MG/L	Target Effluent Quality Highest Single Analysis Result MG/L	Influent Water Quality (Highest Half Mile Value) MG/L
TOTAL ALKALINITY	MG/L as $CaCO_3$	0.7	**6.92**	**9.2**	Not Reported
PHENOLPHTHALEIN ALKALINITY	MG/L as $CaCO_3$	0.7	**0.7**	**Not Detectable**	Not Reported
BICARBONATE ALKALINITY	MG/L	1.3	Not Reported	Not Reported	Not Reported
CARBONATE ALKALINITY	MG/L	1.3	Not Reported	Not Reported	Not Reported
TOTAL PHOSPHORUS	MG/L	0.01	0.020	0.04	0.04
TDS	MG/L	10	38.5	51	Not Reported
TSS	MG/L	2.5	4.5	9.7	12
MERCURY	MG/L	0.0002	0.0002	Not Detectable	Not Reported
ALUMINUM	MG/L	0.005	0.1767	0.28	0.358
ANTIMONY	MG/L	0.0002	0.00045	0.0014	0.0009
ARSENIC	MG/L	0.0002	0.00042	0.0009	0.005
BARIUM	MG/L	0.003	0.0062	0.009	0.021
BERYLLIUM	MG/L	0.0002	0.0002	Not Detectable	Not Detectable
BORON	MG/L	0.02	0.02	0.02	0.196
CADMIUM	MG/L	0.00002	0.000132	0.00014	0.0477
CALCIUM	MG/L	0.1	2.81	3.6	91.8
CHROMIUM	MG/L	0.002	0.002	Not Detectable	Not Detectable
COBALT	MG/L	0.0003	0.0003	0.0003	0.151
COPPER	MG/L	0.0001	0.00116	0.01	0.383
IRON	MG/L	0.02	0.232	0.56	6.02
LEAD	MG/L	0.0001	0.00018	0.0005	0.0257
LITHIUM	MG/L	0.0001	0.00029	0.0005	0.0037
MAGNESIUM	MG/L	0.1	0.67	0.9	7.17
MANGANESE	MG/L	0.002	0.0334	0.075	1.27
MOLYBDENUM	MG/L	0.005	0.005	Not Detectable	Not Detectable
NICKEL	MG/L	0.002	0.002	Not Detectable	0.013
POTASSIUM	MG/L	0.1	0.28	0.4	5.92
RUBIDIUM	MG/L	0.0005	0.0005	Not Reported	0.0149
SELENIUM	MG/L	0.00006	0.00006	Not Reported	0.002
SILICON	MG/L	0.02	1.93	3	2.6
SILVER	MG/L	0.0003	0.0003	Not Detectable	Not Detectable
SODIUM	MG/L	0.1	0.99	1.2	25
STRONTIUM	MG/L	0.0003	Not Reported	Not Reported	0.25
SULFUR	MG/L	1	1.05	1.4	3
THALLIUM	MG/L	0.0001	0.0002	0.0008	Not Detectable
ZINC	MG/L	0.0002	0.00768	0.045	10
CHLORIDE	MG/L	0.3	0.512	0.62	Not Reported
FLUORIDE	MG/L	0.03	0.03	Not Detectable	Not Reported
NITRATE AS N	MG/L	0.1	0.1	Not Detectable	Not Reported
NITRITE AS N	MG/L	0.03	0.03	Not Detectable	Not Reported
PH	STU	0.01	6.712	6.30 - 7.04 (Range)	7.5
SPECIFIC CONDUCTANCE	µS/CM	25	26.6	28	732
SULFATE	MG/L	0.6	1.9	2.7	Not Reported
TOC	MG/L	0.7	10.06	12	Not Reported
DOC	MG/L	0.7	9.49	12	Not Reported
TOTAL CYANIDE	MG/L	0.005	0.0136	0.015	Not Reported
TURBIDITY	NTU	0.1	3.91	9.7	21.2
TRUE COLOR		5	48	70	Not Reported

Note: Units are milligram per liter (MG/L)
Target effluent quality average utilizes the MDL for all values that were reported by the laboratory as zero.

It should also be noted that oil, grease and other potential organic materials which might enter the wastewater stream through mining operations are considered in the treatment plant design. Modern underground mine design and operations carefully monitors and controls any discharge of oil and grease from underground mobile equipment. In addition to oil and grease separation systems used to separate and recover oil and grease from wash water, mobile equipment contain multiple failsafe devices designed to minimize the risk of any spills occurring due to equipment failures. Even with these safeguards in place, there remains potential for trace amounts of oil and grease to be in the mine effluent water sent to the water treatment plant. The inclusion of ceramic UF as a first treatment stage in the treatment plant design provides proven technology for rejection of oil and grease to the waste stream. This means that any trace amounts of oil and grease that may enter the water treatment plant will ultimately be retained within the mine wastewater system for disposal via cement preparation for backfill. As an example, one study conducted using ceramic UF membranes on oily wastewater documented a 97.6% rejection rate.[12]

Modeling Studies

Modeling of UF RO systems was completed utilizing four different commercially available software packages. The accuracy of computer simulations versus laboratory and pilot studies was examined by the Texas Water Development Board and presented in their "Report 1148321310 Part II. Performance Evaluation of Reverse Osmosis Membrane Computer Models" which was published in 2014. In part their conclusions state, "In summary, the overall accuracy and precision demonstrated by the computer models evaluated as part of this study were within a reasonable level of expectation considering the limited amount of the start-up data available. The level of accuracy for first stage feed pressures was sufficient to facilitate a conservative selection of a first stage feed pump. The level of accuracy for rejection of most ion constituents and total dissolved solids was within the expected range considering the limited amount of start-up feed and permeate water quality data. Computer model accuracy was comparable to the accuracy provided by the results of a pilot study for the one full-scale facility for which pilot test data was available. Another pilot study evaluation demonstrated the similarity of performance provided by pilot testing and computer models in predicting the performance of a full-scale reverse osmosis membrane system. Computer models created to predict the performance of two different membranes used during single-element pilot tests demonstrated a sufficient degree of accuracy to validate the use of computer models in predicting the performance of a full-scale membrane system. The precision demonstrated by the computer models was, in most cases, sufficient to facilitate the design of a membrane system to accommodate similar membranes from multiple membrane manufacturers."[13]

A number of commercial modeling programs are available, and each program utilize membranes that are commercially available from a single membrane manufacturer. The following programs were utilized to develop this water treatment plan.

[12] Chen, J.; Lv, Q.; Meng, Q.; Liu, X.; Xiao, X.; Li, X.; Liu, Y.; Zhang, X.; Gao, P. Study on Treatment of Low Concentration Oily Wastewater Using Alumina Ceramic Membranes. Crystals 2022, 12, 127. https:// doi.org/10.3390/cryst12020127

[13] https://www.twdb.texas.gov/publications/reports/contracted_reports/doc/1148321310_Part%20II_Performance%20Evaluation.pdf

1. Hyr-RO-Dose from French Creek Software Inc., which is a specialized water treatment modeling program. The hyd-RO-Dose program is primarily designed to predict antiscalant requirements for membrane systems; however, to accomplish this, a detailed model of the membrane system input and output water chemistry is developed by the software. The primary benefit of the hyd-RO-Dose program is modeling of water chemistry parameters to five decimal places making it especially effective for ultra-pure water.
2. Wave software from Dupont. Wave is a modeling program developed by Dupont to support system designers utilizing various Dupont technologies, including UF and RO membranes from Dupont.
3. Winflows from Suez Water Technologies and Solutions. Winflows is a modeling program developed by Suez to support system designers utilizing various Suez technologies, including UF and RO membranes from Suez.
4. IMSDesign from Nitto Hydranautics. IMS Design is a modeling program developed by Nitto/Hydranautics to support system designers utilizing various Nitto/Hydranautics UF and RO membranes.

In all modeling cases, a single UF stage was utilized followed by a two-stage RO system to provide optimal metal and mineral removal. All programs were utilized as a check against each other and because some programs model certain chemical species that others do not. Reduction of reject (waste) water was accomplished through the utilization of a calcite reactor and filter press followed by an additional UF RO stage on the first pass reject water. Final wastewater treatment design utilized IMSDesign software due to its expanded capabilities to model a wider range of metals (as shown on Table 2 “Permeate Water Quality Summary from Multiple Models” on the following page).

The four models generated the following data for permeate water quality (see Table 2 below). It should be noted that slight variations in final effluent quality from one program to another are the result of slight differences in the efficiency of the particular membranes chosen for the model. As per the scope of the Project these various modeling programs were utilized to determine the final permeate quality achievable. Final membrane selection will be based on Mine Water Service’s field experience with similar water quality and include, for example, Hydronautics CPA7-LD low fouling spiral wound membranes for final modeling and plant design.

Table 2. Permeate Water Quality Summary from Multiple Models

						Modeling Program			
						hyd-RO-Dose	Wave	Winflows	IMSDesign
Analyte	Units	Method Detection Limit	Target Effluent Quality Average MG/L	Target Effluent Quality Highest Single Analysis Result MG/L	Influent Water Quality (Highest Half Mile Value) MG/L	Final Effluent Quality	Final Effluent Quality	Final Effluent Quality	Final Effluent Quality
TOTAL ALKALINITY	MG/L as $CaCO_3$	0.7	**6.92**	**9.2**	Not Reported	0			
PHENOLPHTHALEIN ALKALINITY	MG/L as $CaCO_3$	0.7	**0.7**	**Not Detectable**	Not Reported	0			
BICARBONATE ALKALINITY	MG/L	1.3	Not Reported	Not Reported	Not Reported	0.000	1.39	2.170	0.677
CARBONATE ALKALINITY	MG/L	1.3	Not Reported	Not Reported	Not Reported	0.000	0.000	0.000	0.000
TOTAL PHOSPHORUS	MG/L	0.01	0.020	0.04	0.04	0.000	0.000	0.010	0.000
TDS	MG/L	10	38.5	51	Not Reported	0.28	1.420	5.090	0.970
TSS	MG/L	2.5	4.5	9.7	12	0.000	0.000	0.000	0.000
MERCURY	MG/L	0.0002	0.0002	Not Detectable	Not Reported				
ALUMINUM	MG/L	0.005	0.1767	0.28	0.358	0.000			0.000
ANTIMONY	MG/L	0.0002	0.00045	0.0014	0.0009	0.000			
ARSENIC	MG/L	0.0002	0.00042	0.0009	0.005				0.000
BARIUM	MG/L	0.003	0.0062	0.009	0.021	0.000	0.000	0.000	0.000
BERYLLIUM	MG/L	0.0002	0.0002	Not Detectable	Not Detectable				
BORON	MG/L	0.02	0.02	0.02	0.196	0.000	0.000		0.014
CADMIUM	MG/L	0.00002	0.000132	0.00014	0.0477				0.000
CALCIUM	MG/L	0.1	2.81	3.6	91.8	0.05	0.000	0.170	0.000
CHROMIUM	MG/L	0.002	0.002	Not Detectable	Not Detectable				
COBALT	MG/L	0.0003	0.0003	0.0003	0.151				0.0000
COPPER	MG/L	0.0001	0.00116	0.01	0.383	0.000958			0.000
IRON	MG/L	0.02	0.232	0.56	6.02	0.000		0.000	0.000
LEAD	MG/L	0.0001	0.00018	0.0005	0.0257				0.000
LITHIUM	MG/L	0.0001	0.00029	0.0005	0.0037				0.000
MAGNESIUM	MG/L	0.1	0.67	0.9	7.17	0.000		0.050	0.000
MANGANESE	MG/L	0.002	0.0334	0.075	1.27				0.000
MOLYBDENUM	MG/L	0.005	0.005	Not Detectable	Not Detectable				0.000
NICKEL	MG/L	0.002	0.002	Not Detectable	0.013				0.000
POTASSIUM	MG/L	0.1	0.28	0.4	5.92	0.000	0.000	0.120	0.004
RUBIDIUM	MG/L	0.0005	0.0005	Not Reported	0.0149				
SELENIUM	MG/L	0.00006	0.00006	Not Reported	0.002				
SILICON	MG/L	0.02	1.93	3	2.6	0.000	0.000	0.040	0.000
SILVER	MG/L	0.0003	0.0003	Not Detectable	Not Detectable				
SODIUM	MG/L	0.1	0.99	1.2	25	0.010	0.000	1.060	0.261
STRONTIUM	MG/L	0.0003	Not Reported	Not Reported	0.25				0.000
SULFUR	MG/L	1	1.05	1.4	3	0.06		0.003	0.000
THALLIUM	MG/L	0.0001	0.0002	0.0008	Not Detectable				
ZINC	MG/L	0.0002	0.00768	0.045	10				0.004
CHLORIDE	MG/L	0.3	0.512	0.62	Not Reported	0.13	0.000	1.280	0.000
FLUORIDE	MG/L	0.03	0.03	Not Detectable	Not Reported				
NITRATE AS N	MG/L	0.1	0.1	Not Detectable	Not Reported			0.016	0.009
NITRITE AS N	MG/L	0.03	0.03	Not Detectable	Not Reported				
PH	STU	0.01	6.712	6.30 - 7.04 (Range)	7.5	5.76	4.600	5.230	8.140
SPECIFIC CONDUCTANCE	µS/CM	25	26.6	28	732	1.12	9.000	10.000	<10
SULFATE	MG/L	0.6	1.9	2.7	Not Reported	0.000	0.000	0.000	0.000
TOC	MG/L	0.7	10.06	12	Not Reported				
DOC	MG/L	0.7	9.49	12	Not Reported				
TOTAL CYANIDE	MG/L	0.005	0.0136	0.015	Not Reported				
TURBIDITY	NTU	0.1	3.91	9.7	21.2	0	0.000	0.000	0.000
TRUE COLOR		5	48	70	Not Reported	0	0.000	0.000	0.000

1. Empty cells indicate that that specific program does not model that analyte.
2. Minor variations in final water quality from one program to another is due to performance variations in the particular suppliers' membranes.

It should be noted that certain species are not modelled by any of the programs and that certain species were not included in the baseline or Half Mile analytical analysis. A brief description of these species follows.

- Modeling programs automatically adjust chloride, sodium or sulfate to modify input water chemistry to produce a water that is balanced in total anion and cation molar concentration. For this reason, in some instances, chloride, sodium or sulfate concentrations in permeate or concentrate water may not

be exactly equal to the theoretical values based on input water analysis chemistry. An example of this can be found in the Winflows chloride value in Table 2.

- Various alkalinities were not tested for certain samples, and in the case of Half Mile only total alkalinity was reported. Alkalinity in water takes into account natural bicarbonate, carbonate and hydroxide ions and is an equilibrium reached based on carbon dioxide adsorption and buffering capacity of the water. Alkalinity can vary dramatically in water based on rainfall, temperature, and seasonal variability especially associated with ice cover of surface waters. Alkalinity variability will not have any impact on the proposed treatment process or results achievable for all other metals and species present.
- TDS (Total Dissolved Solids) represents the sum of dissolved metals and other species in water and is not required or relevant in modeling UF RO system removal efficiency.
- Mercury was not reported in the Half Mile report and was therefore not modeled. It should be noted however that the IMSDesign program does model mercury removal and imputing mercury concentration at 0.1 mg/l resulted in a permeate mercury residual of not detectable when modeled.
- Rubidium is not currently modeled by any modeling programs due to the infrequent occurrence of rubidium in waters. Removal efficiency of rubidium is expected to be similar to that of strontium based on their similar atomic weights (rubidium = 85.5, strontium = 87.6). Available literature[14] indicates strontium removal utilizing RO ranges from 99.7% to 100% for a single pass. Anticipated removal efficiency for the Pickett Mountain two pass system would therefore be essentially 100%.
- Selenium is not currently modeled by any modeling programs however published literature[15] indicates that rejection rates for selenium are expected to be 90% to 95% for a single pass RO. This indicates a rejection rate in the two-pass Pickett Mountain plant of 99% to 99.75%.
- Sulfate was not reported however low-level sulfate was added to the models representing background sulfate levels.
- TOC (Total Organic Carbon) and DOC (Dissolved Organic Carbon) were not reported for the Half Mile samples and were therefore not modeled.
- Cyanide was not reported for Half Mile samples and was therefore not modeled.
- True color was not reported for Half Mile and was not modeled.

[14]Cai, Y.-H.; Yang, X.J.; Schäfer, A.I. Removal of Naturally Occurring Strontium by Nanofiltration/Reverse Osmosis from Groundwater. *Membranes* **2020**, *10*, 321. https://doi.org/10.3390/membranes10110321

[15] Abejón, R. A Bibliometric Analysis of Research on Selenium in Drinking Water during the 1990–2021 Period: Treatment Options for Selenium Removal. Int. J. Environ. Res. Public Health 2022, 19, 5834. https://doi.org/10.3390/ijerph19105834

Table 3. Anticipated Final Treated Water Quality (IMSDesign)

						Modeling Program				
						hyd-RO-Dose	Wave	Winflows	IMSDesign	
Analyte	Units	Method Detection Limit	Target Effluent Quality Average MG/L	Target Effluent Quality Highest Single Analysis Result MG/L	Influent Water Quality (Highest Half Mile Value) MG/L	Final Effluent Quality	Final Effluent Quality	Final Effluent Quality	Final Effluent Quality	Final Expected Water Treatment Plant Effluent Quality MG/L
TOTAL ALKALINITY	MG/L as $CaCO_3$	0.7	**6.92**	**9.2**	Not Reported	0				
PHENOLPHTHALEIN ALKALINITY	MG/L as $CaCO_3$	0.7	**0.7**	**Not Detectable**	Not Reported	0				
BICARBONATE ALKALINITY	MG/L	1.3	Not Reported	Not Reported	Not Reported	0.000	1.39	2.170	0.677	0.677
CARBONATE ALKALINITY	MG/L	1.3	Not Reported	Not Reported	Not Reported	0.000	0.000	0.000	0.000	Not Detectable
TOTAL PHOSPHORUS	MG/L	0.01	0.020	0.04	0.04	0.000	0.000	0.010	0.000	Not Detectable
TDS	MG/L	10	38.5	51	Not Reported	0.28	1.420	5.090	0.970	0.970
TSS	MG/L	2.5	4.5	9.7	12	0.000	0.000	0.000	0.000	Not Detectable
MERCURY	MG/L	0.0002	0.0002	Not Detectable	Not Reported					
ALUMINUM	MG/L	0.005	0.1767	0.28	0.358	0.000			0.000	Not Detectable
ANTIMONY	MG/L	0.0002	0.00045	0.0014	0.0009	0.000				Not Detectable
ARSENIC	MG/L	0.0002	0.00042	0.0009	0.005				0.000	Not Detectable
BARIUM	MG/L	0.003	0.0062	0.009	0.021	0.000	0.000	0.000	0.000	Not Detectable
BERYLLIUM	MG/L	0.0002	0.0002	Not Detectable	Not Detectable					Not Detectable
BORON	MG/L	0.02	0.02	0.02	0.196	0.000	0.000		0.014	Not Detectable
CADMIUM	MG/L	0.00002	0.000132	0.00014	0.0477				0.000	Not Detectable
CALCIUM	MG/L	0.1	2.81	3.6	91.8	0.05	0.000	0.170	0.000	Not Detectable
CHROMIUM	MG/L	0.002	0.002	Not Detectable	Not Detectable					Not Detectable
COBALT	MG/L	0.0003	0.0003	0.0003	0.151				0.0000	Not Detectable
COPPER	MG/L	0.0001	0.00116	0.01	0.383	0.000958			0.000	Not Detectable
IRON	MG/L	0.02	0.232	0.56	6.02	0.000		0.000	0.000	Not Detectable
LEAD	MG/L	0.0001	0.00018	0.0005	0.0257				0.000	Not Detectable
LITHIUM	MG/L	0.0001	0.00029	0.0005	0.0037				0.000	Not Detectable
MAGNESIUM	MG/L	0.1	0.67	0.9	7.17	0.000		0.050	0.000	Not Detectable
MANGANESE	MG/L	0.002	0.0334	0.075	1.27				0.000	Not Detectable
MOLYBDENUM	MG/L	0.005	0.005	Not Detectable	Not Detectable				0.000	Not Detectable
NICKEL	MG/L	0.002	0.002	Not Detectable	0.013				0.000	Not Detectable
POTASSIUM	MG/L	0.1	0.28	0.4	5.92	0.000	0.000	0.120	0.004	Not Detectable
RUBIDIUM	MG/L	0.0005	0.0005	Not Reported	0.0149					Not Detectable
SELENIUM	MG/L	0.00006	0.00006	Not Reported	0.002					Not Detectable
SILICON	MG/L	0.02	1.93	3	2.6	0.000	0.000	0.040	0.000	Not Detectable
SILVER	MG/L	0.0003	0.0003	Not Detectable	Not Detectable					Not Detectable
SODIUM	MG/L	0.1	0.99	1.2	25	0.010	0.000	1.060	0.261	0.261
STRONTIUM	MG/L	0.0003	Not Reported	Not Reported	0.25				0.000	Not Detectable
SULFUR	MG/L	1	1.05	1.4	3	0.06		0.003	0.000	Not Detectable
THALLIUM	MG/L	0.0001	0.0002	0.0008	Not Detectable					Not Detectable
ZINC	MG/L	0.0002	0.00768	0.045	10				0.004	0.004
CHLORIDE	MG/L	0.3	0.512	0.62	Not Reported	0.13	0.000	1.280	0.000	Not Detectable
FLUORIDE	MG/L	0.03	0.03	Not Detectable	Not Reported					Not Detectable
NITRATE AS N	MG/L	0.1	0.1	Not Detectable	Not Reported			0.016	0.009	Not Detectable
NITRITE AS N	MG/L	0.03	0.03	Not Detectable	Not Reported					Not Detectable
PH	STU	0.01	6.712	6.30 - 7.04 (Range)	7.5	5.76	4.600	5.230	8.140	8.180
SPECIFIC CONDUCTANCE	µS/CM	25	26.6	28	732	1.12	9.000	10.000	<10	<10
SULFATE	MG/L	0.6	1.9	2.7	Not Reported	0.000	0.000	0.000	0.000	Not Detectable
TOC	MG/L	0.7	10.06	12	Not Reported					
DOC	MG/L	0.7	9.49	12	Not Reported					
TOTAL CYANIDE	MG/L	0.005	0.0136	0.015	Not Reported					
TURBIDITY	NTU	0.1	3.91	9.7	21.2	0	0.000	0.000	0.000	Not Detectable
TRUE COLOR		5	48	70	Not Reported	0	0.000	0.000	0.000	Not Detectable

The above modeling results (Table 3) indicate that the proposed treatment plant design will be able to meet existing water quality at the Pickett Mountain site.

Water Treatment Facility Design

The conceptual facility design for the Project is as follows and presented on Figure 7,

1. Surface contact water from the collection/storage pond is fed to the water treatment plant at a rate of 205 USGPM.
2. Feed water passes through a ceramic UF unit for removal of suspended solids.
3. Filtrated is then fed to the first of two stages of RO.
4. Permeate from the first stage RO is fed to the second stage RO.
5. Second stage RO permeate is final effluent (treated water) and is produced at a rate of 200 USGPM.
6. Second stage wastewater (concentrate) is recycled to the first stage RO feed at a rate of 22 USGPM.
7. First stage RO wastewater (concentrate) reports to a reactor where lime (CaO) is added to precipitate excess calcium and alkalinity as calcite (calcium carbonate – $CaCO_3$) which is removed via filtration and becomes a solid waste material (filter cake). Filter cake volume is anticipated to be 2.6 cubic feet per day (2.9 cubic yards per month) The media filter cake is defined as a special waste under Maine's Solid Waste Management Rules, Chapter 400, and will be transported and disposed of in conformance with those rules.
8. Reactor overflow water reports to a second UF RO system (concentrate recovery system) at a rate of 58 USGPM.
9. Permeate from the concentrate recovery UF RO system is recycled to the primary UF feed at a rate of 50 USGPM along with calcite filter filtrate at a rate of 3.5 USGPM.
10. Final wastewater (concentrate) exits the plant at a flow rate of 5 USGPM.

Based on the proposed plant design the full capacity water balance is as follows,

Mine Impacted Water Treatment Plant Feed	= 205 USGPM
Final Permeate (Treated) Water to Discharge	= 200 USGPM
Wastewater	= 5 USGPM

Figure 7. Proposed Plant Process Flow Diagram

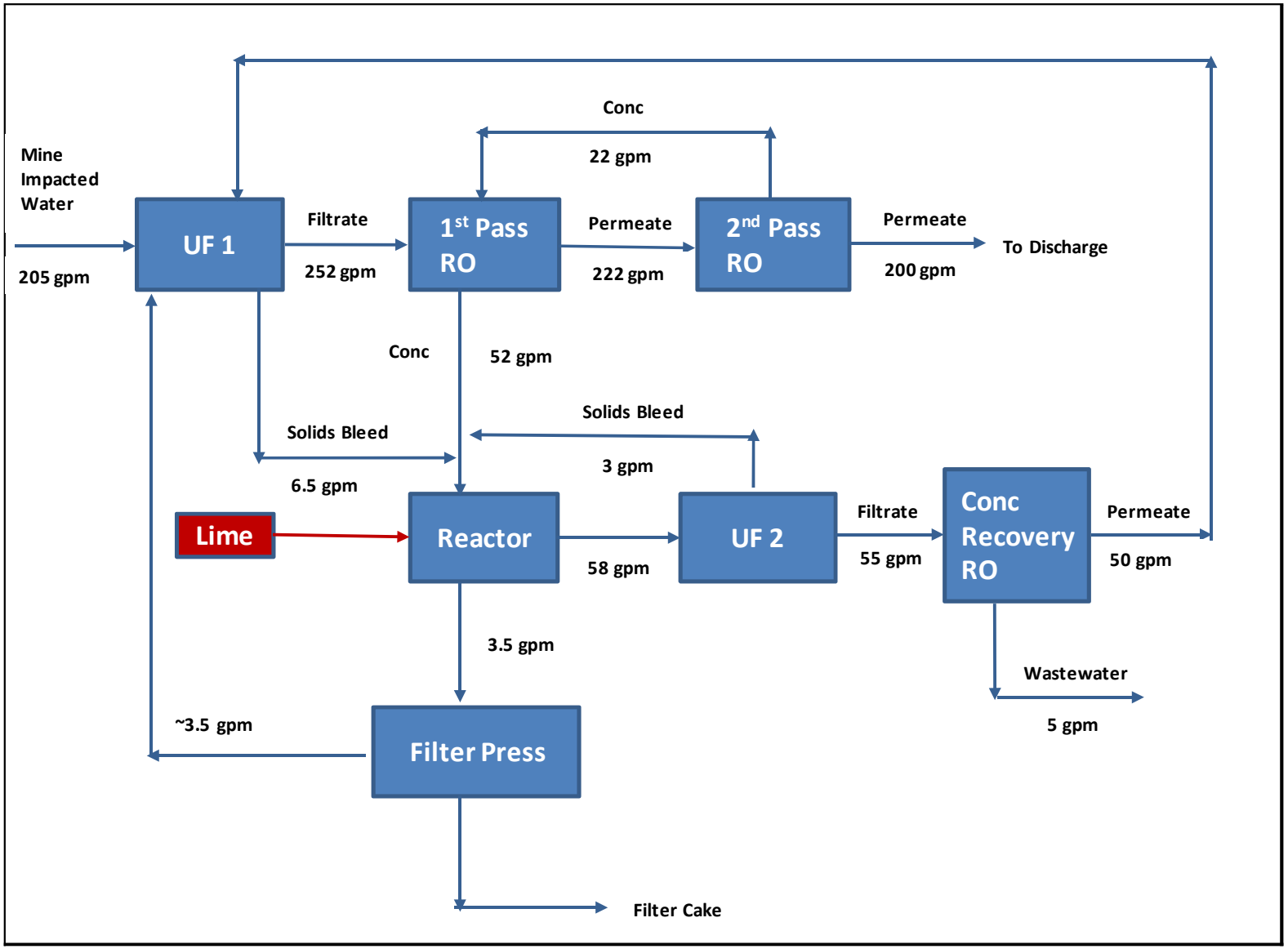

The proposed treatment plant will result in an overall mass balance (Table 4).

Table 4. Mass Balance

Analyte	Units	Target Effluent Quality MG/L	Final Plant Clean Water @ 200 USGPM	Final Plant Waste Stream @ 5 USGPM
TOTAL ALKALINITY	MGCACO3/L	**6.92**		
PHENOLPHTHALEIN ALKALINITY	MGCACO3/L	**0.7**		
BICARBONATE ALKALINITY	MG/L		0.677	27.757
CARBONATE ALKALINITY	MG/L		0.004	0.164
TOTAL PHOSPHORUS	MG/L	**0.02**	Not Detectable	1.64
TDS	MG/L	**42.7**	1.660	
TSS	MG/L	**4.5**	Not Detectable	492
MERCURY	MG/L	**0.0002**		
ALUMINUM	MG/L	**0.1767**	Not Detectable	14.678
ANTIMONY	MG/L	**0.00045**	Not Detectable	0.0369
ARSENIC	MG/L	**0.0004**	Not Detectable	0.205
BARIUM	MG/L	**0.0062**	Not Detectable	0.861
BERYLLIUM	MG/L	**0.0002**	Not Detectable	Not Detectable
BORON	MG/L	**0.02**	Not Detectable	8.036
CADMIUM	MG/L	**0.000132**	Not Detectable	1.9557
CALCIUM	MG/L	**2.81**	Not Detectable	3763.8
CHROMIUM	MG/L	**0.002**	Not Detectable	Not Detectable
COBALT	MG/L	**0.0003**	Not Detectable	6.191
COPPER	MG/L	**0.00116**	Not Detectable	15.703
IRON	MG/L	**0.232**	Not Detectable	246.82
LEAD	MG/L	**0.00018**	Not Detectable	1.0537
LITHIUM	MG/L	**0.00029**	Not Detectable	0.1517
MAGNESIUM	MG/L	**0.67**	Not Detectable	293.97
MANGANESE	MG/L	**0.0334**	Not Detectable	52.07
MOLYBDENUM	MG/L	**0.005**	Not Detectable	0.0943
NICKEL	MG/L	**0.002**	Not Detectable	0.533
POTASSIUM	MG/L	**0.28**	Not Detectable	242.72
RUBIDIUM	MG/L	**0.0005**	Not Detectable	0.6109
SELENIUM	MG/L	**0.005**	Not Detectable	0.082
SILICON	MG/L	**1.93**	Not Detectable	106.6
SILVER	MG/L	**0.0003**	Not Detectable	Not Detectable
SODIUM	MG/L	**0.99**	0.281	1025
STRONTIUM	MG/L	**0.0003**	Not Detectable	
SULFUR	MG/L	**1.05**	Not Detectable	123
THALLIUM	MG/L	**0.0002**	Not Detectable	Not Detectable
ZINC	MG/L	**0.00768**	0.004	410
CHLORIDE	MG/L	**0.512**	Not Detectable	41
FLUORIDE	MG/L	**0.03**	Not Detectable	
NITRATE AS N	MG/L	**0.1**	Not Detectable	203.2
NITRITE AS N	MG/L	**0.03**	Not Detectable	
PH	STU	**6.3 - 7.04 (Range)**	8.140	8.18
SPECIFIC CONDUCTANCE	µS/CM	**26.6**	<10	30012
SULFATE	MG/L	**1.9**	Not Detectable	110.7
TOC	MG/L	**10.06**		492
DOC	MG/L	**9.49**		492
TOTAL CYANIDE	MG/L	**0.0136**		0.615
TURBIDITY	NTU	**3.91**	Not Detectable	869.2
TRUE COLOR		**48**	Not Detectable	2870

Plant Sizing

The water treatment plant size proposed is based on peak monthly treatment volumes as described in the technical memorandum "Proposed Pickett Mountain Mine Project Precipitation Runoff Collection Areas - Mine Only Option" dated May 23, 2022 and revised August 25, 2022, prepared by Wood PLC Engineering consultants and prepared by Wood PLC Engineering consultants. Table 5 below provides a summary of the anticipated runoff flows summarized in this technical memorandum, with the peak or highest flow months highlighted in red (Table 5). Treatment plant sizing is based on the highest monthly estimated flow of 6.57 million gallons which equates to 152.08 USGPM. Normal contingency factors added to water treatment plant designs range from 20% to 30% and a 30% excess flow contingency was used for design of the Pickett Mountain plant. The proposed treatment plant is therefore sized to discharge treated water at the anticipated peak monthly flow with a 30% additional contingency capacity which equates to 197.71 USGPM which was rounded up to 200 USGPM.

Total annual estimated runoff volume is 43.73 million gallons which equates to a nominal treatment rate of 119,808.2 gallons per day or 83.2 USGPM. Based on an optimized waste stream flow of 5 USGPM at full plant capacity the annual wastewater volume is expected to be 1,075,200 gallons per year (2.13 USGPM at 83.2 USGPM permeate production rate). It should also be noted that the proposed UF RO design for the Pickett Mountain plant is modular in nature. While the proposed plant is currently sized to accommodate peak flows as per the table below should further study result in changes to anticipated flows the proposed plant design can easily be modified to accommodate any anticipated flow.

Table 5. Peak Monthly Runoff Flows

Jan	Feb	Mar	Apr	May	Jun	Jul	Aug	Sept	Oct	Nov	Dec
Average Precipitation in Inches											
3.28	2.57	3.07	3.85	4.02	3.81	4.08	3.99	4.02	4.27	4.38	3.69
Runoff Volume in Million Gallons											
2.22	1.72	2.07	2.29	2.41	2.26	2.45	2.39	2.41	2.59	2.67	2.51
Assumed Runoff Factor Due to Temperature											
0.15	0.10	0.70	2.30	1.60	1.00	1.00	1.00	1.00	1.00	0.95	0.90
Estimated Runoff Volume Adjusted for Temperature in Million Gallons											
0.33	0.17	1.45	5.28	3.87	2.26	2.45	2.39	2.41	2.59	2.54	2.26
30 GPM Mine Dewatering Monthly Volume in Million Gallons											
1.34	1.21	1.34	1.30	1.34	1.30	1.34	1.34	1.30	1.30	1.30	1.34
Total Monthly Treatment Volume in Million Gallons											
1.67	1.38	2.79	6.57	5.20	3.56	3.79	3.73	3.71	3.89	3.84	3.60

Blue: Winter Months - frozen conditions with reduced runoff.
Grey/Blue: Late Fall-Early Winter or Late Winter- Early Spring - some reduced runoff.
Green: Spring months - increased runoff with snow melt.

Pre and Post Production Water Management

Water management during the construction phase of the Project will entail water collection, storage, treatment and discharge but with reduced volumes due to a reduced site footprint resulting in reduced collection and water treatment requirements. Water will be collected from the waste rock storage pad and the storage ponds. Water from these pads and ponds will be collected and treated as if it was contaminated. After treatment through the water treatment plant, effluent will be discharged into the Post -Treatment Water Storage Pond, tested, then discharged into the surrounding groundwater via infiltration galleries. Reject water from the water treatment plant will be pumped back into the large Pre-Treatment Water Storage Pond where it will mix with additional impacted water collected from the site.

Approximately 32% of the site assets will not be established until near production. The headframe and associated pads will not be developed until 3 years post startup of the project. This means that prior to start up and well into production the actual water requiring collection for treatment will be less than the projected maximum volume. Prior to start up, with development of site assets representing only 68% of the total site footprint, the precipitation requiring collection and treatment represents 29,750,000 gallons of water over a 12-month construction/preproduction period (68% of the total projected annual volume of 43.73 million gallons). This represents a nominal treatment plant clean water production rate of 56.58 USGPM which will result in a nominal reject water rate of 1.414 USGPM.

The total volume of stored water capacity in the pre water treatment storage pond is projected to be 6,870,000 Gallons. Over the duration of 1 full year pre-production (at 68% asset development), the maximum reject water produced is 743,410 gallons or 10.82% of the total volume of the pond. The total volume of water requiring treatment in the first year of operation can be treated with the proposed water treatment plant in 104 days at peak design flow.

Chemical and mineral loading in the 743,410 gallons of stored reject water will be minimal due to continued dilution from precipitation. After the first construction year and when production and backfilling commence, this stored water will be treated again, and contaminants further concentrated. Final concentrates can then be used in the mining process as backfill cement mix water as described in the next section of this report.

Postproduction impacted water will continue to be collected in the pre water treatment storage pond, processed through the water treatment plant and stored in the Post-Treatment Water Storage Pond, tested and once verified to meet existing water quality will be discharged into the surrounding groundwater via infiltration galleries. It is anticipated that once production ceases eventual dilution from natural precipitation will result in the site impacted water reaching background quality without the requirement for treatment. In the case that this is incorrect, water treatment will take place until a small volume of wastewater remains in storage. This water can then be collected and removed from site to be stored at a certified water management facility or evaporated until only solids remain, which would then be removed and disposed of in an approved landfill.

Water Treatment Plant Waste Water Management

The proposed treatment plant will produce, at peak flow, 5 USGPM of wastewater which will be directed to the Pre-Treatment Water Storage Pond within the Pickett Mountain Site. Wastewater will be stored until backfill production commences and will then be used to prepare cement to be utilized for backfill placement underground as a means of ground stabilization. Annual water treatment requirements for the Pickett Mountain Site are projected to be 43.73 million gallons which equates to an average water treatment plant permeate production rate of 83.2 USGPM (utilizing 365 days per year plant operation) during production. Wastewater production from the plant at this treatment rate will be 2.13 USGPM or 3,072 US gallons per day based on the Wood PLC Engineering study cited above.

Backfill production is based on the use of cemented rock fill with an anticipated fill placement rate of 6.6 tons per day of rock placement and 5% cement binder content. Daily water requirements for cement preparation are estimated to be 6,340 US gallons. Daily wastewater production from the UF RO plant is projected to be 3,072 US gallons. This means that all wastewater generated from the RO plant can be used for cement production during production.

Reagent Use and Final Disposition

Various chemical reagents are employed to treat the various membrane systems for scale and deposit control as well as required periodic cleaning. While cleaning frequency can't be determined until the plant is in actual operation MWS's experience with UF RO plants treating similar quality water indicates that cleaning frequency will likely be less than monthly and more likely quarterly for first stage UF and first and second stage RO. Cleaning frequency for the brine recover UF (UF 2) and RO will be slightly more frequent due to the nature of the water being treated at this stage of the process however anticipated frequency would still be not more than monthly. All chemicals are applied to the influent side of the UF and RO system and therefore report to the wastewater side of the process. In all cases, the reagents do not represent a hazard for downstream use of wastewater in the Pickett Mountain operations. The anticipated maximum consumption of reagents that will be utilized in operation of the plant are outlined below in Table 6.

Table 6. Water Treatment Plant Anticipated Reagent Use

Reagent	Composition	Purpose	Addition Point	Dosage (mg/l)	Anticipated Monthly Consumption at Peak Flow	Anticipated Monthly Consumption at Nominal Flow
Sodium Hydroxide	Sodium hydroxide 50%	RO stage 2 feed pH adjustment	RO stage 2 feed	110	6,820 lb.	3,290 lb.
Lime	CaO 100%	Calcite reactor	Calcite reactor	TBD	TBD	TBD
Osmonix WL3000 or BWA Flocon 885 Antiscalant or similar	Proprietary (Biodegradable)	Scale control for RO membranes	RO stage 1 feed	5	351.5 lb.	150 lb.
Disinfectant	Sodium hypochlorite (bleach)	Biofouling cleaning of UF	UF chemically enhanced backwash	Periodic - weekly	125 lb.	125 lb.
Low pH Cleaner	Hydrochloric or Citric acid 10%	RO membrane cleaning	RO clean In place	Periodic - monthly	20 lb.	20 lb.
Alkaline Cleaner	Sodium hydroxide 10%	RO membrane cleaning	RO clean In place	Periodic - monthly	20 lb.	20 lb.

Note: Monthly consumption based on peak plant flow.

All chemical reagents utilized in the operation of the plant ultimately report to the waste stream and will not pass through the RO membranes to end up in the final permeate discharge water. While all wastewater generated from the water treatment plant will be utilized for cement preparation it should be noted that even prior to this the reagents will be eliminated through natural reactions in the wastewater holding pond. The sodium hydroxide, low pH cleaner and alkaline cleaner will naturally decompose to form sodium chloride (table salt) and water. Sodium hypochlorite will degrade naturally to form, once again, sodium chloride and water. The proprietary antiscalant is biodegradable[16] and contains no components that would be harmful to people or the environment.

In addition to periodic cleaning both UF and RO membranes are periodically replaced due to wear and in some cases fouling due to inorganic scale formation which results in reduced flow rates and excessive operating pressure. The proposed plant design will include a high degree of instrumentation allowing the operators to monitor membrane performance and schedule membrane replacements prior to any operational impact on the plant. Membranes which are replaced can be safely disposed of in landfill.

Re-Mineralization

In many instances, treated water from RO plants is re-mineralized prior to discharge to the environment to add back constituents in to enhance the discharge water quality. In the case of the Pickett Mountain Project, this remineralization could be undertaken to add calcium and alkalinity to provide levels equal to the background water quality targets. Remineralization is accomplished by adding calcium, normally in the form of calcium chloride, and alkalinity normally in the form of sodium carbonate.

Remineralization is easily included in the overall water treatment plant design and control systems. Instrumentation included in the plant design will automatically calculate and adjust addition rates of calcium chloride and sodium carbonate based on plant operating rate to achieve calcium and alkalinity targets. The

[16] http://www.dormeco.co.il/wp-content/uploads/2012/12/Flocon-885.pdf

need for and amount of remineralization will be determined in conjunction with the Chapter 200 permitting for the Project.

Anticipated remineralization reagent usage is as follows (Table 7).

Table 7. Anticipate Re-Mineralization Reagent Requirements

Reagent	Composition	Purpose	Addition Point	Dosage (mg/l)	Anticipated Monthly Consumption at Peak Flow	Anticipated Monthly Consumption at Nominal Flow
Calcium Chloride	$CaCl_2$ 32%	Addition of calcium to final effluent	Final effluent	50	3,515 lb.	1,496 lb.
Sodium Carbonate	Na_2CO_3 100%	Addition of alkalinity to final effluent	Final effluent	50	3,515 lb.	1,496 lb.

Appendix 1. Wolfden Supplied Input and Existing Water Quality

Input Water Quality (Half Mile Mine)

Analyte	Units	Influent Water Quality (Highest Half Mile Value) MG/L
TOTAL ALKALINITY	MG/L as $CaCO_3$	Not Reported
PHENOLPHTHALEIN ALKALINITY	MG/L as $CaCO_3$	Not Reported
BICARBONATE ALKALINITY	MG/L	Not Reported
CARBONATE ALKALINITY	MG/L	Not Reported
TOTAL PHOSPHORUS	MG/L	0.04
TDS	MG/L	Not Reported
TSS	MG/L	12
MERCURY	MG/L	Not Reported
ALUMINUM	MG/L	0.358
ANTIMONY	MG/L	0.0009
ARSENIC	MG/L	0.005
BARIUM	MG/L	0.021
BERYLLIUM	MG/L	Not Detectable
BORON	MG/L	0.196
CADMIUM	MG/L	0.0477
CALCIUM	MG/L	91.8
CHROMIUM	MG/L	Not Detectable
COBALT	MG/L	0.151
COPPER	MG/L	0.383
IRON	MG/L	6.02
LEAD	MG/L	0.0257
LITHIUM	MG/L	0.0037
MAGNESIUM	MG/L	7.17
MANGANESE	MG/L	1.27
MOLYBDENUM	MG/L	Not Detectable
NICKEL	MG/L	0.013
POTASSIUM	MG/L	5.92
RUBIDIUM	MG/L	0.0149
SELENIUM	MG/L	0.002
SILICON	MG/L	2.6
SILVER	MG/L	Not Detectable
SODIUM	MG/L	25
STRONTIUM	MG/L	0.25
SULFUR	MG/L	3
THALLIUM	MG/L	Not Detectable
ZINC	MG/L	10
CHLORIDE	MG/L	Not Reported
FLUORIDE	MG/L	Not Reported
NITRATE AS N	MG/L	Not Reported
NITRITE AS N	MG/L	Not Reported
PH	STU	7.5
SPECIFIC CONDUCTANCE	µS/CM	732
SULFATE	MG/L	Not Reported
TOC	MG/L	Not Reported
DOC	MG/L	Not Reported
TOTAL CYANIDE	MG/L	Not Reported
TURBIDITY	NTU	21.2
TRUE COLOR		Not Reported

Water Sampling Locations and Existing Water Quality – Pickett Mountin Site

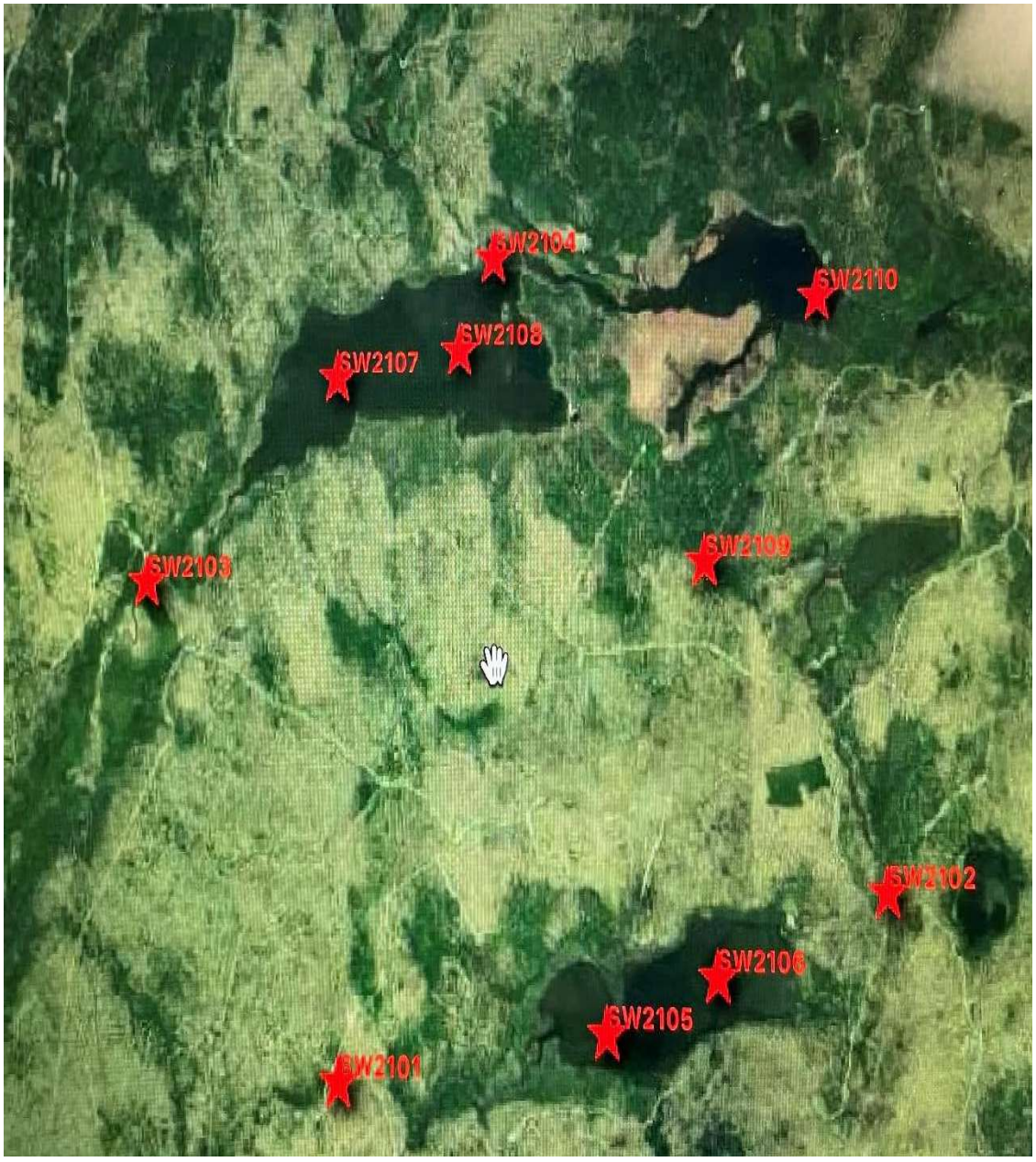

Appendix 2. Individual Modeling Program Data – Two Pass Primary Treatment

Hyd-RO-dose

hyd-RO-dose®

WATER CHEMISTRY SUMMARY
AT 75.0 % RECOVERY

Report Date: 06-06-2022 Sampled: 06-06-2022
Sample ID: 0 at 1658

CATIONS (mg/L)	Raw	Feed	Product	Brine
Calcium(as Ca)	2.04	2.04	0.05	8.00
Magnesium(as Mg)	0.16	0.16	0.00	0.63
Barium(as Ba)	0.00	0.00	0.00	0.00
Strontium(as Sr)	0.00	0.00	0.00	0.00
Sodium(as Na)	0.56	0.56	0.01	2.20
Potassium(as K)	0.13	0.13	0.00	0.51
Lithium(as Li)	0.00	0.00	0.00	0.00
Iron(as Fe)	0.13	0.13	0.00	0.51
Ammonia(as NH_3)	0.00	0.00	0.00	0.00
Aluminum(as Al)	0.01	0.01	0.00	0.04
ANIONS (mg/L)				
Chloride(as Cl)	5.03	5.03	0.13	19.72
Sulfate(as SO_4)	0.06	0.06	0.00	0.24
Dissolved CO_2	0.0	0.0	0.0	0.0
Bicarbonate	0.2	0.2	0.0	0.7
Carbonate	0.0	0.0	0.0	0.0
Silica(as SiO_2)	0.14	0.14	0.00	0.55
Phosphate(as PO_4)	0.00	0.00	0.00	0.00
H_2S (as H_2S)	0.00	0.00	0.00	0.00
Fluoride(as F)	0.00	0.00	0.00	0.00
Nitrate(as NO_3)	0.01	0.01	0.00	0.04
Boron(as B)	0.00	0.00	0.00	0.00
PARAMETERS				
pH	7.00	7.00	5.76	7.84
Temperature (°C)	25.00	25.00	25.00	25.00
Calculated T.D.S.	8.59	8.59	0.28	33.70
Calculated Cond.	19.22	19.22	1.12	73.79

French Creek Software, Inc.
1220 Valley Forge Road, Suite 21, Valley Forge, PA 19460

Wave

DUPONT

Concentrations (mg/L as ion)						
	Feed	Concentrate		Permeate		
		Stage1	Stage2	Stage1	Stage2	Total
NH_4^+	0.07	0.14	0.55	0.00	0.00	0.00
K^+	0.01	0.02	0.09	0.00	0.00	0.00
Na^+	0.04	0.08	0.33	0.00	0.00	0.00
Mg^{+2}	0.00	0.01	0.04	0.00	0.00	0.00
Ca^{+2}	0.06	0.11	0.44	0.00	0.00	0.00
Sr^{+2}	0.00	0.00	0.00	0.00	0.00	0.00
Ba^{+2}	0.00	0.00	0.00	0.00	0.00	0.00
CO_3^{-2}	0.00	0.00	0.00	0.00	0.00	0.00
HCO_3^-	1.72	2.07	4.81	1.38	1.39	1.39
NO_3^-	0.00	0.00	0.00	0.00	0.00	0.00
F^-	0.00	0.00	0.00	0.00	0.00	0.00
Cl^-	0.00	0.00	0.00	0.00	0.00	0.00
Br^{-1}	0.00	0.00	0.00	0.00	0.00	0.00
SO_4^{-2}	0.00	0.00	0.00	0.00	0.00	0.00
PO_4^{-3}	0.00	0.00	0.00	0.00	0.00	0.00
SiO_2	0.01	0.02	0.06	0.00	0.00	0.00
Boron	0.01	0.03	0.09	0.00	0.00	0.00
CO_2	57.61	58.28	59.42	56.90	57.63	57.24
TDS*	1.96	2.50	6.42	1.41	1.42	1.41
Cond. µS/cm	8	8	10	9	9	9
pH	4.7	4.8	5.2	4.6	4.6	4.6

Footnotes:

*Total Dissolved Solids includes ions, SiO_2 and B. It does not include NH_3 and CO_2

Winflows

SUEZ Water Technologies & Solutions

Winflows Version 4.04 DataBase Version 4.04

Streams Analytical Data

Ions, mg/l		Raw Feed	RO1 Element Feed	DownStream Perm RO1	RO1 Concentrate
Calcium (Ca)		83.00	83.00	0.17	276.36
Magnesium (Mg)		25.00	25.00	0.05	83.24
Sodium (Na)		106.00	106.00	1.06	350.97
Potassium (K)		8.00	8.00	0.12	26.39
Ammonia - N (NH4)		2.00	2.00	0.11	6.42
Barium (Ba)		0.05	0.05	0.00	0.17
Strontium (Sr)		0.10	0.10	0.00	0.33
Iron (Fe)		1.00	1.00	0.00	3.33
Manganese (Mn)		0.10	0.10	0.00	0.33
Sulfate (SO4)		3.00	3.00	0.00	9.99
Chloride (Cl)		303.61	303.61	1.28	1009.33
Fluoride (F)		1.00	1.00	0.01	3.30
Nitrate (NO3)		5.00	5.00	0.07	16.51
Bromide (Br)		0.00	0.00	0.00	0.00
Phosphate (PO4)		1.00	1.00	0.01	3.32
Boron (B)		0.00	0.00	0.00	0.00
Silica (SiO2)		5.00	5.00	0.04	16.57
Hydrogen Sulfide (H2S)		0.00	0.00	0.00	0.00
Bicarbonate (HCO3)		145.78	145.78	2.17	479.45
Carbon Dioxide (CO2)		20.53	20.53	20.43	21.34
Carbonate (CO3)		0.10	0.10	0.00	1.11
TDS, mg/l		689.73	689.73	5.09	2287.12
Flow	gpm	351.09	351.09	245.80	105.30
Temperature	°C	25.00	25.00	25.00	25.00
Pressure	psi	0.00	148.40	0.00	91.55
Hardness	ppm as CaCO3	310.23	310.23	0.62	1032.95
Density	kg/m3	997.49	997.49	997.00	998.63
Ionic Strength		0.01	0.01	0.00	0.05
Osm. Pressure	psi	6.72	6.72	0.22	21.27
pH		7.00	7.00	5.23	7.45
Conductivity at 25°C	µS/cm	1268.00	1268.00	10.00	3939.00
Saturation Data					
BaSO4	%	6.34	6.34	0.00	25.02
CaF2	%	10.09	10.09	0.00	**223.43**
CaSO4	%	0.10	0.10	0.00	0.43
SiO2	%	3.99	3.99	0.02	13.20
SrSO4	%	0.01	0.01	0.00	0.03
Struvite	%	0.00	0.00	0.00	0.03
LSI		-0.37	-0.37	-6.47	0.80
S&DI		-0.71	-0.71	-6.98	0.72

IMSDesign

Ion (mg/l)	Raw Water	Feed Water	Permeate Water	Concentrate
Hardness, as CaCO3	256.89	236.43	0.000	471.7
Ca	91.00	83.76	0.000	419.6
Mg	7.17	6.60	0.000	33.1
Na	25.53	34.21	0.261	168.0
K	5.96	5.62	0.004	27.5
NH4	0.01	0.01	0.000	0.0
Ba	0.021	0.019	0.000	0.1
Sr	0.250	0.230	0.000	1.2
Zn+2	10.000	9.200	0	46.103
CO3	0.68	13.53	0.004	23.0
HCO3	392.00	384.74	0.677	1898.8
SO4	3.00	2.76	0.000	13.8
Cl	1.00	0.92	0.000	4.6
NO3	10.00	9.32	0.009	46.1
PO4	0.04	0.04	0.000	0.2
OH	0.00	0.16	0.011	0.0
SiO2	2.60	2.40	0.000	12.0
B	0.20	0.24	0.014	0.9
CO2	21.12	19.43	0.01	19.43
NH3	0.00	0.00	0.00	0.00
TDS	**549.46**	**553.60**	**0.97**	**2694.98**
pH	**7.50**	**7.53**	**8.14**	**8.18**

The deposit would be mined by underground mining methods with metals extracted in a processing plant custom built for the purpose. The mine site infrastructure facilities would be minimised but include a processing plant, small surface shop, warehouse, office complex, water treatment facility, dry stack tailings facility, and transformer and power distribution. Water for the project is assumed for this study to be provided from a well(s) near to the project initially then mainly recycled within the project site.

The mine would operate at 432,000 tonnes per annum and produce $1.36 billion in cash flow during the life of the mine.

Based on the study results, the conclusions of AMPL are:

1. The project provides positive returns based on the parameters and metal prices used in this study and should be developed further with the aim of bringing the deposit to production.

2. The proposed project would be considered a small to medium sized underground mining operation, which can be developed for production at a reasonable cost in a near-term horizon, provided regulatory approval and permits are acquired.

3. The mined grade of potentially economic mineralisation is an important variable for the success of the operation as are operating costs. Operating management efforts during mine production must be focused on these parameters.

4. The scoping level test work has indicated that a sequential flotation process will produce marketable-grade copper, lead, and zinc concentrates. Arsenic and antimony levels were high in copper concentrates produced in open-cycle and locked-cycle tests. Additional geo-metallurgical test work will provide additional information on the impurities in the marketable-grade copper concentrate to determine if penalties need to be paid. In addition, blending of ores from different areas in the mine will keep impurities (As/Sb) below penalty levels.

5. The following conclusions can be drawn based on the historical and current scoping level metallurgical studies:

    - The sequential flotation process is a process of choice for recovering marketable-grade concentrates of copper, lead, and zinc that include in each, quantities of previous metals.

    - Blending of material into the mill and/or final copper concentrate may be required to maintain low levels of arsenic and antimony, below the penalty limits for the concentrate.

    - Metal recoveries of 78% to 88% for copper, lead, and zinc are expected in the selected flowsheet while maintaining high quality concentrates.

    - Further testing is needed to optimise metal recoveries and reagent quantities in order to maximise revenue and reduce Capex and Opex for the milling circuit.

The project will be required to first obtain, from the Maine LUPC, approval of a rezoning petition that will allow for mining in this unorganised township. The petition was submitted and has been accepted by the LUPC as complete for its review. Based on initial soil and wetland field survey,s in addition to desktop studies as described in the petition, it was concluded that the preliminary designs of the proposed project would have no undue impact on the natural resources and could be completed in a manner that would fit

volcanism and sedimentation. The deposit horizon is rotated into an interpreted syncline east of the East Zone, also arguing for fold repetitions of the contact.

Foliations in the rocks are axial planar to the interpreted folds near contacts but tend to be more northerly away from contacts. It is suggested that these foliations record a later flattening that produced cross-folding in the deposit area.

7.3 Mineralisation

The mineral zone at Pickett Mountain is a volcanogenic massive sulphide deposit that strikes at approximately 057°. It has been traced by drilling approximately 900m along strike and to 750 vertical metres below surface. It consists of 4 primary lenses and several minor lenses that likely reflect the original formation of the mineralisation. It is stratabound and is hosted primarily by an intermediate to felsic lapilli tuff to volcanic breccia unit (Scully, 1988).

Primary minerals of economic interest are chalcopyrite, galena, and sphalerite intercalated with variable amounts of pyrite. Accessory minerals include tetrahedrite and minor arsenopyrite. There are two primary lenses of massive sulphide that have been discovered to date that have been subdivided into four lenses (W1, W2, E1, and E2). These vary from 0.5m to about 25m in horizontal width and with the highest base metal grades situated at or near the base of the massive sulphide lenses. The high-grade Cu-Pb-Zn sulphides are typically finely laminated and are overlain and in sharp contact with massive pyrite (Scully, 1988).

The high-grade sulphides typically include 45% to 60% pyrite, 15% sphalerite, 3% galena, and 4% chalcopyrite. There are also minor amounts of tetrahedrite, tennantite, arsenopyrite, magnetite, and barite. Laminations are typically 2 mm to 5 cm in thickness and are compositionally defined (Scully, 1988).

The West Lens is the most prominent massive sulphide lens discovered to date having been traced by drilling over a 300m strike length and to a vertical depth of 825m. Notably, it also is the highest grade of all lenses based on current and historic drilling and the most intense footwall alteration. The West Lens, especially along its eastern edge, includes fold repetitions and structurally stacked mineralisation in the hanging wall (previously interpreted as W2 Lens). Re-logging, which is in progress, has been completed and lithogeochemical data are supporting the updated interpretation. It is also likely that additional holes will need to be drilled to finalise the updated interpretation. As well, the West Lens lies directly on either felsic volcanic in the upper part of the zone and sedimentary rocks, in the lower part of the zone. This suggests that, the massive sulphides were deposited, both on top of the felsic volcanic rocks and in local, likely structurally-controlled sub-basins, with local structures, likely controlling mineralising hydrothermal fluid flow.

The East Lens (E1 and E2 Lenses) can be traced over a strike-length of close to 550m and to a maximum vertical depth of about 550m below the surface with the bulk of the zone above 400m. The QFP unit occurring below the East Lens, may have modified the orientation of the lens resulting in a locally shallower dip and may have propagated a fault or dislocation between the East and West Lenses. In addition, the QFP and a massive feldspar quartz porphyry unit appears to partially truncate the East Lens at its eastern extremity, occurring as a felsic dome intruding the upper rhyolite. The continuation of the favourable stratigraphy hosting the West and East Lenses, beyond the eastern limits of this intrusive cut-off, is unknown.

Longitudinal sections for the massive sulphide lenses, that are subject to the resource estimate, are depicted in Figure 7.6 and Figure 7.7.

The soil geochemistry map (Figure 9.13) clearly shows that both the East and West Lenses are reflected by strong, well defined soil anomalies (Zn + Pb + Cu). There is also a significant component of dispersion of such soil anomalies to the southeast of the massive sulphide lenses, likely due to glacial smearing of overburden in the down-ice direction. The ice direction is from the north-northwest to the south-southeast (170°), as evidenced by the presence of glacial striae observed in outcrops proximal to the East and West Lenses.

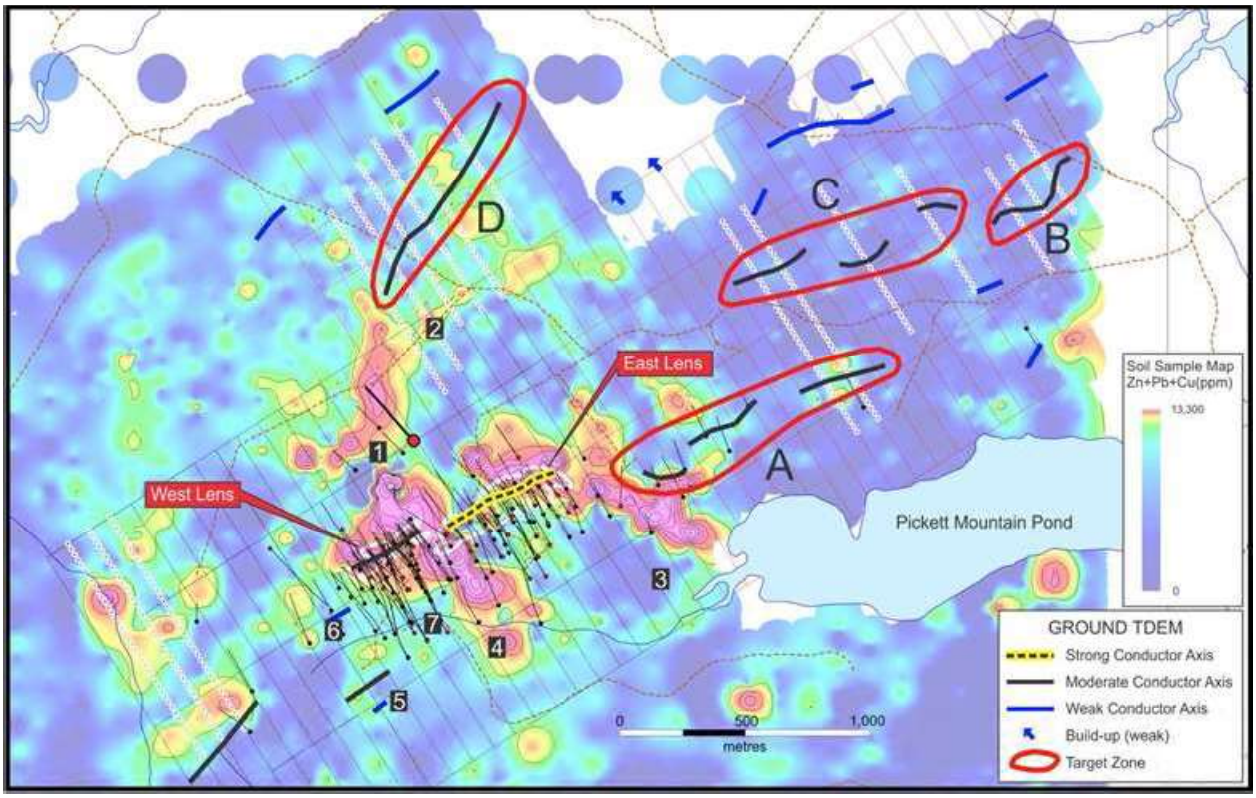

Figure 9.13 (Zn+Pb+Cu) Compilation Map

Other soil anomalies defined are compelling targets and warrant further investigation. In particular, a prominent anomaly located immediately to the west of the West Lens on the western fringe of the grid has not been tested by diamond drilling and may represent the southwestern extension of the main Pickett Mountain horizon. Strong soil anomalies persist immediately to the north and upslope from the East and West Lenses. The presence of such anomalies augurs well for the potential discovery of additional footwall lenses of massive sulphide in relation to the main mineralised horizon. Finally, a strong north-northeast trending soil anomaly situated 500m to the north of the East and West Lenses has seen minimal diamond drilling. The extension of this soil anomaly to the north-northeast is coincident with a prominent conductor defined by the ground TDEM survey (Target Zone D).

the addition of other lenses. This target size is derived from the interpretation of the drilling, geological structure, geology, and surface sampling carried out on the Property to date. The potential quantity and grade of the target is conceptual in nature. There has been insufficient exploration of this target to define a Mineral Resource and it is uncertain if further local exploration will result in this target being delineated as a Mineral Resource.

14.15.1 Mineral Resources Used in the Mine Plan

The mineral resource used in the PEA includes Indicated and Inferred Resources and is an update from the January 7, 2019 Mineral Resource statement. The estimate uses a 7% cut-off grade (or an NSR value of $139/t) rather than the previous 9% cut-off grade ($178/t NSR). The same methodology used in the 2019 estimate was applied to the updated estimate where the metal prices were not updated (to those used in the PEA financial model) and no additional information was either included or excluded even though infill drill results since 2019 is expected to upgrade the mineral resource and could potentially lead to an increase.

The resource estimates used in the mine plan are only those contained within the main zones of the mineralised zones and have had fringe outliers removed from the estimates. They are presented in Table 14.17.

TABLE 14.17
UPDATED MINERAL RESOURCES USED IN MINE PLAN

Category	Tonnes	Zn %	Pb %	Cu %	Ag g/t	Au g/t	Density	ZnEq %
Indicated	2,177,000	9.25	3.68	1.32	96.4	0.9	3.98	18.23
Inferred	2,294,000	9.79	3.88	1.15	101.1	0.9	3.99	18.62

The mineral resources were estimated using the metal prices of US$1.20/lb Zn, $2.50/lb Cu, $1.00/lb Pb, $16.00/oz Ag, and $1,200/oz/Au, using a 7% cutoff grade that equates to an NSR cut-off of $139/tonne at the same metal prices. An average recovery of 75% for all metals was assumed. A 10% mining dilution at zero grade was only added to the financial model which also used different metal prices.

December 26, 2022

Mr. Jeremy Ouellette, P. Eng.
Vice President Project Development
Wolfden Resources Corporation

Mr. Ouellette:

Wolfden Resources Corporation (Wolfden) has asked A-Z Mining Professionals Ltd. (AMPL) to review the economic model constructed for the Preliminary Economic Assessment (PEA) for the Pickett Mountain Project, Penobscot County Maine, filed October 29, 2020 to evaluate the economic impact of relocating the processing plant and tailings management facility (TMF) to an off-site location. As the Engineer of Record, I have reviewed the economic model and made the following adjustments to the capital and operating costs:

a) The capital costs of constructing the processing plant and TMF have not been changed. Note that a solar facility is being considered by the current design team. This will be a cost savings driver and will not negatively impact the economics of the project.

b) An additional $5.69/tonne has been included in operating costs for haulage from the site to the new processing plant location as per a quote provided to AMPL by Wolfden. A second plant location site, 15 miles further from the mine site is also being considered. The haulage costs would be expected to increase slightly to the second location, but should have only a minimal effect on the project economics.

c) Costs have been included for a second water treatment plant, one at the mine site and one at the new location of the processing facility.

d) Costs related to operating spray irrigation and snowmaking systems compared to infiltration galleries will reduce the capital costs of the project while maintaining comparable operating costs. It is considered a conservative approach to keep the current capital costs for discharging treated water as related to capital infrastructure.

e) All other costs remain the same.

f) The approach to the relocation of the processing plant and TMF is considered to be conservative regarding the following:

    i. There is an opportunity to save on construction costs for the TMF if relocated to more level terrain.

ATTACHMENT 24

JANET T. MILLS
GOVERNOR

STATE OF MAINE
DEPARTMENT OF
INLAND FISHERIES & WILDLIFE
353 WATER STREET
41 STATE HOUSE STATION
AUGUSTA ME 04333-0041

JUDITH CAMUSO
COMMISSIONER

June 27, 2023

Tim Carr
Senior Planner
Maine Land Use Planning Commission
22 State House Station
Augusta, Maine 04333-0022

RE: Wolfden Mt. Chase LLC, Rezoning Request ZP 779A, Pickett Mountain Metallic Mineral Mine, T6R6 WELS

Dear Tim,

Per your request received on May 4, 2023, the Maine Department of Inland Fisheries and Wildlife (MDIFW) has reviewed application materials related to the request by Wolfden Mt. Chase LLC to rezone 374 acres in T6R6 WELS from a General Management (M-GN) Subdistrict to a Planned Development (D-PD) Subdistrict. If rezoning is approved, Wolfden would then have the opportunity to apply for regulatory review and possible permitting of the proposed underground Pickett Mountain Metallic Mineral Mine. MDIFW has provided previous reviews and correspondences on July 27, 2022; September 11, 2020; November 25, 2019; and participated in a site visit and onsite meeting on September 3, 2020, related to this project.

MDIFW has previously noted potential concerns related to State listed bats and their critical habitats; intermittent and perennial streams; lakes and ponds; fisheries and other aquatic resources; freshwater wetlands; Inland Waterfowl and Wadingbird Habitats; vernal pools; and other known and potential resources of concern. The September 11, 2020, correspondence (attached) provides information on fisheries, aquatic, and wetland resources in the area. These resources, as well as the surface water and groundwater resources that supply them, are significant concerns for the agency and will be the subject of further review and recommendations in any future regulatory proceedings.

MDIFW notes that the proposed project has undergone substantial modifications and that application materials suggest that significant analyses have been and are being conducted. The applicant indicates that 129 acres of the 374 acres proposed for rezoning will be cleared for the project, with mine facilities, water treatment, water storage, and a water recharge area located within an approximately 31-acre portion of impervious development. The project site may also include a possible future 47-acre solar development. The applicant's consultant indicates that the proposed design will avoid jurisdictional wetland, stream, and vernal pool resources. In the current proposed design, concentrator and tailings processing facilities will be proposed at another location to be determined and not located at this site. MDIFW will be interested in the location proposed for these operations.

Mineral deposits are reportedly located at depths of 160-2,700 feet below surface. Thus, the project design appears to allow for maintaining approximately 160 feet of overburden material beneath natural resources, seemingly reducing the potential for the mining activity itself to affect groundwater flows to wetland and aquatic resources on the surface. This concept merits further review.

Application materials indicate that mined ore and waste rock will be temporarily stockpiled on impermeable, lined storage pads with leachate and storm water collection and treatment, including settling and reverse osmosis, prior to surface discharge through spray irrigation and wastewater snowmaking. Spray irrigation/snowmaking discharges are proposed to be located within water recharge areas to provide approximately equivalent pre and post construction water budgets to offset lost surface flows to aquatic and wetland resources from adjacent areas altered by development. MDIFW will be interested in more detailed analyses of this proposal as designs are further developed, to ensure that distributed water is free of contaminants from mine activities and that any adverse impacts to surface water and groundwater resources, fisheries, wildlife, and their critical habitats, are avoided, minimized, and, if appropriate, adequately mitigated.

MDIFW's preliminary desktop reviews and record searches identify known resources, but site surveys are often necessary to identify other important resources that have not yet been investigated but may be present in an area. Locating a project in or in proximity to certain habitats can result in adverse impacts to those habitats and the species that utilize them and, in those situations, MDIFW will likely recommend increased siting and design considerations, operational measures, monitoring practices, and/or other efforts in attempt to avoid, minimize, and possibly mitigate for such impacts. Resource surveys, project siting, facility design/layout, and operational practices are all very important steps in this process. MDIFW provides recommendations based on known and reported resource information but, it is the applicant's ultimate responsibility to ensure that its activities do not result in substantial detrimental impacts to resources.

Based on review of the materials provided, MDIFW offers no objection at this time to Wolfden Mt. Chase LLC's request to rezone 374 acres in T6R6 WELS from a General Management (M-GN) Subdistrict to a Planned Development (D-PD) Subdistrict. MDIFW anticipates that any future application materials will include compelling information on measures to avoid or minimize adverse impacts to important natural resources such as, but not limited to, those noted above and in MDIFW's previous correspondences. Further, we anticipate that any regulatory proceedings will include opportunities for MDIFW to review and provide recommendations for the protection of important fisheries, wildlife, and critical aquatic, wetland, riparian, and terrestrial habitats, and that such recommendations will be appropriately considered in regulatory actions.

Thank you for this opportunity. If you have any questions or concerns, please feel free to contact me at robert.d.stratton@maine.gov or (207) 287-5659.

Sincerely,

Bob Stratton IFW

Robert D. Stratton
Environmental Program Manager
Maine Department of Inland Fisheries & Wildlife

cc: Kevin Dunham, Mark Caron (MDIFW)

encl: MDIFW Preliminary Resource Map (2023)
MDIFW Fish and Wildlife Resources Review (September 11, 2020)
Wolfden Preliminary Stream Resources Map (2020)

Maine Department of Inland Fisheries and Wildlife
Environmental Review of Fish and Wildlife Observations and Priority Habitats

Wolfden Metallic Mineral Mining Rezoning

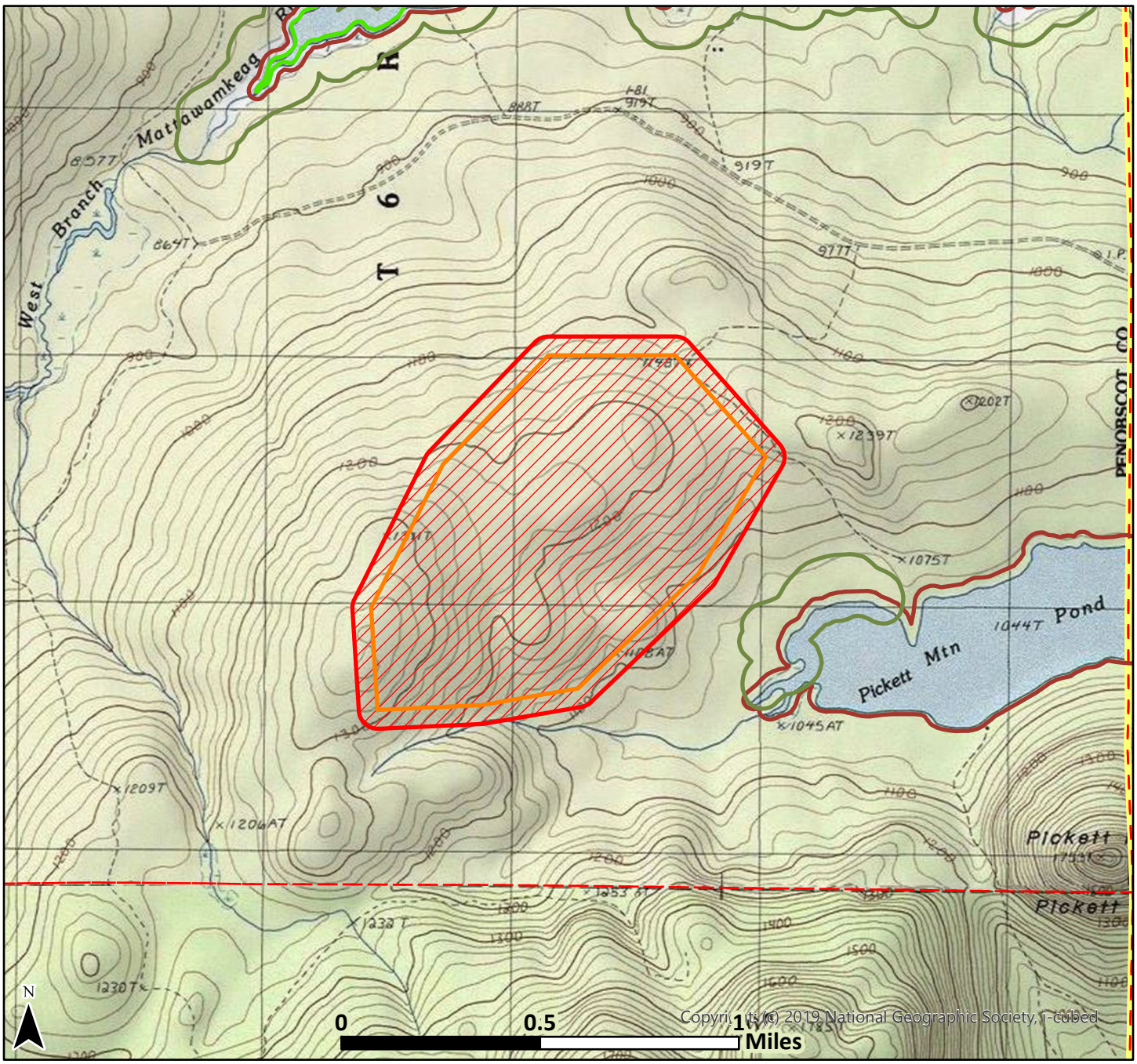

- County Boundary
- Township Boundary
- Project Footprint
- Search Area
- Inland Waterfowl/Wading Bird
- Maine Heritage Fish Waters
- Special Concern Fish

Date: 6/23/2023
Projection:
UTM Zone 19N, NAD83

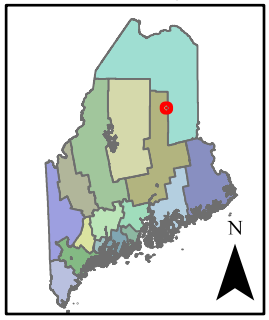

Legend only lists resources visible in the map; see response letter for all resources that were evaluated.

JANET T. MILLS
GOVERNOR

STATE OF MAINE
DEPARTMENT OF
INLAND FISHERIES & WILDLIFE
284 STATE STREET
41 STATE HOUSE STATION
AUGUSTA ME 04333-0041

JUDITH CAMUSO
COMMISSIONER

September 11, 2020

Ms. Stacie J. Beyer
Planning Manager
Maine Land Use Planning Commission
22 State House Station,
Augusta, Maine 04333-0022

RE: Wolfden Resources Mineral Mining Rezoning Petition, T6R6 WELS; Additional Resource Information.

Dear Stacie,

Per your request, and as a follow up to the site visit conducted on September 3, 2020, the Maine Department of Inland Fisheries and Wildlife (MDIFW) offers the following additional observations and recommendations related to Wolfden Resources' petition to rezone 528 acres in T6R6 WELS to allow for an application to construct a metallic mineral mine. We appreciate the opportunity to attend the site visit, which was very informative and provided an opportunity to discuss resource concerns with the applicant and other parties present.

In MDIFW's letter of November 25, 2019, we described our agency's focus on Rare, Threatened, and Endangered Species and Habitats; Significant Wildlife Habitats; and Protected Natural Resources. Based on preliminary information provided, we also noted several resources for further investigation and of particular concern, some of which are further addressed below. The following is in response to your request for additional information related to the presence, use, and concerns for potential impacts to natural resources in the vicinity of the proposed project.

<u>Significant Wildlife Habitat, Potential for Maine Threatened Species</u>
It is noted that a designated Inland Waterfowl and Wading Bird Habitat (IWWH) is located on the inlet on the western end of Pickett Mountain Pond, adjacent to the proposed project site. MDIFW anticipates receiving and reviewing additional project information in the future to ensure that there are no unreasonable, adverse impacts to this resource, which is a Significant Wildlife Habitat (SWH) pursuant to the Natural Resources Protection Act (38 M.R.S., §480-B.10) and SWH Rules (06-096 CMR 335; 09-137 CMR 10). In addition, MDIFW recommends investigation of the IWWH for presence / absence of shrubby cinquefoil, the host plant for the State Threatened Clayton's copper butterfly. Aerial photo interpretation suggests that the IWWH may have conditions that favor this plant and there is an existing population of Clayton's copper butterflies in nearby Crystal. The Clayton's copper butterfly is currently known from only ten sites in Maine, including four in a ten square mile area of eastern Penobscot County in the vicinity of Lee and Springfield, and three sites in northern Piscataquis and eastern Aroostook Counties. Clayton's copper is found only in association with its larval host plant, the shrubby cinquefoil. This uncommon shrub requires limestone soils and has a scattered distribution throughout Maine, however, there are relatively few stands large enough to support viable Clayton's copper populations. Shrubby cinquefoil is intolerant of shade and can only thrive in open areas. It

typically occurs along the edge of calcareous (limestone) wetlands. It can also be found in old fields, but these stands are typically short-lived because of forest succession. All of the currently known occurrences for Clayton's copper are in enriched fens and bogs, and streamside shrublands or meadows. Please contact MDIFW's Reptile, Amphibian, and Invertebrate Biologist, Beth Swartz (beth.swartz@maine.gov, 207- 941-4476), for further guidance. If MDIFW-approved surveys are conducted and indicate that shrubby cinquefoil is not present, or if it can be demonstrated that the Wolfden proposal will not adversely affect shrubby cinquefoil and will avoid Take or Harassment of the Maine Threatened Clayton's copper butterfly, MDIFW anticipates having no concerns for this species.

Bat Habitat Creation, Post-Closure

During the September 3, 2020 site visit, we briefly explored the potential to create habitat for at-risk bat species as part of the post-operational site remediation plan. As I understand it, the main underground portal will consist of an approximately 16-foot x 16-foot opening surrounded by a larger rock face. There will also be both east and west ventilation raises with approximately 10-foot x 10-foot openings. Wolfden intends to fill and add concrete around the openings to prevent water intrusion after closure. We briefly discussed the potential to slope and berm around the openings to discourage water entry and to leave gated openings as possible caves for bat hibernacula. We also discussed the possibility of installing some piles of rock rubble on the closed tailings storage area as potential hibernacula. These discussions were conceptual but, Wolfden expressed interest in further exploring the concept to determine the potential for creating viable habitat conditions while also meeting site closure needs.

Aquatic Resources

The proposed project site is located in the Rockabema Lake subwatershed (HUC 12), in proximity and west of Pickett Mountain Pond, which flows to Grass Pond, then to Mud Lake, and other waters downstream. It is also east and south of the West Branch of the Mattawamkeag River, which flows to Pleasant Lake, Mud Lake, Duck Pond, Rockabema Lake, and other downstream resources along the West Branch of the Mattawamkeag River. The watershed contains other resources including intermittent and perennial streams, associated riparian habitats, and freshwater wetlands, and is considered important for brook trout.

Pickett Mountain Pond has a maximum depth of seven feet, with warm, well oxygenated water. The initial fisheries survey (1958) indicated that the inlet tributary had no potential for brook trout spawning, rearing, or adults, and the outlet had little potential. One trout was captured during the initial survey, none in subsequent samples (1996, 2004). MDIFW Regional Fisheries Biologist Kevin Dunham indicates that Pickett Mountain Pond contains white sucker, fine-scale dace, red-belly dace, fallfish, creek chub, golden shiner, common shiner, red-breasted sunfish, black-nose dace, and pearl dace, and would make a great place to harvest bait fish.

Pleasant Lake, Mud Lake, and Grass Pond are all designated as Heritage Fish Waters. Maine Heritage Fish Waters are native and wild brook trout lakes and ponds which represent unique, valuable, and irreplaceable ecological and angling resources. MDIFW recognizes the unrivaled historic and economic importance of Maine's wild and native brook trout resource and focuses on the conservation and protection of this uniquely valuable resource. MDIFW's primary intent for managing wild brook trout in lakes and ponds is the protection and conservation of these self-sustaining fisheries. The inlets of these lakes originate in the West Branch of the Mattawamkeag River as well as Picket Mountain Pond, positioned west and east of the proposed project site, respectively.

MDIFW regional fisheries staff consider Pleasant Lake and Mud Lake to be some of the best brook trout and landlock salmon waters available in the Region. Kevin Dunham notes, "*Though the initial survey of the lakes in 1953 describes them as being shallow and having warm water throughout, it does go on to say, 'trout and salmon seek the cool water of spring holes…'. Pleasant Lake has an adequate amount of cool-water spring holes to support an excellent trout and salmon fishery. Subsequent fishery surveys, the most recent conducted in June 2019, found extraordinary growth of one-year old wild brook trout averaging 9.1", most of which probably took place in a cooler tributary stream. Additionally, while the lake does not stratify and temperatures remain homogenous throughout the water column, dissolved oxygen levels also remain ideal from top to bottom. Multiple age-classes of brook trout were captured during recent surveys as well, indicating year to year holdover is taking place at Pleasant and Mud Lakes."* Anecdotal evidence suggests moderate angling pressure in these waters and the fisheries resources are protected and managed through specialized regulations. "*The landlocked salmon fishery is not as robust as the trout fishery, but past surveys have sampled multiple age-classes in the 7-17" size ranges. While the lakes are somewhat limiting in cold-water refugia they do support healthy populations of salmonids* (and other fish including smelt) *and it is vitally important to protect the tributaries as well as the lakes since they contain an abundance of spawning and rearing habitat*."

Merry Gallagher, MDIFW's Native Fish Conservation Biologist, provided the attached map of preliminary stream resources, and noted that the orange stream lines *"signify streams that are of medium/moderate value for wild brook trout conservation according to* (MDIFW's) *recent effort to classify streams.*" As noted during our November 5, 2019 meeting, brook trout streams are plentiful throughout this region. During surveys conducted in September 2008, one survey site indicated on the map yielded 16 wild brook trout, while the second site provided two wild brook trout, along with common shiner, black nose dace, creek chub, white sucker, and black nose shiner.

MDIFW requests additional information on the proposed mining operation and associated activities to ensure that it will not result in unreasonable adverse impacts to these valuable resources.

<u>Streams and Wetlands</u>

Wolfden's plan during the mining operation includes capturing water from runoff and infiltration on site, treating it to equal to or better than ambient conditions, and discharging treated water into bedrock aquifers. During the September 3, 2020 site visit, MDIFW noted that intermittent and perennial streams and freshwater wetlands in the area are likely supplied by water from shallow features that flow through the overburden and less likely from bedrock sources. MDIFW expressed concern with the potential for these natural resources to be adversely affected by removing water from surficial and shallow horizons and discharging it to bedrock aquifers. The concern is with a potential dewatering and/or change in water chemistry, temperature, etc. of these natural resources that are important habitats by themselves as well as through their contributions to the larger resources described above. Also, additional information is necessary to demonstrate that the proposed mining operation and associated activities will not cause physical interruptions in subsurface flow patterns that supply these resources, even if Wolfden is able to maintain recommended undisturbed, forested buffer distances. During the site visit, we discussed investigating spray irrigation of the treated water to the ground surface during operation, allowing it to infiltrate the overburden and potentially provide flows to surface water resources. However, even if this is determined feasible and beneficial, the question remains of potential long term/permanent effects as this practice will not be in use after operations cease. MDIFW requests additional information to address concerns for potential direct and indirect impacts to surface and groundwater features and flow patterns that contribute to these resources.

We hope that this information is valuable to your process. If you have any questions or concerns, please feel free to contact me at robert.d.stratton@maine.gov or (207) 287-5659.

Thank you,

Bob Stratton, IFW

Robert D. Stratton
Environmental Program Manager
Maine Department of Inland Fisheries & Wildlife

Cc: Jim Connolly, Director, Bureau of Resource Management, MDIFW

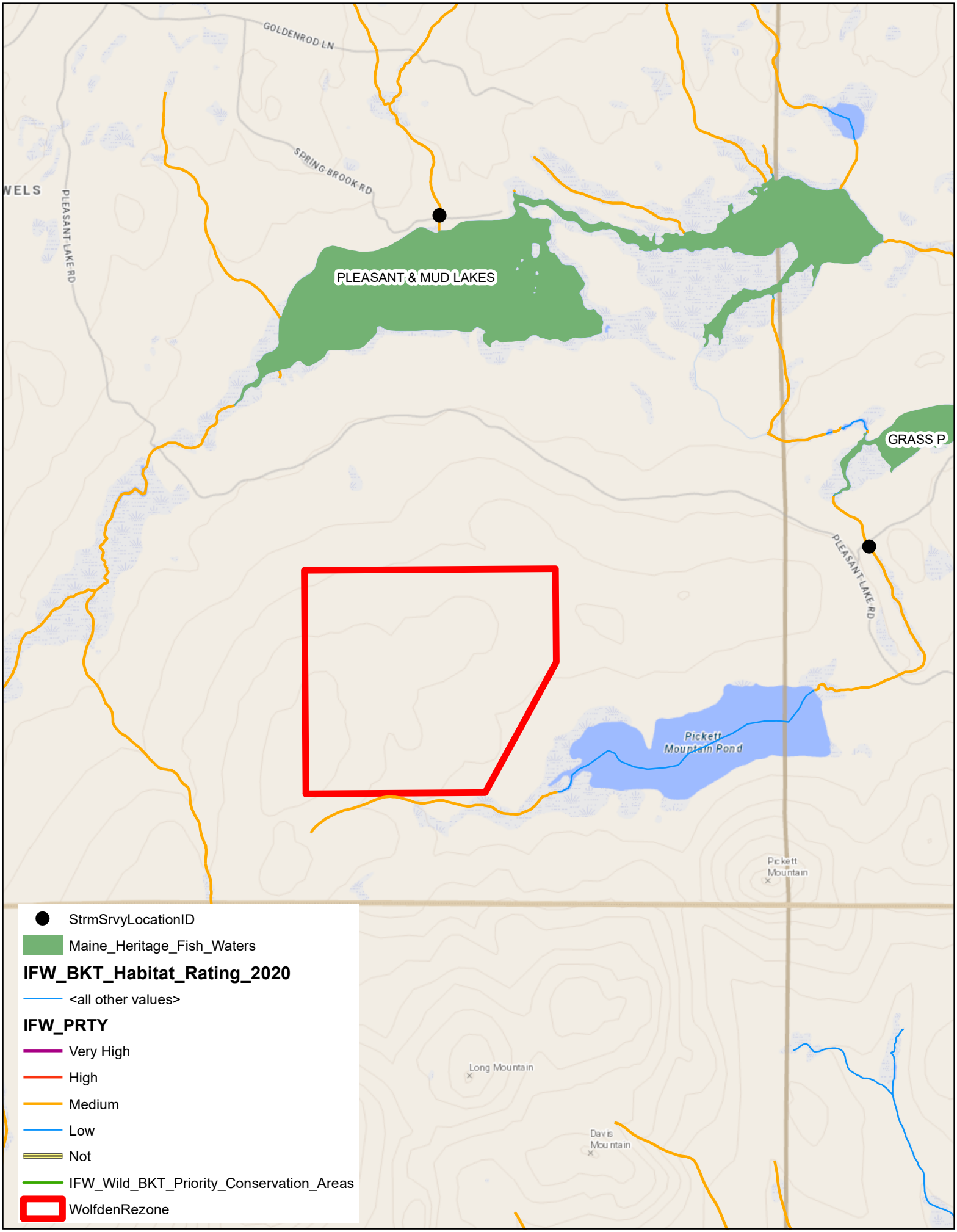
GOLDENROD LN
SPRING BROOK RD
WELS
PLEASANT LAKE RD
PLEASANT & MUD LAKES
GRASS P
PLEASANT LAKE RD
Pickett Mountain Pond
Pickett Mountain
Long Mountain
Davis Mountain
StrmSrvyLocationID
Maine_Heritage_Fish_Waters
IFW_BKT_Habitat_Rating_2020
<all other values>
IFW_PRTY
Very High
High
Medium
Low
Not
IFW_Wild_BKT_Priority_Conservation_Areas
WolfdenRezone

ATTACHMENT 25

A LEGACY OF NEARLY 500 YEARS OF MINING IN POTOSÍ, BOLIVIA: ACID MINE DRAINAGE SOURCE IDENTIFICATION AND CHARACTERIZATION[1]

W.H. Strosnider, R.W. Nairn, and F.S. Llanos[2]

Abstract: Intensive mining and processing of silver, lead, tin and zinc ores have occurred in various locations within and around the city of Potosí, Bolivia since 1545. Surface and subsurface waters, stream sediments and soils are contaminated with various heavy metals. Acid mine drainage and processing plant effluent are primary contaminants in the headwaters of the economically vital, yet highly impacted, Rio Pilcomayo watershed. Previous studies have documented downstream heavy metal contamination. The acid mine drainage sources documented in this study help to link downstream pollution to primary origins. Selected acid mine drainage sources, from both operating and abandoned mines contributing to local streams, contained total metal concentrations of 0.284-977 mg/L Al, 0.03-191 mg/L As, 0.025-50.68 mg/L Cd, 0.03-161 mg/L Cu, 0.15-7,320 mg/L Fe, 0.3-438 mg/L Mn, 0.03-15.0 mg/L Pb and 1.46-11,760 mg/L Zn, with pH and specific conductance ranging from 2.46-6.39 and 893-19,070 μS/cm, respectively. Data were gathered during the dry season with flows ranging from nil to 4.59 L/s. Metals concentrations and pH values in all mine drainage sources sampled are several orders of magnitude above compliance with Bolivian environmental law.

Additional Key Words: acid rock drainage, aqueous geochemistry, water quality, and mineral processing

---

[1] Paper was presented at the 2007 National Meeting of the American Society of Mining and Reclamation, Gillette, WY, 30 Years of SMCRA and Beyond June 2-7, 2007. R.I. Barnhisel (Ed.) Published by ASMR, 3134 Montavesta Rd., Lexington, KY 40502.

[2] William H. Strosnider, Doctoral Student, and Robert W. Nairn, Associate Professor, respectively, Center for Restoration of Ecosystems and Watersheds, School of Civil Engineering and Environmental Science, University of Oklahoma, 202 West Boyd St. Norman, OK 73019 Freddy S. Llanos López, Director of the Major, Department of Mining Engineering, Universidad Autónoma de "Tomás Frías." Avenida Villazón esq. Arce s/n., Potosí, Bolivia.

Proceedings America Society of Mining and Reclamation, 2007 pp 788-803
DOI: 10.21000/JASMR07010788

Introduction

Background

Twelve years after Pizarro dethroned Atahualpa and conquered the Inca, the largest Ag deposit in the world was discovered at Cerro Rico (Rich Hill) by the indigenous nobleman Diego Huallpa. The next year the Spanish founded the city of Potosí at Cerro Rico's base with Huallpa's confidant, the Spainard Juan de Villarroel, registering the first claim April 21, 1545 (Wilson and Petrov, 1999). Within a hundred years Potosí became one of the world's richest and most populous cities during a Ag boom fueled by Cerro Rico veins of up to 25% pure metal (Wilson and Petrov, 1999; Bartos, 2000; Abbot and Wolfe, 2003; Waltham, 2005). Mining proceeded nearly continuously over the last five centuries and it is estimated that between 20,000 and 40,000 metric tons of Ag were produced from 1545 to 1824 and nearly 10,000 metric tons from 1824 to present (Lindgren, 1928; Zartman and Cunningham, 1995; Pretes, 2002; Abbot and Wolfe, 2003). Abbot and Wolfe (2003) also postulate that thousands of metric tons of Ag were produced from Cerro Rico and nearby deposits in Pre-Colombian times before and after the Incan conquest from the 10^{th} to the 15^{th} centuries. Ores from Potosí subsidized Spanish wars in Europe while millions of forced indigenous and slave African laborers died premature deaths mining the depths of Cerro Rico and processing the ores found within (Galeano, 1971; Tandeter, 1981; Bakewell, 1984). In addition, the environmental cost of Potosí's good fortune has been steep. Terrestrial zones have experienced extreme deforestation and soil loss while local watercourses have been impacted by mineral processing effluent and acid mine drainage (AMD).

Acid Mine Drainage

Economically-valuable geologic deposits such as coal and metal ores are normally chemically stable under undisturbed in-situ conditions. AMD forms when isolated sulfide ores, such as pyrite, sphalerite and galena, are exposed to oxygen and water (Younger et al., 2002). Microbes such as *Acidithiobaccillus ferrooxidans* increase the rate of AMD evolution by catalyzing mineral oxidation (Younger et al., 2002). This mineral oxidation creates and mobilizes free metal and hydrogen ions into solution, often to be transported to discharge points such as seeps, adits or boreholes which then impact downstream environments.

The environmental cost of AMD has been known for years. The man who is considered the founder of geology as a discipline, Georgius Agricola, stated in the 16^{th} century that "…when the ores are washed, the water which has been used poisons the brooks and streams, and either destroys the fish or drives them away" (Agricola, 1556). The ecotoxic metal ions, acidity and resultant precipitates (such as iron oxyhydroxide often referred to as *ochre*) associated with AMD are a significant threat to freshwater resources and can cause fish-kills and lasting degradation of aquatic habitats (Adams and Younger, 2000; Younger et al., 2002). AMD also often renders receiving watercourses unfit for use as water resources (Adams and Younger, 2000).

Geology

Cerro Rico of Potosí was created by volcanic eruptions of the Tertiary Age (Fig. 1). It lies within a Neogene-Quaternary volcanic-plutonic complex stretching for approximately 800 km along the Eastern Cordillera of the Central Andes (Zartman and Cunningham, 1995; Kamenov et al., 2002). Ore occurs throughout systems of veins in a conical dacitic volcanic dome rising 700 m above the city of Potosí (Zartman and Cunningham, 1995). Argentiferous magma crystallized into cassiterite-rich veins formed in Ordovician slate, dacitic tuff and tuff breccia, and other

dacitic stock (Griess, 1951; Brading and Cross, 1972; Rice and Steele, 2005). The veins are enclosed in zones of Ag and base metal sulfides, oxides and gangue minerals such as quartz, tourmaline, siderite and kaolinite. Silver oxides predominated in the upper altitudes of Cerro Rico while Ag sulfide ores dominate in the lower reaches (Bartos, 2000). Host rock is pyritized near the veins and pyrite "predominates greatly in the ores" according to Lindgren (1928). The Sn mineral, cassiterite, is found finely disseminated through pyrite (Petersen, 1945). Pyrite is the prime source of AMD formation and its pervasiveness indicates that AMD will be released to the surrounding areas for decades or centuries unless remedial actions are undertaken.

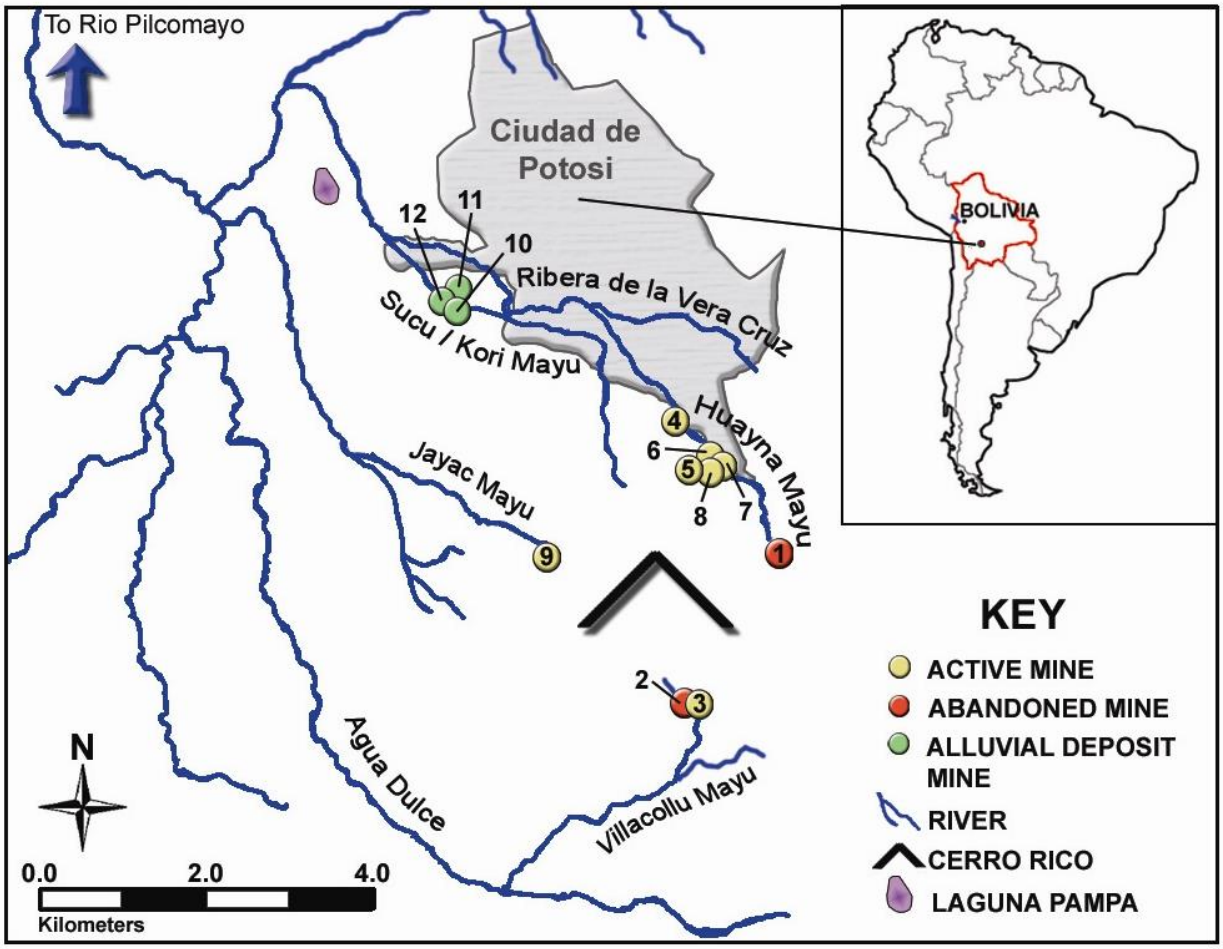

Figure 1. Study area and numbered AMD sources sampled with respect to receiving streams, greater Bolivia and South America

Potosí's Mining History and Legacy

The history of Potosí, like many historic mining centers, is one of cyclical boom and bust that has likely maximized AMD evolution. Many local mines have been abandoned, flooded, dewatered and mined again multiple times (Hillman, 1984). There is evidence from Pb-contaminated historical lake sediments that mining and smelting for Ag production began at Cerro Rico around 1000 A.D (Abbot and Wolfe, 2003). Cerro Rico is considered the world's largest Ag deposit and Potosí led the world in production during the 16th and 17th centuries

(Lofstrom, 1970; Zartman and Cunningham, 1995; Bartos, 2000; Rice and Steele, 2005). Ag production peaked in the late 16th century when there were over 600 mines on the mountain working a vertical interval of approximately 250 m (Waltham, 2005). However, eventually Ag market prices fell and ore quality decreased so that by 1825 Cerro Rico was home to more than 5,000 open mine shafts and adits, most of which were abandoned, flooded or caved in (Lofstrom, 1970). Of those shafts, only 50-60 were in use and the lower majority of the mountain was flooded (Lofstrom, 1970). In the 1800s Potosí's population had fallen from a maximum of approximately 160,000 during the Ag boom of the 1600s to about 10,000 as Ag mining became less profitable (Pretes, 2002).

Resurgence of the Ag industry from 1850-73 enabled by lower Hg prices (Hg was used in the amalgamation technique for processing Ag sulfides) caused the dewatering and re-start of many mines (Hillman, 1984). In the latter half of the 1800s, Potosí's fortunes rebounded yet again with the emergence of the Sn industry as the Ag industry declined (Hillman, 1984). As of 1928, many veins in Potosí had been worked over a vertical interval of approximately 600 m (Lindgren, 1928). The pinnacle of the Sn industry was in the first half of the 20th century when Bolivia was one of the top three worldwide Sn producers during World War II (Griess, 1951). Although the Sn industry was first established by the Incas, Sn only surpassed Ag in economic importance around the turn of the 20th century (Hillman, 1984; Godoy, 1985). At this time Sn miners dewatered and worked former Ag mines as well as alluvial deposits (*pallacos*) at the base of Cerro Rico (Bartos, 2000; Waltham, 2005). However, the 1985 Sn price collapse caused the closure and flooding of many Potosí mines (Waltham, 2005; Younger, *in press*). Ag, Pb, Sn and Zn prices have risen in recent years, leading to yet another boom cycle of dewatering and ore exploitation. As of 2000, mine workings had extended to a vertical interval of 1,150 m (Bartos, 2000). The repeated flooding, dewatering and mining of Cerro Rico has likely led to near-continuous production of high-strength AMD for centuries as freshly exposed sulfide minerals contact water during non-operational periods. The subsequent dewatering allows for oxygen ingress and fresh mineral exposure as the cycle is repeated.

Mining and mineral processing technology applied in Potosí has generally lagged behind contemporary methods. In the 19th century, human porters were used to remove ore in Potosí while railcars and steam power were used in Europe (Lofstrom, 1970). Through the 20th century poorly maintained and operated equipment and facilities were a hallmark of Bolivian mining (Godoy, 1985). Currently, the mining cooperatives on Cerro Rico tend to maximize labor by utilizing manpower over machinery (Waltham, 2005). Pneumatic drills and dynamite are used to drill and blast. Hand-powered winches transport the ore through vertical intervals. Ore is manually shoveled into ore carts that are often pushed by laborers out of the mines. The sorted ore is then again manually shoveled onto ore trucks for transport to local processing plants.

Outdated mineral processing methods used in Potosi have led to the release of tons of heavy metals to the local landscape and waterways. At first, Incan smelting technology was applied to process the Ag oxide cap of Cerro Rico with small charcoal-fueled clay furnaces (*huayras*) (Abbott and Wolfe, 2003). During this period, thousands of active huayras illuminated the slopes of Cerro Rico (Bakewell, 1984). Abbott and Wolfe (2003) documented the diffuse Pb deposition from these operations in nearby lake sediments. It is likely that other ecotoxic heavy metals common within Cerro Rico ores, such as As and Cd, were dispersed into the local environment during this period as well. In 1572, Hg amalgamation replaced smelting as the primary Ag extraction process as mine workings moved deeper into Cerro Rico where Ag sulfide

ores predominate (Bartos, 2000; Abbot and Wolfe, 2003). Amalgamation involves the mixing of Hg with pulverized ore to form denser Hg-Ag amalgam (Miller et al., 2004). The amalgam is heated to vaporize the Hg, leaving condensed Ag. From the 1570s to the 1810s, roughly 220,000 kg/year of Hg was mined and used in Peru, which included Bolivia at the time (Brading and Cross, 1972). Of this, the majority went towards the amalgamation process in Potosí (Brown, 2001). Wasteful use of Hg in amalgamation processes has been documented and estimates suggest that 0.85-4.1 kg of Hg was lost to the environment for every kg of Ag produced (Lofstrom, 1970; Nriagu, 1993). Hg and other heavy metals associated with mining waste were released into the local atmosphere and waterways (Nriagu, 1993; Miller et al., 2004). Nriagu (1993) has suggested that total discharge of Hg from ore processing in Peru, which then included Bolivia, was approximately 196,000 tons. As Cerro Rico was the primary colonial mine and Hg consumer, it can be assumed that the majority of that 196,000 tons was associated with mining at Potosí.

Local streams receive froth flotation effluent and pyrite-rich tailings from local mills as well as AMD from the extensive mine shafts within Cerro Rico and large tailings piles around the mountain called *sucu* (Bocangel, 2001; Miller et al., 2004). Currently, most ore processing facilities within Potosí are outdated flotation systems using disproportionate amounts of reagents (Bocangel, 2001). Aside from tremendous anthropogenic alterations in local groundwater hydrology, surface waters in Potosí bear no semblance to the pre-mining landscape. Twenty ponds were built close to an artificial channel that crosses Potosí east to west, the Ribera de la Vera Cruz, constructed in 1575 (Brading and Cross, 1972) (Figure 1). The Ribera still crosses Potosí with metal-laden effluent and its water is used by multiple ore processing facilities producing Pb, Ag, Zn, and Sn (Gioda et al., 1998; Bocangel, 2001). These facilities currently discharge sulfurous solids, cyanide, and elevated levels of heavy metals (Bocangel, 2001).

An additional canal has been recently built to shunt ore processing effluent west of the city into Laguna Pampa, an inadequately constructed tailings impoundment that is over-capacity and posing a possible failure hazard. Over the centuries and until the last few years, nearly all tailings were discharged directly into the Ribera de la Vera Cruz. Mining activities, pre-Laguna Pampa, were estimated to annually release approximately 360,000 tons of mining related sludge to Ribera de la Vera Cruz (Smolders et al., 2002). Despite the new tailings canal and tailings impoundment, some processing effluent still regularly enters the Ribera de la Vera Cruz, often washed in during rain events from an overflowing tailings canal and/or poorly designed floatation ponds. The current state of Laguna Pampa, and slow pace of construction on a new tailings impoundment, could necessitate the reintroduction of tailings to the Ribera de la Vera Cruz within the next year.

Broad and progressive Bolivian environmental legislation became law in 1992 (BMSDP, 2000). The law (Number 1333) regulates pollutant discharges of nearly all industries, sets water quality standards for receiving bodies and establishes limits for liquid discharges. However, it appears to have been largely ignored by the mining industry (Garcia-Guinea and Harffy, 1998). Article 45 of the Bolivian Mining Code states: "that mining operations should use systems and technology compatible with environmental protection (Bocangel, 2001)." The Bolivian government issued and widely publicized Supreme Decree 25419, requiring all mining operations to obtain an environmental license (Bocangel, 2001). Supreme Decree 25877 extended the deadline for compliance and has also met very limited success (Bocangel, 2001). It

is likely that, in addition to discharging effluent out of compliance with Bolivian law, many mining facilities have not acquired an environmental license.

Previous Studies

Intensive mining over several centuries has devastated the environment around Potosí. Potosí is near the headwaters of a major Bolivian watershed, the Rio Pilcomayo which flows from central Bolivia east to Argentina. Contamination limits the uses of the Rio Pilcomayo and water is precious in the arid western Cordillera Real and Chaco regions of southern Bolivia (USACE, 2004). Immediately downstream of Cerro Rico near the western edge of Potosí's city limits, Hudson-Edwards et al. (2001) found dissolved metals concentrations orders of magnitude above background levels (Table 1). However, the pH was 10.3, which limited the solubility of metals species and indicates that local mineral processing plants were discharging directly to local streams at the time. Near the same location, Smolders et al. (2003) found dissolved metals concentrations similar to that found by Hudson-Edwards et al., (2001). Total metals concentrations were found by Smolders et al. (2003) to be orders of magnitude greater than the dissolved levels (Table 1). Miller et al. (2002 and 2004) documented severe contamination of water and sediments up to 200 km downstream of Cerro Rico. Miller et al. (2002) linked this contamination to mining activity via isotopic analysis of Pb in sediment. Smolders et al. (2002 and 2004) sampled dissolved ions and suspended solids over 500 km downstream at Villa Montes to find vast differences in pollution levels between the rainy (December – March) and dry (May – September) seasons. This study found that in the rainy season, when heavy erosion from uncontaminated sources dilutes the metals concentrations of suspended solids, suspended solids averaged 23.6 g/L with Zn, Cu, Pb and Cd levels of 139, 23.9, 35.3 and 0.55 mg/kg dry weight, respectively (Smolders et al., 2002). In the dry season, when mining related effluent contributes a higher proportion of flow, suspended solids averaged 0.011 g/L with Zn, Cu, Pb and Cd levels of 19327, 1107, 1495 and 12.4 mg/kg dry weight, respectively (Smolders et al., 2002). This heavy metals pollution dramatically reduced the diversity of benthic macro-invertebrate communities downstream of the Cerro Rico mines (Smolders et al., 2003). However, the environmental effects of mining on the lower Rio Pilcomayo are lessened by the dilution of both dissolved and suspended heavy metal ions and compounds by uncontaminated waters and sediment (Smolders et al., 2002). Smolders et al. (2002) posit that a maximum of 0.3% of the sediment reaching Villa Montes is mining related.

Primary human exposure pathways in the region are likely through ingestion and inhalation of airborne particulates and contaminated water, agricultural produce and fish consumption (Smolders et al., 2002; Miller et al., 2004). Downstream communities rely on river water for irrigation, washing and occasional cooking and drinking (Garcia-Guinea and Harffy, 1998; Archer et al., 2005). Little study has been undertaken to quantify contaminant levels in humans. However, human hair and urine As concentrations in some downstream Rio Pilcomayo communities exceed published values for non-occupationally exposed subjects (Archer et al., 2005). Concentrations of Cd, Pb and Zn in some local agricultural soils exceed recommended guidelines for agricultural usage (Miller et al., 2004). Increased local human exposure risks are present because rural communities in the region have been found to consume 56 plant species for medicinal purposes (Fernandez et al., 2003). Distant consumers could be at risk as well because contaminated irrigation water is used extensively to grow vegetables for sale in greater Bolivia (Miller et al., 2004). The lower Rio Pilcomayo is also a major fishery. The sábalo (*Prochilodus platensis*) fishery in the lower Pilcomayo is the most important commercial fish in Bolivia

according to Payne and Harvey (1989). However, heavy metal concentrations in sábalo are below international threshold values (Smolders et al., 2002).

Table 1. Aqueous metals concentrations in downstream grab samples taken in previous studies in and downstream of Potosí.

Site	Type	pH	As	Cd	Cu	Pb	Zn	Season	Source
			- - - - - - - - - - - - - mg/L - - - - - - - - - - - - -						
Potosí	dissolved	10.3	0.065	0.01	0.3	0.041	0.035	dry-1998	H-E
Potosí	dissolved	NR	NR	0.00076	0.014	0.0285	0.238	dry-1999	S
Potosí	totals	NR	NR	0.0592	0.304	1.399	6.021	dry-1999	S
El Molino	totals	NR	12.8	NR	NR	NR	NR	dry-2003	A
El Molino	totals	NR	2.74	NR	NR	NR	NR	wet-2004	A
Rio Tarapaya	dissolved	NR	NR	0.005	0.013	0.056	0.601	dry-1999	S
Rio Tarapaya	totals	NR	NR	0.315	1.709	2.291	12.416	dry-1999	S
Tasapampa	totals	NR	0.272	NR	NR	NR	NR	dry-2003	A
Tasapampa	totals	NR	0.113	NR	NR	NR	NR	wet-2004	A
Tuero Chico	totals	NR	0.154	NR	NR	NR	NR	dry-2003	A
Tuero Chico	totals	NR	0.199	NR	NR	NR	NR	wet-2003	A
Sotomayor	totals	NR	1.213	NR	NR	NR	NR	dry-2003	A
Sotomayor	totals	NR	0.421	NR	NR	NR	NR	wet-2003	A
Villa Montes	dissolved	8.77	0.03	<0.01	<0.02	0.025	0.016	dry-1998	H-E
Villa Montes	dissolved	NR	NR	0.00039	0.0022	0.0007	0.017	dry-1999	S
Villa Montes	totals	NR	NR	0.00077	0.017	0.0198	0.186	dry-1999	S

H-E = Hudson-Edwards et al., 2001
S = Smolders et al., 2003
A = Archer et al., 2005
NR = Not reported

Although downstream heavy metals contamination has been fairly well-documented, contamination sources have not. This study was executed to characterize one of the sources of heavy metals pollution to the upper Rio Pilcomayo to better understand the relationship between downstream pollution and upstream sources. The dry season was chosen for the study to establish baseline AMD flow rates and physical and chemical parameters.

Methods

Study Area

The study centered around Cerro Rico, approximately 1 km south of Potosí, Bolivia. Potosí (19.585°S 65.754°W) lies in the Eastern Cordillera range of the Central Andes in the upper reaches of the Rio Pilcomayo watershed. The Rio Pilcomayo is a chief tributary of the Rio de la Plata system, a crucial water resource for south-central and southeastern South America. The sampled AMD sources drain to streams that reach Rio Tarapaya, which later combines with Rio Yocalla approximately 30 km downstream to become the Rio Pilcomayo. The Rio Pilcomayo flows in a general southeasterly direction down the Eastern Cordillera range and through the semi-arid Chaco Plains. Eventually the Rio Pilcomayo forms Argentina's northern border with Paraguay before it diffuses, and partially disappears beneath the surface, into a wide alluvial fan that empties into the Rio Paraguay at Asunción, Paraguay.

AMD sources identified and sampled were from active and abandoned mine portals of Cerro Rico and mineral-rich *pallacos* at the Northwest base of Cerro Rico (Figures 1-2). The sources documented in this study are those which were actively producing AMD during Potosí's dry season of July 2006 and those not intercepted for mineral processing use. Innumerable working and abandoned mines dot Cerro Rico, however many are reported to not produce AMD. Mines likely to be producing drainage near the base of Cerro Rico were visited in this field study. The majority of those mines were not actively draining at the time. Of the eight AMD sources sampled on Cerro Rico proper, six were from active mines. Discharge sites 1 and 4-8 drain to Rio Huayna Mayu which empties into the highly polluted Ribera de la Vera Cruz, which contains raw sewage from the city, AMD and processing plant effluent before the junction. Sites 2 and 3 drain to Rio Villacollu Mayu which empties into the relatively pristine Rio Agua Dulce. Site 9 drains to the highly impacted Rio Jayac Mayu ("spicy river" in Quechua, the language of the Inca) which also receives diffuse AMD from numerous waste rock piles near its source. The *pallacos* AMD sources (sites 10-12) are associated with natural and anthropogenic erosion of mineral-rich material from Cerro Rico and the Sn mining of that material that ceased decades ago (Bartos, 2000; Waltham, 2005). These sources may also be influenced by polluted groundwater seepage from the San Miguel tailings dump. Rio Sucu / Kori Mayu receives drainage from the *pallacos* AMD sources and soon thereafter empties into the Ribera de la Vera Cruz.

Figure 2. AMD sources 1 (left) and 8 (right). Source 1 is an abandoned mine near the eastern base of Cerro Rico. Source 8 is a functioning mine on the north slope of Cerro Rico.

Water quality parameters and samples were obtained at AMD sources at the mouths of working and abandoned mines in July and August of 2006. The location of each sample point

was recorded with a Garmin® GPS unit. Acidity and alkalinity titrations were conducted in the field following standard methods (APHA, 1998). Temperature, pH, dissolved oxygen (DO) and specific conductance were determined using a properly calibrated Orion 1230 multimeter. All grab samples were taken using 125-mL HDPE containers for later analyses at the University of Oklahoma Center for the Restoration of Ecosystems and Watersheds laboratories. Total metals samples were preserved with concentrated nitric acid and stored at 4 °C until microwave acid digestion following EPA method 3015. Digested metals samples were filtered through 0.45 µm nylon filters then analyzed via a Varian Vista-Pro® simultaneous inductively coupled plasma-optical emission spectrometer (ICP-OES) following EPA method 6010. Samples for anion analyses were stored at 4 °C until filtered through Dionex OnGuard® II H cartridges and 0.2 µm nylon filters. A MetrOhm® 761 Compact ion chromatograph (IC) unit was used to quantify sulfate concentrations following EPA method 300.0. As a field backup, sulfate was also quantified on-site using EM QUANT® 200-1600 ppm test strips. Samples were diluted when concentrations were greater than 1600 ppm.

Flow rates (Q) were obtained via two methods. When possible, flow rates were obtained by building temporary weirs and determining time to gather a known volume in a bucket or graduated cylinder. When flow rates were greater than this method would allow, discharge was estimated by determining channel cross-section, depth and velocity as approximated by floating a partially submersible object a given distance.

Results and Discussion

Physical parameters, sulfate and total metals concentrations for sampled AMD sources are presented in Tables 2 and 3. These results may be compared to various water quality criteria set by the Bolivian government and, for reference purposes only, the US Environmental Protection Agency (EPA) in Table 4. Concentrations of contaminants in sampled AMD sources were orders of magnitude out of compliance with Bolivian discharge limits and contributed to the aforementioned pollution downstream.

Table 2. Mean physical parameter measurements from AMD sources around Cerro Rico

Site	pH	Net Acidity[a] (mg/L as $CaCO_3$ eq.)	DO (mg/L)	Sp. Cond. (µS/cm)	Temp. (°C)	Q (L/s)
1 (n = 3)	3.56±0.08	911	6.6±1.2	1888±72	8.4±0.3	0.86
2 (n = 2)	2.90	7656	1.3	7530	7.2	0.02
3 (n = 2)	3.23	ND	2.2	3160	1.8	0.17
4*	3.30	ND	0.8	9470	4.4	†
5*	3.15	11375	4.4	8690	2.7	0.13
6*	3.02	ND	2.9	14920	10.0	0.07
7*	3.02	ND	4.1	19070	5.0	†
8*	2.97	ND	3.5	10440	5.0	†
9*	2.46	ND	6.1	18640	5.5	0.28
10*	6.39	43.2	6.6	893	12.3	0.10
11*	2.96	1344	2.5	2820	13.1	0.26
12*	4.20	63	4.7	1115	12.4	4.59

† Flow rates not detectable ND = Not determined * n = 1 [a]Net acidity = total acidity – total alkalinity, alkalinity and acidity titrations necessary for net acidity were performed once

Table 3. Mean sulfate and total metal concentrations determined for grab samples of AMD sources around Cerro Rico

Site	Al	As	Ca	Cd	Co	Cr	Cu	Fe	Mg	Mn	Na	Ni	Pb	Zn	SO_4^{2-}	SO_4^{2-}‡
	mg/L															
1 (n = 5)	4.88 ±0.16	0.03 ±0.01	104 ±2.2	0.17 ±0.02	0.139 ±0.004	0.053 ±0.000	0.037 ±0.004	107 ±6.9	16.8 ±0.36	13.4 ±0.63	15.6 ±0.41	0.165 ±0.006	0.073 ±0.009	616 ±29	1323	1200-1600
2 (n = 3)	72.4 ±1.9	21.4 ±0.97	130 ±1.5	7.77 ±0.04	0.591 ±0.003	0.031 ±0.001	0.047 ±0.001	2449 ±100	34.3 ±0.36	146 ±7.7	10.1 ±0.28	0.817 ±0.022	0.51 ±0.019	3500 ±175	9184	4000-8000
3 (n = 3)	99 ±5.9	14.4 ±5.67	210 ±2.5	0.54 ±0.05	1.073 ±0.01	0.033 ±0.002	0.41 ±0.021	595 ±94	52.8 ±0.91	58.6 ±1.70	6.63 ±0.19	0.585 ±0.010	7.78 ±4.79	380 ±6.1	3395	2400-3200
4*	389	30.2	44.0	7.33	2.49	0.087	11.0	7200	512	438	15.5	4.34	1.46	3330	ND	24000-32000
5*	581	45.2	477	19.5	1.92	0.243	92.7	3680	234	92	38.6	2.07	1.20	4950	ND	12800-19200
6*	686	8.0	21.4	50.7	4.03	0.142	10.2	3850	86.4	46.9	9.9	5.72	0.63	10200	ND	9600-12800
7*	641	33.4	116	37.6	3.82	0.129	12.5	3140	62.7	35.2	27.5	6.18	2.50	11800	ND	12800-19200
8*	231	0.58	76.3	12.7	2.00	0.031	1.80	874	31.1	19.7	16.0	2.98	0.21	4400	ND	9600-12800
9*	977	191	68.8	38.3	2.61	0.401	161	7320	25.6	54.6	13.2	2.36	15.0	11500	ND	24000-32000
10*	0.284	BDL	95.8	0.025	BDL	BDL	0.03	0.15	32.0	0.30	43.4	0.026	0.028	4.86	ND	400-800
11*	134	BDL	251	0.69	0.344	0.296	24.8	56.7	65.7	51.0	41.7	0.297	0.05	108	ND	1600-3200
12*	6.68	BDL	115	0.089	0.018	0.016	0.59	0.36	37.1	3.62	43.1	0.10	0.047	14.2	ND	400-800

‡ These sulfate ranges were obtained in the field with EM QUANT® sulfate test strips
BDL = Below detection limits
ND = Not determined
* n = 1
Mean and standard deviations include two field duplicates taken at site 1 and one each at sites 2 and 3.

Table 4. Bolivian discharge and receiving body criteria with respect to US EPA drinking water standards

Standard	pH	Al	As	Ca	Cd	Co	Cr	Cu	Fe	Mg	Mn	Na	Ni	Pb	Zn	SO_4^{2-}
		mg/L														
Bolivian discharge[δ]	6-9		1.0		0.3		1.0/0.1[α]	1.0	1.0					0.6	3.0	
Bolivian discharge[μ]	6-9		0.5		0.15		0.5/0.05	0.5	0.5					0.3	1.5	
Bolivian class "A"	6.0-8.5	0.2	0.05	200	0.005	0.1	0.05	0.05	0.3	100	0.5	200	0.05	0.05	0.2	300
Bolivian class "B"	6-9	0.5	0.05	300	0.005	0.2	0.6/0.05[α]	1.0	0.3	100	1.0	200	0.05	0.05	0.2	
Bolivian class "C"	6-9	1.0	0.05	300	0.005	0.2	0.5/0.05[α]	1.0	1.0	150	1.0	200	0.5	0.05	0.2	
Bolivian class "D"	6-9	1.0	0.1	400	0.005	0.2	1.1/0.05[α]	1.0	1.0	150	1.0	200	0.5	0.05	0.2	400
US EPA primary			0.01		0.005		0.1	1.3						0.015		
US EPA secondary	6.5-8.5	0.05						1.0	0.3		0.05				5	250

[α] Cr (III) and Cr (VI) limits respectively
[δ] Daily discharge limits
[μ] Monthly average discharge limits

The active mines generally had higher total metals concentrations than the abandoned and alluvial deposit sources (Table 3). This is likely due to the presence of fine sulfurous solids in the drainage, probably from blasting and drilling within the mines. The alluvial deposit sources generally exhibited lower metals concentrations than the other abandoned and active mine sources. This is likely due to the increased weathering that the alluvial deposits have experienced. These deposits were created over millennia as surface rock of Cerro Rico weathered and migrated downhill. Much of the sulfides on the exposed surfaces of the alluvial deposits have likely been weathered, leaving more inert material that produces AMD of lower metals concentrations and acidity. The freshly exposed sulfides within Cerro Rico are likely leading to higher metals concentrations in the drainage of the active mines. Because Cerro Rico has been mined for centuries and many mines are interconnected due to the degree of exploration, the abandoned mine workings sampled in this study may be connected to and receive waters from active mines, thus sharing in the effect of fresh sulfide mineral exposure.

Many of the AMD sources documented in this study would likely result in violations of Bolivian receiving body water quality limits (Table 4). Class "A" receiving water bodies, those which are suitable for drinking without treatment or only with bacterial disinfection, have stringent water quality requirements (BMSDP, 2000). Class "D" is the lowest designation of Bolivian receiving water bodies in which industrial applications and navigation are the only suitable uses except in extreme circumstances. Bolivian law states that class "D" waters must be "coagulated, flocculated, filtered and disinfected" prior to domestic use (BMSDP, 2000). It is not known how the water bodies downstream of Potosí are designated. However, they are used for agriculture and therefore should be rated at a minimum above class D. The introduction of effluent orders of magnitude over class "D" limits is likely leading to non-compliance downstream.

All of the sources exceeded discharge limits to some degree and most by orders of magnitude. Six out of the twelve sources had higher than permissible Pb concentrations. Seven of the sources contained higher than permissible As and Cu concentrations. Nine of the sources contained higher than permissible Cd concentrations. Ten of the sources had higher than permissible Fe concentrations. Eleven of the sources had higher than permissible Zn concentrations and lower than permissible pH. For example, AMD source 2 discharged As, Cd, Fe and Zn concentrations 21.4, 25.9, 2449 and 1166 times greater than daily discharge limits. The data support the assertion of Garcia-Guinea and Harffy (1998) that Bolivian environmental law "has been sadly ignored where mining is concerned."

The AMD sources documented in this study contained elevated concentrations of the same heavy metal elements documented by earlier studies downstream. The majority of AMD sources had concentrations of As, Cd, Cu, Pb and Zn orders of magnitude higher than those found downstream. This indicates that these AMD sources are contributing to some degree to downstream heavy metals pollution in the upper Rio Pilcomayo basin.

The relative importance of pollution sources to the Rio Pilcomayo is unknown. Hudson-Edwards et al., (2001) and Smolders et al., (2003) stress the significance of mineral processing effluent in downstream contamination. However, these studies were undertaken when the tailings load to the upper Rio Pilcomayo was much higher, before the construction of the Laguna Pampa tailings dam. In addition, no published peer-reviewed studies have documented mineral processing effluent characteristics and quantity. This study is the first to characterize AMD sources. However, the dry season data presented in this study is insufficient to extrapolate

annual loading to downstream watercourses. The Smolders et al. (2002) study highlighted the need for both dry and rainy season data. It is likely that AMD flows are greater and metals concentrations lower in the rainy season, yet mass loads may be higher. Further research, including mineral processing effluent and rainy season AMD characterization and quantification will help solidify the relative importance of the Rio Pilcomayo's pollution sources. This information could help establish priorities for future remediation efforts.

Conclusions and Recommendations

The extraction and export of mineral wealth has dominated the political economy of Bolivia for centuries, however, the importance of mining has declined somewhat in recent decades (Griess, 1951; Hillman, 1984). However, Potosí's economy and roughly 150,000 residents are still heavily dependent upon mineral extraction and processing. Therefore, environmental law enforcement should be carefully applied and fitting solutions presented to lessen the impact of mining operations. Bolivia is currently the second poorest nation in the Western Hemisphere. Therefore, solutions attempted to address to the mine water pollution problems in Potosí can not be capital-intensive. A labor-intensive solution may be desirable because of high unemployment and underemployment in Potosí, as well as the low cost of local labor.

Passive systems may be more suitable than active systems for AMD treatment in Potosí. Passive treatment uses unrefined natural materials to promote natural chemical and biological processes to improve water quality (Younger et al., 2002). Active treatment, the improvement of water quality by methods that require ongoing inputs of energy and chemical reagents, generally have higher operational costs than passive systems (Younger et al., 2002). Highly mechanized construction or operational activities are not desirable in Potosí because of logistical and supply issues. In developed nations, passive treatment systems have higher up-front costs because of greater land and construction expenses (Younger et al., 2002). However in Bolivia depressed land and low construction costs may make passive treatment a logical solution from both long- and short-term perspectives. The chemicals, electricity and equipment needed for active treatment may make passive treatment by default the most applicable solution. Also, passive treatment system construction and metal reclamation could provide needed employment for Potosínos.

In 2000, Younger demonstrated passive treatment system feasibility on the slopes of Chacaltaya and Huayna Potosí, near La Paz, a setting nearly identical to the Cerro Rico de Potosí (Younger, in press). Limestone gravel and llama dung were set in a series of tanks receiving a continuous flow of AMD from the abandoned Milluni mine. The average pH rose from 3.2 to 6.3 and metals were taken out of solution even though the experiment ran through the coldest time of year when reaction rates are lowest (Younger, in press). There are documented limestone and dolomite deposits around Potosí (Zartman and Cunningham, 1995; Deconinck et al., 2000; Kamenov et al. 2002). The Cayara® lime plant on the outskirts of Potosi currently accepts limestone of 85-92% calcite from local sources, which indicates that high quality limestone for passive treatment is available. Llama dung is readily available around Potosí as domesticated llama herds roam nearby valleys and mountainsides. Other carbon sources for sulfate reducing bacteria are also available, including domestic sewage and waste sugar cane from lowland regions Northeast of Potosí. However, the ubiquity of Al in high concentrations within the AMD around Potosí precludes the application of anoxic limestone drains and limits the useful life of reducing and alkalinity producing systems.

Action is necessary to address the uniformly non-compliant AMD sources documented in this study. They are contributing to previously-documented downstream pollution. To determine the extent to which they are responsible, rainy season data must be collected. If environmental laws are to be enforced, care should be taken to ensure that the fragile mineral extraction and processing industries vital to Potosí can continue operation. Passive treatment may prove a suitable solution to the unique circumstances presented in the "Villa Imperial" (Imperial City) of Potosí.

Acknowledgements

We are grateful to Professors Franz Mamani and Elias Puch of the Universidad Autónoma de "Tomás Frías", Yoichi Matsuda of the Japan International Cooperation Agency and Patrick Stack for aiding greatly in field work and gathering local information key to this manuscript. Engineers Lionel Villarroel Gonzales, Mirko Kirigin, Huascar Beltrán and Primo Choque provided important data, logistical support, materials and contacts, without which this study would have been impossible. We would also like to thank Kristina Strosnider for assistance in mapping sampling sites. A University of Oklahoma Presidential International Travel Fellowship and United States Department of Education Graduate Assistance in Areas of National Need (GAANN) Fellowship partially funded this study.

Literature Cited

Abbot, M.B. and A.P. Wolfe. 2003. Intensive Pre-Incan metallurgy recorded by lake sediments from the Bolivian Andes. Science. 301: 1893-1895. http://dx.doi.org/10.1126/science.1087806.

Adams, R. and P.L. Younger. 2000. A strategy for modeling ground water rebound in abandoned deep mine systems. Ground Water. 39(2): 249-261. http://dx.doi.org/10.1111/j.1745-6584.2001.tb02306.x.

Archer, J., Hudson-Edwards, K.A., D.A. Preston, R.J. Howarth, and K. Linge. 2005. Aqueous exposure and uptake of arsenic by riverside communities affected by mining contamination in the Río Pilcomayo basin, Bolivia. Mineralogical Magazine. 69(5): 719-736. http://dx.doi.org/10.1180/0026461056950283.

American Public Health Association (APHA). 1998. Standard Methods for the Examination of Water and Wastewater. 20th Ed.

Bakewell, P. 1984. Miners of the Red Mountain: Indian Labor in Potosí, 1545-1650. Albuquerque: The University of New Mexico Press.

Bartos, P.J. 2000. The pallacos of Cerro Rico de Potosí, Bolivia: a new deposit type. Economic Geology and the Bulletin of the Society of Economic Geologists. 95: 645-654. http://dx.doi.org/10.2113/95.3.6454.

Bocangel, D. 2001. Small-scale mining in Bolivia: national study mining minerals and sustainable development. Mining, Minerals and Sustainable Development. 71.

Bolivian Ministry of Sustainable Development and Planning (BMSDP). 2000. Ley del medioambiente – No. 1333.

Brading, D.A. and H.E. Cross. 1972. Colonial silver mining: Mexico and Peru. The Hispanic American Historical Review. 52: 545-579. http://dx.doi.org/10.2307/25127819.

Brown, K.W. 2001. Workers' health and colonial mercury mining at Huancavelica, Peru. The Americas. 57(4): 467-496. http://dx.doi.org/10.1353/tam.2001.0030.

Deconinck, J.F., M.M. Blanc-Valleron, J.M. Rouchy, G. Camoin and D. Badaut-Trauth. 2000. Palaeoenvironmental and diagenetic control of the mineralogy of Upper Cretaceous-Lower Tertiary deposits of the Central Palaeo-Andean basin of Bolivia (Potosí area). Sedimentary Geology. 132: 263-278. http://dx.doi.org/10.1016/S0037-0738(00)00035-X.

Fernandez, E.C., Y.E. Sandi and L. Kokoska. 2003. Ethnobotanical inventory of medicinal plants used in the Bustillo Province of the Potosí Department, Bolivia. Fitoterapia. 74: 407-416. http://dx.doi.org/10.1016/S0367-326X(03)00053-4.

Galeano, E. 1971. The Open Veins of Latin America. Monthly Review Press, New York.

Garcia-Guinea, J. and M. Harffy. 1998. Bolivian mining pollution; past present and future. Ambio. 27(3): 251-253.

Gioda, A., C. Serrano and M. Frey. 1998. Water and silver in Potosí (Bolivia). Houille Blanche-revue Internationale de l'eau. 53: 65-75.

Godoy, R.A. 1985. Technical and economic efficiency of peasant miners in Bolivia. Economic Development and Cultural Change. 34: 103-120. http://dx.doi.org/10.1086/451511.

Griess, P.R. 1951. The Bolivian tin industry. Economic Geography. 27: 238-250. http://dx.doi.org/10.2307/141097.

Hillman, J. 1984. The emergence of the tin industry in Bolivia. Journal of Latin American Studies. 16: 403-437.

http://dx.doi.org/10.1017/S0022216X00007124.

Hudson-Edwards, K.A., M.G. Macklin, J.R. Miller and P.J. Lechler. 2001. Sources, distribution and storage of heavy metals in the Rio Pilcomayo, Bolivia. Journal of Geochemical Exploration. 72: 229-250. http://dx.doi.org/10.1016/S0375-6742(01)00164-9.

Kamenov, G., A.W. Macfarlane, and L. Riciputi. 2002. Sources of lead in the San Cristobal, Pulacayo, and Potosí mining districts, Bolivia, and a reevaluation of regional ore lead isotope provinces. Economic Geology. 97: 573-592. http://dx.doi.org/10.2113/97.3.573.

Lindgren, W. 1928. Mineral Deposits. McGraw- Hill, New York.

Lofstrom, W. 1970. Attempted economic reform and innovation in Bolivia under Antonio Jose de Sucre, 1825-1828. The Hispanic American Historical Review. 50: 279-299. http://dx.doi.org/10.2307/2513027.

Miller, J.R., P.J. Lechler, K.A. Hudson-Edwards and M.G. Macklin. 2002. Lead isotopic fingerprinting of heavy metal contamination, Rio Pilcomayo basin, Bolivia. Geochemistry: Exploration, Environment, Analysis. 2: 225-233. http://dx.doi.org/10.1144/1467-787302-026.

Miller, J.R., K.A. Hudson-Edwards, P.J. Lechler, D. Preston and M.G. Macklin. 2004. Heavy metal contamination of water, soil and produce within riverine communities of the Rio Pilcomayo basin, Bolivia. Science of the Total Environment. 320: 189-209. http://dx.doi.org/10.1016/j.scitotenv.2003.08.011.

Nriagu, J. 1993. Legacy of mercury pollution. Nature. 363: 589. http://dx.doi.org/10.1038/363589a0.

Payne, A.I. and M.J. Harvey. 1989. An assessment of the prochilodus platensis holmberg population in the Pilcomayo River fishery, Bolivia using scale-based and computer-assisted methods. Aquaculture and Fisheries Management. 20: 223-248. http://dx.doi.org/10.1111/j.1365-2109.1989.tb00349.x.

Petersen, E.F. 1945. Mining and development, Potosí, Bolivia. Mines Magazine. 35: 19-20.

Pretes, M. 2002. Touring mines and mining tourists. Annals of Tourism Research. 29: 439-456. http://dx.doi.org/10.1016/S0160-7383(01)00041-X.

Rice, C.M. and G.B. Steele. 2005. Duration of magmatic hydrothermal and supergene activity at Cerro Rico de Potosi, Bolivia. Economic Geology 100: 1647-1656. http://dx.doi.org/10.2113/gsecongeo.100.8.1647.

Smolders, A.J.P., M.A. Guerrero Hiza, G. Van der Velde and J.G.M. Roelofs. 2002. Dynamics of discharge, sediment transport, heavy metal pollution and sábalo (prochilodus lineatus) catches in the lower Pilcomayo river (Bolivia). River Research Applications. 18: 415-427. http://dx.doi.org/10.1002/rra.69027.

Smolders, A.J.P., R.A.C Lock, G. Van der Velde, R.I. Medina Hoyos and J.G.M. Roelofs. 2003. Effects of mining activities on heavy metal concentrations in water, sediment, and macroinvertebrates in different reaches of the Pilcomayo river, South America. Archives of Environmental Contamination and Toxicology. 44: 314-323. http://dx.doi.org/10.1007/s00244-002-2042-1.

Smolders, A.J.P., K.A. Hudson-Edwards, G. Van der Velde and J.G.M. Roelofs. 2004. Controls on water chemistry of the Pilcomayo river (Bolivia, South-America). Applied Geochemistry. 19: 1745-1758. http://dx.doi.org/10.1016/j.apgeochem.2004.05.001.

Tandeter, E. 1981. Forced and free labour in Late Colonial Potosí. Past and Present. 93: 98-136. http://dx.doi.org/10.1093/past/93.1.98.

United States Army Corps of Engineers. 2004. Water Resources Assessment of Bolivia.

Waltham, T. 2005. The rich hill of Potosí. Geology Today. 21(5): 187-190. http://dx.doi.org/10.1111/j.1365-2451.2005.00528.x.

Wilson, W.E. and A. Petrov. 1999. Famous mineral localities: Cerro Rico de Potosí, Bolivia. Mineralogical Record. 30: 9-36.

Younger, P.L., S.A. Banwart and R.S. Hedin. 2002. Mine Water: Hydrology, Pollution, Remediation. Kluwer Academic Publishers, Boston. http://dx.doi.org/10.1007/978-94-010-0610-1.

Younger, P. in press. Pro-poor water technologies working both ways: lessons from a two-way, south-north interchange. Geoforum. http://dx.doi.org/10.1016/j.geoforum.2005.10.006.

Zartman, R.E. and C.G. Cunningham. 1995. U-Th-Pb zircon dating of the 13.8-Ma dacite volcanic dome at Cerro Rico de Potosí, Bolivia. Earth and Planetary Science Letters. 133: 227-237. http://dx.doi.org/10.1016/0012-821X(95)00093-R.

ATTACHMENT 26

Part II. Performance Evaluation of Reverse Osmosis Membrane Computer Models

Final Report

by
Erika Mancha
Don DeMichele
W. Shane Walker, Ph.D., P.E.
Thomas F. Seacord, P.E.
Justin Sutherland, Ph.D., P.E.
Aaron Cano

Texas Water Development Board

P.O. Box 13231, Capitol Station
Austin, Texas 78711-3231
January 2014

It is important to consider that the model output can only be as accurate as the information provided to it. Table 3-2 summarizes these key model input parameters that are subsequently discussed in greater detail.

3.3.1 *Feed Water Quality Data*

The various computer models have similar user interfaces for inputting feed water quality data. There are two steps to establish the feed water quality:

1. *Input source water classification.* For the purposes of this study, the water source or water type is limited to brackish water; however, brackish water is also identified in the models as well water, brackish well water, and well water with a silt density index less than 3. In the computer models, the source water classification is linked with guidelines and warnings that include limits for salt saturation, flux, and concentrate flow rate.
2. *Input the source water quality data*. Table 3-3 lists ions common among the six software models. The element iron is an input in all the programs except in the ROSA model. Winflows and KMS ROPRO also allow the user to specify manganese concentrations. Other ions such as bromide and phosphate can also be entered in feed water quality for the Winflows and TorayDS programs. In addition, hydrogen sulfide can be entered for Winflows and IMSdesign models.

The mineral data required by the computer models constitute the major cations and anions found in natural waters. The validity of the analytical data entered into the software model and the subsequent mineral scaling (solubility) calculations used to determine the maximum recovery that can be achieved, both depend on the accuracy of these inputs.

Because of the importance of carbonate chemistry in determining appropriate pretreatment and recovery limits, computer models require the user to define the concentration of the various carbonate species, which is both pH and temperature dependent. However, the entry and methods used to determine of the concentration of carbonate species (such as, $CO_2/HCO_3^-/CO_3^{2-}$) vary based upon the computer model used:

- ROSA, Toray DS2, CSMPRO, and IMSdesign require the user to input pH, temperature, and concentration of bicarbonate. Using this information, the model calculates the concentrations of carbonate and carbon dioxide.
- Winflows requires the user to enter pH, temperature, and the total alkalinity as calcium carbonate. The concentrations of bicarbonate, carbonate, and carbon dioxide are subsequently determined by calculation.
- KMS ROPRO allows the user to enter pH, temperature, bicarbonate, and carbonate concentrations, but the user can also enter the P-alkalinity or M-alkalinity, where P-alkalinity is the amount of carbonate and hydroxyl alkalinity present and M-alkalinity (also known as total alkalinity) is the amount of bicarbonate, carbonate, and hydroxide present in the water. When the user enters the bicarbonate and carbonate value, the pH value is recalculated, and the model provides the user with a warning stating the pH will be adjusted.

ATTACHMENT 27

THE CANADIAN MINE ENVIRONMENT NEUTRAL DRAINAGE (MEND) INITIATIVE

Gilles A. Tremblay

Natural Resources Canada – CANMET/MEND - 555 Booth Street - Ottawa, Ontario - K1A 0G1 – Canada – gtrembla@nrcan.gc.ca

ABSTRACT

Acidic drainage has long been recognized as the largest environmental liability facing the Canadian mining industry, and to a lesser extent, the public through abandoned mines. The Mine Environment Neutral Drainage (MEND) Program was the first international multi-stakeholder initiative to develop scientifically-based technologies to reduce the effect of acidic drainage. A toolbox of technologies is now available to open, operate and decommission a mine property in an environmentally acceptable manner. This volunteer program established Canada as the recognized leader in research and development on acidic drainage. Through MEND, Canadian mining companies and the federal and provincial governments have reduced the liability due to acidic drainage by an estimated $340 million, an impressive return on an investment of $17.5 million over nine years.

The original MEND Program extended over a nine-year time frame ending in 1997; with technology transfer activities continuing to the end of year 2000 under the MEND 2000 program. MEND and MEND 2000 were described as a model way for governments, industry and non-governmental organizations (NGOs) to cooperate in technology development. This presentation will summarize the results that have been achieved, the lessons learned, and the opportunities for future actions. Case studies depicting Canadian full-scale applications of various technologies will be presented and discussed. Through these efforts a further reduction of the environmental liability associated with acidic drainage during mine life will be realized.

INTRODUCTION

One of the most significant environmental issues facing the global mining industry today is acidic drainage which affects all sectors of the industry including coal, precious metals (gold, silver), base metals (copper, nickel, zinc, lead), iron ore and uranium. Acidic drainage is the result of a natural oxidation process whereby sulfur-bearing minerals oxidize upon exposure to oxygen and water. The net result is the generation of metal-laden effluents of low pH that can potentially cause damage to ecosystems in the downstream environment. Acidic drainage is caused not only by mining activities but also civil works. Remedial measures are currently in place at an international airport in Canada after construction of a runway exposed sulphide minerals which in turn resulted in acidic drainage. Road and pipeline construction are also periodic contributors.

Although the issue of acidic drainage is not new and has an extensive history spanning decades (and even centuries in Europe), it is not fully understood. In the past 10 years, changes in socio-economic expectations and heightened environmental awareness have made the management of waste an increasingly pressing issue in the mining industry (Price, 1995), with the result that the industry is one of the more intensively regulated and scrutinized of all industries. Extensive liabilities have been generated in countries such as Canada, the United States, Australia, Sweden and Germany by the inability to adequately deal with acidic drainage issues. Other countries such as Brazil, Peru and Argentina have recently discovered their own problems with acidic drainage. These liabilities are essentially the costs incurred by the property owner/manager during or after the life of the mine to ensure that the impact to the environment is minimized and consistent with environmental regulations. Costs typically include: the collection and treatment of acidic drainage; construction of engineered structures to contain mine wastes; relocation of mine wastes to containment areas; and rehabilitating the mine, mill and containment areas after operations have ceased. Some operations, at closure, may require treatment in perpetuity.

SCOPE OF THE PROBLEM

In the United States approximately 20,000 kilometers of streams and rivers have been impacted by acidic drainage, 85-90% of which receive acidic drainage from

abandoned mines (Skousen and Ziemkiewicz, 1995). Although there are no published estimates of total U.S. liability related to acidic drainage, some global examples may help to quantify the dimensions of the problem:

- The Leadville site, a Superfund site in Colorado, has an estimated liability of $290 million due to the effects of acidic drainage over the 100-year life of the mine.
- The Summitville Mine, also in Colorado, has been declared a Superfund site by the Environmental Protection Agency (EPA) which estimated total rehabilitation costs at approximately ~ $175 million.
- More than $253 million dollars have been spent on Abandoned Mine Lands reclamation projects in Wyoming (Richmond, 1995).
- At an operating mine in Utah, U.S. regulators estimate liability at $500-$1,200 million (Murray et al., 1995).
- The Mineral Policy Center in the US has estimated that there are 557,000 abandoned mines in 32 states, and that it will cost between $32 - $72 billion to clean them up (Bryan, 1998).
- Liability estimates for Australia in 1997 and Sweden in 1994 were $900 million and $300 million respectively (Harries, 1997; Gustafsson, 1997).
- Ontario has more than 6000 historic inactive sites having an estimated rehabilitation cost of $300 million dollars (CDN) (Cowan, 1999).
- The total Canadian liability has been estimated to be between $2 and $5 billion (CDN) (MEND 5.8e).

Considering the above data, the number of new mining projects currently under development plus existing mining projects in other countries not mentioned above (e.g. Europe, South America, South Africa), one might anticipate the total worldwide liability to be in the region of $100 billion (US), or even beyond.

RESPONSE TO THE PROBLEM

Thirty years ago, rehabilitation was regarded primarily in terms of physical stabilization and the establishment of a self-sustaining vegetative cover. It was generally thought that the surface addition of alkalinity and the establishment of a vegetative cover would alleviate acidic drainage problems from these sites, and allow mining companies to abandon them without further liability. However, monitoring of the quality of the water draining from revegetated acid-generating waste sites clearly showed in the years following, that acidic drainage remained a concern at many of these sites. In some cases, property owners were faced with the prospect of continuing to operate and maintain lime treatment plants indefinitely. There was need for a better understanding of processes involved, and for new remedial technology to be developed and demonstrated. What was done to try and resolve this issue?

In Canada there had been a tradition of institutional or collective approach to problem solving. From this mould, the National Uranium Tailings Program (NUTP) was cast in 1992. NUTP (1983-1988) was a program that focuses on developing predictive models to develop technology to reduce the liability for uranium mine tailings. The program was a Federal government initiative that had a fixed budget of $9.5 million, was managed by a group of specialists, and had an advisory board from government and industry. Although some useful and innovative modelling methods were developed, no significant new disposal or management technology was developed. Also in terms of liability and environmental impact, acid generation from residual sulphides was clearly identified as the priority issue for uranium tailings in Ontario. This realization combined with the concerns by base metal and gold mining companies and government agencies led to the establishment of the Reactive Acid Tailings Stabilization (RATS) task force, which issued a report in 1988 which set out a 5-year research program that was to cost $12.5 million. The program was subsequently called the Mine Environment Neutral Drainage (MEND) program with the realization that waste rock, mine adits and mine walls could also result in the generation of acidic drainage. This program had the following objectives:

- Provide a comprehensive, scientific, technical and economic basis for the mining industry and government agencies to predict with confidence the long-term management requirements for reactive tailings and waste rock.
- Establish techniques to enable the operation and closure of acid generating tailings and waste rock disposal areas in a predictable, affordable, timely and environmentally acceptable manner.

MEND was an unusual consortium driven primarily by the 130 volunteer representatives of the different participating agencies: regulators, NGO advisors, mining company managers and engineers, and federal and provincial government officials and scientists who freely contributed their time and expertise to the program. The program adopted an organizational structure that included a Board of Directors, a management committee and

several technical committees and a coordinating secretariat. Roles were simple. The Board of Directors provided vision and approval of yearly plans and budgets; the management committee provided "hands-on" management of the program; and the technical committees addressed technological issues and solutions. The Secretariat was essentially the "hub" of the organization and ensured coordination of the elements within, and external to MEND.

Over the succeeding ten years, the two levels of government, together with the Canadian mining industry, spent over $17.5 million within the MEND program to find ways to reduce the estimated liabilities. Planned funding for MEND was divided equally among the three major partners: the mining industry, the federal government and five provincial governments. When MEND ended in December 1997, the federal government had contributed 37% of the funding, the provinces 24%, and industry 39%.

OTHER ASPECTS OF MEND'S SUCCESS

Aside from its technical successes, MEND has been described as a model for governments and industry to cooperate in technology development for advancing environmental management in the mining industry. Decisions on acidic drainage issues are now made based on sound science. The reasons for MEND's success include the following:

- The high return on the investment targeted and achieved, in terms of knowledge gained and environmental and technical awareness of the scope of the problem and credible scientific solutions.
- The partnership and improved mutual understanding developed between the two levels of government and the mining industry in search of solutions to a major environmental problem. Participation from non-governmental organizations was highly beneficial to the partnership.
- The small dedicated secretariat group which coordinated activities, managed the accounting, reporting and technology transfer, and was the "glue" which held the program together.
- The extensive peer review process that was both formal and informal, and resulted in enhanced credibility of the information base.
- The aggressive approach taken for transferring the knowledge gained during MEND.

Partly due to MEND, new mines are often able to acquire operating permits faster and more efficiently than before since there are now accepted acidic drainage prevention techniques. As an example, the Louvicourt mine in northern Québec adopted MEND subaqueous tailings disposal technology and has been able to progress from the exploration phase to an operating mine within 5 years, with a reduced liability of approximately $10 million for the tailings impoundment. Similar impacts are reported for existing sites in the process of decommissioning. MEND has also fostered working relationships with environmental groups, ensuring that they are an integral part of the process.

MEND 2000

When MEND ended on December 31, 1997, the partners agreed that additional cooperative work was needed to further reduce the acidic drainage liability and to confirm field results of MEND-developed technologies. Increased technology transfer was also emphasized.

This resulted in MEND 2000, a three-year program that officially ended in December 2000. The program was funded equally by the Mining Association of Canada (MAC) and Natural Resources Canada (CANMET), a department of the Canadian government.

The MEND 2000 organizational structure included a Steering Committee that set the objectives, provided strategic direction and managed the overall program. Except for the Secretariat at CANMET, all members and stakeholders were volunteers from the mining industry, NGOs, and federal and provincial government departments. Many of these individuals were participants in the MEND program.

The importance of technology transfer became evident as MEND progressed and was regarded as the most important function for MEND 2000. All research results must be effectively communicated to industry, government agencies and the public if the program was to continue to achieve the desired results.

MEND3

In 2000, members of the MEND 2000 Steering Committee, together with their representative constituencies, reviewed the current and future needs of Canadian stakeholders in addressing acid rock drainage.

It ultimately recommended that a renewed national ARD research initiative called "MEND3" be launched in 2001. The overall mission of MEND3 is to provide leadership in ARD research on Canadian priority issues, within an international context. It is a multi-stakeholder coordinated, focused Canadian ARD research initiative based on re-prioritized and augmented existing industry, government and university programs. It is intended to be a phased research program, carefully focused on prioritized Canadian national and/or regional needs, with modest administration costs. It is a proactive program that will maximize value from scarce resources, involve many stakeholders and provide a regional link to international efforts. This program will provide a national focus. The year 2001 will be used to lay the initial groundwork for a multiyear program.

MAJOR ELEMENTS AND RESULTS OF THE CANADIAN RESEARCH

MEND organized its work into four technical areas: prediction, prevention and control, treatment and monitoring. The four technical committees were also involved in technology transfer and international activities.

Over 200 projects were completed. Some of the key technical results and observations include the following.

Prediction and Modelling

Field studies of several waste rock piles provided important understanding for development of prediction techniques. One of the most important observations was that waste rock piles accumulate extensive quantities of oxidation products and acidity that can be released to the environment in the future (MEND 1.14.3; MEND 1.41.4).

Geochemical and physical characteristics of a waste rock pile, from its origin in underground workings to its disassembly and placement underwater in a nearby lake was completed. This study on Eskay provided qualitative and quantitative information on mass transport and water infiltration within a waste rock pile. Geochemical processes were dependent on physical factors such as channeling or stratification within the dump (MEND 1.44.1).

Laboratory and field prediction tests for waste rock and tailings have been investigated and further developed. These tests include static and kinetic tests, mineralogical evaluations and oxygen consumption methods.

An "Acid Rock Drainage Prediction Manual" for the application of chemical evaluation procedures for the prediction of acid generation from mining wastes was produced (MEND 1.16.1b).

Advances in the prediction of drainage quality for waste rock, tailings and open pit mines have been made. A tailings model (RATAP) was distributed and a geochemical pit lake model was developed (MINEWALL). A critical review of geochemical processes and geochemical models adaptable for prediction of acidic drainage was completed (MEND 1.42.1).

Models that will predict the performance of dry and wet covers on tailings and waste rock piles are available (WATAIL, SOILCOVER).

Prevention

Prevention has been determined to be the best strategy. Once sulphide minerals start to react and produce contaminated runoff, the reaction is self-perpetuating. Also, at some mine sites, acidic drainage was observed many years after the waste pile had been established. With many old mine sites, there may be no "walk-away" solution;

In Canada, the use of water covers and underwater disposal are being confirmed as the preferred prevention technology for unoxidized sulphide-containing wastes. A total of 25 reports and/or scientific papers have been prepared on subaqueous disposal (MEND 2.11). A generic design guide was developed (MEND 2.11.9). The guide outlines the factors involved in achieving physically stable tailings, and discusses the chemical parameters and constraints that need to be considered in the design of both impoundments, and operating and closure plans. Water covers have been applied at many sites, but are not universally applicable. Related issues such as the ability to maintain a water cover over the long-term, (structures) and locality and site-specific potential risks due to seismic events, severe storm events, etc. can negate the use of this technology. However, under suitable conditions, the present state of knowledge is sufficient to allow for the responsible design, operation and closure of waste management facilities using water covers.

Underwater disposal of mine wastes (tailings and waste rock) in man-made lakes is presently an option favored by the mining industry to prevent the formation of acidic drainage. At the Louvicourt Mine (Québec) fresh, sulphide-rich tailings have been

deposited in a man-made impoundment since 1994. Laboratory and pilot-scale field tests to parallel the full-scale operation and evaluate closeout scenarios were completed (MEND 2.12.1).

The use of water covers to flood existing oxidized tailings can also be a cost effective, long lasting method for prevention of acid generation. Both the Quirke (Ontario) and Solbec (Québec) tailings sites were subjects of MEND field and laboratory investigations (MEND 2.13.1 (Quirke); MEND 2.13.2 (Solbec)). These sites were decommissioned with water covers and are presently being monitored. Where mining wastes are significantly oxidized, laboratory results have shown that the addition of a thin sand or organic-rich layer over the sulphide-rich materials can prevent or retard diffusion of soluble oxidation products into the water column.

Control

Dry covers are an alternative where flooding is not possible or feasible. MEND has extensively investigated multilayer earth covers for tailings and waste rock (e.g. Waite Amulet and Les Terrains Aurifères (tailings) and Heath Steele (waste rock): 3-layer systems). These type of covers use the capillary barrier concept and although they are effective, they are also costly to install.

Innovative "dry" cover research is indicating that a range of materials, including low cost waste materials from other industries (crude compost, lime stabilized sewage sludge, paper mill sludge) may provide excellent potential for generating oxygen-reducing surface barriers. This technology would see the application of one waste to solve a problem of other wastes.

Non acid-generating tailings can be used as the fine layer in composite moisture-retaining surface barriers. Laboratory studies have confirmed that sulphide-free fine tailings offers some promising characteristics as cover materials (MEND 2.22.2). Barrick's tailings site in Northwest Québec, Les Terrains Aurifères, is the first full-scale demonstration project of using tailings in a cover system (MEND 2.22.4). A second site, Québec crown-owned Lorraine, has also been rehabilitated using the same closure technique.

The first full-scale application in Canada of a geomembrane liner for close-out was completed in 1999 at Mine Poirier in Northwest Québec. Performance monitoring of the close-out scenario is ongoing.

Disposal Technologies

Several other disposal technologies that will reduce acid generation and have been investigated include:

Permafrost in northern environments. Permafrost covers approximately 40% of Canada, and cold conditions inhibit oxidation. Predictive methods have been researched. Although acid generation is common in cold environments, it occurs when exposed sulphides are warmed to temperatures above freezing (MEND 1.61.1-3, 1.62.2)

Blending and segregation (or layering). Technology is defined as the mixing of at least two rock waste types with varying acid generation potential, neutralization potential and metal content to produce a pile that has seepage water quality acceptable for discharge without additional measures (MEND 2.37.1, 2.37.3).

Elevated water table in tailings. This technique offers a method of inhibiting the oxidation of sulphides through the effective saturation of pore spaces. It may be applied as one component of a multi-component reclamation strategy (MEND 2.17.1).

In-pit disposal following mining. Mined-out pits can provide a geochemically stable environment for wastes and can be a focal point in mine rehabilitation. The addition of buffering material may be required (MEND 2.36.1).

Depyritized tailings as cover materials. Laboratory and field tests are showing that depyritized tailings have excellent potential as covers. Economic analyses have indicated that hydraulic placement will be necessary to be cost effective (MEND 2.22.3).

Lime Treatment

Studies conducted to date support the view that sludges will remain stable if properly disposed. Concerns had been raised with regard to the long-term chemical stability and the potential liability arising from dissolution of heavy metals contained in the sludge (MEND 3.42.2). Other findings include:

- Optimum conditions will depend on site-specific factors e.g. pH, metal loading chemistry.
- Modifications to the treatment process (e.g., lime slaking, pH adjustment, mixing, aeration, flocculent addition) can influence operating costs, sludge volumes, and metal release rates.
- The method of disposal of the sludge will affect its long-term stability: aging can promote recrystallization which improves sludge stability.

- Codisposal of sludges with other mining wastes requires further study.
- Leach test protocols need to be developed specifically for lime treatment sludges.

The status of chemical treatment and sludge management practices was summarized in a reference document (MEND 3.32.1).

Passive Treatment

In Canada, experience indicates that passive systems do have specific applications for acid mine drainage (AMD) treatment. These applications range from complete systems for treating small seeps to secondary treatment systems such as effluent polishing ponds. Alone, they cannot be relied upon to consistently meet AMD discharge standards. Large-scale passive systems capable of handling the low winter temperatures, high metal loads, and fluctuations in flow rates associated with the spring freshet have yet to be implemented.

The status of passive systems for treatment of acidic drainage was summarized in a reference document (MEND 3.14.1).

Monitoring

Several guides are available to assist in the development of acidic drainage monitoring programs. An important MEND deliverable is MEND 4.5.4, *Guideline Document for Monitoring Acid Mine Drainage.* This document is designed to serve as a single source introductory guide to a wide range of AMD monitoring concerns, while also providing users with information on literature sources for site-specific concerns and emerging monitoring techniques. Monitoring requirements are addressed for both source and receiving environments, with receiving environment concerns restricted to freshwater systems.

Other guideline documents include a field sampling manual (MEND 4.1.1) that presents an approach to assist people in selecting the appropriate methodologies for the sampling of tailings solids, liquids and pore gas. A comprehensive list and description of sampling techniques, and a guide to waste rock sampling program design for the exploration, operation and closure phases of a mining project is produced in MEND 4.5.1-1. Available sampling techniques for waste rock is given in MEND 4.5.1-2.

At the conclusion of the MEND program, a "tool box" of technologies has been developed to assist the mining industry in addressing its various concerns related to acidic drainage, and in significantly reducing its estimated liability. A particularly important outcome has been the development of a common understanding among participants, inasmuch as it has allowed operators to take actions with greater confidence and to gain multi-stakeholder acceptance more rapidly.

TECHNOLOGY TRANSFER

Technology transfer activities have been significantly expanded in recent years and this will continue for the duration of MEND3. The dissemination of information on developed technologies to the partners and the public is a major function of the program. A MEND 2000 Internet site (**http://mend2000.nrcan.gc.ca**) has been established and is regularly updated with current information on technology developments. Report summaries, the MEND publication list, information on liabilities, case studies, and conference and workshop announcements are provided. Further, MEND hosts several workshops per year on key areas of technology at various locations across Canada. These workshops have been the vehicle of choice to transfer the available information to the users and they have been quite successful in accomplishing this goal. Proceedings for the workshops on chemical treatment, economic evaluations, case studies of Canadian Technologies, monitoring, in-pit disposal, dry covers, research work in Canada, and risk assessment and management are available from the MEND Secretariat.

MEND participated in the organization of several International Conferences on the Abatement of Acid Rock Drainage (ICARDs) held in 1991 (2nd Montreal), 1994 (3rd Pittsburgh), 1997 (4th Vancouver), and 2000 (5th Denver).

Technology transfer will include information and analysis of projects not necessarily initiated under MEND (e.g Poirier) as well as an exchange of technology information with international organizations involved in research on acidic drainage. This includes foreign government institutes and other research initiatives such as the International Network on Acid Prevention (INAP), the Mitigation of the Environment Impact from Mining Waste (MiMi - Sweden), and the Acid Drainage Technology Initiative (ADTI - USA).

Other technology transfer initiatives include:

- MEND videos are available in English, French, Spanish and Portuguese, and describe technological advances relating to the prediction, prevention and

treatment of acidic drainage from mine sites. These videos are available free of charge and can be ordered directly through the Internet.

- The MEND Manual that summarizes all of the MEND and MEND-associated work on acidic drainage from mine wastes and openings.
- The Proceedings of the 4th International Conference on Acid Rock Drainage are available on CD-ROM.
- About 200 reports completed during MEND and MEND 2000.
- A selection of over 110 MEND reports on two CD-ROMs.
- National case studies on acidic drainage technologies.

NEW IDEAS

In 1992, MEND formed a Task Force to solicit and nurture innovative new ideas. An additional goal was established to encourage researchers from outside the general area of mining environment to becoming involved in acidic drainage research. The resulting technology would need to be reliable, inexpensive, permanent, and widely applicable. An innovator had to demonstrate the relevance of their idea at the concept level, which would then be the basis for proceeding to a more detailed development project. Up to $10,000 was provided for the review and the development of a concept. Although most of the new ideas were innovative and applicable and provided useful information, they did not achieve the objective of providing a solution to the problem of acidic drainage. At least three had potential applications (sprayed polyurethane, modified clay and permafrost) and three yielded useful state-of- art reviews (U.S. research, foam flotation and Japanese technology).

MEND MANUAL

More than 200 technology-based reports were generated from the MEND and MEND 2000 programs. These reports represent a comprehensive source of information, however, it is not practical for users to have on hand or assimilate all the detailed information. This manual is intended to serve as a single source reference to the diverse and complex research undertaken by the MEND Program from 1988 to 2000, and selected complementary work completed outside of MEND. This manual includes an introductory volume (Volume 1) and five technical volumes which address acidic drainage issues: sampling and analyses; prediction; prevention and control; treatment; and monitoring (MEND 5.4.2).

The objective of the manual was to summarize work completed by MEND in a format that would provide practitioners in Canadian industry and government with a manageable document. The document is not a "How to" manual. It is a set of comprehensive working references for the sampling and analyses, prediction, prevention, control, treatment and monitoring of acidic drainage. The document provides information on chemistry, engineering, economics, case studies and scientific data for mine and mill operators, engineering design and environmental staff, consulting engineers, universities and governments. The MEND Manual describes the MEND-developed technologies and their applicability in terms of cost, site suitability and environmental implications.

Many acidic drainage related decisions are subject to a range of considerations including but not limited to the technical basis, the regulatory framework, costs and risks. The MEND Manual, and the majority of the MEND reports referred to in the manual, focused on acidic drainage technical subjects. For the benefit of manual users, the manual includes references to non-MEND documents that address issues such the management of tailings disposal facilities, treated effluent quality and effluent toxicity requirements, environmental management systems, and risk assessment. Readers may find it best to use the manual as a key reference document that allows follow-up with listed references in areas of interest.

Acidic drainage is a technically complex area and one that typically requires the involvement of experts from numerous technical disciplines. Site-specific factors and conditions add to this complexity, and often necessitate site-specific research. As such, acidic drainage technologies are not universally applicable. Research to date, and the application of the new technologies, have provided some practical experience in their application. In this light, the discussions in the manual also note aspects to consider when evaluating the potential use of these technologies.

CONCLUSIONS

The successes of MEND have come through the sharing of experiences, the thorough evaluation of technologies and their incremental improvement. The

major achievement of the program has been the use of water covers. Canadian industry reports that a significant reduction in liability is confidently predicted. An evaluation of MEND (MEND 5.9) concluded that the estimated liability had been reduced by $340 million for five Canadian mine sites alone. It is also acknowledged that the reduction in liability is significantly higher than this quoted value, with a minimum of $1 billion commonly accepted. The same study concluded that:

- There is now a much greater common understanding of acidic drainage issues and solutions;
- The research has led to less negative environmental impact;
- There is increased diligence by regulators, industry and the public;
- MEND has been recognized as a model for industry-government cooperation; and
- The work should continue with strong international connections.

As a result of MEND, the knowledge base on acidic drainage has grown considerably to include a fundamental understanding about the acid generation process and factors that affect it, and about measures that can be taken to prevent and control acid generation, or treat acid drainage should it occur. MEND focused the acidic drainage effort, and developed a toolbox of technologies that is available to all stakeholders. Technologies are now in place to open, operate and decommission a mine property in an environmentally acceptable manner, both in the short and long term. This can have a major impact on new mine financing and development. Moreover, mining companies and consultants have acquired a great deal more capability to deal with water contamination from mine wastes, including acid generation. And while the knowledge base can be generally described as reasonable and adequate, there is a need for additional research to: add to the present state of understanding, confirm the performance of technologies through large scale applications and long term data; and continue the search for more efficient and affordable technologies. As such, readers are encouraged to think of acidic drainage as a work in progress where future research is likely to add to the present state of knowledge.

MEND is thus a good example of a successful, multi-stakeholder initiative addressing a technical issue of national importance, and has been a model for cooperation among industry, various levels of government and NGOs. The program has significantly advanced environmental management practices and thus contributed to the long-term sustainability of the mining industry.

REFERENCES

Bryan, V. 1998. Personal Communication.

Cowan, W.R. and Robertson, J.G.A. 1999. Mine Rehabilitation in Ontario: Ten Years of Progress. In Proceedings of Sudbury'99. Sudbury, Ontario. September 13 – 17. Volume 3: 1037.

Gustafsson, H. 1997. A Summary of the Swedish AMD Experience. In Proceedings of the 4th International Conference on Acid Rock Drainage. Vancouver, British Columbia. May 31-June 6, Volume IV: 1897

Harries, J. 1997. Estimating the Liability for Acid Mine/Rock Drainage in Australia. In Proceedings of the 4th International Conference on Acid Rock Drainage. Vancouver, British Columbia. May 31-June 6, Volume IV: 1905.

MEND Reports. Complete list available from Internet site http://mend2000.nrcan.gc.ca.

Murray, G., Ferguson, K. and Brehaut, H. 1995. Financial and Long Term Liability Associated with AMD. In Proceedings of the 2nd Australian Acid Mine Drainage Workshop. N.J. Grundon and L.C. Bell Eds. March 28-31: 165.

Price, B. 1995. Defining the AMD Problem II. An Operator's Perpective. In Proceedings of the 2nd Australian Acid Mine Drainage Workshop. N.J. Grundon and L.C. Bell Eds. March 28-31: 17

Richmond, T. 1995. Abandoned Mine Land Reclamation Costs in Wyoming. In Proceedings of Sudbury'95. Sudbury, Ontario. May 29 - June 1, Volume 3: 1221.

Skousen, J. and Ziemkiewicz, P. 1995. Acid Mine Drainage Control and Treatment, West Virginia University: 13.

ATTACHMENT 28

States
ment of
Agriculture

Forest Service

In Cooperation
with the U.S.
Department of
the Interior's
Bureau of Mines

Program Aid 1505

March 1993

Acid Drainage From Mines on the National Forests

A Management Challenge

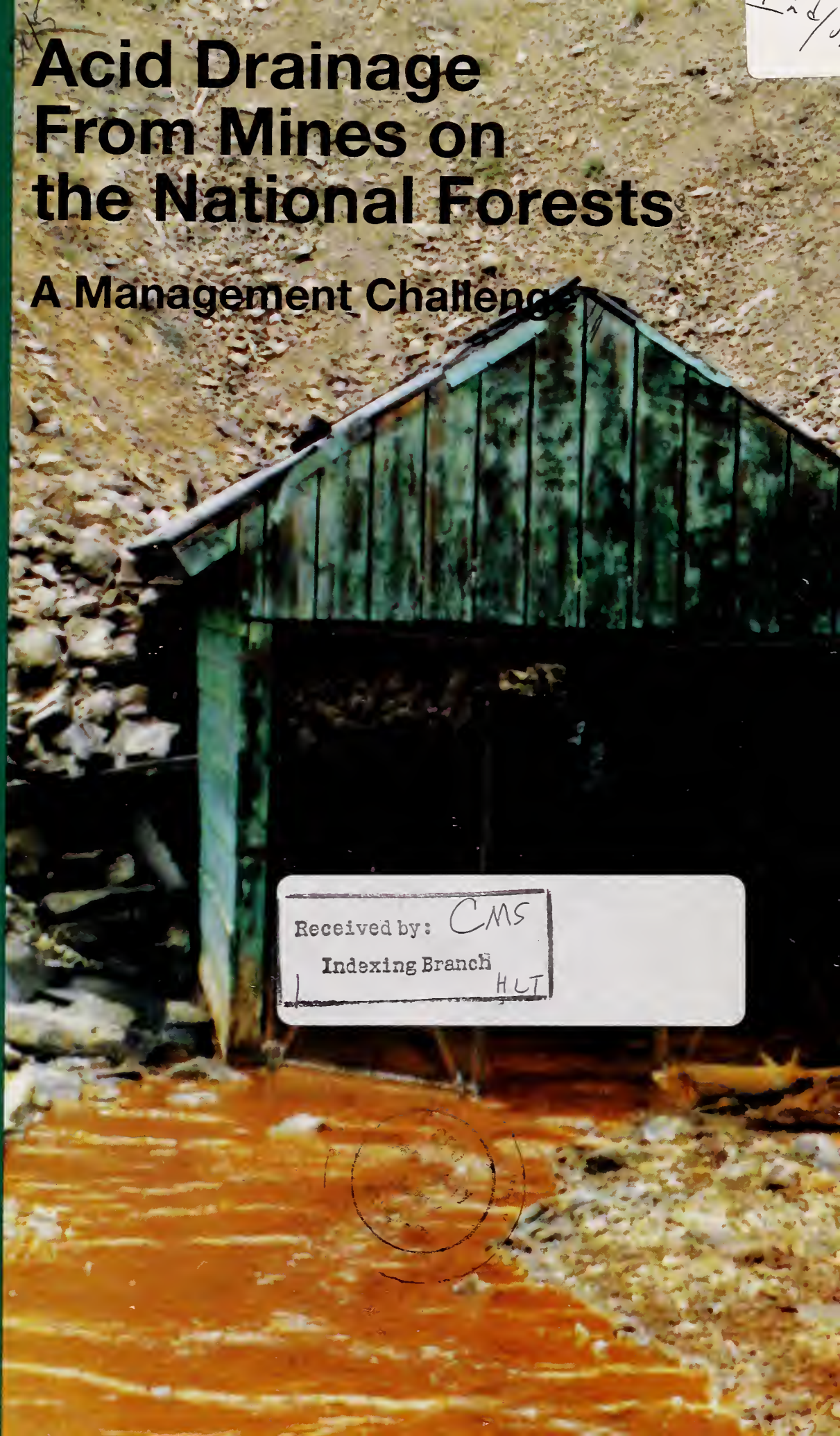

Table of Contents

On the Front Cover

Old mine adit on the Rio Grande National Forest in Colorado. Although partially collapsed, this adit still drains a historic lead, copper, and zinc mine. High acidity and high metal content have severely affected aquatic lifeforms below the mine.

All photos USDA FS/WO–M&GM

"The Forest Service has identified acid drainage from mine sites as the most difficult and costly reclamation problem it faces with western metalliferous mining operations . . . with some significant environmental problems dating as far back as the late 1800's."

When the cooperative research plan on acid drainage from mine sites was signed in April 1991 by the Bureau of Mines and the Forest Service, its mandate was clear—to provide and apply technology to help manage national forests and grasslands affected by acid drainage. The plan represents a long-term cooperative research program focusing on National Forest System lands in the Western United States being carried out using the Research, Development, and Application (RD&A) model. It is a comprehensive program with practical goals—to provide and make use of needed information.

Under the program:

- The Bureau of Mines provides information on the prediction, control, and treatment of acid drainage from mine sites.
- The Forest Service, the mining industry, and others provide research sites and use the information.
- The Forest Service monitors its effectiveness.

This report highlights program contributions to be achieved over time. It also summarizes contributions of the program to date and describes how the program functions. The current effort is a long-term one, using available resources. Additional resources specifically designated to this cooperative effort would result in accomplishing the work in a more timely fashion.

Of course, the true effectiveness of the acid drainage cooperative research program will not be known for some years. Applying the results of new research and development is not accomplished quickly—it takes time. Fortunately, application of this new information being provided by the Bureau of Mines will be a continuing part of Forest Service programs.

Figure 1
Mine tailings producing acid drainage on the Prescott National Forest in Arizona. This gold, lead, and zinc was active in the 1890's.

The Forest Service and the Bureau of Mines –*Agency Responsibilities*

The U.S. Department of Agriculture's Forest Service and the U.S. Department of the Interior's Bureau of Mines each has unique responsibilities in the management of mineral resources in the United States. Generally, the overall responsibility for managing federally owned minerals belongs to the Bureau of Land Management. Other Department of the Interior agencies have minerals responsibilities as well.

In part, the Forest Service is charged with administration and management of National Forest System lands, including land and resource management planning. This responsibility encompasses the mining and extraction of mineral resources, the approval of mining and reclamation plans that protect the environment, particularly surface resources, and the research necessary to protect these resources. The Bureau of Mines has responsibility to ensure that the United States has a dependable and secure supply of domestic minerals, to conduct investigations and research for this purpose, and to protect the environment and minimize damage due to mining and mineral processing activities.

In June 1990, the two agencies entered into a Memorandum of Understanding to enable them to develop and carry out a comprehensive research program to solve problems and demonstrate solutions to acid drainage problems on National Forest System lands. It is an important program, in that solutions to problems such as these are necessary for the extraction of mineral resources in an environmentally sensitive manner. In effect, it influences the degree to which minerals necessary for the economic viability of the Nation are available on these lands.

"The Forest Service and Bureau of Mines have entered into a Memorandum of Understanding to enable them to develop and carry out a comprehensive research program to solve . . . acid drainage problems."

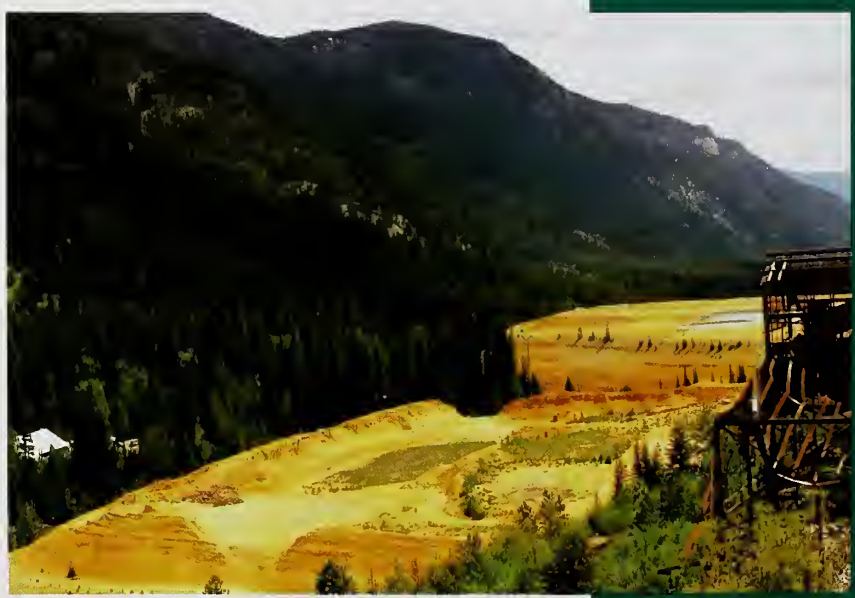

Figure 2
Acid is generated from these abandoned mill tailings on the Wenatchee National Forest in Washington. The primary commodity was copper. The color of the tailings results from precipitated iron.

The Problem

The Forest Service has identified acid drainage from mine sites as the most difficult and costly reclamation problem it faces with western metalliferous mining operations. Acid drainage persists at many active and abandoned mine sites, with some significant environmental problems dating as far back as the late 1800's. There are also concerns that current and future mining operations may generate acid drainage for years or decades after the mines cease operation. Unfortunately, major technical uncertainties are associated with the prediction of acid drainage potential at the time of mine plan approval as well as with mitigation or treatment techniques for post-mining use.

Over 1,500 western mining sites with significant acid drainage problems have been identified on National Forest System lands. Many of these sites in remote locations that are not accessible the year around often represent small, but ecologically damaging flows. Such sites require either permanent control measures to prevent or mitigate acid formation, or low-cost, passive treatment technology to neutralize and detoxify the waters. The problems of acid drainage from the sulfide-bearing rock present at many western metal mines are exacerbated by contamination that occurs when acid waters contact exposed mineral zones and dissolve heavy metals. Many of these metals are toxic to aquatic and terrestrial life, if the concentrations are high enough.

Forest Service land managers, who face increasingly complex and controversial decisions regarding mineral development, need new research information. One major problem affecting the future of metal mining in the West is the absence of technology to predict the potential of new mining ventures to generate acid drainage. State and Federal permitting and regulatory agencies need information on the acid-forming potential of ore deposits in order to analyze the impacts of new mining operations and provide for the development of necessary environmental controls. Gold and other precious metal operations, which have experienced a 30- to 35-percent growth in domestic production in each of the last 5 years, are expected to continue. Without additional research information, it is almost certain that a significant percentage of existing and new mining ventures will experience unexpected acid drainage situations. These situations could result in expensive and difficult remedial actions to prevent adverse environmental impacts, primarily to surface and ground waters, due to metal-contaminated drainage.

The fact that acid drainage has been a persistent problem for more than 100 years is indicative of one of the major difficulties in dealing with it—that there are currently no widely applicable technologies to mitigate or stop a fully developed acid drainage situation. Only stopgap prescriptions are available and at considerable cost. On the other hand, the application of State and Federal regulatory controls on some modern mines has, in some instances, been able to limit the development of acid mine drainage and consequently reduce the long-term environmental effects. However, regulatory controls do not always work. In the case of old, abandoned mines it is too late for regulatory controls. New technologies are needed to effectively deal with these problems.

Currently, reliable data on the total number of mines producing acid drainage and on the number of miles of streams affected by acid and metal drainage are not available for the Western United States. However, various estimates have placed the number of these mines in the range of 20,000-50,000, seriously affecting 5,000-10,000 miles of streams. The cumulative effect of these mines, whatever their actual number, is significant.

The basis for the production of acid drainage is well understood. Pyrite and other sulfide minerals are exposed to air and water in the mining process. Air and water oxidize the sulfide minerals, releasing sulfuric acid and sulfates. This process is catalyzed by iron-oxidizing bacteria and permits a host of site-specific secondary reactions, principally ion exchange and acid-induced metal dissolution. The metals that may be involved in this process cover the range of heavy metals: arsenic, cadmium, copper, iron, lead, manganese, mercury, nickel, selenium, silver, and zinc. Once the chemical reactions are fully realized, the discharge of acid and metal ions is known to persist

Please Note:

States in solid color are the ones represented by photos in this publication. However, acid drainage from metal mines is a problem throughout the West.

A sampling of national forests having acid drainage problems. Numbers refer to figure numbers in this publication.

in some cases for hundreds of years and should be considered a long-term source of contamination. Although this process does occur naturally, it is the volume of drainage from mine sites that is problematic.

The makeup of acid drainage varies from mine to mine and from location to location. Classic acid drainage is composed of acid, precipitated iron compounds, sulfate ions, and dissolved metals. It is the metals, far more than the acidity, that cause the environmental damage. The type of metals in acid mine drainage is controlled by the mineralogy of the ore body; lead and zinc mines may produce metal migrations of lead and zinc. Unexpectedly, gold mines may produce flows containing arsenic. Once the acidity and metal ions migrate into the soils, they are usually unable to support the normal complement of vegetation and soil fauna and flora. These biological components of the soil are inhibited by the dissolved metals in the soil water solution. Bare, unvegetated soils are eroded by the weather elements, and streams are physically contaminated with large volumes of metal-bearing sediments coming off the acidified upland areas of the mines. Extant groundwater aquifers may also be contaminated by the dissolved metals.

When acid and metal drainage enters streams, the fish and other stream organisms are often depleted in a relatively short period of time. Copper ions are especially lethal to fish, but not to mammals. In a coldwater fishery, in softwater conditions, a copper concentration of as little as one part per million may be lethal to trout. Streamside vegetation is affected by a change in species composition and exhibits a general loss of vigor. However, some lower quality streamside vegetation is usually retained.

To briefly summarize, flows of acid drainage often create large, toxic, metal-bearing sediment loads in stream channels. The channels may be brightly colored—red, purple, and orange—by precipitates of iron and other metal compounds. The waters are somewhat acidified, but the metal constituents may increase drastically. Fish and other organisms in the system are lost in the waters most affected as a result of the metal contamination. Streamside vegetation is often changed as to species composition and loss of vigor. The most seriously affected streams are considered to be "dead." Ground water may also be contaminated with metal ions.

A Model of Cooperation

"Without additional research . . . it is almost certain that a significant percentage of existing and new mining ventures will experience unexpected acid drainage situations that could result in expensive and difficult remedial actions . . . ."

The current gold boom in the Intermountain West began in the mid 1980's. It was made possible by a combination of high precious metals prices; discovery of large, low-grade, disseminated ore deposits; and new extraction technology. By the close of the decade, the Forest Service and some segments of the mining industry had recognized the need for better research information to deal with the likelihood of acid drainage. Acid drainage research and development efforts were generally not well coordinated with the needs of the national forests, and adequate planning for this type of focus was often lacking. For this reason, effective June 6, 1990, a Memorandum of Understanding was signed by the Bureau of Mines and the Forest Service in which the two agencies mutually agree to cooperate in addressing the significant national problem posed by acid drainage from mine sites in the Western States. The agreement does not include funding considerations.

A joint agency working group established by the agreement has identified four priority areas that must be addressed to develop effective solutions to acid drainage problems in the West. Together, these areas make up the cooperative research program. They relate to (1) predictive techniques and methodologies to assess the potential of new mining ventures to generate acid waters; (2) control technologies to prevent or minimize acid drainage; (3) treatment technologies to mitigate existing acid drainage problems; and (4) technology transfer and program monitoring to assess the effectiveness of technologies in the above three areas and transfer the information to the mining industry and government agencies.

Under the direction of the national offices of the Forest Service and the Bureau of Mines, the joint agency working group is responsible for program planning, setting research priorities, identifying field study and demonstration sites, and information exchange.

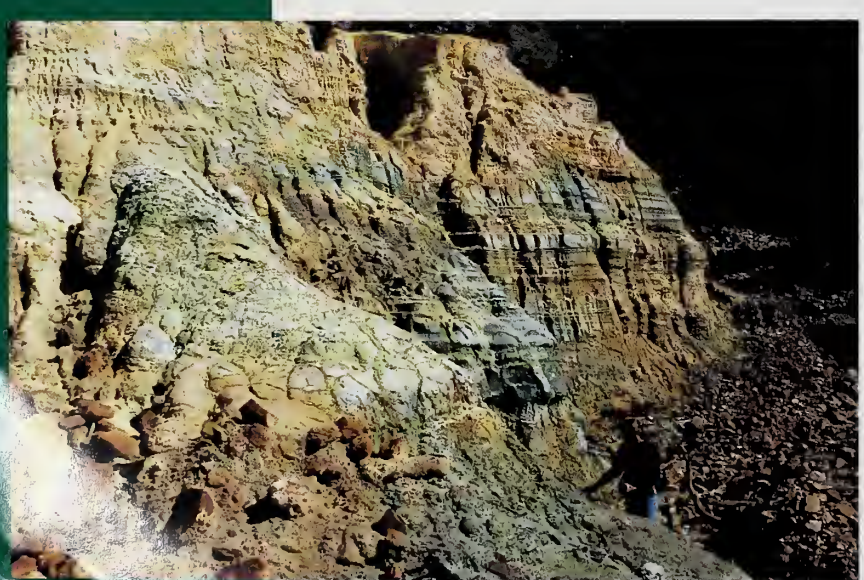

Figure 3
Eroded mine and mill tailings generate acid on the Coronado National Forest in Arizona. The operation produced copper, silver, gold, and other metals.

The cooperative **research** program is a shared effort between the Bureau of Mines and the Forest Service. Basic research information forms the technical foundation of any such program. Although much new technology needs to be generated for the Western United States, some technology is already available in the East upon which to build. Much attention has been directed at acid problems associated with eastern coal mines. In fact, the Bureau of Mines has had an active research program to address acid drainage from eastern coal mines for more than 20 years and has produced a number of successful reclamation, mitigation, treatment, and pre-mine prediction technologies.

Development involves molding existing knowledge and technology into a form that can be used in specific ways. In this case, development efforts will utilize the knowledge base on treatment of acid drainage from eastern coal mines and the extensive expertise of the Bureau of Mines in mining and processing of oresfrom western metal mines. Research and development in this RD&A model is being accomplished by the Bureau of Mines with Forest Service support.

Effective **application** of the cooperative model involves successful technology transfer. Unfortunately, considerably greater emphasis is frequently placed on generating information than on transferring it to users and getting it applied. As a result, a great disparity can exist between the amount of information available and the amount used. In this model, technology transfer is being emphasized and includes usage of the information on the ground. Monitoring to determine the effectiveness of new technologies is considered an integral part of application. The Forest Service, because it administers the land and regulates mining activity, has responsibility for application of research and development information with Bureau of Mines support.

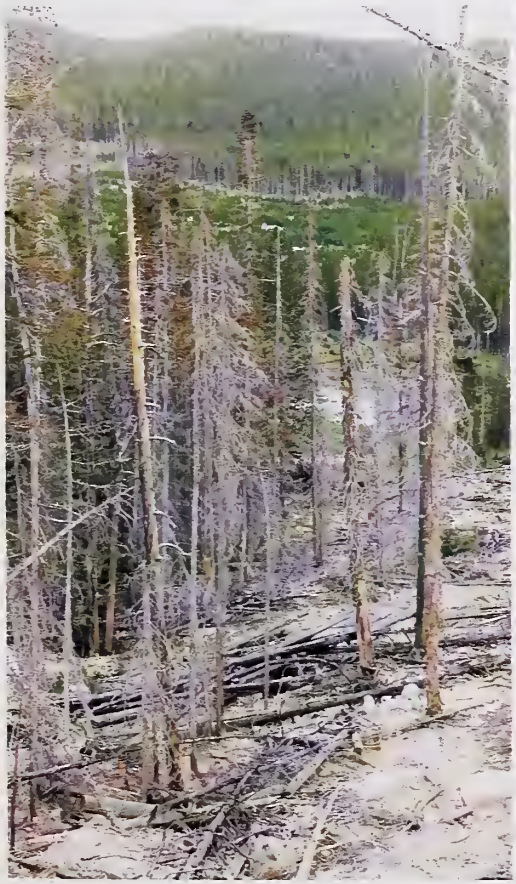

Figure 4
Trees killed by heavy-metal-contaminated acid drainage seeping from sulphide-bearing waste rock on the Helena National Forest in Montana. The mineral commodity was gold.

Figure 5
Acid rock drainage seeps from an abandoned mine adit on the Boise National Forest in Idaho. This water has unusually high concentrations of arsenic.

The Solution

The real value of a cooperative research program depends on its ability to accomplish specific objectives in a given period of time. In addition, the speed at which a program functions is directly related to the resources allocated to it. Therefore, ideally, information and technologies to solve acid drainage problems from mines on National Forest System lands should be generated quickly, followed by a period during which agencies and the mining industry focus on implementing the solutions. The RD&A approach allows for concentration on high-pay-off projects that would otherwise not be accomplished. Following is an explanation of the four priority research areas:

". . . development of effective techniques and methods for predicting the potential of new mining ventures to form acid drainage. . . . would allow the Forest Service, other land management agencies, and industry to avoid repeating the mining mistakes of the past . . . ."

Figure 6 *(Background Photo)*
Acid rock drainage from abandoned gold mine workings in Montana. This mine on the Deerlodge National Forest had both underground and open pit activity.

Figure 7
A stream damaged by acid mine drainage in Montana, Lewis and Clark National Forest. Note the red color from iron precipitate on the stream bottom.

Acid Drainage Prediction

Scope: The Forest Service and the Bureau of Mines concur that the development of effective techniques and methods for predicting the potential of new mining ventures to form acid drainage is one of the highest priority efforts of cooperative research. In essence, predictive technologies would allow the Forest Service, other land management agencies, and industry to avoid repeating the mining mistakes of the past that have led to acid drainage problems. An accurate assessment of the potential for acid drainage formation using information obtained during exploratory drilling, for example, could be used in the permitting process. In addition, the assessment would allow industry to design mine and waste management plans to prevent or mitigate adverse environmental impacts from acid drainage.

Objective: Within 5 years, develop quantitative models, techniques, and methods for the prediction of acid drainage from samples obtained from exploratory drilling programs.

Control Technologies for Acid Drainage

Scope: There is a need for more effective technologies to control acid drainage at both abandoned and operating mine sites. Control aims to prevent acid drainage formation by inhibiting the weathering processes, for example, by preventing water or oxygen contact with mine wastes or mine workings. This technology is applicable to past sites and to all new operations through the development of mine and waste management plans.

Objective: Develop and demonstrate a suite of economical techniques that limit effluent volumes or heavy-metals concentrations from mines and waste rock (nonpoint sources of pollution). These include underground mine workings and pits, coarse waste rock, and fine fractions of mill wastes.

Treatment Technology for Acid Drainage

Scope: Cost-effective technology is needed to correct acid drainage from past operations. The development of a low-maintenance or passive treatment process may be the only cost-effective solution for many national forest sites because of their location, low-volume discharge, or extensive and diffuse underground contamination source. Research should focus on developing low-cost chemical and biochemical systems for small-volume discharges that can operate with minimum maintenance.

Objective: The 5-year objective is to develop a passive, low-maintenance system or systems for treating low-volume drainage from mine adits (point sources of pollution). Treatment may involve combined passive systems, which ideally would produce dense and environmentally stable sludges and have the potential for metal recovery to limit disposal costs.

Program Monitoring and Technology Transfer

Scope: The need to determine the effectiveness of new acid drainage technologies has resulted in a commitment on the part of the Forest Service and the Bureau of Mines to carry out long-term monitoring in the above three research areas. In addition, improved knowledge and technologies to predict, control, and treat acid mine drainage will require aggressive technology transfer, training, and information sharing efforts.

Objectives: Develop and carry out long-term monitoring and evaluation plans consistent with the level of new methods and techniques. Enhance the awareness of acid drainage problems and solutions with the mining industry and State and Federal land management and regulatory agencies.

Benefits

". . . application of this new information being provided by the Bureau of Mines will be a continuing part of Forest Service programs."

The benefits of an effective RD&A program include:

- The ability to predict the potential for acid drainage from mine sites will enable land managers to make informed decisions regarding the exploitation of metallic mineral resources on public lands.
- Predicting the likelihood of acid drainage prior to mining will enable industry to design effective control and mitigation measures into the mining operation.
- The economic viability of the mine can be better assessed. This will reduce premature and ineffective closure due to unexpected environmental control costs.
- A better design for final mine closure can be prepared. Post-mining site monitoring will be reduced, and the time for monitoring will be shortened.
- New techniques will prevent or reduce acid discharges from metal mines and processing wastes. Elimination of these discharges will preclude or reduce acid and heavy metal pollution of receiving streams and ground waters.
- Improved drinking water supplies and restoration of acquatic habitat will result. There will be an elimination of visual pollution of streams due to precipitation of iron compounds.
- Reduced costs for waste water treatment and correcting other damage to the environment.

Figure 8
Highly acidic tailings, with high metals content, were released downstream following collapse of a tailings dam on the Rio Grande National Forest in Colorado.

Accomplishments To Date

Program accomplishments as coordinated by the joint agency working group include:

- Development of site selection criteria for cooperative Bureau of Mines / Forest Service research-related efforts.
- Establishment of a joint agency reconnaissance team for site evaluation and selection.
- Assistance in the control and treatment of acid drainage from the Golinsky Mine on the Shasta-Trinity National Forest.
- Sponsorship of and participation in a national acid mine drainage seminar for industry, land managers, and State and Federal regulatory agencies.

Figure 9
Acid drainage from an inactive gold mine runs down this hillside on the Shasta-Trinity National Forest in northern California. The acid flow has been the cause of fish kills further downstream.

Obviously, these accomplishments represent only a beginning and reflect limited funding. Much work remains to be done. The Forest Service and the Bureau of Mines are committed to moving ahead in this important work as fast as possible. The alternative to solving these problems at the pre-mining or mining stages of mineral development could result in unacceptably long long-term commitments to water treatment and site cleanup. In this age of environmental awareness, this alternative is of course unacceptable for current and future mining operations. Long-standing acid drainage problems from mines in the forests, many from operations before the national forests were set aside, are also in the public eye, with the expectation that an aggressive cleanup program will be pursued. The actions outlined in this publication are consistent with that expectation and are supported by the mining industry.

Figure Ten
Hillsides affected by mining in central California, Toiyabe National Forest. The acids generated in the soils of this old sulfur mine have severely slowed the rehabilitation of the area.

A cooperative interagency effort . . . aimed at solving acid drainage problems.

ATTACHMENT 29

United States
Environmental Protection
Agency

REFERENCE GUIDE
to Treatment Technologies for Mining-Influenced Water

March 2014
EPA 542-R-14-001

U.S. Environmental Protection Agency
Office of Superfund Remediation and Technology Innovation

Technology: Reverse Osmosis

Technology Description

Reverse osmosis is the pressure-driven separation of contaminants through a semi-permeable membrane that allows water to pass through while retaining contaminants. The dissolved ions are retained in a concentrated brine solution that requires management or disposal (Figure 11). Reverse osmosis is a proven method to demineralize acid mine drainage. However, it does require significant construction and operating costs.

Figure 11: Diagram of Simplified Reverse Osmosis Technology

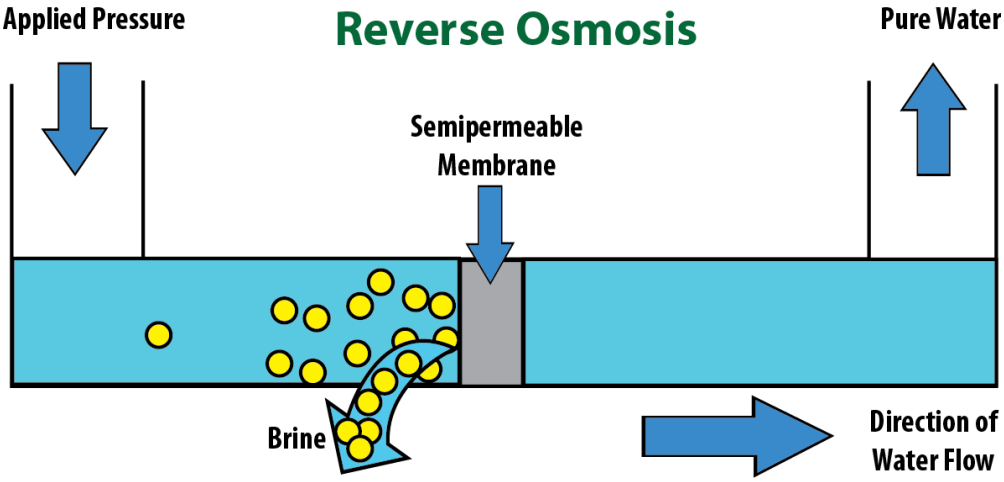

Constituents Treated

Reverse osmosis can be used to remove metals, total dissolved solids, and sulfate from MIW.

Operations

Reverse osmosis involves a semipermeable membrane through which almost pure water is removed from a concentrated input solution by applying pressure, leaving a more highly concentrated brine solution. The membrane is the primary component of a reverse osmosis system. Durable membranes resistant to chemical and microbial agents that retain structural stability over long operating periods are essential. Pre-treatment is necessary to prevent membrane fouling, particularly if the water contains elevated levels of hardness (i.e., calcium or magnesium) or total suspended solids. With pre-treatment and routine maintenance, membranes typically last two to five years.[81]

[81] CH2M Hill, 2010.

The brine produced is typically 20 to 30 percent of the influent flow in a single system, depending on influent water quality. The process produces a concentrated waste stream that must be disposed of properly. Various disposal options are available. However, the concentrated waste stream is typically disposed of through evaporation, deep well injection or ocean discharge.

Reverse osmosis has been used successfully to treat MIW at several sites. At the Barrick Richmond Hill Mine near Lead, South Dakota, reverse osmosis polishes selenium from mine water after pre-treatment for iron reduction and precipitation. The reverse osmosis unit is operated at pressures of 250 pounds per square inch and greater.[82] As of 2005, filtration pre-treatment was required to remove total suspended solids. During winter months, water is heated to prevent crystallization caused by depressed salt solubilities. Additionally, a softening plant is under consideration for treating gypsum scaling resulting from elevated calcium concentrations.

At a historic former gold mine in California, reverse osmosis treated impounded water as an emergency measure to prevent impounded water from affecting a drinking water reservoir below the mine.[83] Trailer-mounted reverse osmosis systems were leased along with pre-filtration and manganese removal columns. The system flow was greater than 100 gpm and the system operated for about four months. The system operated at about 40 percent selenium recovery due to the high total dissolved solids in the influent water. The brine was then returned to the initial impoundment. Selenium concentrations were reduced from about 60 µg/L to less than 5 µg/L. The system operated until levels in the impoundment were reduced to acceptable levels.

Reverse osmosis is also in use at the Kennecott South site, which is located in the Salt Lake Valley, east-southeast of Copperton, Utah.[84] The Bingham Canyon Water Treatment Plant (BCWTP), built as part of the site's remedy, is located in operable unit (OU) 2. Reverse osmosis is being used as the primary technology for addressing total dissolved solids- and sulfate-impacted ground water.

The BCWTP has two reverse osmosis treatment racks that treat 3,200 gpm with total dissolved solids concentrations of about 2,000 mg/L and a sulfate concentration of 1,200 mg/L.[85] The quality of the feed water and regular cleaning has extended the system's lifespan to about six years.

[82] Microbial Technologies, 2005.
[83] Golder, 2009.
[84] ITRC, 2010.
[85] ITRC, 2010.

ATTACHMENT 30

United States
Environmental Protection
Agency

Office of Water
4304T

EPA 822-R-18-002
April 2013

AQUATIC LIFE AMBIENT WATER QUALITY CRITERIA FOR AMMONIA – FRESHWATER 2013

extensively in order to keep the concentrations of ammonia in surface waters from being unacceptably high. In 2011, there were approximately 4.7 million pounds (lbs.) of ammonia documented as discharged from all reporting industries to surface waters (U.S. EPA 2011). In 2010, industrial releases of ammonia to ten large aquatic ecosystems (e.g., Chesapeake Bay, Puget Sound, Great Lakes) were reported to total approximately 1.3 million lbs. (U.S. EPA 2010).

Environmental Fate and Transport of Ammonia in the Aquatic Environment

Ammonia (NH_3) is formed in the natural environment by the fixation of atmospheric nitrogen and hydrogen by diazotrophic microbes, such as cyanobacteria (Latysheva et al. 2012). Trace amounts are also produced by lightning (Noxon 1976). Decomposition of manure, dead plants and animals by bacteria in the aquatic and terrestrial environments produce ammonia and other ammonium compounds through conversion of nitrogen during decomposition of tissues in a process called ammonification (ATSDR 2004; Sylvia 2005). In the aquatic environment, ammonia is also produced and excreted by fish. The chemical form of ammonia in water consists of two species, the more abundant of which is the ammonium ion (NH_4^+) and the less abundant of which is the non-dissociated or unionized ammonia (NH_3) molecule; the ratio of these species in a given aqueous solution is dependent upon both pH and temperature (Emerson et al. 1975; Erickson 1985; Thurston 1988; Whitfield 1974; Wood 1993). Chemically, ammonia in an aqueous medium behaves as a moderately strong base with pK_a values ranging from approximately 9 to slightly above 10 as a function of temperature and ionic strength (Emerson et al. 1975; Whitfield 1974). In general, the ratio of unionized ammonia to ammonium ion in fresh water increases by 10-fold for each rise of a single pH unit, and by approximately two-fold for each 10°C rise in temperature from 0-30°C (Erickson 1985). Basically, as values of pH and temperature tend to increase, the concentration of NH_3 increases and the concentration of NH_4^+ decreases.

The ionized ammonium ion (NH_4^+) and unionized ammonia molecule (NH_3) are interrelated through the chemical equilibrium $NH_4^+ - OH^- \leftrightarrow NH_3 \cdot H_2O \leftrightarrow NH_3 + H_2O$ (Emerson et al. 1975; Russo 1985). The concentration of total ammonia (often expressed on the basis of nitrogen as total ammonia nitrogen or TAN) is the sum of NH_4^+ and NH_3 concentrations. It is total ammonia that is analytically measured in water samples. To estimate the relative

concentrations of NH_4^+ and NH_3 from total ammonia, Emerson et al.'s (1975) formulas are recommended (Adams and Bealing 1994; Alabaster and Lloyd 1980; Richardson 1997; Russo 1985). Figure 1 (below) shows the chemical speciation of ammonia over a range of pH levels in ambient waters at 25°C. It depicts the 10-fold increase in the ratio of unionized ammonia to ammonium ion in fresh water for each rise of a single pH unit as described above. This increase in unionized ammonia with increased pH is one hypothesis explaining why toxicity of total ammonia increases as pH increases.

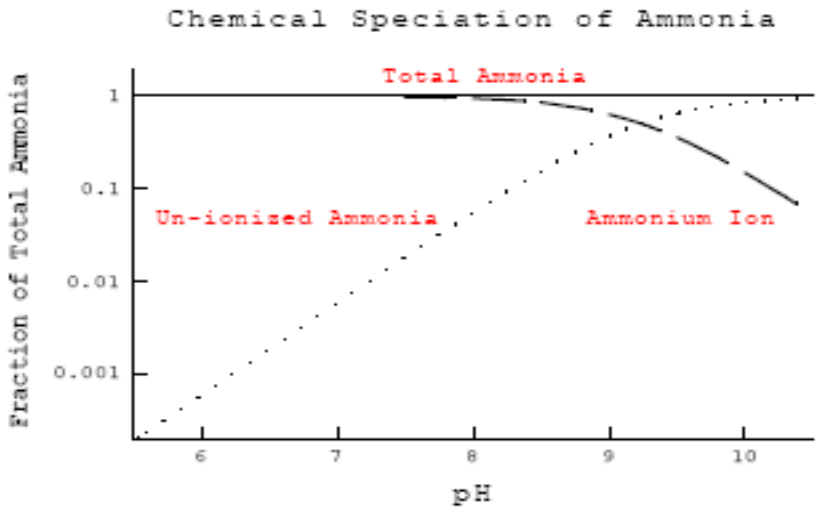

Figure 1. Fraction of Chemical Species of Ammonia Present with Change in pH (at 25°C).

Each separate fraction of total ammonia can be calculated in freshwater from the Henderson-Hasselbach equation if the pH and p*Ka* are known:

NH_4^+ = Total ammonia/(1+ antilog (pH-p*Ka*)) = Total ammonia – NH_3 (Wood 1993)

and,

p*Ka* = 0.09018 + (2729.92/(273.2 + T)) (Emerson et al. 1975)

where T is temperature in °C.

Mode of Action and Toxicity

Ammonia is unique among regulated pollutants because it is an endogenously produced toxicant that organisms have developed various strategies to excrete, which is in large part by passive diffusion of unionized ammonia from internal organs, such as the gills in fish. High external unionized ammonia concentrations reduce or reverse diffusive gradients and cause the buildup of ammonia in internal tissues and blood. Unionized ammonia may cause toxicity to *Nitrosomonas* spp. and *Nitrobacter* spp. bacteria, inhibiting the nitrification process (Russo 1985). Bacterial inhibition can result in the increased accumulation of ammonia in the aquatic environment, thereby intensifying the toxicity to beneficial bacteria and aquatic animals (Russo 1985).

The toxic action of unionized ammonia on aquatic animals, particularly in sensitive fish, may be due to one or more of the following causes: (1) proliferation in gill tissues, increased ventilation rates and damage to the gill epithelium (Lang et al. 1987); (2) reduction in blood oxygen-carrying capacity due to progressive acidosis (Russo 1985); (3) uncoupling oxidative phosphorylation causing inhibition of production and depletion of adenosine triphosphate (ATP) in the brain (Camargo and Alonso 2006); (4) and the disruption of osmoregulatory and circulatory activity disrupting normal metabolic functioning of the liver and kidneys (Arillo et. al.1981; Tomasso et al. 1980).

Among invertebrates, studies testing ammonia toxicity to bivalves, and particularly studies with freshwater mussels in the family Unionidae, have demonstrated their sensitivity to ammonia (Augspurger et al. 2003; Wang et al. 2007a, b; Wang et al. 2008). Toxic effects of unionized ammonia to both freshwater and marine bivalves include reduced opening of valves for respiration and feeding (Epifanio and Srna 1975); impaired secretion of the byssus, or anchoring threads in bivalves (Reddy and Menon 1979); reduced ciliary action in bivalves (U.S. EPA 1985); depletion of lipid and carbohydrate stores leading to metabolic alteration (Chetty and Indira 1995) as well as mortality (Goudreau et al. 1993). These negative physiological effects may lead to reductions in feeding, fecundity, and survivorship, resulting in decreased bivalve populations (Alonso and Camargo 2004; Constable et al. 2003).

ATTACHMENT 31

United States
Environmental Protection
Agency

Office of Water
Office of Science and Technology
(4304T)

EPA-822-R-02-047
November 2002

National Recommended Water Quality Criteria: 2002

For additional information see: *Ambient Water Quality Criteria for Dissolved Oxygen (Saltwater): Cape Cod to Cape Hatteras* (EPA-822R-00-012).

Freshwater Aquatic Life Criteria for Ammonia

This compilation includes EPA's latest revision (*1999*) of the freshwater aquatic life criteria for ammonia. The new water quality criteria reflect research and data since 1984, including the pH and temperature relationship of the acute and chronic criteria and the averaging period of the chronic criterion. The revised acute criterion for ammonia is now dependent on pH and fish species, and the chronic criterion is dependent on pH and temperature. At lower temperatures, the chronic criterion incorporates the presence or absence of early life stages of fish. The temperature dependency results in a gradual increase in the criterion as temperature decreases. At temperatures below 15 °C the criterion is more stringent, when early life stages of fish are expected to be present. EPA's recommendations in the 1999 criteria represent a change from both the 1984 chronic ammonia criterion, which was dependent mainly on pH, and from the 1998 ammonia criteria, in which the chronic criterion was dependent on pH and the presence of early life stages of fish.

For additional information see: *1999 Update of Ambient Water Quality Criteria for Ammonia* (EPA-822-R-99-014).

Cadmium

EPA revised its aquatic life criteria for cadmium. A notice was published in the **Federal Register** (65 FR 50201, 8/17/2000) announcing the availability of the peer review draft and soliciting any significant scientific input from the public. EPA has addressed the peer review comments and significant issues raised by the public. A notice of availability for the completed document, entitled *2001 Update of Ambient Water Quality Criteria for Cadmium* (EPA-822-R-01-001) was published in the **Federal Register** on April 12, 2001 (66 FR18935).

Guidance on the Calculation of Hardness-Dependent Metals Criteria

Freshwater aquatic life criteria for certain metals are expressed as a function of hardness because hardness can affect the toxicities of these metals. Hardness is used as a surrogate for a number of water quality characteristics which affect the toxicity of metals. Increasing hardness has the effect of decreasing the toxicity of metals. Water quality criteria to protect aquatic life may be calculated at different concentrations of hardness measured in milligrams per liter (mg/L) as calcium carbonate ($CaCO_3$).

Appendix B of this document presents the hardness-dependent equations for freshwater metals criteria. The specific values in the table are calculated at a hardness of 100 mg/L ($CaCO_3$) for illustrative purposes only. The hardness equations included in this compilation were developed based on results from laboratory toxicity tests that were conducted in fresh waters encompassing a range of hardness values. Although the amount of data and the strength of the

relationship vary for different metals, almost all data for hardness and toxicity are in the 20 to 400 mg/L hardness range.

In the past, EPA recommended that when the hardness of fresh surface water is less than 25 mg/L, 304(a) criteria concentrations be calculated as if the hardness is 25 mg/L. Available toxicity data in this range for copper, zinc and cadmium (EPA 440/5-84-031, EPA 440/5-87-003,and EPA-822-R-01-001) are somewhat limited, and are quite limited for silver, lead, chromium III and nickel (EPA 440/5-80-071, EPA 440/5-84-027,EPA 440/5-84-029 and EPA 440/5-86-004). Even fewer data are available below 20 mg/L hardness for copper, zinc and cadmium and none are available for silver, lead, chromium III and nickel. EPA evaluated these limited data, available in the current metals' criteria documents, and determined that they are inconclusive. Capping hardness at 25 mg/L without additional data or justification may result in criteria that provide less protection than that intended by EPA's *Guidelines for Deriving Numerical National Water Quality Criteria for the Protection of Aquatic Organisms and Their Uses* (EPA 822/R-85-100) or "the Guidelines." Therefore, EPA now recommends that hardness not be capped at 25 mg/L, or any other hardness on the low end. If there is a state or tribal regulatory requirement that hardness be capped at 25 mg/L, or if there are any situation-specific questions about the applicability of the hardness-toxicity relationship, a Water Effect Ratio (WER) procedure should be used to provide the level of protection intended by the Guidelines. When an ambient hardness of less than 25 mg/L is used to establish criteria for lead or cadmium, the hardness dependent Conversion Factor (CF) should not exceed one.

For hardness over 400 mg/L, EPA recommends two options: (1) calculate the criterion using a default WER of 1.0 and using a hardness of 400 mg/L in the hardness equation; or (2) calculate the criterion using a WER and the actual ambient hardness of the surface water in the equation. The second option is expected to result in the level of protection intended in the Guidelines whereas the first option is thought to result in an even more protective aquatic life criterion. At high hardness there is an indication that hardness and related inorganic water quality characteristics do not have as much of an effect on toxicity of metals as they do at lower hardnesses. Related water quality characteristics do not correlate as well at higher hardnesses as they do at lower hardnesses. There is also increased uncertainty in this range because very limited data are available to clearly quantify the relationship between hardness and toxicity. Therefore, if hardness is over 400 mg/L as $CaCO_3$, EPA continues to recommend that a hardness of 400 mg/L be used with a default WER of 1.0; alternatively, the WER and actual hardness of the surface water may be used.

Where applicable water quality standards require the use of a default hardness (e.g., 25 mg/L) to calculate a criterion, states and authorized tribes should use the WER procedure to adjust that criterion so that it provides the level of protection intended by the Guidelines. As the WER is inherently a site-specific procedure, any WER developed for a given site would be applicable only for that site unless its applicability at other sites is demonstrated. In any case, states and authorized tribes electing to use the WER Guidance should ensure that their water quality standards provide for them. Consistent with the "Performance-Based Approach" discussed in detail in EPA's recent modification of its implementing regulations at 40 CFR

131.21 (See 65 FR 24641, April 27, 2000), EPA encourages states and authorized tribes to identify all opportunities for adoption, and EPA approval of, such site-specific criteria. A performance-based approach relies on the adoption of a standard method or process (e.g., WER procedures) into state or tribal water quality standards, rather than adoption of a specific outcome (e.g., a site-specific criterion). When such an approach is sufficiently detailed and has suitable safeguards to ensure predictable, repeatable outcomes, EPA approval of the approach can serve as approval of the outcomes as well.

National Guidance on the Applicability of Freshwater and Saltwater Criteria

EPA recommends that the aquatic life criteria in this compilation apply as follows:

(1) For water in which the salinity is equal to or less than 1 part per thousand 95% or more of the time, the applicable criteria are the freshwater criteria.

(2) For water in which the salinity is equal to or greater than 10 parts per thousand 95% or more of the time, the applicable criteria are the saltwater criteria in Column C; and

(3) For water in which the salinity is between 1 and 10 parts per thousand the applicable criteria are the more stringent of the freshwater or saltwater criteria, as described in items (1) and (2) of this section. However, an alternative freshwater or saltwater criteria may be used if scientifically defensible information and data demonstrate that on a site-specific basis the biology of the water body is dominated by freshwater aquatic life and that freshwater criteria are more appropriate; or conversely, the biology of the water body is dominated by saltwater aquatic life and that saltwater criteria are more appropriate.

Nutrient Criteria

EPA recently developed section 304(a) water quality criteria for nutrients because excessive levels of nutrients are a major cause of the nonattainment of designated uses and more scientific information is needed to evaluate and address these conditions. Availability of these nutrient criteria recommendations was announced in the **Federal Register** on January 9, 2001 (66 FR1671). EPA's nutrient criteria will cover four major types of waterbodies: lakes and reservoirs, rivers and streams, estuarine and coastal areas, and wetlands across 14 major ecoregions of the United States. EPA's section 304(a) criteria are intended to provide for the protection and propagation of aquatic life and recreation. To support the development of the nutrient criteria, EPA published Technical Guidance Manuals that describe a process for assessing nutrient conditions in the four waterbody types. (For example See: *Nutrient Criteria Technical Guidance Manual: Lakes and Reservoirs*, April 2000; *Nutrient Criteria Technical Guidance Manual; Rivers and Streams*, July 2000; *Nutrient Criteria Technical Guidance Manual: Estuarine and Coastal Marine Waters*, October 2001). This information is intended to serve as a starting point for the states, authorized tribes and others to develop more refined

ATTACHMENT 32

U.S. Department of the Interior
U.S. Geological Survey

MINERAL COMMODITY SUMMARIES 2023

Abrasives
Aluminum
Antimony
Arsenic
Asbestos
Barite
Bauxite
Beryllium
Bismuth
Boron
Bromine
Cadmium
Cement
Cesium
Chromium
Clays
Cobalt
Copper
Diamond
Diatomite
Feldspar
Fluorspar
Gallium
Garnet
Gemstones
Germanium
Gold
Graphite
Gypsum
Hafnium
Helium
Indium
Iodine
Iron and Steel
Iron Ore
Iron Oxide Pigments
Kyanite
Lead
Lime
Lithium
Magnesium
Manganese
Mercury
Mica
Molybdenum
Nickel
Niobium
Nitrogen
Palladium
Peat
Perlite
Phosphate Rock
Platinum
Potash
Pumice
Quartz Crystal
Rare Earths
Rhenium
Rubidium
Salt
Sand and Gravel
Scandium
Selenium
Silicon
Silver
Soda Ash
Stone
Strontium
Sulfur
Talc
Tantalum
Tellurium
Thallium
Thorium
Tin
Titanium
Tungsten
Vanadium
Vermiculite
Wollastonite
Yttrium
Zeolites
Zinc
Zirconium

USGS
science for a changing world

ZINC

(Data in thousand metric tons of contained zinc unless otherwise noted)

Domestic Production and Use: The estimated value of zinc mined in 2022 was about $3.2 billion. Zinc was mined in five States at seven mining operations by five companies. Three smelter facilities, one primary and two secondary, operated by three companies, produced commercial-grade zinc metal. Of the total reported zinc consumed, most was used to produce galvanized steel, followed by brass and bronze, zinc-base alloys, and other uses.

Salient Statistics—United States:	2018	2019	2020	2021	2022[e]
Production:					
Zinc in ores and concentrates	824	753	723	704	770
Refined zinc[e, 1]	116	115	180	220	220
Imports for consumption:					
Zinc in ores and concentrates	([2])	([2])	3	13	6
Refined zinc	775	830	700	702	700
Exports:					
Zinc in ores and concentrates	806	792	546	644	660
Refined zinc	23	5	2	13	10
Shipments from Government stockpile[3]	—	—	—	—	1
Consumption, apparent, refined zinc[4]	868	939	878	908	910
Price, average, cents per pound:					
North American[5]	141.0	124.1	110.8	145.8	190
London Metal Exchange (LME), cash	132.7	115.6	102.7	136.3	160
Stocks, reported producer and consumer, refined zinc, yearend	119	116	120	110	100
Employment, number:					
Mine and mill[6]	2,630	2,470	2,360	2,470	2,600
Smelter, primary	250	250	220	220	220
Net import reliance[7] as a percentage of apparent consumption:					
Ores and concentrates	E	E	E	E	E
Refined zinc	87	88	79	76	76

Recycling: In 2022, an estimated 60% of the refined zinc produced in the United States was recovered from secondary materials at both primary and secondary smelters. Secondary materials included galvanizing residues and crude zinc oxide recovered from electric arc furnace dust.

Import Sources (2018–21): Ores and concentrates: Peru, 71%; Canada, 15%; China, 7%, Taiwan, 4%; and other, 3%. Refined metal: Canada, 66%; Mexico, 16%; Peru, 6%; Spain, 6%; and other, 6%. Waste and scrap (gross weight): Canada, 62%; Mexico, 36%; and other, 2%. Combined total (includes gross weight of waste and scrap): Canada, 66%; Mexico, 16%; Peru, 6%; Spain, 6%; and other, 6%.

Tariff: Item	Number	Normal Trade Relations 12–31–22
Zinc ores and concentrates, zinc content	2608.00.0030	Free.
Zinc oxide; zinc peroxide	2817.00.0000	Free.
Zinc sulfate	2833.29.4500	1.6% ad valorem.
Unwrought zinc, not alloyed:		
Containing 99.99% or more zinc	7901.11.0000	1.5% ad valorem.
Containing less than 99.99% zinc:		
Casting-grade	7901.12.1000	3% ad valorem.
Other	7901.12.5000	1.5% ad valorem.
Zinc alloys	7901.20.0000	3% ad valorem.
Zinc waste and scrap	7902.00.0000	Free.

Depletion Allowance: 22% (domestic), 14% (foreign).

Government Stockpile:[8]

		FY 2022		FY 2023	
Material	Inventory as of 9–30–22	Potential acquisitions	Potential disposals	Potential acquisitions	Potential disposals
Zinc	6.46	—	7.25	—	2.27

Prepared by **Amy C. Tolcin [(703) 648–4940, atolcin@usgs.gov]**

ZINC

Events, Trends, and Issues: On February 24, 2022, a final U.S. critical minerals list was published in the Federal Register (87 FR 10381). The 2022 critical minerals list was an update of the list of critical minerals published in 2018 in the Federal Register (83 FR 23295). The 2022 critical minerals list contained 50 individual mineral commodities instead of 35 minerals and mineral groups. The changes in the 2022 list from the prior list were the addition of nickel and zinc and the removal of helium, potash, rhenium, strontium, and uranium. The list is to be updated every 3 years and revised as necessary consistent with available data.

U.S. zinc mine production increased by 9% in 2022 compared with that in 2021. Zinc production at the Red Dog zinc-lead mine in Alaska, the largest zinc mine in the United States, increased notably compared with that in 2021 owing to higher mill throughput and zinc ore grades. The owner of the Empire State zinc mine in New York received permitting to begin open pit mining activities. An open pit mine would operate alongside the active underground mine and was expected to contribute to an increase in mill throughput in the first half of 2023. Several other zinc exploration and mine expansion projects were in active development in the United States during 2022. The North American price for Special High Grade (SHG) zinc was estimated to have increased by 30% in 2022 from that in 2021. The North American premium to the LME cash price reached historical highs in 2022 amid decreasing stocks on the London Metal Exchange, reduced production by zinc smelters in Europe because of high energy costs, and the permanent closure of a zinc smelter in Canada. Other zinc smelters in Canada and Mexico reported equipment and operational issues that negatively affected production during the year.

According to the International Lead and Zinc Study Group,[9] estimated global refined zinc production in 2022 was forecast to decrease by 2.7% to 13.49 million tons and estimated metal consumption to decrease by 1.9% to 13.79 million tons, resulting in a production-to-consumption deficit of 297,000 tons.

World Mine Production and Reserves: Reserves for Australia, Bolivia, Canada, China, India, Kazakhstan, Mexico, Peru, Sweden, the United States, and "Other countries" were revised based on company and Government reports.

	Mine production[10]		Reserves[11]
	2021	2022[e]	
United States	704	770	7,300
Australia	1,320	1,300	[12]66,000
Bolivia	500	520	NA
Canada	310	250	1,800
China	4,140	4,200	31,000
India	777	830	9,600
Kazakhstan	194	200	7,400
Mexico	724	740	12,000
Peru	1,530	1,400	17,000
Russia	280	280	22,000
Sweden	234	240	4,000
Other countries	1,960	2,000	30,000
World total (rounded)	12,700	13,000	210,000

World Resources:[10] Identified zinc resources of the world are about 1.9 billion tons.

Substitutes: Aluminum and plastics substitute for galvanized sheet in automobiles; aluminum alloys, cadmium, paint, and plastic coatings replace zinc coatings in other applications. Aluminum- and magnesium-base alloys are major substitutes for zinc-base diecasting alloys. Many elements are substitutes for zinc in chemical, electronic, and pigment uses.

[e]Estimated. E Net exporter. NA Not available. — Zero.

[1]Includes primary and secondary zinc metal production.

[2]Less than ½ unit.

[3]Defined as changes in total inventory from prior yearend inventory. If negative, increase in inventory.

[4]Defined as refined production + refined imports – refined exports ± adjustments for Government stock changes.

[5]Source: S&P Global Platts Metals Week, North American SHG zinc; based on the LME cash price plus premium.

[6]Includes mine and mill employment at zinc-containing deposits. Excludes office workers. Source: Mine Safety and Health Administration.

[7]Defined as imports – exports ± adjustments for Government stock changes.

[8]See Appendix B for definitions.

[9]Source: International Lead and Zinc Study Group, 2022, ILZSG session/forecasts: Lisbon, Portugal, International Lead and Zinc Study Group press release, October 12, [4] p.

[10]Zinc content of concentrates and direct shipping ores.

[11]See Appendix C for resource and reserve definitions and information concerning data sources.

[12]For Australia, Joint Ore Reserves Committee-compliant or equivalent reserves were 23 million tons.

ATTACHMENT 33

KELLY T. WOOD
CHRISTOPHER REITZ
Assistant Attorneys General
Office of the Attorney General
Ecology Division
PO Box 40117
2425 Bristol Court SW
Olympia, Washington 98504-0117
(360) 586-6770

ELIZABETH HARRIS
Assistant Attorney General
Office of the Attorney General
Environmental Protection Division
800 5th Ave Ste. 2000 TB-14
Seattle, Washington 98104
(206) 521-3213

Attorneys for Plaintiff State of Washington

UNITED STATES DISTRICT COURT
EASTERN DISTRICT OF WASHINGTON

STATE OF WASHINGTON,

Plaintiff,

v.

CROWN RESOURCES CORPORATION and KINROSS GOLD U.S.A., INC.,

Defendants.

NO. 2:20-CV-00147-RMP

FIRST AMENDED COMPLAINT

I. INTRODUCTION

1.1 Plaintiff, the State of Washington, by and through its attorneys Robert W. Ferguson, Attorney General, and Kelly T. Wood, Christopher Reitz, and Elizabeth Harris, Assistant Attorneys General, brings this action against Defendants named below for violations of the Clean Water Act, 33 U.S.C. §§ 1251–1388.

1.2 Crown Resources Corporation and Kinross Gold U.S.A., Inc., collectively Defendants, are—and have been for years—in violation of the

ATTORNEY GENERAL OF WASHINGTON
Ecology Division
PO Box 40117
Olympia, WA 98504-0117
360-586-6770

these tunnels lie below the water table. During mining, aboveground features of the Buckhorn Mine included access roads, maintenance shops, ore and development rock stockpiles, detention ponds, and a mine water treatment plant (MWTP). Some, but not all, of these aboveground features have been decommissioned.

6.10 Ore extraction at the Buckhorn Mine lasted through approximately 2017. While in active operation, Defendants extracted approximately $1.3 billion worth of gold from the Buckhorn Mine. Crown ceased extractive activity and began mine reclamation in 2017.

6.11 From construction through the present day, Defendants discharge pollutants from the Buckhorn Mine to both ground and surface waters in and around the Buckhorn Mine site. These pollutants include aluminum, ammonia, arsenic, chloride, copper, iron, lead, nitrates, sulfate, total dissolved solids, and zinc.

6.12 Discharges to groundwater travel anywhere from a few hundred to a few thousand feet to ultimately discharge to surface waters at or near the Buckhorn Mine site via hydraulic connectivity. Surface waters receiving discharges include Gold Bowl, Nicholson, Marias, Ethel, Bolster, and Gold Creeks. These creeks flow into Myers Creek and Toroda Creek, both of which flow into the Kettle River, a tributary of the Columbia River.

ATTORNEY GENERAL OF WASHINGTON
Ecology Division
PO Box 40117
Olympia, WA 98504-0117
360-586-6770

ATTACHMENT 34

Court rules gold mining company violated the law more than 3,000 times in Okanogan County

FOR IMMEDIATE RELEASE:
Oct 20 2022

Violations could result in millions of dollars in penalties

OLYMPIA — A federal judge has ruled that Crown Resources committed thousands of violations of the Clean Water Act in its operation of the Buckhorn Mountain gold mine in Okanogan County. The order comes as part of Attorney General Bob Ferguson's ongoing environmental citizen suit against Crown Resources and Kinross Gold.

Despite public assertions that "Crown adhered to the highest environmental standards during operation and closure of the Buckhorn Mine," Crown now stipulates to more than 3,000 violations of the Clean Water Act.

Judge Mary K. Dimke issued the order finding partial liability (https://agportal-s3bucket.s3.amazonaws.com/uploadedfiles/Another/News/Press_Releases/ECF124.pdf) in U.S. District Court for the Eastern District of Washington.

The penalties Crown will face for these violations will be determined at a later phase of the case. Kinross is not part of today's order, and the case against that company is ongoing. The companies could face millions of dollars in penalties for their pollution.

"Buckhorn Mountain is one of the unspoiled natural areas of our state," Ferguson said. "These companies had a responsibility, and legal obligation to protect it. They failed in that responsibility, thousands of times. We will continue our work to hold them accountable."

Judge Rosanna Malouf Peterson had previously dismissed the companies' main defenses (https://www.atg.wa.gov/news/news-releases/ag-ferguson-statement-after-major-win-buckhorn-gold-mine-clean-water-act-case), writing in the ruling that there is "no support" for their claims that the Attorney General's Office cannot enforce all of the mine's Clean Water Act permit.

The lawsuit was filed with consultation from the Washington State Department of Ecology. Okanogan Highlands Alliance, a citizen group that has long monitored water quality issues at the Buckhorn mine, filed a similar lawsuit in April 2020.

Case background

Crown Resources and its parent company, Kinross Gold, own Buckhorn Mountain gold mine, a 50-acre underground mine in Okanogan County located approximately 100 miles northeast of Twisp and about four miles from the Canadian border. From 2008 to 2017, the companies extracted approximately $1.3 billion in gold from the mine's miles of underground tunnels. A majority of these tunnels lie below the water table. Ore extraction stopped in 2017, but contaminants continue to be released from the mine.

Since the mine's construction, it has released pollutants to waters in and around the mine — including both groundwater and nearby streams, which flow into the Kettle River. These pollutants include aluminum, ammonia, arsenic, lead and nitrates. These contaminants are harmful to people, water ecosystems and fish species like trout.

Prior to the mine's construction, these streams were largely untouched and showed little evidence of contamination from human activity.

Crown and Kinross knew about the potential for pollution before the mine was constructed. The state conducted an environmental review of Crown's mine proposal prior to the mine's construction. The review identified potential impacts to nearby waters, noting that the mine would create the risk of "acid mine drainage" — highly acidic liquid, often containing toxic metals, that drains off a mine's newly excavated rock and ore. The review also noted that the use of explosives like dynamite at the mine could release pollutants into nearby waters.

Entities that release pollutants into Washington waterways are required by law to obtain a water quality permit from the state. The water quality permit for the Buckhorn mine requires Crown to capture and treat water impacted by the mine's operations, including stormwater, wastewater and contaminated groundwater.

Ferguson's lawsuit asserts the companies repeatedly violated the Clean Water Act, doing little to comply with its water quality permit and contain the pollution from the mine. Since 2015, the mine has not properly captured contaminated water, allowing contaminants to consistently escape the mine at levels well above those allowed by their water quality permit.

Ferguson's lawsuit asks the court to require Crown to meet the terms of their permit, remediating damage from years of pollution. The lawsuit asks the court to award monetary penalties and attorney's fees. The maximum penalty under the Clean Water Act is $54,800 per violation, per day, for up to five years. The Attorney General's Office estimates that the potential Clean Water Act penalty could be in the millions of dollars.

Assistant Attorneys General Elizabeth Harris, Junine So, and Dan Von Seggern and Paralegals Tricia Kealy, Tanya Rose-Johnston and Virginia Castro with the Environmental Protection Division, and Assistant Attorneys General Kelly Wood and Chris Reitz with the Ecology Division, are handling this case on behalf of the Attorney General's Office.

-30-

The Office of the Attorney General is the chief legal office for the state of Washington with attorneys and staff in 27 divisions across the state providing legal services to roughly 200 state agencies, boards and commissions. Visit www.atg.wa.gov (http://www.atg.wa.gov) *to learn more.*

Media Contact:

Brionna Aho, Communications Director, (360) 753-2727; Brionna.aho@atg.wa.gov (mailto:Brionna.aho@atg.wa.gov)

General contacts: Click here (https://gcc02.safelinks.protection.outlook.com/?url=https%3A%2F%2Fwww.atg.wa.gov%2Fcontact-us&data=02%7C01%7Cask4isd%40atg.wa.gov%7C0bf096ab891d45ee964608d812417366%7C2cc5baaf3b9742c9bcb8392cad34af3f%7C0%7C0%7C637279419610422508&sdata=Pz

News Release Search

Advanced Search (/news/news-releases/news-release-search)

Topic:

- AGO (/news/news-releases/AGO)
- Campaign Finance (/news/news-releases/Campaign%20Finance)
- Civil Rights (/news/news-releases/Civil%20Rights)
- Consumer Protection (/news/news-releases/Consumer%20Protection)
- Courts (/news/news-releases/Courts)
- Crime (/news/news-releases/Crime)
- Health (/news/news-releases/Health)
- Labor and Worker's Rights (/news/news-releases/Labor%20and%20Worker%27s%20Rights)
- Legislature (/news/news-releases/Legislature)
- Opioids (/news/news-releases/Opioids)
- Other Languages (/news/news-releases/Other%20Languages)
- Prescription Drugs; Opioids (/news/news-releases/Prescription%20Drugs%3B%20Opioids)
- Scams (/news/news-releases/Scams)
- Student loans (/news/news-releases/Student%20loans)
- undefined (/news/news-releases/undefined)
- Utilities (/news/news-releases/Utilities)

ATTACHMENT 35

WOLFDEN

April 13, 2023

Mr. Tim Carr
Land Use Planning Commission
22 State House Station
Augusta, ME 04333-0022

RE: Response to LUPC Comments of February 24, 2023

Dear Mr. Carr,

I'm pleased to reply to you and the LUPC with respect to your written request dated February 24, 2023.

Please accept the following as our responses and clarifications to your questions.

1. **Acreages of Current Zones**

   Surveys of the area to be rezoned have found intermittent streams. By rule these streams are bordered by Shoreland Protection subdistricts (P-SL2) of 75 ft. landward from the normal high-water mark on either side. Please provide a revised total acreage of General Management subdistrict (M-GN) and the total acreage of P-SL2 subdistrict that will be rezoned to the D-PD subdistrict. It is our understanding that the total area proposed for rezoning is 374 acres.

   The P-SL2 areas within the footprint represent 24 acres of the 374 rezone area as shown on Figure 1 below. This results in a General Management Subdistrict of 350 acres.

As can be seen on Figure 3, a portion of the spray irrigation areas in wetland catchments 1E, 1F, 1G, and 1P will be within the 400-foot setback from the edge of the rezoning area. No structures or clearing will be located in the setback, the usage is simply adding spray water recharge to maintain the wetland areas.

Variation in Naturally Occurring Precipitation

To assess the impact of an additional 0.9 percent of inflow to the wetlands, SME reviewed the historical precipitation data for Caribou, Maine, from 1939 to 2018 (National Oceanic and Atmospheric Administration), which is the nearest station to Patten with long-term data available. The data was averaged in ten-year increments, beginning in 1939. The lowest ten-year average was 34.8 inches from 1959 through 1968, the highest was 43.7 inches from 2009 to 2018, a 25 percent difference. The lowest individual precipitation year was 28.1 inches in 1987, the highest year was 55.4 inches in 2011, a 97 percent difference. Given the large variability in natural precipitation in the area, it is assumed that an additional 0.9 percent inflow to the wetlands will not cause an undue adverse impact on the water resources at the site. A graph of the eighty years of precipitation data showing the annual variability is included as Figure 4.

LUPC COMMENT 4 - SPRAY IRRIGATION AND SNOWMAKING

Provide conceptual schematics for proposed spray irrigation and snowmaking equipment for the Water Recharge Areas (WRAs).

SME's Response: Attachment 1 contains photos and schematics of typical spray irrigation equipment commonly used at wastewater treatment plants. Attachment 2 contains photos and schematics of typical snow making equipment commonly used at wastewater treatment plants, as well as some examples of snow stockpiles. Attachment 3 includes a case study of wastewater disposal through spray irrigation and snowmaking in Carrabassett, Maine.

Potential areas were designated for the spray irrigation and snow stockpiles of treated effluent, as depicted on Figure 3. Due to the inherent challenges in managing water during the winter at below freezing temperatures, the proposed snow stockpiles were selected to be near the storage ponds and to be at the highest points in the wetland catchments so that melting snow will drain to the wetland areas. Final locations will be determined as part of the final design for the disposition of treated water.

LUPC COMMENT 6 – SNOW STORAGE IN AFFECTED AREA

Provide evidence that sufficient area is set aside for storing snow from the collection area.

SME's Response: The following table provides an estimate of the annual snow storage requirement for the developed area. It is anticipated that only one third of the site will require snow removal, with the remainder of the developed portion of the site consisting of the treatment ponds, rock storage areas, etc. The required storage volume assumes a snow compaction rate of 70 percent, which is expected to occur during placement and settling. The 2.6-acre snow storage area shown on Figure 5 would require only a 16-foot-high snow pile, as calculated in Table 4. The average annual snowfall was taken from climate data for Caribou Municipal Airport, Maine as reported by the

ATTACHMENT 36

Stantec Consulting Services Inc.
30 Park Drive
Topsham ME 04086-1737

August 11, 2023

Project/File: 195602317

Via Email and Overnight Mail
Tim Carr, Senior Planner
Land Use Regulation Commission
22 State House Station
Augusta, Maine 04333-0022

Dear Tim,

Reference: Pickett Mountain Mine Rezone Petition, ZP779A

On behalf of Wolfden Mt. Chase, LLC ("Wolfden"), this letter provides responses to the Land Use Planning Commission (LUPC) comments in its July 13, 2023 letter to Wolfden pursuant to the Application for Zone Change for the Pickett Mountain Mine, ZP779A, referred to herein as the "Project," and review of technical consultant and agency comments provided with that letter.

LUPC Comments

1) *Provide information on the length of time that open-air blasting to provide access for underground workings is expected to last.*

   During portal development, we anticipate that there will be three (3) open air blasts over a period of one week. There will be no more than one blast per day. After one week, it is expected that the portal walls will be fully supported, and services installed to facilitate underground development work.

2) *Provide clarification on whether security signs will be posted around the property boundary (Application, p. 17.2), the subdistrict boundary (Application, p. 2.9), or both.*

   Security signage will be posted around the perimeter of the subdistrict (rezone) boundary within visual distance of any point along the boundary and at roads that intersect the rezone boundary. Directional signage will be posted at the main turnoff from Route 11 and at road intersections along access roads, including Hale Pond Rd. and Bear Mtn. Rd.

3) *Provide the trip number for traffic expected during the peak hour (including employees, contractors, visitors, delivery, and ore haulage).*

   There are expected to be a maximum of 94 trips per peak hour on the 5-mile mine access road within LUPC jurisdiction. This estimate includes employees, contractors, visitors, deliveries, and ore transport vehicles. A Maine DOT traffic permit will be obtained as required should traffic increase to 100 or more trips per peak hour.

The applicant appreciates the growing concern about PFAS contamination throughout the State of Maine and will develop a PFAS avoidance policy as part of its overall chemical management plan to limit the use of any PFAS-containing material onsite. Additionally, the water treatment facility is designed to remove PFAS that may be present in the water.

Impacts to Water Quality

The water collection area is graded and engineered to collect site contact water and redirect it to the pre-treatment water storage pond. This area is considered "impervious" and is underlain with an engineered liner sequence. Infrastructure within the water collection area includes the snow storage area, waste rock and ore stockpiles, buildings, ditches, sumps, and roads. Any activity that could potentially impact water quality, such as loading and unloading mined rock, is executed within the water collection area. Water contacting buildings and lots within the water collection area will be diverted to ditches and the pre-treatment water storage pond.

Miscellaneous Questions

A preliminary Acid Base Accounting ("ABA") study was performed on seven (7) samples taken from representative areas within waste rock where development drifts and raises are currently planned. Five (5) samples were taken from drill holes in the footwall of the orebody and two (2) samples were taken from the hanging wall. A range of rock types were selected for the ABA work, including mafic volcanics, felsic volcanics, and mafic intrusives. A more comprehensive Metal Leaching and Acid Rock Drainage ("MLARD") study will be completed once fresh core has been collected from an infill drill program planned to take place during the Chapter 200 application process. Additional samples will be collected in ore, waste rock, and low-grade ore, including typical rock types to be encountered during underground development and production.

Most of the underground development is currently designed in the footwall of the orebody; however, final detailed mine design will be completed once additional MLARD samples are analyzed, and geo-mechanical drilling programs have taken place. The near-vertical geometry of the deposit allows for some flexibility with mine design, such that the most appropriate locations, geochemically and geotechnically, will be selected for underground development.

Low-grade ore will be handled like higher-grade ore. It can be processed on its own and still produce an incremental profit or it can be blended with higher grade "pods" of ore to generate a consistent mill feed grade. If low-grade ore is not consumed throughout the life of the operation, it is processed through the concentrator before closure and reclamation begin.

Inland Fisheries & Wildlife

The Maine Department of Inland Fish and Wildlife ("MDIFW") did not offer any objections to the proposed rezoning and flagged that additional information would be provided as part of the Chapter 200 process. The applicant agrees and looks forward to continuing consultation with MDIFW to ensure that appropriate

ATTACHMENT 37

Zinc ores and concentrates exports by country in 2021

Change selection (Reporter, Year, Trade Flow, Partner and HS 6 digit Product)

In 2021, Top **exporters** of **Zinc ores and concentrates** are Australia ($1,921,282.16K , 2,102,390,000 Kg), Peru ($1,648,696.24K , 1,610,550,000 Kg), United States ($1,517,454.90K , 657,896,000 Kg), Bolivia ($1,381,611.04K , 699,540,000 Kg), Sweden ($493,876.63K , 436,046,000 Kg).

Zinc ores and concentrates imports by country in 2021

Reporter	TradeFlow	ProductCode	Product Description	Year	Partner	Trade Value 1000USD	Quantity	Quantity Unit
Australia	Export	260800	Zinc ores and concentrates	2021	World	1,921,282.16	2,102,390,000	Kg
Peru	Export	260800	Zinc ores and concentrates	2021	World	1,648,696.24	1,610,550,000	Kg
United States	Export	260800	Zinc ores and concentrates	2021	World	1,517,454.90	657,896,000	Kg
Bolivia	Export	260800	Zinc ores and concentrates	2021	World	1,381,611.04	699,540,000	Kg
		260800	Zinc ores and concentrates	2021	World	493,876.63	436,046,000	Kg

Reporter	TradeFlow	ProductCode	Product Description	Year	Partner	Trade Value 1000USD	Quantity	Quantity Unit
Australia	Export	260800	Zinc ores and concentrates	2021	World	1921282.16	2.10239e+009	Kg
Peru	Export	260800	Zinc ores and concentrates	2021	World	1648696.24	1.61055e+009	Kg
United States	Export	260800	Zinc ores and concentrates	2021	World	1517454.90	6.57896e+008	Kg
Bolivia	Export	260800	Zinc ores and concentrates	2021	World	1381611.04	6.9954e+008	Kg
Sweden	Export	260800	Zinc ores and concentrates	2021	World	493876.63	4.36046e+008	Kg
Turkey	Export	260800	Zinc ores and concentrates	2021	World	469339.29	8.56043e+008	Kg
South Africa	Export	260800	Zinc ores and concentrates	2021	World	444165.50	4.97297e+008	Kg
European Union	Export	260800	Zinc ores and concentrates	2021	World	387138.70	4.12344e+008	Kg
Portugal	Export	260800	Zinc ores and concentrates	2021	World	343986.17	4.09626e+008	Kg
Russian Federation	Export	260800	Zinc ores and concentrates	2021	World	323798.03	3.67344e+008	Kg
Mexico	Export	260800	Zinc ores and concentrates	2021	World	248335.73	1.73725e+008	Kg
Ireland	Export	260800	Zinc ores and concentrates	2021	World	240428.61	1.09763e+008	Kg
Spain	Export	260800	Zinc ores and concentrates	2021	World	238503.12		
Kazakhstan	Export	260800	Zinc ores and concentrates	2021	World	200401.26	2.23703e+008	Kg
Mongolia	Export	260800	Zinc ores and concentrates	2021	World	176417.75	1.12615e+008	Kg
Burkina Faso	Export	260800	Zinc ores and concentrates	2021	World	158113.63	1.81254e+008	Kg
Tajikistan	Export	260800	Zinc ores and concentrates	2021	World	140822.35	1.56665e+008	Kg
Finland	Export	260800	Zinc ores and concentrates	2021	World	131595.40	8.83102e+007	Kg
France	Export	260800	Zinc ores and concentrates	2021	World	126676.72	9.18421e+007	Kg
Greece	Export	260800	Zinc ores and concentrates	2021	World	86728.05	9.99794e+007	Kg
Morocco	Export	260800	Zinc ores and concentrates	2021	World	63963.25	9.39939e+007	Kg
Namibia	Export	260800	Zinc ores and concentrates	2021	World	59499.12	7.95604e+007	Kg
Canada	Export	260800	Zinc ores and concentrates	2021	World	58963.87		
Chile	Export	260800	Zinc ores and concentrates	2021	World	58954.17	6.38598e+007	Kg
North Macedonia	Export	260800	Zinc ores and concentrates	2021	World	55622.73	5.77754e+007	Kg
Saudi Arabia	Export	260800	Zinc ores and concentrates	2021	World	52938.89	5.12276e+007	Kg
Italy	Export	260800	Zinc ores and concentrates	2021	World	50181.53	4.66835e+007	Kg
Honduras	Export	260800	Zinc ores and concentrates	2021	World	46657.81	6.59488e+007	Kg
Netherlands	Export	260800	Zinc ores and concentrates	2021	World	39545.23	3.46962e+007	Kg
Korea, Rep.	Export	260800	Zinc ores and concentrates	2021	World	34678.68	2.38041e+007	Kg
Indonesia	Export	260800	Zinc ores and concentrates	2021	World	32020.44	3.03024e+007	Kg
Serbia, FR(Serbia/Montenegro)	Export	260800	Zinc ores and concentrates	2021	World	31484.22	3.03951e+007	Kg
Nigeria	Export	260800	Zinc ores and concentrates	2021	World	27499.69	3.82546e+008	Kg
Montenegro	Export	260800	Zinc ores and concentrates	2021	World	16366.82	1.93458e+007	Kg
Armenia	Export	260800	Zinc ores and concentrates	2021	World	16165.25	1.19984e+007	Kg
Bosnia and Herzegovina	Export	260800	Zinc ores and concentrates	2021	World	14078.64	1.52003e+007	Kg
United Kingdom	Export	260800	Zinc ores and concentrates	2021	World	12902.02	2.0612e+007	Kg
Dominican Republic	Export	260800	Zinc ores and concentrates	2021	World	12669.61	1.16959e+007	Kg
Lao PDR	Export	260800	Zinc ores and concentrates	2021	World	7519.91	1.2649e+007	Kg
Brazil	Export	260800	Zinc ores and concentrates	2021	World	5025.92	4.53553e+006	Kg
Bulgaria	Export	260800	Zinc ores and concentrates	2021	World	4611.37	2.86975e+006	Kg
Tunisia	Export	260800	Zinc ores and concentrates	2021	World	2749.21	3.77963e+006	Kg
Zambia	Export	260800	Zinc ores and concentrates	2021	World	2655.45	4.33689e+006	Kg
Belgium	Export	260800	Zinc ores and concentrates	2021	World	2495.29	3.19946e+006	Kg
Pakistan	Export	260800	Zinc ores and concentrates	2021	World	1863.87	8.764e+006	Kg
Hungary	Export	260800	Zinc ores and concentrates	2021	World	1016.82	260099	Kg
Myanmar	Export	260800	Zinc ores and concentrates	2021	World	900.62	1.20884e+007	Kg
United Arab Emirates	Export	260800	Zinc ores and concentrates	2021	World	805.65	1.66455e+006	Kg
Singapore	Export	260800	Zinc ores and concentrates	2021	World	783.28	4.02467e+006	Kg
Poland	Export	260800	Zinc ores and concentrates	2021	World	704.34	4.17188e+006	Kg
India	Export	260800	Zinc ores and concentrates	2021	World	585.85	822038	Kg
Malaysia	Export	260800	Zinc ores and concentrates	2021	World	540.57	718221	Kg
Congo, Rep.	Export	260800	Zinc ores and concentrates	2021	World	239.83	4.055e+006	Kg
Romania	Export	260800	Zinc ores and concentrates	2021	World	233.95	5.29689e+006	Kg
China	Export	260800	Zinc ores and concentrates	2021	World	156.76	322235	Kg
Ecuador	Export	260800	Zinc ores and concentrates	2021	World	107.37	114788	Kg
New Zealand	Export	260800	Zinc ores and concentrates	2021	World	84.82	20527	Kg
Oman	Export	260800	Zinc ores and concentrates	2021	World	73.90	2.952e+006	Kg
Bahrain	Export	260800	Zinc ores and concentrates	2021	World	57.44	30366	Kg
Thailand	Export	260800	Zinc ores and concentrates	2021	World	38.74	159035	Kg
Iceland	Export	260800	Zinc ores and concentrates	2021	World	37.41	37915.2	Kg
Trinidad and Tobago	Export	260800	Zinc ores and concentrates	2021	World	29.82	45000	Kg
Guatemala	Export	260800	Zinc ores and concentrates	2021	World	20.60	227828	Kg

Denmark	Export	260800	Zinc ores and concentrates	2021	World	8.59	2100	Kg
Kenya	Export	260800	Zinc ores and concentrates	2021	World	8.42	21501	Kg
Austria	Export	260800	Zinc ores and concentrates	2021	World	1.42	90	Kg
Croatia	Export	260800	Zinc ores and concentrates	2021	World	0.60	151.5	Kg
Switzerland	Export	260800	Zinc ores and concentrates	2021	World	0.30	5	Kg
Luxembourg	Export	260800	Zinc ores and concentrates	2021	World	0.02	1	Kg

ATTACHMENT 38

ISSN 0016-7029, Geochemistry International, 2006, Vol. 44, No. 1, pp. 48–55. © Pleiades Publishing, Inc., 2006.
Original Russian Text © A.A. Yaroshevsky, 2006, published in Geokhimiya, 2006, No. 1, pp. 54–62.

Abundances of Chemical Elements in the Earth's Crust

A. A. Yaroshevsky

Geological Faculty, Moscow State University, Vorob'evy gory, Moscow, 119992 Russia

Received June 29, 2005

Abstract—The evaluation of the abundances of chemical elements in the Earth's crust is a pivotal geochemical problem. Its first solutions in the early 20th century formed the empirical groundwork for geochemistry and justified concepts about the unity of the material of the Universe, the genesis of the chemical elements, and the geochemical differentiation of the Earth. The accumulation of newly obtained data called for the revision of this problem, and a series of papers by A.P. Vinogradov, which were published in *Geokhimiya* in 1956–1962, presented reevaluated contents of elements in the continental crust. In these papers, A.P. Vinogradov relied on the classic idea of the geochemical balance of the sedimentary process. These generalizations provided the foundation for the quantitative characterization of the geochemical background of the biosphere and allowed Vinogradov to formulate the principles of the melting and degassing of material in the outer Earth's shells during the geologic history, a concept that became universally acknowledged in modern geochemistry and geology. The composition of the Earth's crust can also be evaluated based not on the principle of geochemical balance in the sedimentary process but on data on the actual abundances of major magmatic, metamorphic, and sedimentary rock types. The possibility of this solution was provided after the extensive research of A.B. Ronov, who managed to develop a quantitative model for the structure of the Earth's sedimentary shell. Based on these data, A.B. Ronov, A.A. Yaroshevsky, and A.A. Migdisov published a series of papers in *Geokhimiya* in 1967–1985 that presented a model for the chemical structure of the Earth's crust with regard for the material composing not only the upper part of the continental crust but also its deep-seated granulite–basite layer and the oceanic crust. The quantitative estimates thus obtained led the authors to important conclusions: first, it was demonstrated that the estimated abundances of elements in the granite–metamorphic layer of the continental crust presented in the classic works by A.P. Vinogradov are confirmed by independent materials, which are based on data on the actual abundance of rocks. Second, incredible as it was, the principle of geochemical balance in the sedimentary process in application to Ca and carbonates appeared to be invalid. This problem remains unsettled as of yet and awaits its resolution.

DOI: 10.1134/S001670290601006X

The evaluation of the abundances of chemical elements in the Earth's crust is a pivotal problem of geochemistry. In fact, the very first accurate solutions of this problem in the early 1900s marked the establishment of geochemistry as a science on the natural history of the atoms of chemical elements. Papers by F.W. Clarke (United States), J. Vogt (Norway), V.I. Vernadsky (Russia), V.M. Goldschmidt and I. and W. Noddack (Germany), and G. Hevesy (Denmark) laid the empirical groundwork for geochemistry, which made it possible to propose the first solutions of the key scientific problems: the unity of the material of which the observable Universe consists, the origin of the chemical elements, and the geochemical zoning of the Earth. Ideas deduced from these solutions formed the fundamentals of modern geochemistry and acquired universal and philosophical significance.

The new tasks formulated during the solution of these problems were related, first of all, to the need for information on the abundances of trace, rare, and radioactive chemical elements. Interest in these elements rapidly grew in the middle of the last century due to the technological revolution. These tasks called for a radical modification of the analytical techniques. Progress in these methods was related to the fundamental modernization of, first of all, physical analytical methods. In the 1940s–1960s, the appearance and further development of X-ray diffraction analysis, mass spectrometry, and approaches of neutron activation analysis principally extended the empirical basis of geochemistry and made it possible to obtain extensive information, which appended preexisting tables and resulted in the revision of some earlier evaluations. This work was launched in the early 1940s and continued in the 1950s at the laboratory of Geochemical Problems and then at the Vernadsky Institute of Geochemistry and Analytical Chemistry, Russian Academy of Sciences, in Moscow. Its outcome allowed A.P. Vinogradov to publish a fundamental paper in the first issue of *Geokhimiya* (in the spring of 1956) that was the first publication of the then-latest data on the abundances of chemical elements in crustal magmatic rocks. This made it possible to quantify (on the basis of these data) the abundances of chemical elements in the classic object of geochemistry: the Earth's crust. The ever-growing accumulation of newly obtained data soon forced A.P. Vinogradov to return to this problem, and his paper published in 1962 [2] became the benchmark in geochemistry for several

years ahead. The simultaneous publications of analogous materials by Turekian and Wedepohl [2] and Taylor [4] appeared to be closely similar to the results published by A.P. Vinogradov: all of these reviews were based on the same base of empirical data.

The paper published by A.P. Vinogradov in 1962 undoubtedly marked a new stage in the evolution of knowledge about the chemistry of the continental crust. This paper does not lose its both historical and scientific importance for geochemistry, and its summarizing table is worth reproducing in this publication (Table 1). The corrections introduced with time into the estimated abundances of chemical elements in the Earth's crust cannot significantly modify the conclusions that have been drawn from these data. The comprehension and use of these values led to the formulation of at least three key points of geochemistry. First, they clarified the problem of mineral resources, first and foremost, the resources of rare elements, which were "offered" by nature and formed the basis for technological progress. Second, these data made it possible to quantitatively characterize the geochemical background of the biosphere and the natural levels of the concentrations of chemical elements in the habitats of living organisms. They also led to the first correct formulation of the problem of the geochemical heterogeneity of the biosphere and made it possible to identify the boundary conditions for distinguishing natural and anthropogenic geochemical anomalies and to justify the formulation of the problem of the geochemical zoning of the biosphere. Finally, when compared with data on the concentrations of chemical elements in the cosmic matter [5], these data led A.P. Vinogradov to formulate his well-known concept of melting and degassing as the fundamental differentiating processes of the Earth's deep-seated rocks and the origin of the crust, hydrosphere, and atmosphere [6, 7], a concept that appeared in place of V.M. Goldschmidt's idea about the primary differentiation of the completely molten Earth and is now universally recognized in geochemistry and geology.

Early in the evolution of geochemistry, the solution of the problem of the crustal abundances of chemical elements encountered certain principal difficulties, which were of dualistic character. First, the problem of the precise determination of the concentrations of, in the end, all chemical elements (with several of them contained in trace amounts) appeared to be nontrivial in itself. The solution of this problem was further complicated by the diversity of materials that had to be analyzed (rocks, minerals, soils, waters, gases, living matter, with the complete analysis of each of them being a separate experimental problem). Second, the geological object—the Earth's crust—was complex and extremely heterogeneous. The incredible diversity of rocks and mineral deposits, the differences between the crustal abundances of some rocks as great as several orders of magnitude, and the absence of acceptable quantitative estimates of these differences required an idea that would be instrumental in bypassing this "geological" complexity of the problem. Such an idea was found and justified by V.M. Goldschmidt as a concept of the geochemical balance of the sedimentary process. According to this idea, the average composition of secondary sedimentary rocks should be identical to the average composition of primary magmatic rocks. In his famous paper "Grundlagen der Quantitativen Geochemie" (*Fundamentals of Quantitative Geochemistry*) [8], Goldschmidt convincingly demonstrated that the composition of the chemically least altered clays is practically identical to the average composition of magmatic rocks (except only for the concentrations of the most mobile Ca, Na, and volatiles) calculated by F.W. Clarke and G.S. Washington. The validation of the plausibility of this balance provided the possibility of using the average concentrations of chemical elements in clayey rocks as a measure of the contributions of the most widespread rock types (granites and basalts) to the structure and composition of the Earth's crust. It was exactly this balance that was utilized by Vinogradov and Taylor to evaluate the average composition of the continental crust. These estimates of the two researchers appeared somewhat different: using data on a great number of elements, Vinogradov assumed the proportion of granites to basalts in the continental crust equal to 2 : 1, whereas Taylor relied on his own evaluations of the REE abundances in schists and assumed this ratio equal to 1 : 1. This explains the differences (which are generally insignificant) in the final values.

Geological observations, first of all, gradually amassing information on the actual abundances of the major rock types in the crust made the researchers consider more closely the idea of geochemical balance in the sedimentation process. The data of R.O. Daly and, later, S.P. Solov'ev on the actual occurrence frequencies of various magmatic rocks and the first quantitative results obtained by A.B. Ronov on the sedimentary shell demonstrated that the problem of geochemical balance can be revised. Poldervaart [9] was the first to propose in 1955 a new evaluation of the average chemical composition of the Earth's crust on the basis of the hypothetical abundance of the major types of magmatic, sedimentary, and metamorphic rocks in it (the abundances were "hypothetical" because no actual values were known at that time). The average crustal composition assayed by Poldervaart differed from the classic model of Clarke–Goldschmidt. However, the problem of the average chemical composition of the Earth's crust was actually solved in such a way only after A.B. Ronov had accomplished a vast volume of work on reconstructing the structure of the Earth's sedimentary shell. These estimates laid the groundwork for the estimation of the composition of the crust, which was first published in a paper by Ronov and the author of this paper in 1967 [10]. That paper summarized all then-available factual materials, but the likely most interesting result presented in it was the geochemical paradox, which was illustrated by quantitative data, of

Table 1. Abundances (10^{-4} wt %) of chemical elements in the major rock types and the upper continental crust (after [Vinogradov, 1962])

Element	Stony meteorites	Ultrabasic rocks	Basic rocks	Intermediate rocks	Acid rocks	Earth's crust
1	2	3	4	5	6	7
1 H	–	–	–	–	–	–
3 Li	3	0.5	15	20	40	32
4 Be	3.6	0.2	0.4	1.8	5.5	3.8
5 B	2	1	5	15	15	12
6 C	400	100	100	200	300	230
7 N	1	6	18	22	20	19
8 O	350000	425000	435000	460000	487000	470000
9 F	28	100	370	500	800	660
11 Na	7000	5700	19400	30000	27700	25000
12 Mg	140000	259000	45000	21800	5600	18700
13 Al	13000	4500	87600	88500	77000	80500
14 Si	180000	190000	240000	260000	323000	295000
15 P	500	170	1400	1600	700	930
16 S	20000	100	300	200	400	470
17 Cl	70	50	50	1100	240	170
19 K	850	300	8300	23000	33400	25000
20 Ca	14000	7000	67200	46500	15800	29600
21 Sc	6	5	24	2.5	3	10
22 Ti	500	300	9000	8000	2300	4500
23 V	70	40	200	100	40	90
24 Cr	250	2000	200	50	25	83
25 Mn	2000	1500	2000	1200	600	1000
26 Fe	250000	98500	85600	58500	27000	46500
27 Co	800	200	45	10	5	18
28 Ni	13500	2000	160	55	8	58
29 Cu	100	20	100	35	20	47
30 Zn	50	30	130	73	60	83
31 Ga	3	2	18	20	20	19
32 Ge	10	1	1.5	1.5	1.4	1.4
33 As	0.3	0.5	2	2.4	1.5	1.7
34 Se	10	0.05	0.05	0.05	0.05	0.05
35 Br	0.5	0.5	3	4.5	1.7	2.1
37 Rb	5	2	45	100	200	150
38 Sr	10	10	440	800	300	340
39 Y	0.8	–	20	–	34	29
40 Zr	30	30	100	260	200	170
41 Nb	0.3	1	20	20	20	20
42 Mo	0.6	0.2	1.4	0.9	1	1.1
44 Ru	1	–	–	–	–	–
45 Rh	0.19	–	–	–	–	–
46 Pd	1	0.12	0.019	–	–	–
47 Ag	0.094	0.05	0.1	0.07	0.05	0.07

Table 1. (Contd.)

Element	Stony meteorites	Ultrabasic rocks	Basic rocks	Intermediate rocks	Acid rocks	Earth's crust
1	2	3	4	5	6	7
48 Cd	0.1	0.05	0.19	–	0.1	0.13
49 In	0.001	0.013	0.022	–	0.26	0.25
50 Sn	1	0.5	1.5	–	3	2.5
51 Sb	0.1	0.1	1	0.2	0.26	0.5
52 Te	0.5	0.001	0.001	0.001	0.001	0.001
53 I	0.04	0.01	0.5	0.3	0.4	0.4
55 Cs	0.1	0.1	1	–	5	3.7
56 Ba	6	1	300	650	830	650
57 La	0.3	–	27	–	60	29
58 Ce	0.5	–	45	–	100	70
59 Pr	0.1	–	4	–	12	9
60 Nd	0.6	–	20	–	46	37
62 Sm	0.2	–	5	–	9	8
63 Eu	0.08	0.01	1	–	1.5	1.3
64 Gd	0.4	–	5	–	9	8
65 Tb	0.05	–	0.8	–	2.5	4.3
66 Dy	0.35	0.05	2		6.7	5
67 Ho	0.07	–	1	–	2	1.7
68 Er	0.2	–	2	–	4	3.3
69 Tm	0.04	–	0.2	–	0.3	0.27
70 Yb	0.2	–	2	–	4	3.3
71 Lu	0.035	–	0.6	–	1	0.08
72 Hf	0.5	0.1	1	1	1	1
73 Ta	0.02	0.018	0.48	0.7	3.5	2.5
74 W	0.15	0.1	1	1	1.5	1.3
75 Re	0.0008	–	0.00071	–	0.00067	0.0007
76 Os	0.5	–	–	–	–	–
77 Ir	0.48	–	–	–	0.0063	–
78 Pt	2	0.2	0.1	–	–	–
79 Au	0.17	0.005	0.004	–	0.0045	0.0043
80 Hg	3	0.01	0.09	–	0.08	0.083
81 Tl	0.001	0.01	0.2	0.5	1.5	1
82 Pb	0.2	0.1	8	15	20	16
83 Bi	0.003	0.001	0.007	0.01	0.01	0.009
90 Th	0.04	0.005	3	7	18	13
92 U	0.015	0.003	0.05	1.8	3.5	2.5

the absence of Ca balance between the magmatic and sedimentary material of the continental crust. This problem was somehow "felt" in geochemistry before: beginning with papers by Clarke and Goldschmidt devoted to quantitative geochemistry, it became evident enough that the theoretically evaluated abundances of carbonates in the sedimentary shell (as was calculated from the average Ca concentrations in magmatic rocks) significantly (by factors of two to three) exceeded the analogous values that seemed to follow from geological observations. The validation of these observations by the measured volumes of the major rock types compos-

ing the sedimentary shell (these calculations were conducted by Ronov) highlighted these discrepancies and made them obvious. Although numerous papers have been published since then in attempt to solve this paradox, up to the negation of evident data, it remains unsettled as of yet.

However, several geochemical parameters of the Earth's crust could not be evaluated in that research reliably and accurately enough. First of all, this applies to the average composition of the crystalline constituent of the continental crust, which was assayed based on the earlier rough evaluations made by J. Sederholm in 1925 for the Baltic Shield and by F. Grout in 1938 for the Canadian Shield. Second, there were no data on the composition of the oceanic crust, which was not considered at all by classic geochemistry. Third, the problem of the composition of the lower portion of the continental crust, the so-called basaltic layer, remained obscure. The adequate solution of this problem required further studying. The decisive role belongs there to the following works:

(1) In the late 1960s, Ronov and Migdisov completed their extensive research of the average chemical composition of the crystalline basement of the upper continental crust: its granitic–metamorphic layer. This task was accomplished largely with the use of factual materials that were obtained by scrupulous measurements conducted in specially designed maps to characterize the abundances of the main types of metamorphic and magmatic rocks in the Baltic and Ukrainian shields and the crystalline basement of the Russian Platform. Published in 1970, these results [11] enabled the modern evaluation of the composition of the upper continental crust. The roughly coeval data of D. Show *et al.* on the Canadian Shield; the materials of K. Ida and W. Fahring and of I. Lambert and K. Heier on the Australian Shield; the data of E.A. Kulish on the Aldan Shield; and the somewhat later extensive materials of B.A. Gorlitskii on the Ukrainian Shield appeared not only generally closely similar to the results of Ronov and Midgisov but also provided insight into the heterogeneity of the crust (although it was left uncertain as to how these variations might depend on the amounts of the input data and the methods used to assay the average compositions; the reader can find an illustrative explanation of the essence of this problem in Table 36 in the book by Ronov *et al.* [12]).

(2) The "discovery" of the oceanic floor and the accumulation of newly obtained data not only on the composition of modern deep-sea sediments (the first information on their geochemistry became available as early as the late 19th century, when collections of samples taken during the first world-encircling tours were processed, including dredges of marine bottom sediments) but also on one of the most important component of the oceanic crust: its volcanic rocks. The very first results on the chemistry and geochemistry of seven deep-sea basalts published by A. Engel *et al.* in 1965 had demonstrated how geochemically unusual were these basalts, which were even placed in a distinct "cell" in the rock systematics and for which a new term was coined: oceanic tholeiitic basalts. However incredible, the volcanic rocks composing the upper layer of the oceanic crystalline crust appeared to be so geochemically homogeneous that the increase in the number of the samples from seven to a few thousands practically did not affect the evaluation of their chemical composition that was derived from the data of Engel. Together with geophysical information, these data allowed Ronov to measure the actual volume of the oceanic crust and its contribution to the structure of unconsolidated sediments and magmatic material and formed the basis for the modern evaluations of the average chemical composition of the oceanic crust (it is worth mentioning that the description and geochemical examination of metamorphic rocks, which were found, although not very often, among seafloor rocks, did not modify the evaluation of the average composition: these rocks appeared to be of relatively low metamorphic grades and practically indistinguishable geochemically from their protolithic magmatic rocks).

The solution of these problems forced Ronov and the author of this paper to return to the evaluation of the chemical structure of the crust, which was accomplished in a paper published in 1976 [13]. In contrast to the model of 1967, this publication proposed new evaluations for the compositions of the most widespread rocks of the granitic–metamorphic layer of the continental crust, the average composition of this layer as a whole, and that of the oceanic crust; as well as the reevaluated composition of the deep-seated and practically unknown continental crustal layer: the granulite–basite layer (this problem will be discussed below).

The last step toward the solution of problems related to the chemical composition of the Earth's crust was made in the late 1980s. These results were published in a book by A.B. Ronov, the author of this paper, and A.A. Migdisov [12] in 1990. This latter model was based on refined data on the abundances of rocks in the sedimentary shell, which were published in the final papers by A.B. Ronov. The most important of these results were quantitative data on the abundances and compositions of the main types of volcanic rocks [14]. The evaluations obtained by Ronov for the proportions of these rocks and data on the abundances of intrusive rocks, which were also based on the materials of Ronov and Midgisov [11], made it possible to continue the differentiated assessment of the average chemical composition of the magmatic material of the crust depending on its geotectonic (geodynamic) setting [15].

In this, the latest model for the chemical structure of the Earth's crust, we tried to approach the solution of the problem of the unknown composition of the lower part of the continental crust, its granulite–basite layer. As is known, geophysical data provide no unambiguous

Table 2. Mass (10^{24} g) and average chemical composition (wt %) of the Earth's crust and its layers (after [12])

Component	Continental crust				Oceanic crust				Earth's crust as a whole
	sedimentary shell	granite-metamorphic shell	granulite-basite shell	crust as a whole	sedimentary layer	volcanic layer	basaltic layer	crust as a whole	
SiO_2	51.82	63.81	48.69	54.55	39.72	50.16	50.20	49.89	53.54
Al_2O_3	12.89	14.92	17.74	16.17	9.51	14.97	14.97	14.81	15.87
Fe_2O_3	2.50	1.75	–	0.92	3.34	1.79	1.73	1.79	1.11
FeO	2.91	3.68	10.84	7.32	1.31	8.82	8.82	8.60	7.6
MgO	3.32	2.83	6.70	4.91	2.13	7.53	7.54	7.38	5.44
CaO	9.93	4.08	11.69	8.72	19.18	11.62	11.73	11.93	9.41
Na_2O	1.96	3.02	2.71	2.74	1.43	2.43	2.41	2.38	2.66
K_2O	2.23	2.84	0.07	1.32	1.51	0.22	0.19	0.23	1.09
TiO_2	0.659	0.537	0.12	0.855	0.563	1.44	1.40	1.381	0.970
MnO	0.115	0.086	0.22	0.159	0.260	0.180	0.180	0.181	0.164
P_2O_5	0.162	0.141	0.25	0.201	0.198	0.150	0.140	0.143	0.189
C_{org}	0.48	0.05	–	0.07	0.11	–	–	–	0.06
CO_2	7.21	0.90	–	1.14	14.29	–	–	0.42	0.99
SO_3	0.219	0.105	–	0.063	0.355	–	–	0.010	0.052
S	0.221	0.066	–	0.049	0.038	–	–	0.001	0.039
F	0.046	0.053	–	0.025	0.052	–	–	0.002	0.020
Cl	0.539	0.022	–	0.068	0.136	–	–	0.004	0.055
H_2O	3.04	1.17	–	0.77	5.94	0.69	0.69	0.85	0.78
Total	100.00	100.00	100.00	100.00	100.00	100.00	100.00	100.00	100.00
Mass	2.52	8.12	11.68	22.32	0.18	1.05	4.91	6.14	28.46

solution of this problem. Although an attempt to systematically compare experimental data on the physical characteristics of the main types of magmatic and metamorphic rocks at various temperatures and pressures with geophysical data seemed to led the researchers to return to the classic model for the composition of the continental crustal material as corresponding to the composition of mafic rocks, these models were generalized as fairly primitive schemes (Fig. 2 in [13], which was then reproduced in [12]) and did not look convincing enough. It appeared, however, to be interesting to test such a model based on the idea of geochemical balance for the material of the continental crust as a whole. The key point of the idea was the assumption (which looked self-evident for nonvolatile components) that the average composition of the continental crust should be identical to the average chemical composition of magmatic crust-forming rocks of mantle provenance. This idea definitely follows from the modern paradigm of geology, as is expressed, for example, in the principle of the derivation of crustal material from the mantle, and was explicitly formulated by A.P. Vinogradov. S.R. Taylor addressed this idea and proposed his well-known "andesitic" model for the composition of the continental crust [16, 17]. However, the identification of the average composition of crust-forming magmatic material with andesites (in the restricted sense of this term) was at variance with natural observations. This was in conflict not only with the abundances of various types of volcanic rocks in ancient foldbelts but also with the actual abundances of volcanic rocks composing young island arcs of different types and various stages of maturity. In this sense, Ronov's data are undoubtedly more representative. According to them, the average proportions of basalts, andesites, and more acid volcanics among the volcanic rocks of island arcs and foldbelts are close to 5.5 : 3.5 : 1.

The average composition of the crust-forming magmatic material estimated on the basis of these values was slightly more mafic than that in Taylor's andesitic model. Assuming this composition as an average for the crust as a whole and subtracting (in compliance with the measured volumetric proportions) the composition of the upper crust (in fact, that of continental shields) from it, we developed a model for the granulite–basite layer [18], whose silica content (49.7%) was close to those in mafic magmatic rocks. In fact, some details of this composition appeared to be "not good enough" in the sense that the concentrations of other components

Table 3. Abundances (10^{-4} wt %) of some chemical elements in the upper continental crust

Element	Vinogradov, 1962	Ronov *et al*., 1990
O	470000	479000
Si	295000	296300
Al	80500	79000
Fe	46500	40600
Ca	29600	29200
K	25000	23600
Na	25000	22400
Mg	18700	17100
Ti	4500	3220
C	230	2960
S	470	1080
Mn	1000	670
P	930	620
F	660	530
Cl	170	220

did not exactly correspond to the analogous values for natural mafic magmatic and metamorphic rocks (this applies, first of all, to the underestimated content of potassium), but it is hardly reasonable now to expect any "better" estimates.

The final results are summarized in Table 2. The likely most significant outcome of this work is the practical validation of the estimated abundances of major elements in the upper continental crust, the only geologic object that was then accessible for geochemical examination, by the values published in the classic work by A.P. Vinogradov [2] (Table 3). This means that the actual geochemical parameters of the continental crust have long been known, and this problem, which was approached and attacked by geochemists over a long period of time, with the use of different methods, can be considered solved.

The latest evaluations of the abundances of all chemical elements in the upper continental crust seem to be the data published by Wedepohl [19] in 1995. These values are listed in this paper in Table 4. It can be seen that Wedepohl's estimates of the abundances of

Table 4. Abundances (10^{-4} wt %) of chemical elements in the upper continental crust (after [Wedepohl, 1995])

Element	Abundance	Element	Abundance	Element	Abundance
1 H	–	30 Zn	52	59 Pr	6.3
3 Li	22	31 Ga	14	60 Nd	25.9
4 Be	3.1	32 Ge	1.4	62 Sm	4.7
5 B	17	33 As	2.0	63 Eu	0.95
6 C	3240	34 Se	0.083	64 Gd	2.8
7 N	83	35 Br	1.6	65 Tb	0.50
8 O	–	37 Rb	110	66 Dy	2.9
9 F	611	38 Sr	316	67 Ho	0.62
11 Na	25670	39 Y	20.7	68 Er	–
12 Mg	13510	40 Zr	237	69 Tm	–
13 Al	77440	41 Nb	26	70 Yb	1.5
14 Si	303480	42 Mo	1.4	71 Lu	0.27
15 P	665	44 Ru	–	72 Hf	5.8
16 S	953	45 Rh	–	73 Ta	1.5
17 Cl	640	46 Pd	–	74 W	1.4
19 K	28650	47 Ag	0.055	75 Re	–
20 Ca	29450	48 Cd	0.102	76 Os	–
21 Sc	7	49 In	0.061	77 Ir	–
22 Ti	3117	50 Sn	2.5	78 Pt	–
23 V	53	51 Sb	0.31	79 Au	–
24 Cr	35	52 Te	–	80 Hg	0.056
25 Mn	527	53 I	1.4	81 Tl	0.75
26 Fe	30890	55 Cs	5.8	82 Pb	17
27 Co	11.6	56 Ba	668	83 Bi	0.123
28 Ni	18.6	57 La	32.3	90 Th	10.3
29 Cu	14.3	58 Ce	65.7	92 U	2.5

chemical elements differ somewhat form those obtained by Ronov *et al.* These differences can be explained by the fact that Wedepohl proceeded from slightly different proportions of major rock types in the crust. The reasons for these changes are not fully clear, and it is pertinent to mention that, with regard for the generally not very high accuracy of even modern estimates (their inaccuracies can hardly be less than ±10%), there are no grounds to consider these discrepancies principal. The abundances of chemical elements in the lower continental crust and, correspondingly, in the continental crust as a whole published by Wedepohl are even more problematic and are not quoted here.

There seem to be good reasons to believe that our estimates of the average compositions of the upper continental crust, sedimentary shell, and continental crust are fairly realistic. This makes it possible to proceed to the solution of another problem: an accurate quantitative evaluation of the regional geochemical heterogeneity of the Earth's crust, in particular, in relation to its geotectonic (geodynamic) heterogeneity and the different ages of its rocks. Much information devoted to this problem is already published, for example in *Geochemistry International* (see, for instance, [20–25]), but the solution of this problem is only in its early stages and requires so much effort and time that it is hard to expect any appreciable results in the foreseeable future.

REFERENCES

1. A. P. Vinogradov, "Distribution of Chemical Elements in the Earth's Crust," Geokhimiya, No. 1, 6–52 (1956).
2. A. P. Vinogradov, "Average Contents of Chemical Elements in the Major Types of Terrestrial Igneous Rocks," Geokhimiya, No. 7, 555–571 (1962).
3. K. K. Turekian and K. H. Wedepohl, "Distribution of the Elements in Some Major Units of the Earth's Crust," Geo-Mar. Lett. **72** (2), 175–192 (1961).
4. S. R. Taylor, "Abundance of Chemical Elements in the Continental Crust: A New Table," Geochim. Cosmochim. Acta **28** (8), 1273–1285 (1964).
5. A. P. Vinogradov, "Atomic Distributions of Chemical Elements in the Sun and Stony Meteorites," Geokhimiya, No. 4, 291–295 (1962).
6. A. P. Vinogradov, *Chemical Evolution of the Earth* (AN SSSR, Moscow, 1959) [in Russian].
7. A. P. Vinogradov, "The Origin of the Earth's Crust: Paper 1," Geokhimiya, No. 1, 3–29 (1961).
8. V. M. Goldschmidt, "Grundlagen der Quantitativen Geoshemie," Fortssh. Miner. Krist. Retrogr. **XVII**, 112–115 (1933).
9. A. Poldervaart, "Chemistry of the Earth's Crust," Geol. Soc. Am. Sp. Paper **62**, 119–144 (1955).
10. A. B. Ronov and A. A. Yaroshevsky, "Chemical Structure of the Earth's Crust," Geokhimiya, No. 11, 1285–1309 (1967).
11. A. B. Ronov and A. A. Migdisov, "Compositional Evolution of Rocks in the Shields and Sedimentary Cover of the Russian and North American Platforms," Geokhimiya, No. 4, 403–438 (1970).
12. A. B. Ronov, A. A. Yaroshevsky, and A. A. Migdisov, *The Chemical Structure of the Earth's Crust and the Geochemical Balance of Major Elements* (Nauka, Moscow, 1990) [in Russian].
13. A. B. Ronov and A. A. Yaroshevsky, "A new Model for the Chemical Structure for the Earth's Crust," Geokhimiya, No. 12, 1763–1795 (1976).
14. A. B. Ronov, "The Distribution of Basalts, Andesites, and Rhyolites in Continents, Their Margins, and Oceans" Izv. Akad. Nauk SSSR, Ser. Geol., No. 8, 3–11 (1985).
15. A. A. Yaroshevsky, "Average Chemical Composition of the Main Groups of Magmatic Associations in the Earth Crust," Geokhimiya, No. 8, 787–793 (1997) [Geochem. Int. **35** (8), 689–694 (1997)].
16. S. R. Taylor, "Island Arc Models and the Composition of the Continental Crust," Am. Geophys. Union, Maurice Ewing Ser. **1**, 325–335 (1977).
17. S. R. Taylor and S. M. McLennan, *The Continental Crust: Its Composition and Evolution* (Blackwell, Boston, 1985; Mir, Moscow, 1988).
18. A. A. Yaroshevsky, "The Chemical Composition of the Granulite–Basite Layer of Continental Crust and the Chemical Structure of the Earth's Crust with Relation the Concept of Geochemical Balance," Geokhimiya, No. 8, 1139–1147 (1985).
19. K. H. Wedepohl, "The Composition of the Continental Crust," Geochim. Cosmochim. Acta **59** (7), 1217–1232 (1995).
20. A. D. Kanishchev and G. I. Menaker, "Chemical Structure of the Earth's Crust in Central and Eastern Transbaikalia," Geokhimiya, No. 1, 3–17 (1971).
21. A. D. Kanishchev and G. I. Menaker, "Average Contents of 15 Ore-Forming Chemical Elements in the Earth's Crust of Transbaikalia," Geokhimiya, No. 2, 187–202 (1974).
22. O. M. Turkina, "Geochemical Types of Granitoids and Composition of the Earth's Crust within the Kan and Arzybei–Derbin Blocks (Southwestern Siberian Platform)," Geokhimiya, No. 6, 516–528 (1996) [Geochem. Int. **34** (6), 464–474 (1996)].
23. V. S. Lutkov and V. V. Mogarovskii, "Geochemical Model for the Granite-Metamorphic Layer of the Earth's Crust in the Pamirs and Southern Tien Shan Foldbelts of Tajikistan," Geokhimiya, No. 6, 574–581 (1999) [Geochem. Int. **37** (6), 503–511 (1999)].
24. V. S. Lutkov, V. V. Mogarovskii, and V. Ya. Lutkova, "Geochemical Model for the Lower Crust in the Pamirs and Tien Shan Folded Areas, Tajikistan: Evidence from Studies of Xenoliths in Alkaline Mafic Rocks," Geokhimiya, No. 4, 386–398 (2002) [Geochem. Int. **40** (4), 342–354 (2002)].
25. V. R. Vetrin, "Two Types of Lower Continental Crust in the Northern Baltic Shield," Geokhimiya, No. 9, 1006–1009 (2001) [Geochem. Int. **39** (9), 917–919 (2001)].